Biodegradation of Crude Oil Hydrocarbons Supported on Clay Minerals

A thesis submitted to the Newcastle University in partial fulfilment of the requirements for the award of the degree of Doctor of Philosophy in the Faculty of Science, Agriculture and Engineering

Uzochukwu Cornelius UGOCHUKWU

School of Civil Engineering and Geosciences, Newcastle University,

Newcastle Upon Tyne, UK.

August, 2011.

DECLARATION

I hereby certify that this work is my own, except where otherwise acknowledged, and that this work has not been submitted previously for a degree at this, or any other university.

……

Uzochukwu Cornelius UGOCHUKWU

ABSTRACT

Clay minerals are the most abundant minerals near the earth's surface and play very important roles in biogeochemical processes. They have been found very useful in various industrial applications. The surface properties of clay minerals such as high specific surface area (SSA) and cation exchange capacity (CEC) make them able to act as catalysts, supports and sorbents of toxic and radioactive chemicals. However, their role during the biodegradation of crude oil hydrocarbons is not well understood. The main aim of this research project was to investigate the capabilities of the various forms and types of clay minerals in supporting the microbial degradation of crude oil hydrocarbons so as to gain better understanding of their potential role in the bioremediation of oil polluted sites.

The role of clays in hydrocarbon removal was investigated in aqueous clay/oil microcosm experiments with a hydrocarbon degrading microorganism community. The clays used for this study were bentonite, palygorskite, saponite and kaolinite. Clays were treated to produce acid activated clays and organoclays; homoionic interlayer bentonites were also used in this study. The study identified volatilization and adsorption as processes that will take place alongside biodegradation and therefore needed to be accounted for in the assessment of the effects of the clays.

The study indicated that acid activated clays, organoclays, untreated kaolinite, K-bentonite, Zn-bentonite and Cr-bentonite were inhibitory to biodegradation of the hydrocarbons, via different mechanisms, whereas Ca-bentonite and Fe-bentonite were stimulatory to biodegradation with about 80% removal of the total petroleum hydrocarbons (TPH) due to biodegradation. The 'local bridging effect' and polarization of the interlayer water were identified as two opposing influences arising from the interlayer cations of clay minerals that probably determine the extent of biodegradation of the hydrocarbons.

Adsorption of hydrocarbons was significant during biodegradation especially with unmodified palygorskite, Zn-bentonite and K-bentonite as each of them caused more than 40% removal of TPH by adsorption in the experimental microcosm containing 5:1 ratio (w/w) of clay to oil. The process of adsorption of aromatic compounds in the crude oil was believed to take place via cation-π interactions.

The correlation between extent of biodegradation and surface area is more robust than that between extent of biodegradation and CEC. The same trend applies with adsorption indicating that both biodegradation and adsorption are more surface area dependent than CEC.

ACKNOWLEDGEMENTS

My foremost acknowledgement goes to the Almighty God whose grace and providence were sufficient for the successful completion of this study.

I appreciate my country, the Federal Republic of Nigeria for funding this research via the management of PTDF to whom am also grateful.

I am very grateful to my supervisors, Dr. Martin Jones, Professor Ian Head and Professor David Manning. I am highly indebted to these academic giants upon whose shoulders I stood throughout the course of this research. Their supervision of this work was quite thorough without which it would have been difficult to complete this study successfully.

I acknowledge with a deep sense of appreciation, the initial guidance and assistance I received from Dr. Claire Isabella Fialips who was the former supervisor of this project. Her lecture notes in clay minerals were also helpful in building a theoretical background in clays.

My lovely wife is hereby acknowledged for all her assistance and cooperation during this study especially the tremendous understanding she showed during the hectic period of keeping late nights. She provided all the comfort a man will require in a home after some frustrating experimental studies.

I appreciate the assistance I received from some of the staff of the school of civil engineering and geosciences, namely, Dr. Angela Sherry, Jane Davis, Donna Swan, Stuart Patterson, Phil Green, Maggie White and Ian Harrison. My special thanks and indebtedness go to Berny Bowler, Paul Donohue, Margaret Wardley and Yvonne Hall for the special help I received from them at one time or the other. I appreciate Carla Washbourne for all her assistance during the EGME-surface area experiments. I am highly indebted to you all!

My colleagues, Dr. Ojugo Nwosu, Dr. Bunmi Eniola, Dr. Aminu Bayawa, Sani Yahaya, Mohammed Bello Adamu, Victoria Oriuwa, Timi Oriaku, Eleanor Swain, Reuben Ishicheli Agbidi and Ida Shafiee Ismail are highly appreciated for all their contributions in one way or the other.

DEDICATION

This research project is dedicated to my late parents, Elder Paul Okebugwu Ihedioha Ugochukwu and Mrs Elizabeth Ugochukwu who passed on to glory in the course of this study on 5th September, 2010 and 25th October, 2009 respectively.

I rolled in tears each time I remembered you and wondered if I would have the strength to complete this study but the Lord was gracious to me. I am pained remembering that you both went through thick and thin to have me acquire good education but could not see me enter the promised land for surely the Lord has brought me to my REST.

May you all rest in peace!!!

Table of contents

List of Tables

List of Figures

LIST OF ACRONYMS

AIPEA = Association Internationale Pour l' Etude des Argiles

API = American Petroleum Institute

BET = Brunauer Emmet Teller

BH = Bushnell-Haas

BTEX = Benzene, Toluene, Ethylbenzene and Xylene

CEC = Cation Exchange Capacity

CI = Confidence Interval

CMC = Critical Micelle Concentration

DCM = Dichloromethane

DDDMA = Didecyldimethylammonium

DLVO = Derjaguin Landau Verwey Overbeek

EGME = Ethylene glycol monoethyl ether

EOM = Extractable Organic Matter

FID = Flame Ionization Detector

FTIR = Fourier Transform Infra Red

GC = Gas Chromatography

GC-MS = Gas Chromatography-Mass Spectrometry

HMW = High Molecular Weight

HMWPAH = High Molecular Weight Polycyclic Aromatic Hydrocarbons

ICPOES = Inductively Coupled Plasma Optical Emission Spectroscopy

JNC = Joint Nomenclature Committees

LMW = Low Molecular Weight

LMWPAH = Low Molecular Weight Polycyclic Aromatic Hydrocarbons

MPN = Most Probable Number

NAPL = Non Aqueous Phase Liquids

NSO = Nitrogen, Sulphur and Oxygen

PAH = Polycyclic Aromatic Hydrocarbons

RRF = Relative Response Factor

SA = Surface Area

SARA = Saturates, Aromatics, Resins and Asphaltenes

SSA = Specific Surface Area

SPE = Solid Phase Extraction

TLC = Tin Layer Chromatography

TLC-FID = Tin Layer Chromatography –Flame Ionization Detector

TOC = Total Organic Carbon

TPH = Total Petroleum Hydrocarbon

TRS = Total Residual Saturates

UV = Ultra Violet

USEPA = United States Environmental Protection Agency

XRD = X-Ray Diffraction

1. GENERAL INTRODUCTION

1.1 Background

Crude oil has been a major source of energy all over the world for many years now and is likely to continue to be so at least for the foreseeable future as there is no viable alternative yet (Wang et al., 2006). Over the past five decades, there has been a large worldwide increase in the exploration, production, processing, storage, transportation and consumption of crude oil and its fractions which inevitably increases the risk of their accidental discharge to the environment (Harayama et al., 1999; Das and Mukherjee, 2006; Wang et al., 2006; Delille and Coulon, 2008; Nikopolou and Kalogerakis, 2009).

Environmental pollution by crude oil and its fractions has become a major concern in the world today as it is the main cause of ecological and social damage (Burger, 1993; Burns et al., 1993; Shaw, 1992). The spillage of crude oil and its fractions in the environment has resulted in large numbers of contaminated sites (Vidali, 2001; Environment Agency, 2006).

The incidents of oil contamination have been reported to be about nine per day with about one million tonnes of oil spilled into UK terrestrial ecosystems per annum (Environment Agency, 2006; Ripley et al., 2002). Between 1976 and 2005, Nigeria's Niger delta recorded over 3.0 million barrels of oil spilled in the environment in 9,107 spill incidents (Egberongbe et al., 2006).

Soil contamination by hydrocarbons can cause extensive damage to the local ecosystems affecting vegetation and wildlife adversely. Such contamination can also present a serious health threat to humans and in extreme case, can render the contaminated area unsuitable for human habitation (Sunggyu, 1995).

Contaminated land is costly to clean up; for example, in the USA, the cost is expected to exceed 1trillion USD and sites contaminated by petroleum hydrocarbon are estimated to be 90% of all sites undergoing remediation (Cole, 1994; Maier et al., 2000).

Figure 1.1 Oil well-head leaking oil in the Niger delta region of Nigeria destroying vegetation (platformlondon, 2008)

Figure 1.2 Oil spill associated with an incident of fire in the Niger-delta, destroying wildlife, vegetation and jeopardizing air quality (platformlondon, 2008).

Various methods have been utilized for the treatment or remediation of oil contaminated sites. These methods include permanent removal of the contaminated soil to a secure landfill, incineration and indirect thermal treatment (Vidali, 2001). Removal of contaminated soil to landfills is no longer an attractive alternative on account of high excavation, transportation and disposal costs and also because of the potential for residual liability. Incineration and thermal treatments involve enormous transportation and energy costs and therefore are often not viable options (Vidali, 2001). Many different bacteria are known to be capable of degrading, and in many cases, completely mineralizing various organic compounds in a biochemical process termed as biodegradation (Harayama et al., 1999;

Bogan et al., 2003; Holden et al., 2002). Biodegradation is the principal removal process of crude oil spill in soils and sediments and involves the mineralization of the crude oil hydrocarbons by indigenous or added microbes (Prince et al., 1994; Watson et al., 2002; Bogan and Sullivan, 2003; Bogan et al., 2003; Das and Mukherjee, 2006; Retz et al., 2008). The process of biodegradation of crude oil is controlled by the crude oil physicochemistry, the prevailing environmental conditions, bioavailability and the presence of catabolically active microbes (Stroud et al., 2007).

Bioremediation has long been proposed and applied as a treatment technology for the decontamination of hydrocarbon contaminated sites by biodegradation (Bogan et al, 2003). Bioremediation is generally the manipulation of the factors that control the microbial break-down of the contaminants such that the process of biodegradation is sped up leading to conversion of the contaminants to non-toxic substances (Mueller, 1996; Vidali, 2001; Rockne and Reddy, 2003). It is widely accepted to be an environmentally friendly and cost effective method for hydrocarbon spill clean-up (Stroud et al., 2007).

Several studies have demonstrated that some solid surfaces such as clay minerals are able to stimulate microbial growth hence enhancing biodegradation of organic compounds including hydrocarbons (Stotzky and Rem, 1966; van Loosdrecht et al., 1990; Chaerun et al., 2005; Tazaki et al., 2008 and Warr et al., 2009). Clay minerals are ubiquitous in the natural environment, and are non-toxic and economical to use (Tazaki and Chaerun, 2008). They play a vital role in terrestrial biogeochemical cycles and containment of toxic waste materials (Bergaya et al., 2006). Clay minerals are believed to have significant impacts on the environmental fate of pollutants such as oil spills (Chaerun and Tazaki, 2005). In addition to being able to stimulate microbial growth, some clay minerals are believed to have the ability to sorb organic, inorganic and microorganisms which might be beneficial in some remediation processes (Lipson & Stotzky, 1983 & 1984; Boyd et al., 1988; Lee et al., 1990; van Loosdrecht et al., 1990; Guerin and Boyd, 1992; Khanna & Stotzky, 1992; Tapp & Stotzky, 1995; Vettori et al., 1999; Sposito et al., 1999; Lin & Puls, 2000; Murray, 2000; Churchman et al., 2006; Warr et al., 2009).

However, despite the increased research efforts into the role of clay minerals in biogeochemical cycles, their role during the biodegradation of crude oil hydrocarbons has not been adequately reported.

1.2 Crude oil and SARA fractions

1.2.1 Crude oil

Crude oil is derived mainly from aquatic dead plants and animals that had been converted to a complex organic matter called kerogen via diagenesis (Tissot and Welte, 1984). This kerogen which is essentially the petroleum precursor mixes with sand and mud to be transformed to sedimentary rock. This is a very gradual geological process that takes millions of years to take place. The kerogen is converted to petroleum through a process called catagenesis then migrates from the original source rock to a more porous and permeable rock such as siltsone or sandstone which acts as reservoirs that entraps the petroleum (Tissot and Welte, 1984). The final crude oil that is ready to be explored and exploited is affected by certain factors that control its composition. It is expected that due to the variability of the different controlling factors (such as organic source matter, thermal maturity, migration and in-reservoir alteration), no two oils will be same at least at a molecular level (Stout and Wang, 2007).

The nature of crude oil's source organic matter varies with geologic age, lithology and depositional environment eg, lake, delta, ocean etc (Tissot and Welte, 1984). The prevailing process kinetic conditions during the generation and expulsion of crude oil will bring about a particular thermal profile (maturity) that will determine the extent of isomerization, cracking and aromatization for a particular crude oil. During the migration of crude oil after its expulsion from the source strata, the composition of the crude oil might undergo changes due to possible extraction of compounds from the carrier beds. Even the reservoir rock might lend itself to this process leading to further changes of the composition of the crude oil (Curiale, 2002). The migration effect could also lead to a mild molecular fractionation (Larter et al, 1996; Matyasik et al., 2000). In the reservoir, there could be changes in the crude oil composition brought about by processes known as water-washing caused by meteoric water, deasphaltening and biodegradation (Connan, 1984; Seifert et al., 1984; Cassani and Eglinton, 1991; Palmer, 1993).

A particular group of compounds called 'biomarkers' formed during diagenesis or catagenesis have proved to be highly important in understanding the biomass that accumulated to form the organic source rock and the lithology (Rubinstein and Albrechet, 1975; Didyk etal., 1978; Moldowan et al., 1985; Peters et al., 1986; Volkman, 1988). These biomarkers are organic compounds in crude oil whose carbon skeletons can be linked to those found in the naturally occurring bio-chemicals from which they are derived and could be regarded as chemical fossils (Eglinton and Calvin, 1967).

Biomarkers could sometimes be useful in assessing biodegradation as they are relatively resistant to biodegradation. However, if the biodegradation is severe, they may not be useful as they are biodegraded themselves (Prince et al, 1994; Wang et al, 2007).

It is therefore understandable why crude oil is a complex mixture of several thousands of hydrocarbon and non-hydrocarbon compounds. These compounds range from small, simple, volatile compounds like methane to extremely large, complex, non-volatile and colloidally dispersed macromolecules like asphaltenes (Wang and Stout, 2007). The non-hydrocarbon compounds found in crude oil are mainly organic compounds that contain hetero-atoms such as nitrogen, sulphur and oxygen as well as compounds containing metallic constituents, particularly vanadium, nickel, iron and copper. As high as 97% w/w of the crude oil could be hydrocarbons especially for lighter paraffinic crude oil or as low as 50% w/w for heavy crude oil and bitumen (Speight, 2007).

The ultimate (elemental) composition of crude oil is generally, Carbon (83.0% to 87.0%), Hydrogen (10.0% to 14.0%), Nitrogen (0.1% to 2.0%), Oxygen (0.05% to 1.5%), sulphur (0.05% to 6.0%) and metals (Ni and V) less than 1000ppm (0.1%). Unlike coal, crude oil cannot be classified based on the carbon and hydrogen content because of the narrow range of carbon and hydrogen in crude oil (Speight, 2007).

Crude oil can be classified as paraffinic or naphthenic. If the crude oil contains about 50% by weight of saturated hydrocarbons and over 40% by weight paraffinic hydrocarbons, the crude oil is said to be paraffinic (Energy, 2011). Crude oil containing over 40% by weight of naphthenes and less than 50% by weight of saturated hydrocarbons is said to be naphthenic crude oil (Energy, 2011).

The physical properties of crude oil such as, volatilty, density and viscosity are largely determined by the distribution of the constituent compounds. In this regard, crude oil is by convention classified as light, medium and heavy based on American Petroleum Institute (API) gravity. Hence, if the proportion of the light compounds in the crude oil is higher than that of heavier compounds, the oil will tend to be relatively light and therefore will be regarded as light oil. The value of crude oil is determined mainly by its density which is conventionally given by the API gravity.

By mathematical definition,

API Gravity (expressed in degrees) = (141.5/specific gravity) – 131.5 ……. Eq. 1.1

Oils with API gravity of less than 22 degrees are said to be heavy whereas those with API gravity of 38 degrees or more are regarded as light. Medium crude oil normally will have API gravity between 22 and 38 degrees (Neste oil, 2011). These ranges may not give absolute definition but could serve as a general reference.

1.2.2 SARA fractions

Crude oil is also broadly divided into four main classes viz, saturates (also called paraffins or aliphatic hydrocarbons), aromatics, resins and asphaltenes (SARA) fractions (Harayama etal., 1999; Aske, 2002; Speight,2007). The resins and asphaltenes are generally regarded as the polars in some cases. De-asphaltened crude oil, i.e. crude oils that had their asphaltenes removed are called maltenes. Hence, maltenes contain resins, aromatics and saturates (Speight, 2007). Studies seem to indicate that the average composition of crude oil is 14% polars, 29% aromatic hydrocarbons and 57% saturated hydrocarbons (Tissot and Welte, 1984). Whereas the saturated hydrocarbons and aromatic hydrocarbons can be characterized by gas chromatography, most resins and asphaltenes are almost impossible to be characterized with gas chromatography (Sirota, 2005).

Saturated Hydrocarbons

Crude oil saturated hydrocarbons include normal alkanes (straight chain eg, n-heptadecane), branched chain alkanes such as acyclic isoprenoids like pristane or phythane. Wax is also a sub-class of saturated hydrocarbons consisting mainly of straight chain alkanes ranging from

C_{20}-C_{30}. At low temperature, wax will precipitate as particulate solids (Musser and Kilpatrick, 1998). Also in this class are the cyclic alkanes also known as the naphthenes. The naphthenes are saturated hydrocarbons containing one or more rings and may have one or more aliphatic side chains attached to each of the rings. The class of naphthenes containing aliphatic side chain can be regarded as alicyclic hydrocarbons. Examples of the naphthenes found in crude oil which can also be regarded as alicyclic hydrocarbons are the hopanes and steranes which are also called biomarkers (Wang and Stout, 2007).

Below are the structures of some examples of saturated hydrocarbons.

Heptadecane: CH_3-$(CH_2)_{15}$-CH_3

Pristane: CH_3-$CH(CH_3)$-$(CH_2)_3$-$CH(CH_3)$-$(CH_2)_3$-$CH(CH_3)$-$(CH_2)_3$-$CH(CH_3)$-CH_3

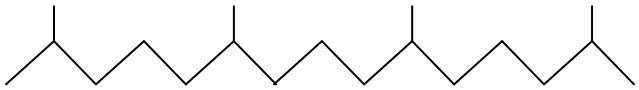

Phytane: CH_3-$CH(CH_3)$-$(CH_2)_3$-$CH(CH_3)$-$(CH_2)_3$-$CH(CH_3)$-$(CH_2)_3$-$CH(CH_3)$-CH_2-CH_3

17α(H), 21ß(H)-Hopane :

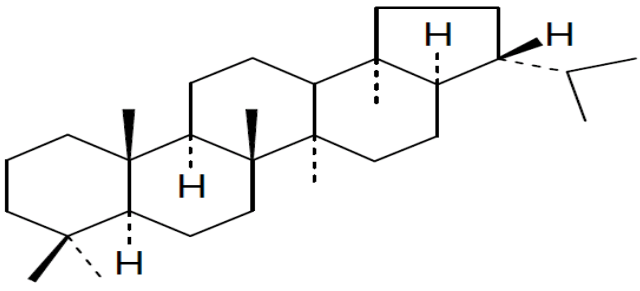

Figure 1.3 Representative saturated hydrocarbons found in crude oil: n-alkanes (heptadecane), branched alkanes (pristane and phytane) naphthene (17α(H), 21ß(H)-Hopane).

Aromatic Hydrocarbons

Aromatic hydrocarbons are hydrocarbons that contain benzene and its structural derivatives. Aromatic hydrocarbons contain one or more nuclei of benzene, naphthalene, and phenanthrene and may be linked to paraffinic side chains or naphthenic rings. The aromatic hydrocarbons can be divided into mono-aromatic or polycyclic aromatic hydrocarbon (PAH). Examples of monoaromatic hydrocarbons are benzene, toluene, ethylbenzene and xylene (BTEX) whereas examples of PAH include: phenanthrene, pyrene and chrysene (Harayama and Kanaly, 2000). PAH's can in turn be divided into low molecular weight (LMW) or high molecular weight (HMW) PAH's. The LMW PAH's have three fused benzene rings like, phenanthrenes, and fluoranthenes. The HMW PAH's have more than three fused benzene rings like pyrene and chrysene (Harayama and Kanaly, 2000). Aromatics in crude oil generally include both aromatic hydrocarbons and other organic compounds of benzene derivatives that may contain other elements such as N, S, O and metals. High molecular weight aromatics that are polar, may fall in the class of either resins or asphaltenes. Benzothiophenes, dibenzothiophenes, indole, carbazole, pyridine, quinoline etc are aromatic compounds that are grouped together with aromatic hydrocarbons described above under crude oil aromatic fraction. Strictly speaking, they are not aromatic hydrocarbons but just aromatic compounds. Figure 1.4 shows structures of some aromatic compounds found in crude oil.

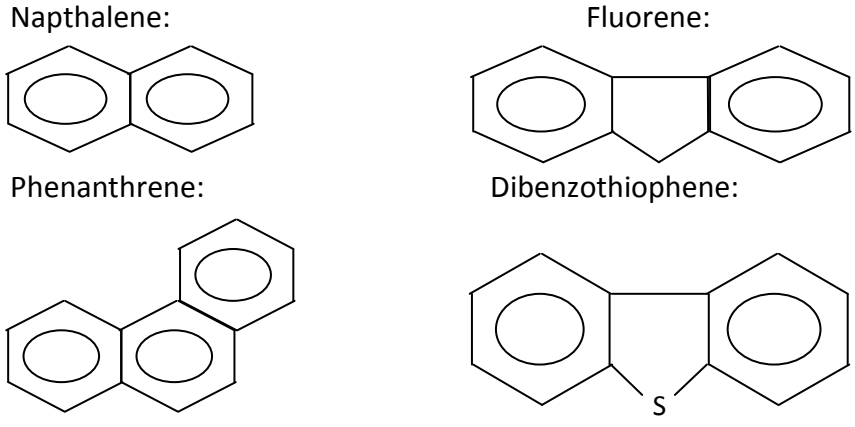

Figure 1.4 Representative aromatics found in crude oil: naphthalene, fluorene, phenanthrene and dibenzothiophene.

Resins

Tissot and Welte, 1984 suggested that resins and asphaltenes could be regarded as small fragments of kerogene and therefore may have the same origin as kerogene. Resins are structurally similar to asphaltenes but lower in molecular weight. Resins are said to be usually less than 1000g/mole and tends to have higher H/C ratio than asphaltenes (Speight, 2007). Resins contain polar molecules containing oxygen, sulphur and nitrogen. They are often defined as a solubility class, being the fraction soluble in light alkanes such as pentane and heptanes but insoluble in liquid propane. The definition of resins as a solubility class makes it possible to have resins in either the aromatic fraction or asphaltene fraction. Naphthenic acids are found in the resin fraction. Functional groups such as O-H typical of hydrogen bonding, N-H typical of pyrolles or indoles, C=0 typical of esters, acids, ketones or quinolines have been established via infra-red spectroscopic studies (Speight, 2007). Resins have also been described by (Speight, 2007) as being soluble in n-pentane or n-heptane but cannot be extracted from soil by n-pentane or n-hexane.

Asphaltenes

The asphaltene fraction of crude oil is insoluble in light alkanes such as pentane, hexane and heptane and is therefore precipitated when the crude oil is mixed with large quantities of any of these light alkanes. This precipitate is however, soluble in aromatic solvents such as benzene and toluene (Speight, 2007). Among all the fractions of crude oil, the asphaltene fraction contains the highest percentage of heteroatoms (N,S,O) and organometallics such as Fe, V, Ni. The H/C ratio of asphaltenes is the lowest of all the four fractions of crude oil and could be as low as 1.15 (Speight, 2007).

It is difficult to measure the molecular weight of asphaltene molecules as they tend to self-aggregate. However, the molecular weight of asphaltene exceeds that of the other fractions ranging from 500 to several thousands g/mole (Aske, 2002). Solution temperature and solvent type tend to influence the molecular weight of asphaltenes when determined by conventional methods like vapour pressure osmometry (Moschopedis et al, 1976). It was suggested by Speight and Moschopedis (1977) that no one particular method can successfully determine absolute molecular weight of asphaltene molecules. It is believed that asphaltenes are suspended in the crude oil as micro-colloids and are stabilized by

adsorbed resins acting as surfactants. The molecules are believed to be held together by interactions due to pie bonds, hydrogen bonds, and electron donor-acceptor bond (Kilpatrick, 2001). Under unfavourable conditions as could be the case with some solvents as described earlier, the resins get desorbed from the asphaltenes, leading to an increase in asphaltene aggregates that will eventually precipitate (Aske, 2002).

1.3 Biodegradation

Biodegradation can take place both in the presence and absence of oxygen. If molecular oxygen is present as the terminal electron acceptor, the biodegradation is aerobic or oxic but if it proceeds in the complete absence of oxygen with other substances acting as electron acceptor (such as nitrates and sulphates), the biodegradation is anaerobic or anoxic (Kanaly and Harayama, 2000; Gieg and Suflita, 2005; Rabus, 2005). There could be a combination of both oxic and anoxic biodegradation in some systems as have been reported to take place in near surface accumulations of tar sands (Connan et al, 1997; Head et al, 2003). For biodegradation to take place, in addition to the presence of electron acceptor, the microbes should be able to obtain carbon from the substrate for building new cell materials and derive energy from transforming the substrate (Rockne & Reddy, 2003). Crude oil hydrocarbons are known to meet the later condition and are therefore readily biodegraded under favourable conditions.

1.3.1 Growth medium/Culture Enrichment

Micro-organisms that are used for studying the biodegradation of organic compounds such as crude oil hydrocarbons must be provided with a medium that is propitious for their growth. A typical growth medium contains compounds that will provide carbon and energy required by the cells. It should also provide nutrients such as nitrogen, phosphorous, sulphur and other trace elements required by the cells to grow. The carbon source should be the only target pollutant(s) to be removed. Compounds that furnish the essential and trace elements for the cells include, $MgSO_4$, $CaCl_2$, Na_2HSO_4, NaCl, KCl, NH_4Cl (Rosenberg et al, 1992 ; Bogan et al., 2003). Other compounds like KH_2PO_4, K_2HPO_4, NH_4Cl, Na_2SO_4, KNO_3, $FeSO_4$, $MgSO_4$ have also been used to prepare a growth medium for microbial degradation of some PAH's (Chen et al., 2000; Watson etal., 2002; Chaerun and Tazaki, 2005). The pH of the medium is usually maintained at 7.0 .The enrichment culture can also be prepared by

obtaining the mixed salts containing the essential and trace elements directly from commercial companies who have already prepared these salts in the right proportions with directives on how to prepare the medium. The Bushnell-Haas broth is an example of an already prepared salt mixture for preparing microbial growth medium for biodegradation studies.

Inoculation is usually carried out with either an indigenous microbial population or an already isolated and fully characterized microbe. When indigenous bacteria taken from soil are used, subcultures which are simply repeated transfers of the enrichment is advised. The repeated transfer of the enrichment through solutions that contain the hydrocarbon and the inorganic nutrients will further increase the degree of purity (selectivity) of the microbial communities (Alexander, 1999).

The proliferated microbes can be enumerated by standard cell plating techniques, a fluorescent staining technique, spectrophotometric techniques or MPN techniques (Joseph et al., 1992). Enumeration of bacteria involves the determination of the number of bacterial cells per gram, mililitre or cubic meter of a sample. The cell counts carried out can either be Viable Counts or Total Counts. Viable Counts would involve only cells that can be cultured or cells that are active metabolically whereas Total Counts will involve counting both cells that are active and inactive (dead).

Several methods can be used for enumeration of cells. These methods are either direct or indirect. The direct methods count actual cells or colonies whereas indirect methods estimate number of cells based on cell mass, scattering of light through a culture (spectroscopy), or a statistical method. Example of a Direct and Viable Count technique is standard plating whereas the Most Probable Number (MPN) technique is an example of Indirect and Viable Count technique. UV-visible spectrophotometric technique that employs light absorbance or optical density for estimation of cells/vol is an example of Indirect and Total Count technique whereas Fluorescent staining and microscopy technique is an example of Direct and Total Count technique. This study employed uv-visible spectrophotometry and standard cell plating.

1.3.2 Microbial Growth Phases

There are four main important phases of microbial growth during biodegradation viz, the lag (also known as acclimation or adaptation), exponential (logarithmic), stationary and death phases (Black, 1996 and Alexander, 1999).

The acclimation phase is the phase that describes the period of time during biodegradation in which there is no apparent loss of the substrate. The substrate is not yet apparently consumed in this phase. Depending on the environment, the substrate and its concentration and the microbial communities, the lag phase can vary from hours to months. The acclimation phase has been said to be due to these factors: presence of only small microbial communities in the medium, presence of toxins, predation of bacteria by protozoa and diauxie (Alexander, 1999). If the microbial communities are present in quite small population, it therefore means that the little loss of the substrate associated with the initial cell growth would probably not be detectable even though there had been actually some level of substrate consumption. Until the loss of the substrate becomes detectable, this period would still be regarded as the lag phase. Under this circumstance of lag phase being as a result of the small population of the microbial community, supply of the inorganic nutrients such as nitrogen, phosphorous and other inorganic nutrients would affect the length of time the lag phase would last (Alexander, 1999).

The presence of toxins will affect the length of the lag phase by inhibiting the rate of cell multiplication required to achieve sufficient cell population that can degrade the substrate to a detectable extent (Stephenson et al., 1984; Alexander, 1999). Also, in situations where the substrate is a mixture of compounds, some of the compounds may be acting as toxicants to the microbial communities degrading the substrates. The lag phase will tend to last till these compounds that are toxicants in the substrate mixture are lost either by biotic or abiotic processes (Alexander, 1999). The main biotic process that can lead to the loss of these toxicants is biodegradation whereas sorption or volatilization represents the main abiotic processes that could lead to the loss of the toxicants. Atlas and Bath (1972) produced some data indicating that the period required for volatilization of some supposedly toxic compounds in oil corresponded to the acclimation phase of oil biodegradation. Toxicants

could be present in form of inorganic substances such as heavy metals and in this case would also extend or lengthen the lag phase (Stephenson et al., 1984)

Protozoa are microscopic, unicellular organisms (eukaryotes) and are known to prey on bacteria. They multiply as they prey on the bacteria. The presence of protozoa could therefore reduce the population of bacteria to the extent that the biodegradation process is grossly inhibited and thereby increasing the period of time required for the acclimation phase (Wiggins and Alexander 1988a; Alexander, 1999). The study of Wiggins and Alexander (1988a) indicated that suppressing the predatory activity of protozoa reduces the acclimation period.

Diauxie occurs when a substrate of interest to be biodegraded is not the preference compound for biodegradation by the microbial communities and hence will only begin to be biodegraded after the first, preference and non-target substrate is biodegraded (Harder etal., 1984; Kuiper and Hanstveit, 1984). The period of time corresponding to the utilization of the preference (non-target) compound corresponds to the acclimation period. The phenomenon of auxic consumption may not occur in situations of heterogeneous microbial communities and mixed nutrients as different microbes might be actively degrading different compounds at the same time (Alexander, 1999).

Exponential growth Phase

Microbial cells grow by cell doubling due to binary fission. Exponential growth phase also known as the logarithmic phase is a phase that corresponds with the period when the cells are doubling (Neidhardt, 1990). The number of newly formed microbial cells per unit time would be proportional to the present microbial cell population.

Mathematically, this could be represented as $dX/dt = U.X$ ……. Eq. 1.2

X is the number of microbial cells or the mass of cell per unit volume at time of generation t. U is the microbial specific growth rate constant.

Cell doubling will continue at a constant rate so both the number of cells and the rate of population increase doubles with each consecutive time period. A plot of the natural logarithm of the microbial cell population (number), X, against time would produce a

straight line with slope described as specific growth rate constant, U and intercept as initial cell number or mass $X_{o.}$

The solution of equation 1.2 is $X/X_o = e^{ut}$.....Eq. 1.3

During binary fission the cells are doubling therefore $X = 2X_o$ .....Eq. 1.4

$2 = e^{ut}$ ..... Eq. 1.5

μ, is a measure of the number of divisions per cell per unit time.

It is important to note that substrate concentration, nutrient availability and environmental factors such as temperature would affect the nature of biodegradation process during the exponential growth phase (Alexander, 1999).

Exponential growth will not continue indefinitely. This is due to the culture medium either being depleted of nutrients or the gradual build up of toxic materials that will reduce the rate of cell multiplication.

Stationary phase

In the stationary phase, there is no net cell growth as there is neither decrease nor increase in cell mass or number. The microbial cell growth rate begins to slow as a result of nutrient depletion and accumulation of toxic substances. Some of the microbial cells indeed begin to die. However, the cell death rate in this phase is equal to the cell growth rate hence

$dX/dt = 0$ …….Eq. 1.6

Many cell functions such as metabolism and biosynthesis will still continue to take place in this phase

Death phase

As soon as the rate of death begins to exceed the rate of cell growth, the stationary phase ends and another phase called the death phase is in place.

The equation, $dX/dt = - K_dX$.....Eq. 1.7

Where K_d is the death rate constant and X the cell mass per unit volume or cell number at time, t (Black, 1996).

1.3.3 Mechanisms of biodegradation of crude oil hydrocarbons

In the presence of water, a crude oil hydrocarbon compound would partition into both the aqueous phase and the non-aqueous phase liquids (NAPL) depending on its solubility in the aqueous phase.

During biodegradation, the hydrocarbon compound would need to be transported to the intracellular sites of the micro-organisms where it is metabolized by enzymatic activity.

Alexander (1999) suggested that there are three mechanisms that can be used to explain how compounds in NAPL is transferred to the cell surface from where they get transported via the cell membrane to the intracellular sites of the microorganisms where metabolic activity takes place.

(i) In the first mechanism, only compounds in the aqueous phase can be utilized by the microorganisms. The assumption is that the microbes only utilize soluble substrates and do not excrete surfactants. This implies that the rate of biodegradation will be a function of the rate of spontaneous partitioning of the NAPL compounds into the aqueous phase.

If the biodegradation system is such that the microbial communities require substrates to be in the aqueous phase, the NAPL compounds that are more soluble are likely to experience greater biodegradation. Hence hydrocarbon compounds with very low log K_{ow} (where K_{ow} is the octanol-water partition coefficient) will be more degraded than those with relatively high log K_{ow}. Wodzinski and Johnson (1968) observed that the growth rate of the microorganisms growing on low molecular weight polycyclic aromatic hydrocarbons (LMWPAH) tends to increase in the following order:

Anthracene $\longrightarrow$ Phenanthrene $\longrightarrow$ Naphthalene. This is also the order of increasing solubility in the aqueous phase.

There are several other evidences of microbial growth increasing with increasing substrate solubility (Wodzinski and Bertolini, 1972; Wodzinski and Coyle, 1974; Wodzinski and Larocca, 1977; Thomas et al, 1987). So long as this mechanism in which substrate utilization

is solely a function of the substrate partitioning into the aqueous phase is operational, the rate of biodegradation is not expected to exceed the rate of substrate partitioning into the aqueous phase. It is important to note that even though the rate of dissolution exceeds the rate of microbial growth especially at early stages of biodegradation, the microbial cells eventually increases to a high value and place high demand on carbon which may exceed the rate of substrate dissolution. At this point, the rate of biodegradation will be limited by the rate of dissolution of the substrates, i.e. substrate partitioning from the NAPLs to the aqueous phase (Stucki and Alexander, 1987; Bouchez et al, 1995; Ghoshal and Luthy, 1996).

(ii) In the second mechanism, the microorganism is able to emulsify the NAPL (hydrocarbon) by producing surfactants and hence convert the hydrocarbon to colloidal particles (in what may be regarded as pseudosolubilization) before assimilating it. As noted in the previous mechanism, the rate of biodegradation is limited by the rate of dissolution and therefore will never exceed it. Hence, the sign that the first mechanism is not operational is when the rate of biodegradation appears to exceed the rate of spontaneous partitioning of the substrate into the aqueous phase. This means that if the rate of substrate partitioning into the aqueous phase is determined in the absence of microbes, it will be less than the rate of biodegradation under same conditions. This implies therefore that another mechanism is in place which is the second mechanism described above. In this second mechanism, the micro-organisms excrete surfactants that enhance the rate of partitioning of the substrates into the aqueous phase. The solubilisation is enough for the microorganisms to utilize and grow (Cameotra et al, 1983 and Goswami and Singh, 1991).This overcomes the situation whereby the increased biomass does not have enough carbon for growth and is then limited by the rate of partitioning of the substrates to the aqueous phase as observed in the earlier mechanism. This mechanism has been proved to be operational during the biodegradation of phenanthrene and pyrene (Efroymson and Alexander, 1995; Bouchez et al 1997).

Generally speaking, solubilization of hydrophobic compounds such as crude oil hydrocarbons is effected by surfactant concentration at or higher than the critical micelle concentration (CMC). However, the studies of Kile and Chiou (1989) indicated that some surfactants can increase the water solubilisation of hydrophobic compounds at surfactant concentration less than the CMC.

(iii) In the third mechanism, the microorganisms make direct contact with the NAPL and the compounds pass through the cell surface to the cytoplasm and are metabolized. Rosenberg and Rosenberg (1985) observed that microorganisms show different binding affinity to the NAPL phase. It has been observed that a particular strain of Arthrobacter was able to degrade hexadecane dissolved in heptamethyl nonane without excreting surfactants. There was no apparent partitioning of the substrate (hexadecane) into the aqueous phase but yet it was biodegraded. The microbes simply get attached at the NAPL-water interface and obtained its carbon from the hexadecane in NAPL phase not in the water phase. Triton X-100, a surfactant that is not toxic to microbes at the appropriate concentration but prevents cell adherence has been used to further strengthen the finding that cell adherence is necessary for microbial degradation of the hexadecane to take place. The study revealed that Triton X-100 prevented the adherence of cell to the NAPL and hence prevented the mineralization of hexadecane (Efroymson and Alexander, 1991). The utilization of naphthalene dissolved in di (2-ethylhexyl) phthalate has been found to also follow this mechanism (Ortega-Calvo and Alexander, 1994).

The study of Acinetobacter calcoacetius (growing on hexane by adherence) and its mutant (which does not adhere and hence could not grow for a long period) is also another proof of this mechanism. The mutant which is non-adhering is only able to utilize the substrate after an emulsifying agent is added (Rosenberg and Rosenberg, 1981). The study of Goswami and Singh (1991) indicated that a strain of Pseudomonas not known to produce an extracellular surfactant or emulsifier but adheres to the surface of hexadecane was able to bring about the mineralization of this substrate. The hexadecane substrate is believed to have been transferred directly to the microbe. It has also been observed that the mineralization of pyrene in the NAPL – water interface by Rhodococcus sp follows the aforementioned mechanism of adherence (Bouchez et al, 1997).

1.3.4 Factors that enhance biodegradation

Supplementing inorganic nutrients (biostimulation), addition of appropriate surfactants, temperature, addition of special microbes (bioaugmentation) and aeration and mixing are the main factors that can promote biodegradation.

The main inorganic nutrients required by the microbes are nitrogen (N) and phosphorous (P) which could be exhausted as the rate of biodegradation increases. If the concentration of nitrogen and phosphorous is not replenished, the rate of biodegradation will ultimately fall. The microbes should not have an inhibited access to these nutrients if the biodegradation process is to be sustained. Floodgate (1984) observed that the concentration of N and P in the immediate surroundings of the crude oil required to bring about biodegradation is 1-11mg/litre and about 0.07mg/litre of seawater respectively. Any or all of these nutrients will limit the rate of biodegradation. Dibble and Bartha, (1976) also observed that iron can also limit the rate of biodegradation. Sub-soils are probably the most common place where the supply of N and P might be inadequate.

The addition of non-ionic surfactants has been shown to stimulate the utilization of oil constituents such as aliphatic and aromatic hydrocarbons (Lupton and Marshal, 1979 and Oberbremer et al, 1990). It has been discovered that surfactants with a hydrophilic and lipophylic balance number of 11 and above are useful with several hydrocarbons (Alexander, 1999). It is important to note that not all surfactants stimulate biodegradation. Most surfactants are beneficial at surfactant concentration at CMC or above the CMC. However, the study by Fu and Alexander (1995) indicates that surfactant concentration less than CMC can be beneficial with some surfactants. It is believed that the surfactants stimulate biodegradation (increasing the rate or extent of biodegradation or both) by causing a large interfacial area that encourages mass transfer from the NAPL phase hence increasing the rate of partitioning of the substrate to the aqueous phase (Kohler et al., 1994). However, if the mechanism of substrate utilization is by cell adherence to the NAPL, addition of surfactant is most likely to inhibit the biodegradation as the surfactant would cause the cells to be flushed out of the substrate hence making the substrate unavailable to the cells. It will be important to consider the mode of substrate utilization by the microbes before taking a decision whether to add surfactants (Alexander, 1999).

Temperature has been reported to affect the biodegradation of oil. The optimum temperature for biodegradation appears to be a function of the environment. Whereas the optimum temperature for biodegradation of oil in soil environment tends to be between 20 and 30^{o}C, that of the marine environment appears to be between 15 and 20^{o}C (Atlas &

Bartha, 1992; Bossert & Bartha, 1984; Cooney et al, 1985). However, biodegradation at very low temperatures- as low as 0-2^{o}C has been reported (Venosa and Zhu, 2003).

The aerobic mineralization of crude oil hydrocarbons requires oxygen. Aeration and mixing promotes the provision and diffusion of oxygen to the interface where metabolic activity is concentrated. Hence injecting air, oxygen or hydrogen peroxide in water into the system would be beneficial. The mineralisation of biphenyls and phenanthrene has been shown to be promoted by processes that improved the supply and diffusion of oxygen (Kohler et al, 1994).

Bioaugmentation (addition of microbes that are efficient in degrading the given substrate) is important in a situation whereby we cannot rely on indigenous microbial communities to completely degrade hydrocarbon pollutants as in oil spill in a given time. The biodegradation as carried out by the indigenous microbial communities will take such a long time that the society cannot afford to wait for. The rate and extent of mineralization of phenanthrene, biphenyl and di(2-ethylhexyl) phthalate in NAPLs in soil slurries have been reported to be enhanced by bioaugmentation (Alexander, 1999).

1.3.5 Biodegradation pathway of saturates and aromatics

Saturates are highly biodegraded by microbes. The biodegradation of n-alkanes can proceed via the production of primary or secondary alkanols. The enzyme, alkane hydroxylase initiates the biodegradation of n-alkanes to n-alkanol and alcohol dehydrogenase further oxidizes the alkanol to alkanal which is then transformed to fatty acid by aldehyde dehydroxygenase. Acyl-CoA synthetase transforms the fatty acid to acyl CoA (Atlas, 1984; Harayama, et al 1999; van Beilen et al, 1998).

The biodegradation pathway of oxidation of n-alkanes to secondary alcohol and then to ketones before finally being oxidized to fatty acid has been reported (Whyte et al, 1998). The biodegradation of cyclohexane (naphthene) proceeds through cyclohexanol, cyclohexanone, caprolactone and finally adipic acid (Harayama et al, 1999).

The first step in the biodegradation of aromatic hydrocarbons is the oxidative catalysis of the benzene ring by oxygenase enzyme to form dihydroxy intermediates known as catechols which in turn undergo oxidative cleavages (Gibson et al, 1968; Cerniglia, 1984; Madigan et

al., 2000). The biodegradation of low molecular weight polycyclic aromatic hydrocarbons such as phenanthrene and its biodegradation pathway has been reported (Harayama et al, 1999). The biodegradation pathways of alkanes and cyclohexane are as shown in Figure 1.5.

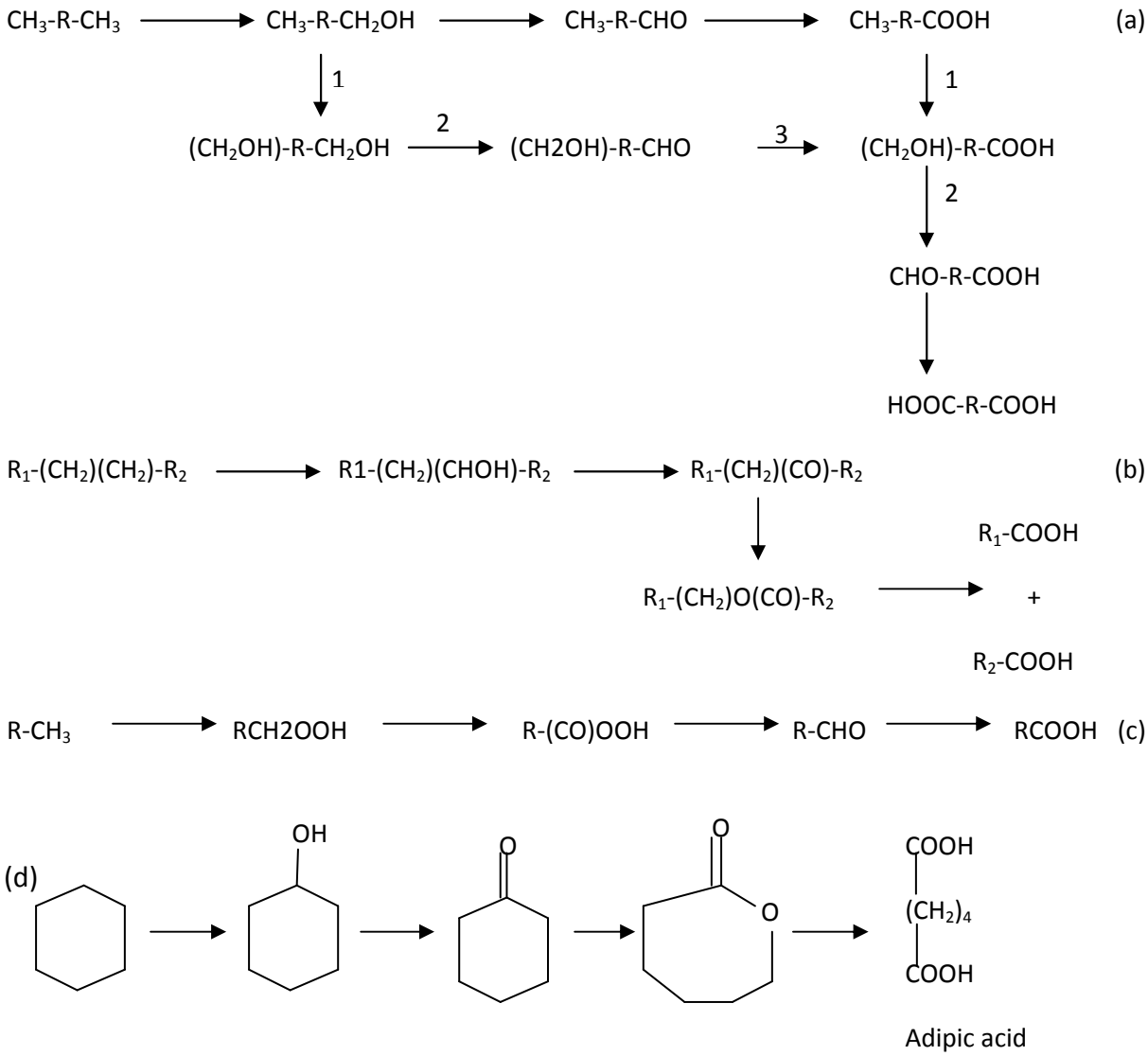

Figure 1.5 Biodegradation pathway showing: (a) terminal oxidation of alkanes (b) subterminal oxidation of alkanes (c) n-alkane degradation via alkyl hydroperoxides and (d) degradation of cyclohexane. Steps 1, 2 and 3 are catalysed by alkane monoxygenase, fatty alcohol dehydrogenase and fatty aldehyde dehydrogenase respectively (modified from Harayama et al., 1999).

The biodegradation pathway of phenanthrene is as shown in Figure 1.6.

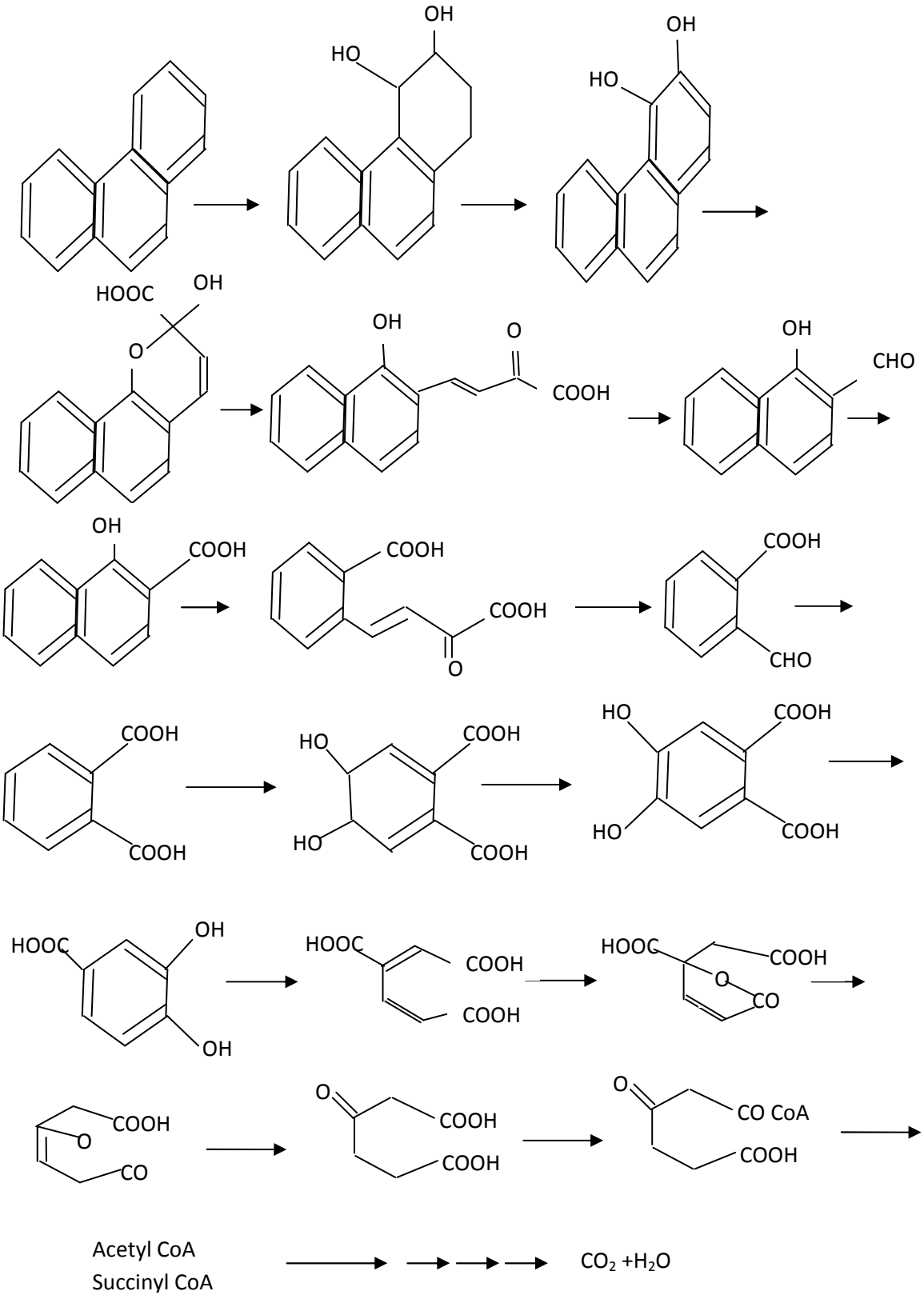

Figure 1.6 Biodegradation pathway of phenanthrene (modified from Harayama et al., 1999).

1.4 Clay minerals

Clay minerals are hydrous alumino silicates and are abundant in soils and sedimentary rocks (Moore and Reynold, 1997). They are very important minerals as a result of their surface properties and the fact that they are reactive hence making them very important in industrial applications and environmental control (Hall, 1987; Kostica et al., 1999; Bergaya et al., 2006). For example, the properties of clay minerals such as acidity, high surface area and cation exchange capacity (CEC) make them play important roles such as catalysts, supports and adsorbents for toxic substances (Hall, 1987; Bergaya et al, 2006). They are mainly composed of layers (sheet-like structures) and are therefore referred to as phyllosilicate minerals.

The Joint nomenclature Committees (JNCs) of the Association Internationale Pour I' Etude des Argiles (AIPEA) and Clay minerals society have defined clay as a naturally occurring material composed primarily of fine-grained minerals which is generally plastic at appropriate water contents and will harden when dried or fired. Clay minerals have also been defined by JNC as phyllosilicate minerals and minerals which impart plasticity to clay and which harden upon drying or firing (Guggenheim and Martin, 1995). Examples of phyllosilicate minerals are kaolin, smectites, vermiculites, chlorites etc. According to these definitions therefore, clay mineral is a constituent of clay.

Clay mineral layers are held together mainly by van der Waals bonding and some contribution from electrostatic interaction (owing to the ionic interaction with interlayer cations-for clay minerals with interlayer cations) or hydrogen bonding (for 1:1 clay minerals such as kaolinites). Consequently, clay minerals are soft with excellent cleavage ability and also exhibit several degrees of disorder (Moore and Reynold, 1997; Meunier, 2005).

The layer units are the most fundamental units of the phyllosilicates. These layer units assemble to form particles and the particles assemble to form aggregates. The aggregates can also assemble to form assemblies of aggregates. These various assemblages leave the phyllosilicate mineral with varying degrees and sizes of pores (Annabi-Bergaya et al, 1979) which might be relevant to adsorption.

1.4.1 Formation

Clay minerals are formed or exist in different geological environments viz, weathering, sedimentary, diagenic/hydrothermal and metamorphic/igneous environments as described in the rock or sedimentary cycle shown below: (Eberl, 1984).

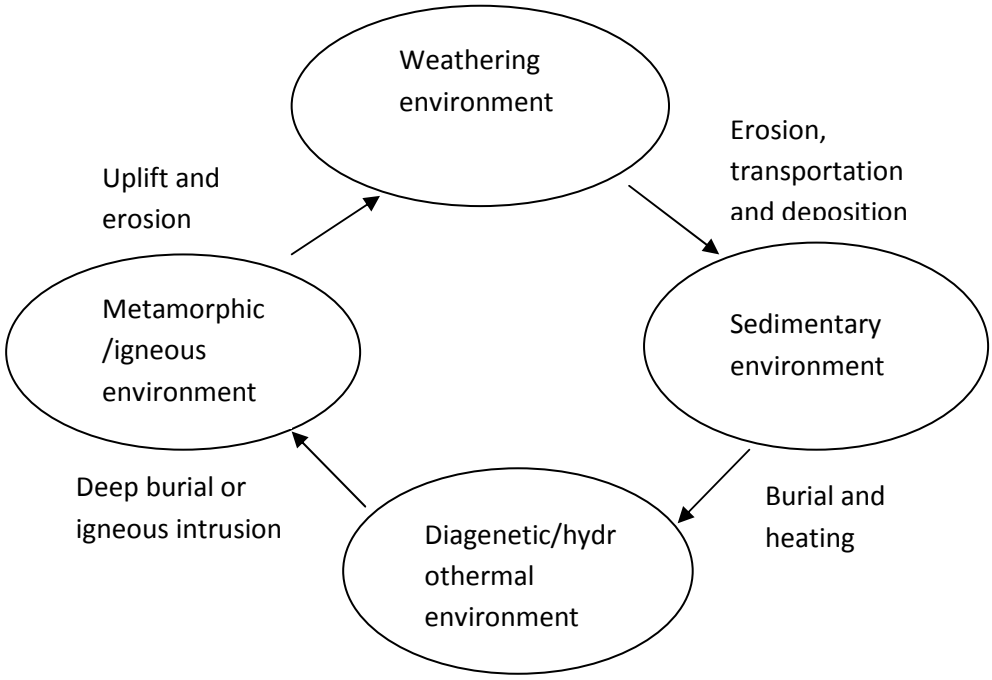

Figure 1.7 The rock cycle showing environments where clay minerals can exist or can be formed (modified from Eberl, 1984).

The weathering environment is where particles are formed as a result of the breakdown of rocks especially igneous rock by physical, chemical and biological processes. The major constituents of igneous rock are primary silicates (such as quartz, feldspars, micas) and ferromagnesian minerals such as olivines, pyroxenes and amphiboles. Feldspars are converted to smectites or kaolinite depending on the environmental conditions. The weathering process produces residues containing mainly quartz and variable amounts of feldspar and mica (Selley, 1982; Hall, 1987).

The special properties of clay minerals are dependent upon their origin (Galan 1999). Clay minerals form by two major processes, neo-formation and mineral transformation during the weathering process.

The process of neo-formation is as a result of the interaction of water, air and steam with rock-forming silicates (Galan, 1999).

(i) Weathering or alteration of primary silicates (neo-formation). The primary silicates such as biotite mica and orthoclase feldspar can undergo weathering to produce clay minerals as outlined in the reaction scheme below:

$KFe_3[Si_3Al]O_{10}(OH)_2 \longrightarrow$ Clay minerals + K^+ in solution + iron oxides/hydroxides

$KAlSi_3O_8 \longrightarrow$ Clay minerals + K^+ in solution + iron oxides/hydroxides

Saponite (Mg-rich trioctahedral smectite) has been suggested to be a product of weathering of olivine (Smith et al, 1987). Another neo-formation process through which clay minerals can form is by direct precipitation from solution or ageing of amorphous materials such as glassy volcanic ash. Volcanic ash-fall alteration is a source of phyllosilcates such as kaolinites and smectites and non-phyllosilicates such as zeolites or a combination of zeolites and K-feldspar. The clay mineral that is formed due to ash-fall alteration is dependent on the environment that receives the ash falls (Reynolds and Moore, 1997). In acidic environments such as coal swamps where dead plants are broken down to organic acids, the alteration of the ash-falls received by this acidic environment would lead to the generation of kaolinite as a component of the rock called tonstein (Bohor and Triplehorn, 1993; Moore and Reynolds, 1997). However, a mild alkaline environment which is usually encountered in a marine system would alter the ash-fall to smectite which is a component of the rock, bentonite. If the environment is highly alkaline, as could be encountered in a highly saline inland sea, the ash-fall will be altered to zeolite or a combination of zeolite and K-feldspar (Moore and Reynolds, 1997).

(ii) Transformation of minerals could be the origin of the clay minerals in sedimentary basins. Illites for example could be transformed to smectites and vice versa under certain physico-chemical conditions. In temperate latitudes, expandable clay minerals such as smectites are formed as opposed to illites that form at higher latitudes (Moore and Reynolds, 1997). In upstream activities of the oil sector such as exploration, clay minerals can be used as stratigraphic markers and environmental indicators of sedimentary systems (Moore and Reynolds, 1997). For example, in mudrocks, which are a potential petroleum

source rock, the major change in clay mineralogy with increasing depth is the conversion of smectites to illites (Hall, 1987; Meunier, 2005). Due to the fact that this change from smectites to illites is not just depth dependent but also time and temperature dependent, it serves as a potential index to the generation of petroleum and natural gas (Moore and Reynolds, 1997). In addition to the use of the smectite-illite transformation for prospecting for potential oil reservoirs, it is important for estimating clay barrier durability (Meunier, 2005). The concentration of potassium ion is believed to be quite crucial in the transformation of smectite to illite. The state of aluminium (mobile or immobile) in the presence of potassium ion determines the quantity of illite generated from the transformation (Hower et al., 1976; Boles and Franks, 1979). In sedimentary basins where sedimentary rocks such as mudrock expels water during compaction that could mix with the product of break-down of kerogen to form carbonic and carboxylic acids (Hunt, 1979), aluminium ion is rendered mobile (Surdam and Crossley, 1985). Hower et al., (1976) proposed a reaction for the smectite-illite transformation in the presence of mobile aluminium as follows:

Smectite + K^+ + Al^{3+} $\longrightarrow$ illite + Na^+ + Ca^{2+} + Si^{4+} + Fe^{2+} + Mg^{2+} + H_2O. In this equation the mole ratio of smectite to illite is 1:1 indicating no mass loss during transformation. However, if aluminium is immobile, the reaction proposed by Boles and Franks, (1979) is:

1.6 Smectite + K^+ $\longrightarrow$ 1illite + Na^+ + Ca^{2+} + Si^{4+} + Fe^{2+} + Mg^{2+} + O^{2-} + OH^- + H_20. According to this reaction equation, the mole ratio of smectite/illite is 1.6:1 implying a mass loss of 37.5% during transformation.

Neo-formation and transformation are both processes of diagenesis with neo-formation simply meaning new formation from solution and transformation meaning the re-modelling of an existing structure in which parts of the parent mineral is retained (Moore and Renoylds 1997). Considering that transformation has another clay mineral as a starting material, neo-formation appears to be the main process of clay mineral formation in which the starting material is silicate rock.

The environmental conditions under which clay minerals form determine the type of clay mineral that is formed. For example, kaolinites form under the environment of acidic leaching whereas smectites form under conditions of low-lying topography, high pH, high

silica activity rich in Si and metal cations (Na, Mg, Ca) but low in K (Moore and Renoylds 1997).

1.4.2 Classification and structure

Generally, phyllosilicates contain layer structures in which each layer is made of tetrahedral and octahedral sheets that are joined in either 1:1 or 2:1 ratio. The tetrahedral sheet is essentially a continuous two dimensional structure with SiO_4 tetrahedrons (Figure 1.8a) linked by the sharing of three corners of each tetrahedron to form a hexagonal mesh pattern (Figure 1.8b). The octahedral sheet is composed of octahedra that are linked together by sharing vertices (Figures 1.9, 1.10 and 1.11).

Below are structural schemes for tetrahedral sheets (Figure 1.8 a&b) and octahedral sheets (Figure 1.9, Figure 1.10-trioctahedral sheet and Figure 1.11-trans dioctahedral sheet & figure 1.12-cis dioctahedral sheet)

(a)

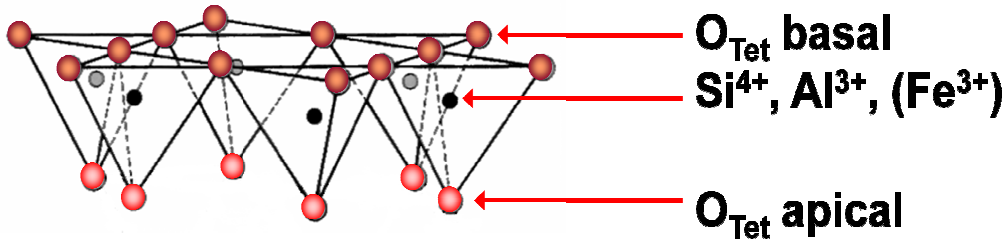

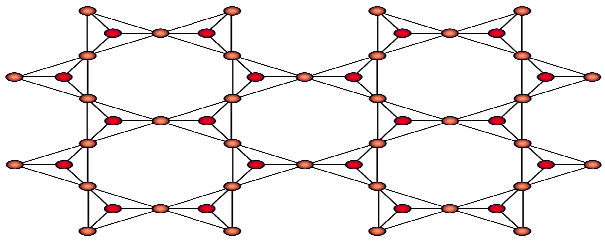

(b)

Figure 1.8 (a&b) shows a typical tetrahedral sheet of phillosilicates (modified from Bergaya, et al, 2006).

Octahedral structure is shown in Figure 1.9. However, the structure of the octahedral sheet will depend on whether all the octahedral sites are completely filled. If all the octahedral sites are filled, we have trioctahedral structure (Figure 1.10) but if all the sites are not filled

such that we have vacant sites then a dioctahedral structure results. Normally, the occupied sites of the dioctahedral structure (2/3 of all the sites) is usually by a trivalent metal such as Al^{3+} whereas divalent cation like Mg^{2+} occupy all the sites of the trioctahedral structure.

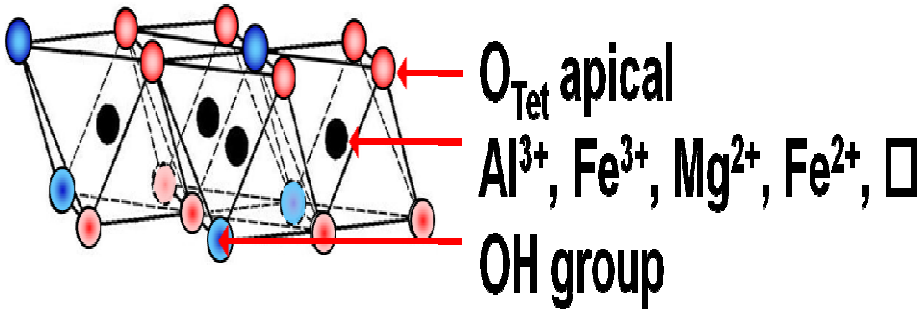

Figure 1.9 Typical octahedral structure

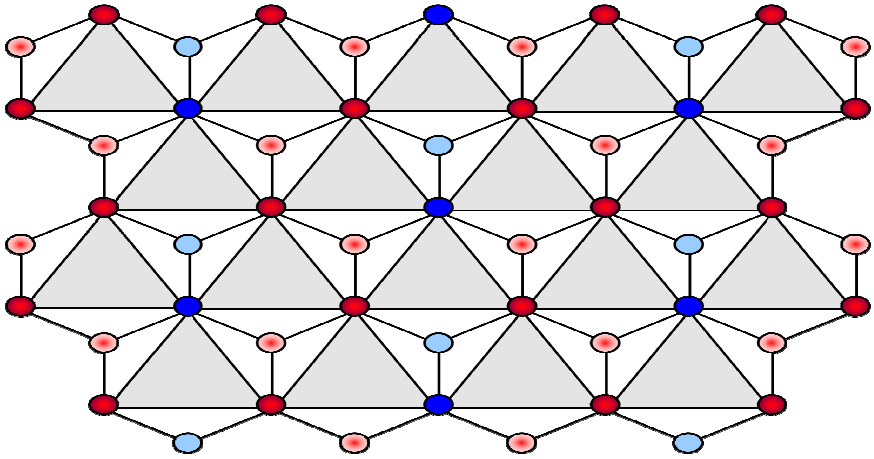

Figure 1.10 The trioctahedral structure showing all the octahedral sites occupied by a divalent cation is as shown by grey triangle in the above structure (modified from Bergaya, et al, 2006).

Because the dioctahedral structure has some vacant sites, the position of the vacant sites is an indication of whether it is cis- or trans- vacant dioctahedral structure. For the trans-vacant dioctahedral, some of the vacant sites seem to be located on an imaginary mirror that bisects the sites whereas for the cis vacant octahedral structure, there is no vacant site located on the imaginary mirror that bisects the sites (Moore and Reynolds, 1997).

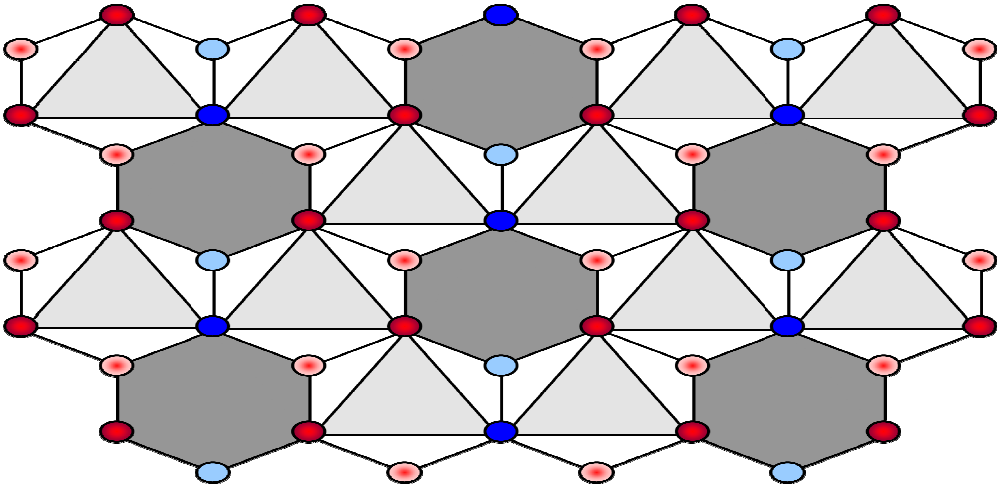

Figure 1.11 Trans-vacant dioctahedral structure. The occupied sites are the light grey triangles while the vacant sites are the dark grey hexagons (modified from Bergaya, et al, 2006).

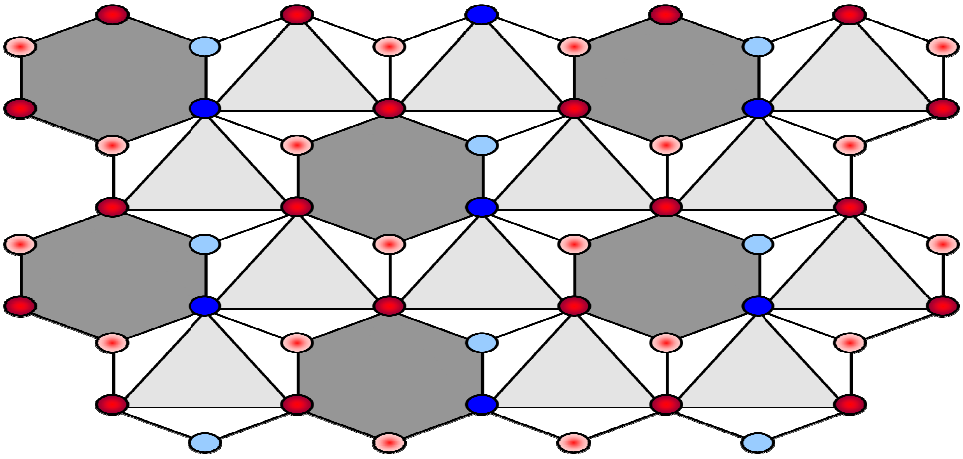

Figure 1.12 Cis-vacant dioctahedral structure. The occupied and unoccupied sites are as described previously (modified from Bergaya, et al 2006).

1:1 Phyllosilicates

The kaolin group are dioctahedral 1:1 phyllosilicates and comprises kaolinites, halloysites, nacrite and dickite as polytypes. It is difficult to differentiate them based on basal XRD reflections of their oriented aggregates.

The general molecular formula of kaolin is $Al_4Si_4O_{10}(OH)_8$. The structural formula of kaolinite is as shown in Figure 1.13.

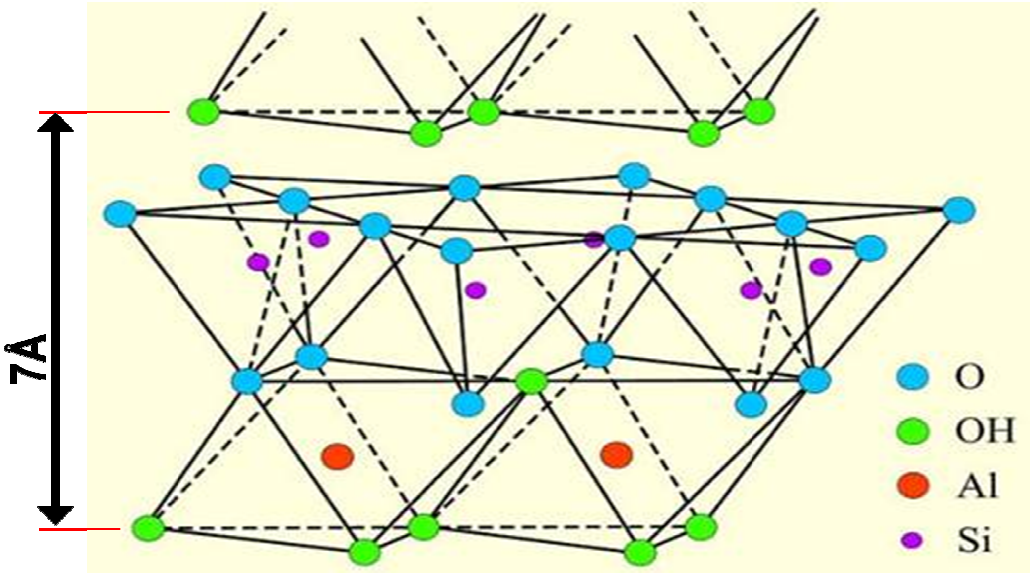

Figure 1.13 Structure of tetrahedral and octahedral sheet forming (1:1) structure of kaolinite with a d-spacing of 7Å (modified from Bergaya, et al, 2006).

The dioctahedral 1:1 phyllosilicates such as kaolinites are ideally electrically neutral and requires no interlayer cation. Consequently, water spheres or shells cannot be held in the interlayer and as a result, 1:1 phyllosilicates such as kaolinites are non swelling clay minerals. The layers of this clay mineral are held together by hydrogen bonding. The ideal layer charge of kaolinites like other 1:1 phyllosilicates is zero. The point of zero charge for kaolinite is about 4.7. The implication of this is that at pH more than 4.7, kaolinite will be negatively charged and may exhibit adsorption towards cationic species.

2:1 Phyllosilicates

Smectites are good examples of 2:1 layer structure phyllosilicates. The ideal 2:1 layer silicates that are the prototype for dioctahedral and trioctahedral 2:1 phyllosilicates with zero layer charge are pyrophyllite and talc respectively with molecular formular: $Al_2Si_4O_{10}(OH)_2$ and $Mg_3Si_4O_{10}(OH)_2$ respectively. The ideal molecular formula of montmorillonites (which is a dioctahedral smectite) is $R_{0.33}^{+}(Al_{1.67}Mg_{0.33})Si_4O_{10}(OH)_2$ where R^+ is a monovalent cation that satisfies electrical neutrality by neutralizing the layer charge (Moore and Reynolds, 1997). As can be seen from the ideal molecular formular of montmorillonites, there is no substitution in the tetrahedral sheet hence the tetrahedral sheet does not contribute to the layer charge. However, there is partial substitution of the Al with Mg in the octahedral sheet leaving the sheet with a net charge of 0.33 which

translates to the charge of the entire layer and is the cause of the attraction of equivalent monovalent cation for electrical neutrality.

The ideal molecular formula of saponite, a trioctahedral smectite is given as:

$R_{0.33}^{+}(Mg_{2.67}R_{0.33}^{3+})(Si_{3.34}Al_{0.66})O_{10}(OH)_2$

where:

R^+ is a monovalent cation that satisfies electrical neutrality by neutralizing the layer charge. R^{3+} is a trivalent cation that partially substitutes Mg in the octahedral sheet. Unlike with the ideal molecular formula of montmorillonite, there are substitutions both in the octahedral and tetrahedral sheets. However, the substitution in the octahedral sheet in which there is a partial substitution of Mg with a trivalent cation leaves the octahedral sheet with a positive charge (+0.33) whereas the substitution of Si with Al in tetrahedral sheet leaves the tetrahedral sheet with a negative charge (-0.66). Because the substitution in the tetrahedral sheet is larger than the substitution in the octahedral sheet, the negative charge in the tetrahedral sheet is able to compensate for the positive charge in the octahedral sheet leaving the layer with a net negative charge.

The general structure of smectites is as shown in Figure 1.14:

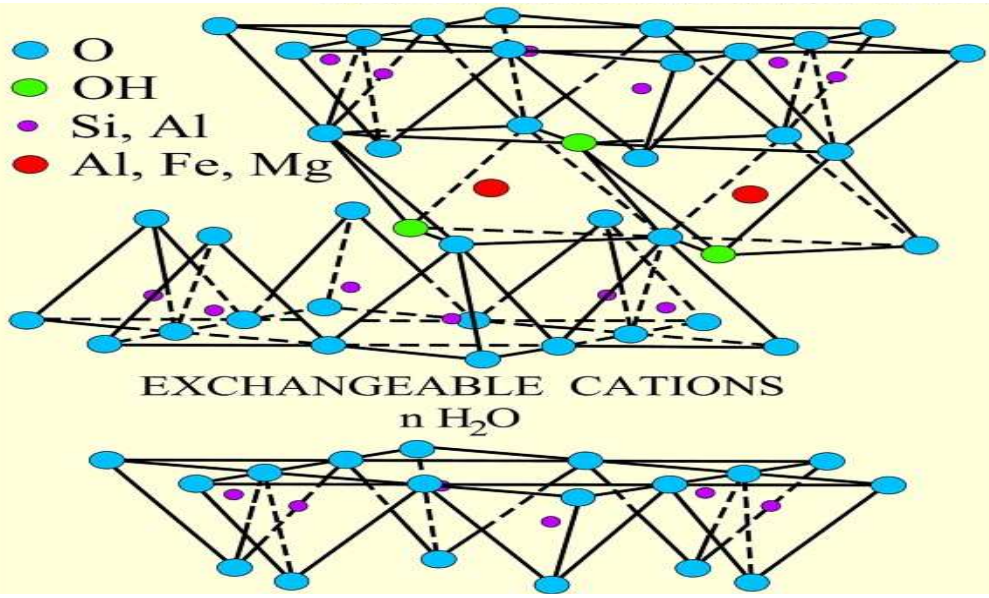

Figure 1.14 2:1 structure of smectites. The d-spacing varies from 10Å to 20Å depending on the amount of interlayer water.

The clay minerals in the smectite group are montmorillonite, nontronite, saponite, hectorite etc. Montmorillonite and nontronite are dioctahedral smectites whereas hectorite and saponite are trioctahedral smectites. Sodium and calcium montmorillonite are the most common form of montmorillonites found in bentonite which is clay that is formed from a glassy igneous material like volcanic ash or tuff (Grim and Guven, 1978).

There is isomorphic substitution in smectites that causes the clay to acquire a net layer charge of 0.2-0.66 necessitating compensation with cations which then enter the interlayer spaces to achieve electrical neutrality. The interlayer cations are able to hold water molecules as they have significant enthalpies of hydration. These water molecules held in the interlayer space of the smectite clay then cause the clay to swell appreciably. The extent of the swelling will be a function of the interlayer cation.

Other clay minerals

Other common clay minerals are illites/mica, chlorites and smectites such as beidellite.

Illites and mica can be either dioctahedral or trioctahedral 2:1 layer structures and usually contain mainly potassium ion as the interlayer cation that is rarely exchangeable (Hall, 1987). The 001 basal spacing of illite is about 10Å and is not affected by ethylene glycolation or heat treatment at temperature of 300^0C (Moore and Reynold, 1997).

Chlorites can occasionally be dioctahedral but usually, it is trioctahedral with a 2:1:1 variable structure. The layer of chlorites is negatively charged as a result of isomorphic substitution and is balanced by a positive charge on the interlayer hydroxide. However, some authors regard this clay mineral as 2:1 clay mineral instead of 2:1:1 clay mineral. The 001 basal spacing of chlorite is approximately 14 Å.

Beidelite is a smectite that differs from montmorillonite by having more aluminium and less magnesium. Unlike in montmorillonite, more than 50% of the total charge deficit is as a result of substitution of Si ion with Al ion in the tetrahedral sheet.

Palygorskite has a non-continuous octahedral sheet structure (Figure 1.15).

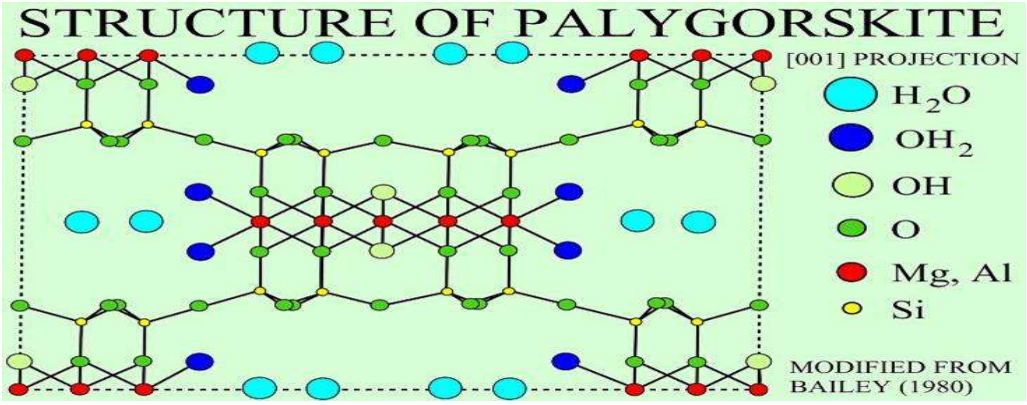

Figure 1.15 Structure of palygorskite (modified from Bailey 1980)

Palygorskite is a rare, fibrous clay with an approximate molecular formula given as $(MgAl_3Si_8O_{20}(OH)_3(OH_2)_4.n(R^{2+}(H_2O)_4)$ where n is an integer and R^{2+} is a divalent cation (Moore and Reynold, 1997). Palygorskite is also known as attapulgite or (in some cases) fuller's earth and is the same family as sepiolites. Commercial deposits form under alkaline conditions in inland lakes or closed marginal marine basins. Small deposits are also associated with hydrothermal alteration of magnesium-rich rocks. The fibrous nature of palygorskite gives the clay a high surface area and porosity which provide excellent sorption and gelling properties. Palygorskite is considered a phyllosilicate on account of its containing a continuous two-dimensional tetrahedral sheet. However, unlike many other phyllosilicates, it lacks continuous octahedral sheets. This explains why the palygorskite structure is considered to contain ribbons of 2:1 phyllosilicate structure. The unique structure of this clay mineral permits the creation of rectangular channels running parallel to the X-axis between opposing ribbons. Because the octahedral sheet is discontinuous at every tetrahedral inversion, oxygen atoms of the octahedral sheet at the edge of the ribbons are coordinated to cations on the ribbon side only. Coordination and charge balance are completed along the channels by protons, coordinated water and small amount of exchangeable cation (Jones and Galan, 1988). Palygorskite undergoes considerable isomorphic substitution as the aluminium ion is substituted by mainly magnesium thereby leaving a moderately high charge on the layers. This clay mineral has high surface area and inverted structure as described. The high surface area of palygorskite and the fact that it has inverted structure that leaves parallel channels through the lattice give palygorskite high sorption capacity (Murray, 2000).

Clay minerals used in this study -their layer charge and type.

The table below classifies the following phyllosilicates according to their layer charge and type.

Table 1.1: Classification of the clay minerals used in this study according to their layer type and charge

Layer type	Mineral	Di or trioctahedral	Layer charge
1:1	Kaolinite (kaolin)	Di	~0
2:1	Montmorillonite (smectite)	Di	0.2-0.6
2:1	Saponite	Tri	0.2-0.6
2:1	Palygorskite	-	variable

1.4.3 Clay mineral surface properties

The surface properties of clay minerals is a function of the chemical composition and nature of the surface atoms, extent and type of defect sites, layer charge and the type of exchangeable cations. The behaviour and role of clay minerals in biogeochemistry is principally due to their surface properties which include surface chemistry, surface area, cation exchange capacity (CEC) and the d-spacing (Schooneheydt and Johnston, 2006).

Surface chemistry of clay minerals is a function of the siloxane surface and the hydroxyl surface. The siloxane surface is composed of the basal oxygen atoms of the Si-tetrahedral and is the principal surface for the 2:1 clay minerals such as smectites whereas the surface for the 1:1 clay minerals includes the siloxane surface and the hydroxyl surface from Al-octahedra.

The siloxane surface can either be neutral or with permanent charge.

The neutral siloxane surface

The neutral siloxane surface is the least reactive surface in clay minerals and normally exists in 2:1 phyllosilicates where there is no isomorphous substitution. The neutral siloxane surface is also found on Si-tetrahedra side of 1:1 kaolin. The neutral siloxane surface is a

Lewis base as it is an electron pair donor but it is really a very weak electron donor (Schooneheydt and Johnston, 2006). The implication of this is that clay minerals where the dominant surface is the neutral siloxane surface will tend to be hydrophobic. Talc and pyrophylite are examples of clay minerals with dominant neutral siloxane surface and are hydrophobic. The neutral siloxane surface will hardly interact with polar molecules such as water given that it is non-polar (Malandrini et al, 1999; Tunega et al 2002). Unlike the neutral siloxane surface that has a very low affinity for polar molecules, non polar organic molecules can interact with the neutral siloxane surface. It is well documented that some non-polar regions can exist between hydrated cation sites on the basal surface of smectites and vermiculites. These sites can therefore be accessed by non-polar compounds. However, the ability of non-polar compounds to access the non-polar regions of the clay surface is a function of the clay surface charge density, nature of the exchangeable cation and its corresponding enthalpy of hydration. Smectites with relatively low surface charge density and containing weakly hydrated exchangeable inorganic cations (eg K^+ and Cs^+) will interact more strongly with organic molecules (Jaynes and Boyd, 1991).

The hydroxyl surface

Unlike the neutral siloxane surface, the hydroxyl surface interacts strongly with water. The hydroxyl surface is prominent among the kaolin group such as kaolinite.

The terminal hydroxyl groups, OH groups located at the broken edges of the clay minerals is chemically more reactive than the basal charge-neutral hydroxyls. The terminal OH groups are under-coordinated and as a result carry a positive or negative charge depending on the type of metal ion and the pH of the aqueous dispersion. The terminal OH groups have the potential to chemi-sorb certain ions irrespective of the pH. Terminal Al-OH and Fe-OH groups have high affinity for phosphate ions (Schooneheydt and Johnston, 2006).

The siloxane surface with permanent charge

The siloxane surface with permanent charge arises as a result of isomorphous substitution in the clay mineral structure that leads to the enhancement of the Lewis base character of the siloxane surface (Sposito, 1984). This effect is more obvious if the isomorphous substitution is in the octahedral sheet as this leads to a more delocalized negative charge. The negative

charge that results from the isomorphous substitution is balanced by exchangeable cations such as Na^{+}, K^{+}, Mg^{2+} and Ca^{2+}. These exchangeable cations have different ionic radius, hydration energy and hydrolysis constant. Consequently, the physico-chemical properties of clay minerals will vary in accordance with the exchangeable interlayer cations of the clay minerals (Schooneheydt and Johnston, 2006).

Surface area

The surface area of clay mineral is derived from external and internal surfaces (Annabi-Bergaya, et al., 1979). It follows therefore that clay minerals with both internal and external surfaces will have surface areas larger than those with only external surfaces. This explains why smectites such as montmorillonites have higher surface areas than kaolinites. The ability of the clay mineral surface to adsorb reacting species increases the concentration of the reactants on the surfaces hence the high surface area confers a local concentration effect to the clay minerals (Laszlo, 1987). Clay minerals especially the phyllosilicates have dimensionality less than three (3) making it possible for reacting molecules to have higher chances of colliding than molecules in three dimensions (Laszlo, 1987). The combined effects of low dimensionality and local concentration effects, enhances the collision frequency of the reactants on clay minerals and hence promotes reactivity (Laszlo, 1987).

The specific surface area of clay minerals can be measured by the low temperature nitrogen adsorption method involving the Brunauer Emmet Teller (BET) method. However, the low temperature nitrogen adsorption BET method is only able to measure the external surface area of clay minerals. The ethylene glycol monoethyl ether (EGME) method is able to measure both the internal and external surface area of clay minerals (Site, 2001).

Cation Exchange Capacity (CEC)

The cation exchange capacity of clay minerals is a measure of their ability to adsorb cations from solution. It has been defined as the quantity of cations that are available at a given pH for exchange with other cations and is usually expressed in milliequivalents/100g of dry clay (Bergaya and Vayer, 1997). The adsorbed cation replaces or exchanges the original negative layer charge balancing cation in solution. This ability of colloidal particles such as clay minerals to retain and exchange positively charged ions is vital as it has a controlling

influence on the mobility of positively charged chemical species both in soils and geochemical cycling of cations in general (Verburg and Baveye, 1994). CEC is normally associated with clay minerals with interlayer exchangeable cations such as smectites. The cation exchange capacity process is a reversible process. It is also stoichiometric and diffusion controlled. The clay mineral preferences for some cations have been presented in quantitative terms via the measurement of binding coefficient (Nir et al., 1986; Margulies et al., 1988; Hirsch et al., 1989 and Rytwo et al., 1996; Table 1.2).

Table 1.2 Binding coefficients of some metalic cations, methylene blue ion (MB^+) and Thioflavin ion (TFT^+)

Cation	Binding coefficient
Li^+	0.6
Na^+	1.0
K^+	2.0
Cs^+	200
Mg^{2+}	2.0
Ca^{2+}	4-40
Sr^{2+}	5.0
Cd^{2+}	10
MB^+	10^8
TFT^+	10^9

Table 1.2 indicates that clay minerals show preference for larger inorganic cations over smaller ones. For smectites, this preference follows the order:

$Cs^+ > Rb^+ > K^+ > Na^+ > Li^+$ (for monovalent metallic cations) and $Ba^{2+} > Sr^{2+} > Ca^{2+} > Mg^{2+}$ (for divalent cations). With multivalent heavy metals, it is possible to have adsorption of the heavy metal cation that is more than the CEC of the clay mineral. The main reason that has been adduced for this behaviour is that multivalent cations can be bound by equimolar rather than equivalent exchange (Rytwo et al, 1996 and Tournassat et al, 2004).

The cationic exchange reaction scheme of the above process is as shown below:

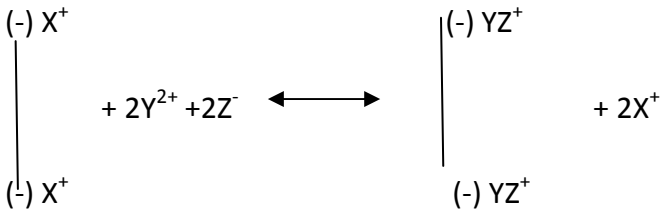

Y^{2+} and Z^{-} represent heavy metal cation and anion in solution respectively whereas YZ^{+} is the bound equimolar species after the cationic exchange.

The work of Maes etal., (1982), Rytwo et al.,(1996), Konya and Nagy, (1998); Konya et al., (1998) and Abollino et al., (2003) indicate that the presence of complexing compounds promotes the exchange of interlayer cations in clay minerals as a result of their high binding coefficients as shown in Table 1.2.

D-spacing

The d-spacing of clay minerals (also known as interlayer distance along the c-axis) is a function of the layer charge, interlayer cation, and the state (wet, dry or exposed to polar solvent) of the clay mineral (Chiou et al., 1997; Moore and Hower, 1986).

Generally speaking, the kaolin group (1:1 phyllosilicates such as kaolinite) has no interlayer cations and therefore has a lower d-spacing than smectites which have interlayer exchangeable cations. The d-spacing of kaolinite is approximately 7Å whereas that of smectites like montmorillonite (in dried state-without water) is between 9.6 and 10Å. In the absence of water, the interlayer distance of smectites will be a function of the size of the interlayer cation. However, the presence of water increases the interlayer distance as the interlayer cation is hydrated by the water. The water forms coordination spheres or shells around the interlayer cations. The interlayer distance will then be a function of the hydration state as each hydration state has a discrete d-spacing. The hydration states of 0,1,2,3 represent the number of sheets of water surrounding the interlayer cation and have the d-spacing corresponding to each state as follows: 9.6, 12.4, 15.2 and 18Å respectively (Moore and Hower, 1986). The specificity of interactions between polar solvents and cations makes solvation of the clay mineral's interlayer cations a function of the interlayer cation type.

The work of Chiou et al (1997) illustrates the effect of interlayer cations such as Ca^+, Na^+, K^+, Cs^+ and TMA^+ (tetramethyl ammonium ion) when the clay mineral is dried and when exposed to water and ethylene glycol monoethyl ether (EGME) vapour. The increase in d-spacing as a result of water vapour adsorption increases with decreasing cation size. The d-spacing in absolute terms increases with cation size when dried.

1.4.4 Electric double layer and DLVO Theory

The electrical double layer concept is very important when dealing with particles in nano to micron size, also regarded as colloidal particles such as clay minerals. The electric double layer theory describes the interaction between surfaces of colloidal particles and ions that are present in the fluid in which the colloidal particles are dispersed (Moore and Reynolds, 1997).

Debye and Huckel (1923) produced the first successful theory on distribution of charges in ionic solution on which Levine and Dube (1940) leveraged to study the behaviour of colloidal particles vis-à-vis colloidal particle stability in colloidal dispersions. Their theory pointed to the fact that charged colloidal particles should experience strong short range repulsion and a weaker long range attraction. The application of the theory did not satisfactorily explain the instability of colloidal systems and the fact that there seems to be irreversible aggregation in solutions of high ionic strength. The ionic strength of a solution is given as:

$$I = \frac{1}{2}\sum_{i=1}^{n} c_i z_i^2 \quad \text{.....Eq. 1.8}$$

where I is ionic strength, C_i and Z_i are the molar concentration of ion i (mol/dm^3) and charge number of same ion respectively and the sum is taken over all the ions in solution. The implication of equation 1.8 is that multivalent ion will contribute more to the ionic strength of the solution than monovalent and divalent ones and will lead to irreversible aggregation which is consistent with DLVO theory. Hence the theory by Derjaguin and Landau (1941) seems to be the most successful in explaining the stability and aggregation of colloidal particles in colloidal dispersion systems. The theory presents two opposing influences responsible for colloidal particle stability and aggregation as van der Waals forces of attraction and electrostatic forces of repulsion. About seven years later, Verwey and

Overbeek independently produced the same result hence the acronym, DLVO (Verwey and Overbeek, 1948). Unlike the Levine and Dube theory, DLVO theory is able to explain the fact that stability of colloidal dispersion system is a function of the ionic strength of the colloid.

The electric double layer is due to the negatively charged surface of clay minerals attracting cations from the solution which in turn attracts anions but these are less rigidly held. The anions attract cations and the series of counter ion attraction continues until there is no segregation and electrical neutrality is achieved. However, two distinct sub-layers of the electrical double layer are apparent, viz, the immobile layer and the diffuse layer. The immobile layer, also called the Stern layer, is the region in which ions are closest to the charged surface whereas the region in which ions are looser and relatively mobile is the diffuse layer (Moore and Reynolds, 1997). The double layer electric repulsion is as shown in Figure 1.16.

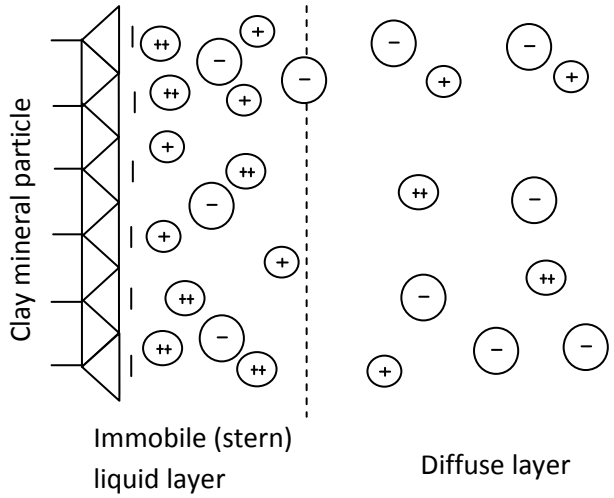

Figure 1.16 Electrical double layer (modified from Moore and Reynolds, 1997)

If the cations in the surrounding fluid of the clay mineral are monovalent, relatively high population of the cations are required to maintain neutrality. This thickens the immobile and diffuse layer causing the cations to repel one another stronger than any form of van der Waals forces that could join them. The implication of this to the colloidal system is that the colloidal particles are dispersed and more stable (Moore and Reynolds, 1997).

However, if the cations in the surrounding fluid are divalent or trivalent, the population of cations required to achieve neutrality will be lower and implication of this is that the

immobile and diffuse layer thins out thereby promoting interparticle contact that in turn leads to aggregation and flocculation (Moore and Reynolds, 1997).

The concept of double layer not only helps to explain dispersion and interparticle contact (which may cause flocculation) but is also useful in studying bacterial adhesion. The DLVO-electrical double layer theory has been used to explain the deposition of bacteria in several studies (van Loosdrecht et al., 1990; Jeremy et al., 2004; Alexis and Elimelech, 2007; and Alexis et al., 2007).

This theory has also been used to explain the enhanced microbial degradation of crude oil in the presence of clay minerals (Warr et al., 2009).

1.4.5 Modification of clay minerals

Clay minerals can be modified both physically and chemically for several industrial and environmental applications. Acid activated clay minerals and organo-clay minerals are some of the main forms of clay minerals resulting from modification.

Acid activated clay minerals

Acid activated clay minerals have been the subject of much research, having been discovered to have good catalytic properties especially for many organic reactions. However, their role during the biodegradation of crude oil hydrocarbon is not well understood. Acid activated clay minerals can occur naturally in the environment by the attack of acid on clay minerals as is the case with the acid mine drainage interacting with clay minerals (Galan et al., 1999; Dubikova et al., 2002). During acid activation, the main goal is to obtain partially dissolved material that is of increased surface area, porosity and surface acidity (Komadel, 2003; Pushpaletha et al., 2005). For industrial or scientific research purposes, acid activated clay mineral is prepared by washing or treating the clay mineral with strong mineral acids such as sulphuric or hydrochloric acid. This treatment of clay minerals with strong inorganic acids is called acid activation, acid washing or dissolution. During the process of activation, the acid exchanges its protons for the interlayer exchangeable cations and partially dissolves the clay crystalline structure by leaching some of the cations such as Mg^{2+}, Al^{3+} or Fe^{2+}. The net effect of this is a product with increased

surface acidity, specific surface area and porosity, called acid activated clay mineral (Theocharis et al, 1988; Komadel, 2003).

The clay mineral type and reaction variables influence the degree of activation. The reaction conditions common with acid activation of clay minerals are temperature, concentration of the mineral acid, time and acid/ clay ratio. It has been reported that the composition of the layers of the clay mineral determines their relative susceptibility to acid attack; hence, trioctahedral phyllosilicates dissolve faster than dioctahedral ones (Vicente et al., 1994; Breen et al., 1995a and Komadel et al., 1996a and 1996b). Breen et al.(1995b) observed that the rate of dissolution in acids for dioctahedral smectites is increased with increased substitution of Mg^{2+} and /or Fe^{3+} for Al^{3+} in the octahedral sheets. The resistance of clay minerals to acid attack is dependent on the structure of the clay minerals. Collapsed layer or non-swelling clay minerals appear to resist acid attack more than the swelling clay minerals, hence, montmorillonite is more susceptible to HCl attack than kaolinites (Jozefaciuk and Bowanko, 2002). Palkova et al (2003) has also pointed out that if the accessibility by the protons of the acid to the clay mineral layers is low due to non-swelling interlayer spaces, the dissolution of the clay mineral is reduced and takes place mainly from the particle edges. The octahedral cations such as Mg^{2+}, Fe^{2+},Fe^{3+} and Al^{3+} are depleted at different rates during acid dissolution of the clay minerals under the same conditions. The resistance to depletion by mineral acids follows the order: Al^{3+}> Fe^{3+}> Fe^{2+}> Mg^{2+} (Corma et al., 1987; Christidis et al., 1997). Trioctahedral phyllosilicates such as saponites are rich in magnesium. The work of Madejova et al.,(1998) demonstrated that magnesium rich trioctahedral phyllosilicates such as saponites are more susceptible to acid attack and hence are less stable in inorganic acids than aluminium-rich dioctahedral clays such as montmorillonite. The reaction conditions required to achieve the same extent of dissolution will therefore vary.

The acid should act for quite some time in order to achieve good activation. Hence an optimal time period must be sought. If the reaction time is too short, activation will be very poor and if the reaction time is too long, the crystalline structure of the clay minerals might be eroded to the point of complete dissolution. By trial and error, an optimum condition can be arrived at whereby activation will lead to production of activated clay mineral with high surface area without destroying the crystalline structure completely (Rozic et al, 2008).

Several studies have been carried out indicating that the acid activation of smectites alters the physical properties of the clay minerals giving increased pore volume and specific surface area (Srasra et al, 1989 and Ravichandran and Sivasankar , 1997).

Organoclay minerals

For a few decades now, organoclay (especially as produced from alkyl ammonium cations) has been used as an adsorbent for organic compounds. The increased environmental awareness and the need to remediate environmental polluted sites with organic compounds especially pesticides and crude oil hydrocarbons has necessitated research advances in this area (Cornejo et al, 2008). Organophilic smectites have been reported to be useful in industrial processing. For example it is useful in the manufacture of inks and polishes, control of the gelling properties of lubricating greases and adding thioxotropic properties to fibreglass resins (Hall, 1987).

Organoclay is quite common in soils where the presence of organic compounds always occurs with the potential of generating organic cations. It is therefore important to understand how the organoclay interacts with hydrocarbon during its biodegradation. Phyllosilicates (such as smectites) with 2:1 layer structure are hydrophilic on account of the hydration of the exchangeable interlayer inorganic cations. However, the very origin of hydrophilicity is the fact that some clay minerals such as smectites have negatively charged surfaces. These surfaces then adsorb inorganic cations (such as Na^{+}, K^{+}, $Mg^{2+}$and Ca^{2+}) to achieve electrical neutrality but these inorganic cations as a result of their substantial hydration energy is able to attract water and consequently get solvated or covered with 'shells' of water and rendering the clay's surface hydrophilic. Because of this hydrophilic character of natural clay minerals such as smectites, there is an inherent ability for them to be good adsorbents for cationic and polar compounds. Due to the universal scientific principle of 'like dissolving like', it is rather not surprising that most natural clay minerals have low ability to adsorb non-ionic or non-polar hydrophobic compounds. The few exceptions to highly reduced ability to adsorb hydrophobic compounds would be those clay minerals with interlayer exchangeable inorganic cations that are able to expose some neutral hydrophobic siloxane surface of the clay minerals as described earlier.

Natural clay minerals such as smectites like sodium or calcium montmorillonite will therefore be expected to have limited ability to adsorb non-ionic and hydrophobic compounds (Jaynes and Vance, 1996). Generally speaking, natural clays appear to be ineffective sorbents for adsorbing non-polar organic compounds (Kim et al, 2003).

There are several applications of smectites on account of their high cation exchange capacity (CEC), swelling capacity and high surface area. These properties of clay minerals which enable them to exhibit strong sorption behaviours are taken advantage of for the production of organoclays which are used for various applications. Producing organoclay minerals in practice requires the replacement of the interlayer exchangeable inorganic cations with organic cations through ion-exchange reactions. The resultant organoclay modifies the surface of the original clay mineral from being hydrophilic to being hydrophobic (Hermosin and Cornejo, 1992 and Groisman et al, 2004a).

Quaternary ammonium ions $[(CH_3)_3NR]^+$ or $[(CH_3)_2NR_2]^+$ are the most common organic cations (where R is an aromatic or aliphatic hydrocarbon) used in the production of organoclay (Cornejo et al, 2008). Basically there are two types of organoclay that can be produced using the process described above:

(i) Short chain alkyl or aryl ammonium cation in which R is a short chain alkyl or aryl group. The most common short chain alkyl and aryl ammonium cations for producing organoclay are tetramethyl ammonium (TMA) and phenyltrimethyl ammonium (PTMA) respectively (Cornejo et al, 2008).

(ii) Long chain alkyl ammonium cation in which R usually has 10 or more carbon atoms. Examples of long chain ammonium cations are hexadecyltrimethylammonium (HDTMA), didecyldimethylammonium (DDDMA) and dioctadecyldimethylammonium (DODDMA) (Cornejo et al, 2008). DDDMA is the cation used in this study to prepare the organoclay samples.

The possibility of producing long chain alkyl ammonium organoclay in excess of the CEC has been identified. It has been suggested that this is due to the fact that in addition to the normal cation exchange, there is a hydrophobic interaction between the adsorbed organic cation bound to the clay mineral and the one not bound to the clay mineral leading to

overall adsorption higher that the CEC of the clay mineral (Zhang et al,1993; Xu and Boyd, 1995; Lemke et al, 1998 and Moronta, 2004). Moronta (2004) has observed that the longer the alkylammonium chain, the greater the contribution of physical, non-coulombic forces to adsorption. The arrangement of the organic cations in the interlayer space is extremely important as it has a direct effect on the adsorptive capacity of the organoclay. The arrangement of the short chain alkylammonium cation is different from that of the long chain alkyl ammonium cation. Furthermore, even among the long chain alkyl ammonium cations, arrangement could be different. Arrangement of the organic cation determines how much space that is available for the adsorbate (Aguer, et al 2000 ; Celis et al, 2002a). The short chain alkylammonium cation is arranged in discrete species whereas the long chain alkylammonium cation could be arranged in one of these forms (Figure 1.17): monolayer, bilayer or paraffinic.

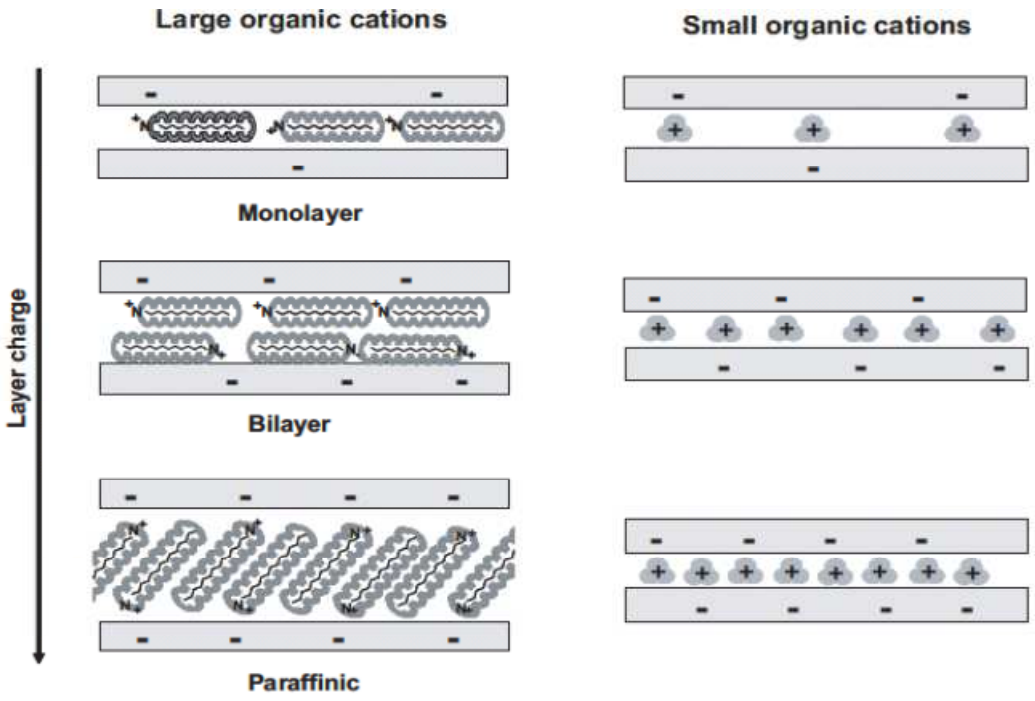

Figure 1.17 Possible arrangements of large and small organic cations in clay mineral interlayer (Cornejo et al, 2008).

The long chain organic cation is able to form almost an organic partition phase which increases in hydrophobicity as the arrangement moves from monolayer to bilayer and paraffinic (Cornejo et al, 2008).

The short chain alkylammonium cation has extremely low ability to form an organic partition phase as it exists as discrete ions. These small organic cations do not have sufficient hydration energy and therefore are non-hydrated. Hence, they are able to expose the neutral siloxane surface (Lee et al 1990; Roberts et al, 2006) and therefore (despite not possessing the ability to form an organic partition phase) would still be able to exhibit hydrophobicity. Surface charge density of the clay mineral is a major factor that determines the form of the organic partition phase to be formed by the long chain alkylammonium cation (Jaynes and Vance, 1996). If the surface charge density of the clay mineral is relatively small, the alkyl ammonium cation arrangement will take the form of either mono or bilayer (depending on the alkylammonium cation) whereas if the surface charge density is relatively high, a paraffinic structure will be formed (Jaynes and Boyd, 1991a; Jaynes and Vance, 1996; Celis et al., 2000a).

The amount of the organic cation in the interlayer space influences the hydrophobicity of the organoclay. The organic cation can be increased upto the CEC of the clay mineral. The hydrophobicity (with the associated adsorption of hydrophobic compounds) will increase with increasing organic cation in the interlayer until at a certain hydrophobic threshold where adsorption is maximum and further increase in hydrophobicity does not lead to increase in adsorption. Hence, total conversion of the hydrophilic surface to hydrophobic surface does not necessarily result in maximum adsorption of the hydrophobic compound (Nir et al, 2000; El-Nahhal et al, 2001; Cruz-Guzman et al., 2005). This indicates that overloading the interlayer space with organic cations to the extent that adsorption sites cannot be easily accessed could be a reason why total transformation of the hydrophilic surface to hydrophobic surface does not necessarily lead to maximum adsorption. El-Nahhal et al (1998) has demonstrated that the amount of alachlor adsorbed on montmorillonite pretreated with benzyltrimethylammonium (BTMA) at organic cation loading of about 63% of the CEC is greater than that at 100% CEC.

However, the adsorption processes of crude oil hydrocarbons on organo-clay especially during the biodegradation of the hydrocarbons is not well understood.

1.4.6 Clay minerals and adsorption

Adsorption of a chemical substance from aqueous phase onto a clay mineral surface is a reversible process involving the transfer of the chemical substance (sorbate) from the aqueous phase to the clay mineral (adsorbent) phase and the desorption of the chemical substance back to the aqueous phase until an equilibrium is reached.

The volatility of organic compounds and microbial transformations are both affected by adsorption (Jury et al., 1990; Gaston et al., 1996).

Under similar adsorption conditions, different clay minerals have different adsorption capacity on account of their having different specific surface area, CEC, interlayer cation, d-spacing and surface chemistry.

In an adsorption system, the distribution of an organic hydrophobic compound such as any crude oil hydrocarbon in the adsorbent phase (clay mineral) and solvent phase (water) will be determined by the relative affinity of the hydrophobic compound (sorbate) for the two phases. The nature of physico-chemical interaction forces between the sorbate and the two phases in-turn determines the degree of affinity which the sorbate will exhibit towards the phases. Physical, electrostatic and chemical interactions are the three loosely defined types of interactions that have been suggested to take place between an adsorbate and an adsorbent (Weber et al, 1991). Adsorption due to processes of physical interactions involves the dipole moments of the adsorbate and adsorbent. The dipole moments can be either induced or permanent. The several interactions that can be grouped under physical adsorption processes therefore include: van der Waals interaction forces, hydrophobic interaction forces, induced-dipole interaction forces and direct dipole-dipole interaction forces. Generally speaking, the bonding arising from these physical interaction forces are weak especially for those involving hydrophobic and van der Waals forces. Oepen et al., (1991) gave the bonding energy as a result of the different physical interaction forces described above as follows:

Van der Waals interactions (4-8kJ/mol), hydrophobic bonding (4kJ/mol), direct and induced-dipole interactions (2-29kJ/mol).

Consequent upon the weakness of the physical interaction forces, adsorption processes in which they are prominent will tend to be weak. Adsorption processes due to electrostatic interactions involves the coulombic forces of attraction between the adsorbate and adsorbent. These coulombic forces of attraction are due to ionic interactions which can either be ion-ion or ion-dipole interactions. The associated energy of bonding arising from electrostatic interaction is higher than that of physical interactions and is given as approximately 40kJ/mol (Oepen etal., 1991). Adsorption processes involving chemical interactions are largely due to hydrogen bonding and covalent bonding. The energy associated with interactions that lead to hydrogen bonding is about 2-40kJ/mol whereas that of covalent bonding is 60-80kJ/mol (Oepen et al., 1991). Another non-covalent type of bonding arises from the interaction between the clay mineral interlayer cation and the π electron of an aromatic compound. Aromatic hydrocarbon compounds are donors of π electrons and therefore lend themselves to adsorption via cation-π interaction. This has been discovered to also largely affect the adsorption of aromatic hydrocarbons by clay minerals. This π electron-cation interaction can be reasonably strong as indicated by recent molecular modelling and spectroscopic studies (Zhu et al, 2004).The bond energy of cation-π interaction is in the order of that of hydrogen bonding (Zhu et al, 2004). Chemisorption is adsorption in which covalent bond is formed between the adsorbate and adsorbent and is not a reversible process. The adsorption process of clay minerals appears to hardly ever involve chemisorption. The adsorption of non-polar compounds such as hydrocarbons has long been suggested to involve some sort of hydrogen bonding in which there is interaction of the methylene group of the hydrocarbon and the clay mineral, the degree of which will depend on the activity of the methylene group and the chain length. The methylene group of the hydrocarbon compound and the clay mineral is thought of interacting to form hydrogen bonding as follows: C-H…..O-Si (Bradley et al., 1945 and Hoffman et al., 1960). However, hydrogen bonding of this nature is not common.

If adsorption is due to hydrogen bonding arising from the interaction between the hydroxyl group of the clay surface and the oxygen of an organic compound, the kaolinites would be expected to exhibit higher adsorption than montmorillonite as the oxygen surfaces of montmorillonite have reduced effectiveness to adsorption due to the competition of water for the oxygen surface. The hydration spheres formed by especially Na and Ca-

montmorillonites tend to block off portions of the clay surfaces that ordinarily would have been available. Therefore if the adsorption of the adsorbate is predominantly due to hydrogen bonding involving the hydroxyl group of the clay mineral and the oxygen of the adsorbate (organic compound), the kaolinite would exhibit a relatively high adsorption towards the NSO compounds (resins and asphaltenes) of the crude oil.

As described in the previous section, the ability of the adsorbate to access the hydrophobic surface of the clay mineral will go a long way to determine the extent of adsorption of the hydrophobic sorbent. The exchangeable interlayer cation determines the extent to which the clay mineral's hydrophobic surface is exposed. As shown in the previous section, montmorillonite with potassium as interlayer cation, will expose the neutral siloxane surface more than montmorillonite with sodium or alkaline earth cations such as magnesium and calcium. If this is the predominant mode of adsorbate uptake, we would expect K-montmorillonite to show a relatively high adsorption to the hydrophobic hydrocarbon compounds of crude oil.

Specific surface area has been identified to determine the extent of adsorption of hydrophobic compounds such as aromatic hydrocarbons. Montmorillonite appears to adsorb aromatic hydrocarbons such as benzene, toluene and xylenes more than the kaolinites (Li et al., 1994). Kaolinite has smaller specific surface area than montmorillonite and also lacks interlayer cations. The increased adsorption by montmorillonite may not just be as a result of the increased surface area but also or exclusively due to the interaction between the interlayer cation of the clay mineral and the π bond of the aromatic ring. The adsorption of 1,2,4,5- tetrachlorobenzen, a non-π-electron-donor aromatic compound on Ag^{+}-montmorillonite was demonstrated to be substantially lower than the adsorption of phenanthrene, a π-electron-donor aromatic compound. This is contrary to the expectation of higher adsorption expected of 1,2,4,5-tetrachlorobenzene, a more hydrophobic compound on account of its octanol-water partition coefficient and aqueous solubility. The phenanthrene π-electron–Ag^{+} montmorillonite accounts for the increased adsorption of phenanthrene (Zhu et al., 2004).

Large monovalent cations such as Cs^+ and Ag^+ appear to relatively favour the π electron-cation complexation hence can be selectively removed from solution by this mechanism (Bochi et al., 1995 ; Ikeda and Shinkais,1997).

In the aqueous phase, interlayer cations with poor hydration energy such as K^+ as a result of large size (relatively high radii) will show more competitive binding to aromatic hydrocarbons via π interactions than interlayer divalent cations such as Ca^{2+} and Mg^{2+} (Zhu et al., 2004). Interlayer cations like K^+ (which has the ability of exposing the neutral siloxane surface of clay mineral thereby enhancing hydrophobic interaction with non-ionic hydrophobic compounds) also have the ability to induce interaction with aromatic hydrocarbons as described above. These two effects are expected to make K^+-montmorillonite a relatively good adsorbent for crude oil hydrocarbons.

The adsorption of hydrophobic non-polar compounds on organoclay is as a result of the non-coulombic hydrophobic interaction between the non-polar hydrocarbon chain of the organoclay and the non-polar compound which is the adsorbate (Lemke et al, 1998). There could also be a contribution to adsorption by exposed siloxane surface especially by organo-clay mineral produced from short chain aliphatic groups (Roberts et al., 2006).

1.4.7 Adsorption of Cells

Before cells can be adsorbed, they must first make their way to the adsorbent surface. There are three main different ways through which cells can be transported to an adsorbent surface, namely: diffusive transport (due to non-negligible Brownian motion), convective transport (due to the flow of the liquid medium) and transport due to the motility of the cells. Under quiescent conditions, sedimentation may contribute to the transport of cells as well (van Loosdrecht, 1990). However, for there to be contact resulting from these modes of transport, the energy barrier imposed by the repulsive forces of interaction between a negatively charged surface (such as clay) and the microbial cell (which is also negatively charged) must be overcome. Once it is overcome, contact is initiated and the cells adhere to the surface. The adhesion is believed to be reversible in the secondary minimum and irreversible in the primary minimum (Busscher et al, 1984; van Loosdrecht et al, 1989). Subsequent to adhesion is firm attachment and surface colonization by the cells (van Loosdrecht et al, 1990; Figure 1.18).

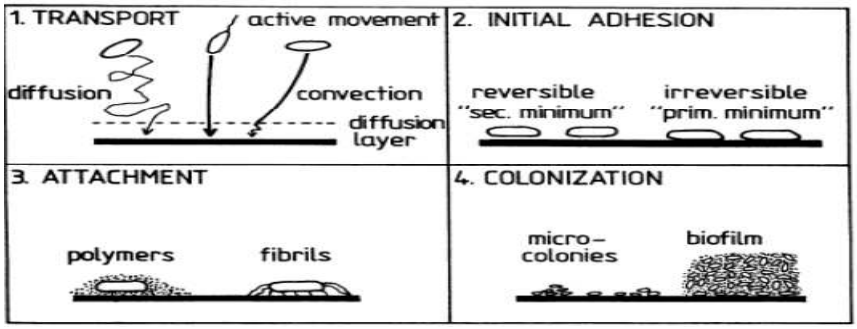

Figure 1.18 Sequence of surface colonization by microbial cells (van Loosdrecht et al., 1990).

Effects of adsorption on biodegradation

Instances of adsorption stimulating and inhibiting biodegradation have been reported (Alexander, 1999; Bright and Fletcher, 1983; Fletcher and Marshal, 1982).

Inhibitory effects of adsorption

(i) Because biodegradation essentially requires the substrates to enter the microbial cells (in whatever mechanism) in order to be acted upon by intracellular enzymes, sorbed substrates are rendered less or totally unavailable for the cells (Alexander, 1999).

(ii) The early steps of the transformation of high-molecular-weight compounds are extracellular. Also, though the enzymatic transformations of low-molecular-weight compounds are intracellular, some may be extracellular. This implies that the preservation of extracellular enzymes in the course of biodegradation is quite vital. However, if these extracellular enzymes are sorbed, they will lose their catalytic properties and this will adversely affect biodegradation. Several studies indicating the adverse effect of sorption have been reported (Griffith and Thomas, 1979; Hughes and Simpson, 1978; Makboul and Ottow, 1979).

(iii) The inorganic nutrients and other elements essential for growth may be sorbed in such a way that they are removed from solution beyond the reach of microbes. Under this situation, microbial transformation is highly hindered.

It has become known recently, however, that it is not in all cases that sorption prevents biodegradation. There have been studies indicating that sorbed substrates could be

available under some circumstances (Guerin and Boyd, 1992; Taylor, 1995; Calvillo and Alexander, 1996).

How adsorbed substrates eventually become available

Though it is not very clear how sorbed substrates eventually become available, some hypotheses have been advanced:

(i) Microbes utilize the substrates in solution and also use the substrates that enter the solution by spontaneous desorption. Initially, the system is in equilibrium as follows:

$$\text{Sorbed substrate} \underset{M2}{\overset{M1}{\rightleftharpoons}} \text{substrate in solution.}$$

Where M1 and M2 are desorption and adsorption rate constants respectively. As the substrate in solution is fully utilized, the rate of biodegradation will eventually be limited by the rate of desorption. Biodegradation of benzylamine sorbed on montmorillonite follows this mechanism (Subba-Rao and Alexander, 1982).

(ii) Unlike in the first mechanism, here in the second mechanism, the rate of biodegradation is greater than the rate of desorption. In this hypothesis, the microorganisms are thought of as producing metabolites that enhance the desorption of the substrates. If the rate of desorption is determined abiotically (in the absence of microorganisms), it will be less than the rate of biodegradation. Studies lending support to this mechanism have been reported by Wszolek and Alexander (1979), Rijnaarts et al., (1990), Calvillo and Alexander (1996). It has also been reported that surfactants desorb anthracene, phenanthrene and pyrene sorbed to soil (Liu et al., 1991). This study led to the suspicion that surfactants produced by microorganisms can facilitate the use of sorbed compounds by these microorganisms.

(iii) The third hypothesis advances that the substrates that are sorbed get utilized directly by the cells adhering to the same surface. Under this hypothesis, the substrate contacting the cell enters directly to the cell without entering the liquid phase. The hydrophobic substrates will most likely contact the cells via the cells' hydrophobic surface. This mechanism is akin to the earlier mechanism (in the previous section) of utilizing water insoluble substrates by cells adhering to the substrates undergoing microbial degradation

(Thomas and Alexander, 1987). Studies supporting this mechanism have been reported by (Harms and Zehnder, 1995; Cavillo and Alexander, 1996).

Stimulatory effects of adsorption

(i) If the clay surface concentrates the nutrients and microorganisms are able to grow on or near this surface especially when the surrounding solution is lean in nutrients, there will be stimulated microbial growth (Fletcher and Marshal, 1982; Bright and Fletcher, 1983).

(ii) Microorganisms can be sorbed themselves and there have been cases of stimulatory growth effected by sorbed microbes (Alexander, 1999). The attached cell could be responsible for the desorption of the substrate as described previously. In a study carried out by Harms and Zehnder (1995), attached cells promoted desorption of substrates.

1.5 Rationale of study/significance

The biogeochemical role of clay minerals during the biodegradation of crude oil hydrocarbons is not well understood. This study will among other things, further the knowledge of this potentially very important process.

The environment under certain conditions can on its own accord, modify the clay minerals which it contains such that the clay minerals become acid activated or transformed into organoclay. Organoclay is quite common in soils where the presence of organic compounds always occurs. Acid activated clays can be encountered in the environment that is polluted with acid mine drainage. How these environmentally transformed clays interact with microbial cells and crude oil hydrocarbons and their effect during the biodegradation of crude oil hydrocarbons is not well understood. This study will therefore provide an understanding of the potential effect on biodegradation of crude oil hydrocarbons of such environments that have the likelihood of generating acid activated clay or organoclay.

Waste discharges from industrial processes can release high concentrations of inorganic cations to the environment such that the clay again can be modified at the interlayer surface which would either inhibit or stimulate the natural ability of indigenous microbes to biodegrade crude oil hydrocarbons. There is inadequate knowledge regarding the potential effect of different interlayer inorganic cations on biodegradation of crude oil hydrocarbons.

This study will therefore advance the knowledge of the effect of different interlayer inorganic cations on biodegradation of crude oil hydrocarbons.

Bioremediation is widely accepted as the most environmentally friendly method of cleaning up crude oil hydrocarbon contamination in the environment. The current field application method of bioremediation as reviewed earlier with respect to crude oil polluted site mainly involves systematic manipulations that can speed up the microbial process of biodegradation of the crude oil hydrocarbons.

Therefore procedures that can further enhance this process of biodegradation by lending support to the microbial cells responsible for the biodegradation of the crude oil hydrocarbons would be quite pertinent to bioremediation.

This study will therefore seek to identify the type of clay minerals that are able to support the biodegradation of crude oil hydrocarbons and the physico-chemical properties responsible for this behaviour.

1.6 Aim and objectives

The general aim of this research project is to investigate the capabilities of various clay minerals in supporting the biodegradation of crude oil hydrocarbons so as to gain better understanding of their potential role in the bioremediation of crude oil polluted sites.

The above aim is achieved via the pursuance of the following objectives:

(i) Fractionation of clay samples

(ii) Preparation of acid activated clay and organo clay

(iii) Preparation of homoionic interlayer cations to produce clay minerals exchanged with mono, di and trivalent cations

(iv) Characterization of clay mineral samples using XRD, FTIR spectroscopy, surface area and CEC determination

(v) Separation of the crude oil samples into the SARA fractions

(vi) Isolating, culturing, purifying and proliferating microbial cells responsible for the biodegradation of the crude oil hydrocarbons

(vii) Investigating the effect of the clay samples on microbial growth and the biodegradation of the crude oil hydrocarbons.

(viii) Investigating the effect of abiotic processes such as adsorption during the biodegradation of the crude oil hydrocarbons.

1.7 Scope

This study is generally limited to studying the effect of clay minerals during the biodegradation of crude oil hydrocarbons. The study is not investigating the effect of clay minerals on biodegradation of resins and asphaltenes.

The assessment of biodegradation of aromatic compounds would be limited to low molecular weight polycyclic aromatic compounds. Hence, the biodegradation of high molecular weight aromatic hydrocarbons such as pyrene will not be assessed.

The identification of the microbial communities responsible for the biodegradation of the crude oil hydrocarbons will not be carried out. The study will rather focus on the isolation, purification and proliferation of the microbes responsible for the biodegradation of the crude oil hydrocarbons.

The time dependent and periodic assessment of the rate of biodegradation for detailed kinetic studies will not be covered in this work. However, the kinetics of the microbial growth and the effects of the clay samples on microbial growth kinetics would be studied.

Characterization of the clay minerals has been limited to XRD, FTIR, CEC and EGME-surface area measurements.

2. MATERIALS AND METHODS

2.1 Preparation of Clay Samples

Clay minerals used in this study are kaolinite (from kaolin), palygorskite, saponite and montmorillonite (from bentonite). Kaolin (polwhite E) and bentonite (Berkbent 163) were supplied by Imerys and Steetley bentonite & absorbent Ltd respectively. Saponite is a component of the Orrock Basalt Quarry rock samples collected from Burntisland, Scotland. The palygorskite (PF1-1) was supplied by Clay Mineral Society (http://www.clays.org). Didecyl dimethylammonium (DDDMA) bromide and other chemicals were supplied by Sigma Aldrich.

2.1.1 Fractionation of Clay mineral samples

Fractionation of the basalt rock samples from Orrock Quarry was carried out in order to liberate the saponite from the rock matrix as follows:

1000g of basalt rock was crushed to particle size of less than 10mm and soaked in a 5litre beaker filled with water to the 4.5litre mark. This was allowed to stand overnight and the supernatant liquid decanted and sonicated for 3mins. Gravity sedimentation was employed for the settling of selected particle sizes (10microns, 5microns and 2microns) using beakers filled upto 11cm height at a temperature of 20^{o}C. Stokes Law was applied to estimate the time period required for settling. Particles ≥ 10micron particle size fraction was first settled by allowing the clay suspension to stand for 22 minutes. The supernatant was collected and the ≥5micron particle size was settled by allowing the suspension to stand for 1hr 30mins. The resultant supernatant was allowed to stand for 9hrs in order to settle particle sizes of ≥ 2microns. The final supernatant is a suspension of 2micron or less particle size.

Table 2.1: Time period required for the gravity sedimentation of 10microns, 5microns and 2microns particle sizes.

Particle size	**Sedimentation time (minutes)**	**Height of beaker (cm)**
10 microns	22	11
5 microns	90	11
2 microns	540	11

Centrifugal sedimentation was finally employed to settle particle sizes of less than 2microns. SORVAL SLA-3000 Superlight centrifuge machine was used for this centrifugal sedimentation. The machine was operated at a speed of 10,000 revolutions per minute for 10 minutes. The sediment was collected dried and weighed.

The normal fractionation based on gravity settling is not enough in the case of palygorskite preparation. This is because of enmasse settling whereby the coarser fraction carries the fine particles along and settle together leaving a layer of clear water on top. To overcome this difficulty in dispersion, (Chipera et al, 1993) introduced the use of sodium hexametaphosphate as a dispersant.

Into 5litres of water was added 100g of palygorskite and thoroughly mixed. 0.01M of sodium hexametaphosphate was prepared and 100ml of the solution added to the suspension as a dispersant. The suspension was allowed to stand for 9hours to allow the coarse particles and particles more than 2microns to settle. Subsequently, the suspension of fine particles (less than 2microns) was centrifuged at 12000 rpm for ten minutes. The supernatant was rejected and the clay washed with de-ionized water three times and dried.

2.1.2 Acid activated Clay samples

The acid activated clay mineral samples were prepared after a trial experiment to establish optimum conditions for preparing the acid clay samples. The method of Rozic et al., (2008) was adopted in the activation process for the trial experiment to determine the optimum conditions. Varied hydrochloric acid (HCl) concentration and solid/liquid ratios were employed. Hence, 1M, 2M, 3M, 4M, 5M and 6M HCl and 1:2, 1:3, 1:4, solid/liquid ratios were employed in this trial experiment. Depending on the solid/liquid ratio and HCl concentration to be used, the appropriate mixture was loaded into a batch reactor and stirred with a magnetic stirrer for 45minutes while maintaining a temperature of 70^0C. The extent of metal leaching was measured by inductively coupled plasma optical emission spectroscopy (ICPOES) and gravimetric analysis.

Inductively Coupled Plasma Optical Emission Spectrometer (ICP-OES)

The concentration of metals leached from the clay mineral crystal structure was determined using Vista-MPX ICP-OES system. The sample containing leached metals is delivered to the

nebulizer through a peristaltic pump. The generated sample aerosol passes to the ICP-OES torch where the sample is ionized by the energy supplied by the plasma. This is accompanied by an emission of photons characteristic of the sample element involved. The energy of emission from solutions of known concentration (standard solutions) was used to prepare a calibration curve from where the concentration of leached metals in each sample was determined.

The optimum conditions for acid treatment were varied with clay mineral type as different conditions were required to achieve approximately the same extent of leaching. These optimum conditions were estimated through gravimetric analysis of treated samples. Whereas 2M HCl and solid/liquid ratio of 1:3 at a temperature of 70^0C and 45 minutes duration, was the optimum conditions for saponite, the optimum conditions for palygorskite and bentonite required 3MHCl with other variables the same as for saponite. The optimum condition for kaolinite required 4MHCl.

Table 2.2 Summary of optimum conditions for producing acid activated clay mineral samples as employed for acid activation.

Clay mineral	Conc of HCl (M)	Temp ^{o}C	Duration (mins)
Saponite	2.0	70	45
Bentonite	3.0	70	45
Palygorskite	3.0	70	45
Kaolinite	4.0	70	45

Sample Washing

The acid activated clay mineral samples prepared as described above (to be used for biodegradation studies) were thoroughly washed to ensure there was no free HCl in the clay samples. Approximately 5g of each acid activated clay sample was dispersed in 250ml deionised water and centrifuged. The supernatant was decanted and the clay repeatedly washed until there is almost no detectable chloride from the chloride analysis. Analysis for chlorides as a measure of free HCl was carried out using ion-chromatography.

Determination of chloride using ion chromatography.

The supernatant collected after the acid-treated clay mineral had been washed repeatedly was analysed for chloride using a Dionex ICS-1000 ion chromatograph. This ion chromatography system has an AS40 autosampler and IonPAC AS14A Analytical column. The flow rate through the column was 1ml/min. The eluent was a 8.0mM Na_2CO_3/1.0Mm $NaHCO_3$ solution and the injection loop was 25ul. Chloride in the sample was detected via a conductivity cell that measured the electrical conductance of the sample chloride ions as they emerged from a suppressor thus producing a signal based on specific chemical/physical properties of chloride ions.

2.1.3 Organo-clay Samples

In the preparation of organo-clay, the first step is usually to determine the cation exchange capacity (CEC) of the clay (Witthuhn, 2006).

2.1.3.1 Cation Exchange Capacity of the clay samples

The essence of determining the CEC of the various clay minerals especially with the 2:1 clay minerals is to be able to ascertain the stoichiometric amount of quaternary ammonium compound (surfactant) required for the production of the organo-clay. 1g of each of the clay samples was dried and introduced into 20ml 1M ammonium acetate solution at pH 7.0 with shaking and left overnight. The next day, the suspensions were centrifuged and the supernatant discarded. Another 20ml of 1M ammonium acetate was added and shaken for 2hrs. This was then centrifuged and supernatant also discarded. This step was repeated twice. 20ml of de-ionized water was then added for washing, shaken for few minutes, centrifuged and supernatant discarded again. This step was repeated four times. 20ml of 1M KCl solution was added and shaken overnight. The suspension was centrifuged but this time, the supernatant was collected in a 100ml volumetric flask. This was repeated three more times but shaking for only 2hrs. The collected solution was acidified with few drops of concentrated nitric acid and flask made up to 100ml mark with de-ionized water.

Ammonium ion was estimated via the determination of ammonical nitrogen as follows:

50ml of sample was placed in the digestion tube and a few drops of phenolphthalein indicator were added. The pH of the solution was adjusted to about 8.5 using 0.02M NaOH.

3ml borate buffer solution was added while the digestion tube was placed in position in the 'Gerhardt Vapodest'. 50ml boric acid in 250ml conical flask was placed in position to the right of the digestion tube. The program was set for '0' second water addition and '0' second sodium hydroxide addition and run. A reagent blank was prepared and distilled. The distillate was titrated with 0.02M H_2SO_4 to pale lavender end point. Also, the CEC of the cation exchanged clay minerals, Na-bentonite, K-bentonite, Mg-bentonite, Ca-bentonite, Zn-bentonite, Al-bentonite, Cr-bentonite and Fe-bentonite was also carried out as described above.

2.1.3.2 Preparation of Organoclay

The CEC determined in the previous section formed the basis of the stoichiometric amount of the quarternary ammonium compound used in the preparation of the organoclay. 35% of CEC was used in the preparation of the organo-clay for bentonite and saponite clay samples. 100g and 50g of saponite and bentonite respectively were dispersed in 1.5l of de-ionized water in separate cylinders and stirred for about 24hrs.

At 35% CEC, the corresponding amounts of didecyldimethylammonium (DDDMA) bromide added to the bentonite and saponite suspension were 7.0g and 5.17g respectively. Before introducing the surfactant to the clay suspension, it(the surfactant) was dissolved in 100ml of water and then slowly added. The mixture was stirred for 24hrs. Thereafter, the clay suspension was centrifuged and the supernatant rejected while the clay was washed ten times by adding de-ionized water, shaking and centrifuging.

The organoclay obtained was dried at a temperature of 48^0C and stored in a dessicator.

2.1.4 Production of several homoionic interlayer cation with bentonite

Several samples were generated from exchanging the interlayer cations of bentonites with Na^+, K^+, Mg^{2+}, Ca^{2+}, Zn^{2+}, Al^{3+}, Cr^{3+} and Fe^{3+} to produce, Na-bentonite, K-bentonite, Mg-bentonite, Ca-bentonite, Zn-bentonite, Al-bentonite, Cr-bentonite and Fe-bentonite. 0.5M solution of the corresponding metal chloride salt was prepared and then 200ml of each of the solution used to disperse 5g of bentonite clay mineral to have a clay suspension. The suspensions were shaken for 24hrs in a mechanical shaker and then subsequently

centrifuged. The supernatant was removed and the clay mineral washed exhaustively until the chloride level is negligible.

2.1.5 Surface area measurement of clay minerals-EGME method

This method of Carter et al., 1965 which is based on adsorption of 2-ethoxyethanol (also known as ethyleneglycol monoethyl ether or EGME) is preferred to BET-N_2 method as a result of its ability to access and hence measure both the external and internal surface area of the clay mineral.

The main pieces of equipment employed are a rotary vacuum pump, analytical balance, aluminium weighing dishes (about 6cm diameter) and glass desiccators. The chemicals used were calcium chloride (desiccant), Ca-montmorillonite (used as a standard) and EGME.

To prepare the desiccant, 100g of oven dried $CaCl_2$ was mixed with 20ml EGME in a beaker, thoroughly stirred and put in glass dish and positioned in the base of the desiccator.

An aluminium dish was weighed to four figures and recorded as M1. Approximately 1g of clay (dried overnight at 80^{o}C and allowed to cool) was added to the dish and the new mass recorded as M2. This procedure was repeated for a further four clay samples including the control sample. Immediately after weighing, 3ml EGME was added to the dry clay in each dish. The dishes were transferred to desiccators containing a mixture of dried $CaCl_2$ and EGME desiccant. Dishes were arranged around the circumference of the desiccant tray cover. The desiccator lid was replaced and allowed to stand for 1-1.5hrs. The system was evacuated overnight under vacuum. Vacuum was released and dishes weighed rapidly every 12-16 hours until a stable mass was achieved which is recorded as M3.

The surface area is calculated from the equation:

$$S = [(M3-M2)/(M2-M1)]/K \quad \text{……………………………………………………………….2.1}$$

Where :

S = surface area

M1 = Weight of dish (g)

M2 = Weight of dish and dry sample (g)

M3 = Weight of dish and dry samples and EGME

K = Weight of EGME required to form a monolayer over $1m^2$ of surface = $2.86*10^{-4}$ g/m^2

2.2 Saturates from crude oil samples

Crude oil saturated hydrocarbons used in this study were prepared in the laboratory by column chromatography.

2.2.1 Deasphaltening of the crude oil sample

The crude oil used in this experiment was an Undegraded North Sea crude oil originally supplied by BP. The asphaltenes in the crude oil were first removed by the process of deasphaltening which involves precipitation of the asphaltenes with hexane, using a hexane/crude oil ratio of 40:1 (v/v). 50ml of the crude oil sample was introduced into five designated flasks of 500ml capacity each with each flask containing 10ml of the crude oil. Into each flask was introduced 400ml of hexane and the whole content agitated with magnetic stirrer for 2hrs and subsequently transferred to the refrigerator to stand overnight. The precipitated asphaltenes were separated by centrifugal sedimentation at a speed of 4000 rev/min for 15 minutes. The resulting supernatant was collected as maltenes (saturates, aromatics and resins).

2.2.2 Separation of crude oil saturates from maltene

Saturated hydrocarbon fractions were separated from the maltene fraction by column chromatography. 1g of maltenes was mixed with 5g of alumina using dichloromethane (DCM) to obtain a consistent paste which was left overnight to drive out the solvent leaving a fine powder of dried maltene/alumina mixture. For each column chromatographic run, 1g of the maltene/alumina mixture was introduced onto the top of the column (dimensions: 2cm diameter and 50cm height) packed with silica gel. 150ml of Petroleum ether (pet ether) was used for eluting the saturates. The collected saturates was re-introduced into a fresh column so as to clean up the saturates and reduce contamination by aromatics. The separated saturates was analysed by GCMS just to ensure that it is substantially free of aromatics by looking for the two peaks of methyl-naphthalene, the presence of which indicates that the saturates still contained traces of aromatics.

2.3 Microbial communities

Microbial communities responsible for biodegradation of both the crude oil saturates and crude oil hydrocarbons were isolated from beach sediment sample consisting of fine sand particles collected in a sterilised glass bottle (Duran) from a site at St Mary's lighthouse near Whitley Bay, Newcastle upon Tyne (N 55° 04' 18", W 01° 26' 59"), United Kingdom and stored at 4^{o} C in cold room until start of the experiment. The Bushnel-Haas (BH) broth as the nutrient source and nutrient agar were supplied by Sigma Aldrich. The microbes were proliferated and purified via several subcultures.

2.3.1 Enrichment Culture Preparation for microbial cell proliferation

Two sets of initial enrichment cultures were prepared by:

(a) Mixing 20g of beach sand, 100ml of BH medium (autoclaved) and 200mg of crude oil saturates (as the carbon source) in a 250ml conical flask transferred under a sterile atmosphere provided by bunsen burner flame.

(b) Mixing 20g of beach sand, 100ml of BH medium(autoclaved) and 500mg of crude oil in a 250ml conical flask under a sterile atmosphere provided by bunsen burner flame.

The B-H medium was prepared by dispersing 0.327g of BH broth in 100ml de-ionized water. The flask was then closed with a cotton wool and continuously shaken.

2.3.2 Microbial growth

The initial culture using saturated hydrocarbons as the carbon source was allowed to incubate for two weeks and 5ml of the cell suspension used to prepare a subculture. Also, the culture using crude oil as carbon source was allowed to incubate for two weeks before the preparation of subculture using also 5ml cell suspension.

For the purpose of enrichment of the cells (enrichment culture), several weights (0.2g-1.75g) of the crude oil saturated hydrocarbon were used as carbon source in several subcultures after the initial culture. In another set of enrichment culture using crude oil as carbon and energy source, different weights of the oil, 0.5g-2.0g were used. Microbial growth was monitored in the second subculture for each case by collecting 1ml of cell suspension every two days and measuring absorbance using a UV-Visible spectrophotometer. Cell growth was also monitored via cell plating. The plates were prepared as follows: 28g of nutrient agar and 3.27g of BH broth were dispersed in 1litre of deionized water and then autoclaved.

Crude oil saturates fraction (500mg) was added and the mixture well shaken. The same procedure was adopted for preparing plates used for enumerating cells grown on crude oil as the carbon source except that instead of using 500mg of saturates, 500mg of crude oil was used. The contents were then poured into several Petri-dishes and allowed to gel. They were then stored at 4^0C and subsequently used for cell plating as samples are withdrawn periodically from the test subculture. The procedure used in carrying out the cell plating was as follows: 1ml of cell suspension from the subculture was used in preparing 10^1 to 10^7fold dilution. 0.1ml of each of the above stated dilutions was spotted on the plate and carefully spread. The plates were incubated for 24hours at 28^0C and enumerated. The growth curve obtained enabled determination of the stationary phase and hence an estimate of when there will be active cells in the system. Several subcultures were consequently prepared by sampling the cells when they are still very active namely the 4^{th} day for cells using saturates as carbon source and the 6^{th} day for cells using crude oil as carbon source.

2.3.3 Bactericidal effect of spent water from organoclay

The bactericidal effect of the spent water from organoclay was tested by collecting the spent water (10ml) arising from the final washings of the organoclay (organo-saponite and organo-bentonite) and using it to prepare the BH medium by dispersing the appropriate quantity (32.7mg) of BH broth into it and adding 50mg of crude oil. The control experiment contained de-ionized water. Both the test and control experiments were inocubated with the same cells that use crude oil hydrocarbons as carbon source. Another set of sacrificial samples were monitored for microbial kinetic purposes.

2.3.4 Effect of clay samples on the microbial growth

A set of experiments (in triplicate) for determining the effect of clay mineral samples on microbial growth was carried out as follows: 250mg of each of the clay samples (unmodified clay, acid activated clay, organoclay and homoionic cation interlayer clay samples) were each mixed with 50mg of crude oil and 10ml BH medium and inoculated with microbial cells. Acid activated bentonite clays (Table 2.3) such as BA (500mg) was also tested for comparison with BA (250mg). See section 2.5 for description of sample codes. Sacrificial samples were collected every four days until the 12^{th} day for microbial growth tests.

2.3.5 Effect of pH on microbial growth.

The effect of pH (adjusted with HCl and NaOH) on microbial growth was tested at pH 3, 4, 9 and 10. Samples for which the BH-medium (10ml) was maintained at pH 3,4,9 & 10 (without clay samples) were mixed with 50mg of crude oil and inoculated with microbial cells and incubated for 12 days. Sacrificial samples were collected every four days and tested for microbial growth.

2.4 Laboratory biodegradation of crude oil saturates supported on clay minerals

The clay samples: unmodified bentonite, saponite, kaolinite and palygorskite; acid activated bentonite, saponite, kaolinite and palygosrkite; and organo bentonite and saponite were employed for testing their capability in supporting biodegradation of crude oil saturates. There were four sets of control experiments: crude oil saturates + microbial cells + BH (positive control)-no clay minerals; BH + crude oil saturates + Clay minerals-no microbial cells; BH + crude oil saturates-no microbial cells and no clay minerals; petroleum ether + BH. The test experiment constituted crude oil saturates + BH + microbial cells + clay minerals. See section 2.5 for sample code description and extraction procedure which are also applicable to this section. Into a 100ml serum bottle was added 25mg of the crude oil saturates, 10ml of BH medium and 250 mg of clay and 1ml cell suspension. However, prior to adding the HC and cell suspension, the clay and BH medium were autoclaved. The control experiments were set up at the same time and under the same conditions. All the serum bottles were shaken and incubated for 21 days at 28^0C.

2.5 Biodegradation of crude oil hydrocarbons supported on clay minerals

All the clay samples: unmodified bentonite, saponite, kaolinite and palygorskite; acid activated bentonite, saponite, kaolinite and palygosrkite; and organo bentonite and saponite were employed for testing their potency in supporting biodegradation of crude oil hydrocarbons. Also employed are the various samples generated from exchanging the interlayer cations of bentonites with Na^+, K^+, Mg^{2+}, Ca^{2+}, Zn^{2+}, Al^{3+}, Cr^{3+} and Fe^{3+} to produce, Na-bentonite, K-bentonite, Mg-bentonite, Ca-bentonite, Zn-bentonite, Al-bentonite, Cr-bentonite and Fe-bentonite. There were three sets of control experiments: crude oil + microbial cells + BH (positive control); BH + crude oil + clay minerals and BH + crude oil. The test experiment was constituted of crude oil+ BH + microbial cells + clay minerals. Clay

mineral/ crude oil ratio of 5:1 was used. Into a 100ml serum bottle was added 50mg of the crude oil, 10ml of BH medium and 250mg of clay and 1ml cell suspension. However, prior to adding the crude oil and cell suspension, the clay and BH medium were autoclaved. All the serum bottles were shaken and incubated for 60 days at 28^0C. Spent water from organoclay was also tested for supporting biodegradation by using it for preparing the BH medium in which 50mg crude oil was added and the mixture inoculated with microbial cells and also incubated for 60 days.

Table 2.3 Code and description of control and clay samples

S/N	Sample code	Description
1.	BA-500	Acid activated bentonite (500mg)
2.	BA-250	Acid activated bentonite (250mg)
3.	KA-250	Acid activated kaolinite (250mg)
4.	PA-250	Acid activated palygorskite (250mg)
5.	SA-250	Acid activated saponite (250mg)
6.	BO-250	Organo-bentonite (250mg)
7.	SO-250	Organo-saponite (250mg)
8.	BU-250	Unmodified bentonite (250mg)
9.	KU-250	Unmodified kaolinite (250mg)
10.	PU-250	Unmodified palygorskite (250mg)
11.	SU-250	Unmodified saponite (250mg)
12.	Control-1	Positive control-in the absence of clay mineral
13.	Control-2	Negative control-absence of clay and microbes
14.	B-Na	Sodium bentonite (250mg)
15.	B-K	Potassium bentonite (250mg)
16.	B-Mg	Magnesium bentonite (250mg)
17.	B-Ca	Calcium bentonite (250mg)
18.	B-Zn	Zinc bentonite (250 mg)
19.	B-Al	Alumium bentonite (250mg)
20.	B-Cr	Chromium (VI) bentonite (250mg)
21.	B-Fe	Iron (III) bentonite (250mg)

All other samples with a 'C' before it such as CBU-250 or CBA-250 or CB-Mg represents controls with only the clay and oil. Hence, there are three sets of controls, Control-1, Control-2 and the control where only clay minerals and oil are mixed and incubated such as CBU-250, CBO-250, CKU-250, CB-Ca, CB-K etc.

Hydrocarbon Extraction procedure

After the incubation period when biodegradation had taken place as described in section 2.5, the serum bottles were removed and the residual crude oil hydrocarbon extracted as follows:

Prior to extraction of the residual hydrocarbon, squalane in a dichloromethane (DCM) solution of 1mg/ml as a surrogate standard was prepared and 250µl (containing 250µg of squalane) of the solution added to the serum bottle containing the residual oil and the clay mineral. Into the same serum bottle, 30ml of DCM was added and the serum bottle covered tightly with aluminium foil and shaken thoroughly to extract the residual crude oil (at this stage not just the hydrocarbons but whole oil was extracted) using a glass separating funnel. This was repeated two more times such that a total of 90ml DCM was used in three stages of extraction. The extracted oil solution (in 90ml DCM) was concentrated by rotary-evaporation to 10ml solution and divided into two aliquots of 8ml and 2ml. The 2ml aliquot was conserved (to be used for Iatro scan analysis) while the 8ml aliquot was used for separation of hydrocarbons fractions. For separation of the hydrocarbons on the solid Phase extraction (SPE) columns, the following procedure of Bennett et al.,(2002) was adopted:

The 8ml aliquot was gently blown down to just dryness under nitrogen to drive off DCM completely. The sample was then re-dissolved in 200-300µl hexane in a 3ml vial. The C18 SPE column was conditioned by flushing with about 5ml hexane and thereafter flushing with air. The sample that was re-dissolved in 200-300µl hexane was then introduced to the SPE column using a pipette. About 200µl of hexane was added and allowed to run through the SPE column and collected into a 10ml vial. This process was repeated to ensure that the sample is thoroughly washed into the sorbent. About 2.5ml of hexane was added again to run through the column and collected. This was repeated and the tip of the SPE column rinsed with 0.5ml of hexane.

An aliquot of a quarter of the total volume collected (1.5ml) was used for GC analysis. 50µg of heptadecylcyclohexane , 10µg of 1,1-binaphthyl and 5µg of 5α-androstane were used as internal standards.

Procedural blanks

Procedural blanks included all the clay mineral samples as used for the biodegradation studies and which were subjected to the same treatment as the test samples and the controls. These were used to establish that the clay samples were free of hydrocarbons that could introduce bias to the result of analysis. The same quantity of internal standards was used for them as the samples.

Extractable organic matter (EOM)

The 2ml aliquot from each sample (conserved in the extraction procedure) as described in the previous section was used for the determination of the EOM. For each sample, empty 10ml capacity vial was weighed and noted. The 2ml aliquot was transferred to a weighed 10ml vial and gently blown down to dryness using a stream of nitrogen followed by weighing.

2.6 Analytical instrumentation

The analytical instruments used in this work were described below:

2.6.1 X-Ray Diffraction (XRD)

XRD is a widely used analytical instrument for the identification and analysis of crystalline materials such as clay minerals (Moore and Reynolds, 1997). In this work, the basal spacings of the clay samples were measured by XRD.

The samples were prepared for XRD measurement by orienting the clays in a glass slide following standard procedure. The slides were air dried and placed in a desiccator containing silica gel to prevent rehydration. Glycolated and heat treated (300^0C) samples were also prepared following standard procedure.

The XRD machine used was a PANalytical X'Pert Pro MPD fitted with an X'Celerator and a secondary monochromatorFor data acquisition, a Cu anode was supplied with 40 kV and a

current of 40 mA to generate Cu-Kα radiation (λ = 1.54180 Å) or Cu-$K\alpha_1$ (λ = 1.54060 Å). The data was collected over a range of 2-70°2θ with a nominal step size of 0.0167°2θ and nominal time per step of 1.00 seconds. Fixed anti-scatter and divergence slits of 1/4° were used together with a beam mask of 10mm. All scans were carried out in 'continuous' mode using the X'Celerator RTMS detector.

Data were interpreted by reference to X'Pert accompanying software program High Score Plus in conjunction with the ICDD Powder Diffraction File 2 database (1999) and the Crystallography Open Database (October 2010; www.crystallography.net).

2.6.2 UV-Visible Absorption Spectroscopy

Spectrophotometry is not only used in quantitative determination of chemical compounds but can also be used to monitor microbial cell growth as indicated in previous section. The absorbance is directly related with cell population and hence is used to monitor microbial growth.

UNICAM 8625 UV/VIS Spectrophotometer was used to monitor the microbial cell growth by measuring the absorbance of subcultures prepared for purposes of determining the exponential and stationary phases during cell proliferation. The spectrometer had a monochromator to provide the selected wavelength of 600nm incident on the sample. The sample was a cell suspension prepared from the subculture by centrifuging the subculture to remove any oil phase. 1ml of the cell suspension was diluted with 9ml of de-ionized water to have a 10-fold dilution and then introduced to the cuvette.

2.6.3 Gas Chromatography (GC)

In this study, GC was used for the analysis of crude oil total petroleum hydrocarbon (TPH) and saturated hydrocarbons. The GC instrument used was an HP 5890 series II gas chromatograph equipped with a split/splitless injector and flame ionization detector (FID). The sample was injected using a HP 7673 autosampler. The separation of the crude oil hydrocarbon compounds was carried out on an Agilent HP-5 capillary column (30m x 0.25mm) coated with 5% phenylmethyl-polysiloxane (0.25µm thick) stationary phase. The GC oven temperature was programmed from 50°C for 2mins and then ramped at 4°C/min, up to 300°C where it was held for 20mins. The carrier gas used was hydrogen at a flow rate

of about 2ml/min at initial pressure of 100kPa. The GC data was acquired using Atlas software on HP computer desktop.

2.6.4 Gas chromatography/mass spectrometry (GC-MS)

GC-MS was used to analyse the hydrocarbon fractions of the laboratory biodegraded crude oil samples. The GC-MS used was Agilent 6890 GC instrument with split/splitless injector (280^{o}), linked to a 5975 MSD mass spectrometer. The GC was equipped with a fused silica capillary column (30m x 0.25mm) coated with 5% phenyl polysiloxane (HP-5) stationary phase. The GC oven was programmed from 40^{o}C for 5mins and then ramped at 4^{o}C/min, up to 300^{o}C where it was held for 20mins. The carrier gas used was helium at a flow rate of about 1ml/min and initial pressure of 50kPa while split at 30ml/minute. The sample was injected by an HP7683 autosampler and the split opened after 1 minute to vent the solvent. The mass spectrometer used an electron ionization energy of 70 eV. The following operating conditions were used: Source temperature of 230 ^{o}C; Quadrupole temperature of 150 ^{o}C; Multiplier voltage of 2000V; Interface temperature of 310 ^{o}C. Selected ion monitoring (SIM) mode was used to monitor ions of interest such as ions 85, 128, 142, 156, 170, 178, 182, 191,198, 212, 231, 254 etc.

2.6.5 IATROSCAN (Tin Layer Chromatography-FID)

In this study, the biodegraded crude oil extract samples and fresh oil samples in dichloromethane (DCM) were analysed using an Iatroscan MK-5 TLC-FID following the method of (Karlsen & Larter, 1991).

The mobile phases used were n-hexane, toluene and DCM-methanol (93:7 v/v) whereas the stationary phase was silica coated onto glass rods (Chromarods). The Chromarods were type S III, pore diameter 60Å and particle size 5µm). Pure grade hydrogen at a flow rate of 130ml/min and air at a flow rate of 500ml/min were used in the flame ionization detector (FID). The initial step in this Iatroscan technique was passing the Chromarods to the FID to burn off organic contaminants and activate the silica. Subsequently, the rods were spotted with an aliquot (3µl) of the extracted biodegraded crude oil samples. The first two rods were spotted with standard oil (North Sea Oil) as a reference standard. The rods were developed in n-hexane for about 25min until the solvent reached 100% of the rod length as indicated

on the rods' rack. The rods were then removed and allowed to dry at room temperature for about 3mins. The rods were then developed in toluene for about 10mins until solvent reached the 60% mark as indicated by the mark on the rack. Again, the rods were removed and allowed to dry at room temperature for about 6mins. Finally, the rods were developed in DCM/methanol (93:7 v/v) for about 4mins until the solvent reached 30% of the mark as indicated by the mark on the rack. The rods were then removed and dried in an oven (60^{o}C) for about 90 seconds. The final step was placing the rods in the Iatroscan-FID analyser and recording the results using Labsystems Atlas data system.

Some of the samples were run in triplicates for testing reproducibility.

2.6.6 Fourier transform infrared (FTIR) spectroscopy

The clay mineral samples were made into fine powders by grinding using agate and mortar and then kept in the oven overnight to avoid moisture adsorption.

The sample (0.0005g) was mixed with 0.2995g of Potassium bromide (KBr) and then ground again to a homogeneous blend and compressed under 750 * 10^3 kPa pressure to give a small transparent disc of 13mm diameter. A background spectrum of pure KBr was run before the spectrum of any sample to account for any absorption due to impurities in the KBr. The disc containing the sample was then placed in the infrared spectrometer and the spectrum of the clay sample was collected, collecting 100 scans over a wavelength of 400-4000cm^{-1} at 4cm^{-1} resolution using a Fourier transform spectrometer (Thermo Nicolet Nexus 870) fitted with a transmission accessory and equipped with a DTGS detector.

2.6.7 Total organic carbon (TOC)

Total organic carbon (TOC) was measured to characterize and also estimate the yield of the organo-clay produced in this study.

Approximately 100mg of organo-clay sample in a porous crucible was treated with sufficient (about 1ml) hydrochloric acid at a concentration of 4M in order to remove any carbonates that may be present. After the acid has drained from the crucible for about 4hrs, the crucible and sample were dried overnight at 65°C. Residual (organic) carbon was then determined using a Leco CS244 Carbon analyser. This instrument uses a flow of oxygen that

enables the sample to be ignited in an induction furnace so as to convert all residual carbon in the sample to carbon dioxide. The infra-red detector in the instrument measures the carbon dioxide. Prior to running the sample, a blank was run to detect any background residual carbon in all the apparatus that are to be used.

The organic carbon content is calculated as follows:

Organic Carbon, % = C_s - C_{bl} …….Eq. 2.2

Where C_s and C_{bl} are organic carbon content of sample and blank respectively. The difference represents the TOC of the sample.

3. CHARACTERIZATION OF CLAY MINERAL SAMPLES

3.1 Introduction

The characterization of clay mineral samples in this study is important in order to ensure that the clay samples are adequately identified. It also provides an opportunity to identify any likely impurity that could significantly affect the behaviour of the clay samples, and to determine whether or not the clay minerals are affected by the treatments that have been carried out. The characterization of the clay mineral samples used in this study was expected to provide adequate framework to understand observed variation in their properties (e.g. surface area and cation exchange capacity). These properties are expected to be useful for the correlation of the observed effects of the clay samples during the biodegradation of the crude oil hydrocarbons.

Surface phenomena and biogeochemical roles of clay minerals are believed to be determined largely by their surface area and cation exchange capacity (CEC). Therefore clay characterization which involves determination of specific surface area and CEC would aid in accounting for differences in behaviour of the clay samples for processes that take place at the solid-liquid interface or exchange of cations. It will also differentiate between non-microporous and microporous phyllosilicates (Bergaya et al, 2006).

In this work, the characterization of the clay mineral samples was generally carried out with respect to the surface area (SA), Fourier Transform Infrared (FTIR) spectrometry, X-ray diffraction (XRD), cation exchange capacity (CEC) and total organic carbon (TOC) content (for organoclay samples). The acid activated clay samples were also additionally characterized by determination of pH and free chloride as described in section 2.1.2.

3.2 Free Chloride and pH values of the acid activated clays and homoionic bentonite clay samples

The pH of the clay sample suspension and free chloride (as a result of acid treatment) are presented in Table 3.1 below.

Table 3.1 Free chloride for all prepared clay samples and their pH values. The sample codes in Table 3.1 are described as follows: BA=acid activated bentonite, KA=acid activated kaolinite, SA=acid activated saponite, PA=acid activated palygorskite, B-Na=sodium bentonite, B-K=potassium bentonite, B-Mg=magnesium bentonite, B-Ca=calcium bentonite, B-Zn=zinc bentonite, B-Cr=Chromium bentonite and B-Fe=ferric bentonite. Others are BA-250=acid activated bentonite (clay/oil ratio = 5:1) and BA-500=acid activated bentonite (clay/oil ratio=10:1)

Sample	pH	Chloride(mg/g)
BA	4.1	0.04
KA	4.4	0.0
SA	4.3	0.0
PA	4.2	0.0
B-Na	7.8	0.1
B-K	7.8	0.0
B-Mg	7.8	0.0
B-Ca	7.6	0.06
B-Zn	5.9	0.04
B-Cr	4.8	0.0
B-Fe	4.9	0.0
B-Al	4.7	0.01
BA-250	4.1	0.04
BA-500	3.6	0.04
BH medium	7.2	-

Table 3.1 shows that the acid activated clay samples have the lowest pH values hence are the most acidic. Following these samples closely are the trivalent cation exchanged clays namely: B-Al, B-Cr B-Fe. The pH of B-Zn indicates that this sample is acidic but not as acidic as the trivalent cation exchanged clays whereas the other divalent cation exchanged clays such as B-Mg and B-Ca and the monovalent cation exchanged clays such as B-Na and B-K are quite close to the pH of the Bushnell-Haas (BH) medium. The highest residual chloride on the

clay mineral samples appears to be with B-Na and is possibly due to the fact that this clay sample expands more extensively in water than the other clay samples making it increasingly difficult to remove all the chloride. However, the chloride level at 0.01% is not expected to alter the behaviour of this sample significantly.

3.3 Surface area, cation exchange capacity and total organic carbon (TOC)

The properties of the clay samples such as EGME-surface area, cation exchange capacity (CEC) are presented in Table 3.2. The total organic carbon (TOC) of the organoclay are also presented in Table 3.2

Table 3.2 Surface area, cation exchange capacity and total organic carbon of the clay samples

Sample	Surface area(m^2 /g)	CEC(meq/100g)	TOC(%)
BU	645	83.3 (80.4)α	-
BA	722	-	-
BO	471	-	7.3(72.3%)β
SU	473	35.4	-
SA	532	-	-
SO	330	-	3.41 (85%)η
PU	502	16.5	-
PA	567	-	-
KU	36	3.5	-
KA	39	-	-
B-Na	570	83	-
B-K	455	76.4	-
B-Mg	522	81.7	-
B-Ca	598	79.1	-
B-Zn	525	73.8	-
B-Al	513	65.9	-
B-Cr	489	83	-
B-Fe	646	88	-

From Table 3.2, α, β and η represent the CEC measured using 250mg of BU instead of 1g, the % conversion of BO and the % conversion of SO respectively.

The EGME- surface area of the clay samples tends to increase with acid activation except for kaolinite which did not seem to undergo any significant change in surface area. The intercalation of didecyldimethylammonium ion to produce organoclays tend to reduce the EGME-surface area significantly. Among the unmodified clay samples, bentonite has the highest surface area. The same thing applies to acid activated clay samples as acid activated bentonite has the highest surface area. Among the cation exchanged clay samples, Fe-bentonite has the highest surface area followed by Na-bentonite and Ca-bentonite. The least surface area is that of K-bentonite. Table 3.2 shows that there is no significant difference between the CEC value measured using 1g of bentonite and 250mg of bentonite (note α) hence the CEC reported for B-Na, B-K, B-Mg, B-Ca, B-Zn, B-Al, B-Cr and B-Fe which was based on 250mg clay is not expected to be significantly different from that measured using 1g of clay. From Table 4.2, the CEC of the clay samples for the cation exchanged clay samples increases in this order: B- Al< B-Zn <B-K <B-Ca < B-Mg <B-Na=B-Cr< B-Fe. Among all the samples whose CEC was measured, unmodified kaolinite (KU) has the lowest value.

3.4 FTIR spectra

The FTIR spectra in the region 500cm^{-1} - 4000cm^{-1} for the characterization of the clay minerals are presented in this section.

3.4.1 Bentonite

The FTIR spectra of bentonite are presented in Figures 3.1, 3.2 and 3.3.

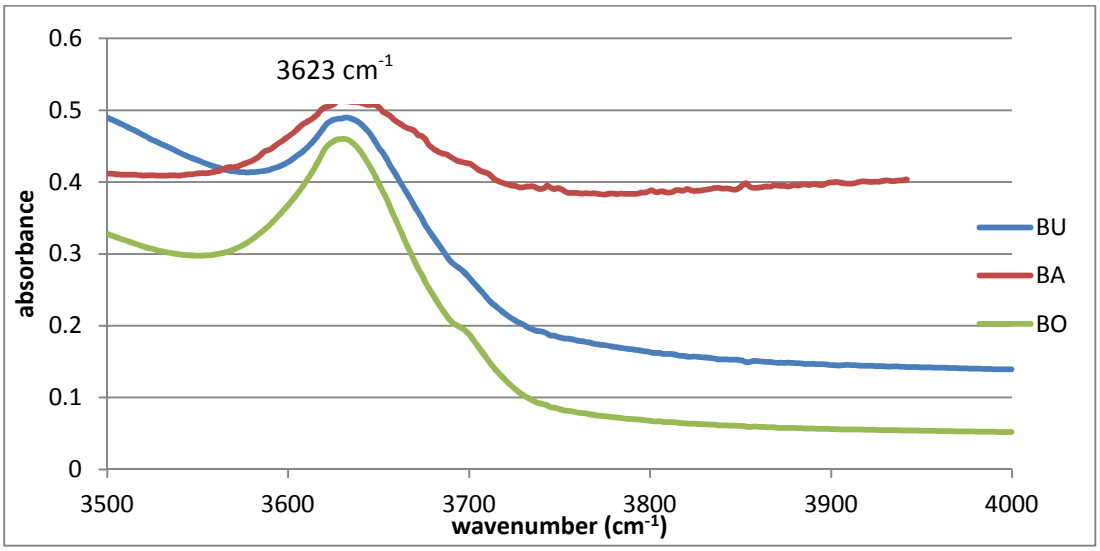

Figure 3.1 Infrared spectra of bentonite (3500-4000cm^{-1})

The broad IR absorption band at 3623 cm^{-1} in the spectra for treated and untreated bentonite as shown in Figure 3.1 is assigned to OH-stretching of AlAlOH which is typical of dioctahedral smectites such as montmorillonites. All the samples (unmodified bentonite, acid activated bentonite and organobentonite) showed this absorption band.

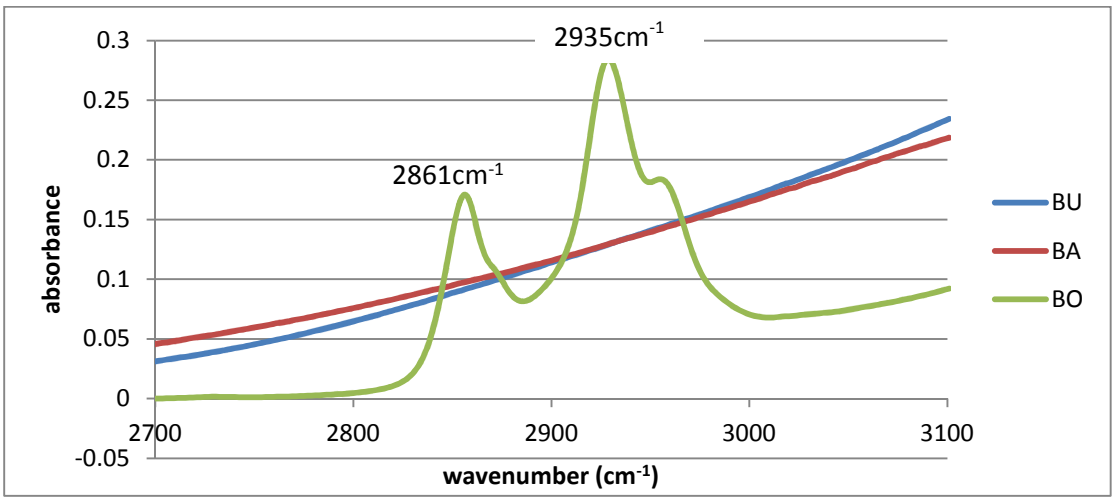

Figure 3.2 Infrared spectra of bentonite (2700-3100cm^{-1})

The absorption bands at 2861 cm^{-1} and 2935cm^{-1} (Figure 3.2) observed with organobentonite sample (BO) are assigned to symmetrical and assymetrical vibration stretch

of C-H_2 respectively from the hydrocarbon moiety of DDDMA used in the preparation of the organoclay sample.

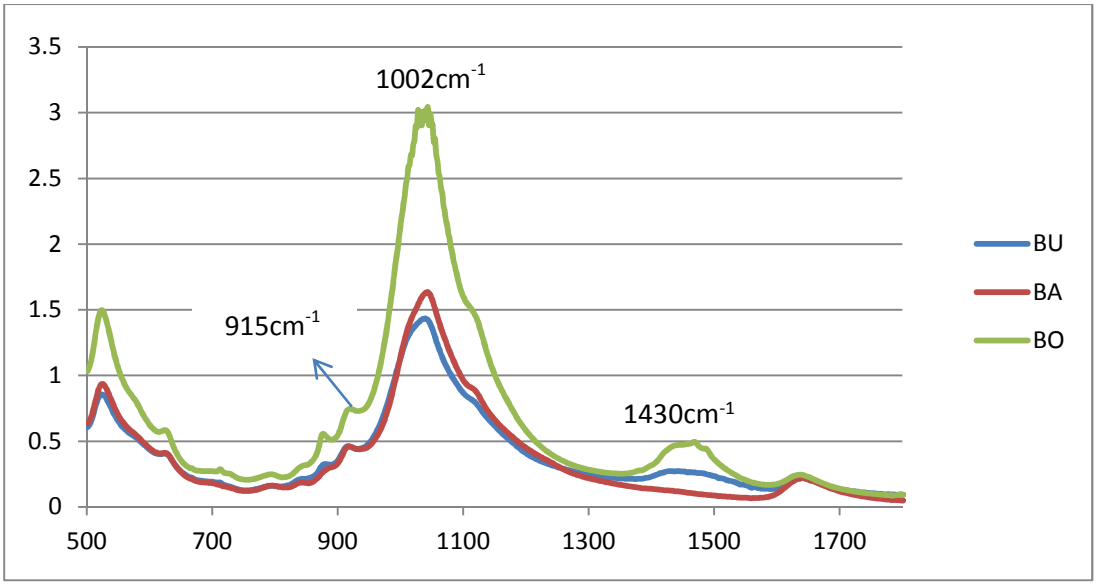

Figure 3.3 Infrared spectra of bentonite (500-1700cm^{-1})

The absorption band at 915 cm^{-1} (Figure 3.3) without a band at 938cm^{-1} is due to deformation of the AlAlOH and is characteristic of montmorillonites. The band at 1002cm^{-1} is due to the Si-O stretch vibration while that at 1430cm^{-1} is due to calcite (carbonate) and does not appear in BA as it is digested during acid activation.

3.4.2 Kaolinite

The FTIR spectra of kaolinites are presented in Figures 3.4 and 3.5

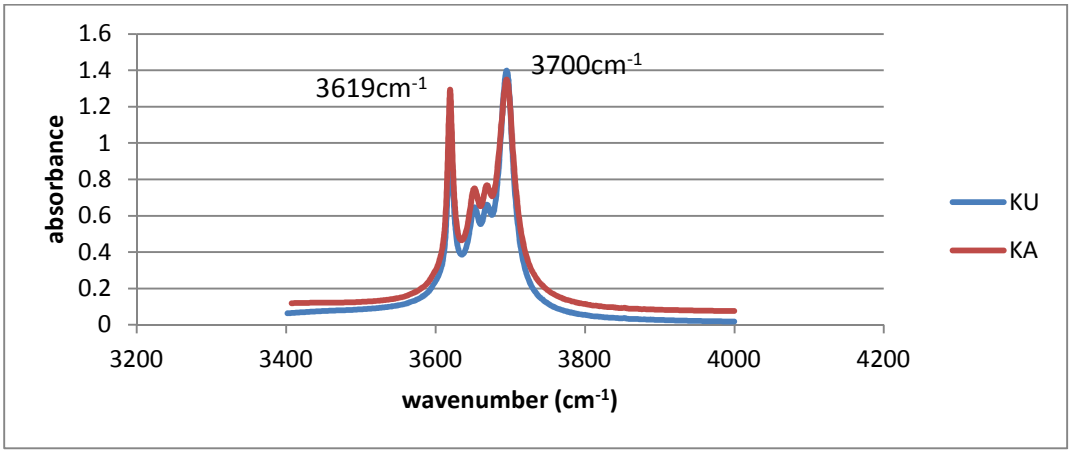

Figure 3.4 Infrared spectra of kaolinite (3200-4200cm^{-1}).

The absorption bands in Figure 3.4 at 3619cm^{-1} and 3700cm^{-1} (double) are due to the vibrational stretch of OH groups and are typical of kaolinites**.**

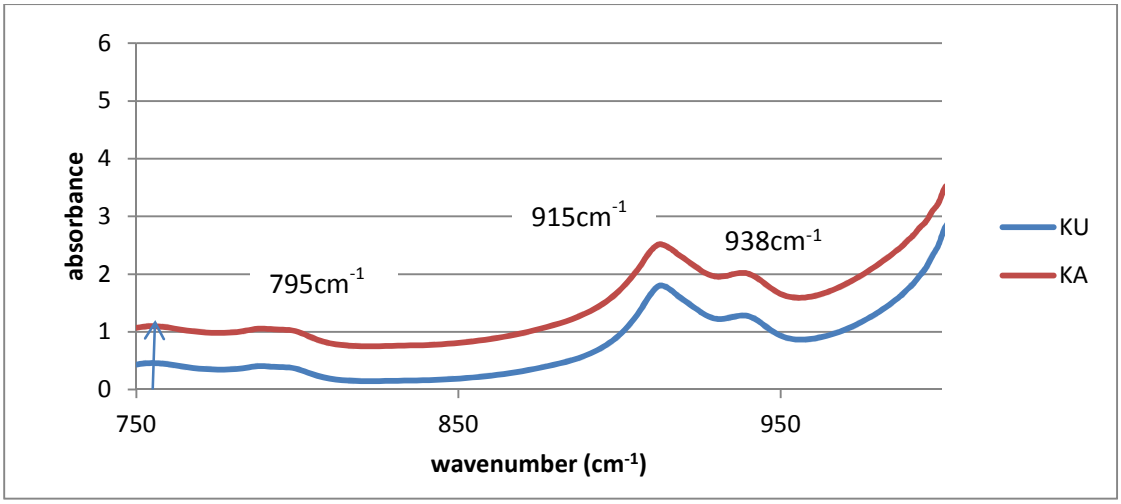

Figure 3.5 Infrared spectra of kaolinite (750-1000cm^{-1}).

The OH deformation bands (Figure 3.5) at 915cm^{-1} and 938cm^{-1} are characteristic of kaolinites and the kaolin group in general. Two bands at 758cm^{-1} (shown by the arrow) and 795cm^{-1} distinguish kaolinite from halloysite.

3.4.3 Palygorskite

The FTIR spectra of palygorskite are presented in Figures 3.6 and 3.7

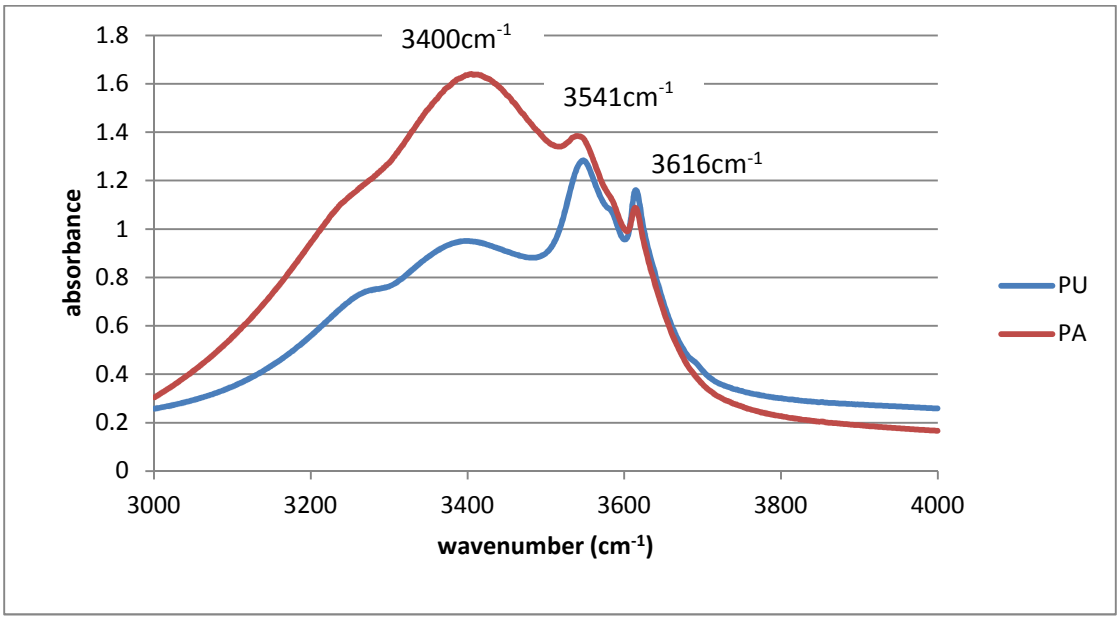

Figure 3.6 Infrared spectra of palygorskite (3000-4000cm^{-1})

As shown in Figure 3.6, the OH-stretching band at 3616cm^{-1} is characteristic of palygorskite. The bands at 3400cm^{-1} and 3541cm^{-1} are assigned to bound molecular water and unbound zeolitic water molecules respectively within the palygorskite channels.

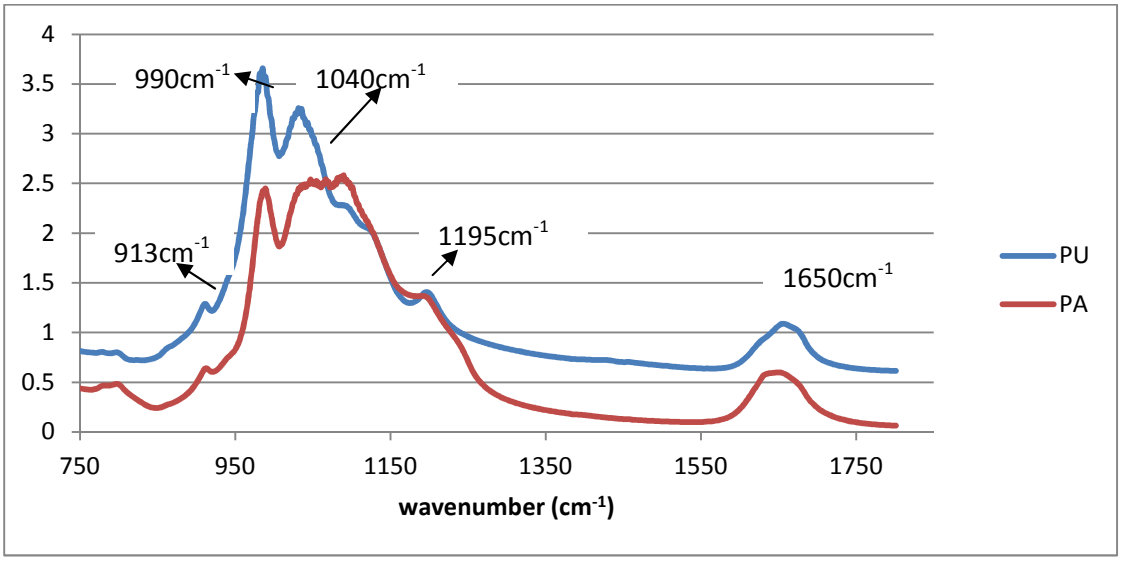

Figure 3.7 Infrared spectra of palygorskite (750-1800cm^{-1})

Figure 3.7 shows the AlAlOH deformation band at 913cm^{-1} which confirms the dominant dioctahedral character of palygorskite. The structural bands at 990cm^{-1} and 1195cm^{-1} are assigned to the stretching band of Si-O of palygorskite and are characteristics of palygorskite. The band at 1040cm^{-1} appears to be affected by acid activation and could be due to the presence in untreated samples, of carbonates such as calcite or siderite. The band at 1650cm^{-1} is due to bound molecular water coordinated to Al and Mg.

3.4.4 Saponite

The FTIR spectra of saponite are presented in Figures 3.8, 3.9 and 3.10

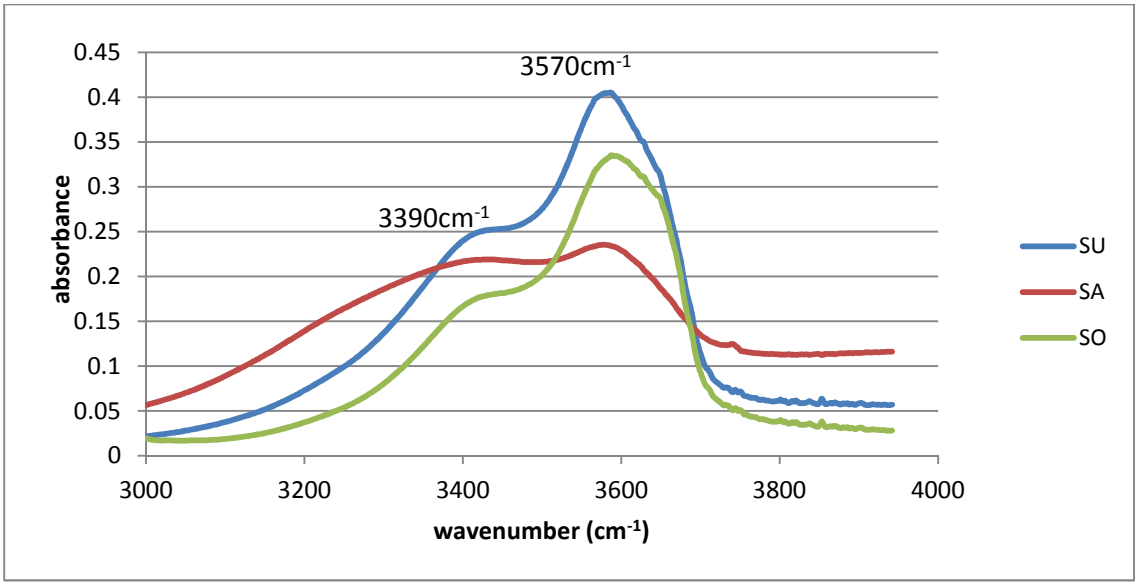

Figure 3.8 Infrared spectra of saponite (3000-4000cm^{-1})

The two bands at 3390cm^{-1} and 3573cm^{-1} (Figure 3.8) are suggested to reflect octahedral character (Wilson, 1987). It has been reported that the absorption band at 3570cm^{-1} is due to Mg/Fe^{2+}-OH stretch vibration of Fe-rich saponite (Shayan et al, 1988).

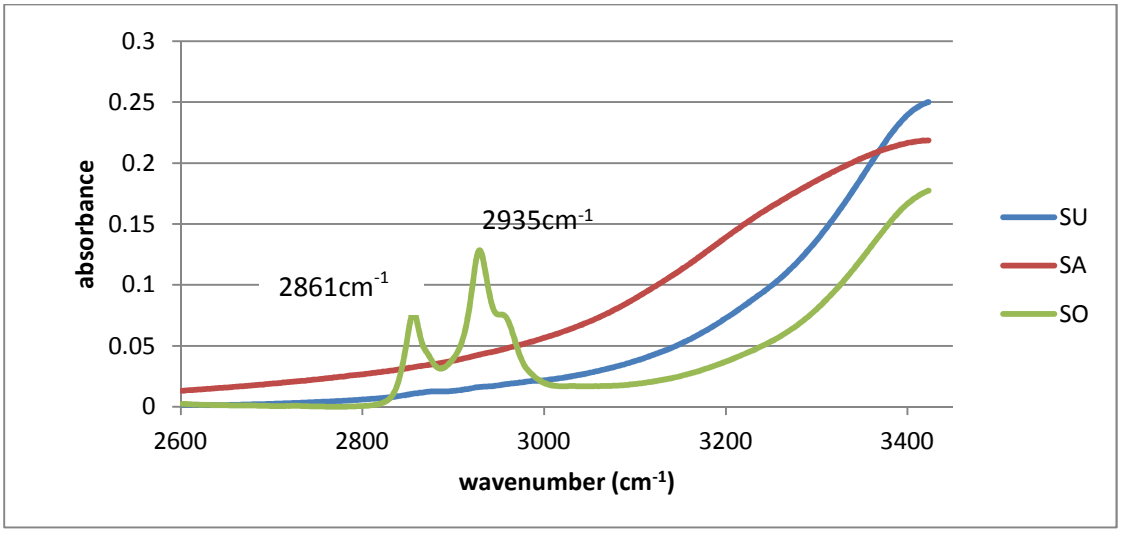

Figure 3.9 Infrared spectra of saponite (2600-3500cm^{-1})

The absorption bands at 2861 cm^{-1} and 2935cm^{-1} (Figure 3.9) observed with organosaponite (SO) are assigned to symmetrical and assymetrical vibration stretch of C-H_2 respectively from the hydrocarbon moiety of DDDMA used in the preparation of the organoclay sample.

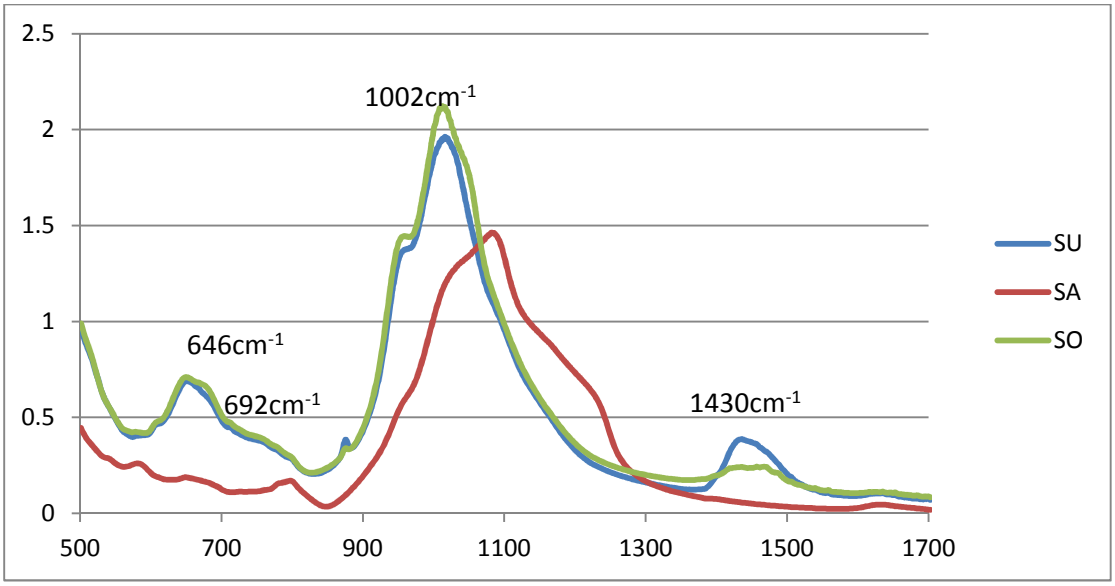

Figure 3.10 Infrared spectra of saponite (500-1700cm^{-1})

The bands at 646cm^{-1} and 692cm^{-1} (Figure 3.10) are OH deformation bands typical of trioctahedral clays. However, these bands appear to have been affected by acid activation. The band at 1002cm^{-1} is likely to be due to Si-O stretching band and was also affected by acid activation. The band at 1430cm^{-1} is most likely due to carbonates such as calcite and disappears on acid activation (Wilson, 1987).

3.5 XRD

The basal spacing of 00l reflections for the clay samples at various conditions viz, air dried, ethylene glycolation and heat treated (300^{0}C) are presented in this section. See Table 3.3 for the detailed d-spacing (001) of all the samples.

3.5.1 Acid activated bentonite

The 00l reflections of acid activated bentonite is presented in Figure 3.11.

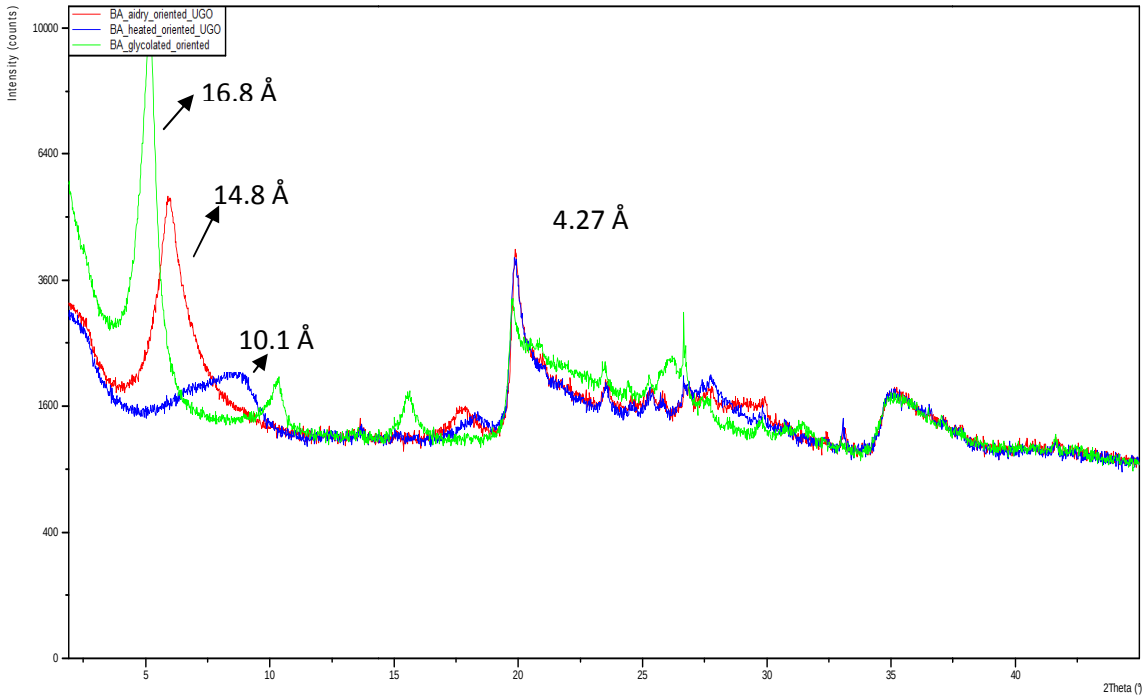

Figure 3.11 XRD patterns of acid activated bentonite (BA)

3.5.2 Organo bentonite

The 00l reflections of organo bentonite is presented in Figure 3.12

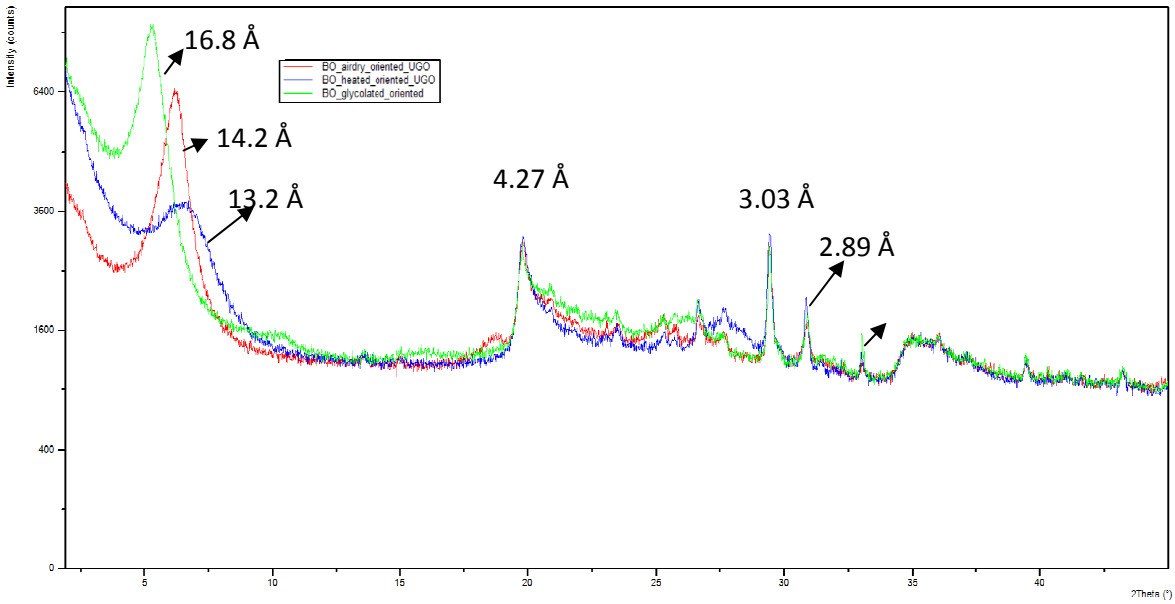

Figure 3.12 XRD patterns of organobentonite (BO)

3.5.3 Unmodified bentonite

The 00l reflections of unmodified bentonite is presented in Figure 3.13

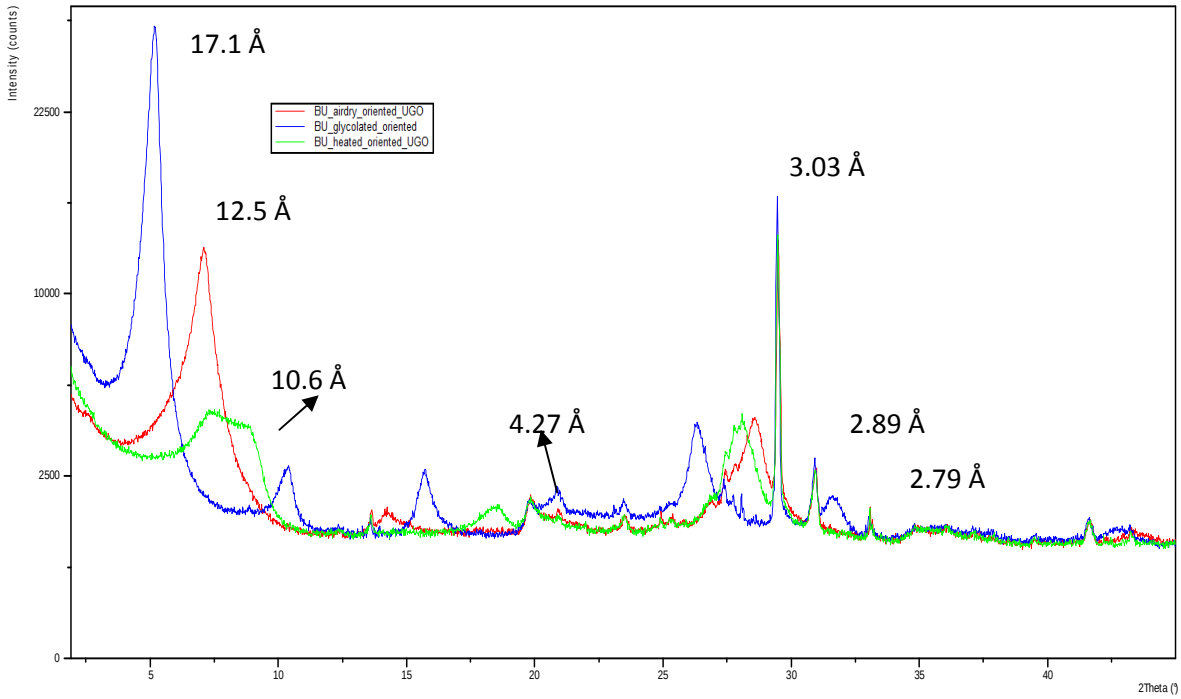

Figure 3.13 XRD patterns of unmodified bentonite (BU)

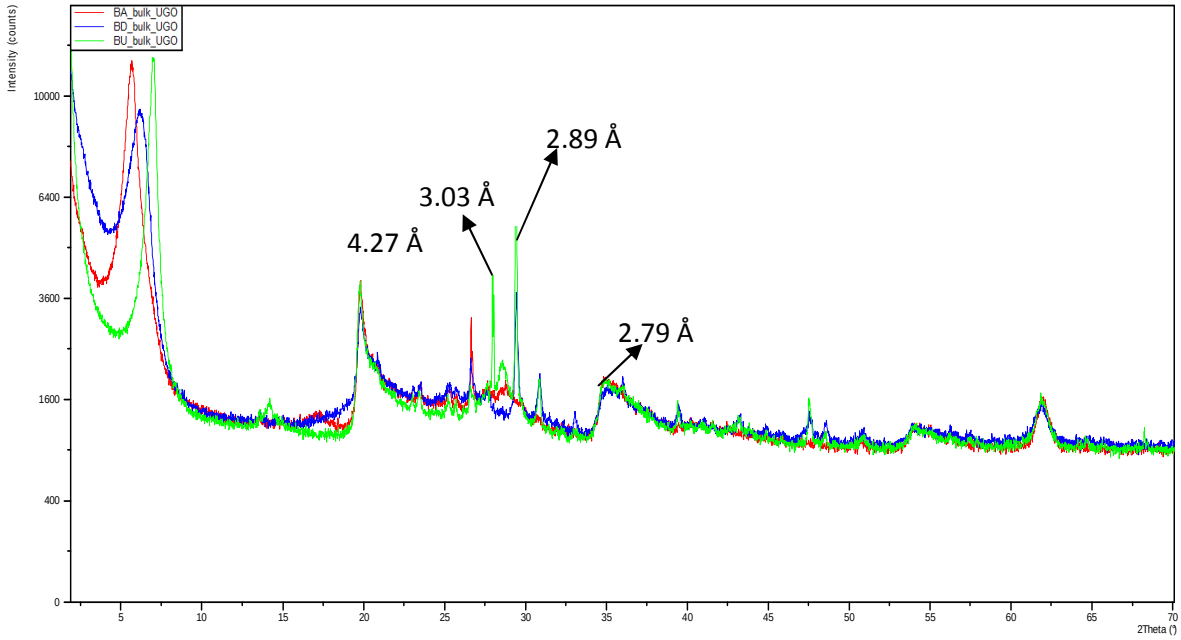

Figure 3.14 XRD pattern from bulk analysis-samples BA, BO and BU.

From Figure 3.11, the crystal structure of the bentonite clay was not totally destroyed by acid activation. However, the peak observed at 3.03 Å with samples BO and BU in Figures 3.12, 3.13 and 3.14 is most likely to be due to calcite. However, this peak had been removed in Figure 3.11 i.e. with sample BA as a result of acid activation. Also, the peaks observed at 2.89 Å and 2.79 Å with samples BO and BU (Figures 3.12 and 3.13 and 3.14) are due to

dolomite and siderite respectively and were also substantially removed on acid activation. The peak at 4.27 Å for all the samples (BA,BO and BU) is due to quartz (Figure 3.14). The d-spacing of air dried BA as shown in Figure 3.11 is 14.8 Å. This indicates that the protons located at the interlayers of the clay may have been highly hydrated by water (moisture). From Figure 3.12, the organobentonite (BO) on heat treatment at 300^{o}C showed the least layer collapse at 13.2 Å in comparison with BA (10.1 Å) and BU (10.6 Å) due to the intercalation of didecyldimethylammonium(DDDMA) in the interlayer of this clay sample. Figure 3.13 shows the d-spacing (001) of glycolated unmodified bentonite (BU) of 17.1 Å which is typical of sodium bentonite. The peak at 4.27 Å observed with BA and BO (Figures 3.11 and 3.12) is due to quartz. This peak is also found in BU (Figure 3.13) though quite small because of difference in intensities.

3.5.4 Acid activated kaolinite

The 00l reflections of acid activated kaolinite is presented in Figure 3.15

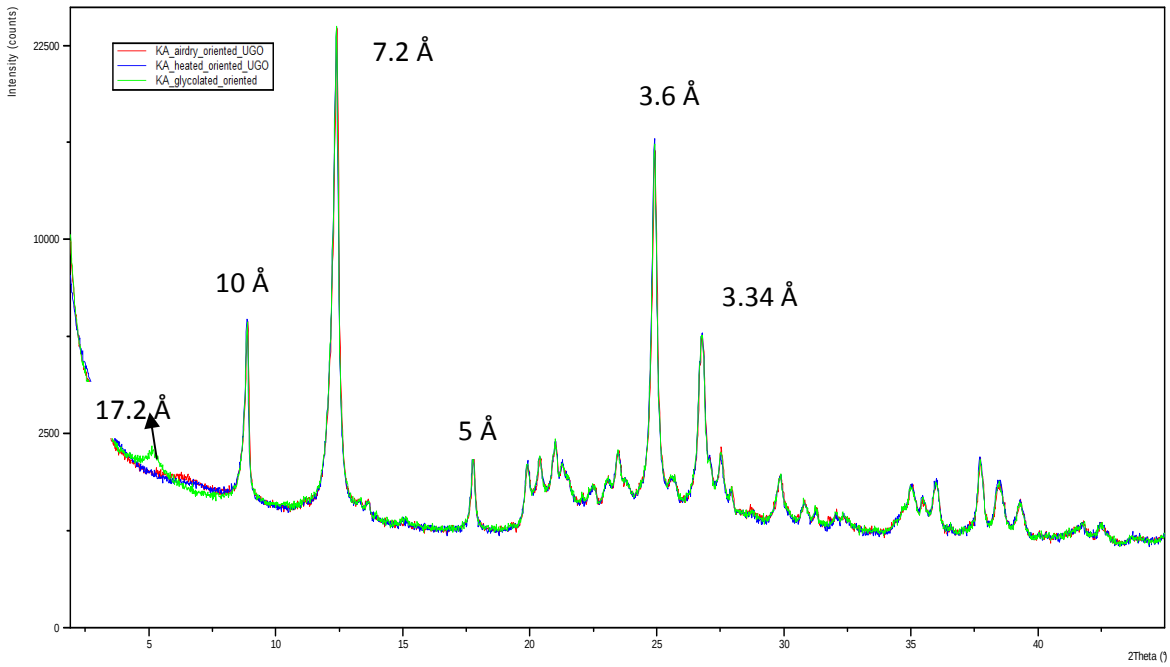

Figure 3.15 XRD patterns of acid activated kaolinite (KA)

3.5.5 Unmodified kaolinite

The 00l reflections of unmodified kaolinite is presented in Figure 3.16

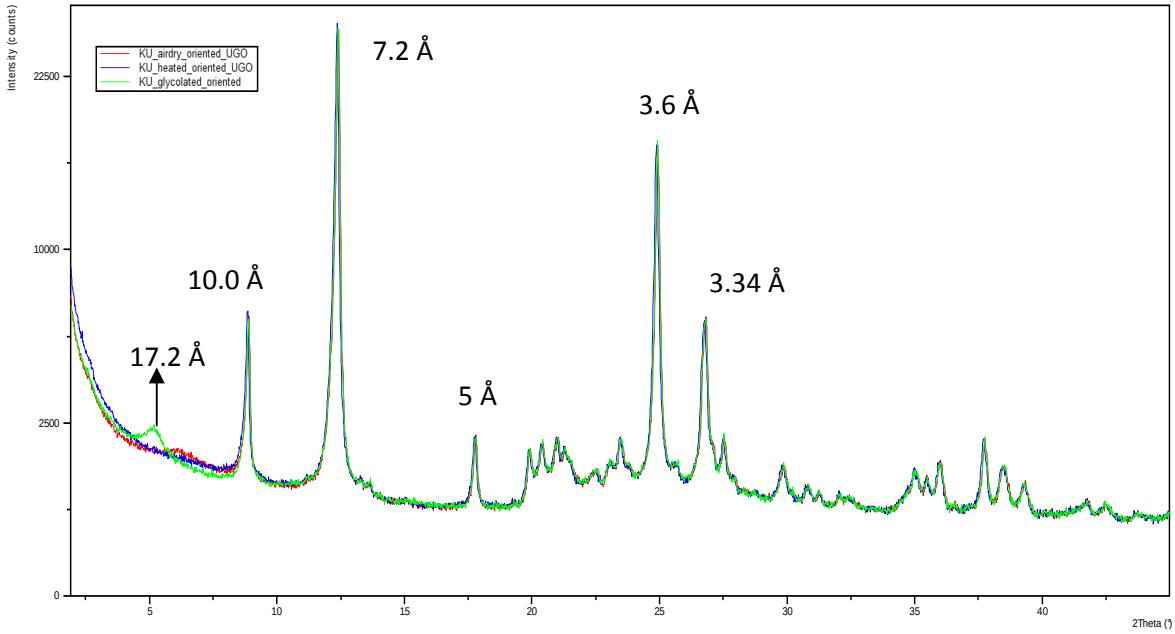

Figure 3.16 XRD patterns of unmodified kaolinite (KU)

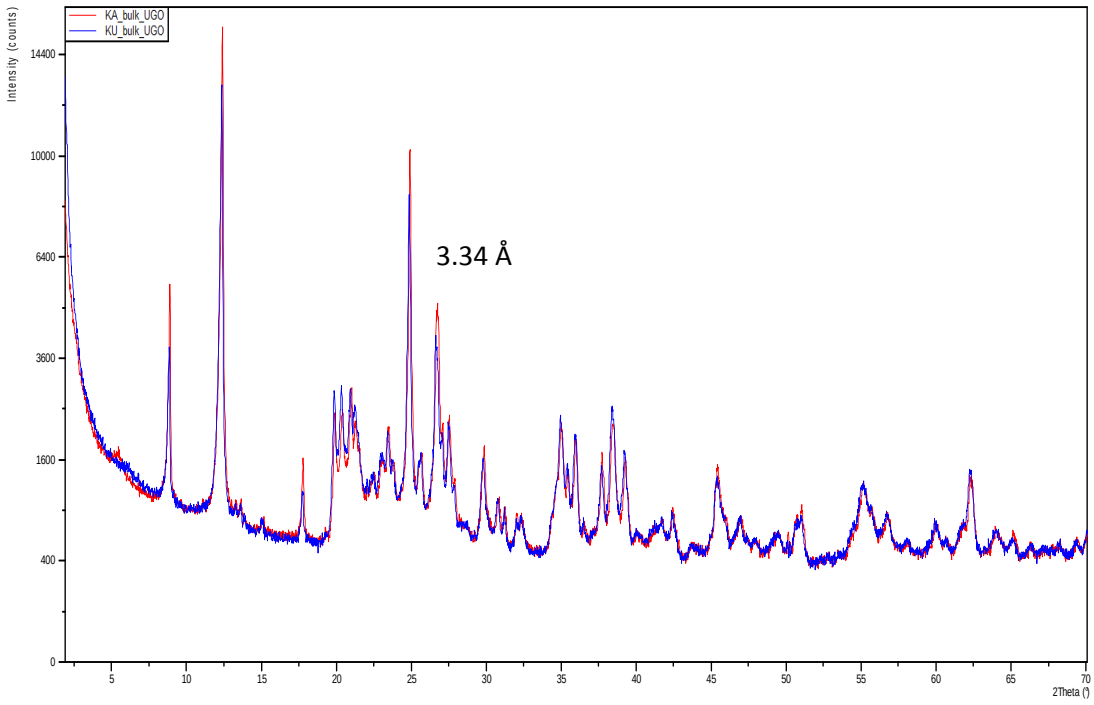

Figure 3.17 XRD pattern from bulk analysis-samples KA and KU.

From Figures 3.15 - 3.17, there is no significant difference between the XRD patterns of the acid treated and unmodified kaolinite. The small peak at 17.2 Å observed on ethylene glycolation (Figure 3.15 and 3.16) could be due to the minute presence of motmorillonite in

this sample. The peaks observed at 7.2 Å and 3.6 Å correspond to 001 and 002 reflections typical of kaolinites. However, the peak observed at 10 Å corresponds to mica and is confirmed by the 002 and 003 reflections at 5 Å and 3.34 Å respectively (Figures 3.15 and 3.16). The peak due to 001 reflection for mica at 10 Å was not affected by heat treatment or ethlyne glycolation as is typical of mica. Also, the intensity of 003 reflection is higher than that for the 002 reflection as is common with dioctahedral mica such as illites (Moore and Reynolds, 1997). These indicate that the sample is not pure kaolinite but contaminated with montmorillonite and mica. Intergrowth of other clay minerals with kaolinites has been reported and may account for the observed contamination in this kaolinite sample (Psyrillos et al, 1997). It has also been reported that detailed analysis of kaolinite sometimes indicate the presence of layers of mica, vermiculite or smectite of between 0.1 -10% (Talibudeen and Goulding, 1983a).

3.5.6 Acid activated palygorskite

The 00l reflections of acid treated palygorskite is presented in Figure 3.18

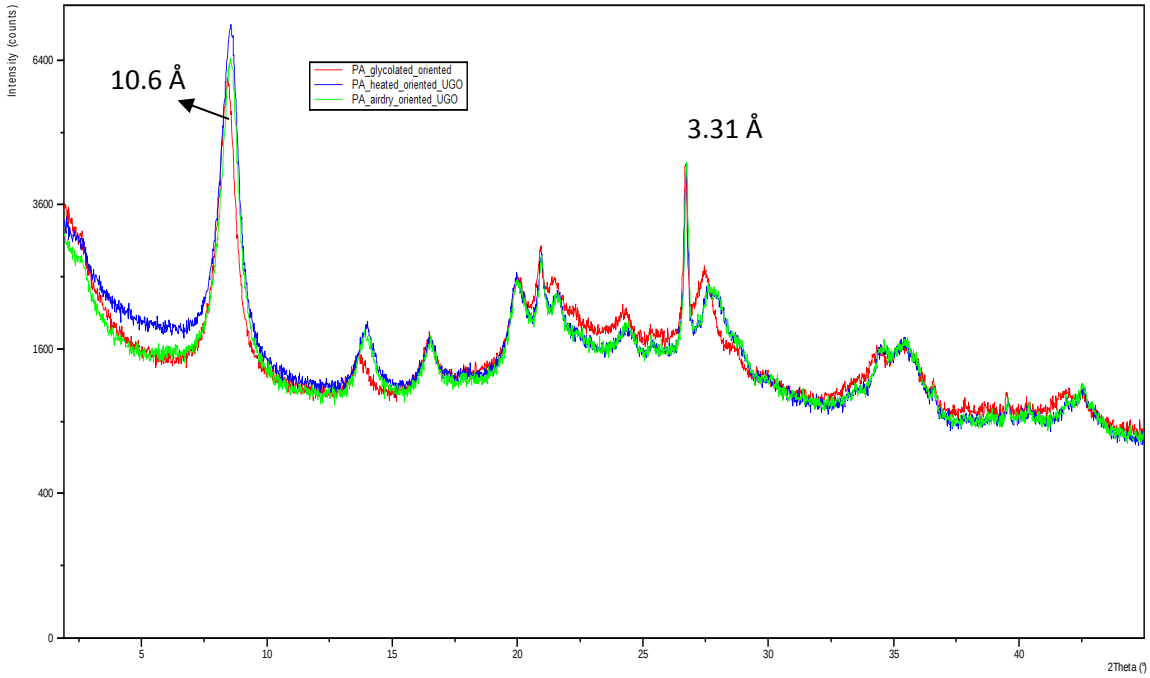

Figure 3.18 XRD patterns of acid activated palygorskite (PA)

3.5.7 Unmodified palygorskite

The 00l reflections of unmodified palygorskite is presented in Figure 3.19

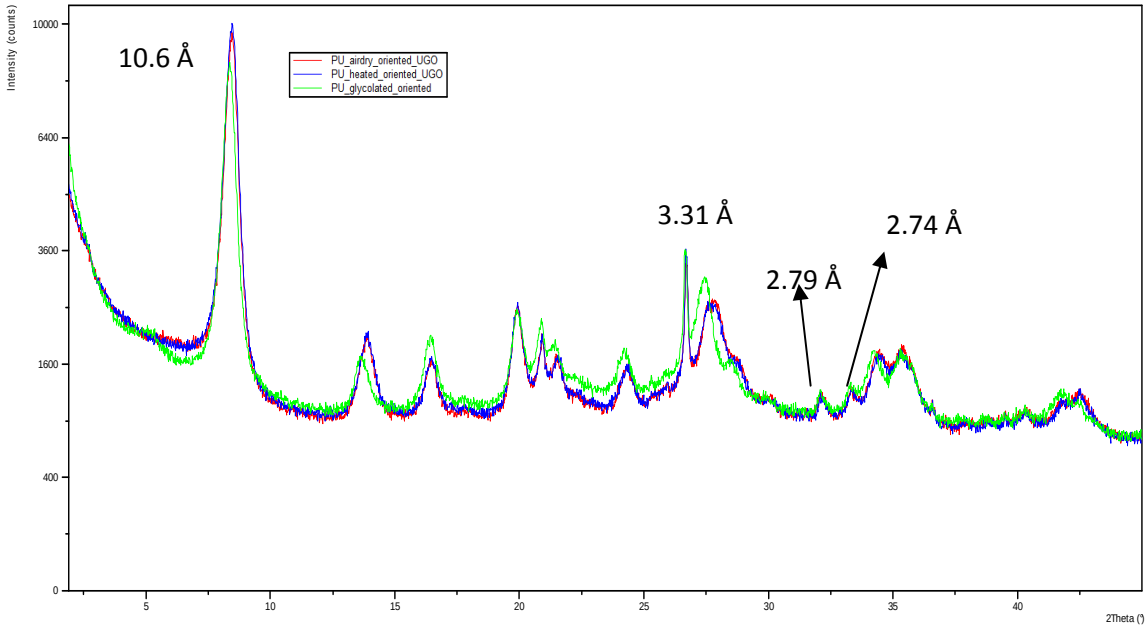

Figure 3.19 XRD patterns of unmodified palygorskite (PU)

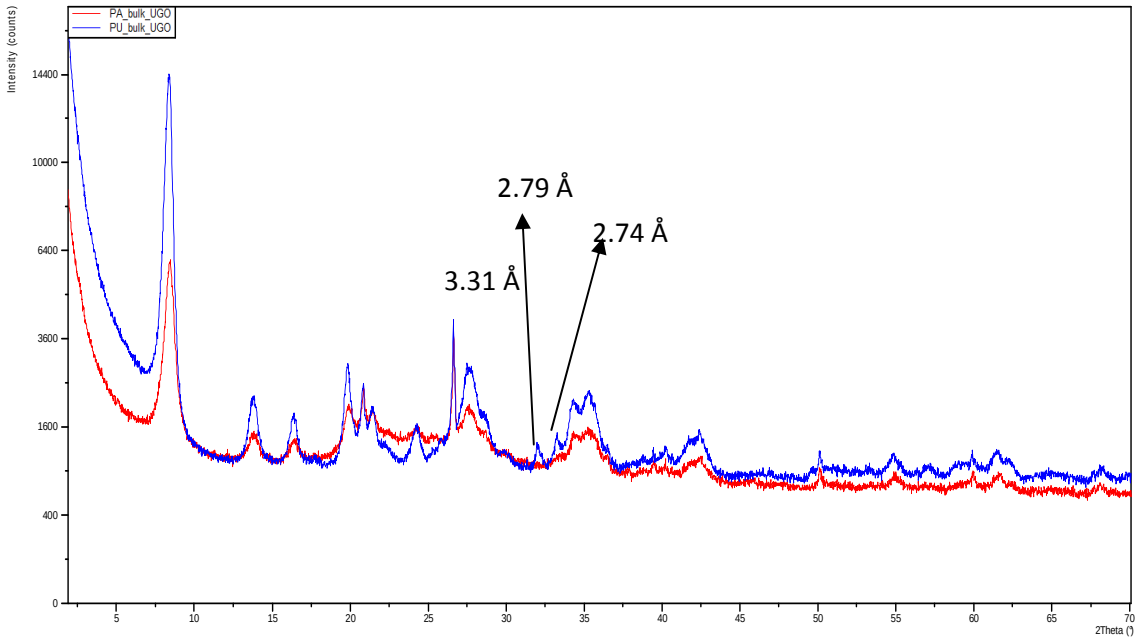

Figure 3.20 XRD pattern from bulk analysis-samples PA and PU.

From Figures 3.18 and 3.19, there is evidence of acid treatment as the peaks for PA (Figure 3.18) appear less sharp than the peaks for PU (Figure 3.19). The small peaks at 2.79 Å and 2.74 Å in unmodified palygorskite due to siderite (carbonate) and magnesite (carbonate) respectively disappeared on acid activation as can be observed in Figures 3.18, 3.19 and 3.20. The peak at 3.31 Å is due to K-feldspar. The d-spacing for the two samples (PA and PU) with respect to air-drying, glycolation and heat treatment (300^{o}C) are similar ~ 10.6 Å. Clay

minerals with fibrous nature such as palygorskite are difficult to be oriented such that the diffraction pattern will be dominated by 00l reflections. The characteristic reflection observed with the palygorskite sample at 10.6Å is actually due to 011 reflections and not 001 reflections for the reason given above (Wilson, 1987; Moore and Reynold, 1997).

3.5.8 Acid activated saponite

The 00l reflections of acid activated saponite is presented in Figure 3.21

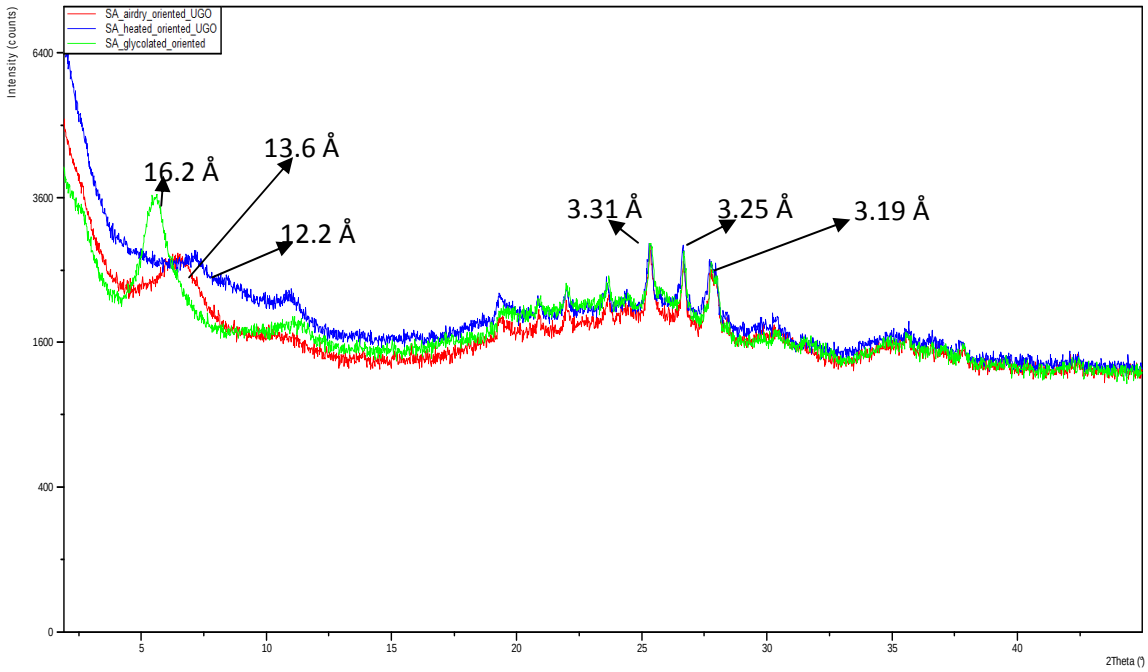

Figure 3.21 XRD patterns of acid activated saponite

3.5.9 Organosaponite

The 00l reflections of Organosaponite is presented in Figure 3.22

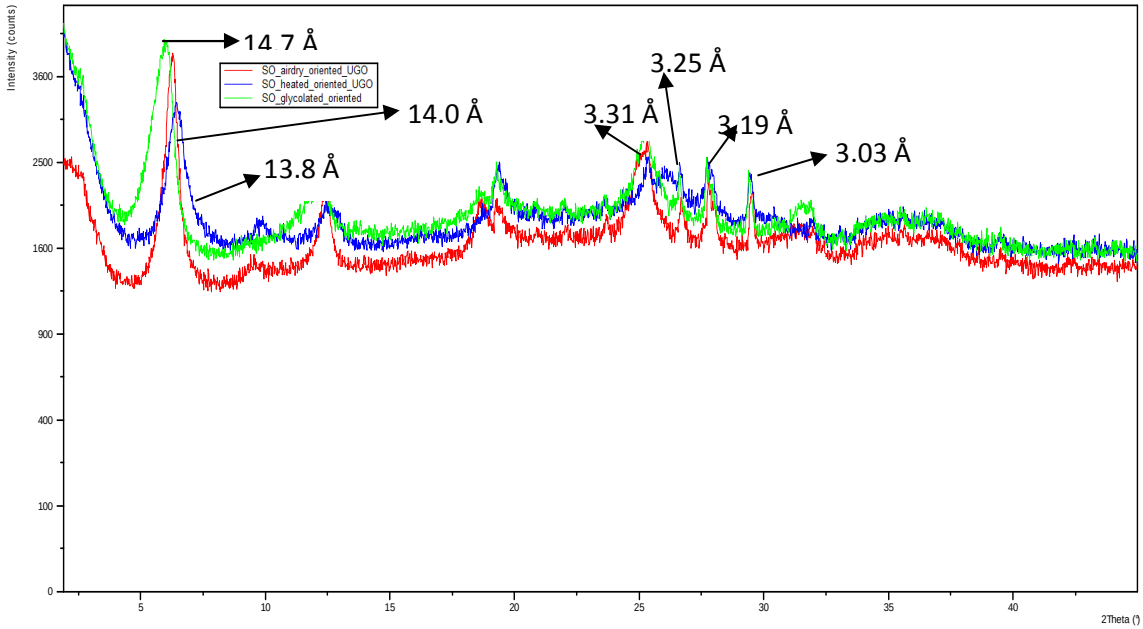

Figure 3.22 XRD patterns of organosaponite (SO)

3.5.10 Unmodified saponite

The 00l reflections of unmodified saponite is presented in Figure 3.23

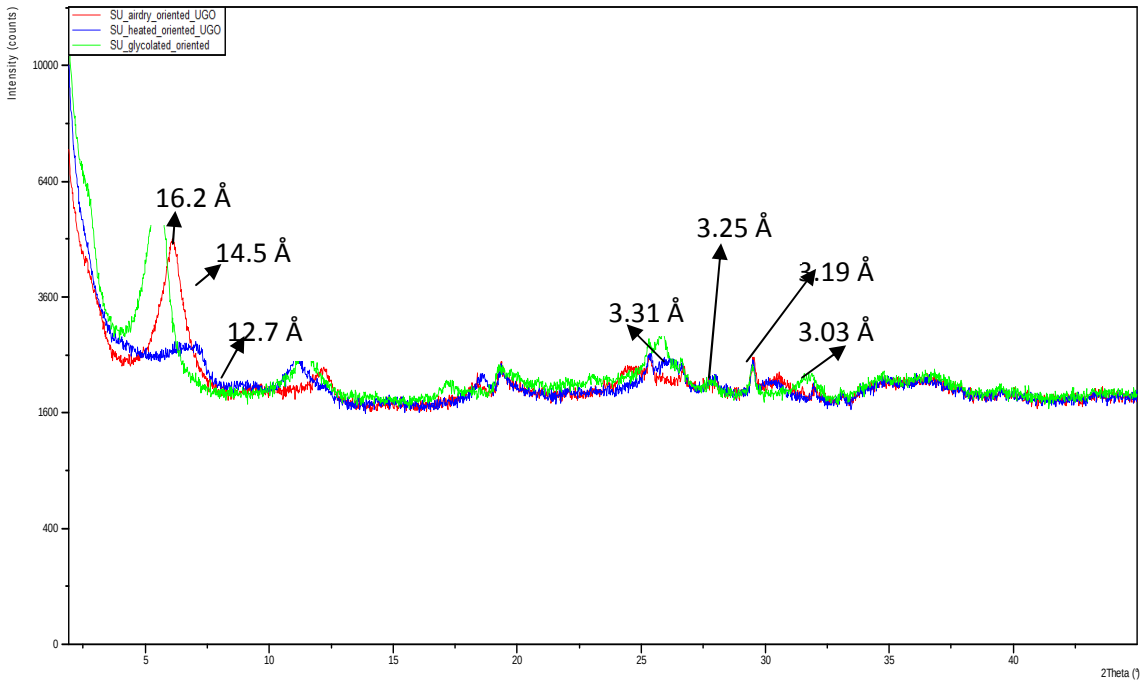

Figure 3.23 XRD patterns of unmodified saponite (SU)

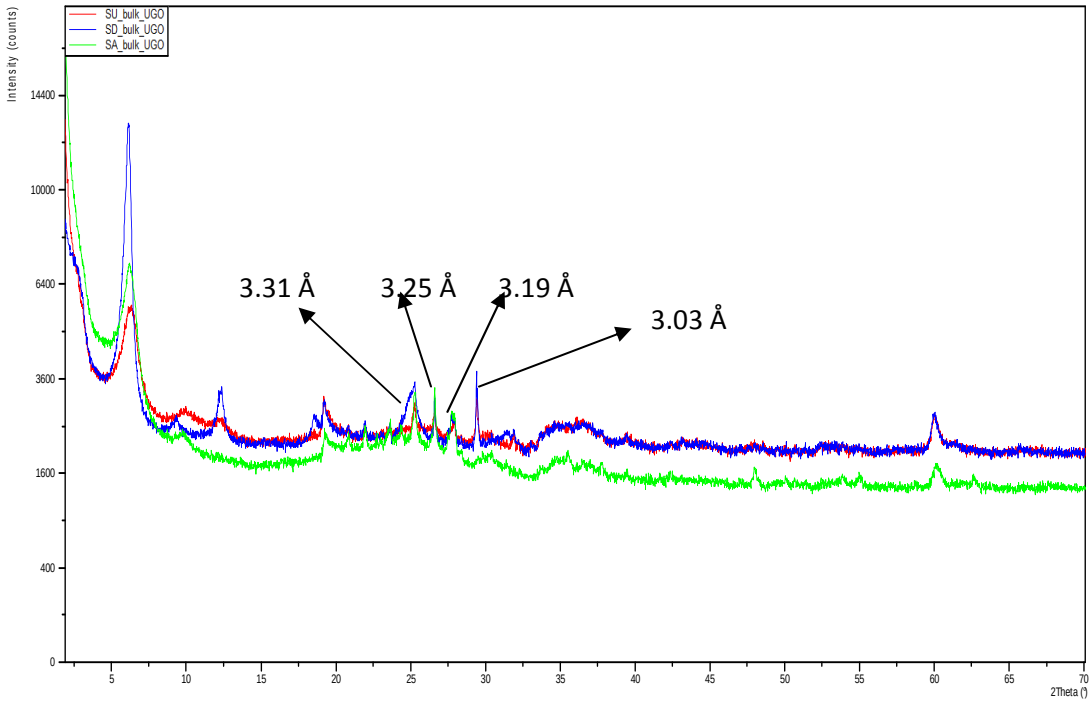

Figure 3.24 XRD pattern from bulk analysis-samples SA, SO and SU.

From Figure 3.23, the air dried and glycolated d-spacing (001) of 14.5Å and 16.2Å respectively are typical of saponites especially with divalent cations in the interlayer (Wilson, 1987). The collapse of the layers at 300^{o}C is least with the organosaponite, SO (13.8Å) in comparison with SA (12.2Å) and SU (12.7Å) as a result of the DDDMA intercalation (Figures 3.21, 3.22 and 3.23). The peaks at 3.31Å, 3.25Å and 3.19Å observed in Figures 3.21, 3.22, 3.23 and 3.24 are due to sanidine, microcline and albite (all three are feldspars) respectively. However, the peak at 3.03Å common with SO and SU is due to calcite and disappears in Figures 3.21 as a result of acid activation.

3.5.11 Homoionic interlayer bentonite

The 00l reflections of homoionic interlayer bentonite viz, Na-bentonite, K-bentonite, Mg-bentonite, Ca-bentonite, Zn-bentonite, Al-bentonite, Cr-bentonite and Fe-bentonite are presented in Figures 3.25-3.32

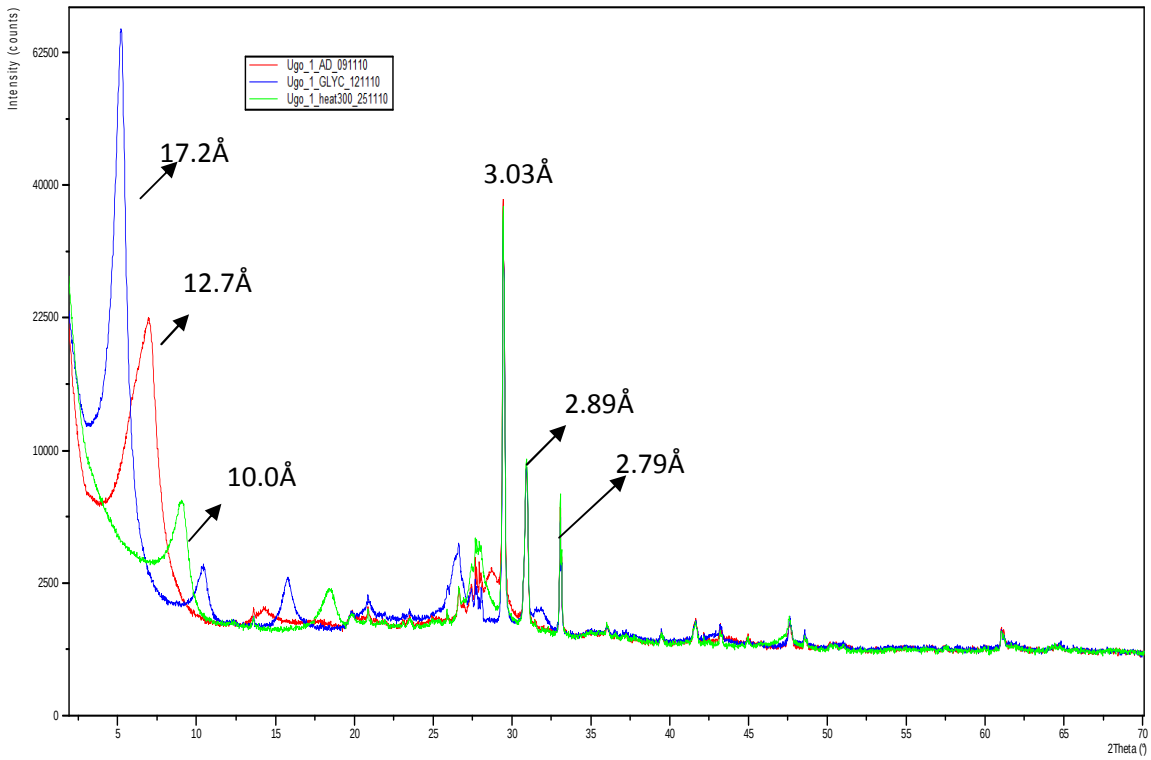

Figure 3.25 XRD patterns of Na-bentonite

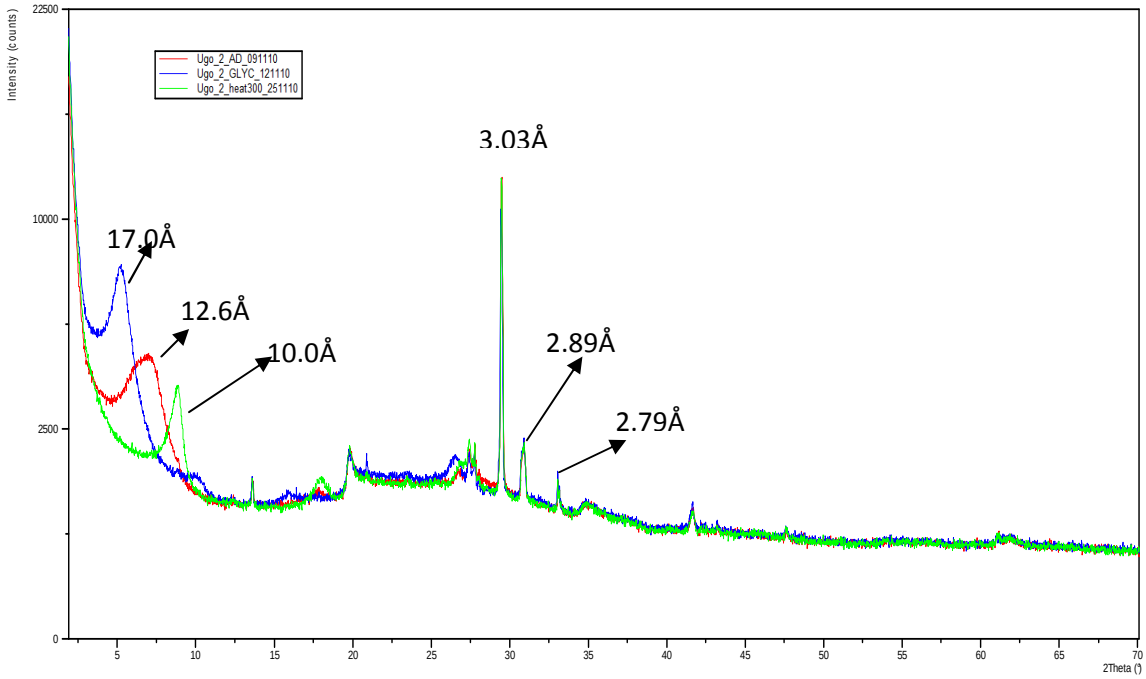

Figure 3.26 XRD patterns of K-bentonite

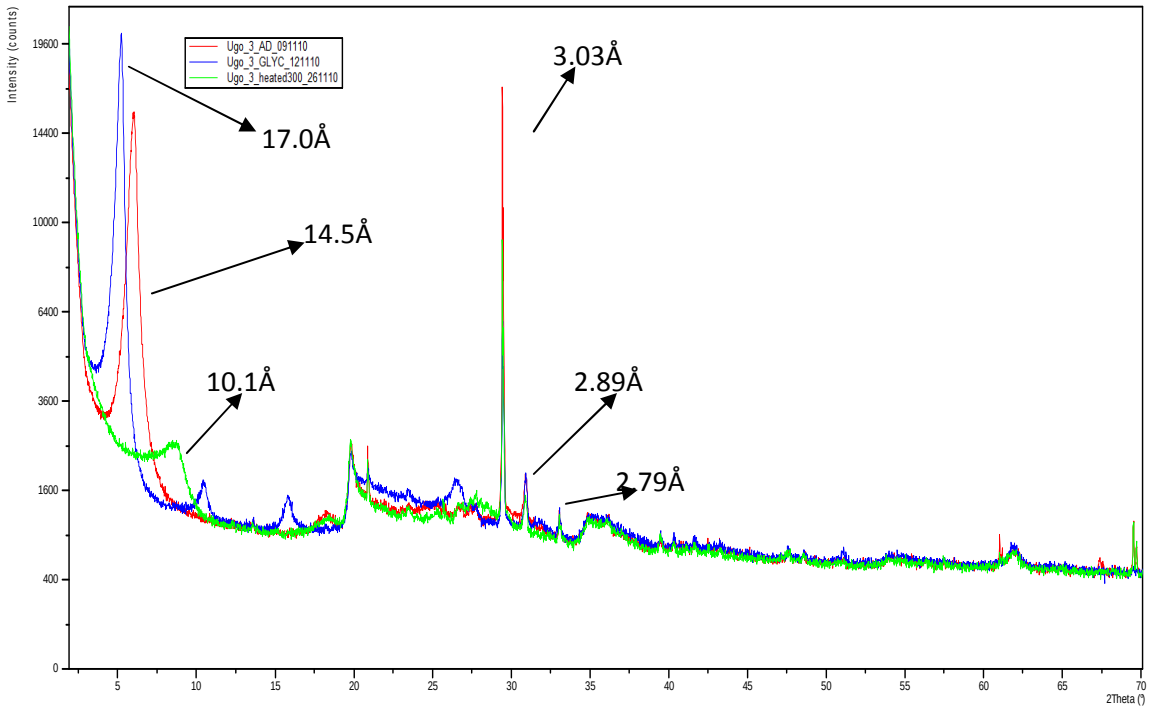

Figure 3.27 XRD patterns of Mg-bentonite

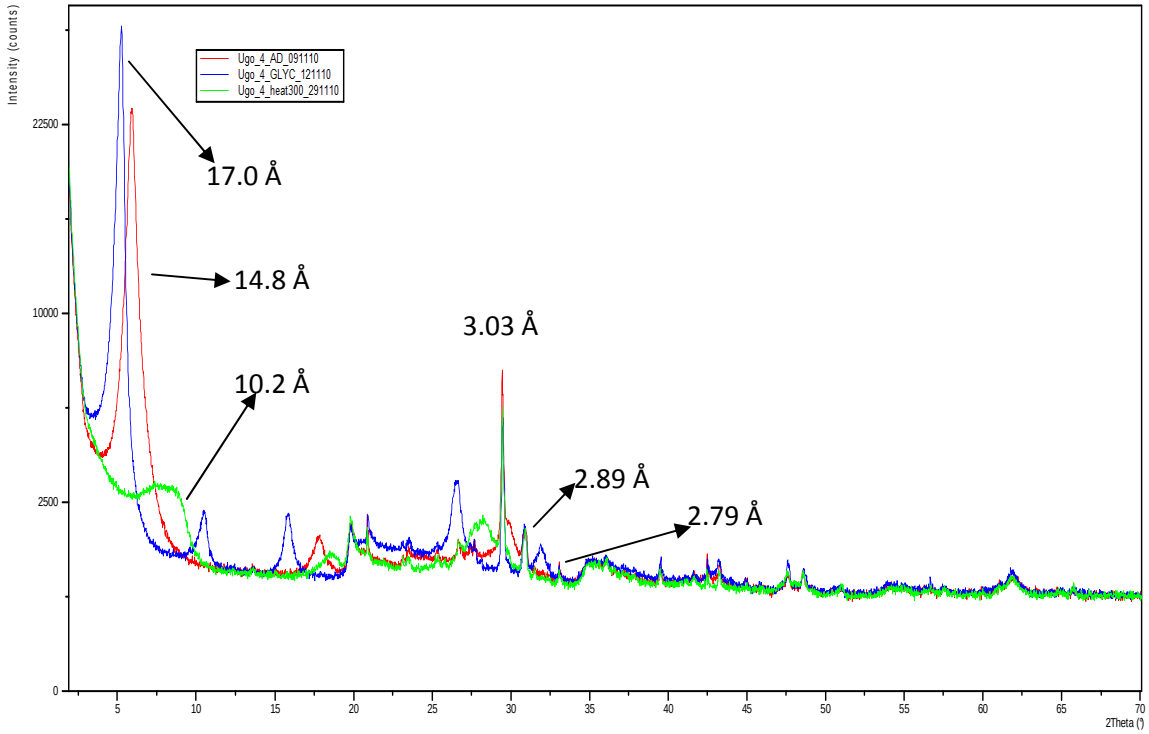

Figure 3.28 XRD patterns of Ca-bentonite

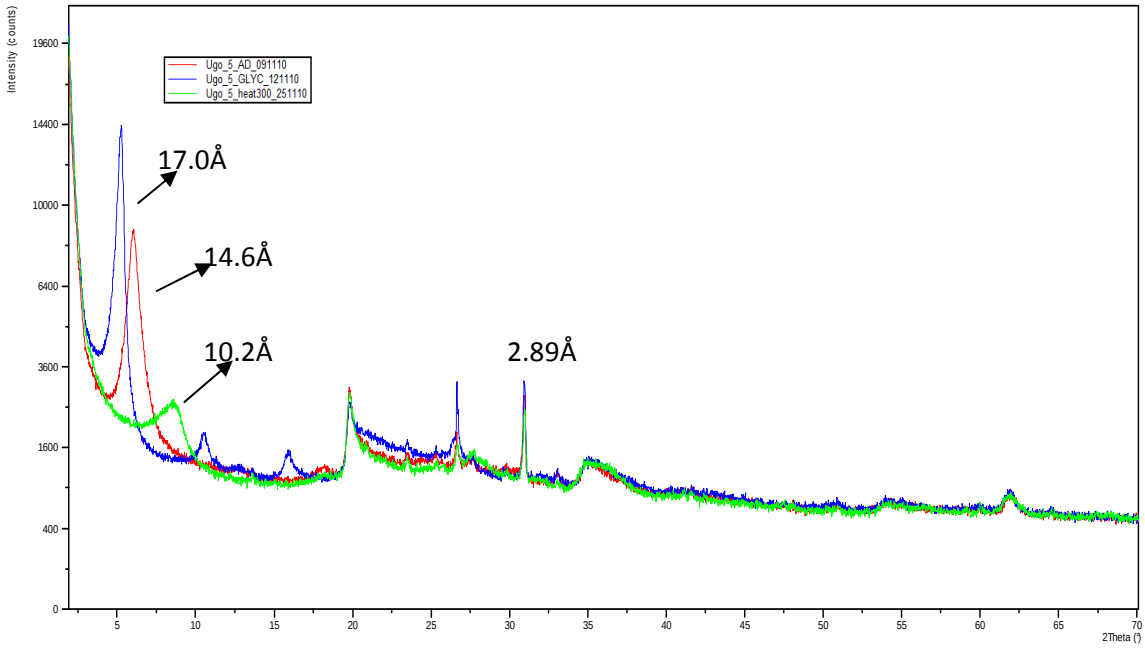

Figure 3.29 XRD patterns of Zn-bentonite

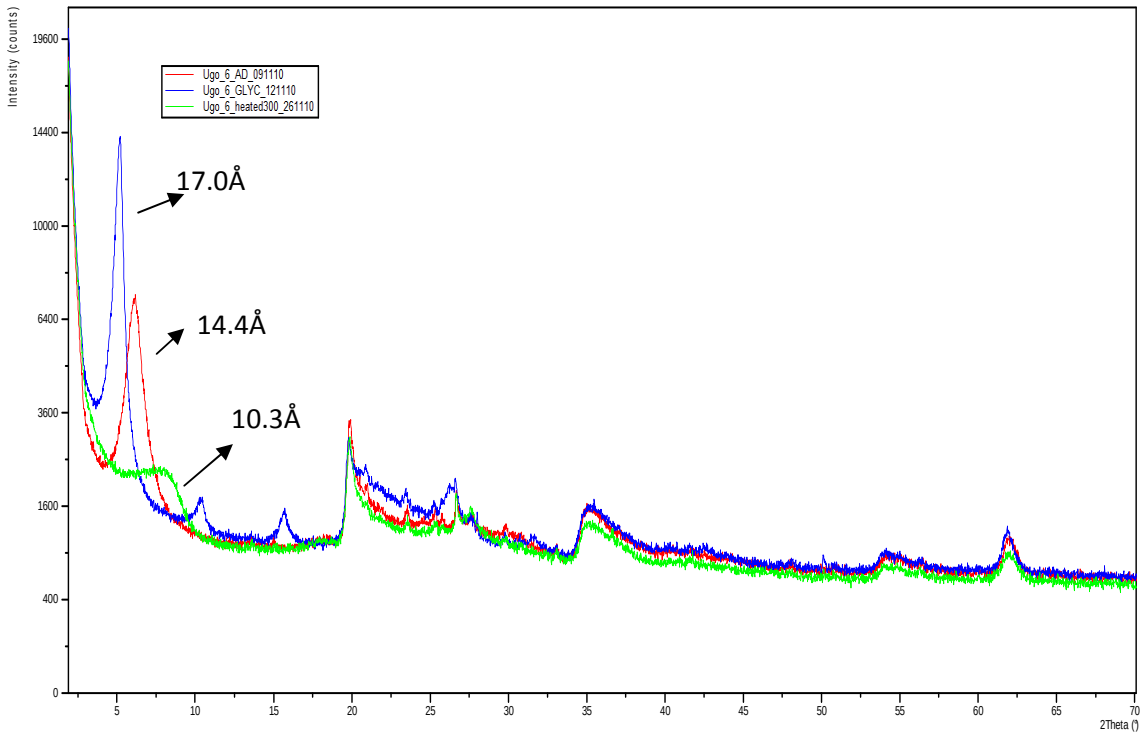

Figure 3.30 XRD patterns of Al-bentonite

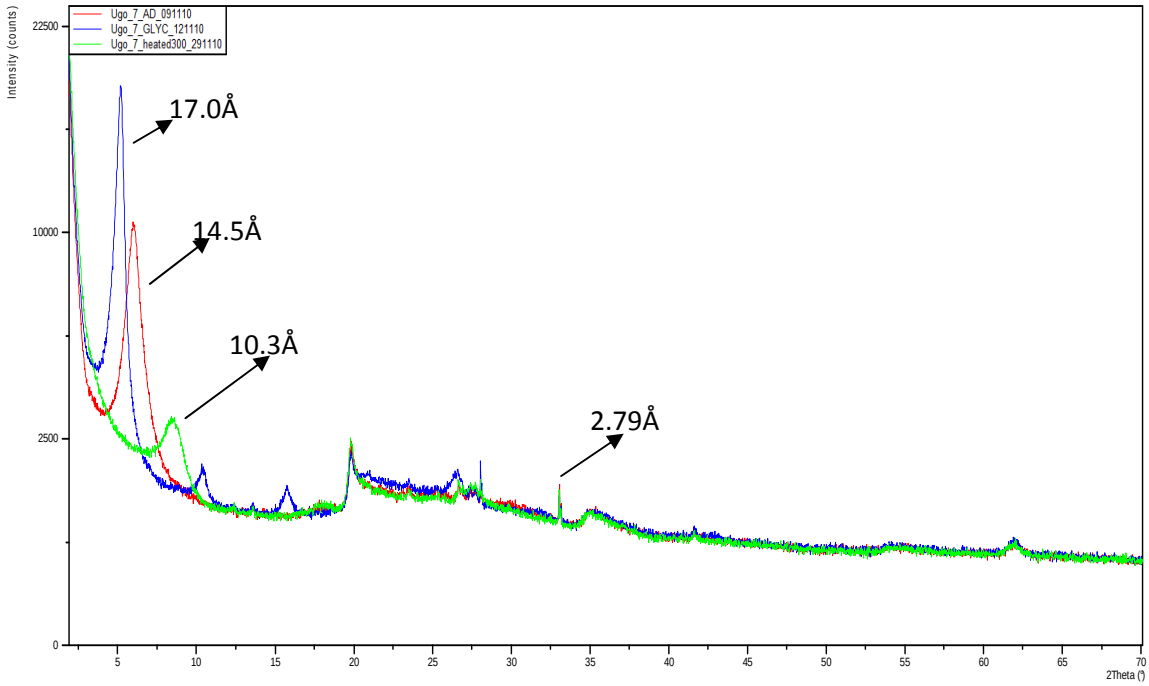

Figure 3.31 XRD patterns of Cr-bentonite

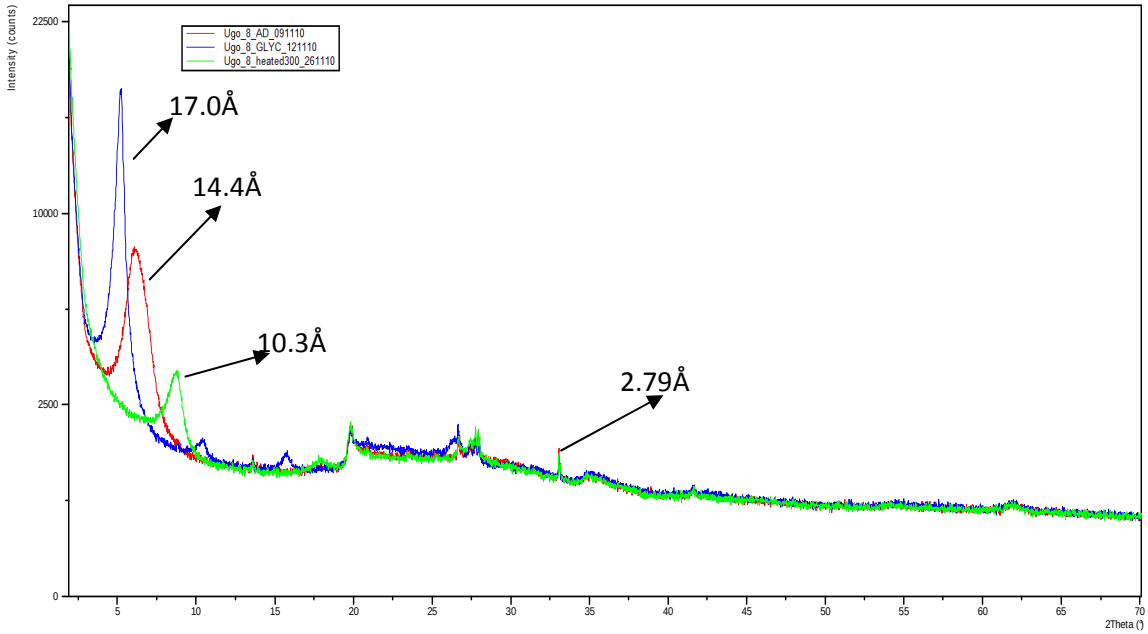

Figure 3.32 XRD patterns of Fe-bentonite

From Figures 3.26 and 3.27, sodium bentonite and potassium bentonite have almost identical d-spacing (001) on air drying with BU(12.5Å) whereas the divalent and trivalent cations in the interlayer of bentonite caused the d-spacing on air drying to shift to between 14.4Å and 14.8Å as a result of increased hydration energy which favours attraction of two water layers (Figures 3.28-3.32). However, the d-spacing (001) as a result of glycolation is

slightly higher with Na-bentonite (17.2Å) than the other samples. The peaks observed at 3.03Å, 2.89Å and 2.79Å are due to carbonates as described earlier. However, it can be observed that these carbonates peaks observed in Sodium, potassium, Magnesium and Calcium-bentonites (Figures 3.25-3.28) disappeared completely with aluminium-bentonite (Figure 3.30). With chromium and ferric-bentonite (Figures 3.31 and 3.32 respectively), only small peak also at 2.79Å remained while the calcites and dolomites have been removed completely.

Table 3.3 Basal spacing of 001 reflections of the clay samples

Sample	d-spacing (Å)		
	Ethylene glycolated	Air dried	Heat treated (300^0C)
BA	16.8	14.8	10.1
BO	16.8	14.2	13.2
BU	17.1	12.5	10.6
KA	7.2 (17.2) (10.0)	7.2 (10.0)	7.2 (10.0)
KU	7.2 (17.2) (10.0)	7.2 (10.0)	7.2 (10.0)
PA	10.6	10.6	10.6
PU	10.6	10.6	10.6
SA	16.2	13.6	12.2
SO	14.7	14.0	13.8
SU	16.2	14.5	12.7
B-Na	17.2	12.7	10.0
B-K	17.0	12.6	10.0
B-Mg	17.0	14.5	10.1
B-Ca	17.0	14.8	10.2
B-Zn	17.0	14.6	10.2
B-Al	17.0	14.4	10.3
B-Cr	17.0	14.5	10.3
B-Fe	17.0	14.4	10.3

Table 3.3 shows that the kaolinite sample is contaminated with montmorillonite and mica as described earlier.

3.6 Discussion

The acid activated clay mineral samples have negligible chloride ion contents indicating that the pH recorded for these samples could not have been due to the free HCl but due to the protons occupying interlayer and edge sites. The EGME-surface area of the acid activated clay samples was higher than for their organo and unmodified counterparts. This is suggested to be due to the ability of the activating acid (HCl) to digest non-clay materials such as carbonates and partially leach out the cations located in the crystal structure of the clay during the acid activation process. The FTIR and XRD data as shown in Figures 3.14, 3.20, 3.24 and Figures 3.29-3.32 confirms that some materials (carbonates) have been removed during the acid activation process. Carbonates removed were calcite, dolomite, siderite and magnesite. The acid activated clay surface is hydrophilic and this is confirmed by the ability of the protons at the interlayer to attract water giving air dried 001 reflections (basal spacings) of 14.8Å. This water layer attraction is higher than that for either Na^+ or K^+ and is due to the relative higher charge to size ratio of H^+. The fact that acid activated clay samples are hydrophilic means that EGME will be able to access their surface and hence be able to give good estimates of their surface area.

Organoclay samples showed FTIR and XRD patterns that are different from the other samples. The total organic carbon (TOC) of the organoclay samples indicates the presence of an organic component (DDDMA). The process employed in the generation of the organoclay achieved 72.3% conversion.

The FTIR data provided evidence that there is indeed the presence of an organic component associated with the organoclay samples. There is further evidence provided by the XRD patterns of organoclay samples confirming that the organic component is actually intercalated in the interlayer site of the clays as the basal spacing of 001 reflections for the heat treated samples of the organosaponite and organobentonite are higher than those for the unmodified and acid activated clay samples (Table 3.3).

The organoclay samples have low EGME-surface area in comparison with their acid activated and unmodified counterparts. This low EGME-surface area may be due to the fact that the EGME being polar is not able to interact with the non-polar portions of the organoclay occupied by the cationic organic component and hence cannot access this non-polar portion.

The unmodified clay samples employed in this work were contaminated by mainly carbonates, feldspar and quartz.

The unmodified kaolinites seemed to be contaminated by montmorillonite and mica. The EGME-surface area of unmodified kaolinites is quite low ($35m^2/g$) in comparison with other unmodified clay samples employed in this study. Ideally, kaolinites lack an interlayer surface hence the main contribution to the surface area of kaolinites is the external surface accounting for why this clay sample has a low EGME-surface area. The CEC of unmodified kaolinite is very low, 3.5meq/100g. This is also due to the lack of the interlayer surface that translates into a lack of interlayer cations available for exchange. The measured CEC may be due to the traces of montmorillonite associated with this sample.

Unmodified saponite appeared to be contaminated by feldspar and calcite (carbonate). The air dried d-spacing (001) for unmodified saponite is about 14.5Å indicating the presence of divalent cations (such as Ca^{2+} and Mg^{2+}) in the interlayer. The FTIR data also indicated that this clay sample is Fe(II) rich. The EGME-surface area of unmodified saponite is higher than that of kaolinite but lower than that of palygorskite and bentonite. However, the CEC is higher than that of kaolinite and palygorskite but lower than that of bentonite.

The main contaminants of palygorskite are siderite and magnesite (carbonates) and K-feldspar. The EGME-surface area of palygorskite is high and this may be due to the fact that the clay sample is microporous (Bergaya et al, 2006). However, the CEC is low. The XRD data for this sample indicates that this clay is not expandable as the d-spacing for 001 reflections for the heat treated, air dried and glycolated samples are approximately the same.

The unmodified bentonite clay sample employed in this study is contaminated by mainly quartz and carbonates (dolomite, siderite and calcite). This clay sample has high values for EGME-surface area and CEC. The high surface area is attributable to the very extensive

interlayer surface of this type of clay (Bergaya et al, 2006). It is also quite expandable as shown by the d-spacing of 001 reflections for air-dried, heat treated and glycolated samples.

The homoionic interlayer clay samples showed marked differences in properties.

Clay samples with monovalent cations at the interlayer (Na-bentonite and K-bentonite) have similar d-spacings for 001 reflections of about 12.6Å whereas the other homoionic clay samples have d-spacings for 001 reflections of about 14.5Å. This discrepancy is due to the ability of the other homoionic clay samples to attract two water layers in the interlayer due to their higher hydration energies whereas K-bentonite and Na-bentonite attracts only one water layer.

The carbonates (siderite, calcite and dolomite) which are the main contaminants found in Na-bentonite, K-bentonite, Mg-bentonite and Ca-bentonite were absent from Al-bentonite. Zn-bentonite contained dolomite and traces of calcite while siderite had been removed in its preparation. Fe(III)-bentonite and Cr (III)- bentonite contained traces of siderite as dolomite and calcite had been completely removed. Zn-bentonite, Al-bentonite, Cr-bentonite and Fe-bentonite are more acidic that the other homoionic clay samples (Table 3.1) and the acidity for these four samples increases in the order: Zn-bentonite < Fe-bentonite < Cr-bentonite < Al-bentonite. The pattern of occurrence of carbonate minerals in these four clay samples follows the same order, with Al-bentonite having least carbonate contamination.

The acidity of the clay samples arises from the ability of the cations (especially the trivalent cations) to hydrolyse water thereby generating protons that lower the pH and increase the acidity during the cation exchange reaction. Consequently, the carbonates are digested by the acidic medium.

The EGME-surface area of K-bentonite is the lowest among all the homoionic clay samples. This is suggested to be due to the ability of the K-bentonite to expose the hydrophobic siloxane surface of the clay limiting access to this part of the clay by the EGME.

4. MICROBIAL GROWTH IN THE PRESENCE OF CLAY MINERALS

4.1 Introduction

The major agents that effect the mineralization of organic pollutants in terrestrial and aquatic environments are microorganisms and their activities with respect to biodegradation in the presence of colloidal minerals such as clay minerals is either enhanced or inhibited (Guerin and Boyd, 1992; Knaebel et al., 1994; Ortega-Calvo & Saiz-Jimenez, 1998). Clay minerals have been reported to have the ability to adsorb not just organic compounds but microorganisms as well with varied implications on microbial degradation of target pollutants (Schffenbauer & Stotzky, 1982; Khanan and Stotzky, 1992; Vettori et al., 1999; Lin & Puls, 2000). It has been reported that some clay minerals stimulate microbial growth and hence enhance the biodegradation of organic compounds used as carbon source (Stotzky and Rem, 1966; van Loosdrecht et al, 1990; Chaerun et al, 2005; Tazaki et al, 2008; Warr et al, 2009). Some studies have demonstrated the inhibitory properties of clay minerals to microbial growth in the presence of oil as sole carbon and energy source. Example, Warr et al (2009) has reported that high defect kaolinites inhibited microbial growth on oil as sole carbon and energy source.

However, the effects of unmodified saponites, acid activated clay, organoclay and homoionic interlayer clays on the growth of microorganisms using crude oil hydrocarbons as sole carbon and energy source have not been reported. This aspect of the study will therefore investigate the effects of the above mentioned clays on microbial growth in addition to studying the effect of other clays such as unmodified bentonite, unmodified palygorskite and unmodified kaolinite for comparison purposes.

The main questions addressed in this chapter of the project are:

a. Do different clay minerals stimulate or inhibit microbial growth?

b. Does modification of clays affect their ability to stimulate or inhibit microbial growth?

c. What factors can explain the different effects of both unmodified clays and modified clays?

4.2 Method

Absorbance measurements at 600nm were used to monitor the microbial growth during the initial culture and culture enrichment experiments. Hence it was used to establish the different phases of the microbial growth in the initial culture to enable the sampling of active cells. The cells were sampled when they were at the exponential phase in order to maintain active cells for the preparation of the enrichment culture and microbial growth kinetic experiments in the presence of the clay samples. Cell yield for studying the kinetics of the microbial growth was monitored via cell count using plating method. See section 2.3 for details. The cell yield was determined every 4 days until the 12^{th} day so as to ascertain the maximum cell yield. The effects of the clay mineral samples on the kinetics of microbial growth was studied for only crude oil as sole carbon and energy source. Maximum cell yield and specific growth rate were used to compare the kinetics of the cell growth among samples and hence the effects of the clay samples on microbial growth. 2-sample t-test was used to analyse for significant statistical difference among the samples with respect to maximum cell yield.

There are three sets of controls, Control-1, Control-2 and the clay control where only clay minerals and oil are mixed and incubated such as CBU-250, CBO-250, CKU-250, CB-Ca, CB-K etc.

Note that Control-1 is a positive control (microbes + oil + BH medium)-no clay.

Control-2 is a negative control (oil + BH medium)-no clay and no microbes

Clay control such as CBU-250 (clay + oil + BH medium)-no microbes.

4.3 Results and Discussion

4.3.1 Hydrocarbon degrading enrichment culture

The microbial growth curves for the initial culture and final subculture (enrichment culture) using saturated crude oil hydrocarbons and ‘whole crude oil’ as sole carbon and energy source are presented in this subsection.

4.3.1.1 Crude oil saturated hydrocarbon as carbon and energy source

The absorbance – time curve for the initial culture using crude oil saturated hydrocarbon fraction as sole carbon and energy source from where the point of cell sampling for subsequent enrichment culture was determined is presented in Figure 4.1

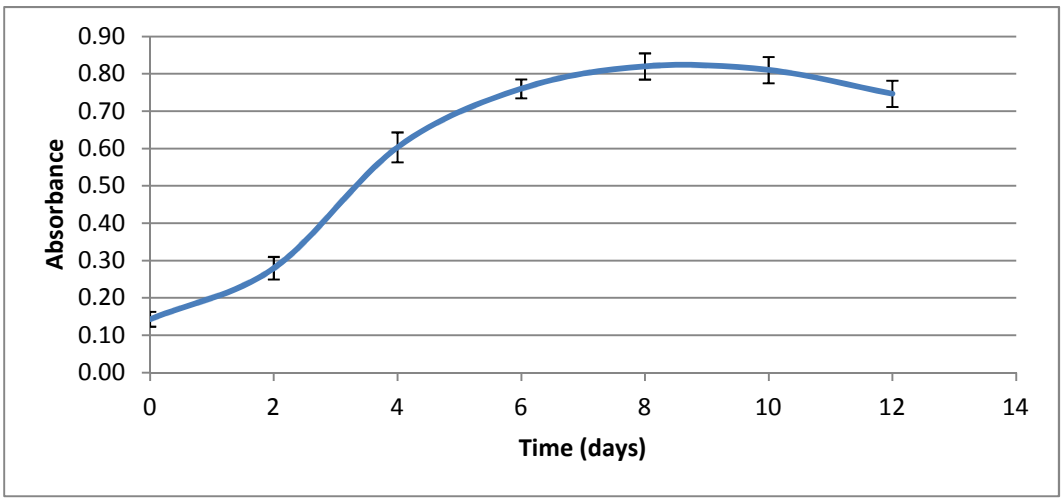

Figure 4.1 Microbial growth curve for initial culture with crude oil saturated hydrocarbon (200mg) as sole carbon and energy source. Values are presented as mean ± one standard deviation.

Figure 4.1 shows that day 4 is the most probable period of having active cells in the culture hence this is the point of sampling the cells in order to maintain active cells. Consequently, the microbial enrichment culture was grown in a mineral salts growth medium (Bushnell-Haas) with saturated hydrocarbon fraction from crude oil as sole carbon and energy source. Different amounts of the substrate (0.2g-1.75g) were used for the enrichment culture and sampling done at the fourth day for fresh subculture until the 9^{th} subculture which was the final enrichment culture.

The absorbance – time curve for the 9^{th} subculture (final enrichment subculture) using crude oil saturated fraction as sole carbon and energy source is presented in Figure 4.2

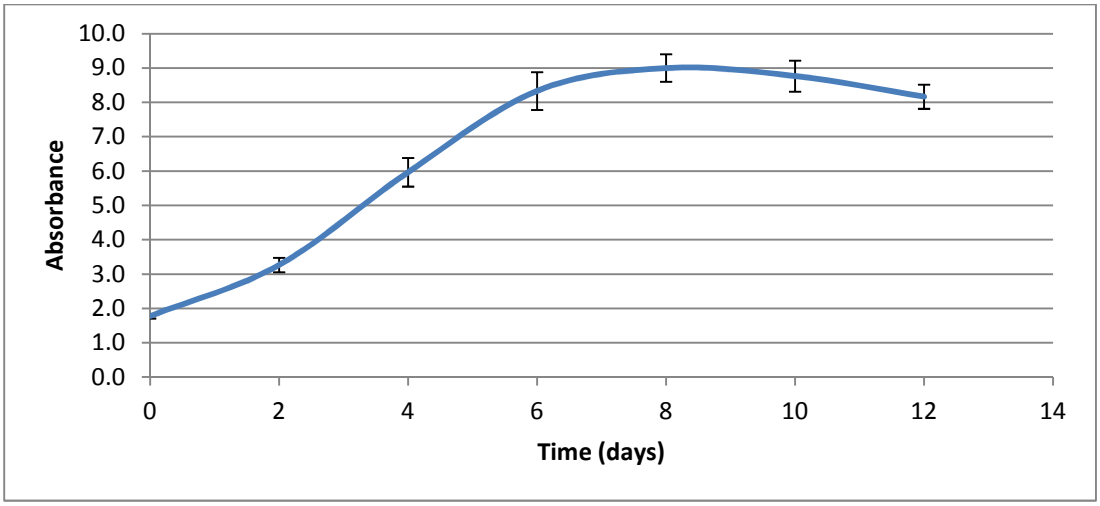

Figure 4.2 Microbial growth curve for final enrichment culture (9th subculture) with crude oil saturated hydrocarbon (1.75g) as sole carbon and energy source. Values are presented as mean ± one standard deviation.

Figure 4.2 shows that the final enrichment culture with saturated hydrocarbon as sole carbon and energy source had consistent growth rate with other cultures (specific growth rate of about 0.011 hr^{-1}) and had relatively very high cell density as the absorbance is relatively high. This 9th subculture was used as the source of microbial cells for the biodegradation experiments.

The absorbance – time curve for the initial culture using 'whole' crude oil as sole carbon and energy source from where the point of cell sampling for subsequent enrichment culture was determined is presented in Figure 4.3

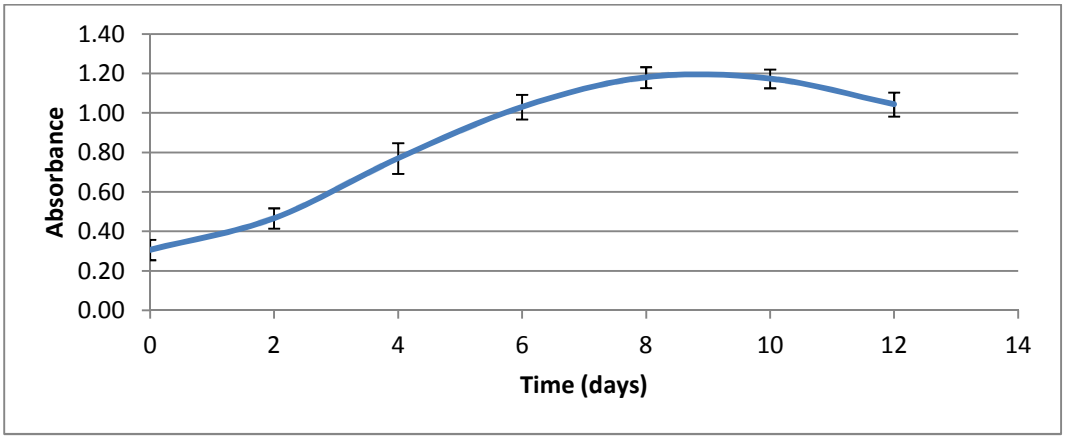

Figure 4.3 Microbial growth curve for initial culture with crude oil (500mg) as sole carbon and energy source. Values are presented as mean ± one standard deviation.

Figure 4.3 shows that day 6 is the most probable period of having active cells in the culture hence the point of sampling the cells in order to maintain active cells. Consequently, the microbial enrichment culture was grown in a mineral salts growth medium (Bushnell-Haas) with saturated hydrocarbon fraction from crude oil as sole carbon and energy source. Different amounts of the substrate (0.5g-2.g) were used and sampling done at the sixth day for fresh subculture until the 9th subculture which was the final enrichment culture.

The absorbance – time curve for the 9th subculture (final enrichment subculture) using crude oil as sole carbon and energy source is presented in Figure 4.4

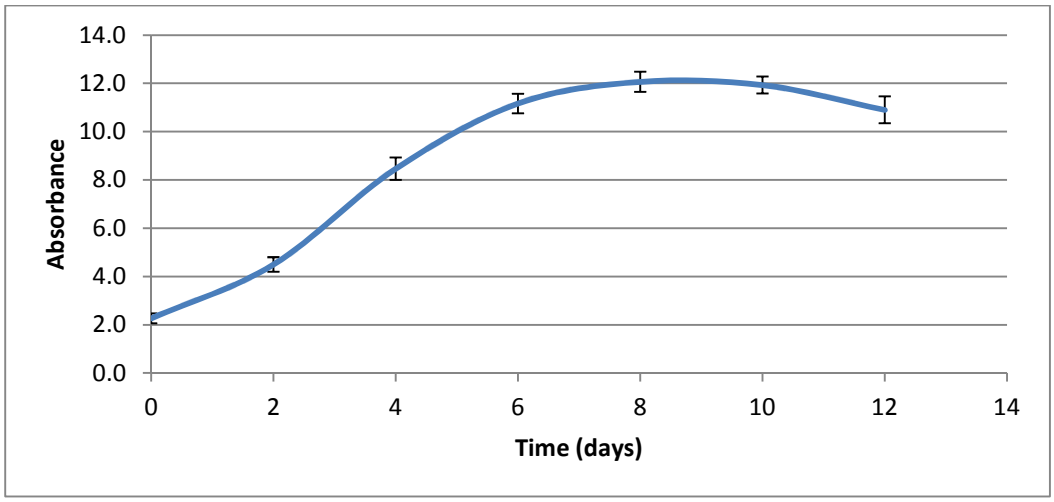

Figure 4.4 Microbial growth curve for final enrichment culture (9th subculture) with crude oil (2.0g) as sole carbon and energy source. Values are presented as mean ± one standard deviation.

The final enrichment culture (9th subculture) has a growth rate (specific growth rate of about 0.008 hr^{-1}) that is consistent with other subcultures and produced maximum absorbance (Figure 4.4) as a result of relatively high cell density. This 9th subculture was the source of the microbial cells used for subsequent experiments in studying the effect of clay minerals on microbial growth during biodegradation of crude oil hydrocarbons and all biodegradation experiments in which crude oil was used as sole carbon and energy source.

4.3.2 Effect of unmodified clay minerals on growth of hydrocarbon degrading bacteria

The effects of different unmodified clay mineral types namely, bentonite, saponite, kaolinite and palygorskite (which are 2:1 dioctahedral smectite, 2:1 trioctahedral smectite, 1:1 dioctahedral clay mineral and 2:1 fibrous clay mineral respectively) on growth of hydrocarbon degrading bacteria are presented in this section. The microbial growth curves showing the effect of these clay samples are presented in Figure 4.5

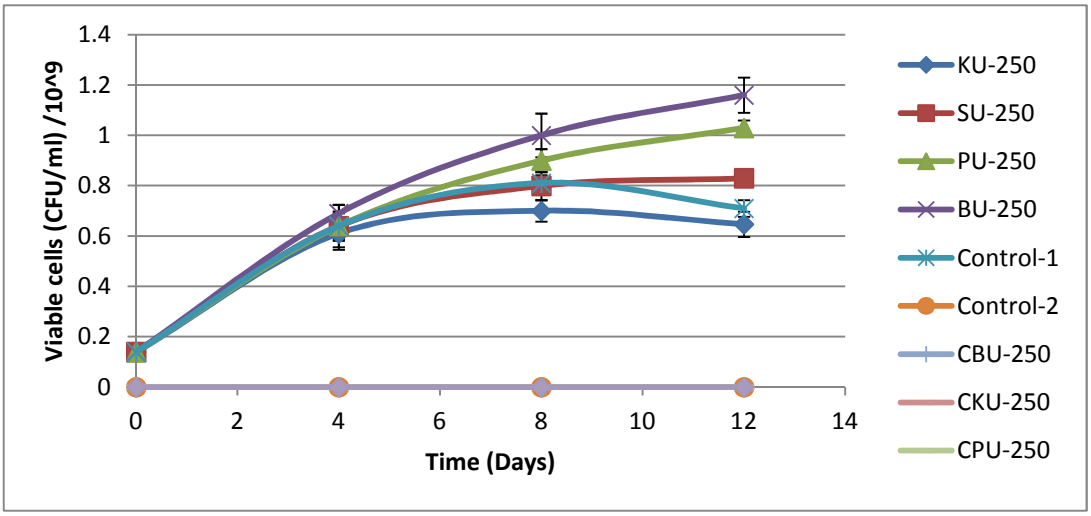

Figure 4.5 Effect of unmodified clay minerals on growth of hydrocarbon degrading bacteria. KU-250 = unmodified kaolinite; SU-250 = unmodified saponite; PU-250 = unmodidfied palygorskite; BU-250 = unmodified bentonite. CBU-250, CKU-250, CPU-250 and CSU-250 are clay controls. Control-1 is the positive control (BH + oil + cells) without clay; Control-2 is the negative control (BH + oil) without clay and cells. Values are reported as mean ± one standard error.

Figure 4.5 shows that the unmodified clay minerals affect the microbial growth according to the type of the unmodified clay mineral on which the microbial growth is supported.

The effect of unmodified clay minerals on microbial growth assessed by the maximum cell yield and specific growth rate of the microbial cells is presented in Table 4.2

Table 4.2 Maximum cell yield and specific growth rate due to the effect of unmodified clay minerals. Values are reported as mean ± standard error of the mean.

Sample	Surface area of clay sample (m^2/g)	Maximum cell yield (CFU/ml)/10^8	Specific growth rate (hr^{-1}) *10^3
KU-250	36	7.1 ± 0.4	8.4 ± 0.3
SU-250	473	8.3 ± 0.3	9.1 ± 0.4
PU-250	502	10.3 ± 0.5	9.7 ± 0.3
BU-250	645	11.2 ± 0.4	10.2 ± 0.4
Control-1	-	8.1 ± 0.3	9.1 ± 0.2

Table 4.2 shows that the maximum cell yield and specific growth rate constant of the microbial cells in sample KU-250 are the lowest among the unmodified clay samples and lower than Control-1 whereas the maximum cell yield and specific growth rate in sample BU-250 are the highest among the unmodified clay minerals and higher than Control-1. The 2-sample t-test at 95% confidence interval (CI) performed to analyse for differences in maximum cell yield that may be statistically significant indicates that PU-250 and BU-250 are significantly different from Control-1 (P-values of 0.04 and 0.01 respectively). This result is consistent with the studies of Warr et al., 2009 although the study (Warr et al., 2009) did not cover the area of saponites. There is no statistical significant difference between Control-1 and either of SU-250 or KU-250 (P-values of 0.71 and 0.2 respectively) indicating that these two samples, KU-250 and SU-250 are not stimulatory to microbial growth. The microbial growth in the presence of unmodified clay minerals appears to increase with the surface area of the clay mineral samples. Unmodified kaolinite appears not to stimulate the microbial growth as a result of very low surface area and lack of interlayer cations. Interlayer cations are believed to cause 'local bridging effect' (effective delivery of nutrients to cells due to reduction of zeta potential or electrical double layer repulsion) hence clays without interlayer cations such as kaolinite will not have 'local bridging effect'(Warr et al., 2009). Conversely, unmodified bentonite has high surface area ($645m^2/g$) and interlayer cations that are able to cause' local bridging effect' hence leading to the accumulation and

delivery of the nutrients to the cells and enhancing their growth (Bright and Fletcher, 1983; Fletcher and Marshal, 1982; Warr et al., 2009).

4.3.3 Effect of acid activated clay minerals on growth of hydrocarbon degrading bacteria

Having tested the effect of the unmodified clay samples on microbial growth, the effect of treated clay samples like acid activated clay minerals is presented in this subsection.

The effects of the different acid activated clay minerals on microbial growth is presented in Figure 4.6

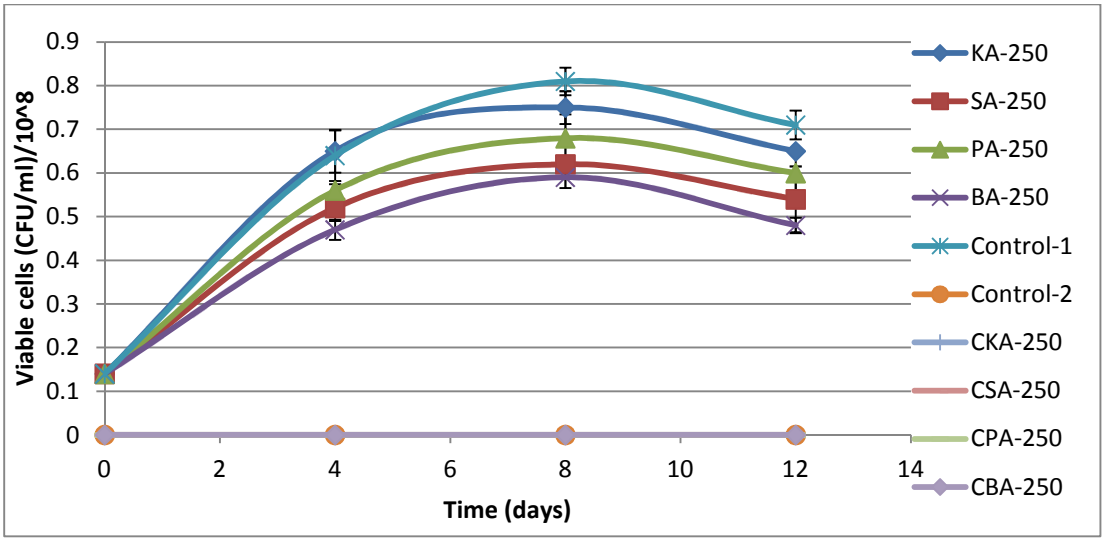

Figure 4.6 Effect of acid activated clay minerals on growth of hydrocarbon degrading bacteria. KA-250 = acid activated kaolinite; SA-250 = acid activated saponite; PA-250 = acid activated palygorskite; BA-250 = acid activated bentonite. CBA-250, CKA-250, CPA-250 and CSA-250 are clay controls. Control-1 is the positive control (BH + oil + cells) without clay; Control-2 is the negative control (BH + oil) without clay and cells. Values are reported as mean ± one standard error.

Figure 4.6 shows that the acid activated clay minerals are likely to have adverse effect on microbial growth. The effect of acid activated clay minerals on microbial growth assessed by the maximum cell yield and specific growth rate of the microbial cells is presented in Table 4.3.

Table 4.3 Maximum cell yield and specific growth rate due to the effect of acid activated clay minerals. Values are reported as mean ± standard error of the mean.

Sample	pH	Maximum cell yield (CFU/ml)/10^8	Specific growth rate (hr^{-1})*10^3
KA-250	4.4	7.1 ± 0.4	8.3 ± 0.3
SA-250	4.3	6.2 ± 0.2	7.8 ± 0.1
PA-250	4.2	6.6 ± 0.3	8.1 ± 0.2
BA-250	4.1	5.9 ± 0.2	7.5 ± 0.2
Control-1	7.2	8.1 ± 0.3	9.1 ± 0.2

Table 4.3 shows that the acid activated clay minerals appear to depress microbial growth as the maximum cell yield and specific growth rate constant for cells in Control-1 are higher than those in the acid activated clay samples. The lower pH of the acid activated clay samples could be responsible for this depression of microbial activity. The 2-sample t-test at 95% confidence interval (CI) performed to analyse for differences in maximum cell yield that may be statistically significant indicates that Control-1 is significantly different from SA-250, PA-250 and BA-250 (P-values of 0.014, 0.03 and 0.01 respectively) but is not significantly different from KA-250 (P-value of 0.3). This indicates that the acid activated clay samples suppress microbial growth and this depression of microbial growth appears to increase as the pH decreases. To test whether the depression of microbial growth by the acid activated clay minerals is as a result of lowering the pH or as a result of some other properties of the acid activated clay mineral, two more experiments were conducted. One of them was studying the effect of increasing the acid activated clay/oil ratio from 5:1 (w/w) to 10:1(w/w) hence instead of 250mg of acid activated clay, 500mg was used as this further reduced the pH to 3.6. The second experiment was conducted with media at various pH so as to obtain further evidence of the effect of acid activated clay minerals being likely the lowering of pH.

The effect of increasing the acid activated ratio from 5:1 (w/w) to 10:1(w/w) is presented in Figure 4.7.

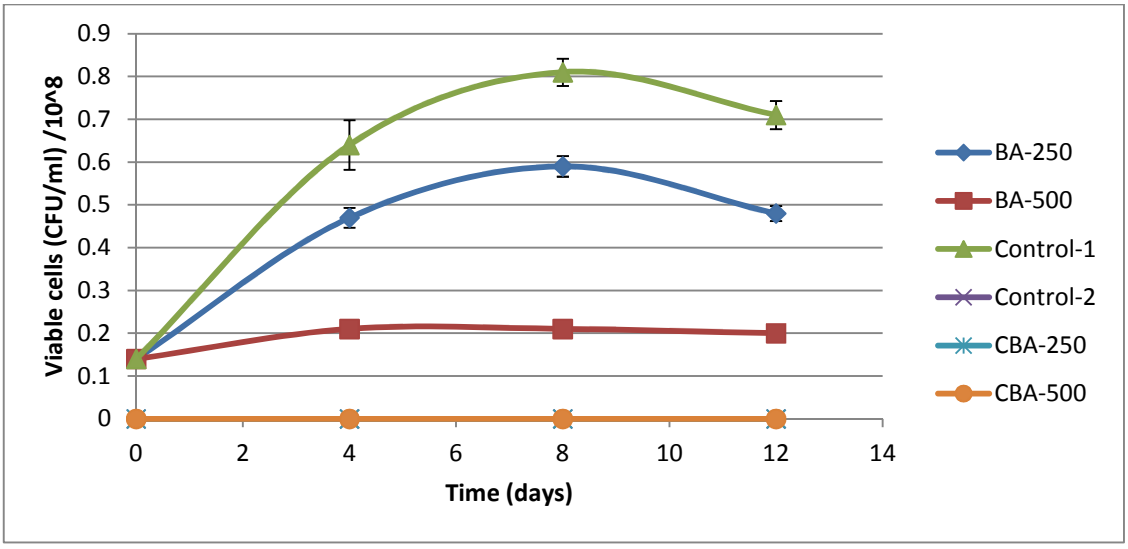

Figure 4.7 Effect of increasing the acid activated clay minerals/oil ratio from 5:1 (w/w) to 10:1(w/w) on growth of hydrocarbon degrading bacteria. BA-250 = acid activated bentonite (5:1); BA-500 = acid activated bentonite (10:1). The controls are as previously described. Values are reported as mean ± one standard error.

Figure 4.7 shows that increasing the activated clay mineral/oil ratio (w/w) from 5:1 to 10:1 adversely affect the microbial growth. The maximum cell yield and specific growth rate of the microbial cells is presented in Table 4.4.

Table 4.4 Maximum cell yield and specific growth rate constant due to the effect of increasing the acid activated clay mineral oil ratio from 5:1 to 10:1. Values are reported as mean.

Sample	pH	Maximum cell yield (CFU/ml)/10^8	Specific growth rate (hr^{-1})*10^3
BA-500	3.6	2.5 ± 0.2	3.1 ± 0.4
BA-250	4.1	5.9 ± 0.2	7.5 ± 0.2
Control-1	7.2	8.1 ± 0.3	9.1 ± 0.2

Table 4.4 shows that as the pH of the medium decreases, the maximum cell yield and specific growth rate constant decreases. The 2-sample t-test at 95% confidence interval (CI) performed to analyse for differences in maximum cell yield that may be statistically significant indicates that BA-250 and Control-1 are significantly different from BA-500 (P-

value of 0.002 and 0.001 respectively). Hence, increasing the acid activated clay/oil ratio from 5:1 to 10:1 decreases the pH of the medium and further depresses the microbial growth.

The effect of the various pH of the BH medium (in the absence of acid activated clay minerals) is presented in Figure 4.8

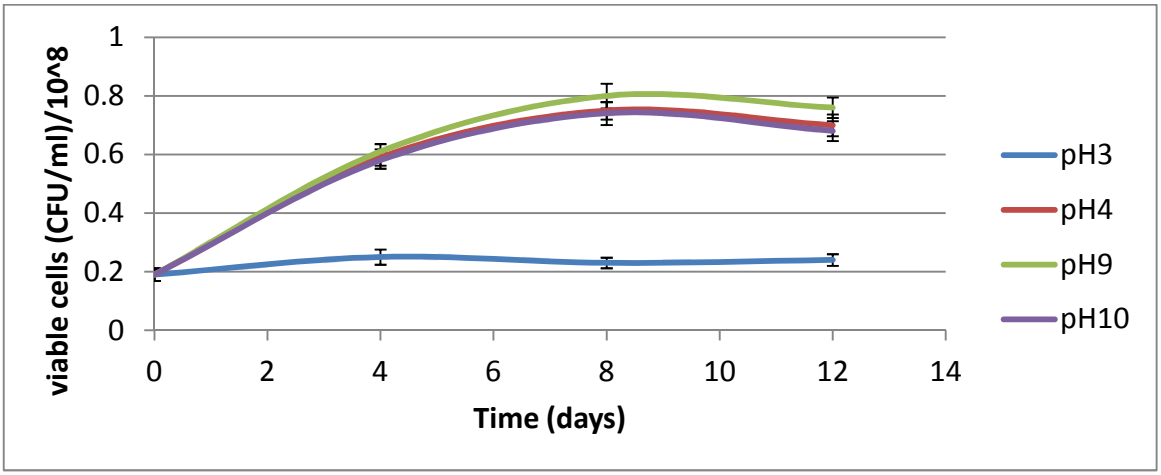

Figure 4.8 Effect of pH on growth of hydrocarbon degrading bacteria. pH3, pH4, pH9 and pH10 represent samples maintained at pH3, pH4, pH9 and pH10 in the absence of any clay. Values are reported as mean ± one standard error.

Figure 4.8 shows that pH3 seems to have an adverse effect on microbial growth. The maximum cell yield and specific growth rate constant of the microbial cells is presented in Table 4.5.

Table 4.5 Maximum cell yield and specific growth rate constant due to the effect of pH. Values are reported as mean.

Sample	Maximum cell yield (CFU/ml)/10^8	Specific growth rate (hr^{-1})*10^3
pH3	2.3 ± 0.2	3.1 ± 0.4
pH4	7.5 ± 0.3	8.3 ± 0.2
pH9	8.0 ± 0.4	8.4 ± 0.3
pH10	7.4 ± 0.4	8.0 ± 0.2

Table 4.5 shows that as the pH increases from 3 to 9, the maximum cell yield and specific growth rate constant increases. The 2-sample t-test at 95% confidence interval (CI) performed to analyse for differences in maximum cell yield that may be statistically significant indicates that there is statistical significant difference between sample maintained at pH3 and those maintained at pH4, pH9 and pH10 (P-values of 0.00). Figures 4.7 and 4.8 and Tables 4.4 and 4.5 all indicate that the acid activated clay minerals must have depressed the microbial growth by decreasing the pH of the medium. It is therefore suggested that the extent of depression of the microbial activity by the acid activated clays is a function of the clay minerals ability to reduce the pH to a level that will be toxic to the microbes.

4.3.4 Effect of Organoclay minerals on growth of hydrocarbon degrading bacteria

The organoclay mineral samples were prepared from saponite and bentonite as a result of their having substantial CEC. These organoclay samples have an organic cation, didecyldimethyl ammonium (DDDMA) intercalated in the interlayer of the clay samples (saponite and bentonite). This makes the organoclay acquire an organic phase in its interlayer hence rendering the clay surface hydrophobic. Because bentonite has a higher CEC than saponite, the organobentonite has more organic phase than organosaponite. The microbial growth curves showing the effect of these organoclay samples are presented in Figure 4.9

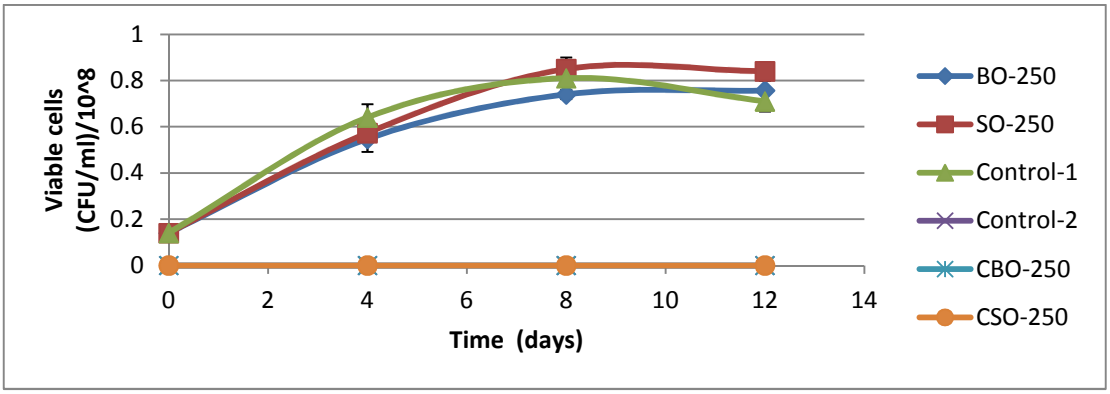

Figure 4.9 Effect of organoclay minerals on growth of hydrocarbon degrading bacteria. BO-250 = organobentonite; SO-250 = organosaponite; Control-1 =BH + oil + cells. Control-2= BH + oil. CBO-250 and CSO-250 are clay controls. Values are reported as mean ± one standard error.

Figure 4.9 shows that the organoclay samples seem to have about the same effect on microbial growth as the positive control (Control-1). The maximum cell yield and specific growth rate constant of the microbial cells is presented in Table 4.6.

Table 4.6 Maximum cell yield and specific growth rate constant due to the effect of organoclay mineral. Values are reported as mean.

Sample	Maximum cell yield (CFU/ml)/10^8	Specific growth rate (hr^{-1})*10^3
BO-250	7.3 ± 0.3	8.4 ± 0.2
SO-250	8.2 ± 0.2	9.2 ± 0.2
Control-1	8.1 ± 0.3	9.1 ± 0.2

Table 4.6 shows that the microbial growth seemed to be depressed in sample BO-250 as the maximum cell yield and specific growth rate constant are lower with this sample than either Control-1 or SO-250. The 2-sample t-test at 95% confidence interval (CI) performed to analyse for differences in maximum cell yield that may be statistically significant indicates that there is no statistical significant difference between Control-1 and either of BO-250 or SO-250 (P-value of 0.16 and 0.15 respectively). BO-250 and SO-250 cannot be said to stimulate the microbial growth although SO-250 does not depress it either. Generally therefore, the organoclay samples did not stimulate microbial growth. However, because DDDMA bromine used for preparing the organoclay is believed to be bactericidal, it became necessary to test whether the non-stimulatory behaviour of the organoclay especially BO-250 is due to free DDDMA bromine on the clay's surface or rather properties inherent in the organoclay. This test was carried out as described in section 2.3.3 and the result presented in Figure 4.10

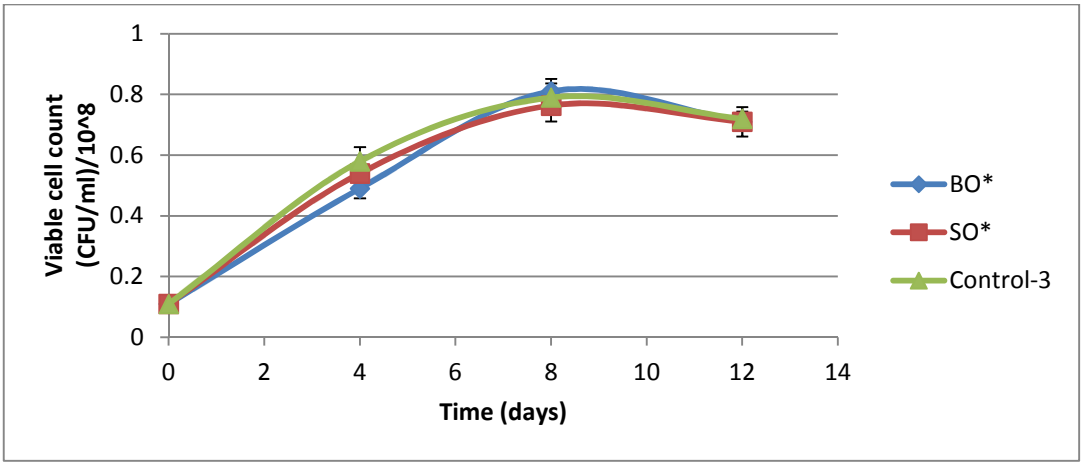

Figure 4.10 Test for free DDDMA Bromine on organoclay surface minerals. BO*= organobentonite spent water; SO* = organosaponite spent water; Control-3 = BH + oil + cells (prepared with de-ionized water). Values are reported as mean ± one standard error.

Figure 4.10 shows that the three samples, BO*, SO*, and Control-3 are similar with respect to supporting microbial growth. The maximum cell yield and specific growth rate constant of the microbial cells are presented in Table 4.7

Table 4.7 Maximum cell yield and specific growth rate constant due to the effect of organoclay mineral spent water. Values are reported as mean.

Sample	Maximum cell yield (CFU/ml)/10^8	Specific growth rate (hr^{-1})*10^3
BO*	8.1 ± 0.2	9.1 ± 0.2
SO*	7.9 ± 0.2	9.0 ± 0.2
Control-3	8.0 ± 0.2	9.1 ± 0.3

Table 4.7 shows that the microbial growth based on maximum cell yield and specific growth rate constant is similar for the three samples, BO*, SO* and Control-3. The 2-sample t-test at 95% confidence interval (CI) performed to analyse for differences in maximum cell yield that may be statistically significant indicates that there is no statistical significant difference between BO* and either of Control-3 and SO* (P-value of 1.00 and 0.5 respectively).

This suggests that there is no free DDDMA bromine on the surface of organoclay.

4.3.5 Effect of homoionic interlayer clays on growth of hydrocarbon degrading bacteria

The effects of the homoionic interlayer clay samples namely, Na-bentonite, K-bentonite, Mg-bentonite, Ca-bentonite, Zn-bentonite, Al-bentonite, Cr-bentonite and Fe-bentonite on microbial growth are presented in Figure 4.11.

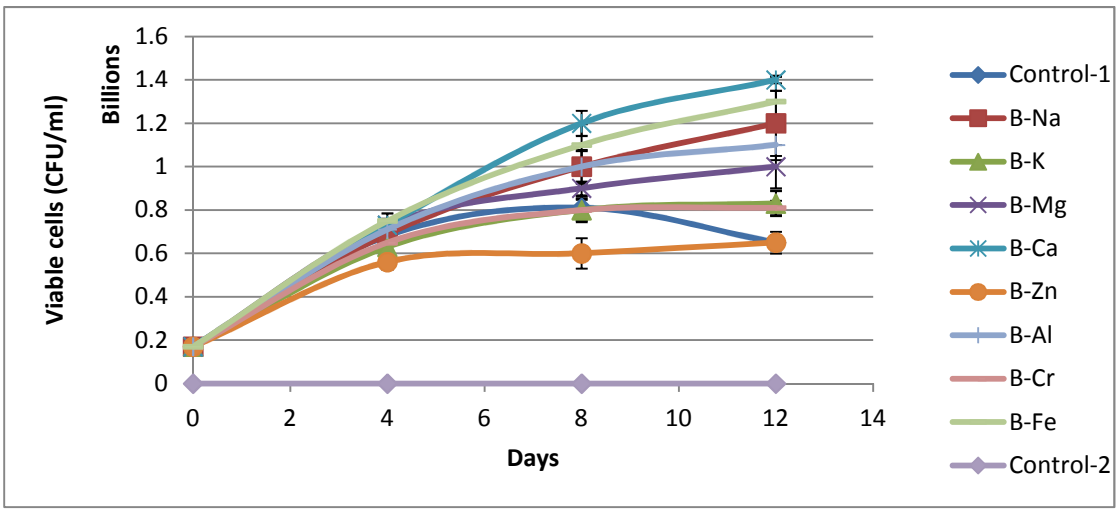

4.11 Effect of homoionic interlayer clay samples on growth of hydrocarbon degrading bacteria. B-Na = sodium bentonite; B-K = potassium bentonite; B-Mg = magnesium bentonite; B-Ca = calcium bentonite; B-Zn = zinc bentonite; B-Al = aluminium bentonite; B-Cr = chromium bentonite; B-Fe = ferric (Iron (III)) bentonite; Control-1 =BH + oil + cells. Control-2 and clay controls with zero values are all on the horizontal axis. Values are reported as mean ± one standard error.

Figure 4.11 shows that one of the homoionic interlayer clay minerals, B-Zn seemed to depress microbial growth while others appeared to stimulate growth. The maximum cell yield and specific growth rate constant of the microbial cells are presented in Table 4.8

Table 4.8 Maximum cell yield and specific growth rate constant due to the effect of homoionic interlayerclays. Values are reported as mean.

Sample	Maximum cell yield (CFU/ml)/10^8	Specific growth rate (hr^{-1})*10^3
B-Na	12.0 ± 0.8	10.1 ± 0.4
B-K	8.2 ± 0.6	8.8 ± 0.4
B-Mg	10.0 ± 1	9.5 ± 0.6
B-Ca	14.1 ± 0.5	11.3 ± 0.4
B-Zn	6.5 ± 0.7	7.5 ± 0.5
B-Al	10.1 ± 0.5	10.1 ± 0.4
B-Cr	8.1 ± 0.3	8.8 ± 0.3
B-Fe	13.2 ± 0.7	11.0 ± 0.4
Control-1	8.1 ± 0.3	9.1 ± 0.2

2-sample t-test at 95% confidence interval (CI) were performed to analyse for differences in maximum cell yield that may be statistically significant and indicated that there was no significant difference between Control-1 and any of B-Zn, B-K and B-Cr (P-values of 0.096, 0.84 and 1.00). These samples can therefore be said not to stimulate or surpress microbial growth. These samples as reported in subsequent sections of this thesis appear to have better adsorptive properties to aromatic hydrocarbons more than the other homoionic interlayer clay samples and may account for why the microbial growth tend not to be bolstered. In contrast, the other clay samples especially B-Na, B-Fe and B-Ca have quite higher specific growth rate constants and maximum cell yields than Control-1. The 2-sample t-test at 95% confidence interval (CI) performed to analyse for differences in maximum cell yield that may be statistically significant indicates that there is significant difference between Control-1 and B-Na, B-Ca and B-Fe (P-values of 0.04, 0.04 and 0.01). This indicates that samples (B-Na, B-Ca and B-Fe) may have stimulated microbial growth. These samples must have stimulated microbial growth by 'local bridging effect' as explained in section 4.3.2.

This result is consistent with the study of Warr et al., 2009 which investigated the effect of Na-, Mg-and Ca-montmorillonite on microbial growth. There was no study to compare the other results which have to do with the effect of K-, Zn-, Al- and Fe-bentonite on microbial growth.

4.4 Conclusion

Unmodified clay samples exhibited different effects on microbial growth. Unmodified palygorskite and unmodified bentonite stimulated microbial growth in contrast to unmodified saponite and unmodified kaolinite which are neutral and inhibitory to microbial growth respectively. The huge surface area of the clay samples and 'local bridging effect' are suggested to account for the stimulatory role of clay minerals.

Acid activated clay minerals inhibited microbial growth by lowering the pH of the medium. This lowering of the pH must have increased the toxicity of the system and hence depressed the activities of the microbial cells.

Organobentonite appeared to be inhibitory to microbial growth and may be as a result of the hydrophobic interaction between the clay and hydrocarbons to the extent that some of the hydrocarbons are rendered unavailable. The inhibitory behaviour of the organoclay increases as the amount of the organic phase in the organoclay increases.

The homoionic interlayer clay samples have varied effects indicating that the interlayer cation of the clay influences microbial growth. For example, if the interlayer cations of bentonite are zinc, potassium or chromium, they tend to inhibit the microbial growth by extensive adsorption of the hydrocarbons (see section 5.3.7). In contrast, if the interlayer cations are sodium, calcium or iron (III), the microbial growth is stimulated as a result of local bridging effect.

5. BIODEGRADATION OF CRUDE OIL HYDROCARBONS SUPPORTED ON CLAY MINERALS-TOTAL PETROLEUM HYDROCARBONS (TPH).

5.1 Introduction

5.1.1 Effect of clay minerals on hydrocarbon biodegradation

Clay minerals provide surfaces that may be inhibitory or stimulatory to biodegradation of organic compounds (Filip, 1973; Guerin and Boyd, 1992; Scow & Alexander, 1992; Knaebel et al, 1994; van Loosdrecht et al, 1994; Chaerun, 2005).

Clay minerals have extensive surface (internal and external) areas on which substrates and nutrients can be adsorbed. The high surface area of some clay minerals provides a high surface activity as they accumulate or concentrate nutrients that stimulates biological breakdown of hydrocarbons hence enhancing biodegradation and environmental remediation of polluted sites (Fletcher & Marshal, 1982; Bright and Fletcher, 1983; van Loosdrecht etal, 1990; Tuccillo et al, 1999; Murray, 2000; Kosita et al, 2002 and Shelobolina et al, 2004; Warr et al, 2009).

The nature and strength of sorption will depend on the type of clay and substrate. Depending on the microbial community involved in biodegradation, adsorbed compounds may be resistant to microbial degradation on the account of its reduced availability or non-availability. Weissenfels et al (1992) demonstrated that some polycyclic aromatic hydrocarbons could not be biodegraded because they were adsorbed.

The ability of some clay minerals to aid dispersion and enhance pseudosolubilization of oil leading to increase in interfacial area that in turn enhances bioavailabilty of the hydrocarbons (that are the main hydrophobic compounds of oil) has been reported (Owens and Lee, 2003).

Chaerun and Tazaki (2005) has reported the ability of some kaolinites to aid the biodegradation of oil. Also, the study of Tazaki and Chaerun (2008) indicated that some kaolinites stimulated the biodegradation of seawater polluted oil. However, that study assessed biodegradation of the oil by microbial growth based only on cell count. This therefore does not provide adequate evidence that the microbial growth is due to hydrocarbon degradation.

Other clay minerals have also been investigated with respect to their abilities to stimulate biodegradation of crude oil hydrocarbons. Warr et al, (2009) has reported that Na- and Ca-montmorillonite, hectorite, and palygorskite stimulated microbial degradation of crude oil hydrocarbons more than high defect kaolinites, which were inhibitory. The study reported that many of the most successful clay minerals in stimulating the bacterial digestion of the oil are dioctahedral smectites especially Ca-montmorillonite. Extensive breakdown of the oil was also reported for biodegradation supported on palygorskite and hectorite. The study suggested that divalent exchangeable interlayer cations might be responsible for the improved microbial degradation of the hydrocarbons as they seem to be common with all the successful tested clay mineral samples.

As much as all the reviewed studies are significant in furthering knowledge with respect to the role some clay minerals play during the biodegradation of hydrocarbons, some other important areas that could be encountered in the environment such as an environment that is contaminated with acid or organic waste to the extent that the clay minerals become either acid activated or turns into organo-clay have not been studied. Also, questions arise from several recent publications considering the role of clay minerals in hydrocarbon biodegradation. For example, the study of Warr et al, (2009) indicated that exchangeable divalent cations (with local bridging effect) are responsible for why some of the clay mineral samples such as Ca-montmorillonite and palygorskite are more successful in stimulating the biodegradation of crude oil hydrocarbons than other clay samples such as monovalent interlayer cation clays such as Na- montmorillonite. However, it would be important to investigate the effect of other monovalent, divalent cations (such as Mg, Zn) and trivalent cations such as Al, Cr and Fe (III) as homoionic interlayer clays to be able to draw further conclusions about the effect of interlayer exchangeable cations.

The repoprts of Chaerun et al (2005) and Warr et al (2009) on the biodegradation of hydrocarbons supported on clay minerals did not appear to take into account the effects of hydrocarbon adsorption in their experiments, which would need to be known, as well as those of volatilization in order to accurately assess the losses due to biodegradation. All the aforementioned shortcomings have informed my research investigations, looking at how kaolinites, bentonites, palygorskites and saponites mediate biodegradation processes of crude oil hydrocarbons. The experimental design and procedure of the work in this thesis

has therefore been carried out to account for removal of hydrocarbon due to abiotic processes such as volatilization and adsorption.

While a previous study (Warr et al, 2009) used semi-quantitative FTIR methods to quantitate the oil removal during the process of biodegradation, FTIR may suffer interference from the lipids present in the microbial cells, therefore this study used GC-FID to quantitate TPH removed by both biodegradation and adsorption.

In this chapter, the results of the GC-FID measurements of the residual TPH after incubation (during which time biodegradation occurred) is presented and interpreted.

The key questions addressed in this chapter are:

a. Do different clay minerals stimulate or inhibit biodegradation of crude oil hydrocarbons?
b. Does modification of clays affect their ability to stimulate or inhibit the biodegradation of crude oil hydrocarbons?
c. What factors can explain the different effects of both unmodified clays and modified clays?

5.1.2 Crude oil biodegradation scales

Crude oil biodegradation scales are based on the classes of hydrocarbons that are removed during biodegradation. The more the recalcitrant compounds are biodegraded, the more severe the biodegradation. Peters & Modolwan (1993) produced a scale that provides an approximate ranking and classification of the degree of biodegradation. The ranking of biodegradation by Peters & Modolwan (1993) is from scale of 0-10 where the degree of biodegradation is described as undegraded, light, moderate, heavy, very heavy and severe. See Table 5.1.

Table 5.1: The scale and classification of the degree of biodegradation of crude oil (from Peters and Modolwan, 1993)

Rank	**Characteristic compositional change**	**Degree of biodegradation**
0	No alteration	Undegraded
1	Lower homologues of n-alkanes depleted	Light
2	General depletion of n-alkanes	
3	Only traces of n-alkanes remain	
4	No n-alkanes, acyclic isoprenoids intact	Moderate
5	Acyclic isoprenoids absent	
6	Steranes partly degraded	Heavy
7	Steranes degraded, diasteranes intact	
8	Hopanes partly degraded	Very heavy
9	Hopanes absent, diasteranes attacked	
10	C_{26}-C_{29} aromatic steroids attacked	Severe

5.1.3 Assessment of biodegradation

There are several techniques that are employed in the assessment of the biodegradation of hydrocarbons (Wang, etal., 2007). The most common ones involve the use of conserved internal standards. Conserved internal standards are mainly found amongst the biomarkers and are useful in assessing biodegradation because they are relatively resistant to microbial degradation (Prince et al, 1994; Wang, etal., 2007). Examples of conserved internal standards useful in biodegradation of hydrocarbon studies are: pristane, phytane and hopanes (Wang, etal., 2007; Prince et al., 1994). The simplest approach in evaluating biodegradation at its earliest stage is to track the degradation of degradable compounds (such as heptadecane and octadecane) by reference to slowly degradable ones (such as pristane and phytane) where their ratios will give useful information about changes due to biodegradation (Prince et al, 1994).

Because the isoprenoids such as pristane and phytane are less resistant to biodegradation than hopanes, they are not useful during the later stages of biodegradation when they start getting degraded themselves. Consequently, hopanes are more useful at this later stage of biodegradation. Hopanes such as 17α(H), 21β(H)-hopane have been found very useful as conserved internal standards in the assessment of biodegradation (Butler et al, 1991; Bragg et al, 1993; Prince et al, 1994; Wang et al, 2007).

However, under very heavy and severe biodegradation, the hopanes can also be biodegraded making them again unsuitable for the assessment of biodegradation (Godwin, 1981; Peters & Modolwan, 1993 and Wang et al, 2007). Parker and Acey (1993) reported that 30% of hopanes were degraded in 5 weeks by mycobacterium fortuitum growing on pristane.

To overcome these problems associated with using the above mentioned conserved internal standards for the assessment of biodegradation of crude oil hydrocarbons, the technique of measuring the total petroleum hydrocarbon was used in this study.

5.1.4 Assessment criteria for biodegradation

The basis for the assessment of biodegradation in this study is the determination of the total petroleum hydrocarbons (TPH) using GC. This TPH as determined by GC is the residue of the original TPH after incubation.

5.2 Methods

5.2.1 TPH Determination

The determination of the TPH concentration was done by measuring the total GC area of the TPH fraction between 10 and 70 minutes above the baseline of hexane as a blank.

Total GC area, TGC = $RPA + UPA$ ……5.1

TPH (mg) = $\frac{(TGC-PASS-BA)WS(ug)}{PAS} * \frac{1}{1000}$ ……5.2

Where:

TGC = Total GC area

UPA = Unresolved peak area

RPA = Resolved peak area,

PA S = Peak area of surrogate standard (squalane) also used for quantifying the TPH

PASS = Peak area of all standards including the surrogate standard

BA = Area of blank (hexane)

WS (µg) = Weight of surrogate standard (Squalane) in microgram

The factor of 1000 converts the TPH weight from microgram to milligram.

Relative Response Factor

The relative response factor for the surrogate standard (squalane) was calculated as follows:

$$RRF = \left(\frac{PAS}{WS}\right) * \frac{WI(HDCH)}{PAI} \quad \text{.....5.3}$$

Where:

RRF = Relative response factor

PAS = Peak area of Squalane

WS = Weight of Squalane

WI = Weight of internal standard, heptadecylcyclo hexane(HDCH) as used in this study

PAI = Peak area of HDCH

% Recovery of Surrogate standard

The % recovery of the surrogate standard is given as:

$$\%R = \frac{WS}{TWS} * \frac{100}{RRF} \quad \text{.....5.4}$$

Where:

%R is percentage recovery

WS = uncorrected weight of surrogate (Squalane)

TWS = Theoretical weight of Squalane (250ug).

5.2.2 Differentiating between removal of TPH due to biodegradation from that due to adsorption.

The experiment was designed and carried out in such a manner as to separate adsorption from the process of biodegradation.

The difference in the TPH (mg) content between Control-2 (control without clay and without microbial cells) and the clay controls (controls without microbial cells but with clay) gives the weight of hydrocarbons adsorbed. For example, the difference in TPH(mg) between Control-2 and CBU-250, gives the weight of hydrocarbons adsorbed by CBU-250. It would then be expected that the test unmodified bentonite sample (BU-250) would adsorb similar amount of hydrocarbons during the "live" (biodegradation) experiments and would therefore be deducted from the total amount of hydrocarbons removed in order to determine the TPH removed by biodegradation.

The following equations were therefore used to determine the weight and percentage of hydrocarbons removed by biodegradation and adsorption.

TPH-as biodegraded (mg) = $TPHcy - TPHr$.....Eq. 5.5

TPH-as biodegraded (%) = $\frac{(TPHcy-TPHr)}{TPHcy} * 100$ .....Eq. 5.6

Where:

TPHcy = TPH(mg) of the clay control,

TPHr = TPH(mg) of clay test sample.

TPH-as adsorbed(mg) = $TPHc2 - TPHcy$ .....Eq. 5.7

TPH-as adsorbed (%) = $\frac{TPHc2-TPHcy}{TPHc2} * 100$ .....Eq. 5.8

Where TPHc2 is the TPH(mg) of the control 2.

TPH(mg) removed (overall),

= TPH-as biodegraded (mg) + TPH-as adsorbed(mg).....Eq. 5.9

TPH(%) removed (overall),

= {TPH(mg) removed (overall)/ TPH(mg) of the control 2}*100 .....Eq. 5.10

Other terms retain their usual meaning.

5.2.3 Data integrity-quality assurance

The experiments were carried out in triplicates to ensure reproducibility and amenability to statistical analysis. Adequate control experiments were employed to ensure that loss of hydrocarbons due to abiotic processes such as volatilization and adsorption are accounted

for. Procedural blanks were also carried out and analysed to ensure that the clay samples and other procedural steps did not on their own introduce bias to the study.

The clay mineral samples prepared in the laboratory and used for this study such as acid-activated clay and interlayer-cation-exchanged clays were thoroughly washed until free chlorides were removed as evidenced by negligible level of chlorides when analysed by ion chromatography (Sections 2.1 and 3.2 and Table 3.1).

The expected major source of bias with using the prepared organo-clay in this study is the bactericidal effect of didecyldimethylammonium (DDDMA) bromide which was used as a source of organic cation for preparing the organo-clay. To ensure the elimination of bias from any free DDDMA bromide, the organoclay was thoroughly washed until there was no free DDDMA bromide. The method employed in this study for ensuring that the organo-clay as used for biodegradation experiments did not contain free DDDMA bromine (that would have bactericidal effect) was to carry out a set of triplicate experiments in which an aliquot (10ml) of the supernatant from the final washings of the organo-clay was collected and the appropriate quantity of BH broth added and then finally inoculated with the microbial cells (the same cells that were employed in the biodegradation experiment) in the presence of same quantity of 50mg of crude oil as used in all experiments.

Another 10ml of the aliquot was also collected for an experiment of cell count after every four days until the 12^{th} day. The results were compared with the result obtained from a control experiment carried out with BH medium but in de-ionized water. See section 2.3.3.

The relative response factors (RRF) of the surrogate standard (Squalane) employed in this study lie between 0.78 and 0.8 which is considered reasonable.

The percentage recovery of the surrogate standard was also found to lie between 70% and 120% which again is within acceptable range (USEPA method 8270). See Appendix 5.9.

5.3 Results

5.3.1 Selected gas chromatograms showing extent of oil biodegradation

The chromatograms of TPH fractions from selected representative samples are shown in figures 5.1-5.4. See Appendix 5.7A-5.7F for the chromatograms of all the samples studied. The selected chromatograms in this sub-section show the different degrees of biodegradation that took place in this study.

Undegraded

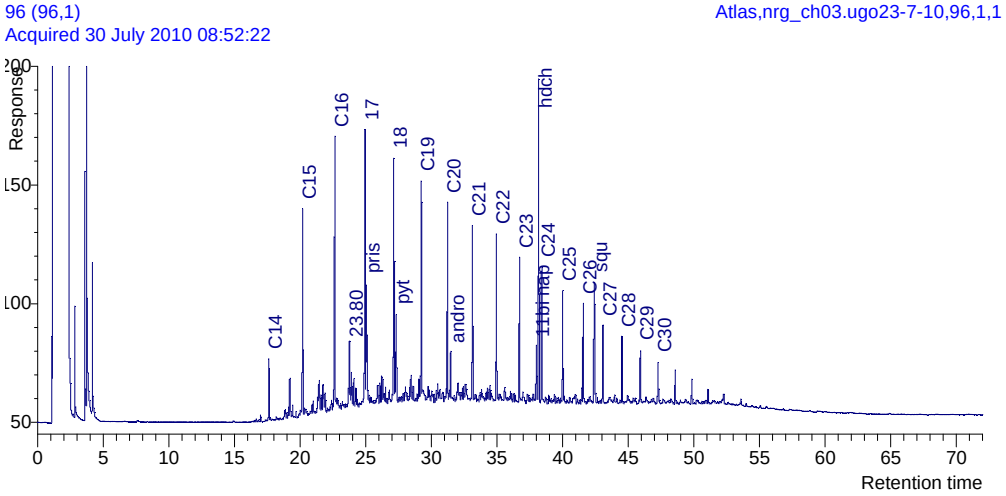

Figure 5.1 Chromatogram (of TPH fraction) showing no biodegradation-sample Control-2. Control-2 = negative control (BH + oil) no clay and no cells. The standards are labelled as: Squ=squalane; hdch=heptadecylcyclohexane; 1,1-binaph=1,1-binaphthyl; andro= 5α-androstane.

Light biodegradation

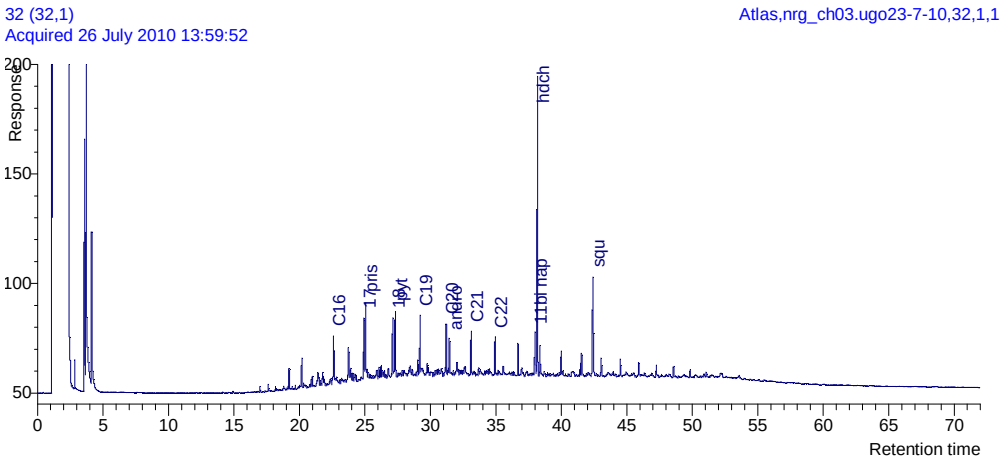

Figure 5.2 Chromatogram (of TPH fraction) showing light biodegradation-sample BA-500. BA-500 = acid activated bentonite (500mg).

Moderate to heavy biodegradation

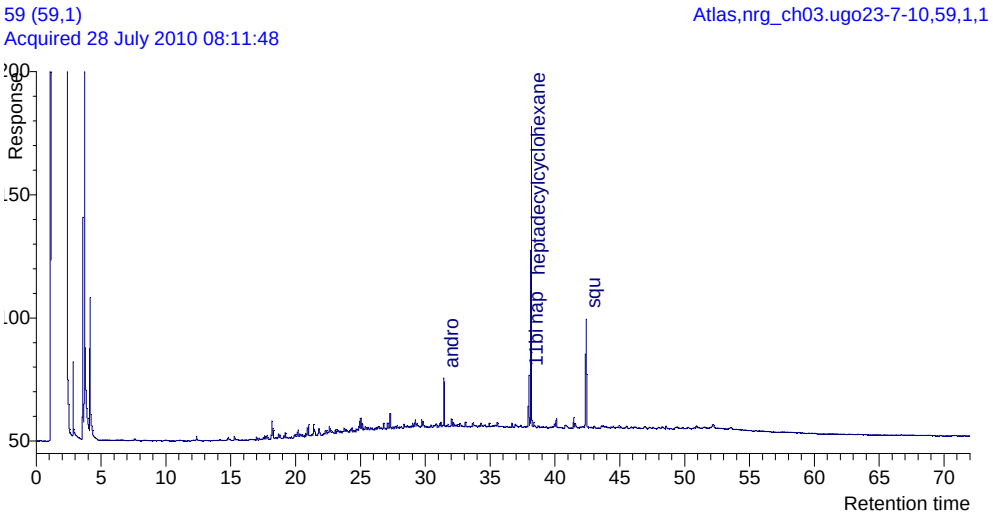

Figure 5.3 Chromatogram (of TPH fraction) showing moderate to heavy biodegradation-sample BO-250. B250 = organobentonite

Heavy biodegradation

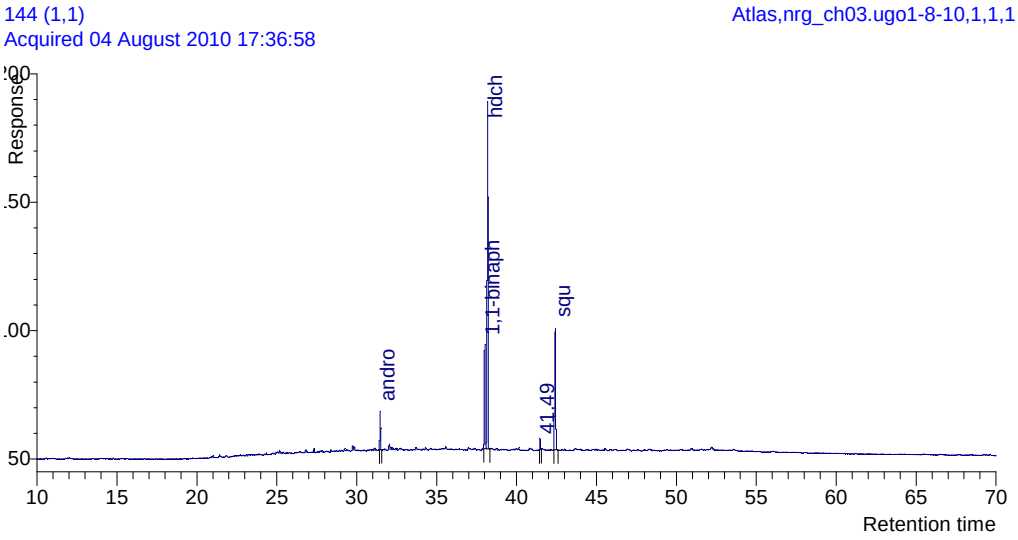

Figure 5.4 Chromatogram (of TPH fraction) showing heavy biodegradation-sample B-Ca. B-Ca = calcium-bentonite.

In Figure 5.1, absence of biodegradation of the hydrocarbons is evident and the nC17/pristane and nC18/phytane ratios for this sample are 2 and 2.1 respectively (see Table 5.2).

Figure 5.2 shows a typical case of light biodegradation as the nC17/pristane and nC18/phytane ratios are reduced to 0.6 and 0.7 respectively (see Table 5.3).

In Figures 5.3 and 5.4, the acyclic isoprenoids (pristane and phytane) are highly degraded. The biodegradation shown in Figure 5.4 appears to be heavier as there are virtually no visible peaks other than the surrogate and internal standards (squalane, heptadecylcylohexane, 1,1-binaphthyl and 5α-androstane) used.

5.3.2 Effect of unmodified clay minerals on biodegradation of crude oil hydrocarbons

The effect of unmodified clay minerals during biodegradation of the crude oil hydrocarbons assessed by nC17/pristane and nC18/phytane ratios are presented in Table 5.2.

Table 5.2 nC17/pristane and nC18/phytane ratios-effect of unmodified clay minerals

Sample	nC17/pristane	nC18/phytane
PU-250	NM	NM
SU-250	NM	NM
BU-250	NM	NM
KU-250	NM	NM
Control-1	NM	NM
CPU-250	2.0	2.1
CSU-250	2.0	2.1
CBU-250	2.0	2.1
CKU-250	2.0	2.1
Control-2	2.0	2.1

NM = not measurable

Table 5.2 shows that all the negative control samples have nC17/pristane and nC18/phytane ratios of 2.0 and 2.1 respectively indicating non-microbial activity. The test samples must have undergone heavy biodegradation as the n-alkanes, prsitane and phytane are not measurable and the chromatograms show that the peaks are all depleted. See chromatograms in Appendix 5.7A and 5.7B.

The effect of unmodified clay minerals during biodegradation of the crude oil hydrocarbons assessed by TPH measurements are presented in Figures 5.5-5.7.

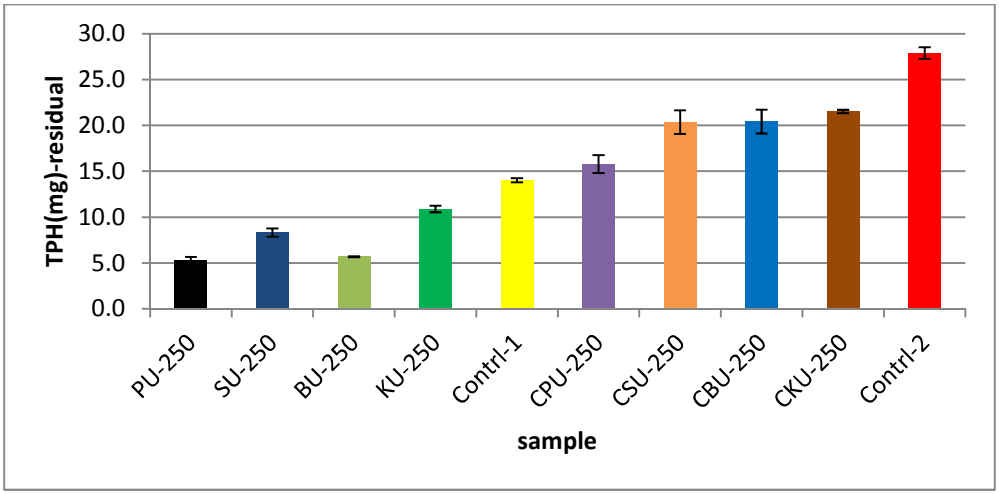

Figure 5.5 Residual TPH after biodegradation of crude oil hydrocarbons supported on unmodified clay minerals. BU-250 = unmodified bentonite, CBU-250 = unmodified bentonite control, PU-250 = unmodified palygorskite, CPU-250 = unmodified palygorskite control, SU-250 = unmodified saponite, CSU-250 = unmodified saponite control, KU-250 = unmodified kaolinite, CKU-250 = unmodified kaolinite control, Control-1 = Positive control (BH + oil + cells) no clays, Control-2 = Negative control (BH + oil) no cells and no clays. Values are reported as mean ± one standard error.

Figure 5.5 shows that the residual TPH is lowest for unmodified palygorskite and unmodified bentonite indicating that the removal of the hydrocarbons is more with these samples. However, on examination of the controls, CPU-250, CBU-250, CSU-250 and CKU-250, it is apparent that some portion of the removal may be due to abiotic process such as adsorption.

The removal of TPH fractions due to biodegradation on weight and percentage basis are presented in Figures 5.6 and 5.7 below:

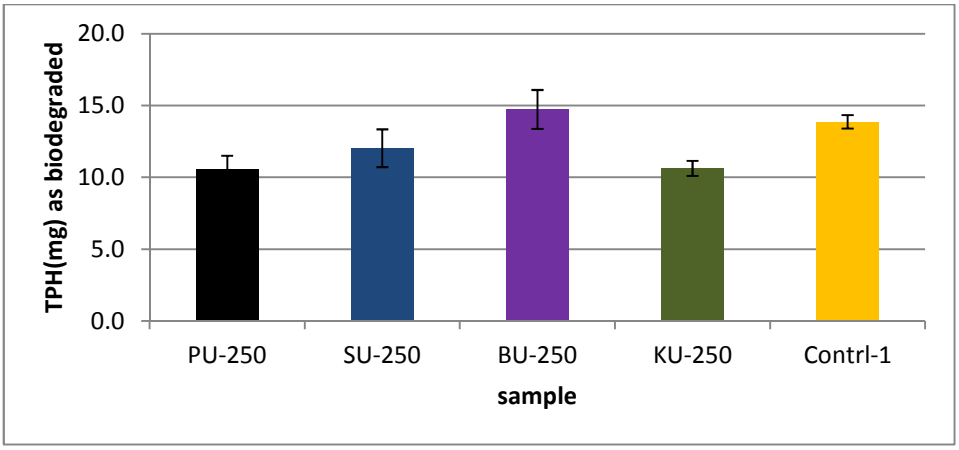

Figure 5.6 TPH biodegraded with unmodified clay samples. Values are reported as mean ± one standard error.

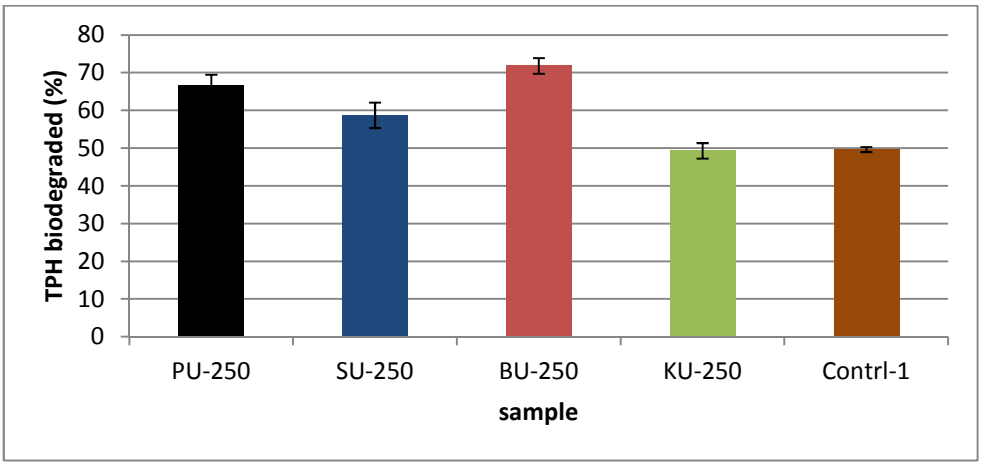

Figure 5.7 Percentage TPH biodegraded with the unmodified clay minerals. Values are reported as mean ± one standard error.

Figures 5.5-5.7 indicate that some unmodified clay minerals such as unmodified bentonite tend to somewhat enhance the biodegradation of crude oil hydrocarbons. Though Figure 5.6 on a weight basis shows lower TPH removed for unmodified palygorskite than control-1, on percentage of TPH removed due to biodegradation (Figure 5.7), we can infer that palygorskite indeed also supports biodegradation. The 2-sample t-test at 95% confidence interval (CI) performed to analyse for differences that may be statistically significant is as presented in Appendix 5.3. This statistical test indicates that KU-250 appears not to enhance biodegradation as the percentage removal of TPH due to biodegradation is quite comparable with that of Control-1 evidenced in a high P-value. SU-250 though slightly better than KU-250 is comparable with it (KU-250) and Control-1 as there is no statistical significant

difference both with Control-1 and KU-250. This therefore indicates that unmodified kaolinite and unmodified saponite do not seem to enhance biodegradation of crude oil hydrocarbons. However, as indicated earlier, the P-values for BU-250 & Control-1 and PU-250 & Control-1 suggest that unmodified bentonite and unmodified palygorskite offer better support for the biodegradation of crude oil hydrocarbons than unmodified saponite and kaolinite.

The difference in removal of TPH due to adsorption and biodegradation with the various unmodified clay minerals is shown in Figure 5.8 below:

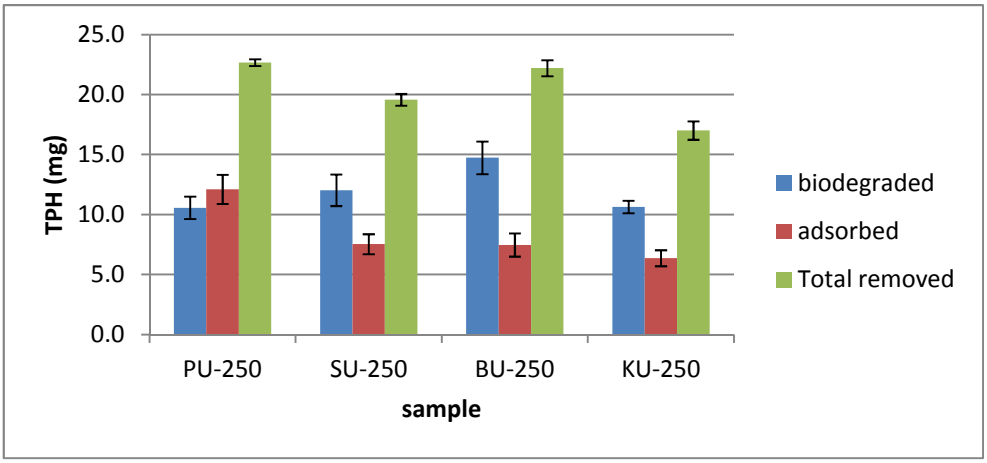

Figure 5.8 Removal of TPH by biodegradation and adsorption with the unmodified clay samples. Values are reported as mean ± one standard error.

Figure 5.8 shows that biodegradation occurs most with BU-250 whereas adsorption occurs most with PU-250. There is no significant difference in the amount of total TPH removed for samples PU-250 and BU-250. The suggested explanation for the difference in behaviour among these clay minerals is presented in a subsequent section (5.5).

The effect of the treated (modified) clay samples such as acid activated clays, organoclays and homoionic interlayer bentonite clays are presented in subsequent sections.

5.3.3 Effect of acid-activated clay minerals on biodegradation of crude oil hydrocarbons.

The effect of acid activated clay minerals during biodegradation of the crude oil hydrocarbons assessed by nC17/pristane and nC18/phytane ratios are presented in Table 5.3.

Table 5.3 nC17/pristane and nC18/phytane ratios-effect of acid activated clay. NM = not measurable

Sample	nC17/pristane	nC18/phytane
KA-250	-	-
PA-250	-	-
SA-250	-	-
BA-250	-	-
BA-500	0.6	0.7
CKA-250	2.0	2.1
CPA-250	2.0	2.1
CSA-250	2.0	2.1
CBA-250	2.0	2.1
CBA-500	2.0	2.1
Control-1	NM	NM
Control-2	2.0	2.1

Table 5.3 shows that all the negative control samples (without microbial cells) have nC17/pristane and nC18/phytane ratios of 2.0 and 2.1 respectively indicating absence of microbial activity hence absence of biodegradation. The ratios for the test acid activated clay samples cannot be computed as the n-alkanes, pristane and phytane are all biodegraded except in sample BA-500 where the ratio is 0.6 and 0.7 for nC17/pristane and nC18/phytane repectively indicating light microbial degradation.

The effect of acid activated clay minerals during biodegradation of the crude oil hydrocarbons assessed by TPH measurements are presented in Figures 5.9-5.11.

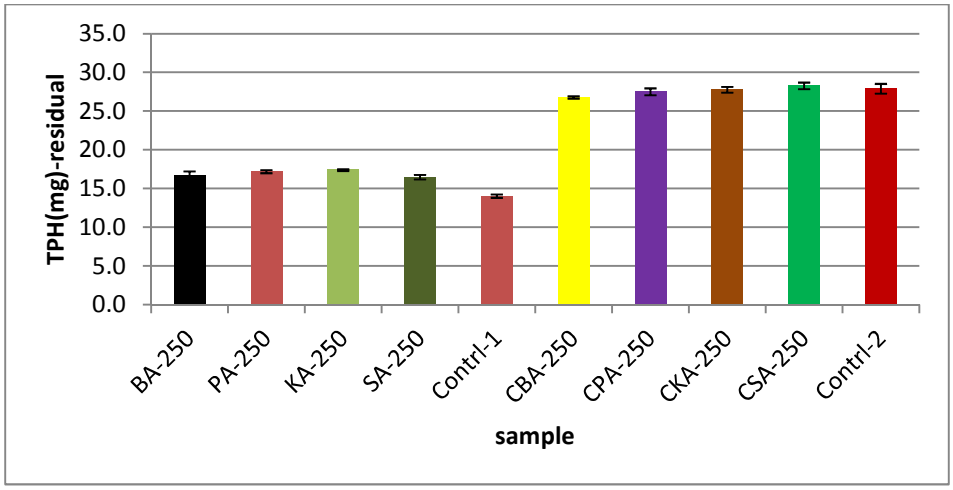

Figure 5.9 Residual TPH after biodegradation of crude oil hydrocarbons supported on acid activated clay samples. BA-250 = acid activated bentonite, CBA-250 = acid activated bentonite control, PA=250 = acid activated palygorskite, CPA-250 = acid activated palygorskite control, SA-250 = acid activated saponite, CSA-250 = acid activated saponite control, KA-250 = acid activated kaolinite, CKA-250 = acid activated kaolinite control. Control-1 and Control-2 retain their meanings. Values are reported as mean ± one standard error.

Figure 5.9 shows that the control samples where there were no microbial cells CBA-250, CPA-250, CKA-250, CSA-250 and Control-2 had the highest residual TPH indicating that there was little or no biological activity with these samples. Control-1 (the positive control) had the lowest residual TPH indicating that biodegradation must have occurred most with this sample. The result of the TPH biodegraded by the acid activated clay mineral samples in comparison with Control-1 on weight and percentage basis are presented in Figures 5.10 and 5.11 respectively.

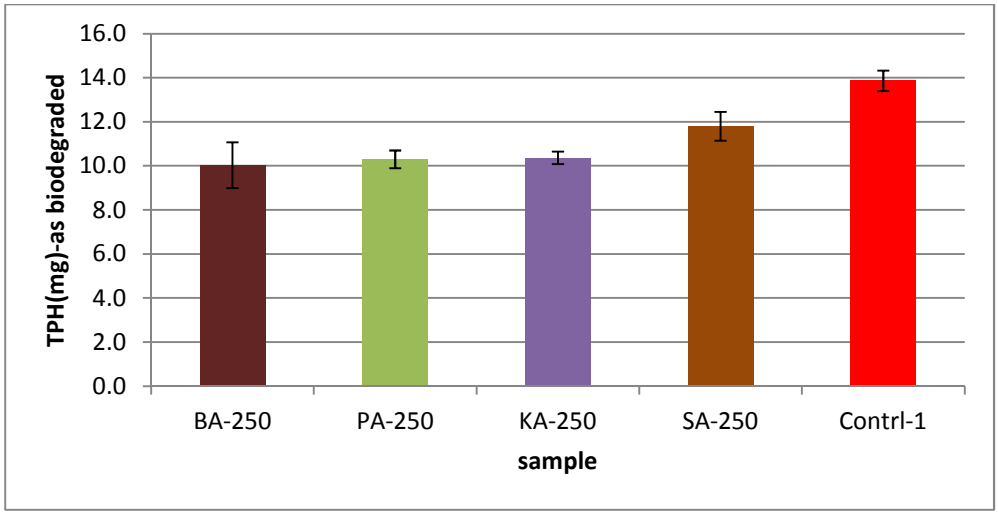

Figure 5.10 TPH biodegraded with acid activated clay samples. Values are reported as mean ± one standard error.

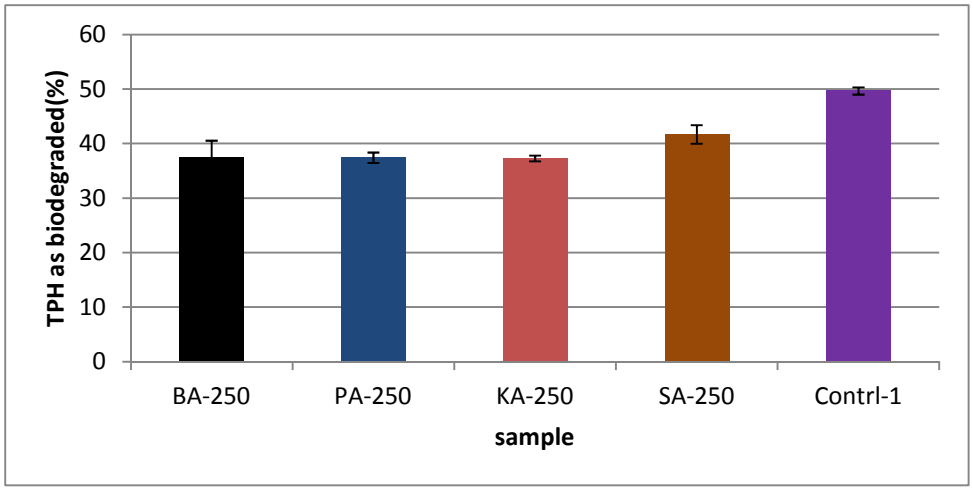

Figure 5.11 Percentage TPH biodegraded with acid activated clay samples. Values are reported as mean ± one standard error.

Figures 5.10 and 5.11 seem to indicate that biological activity occurred most in control-1 in comparison with the acid-activated samples.

The 2-sample t-test at 95% confidence interval (CI) performed to analyse for differences that may be statistically significant indicates that all the acid activated clay samples and Control-1 share a lot of similarities and hence no significant statistical difference amongst them as reflected on their P-values (see Appendix 5.2).

The acid activated clay mineral samples therefore seem not to enhance biodegradation of the crude oil hydrocarbons rather they appear to inhibit the biodegradation.

To test whether the depression of biodegradation by the acid activated clay samples is as a result of their lowering the pH of the medium or as a result of some other properties of the acid activated clay mineral, two more experiments were conducted. One of them was studying the effect of increasing the acid activated clay/oil ratio from 5:1 (w/w) to 10:1(w/w) hence instead of 250mg of acid activated clay, 500mg was used as this further reduced the pH to 3.6. The second experiment was conducted with media at various pH so as to obtain further evidence of the effect of acid activated clay minerals .

Effect of increasing the acid activated clay mineral /oil ratio from 5:1 to 10:1

The hypothesis of acid activated clay mineral hindering biodegradation (by toxicity caused by the acidity of the dispersion system) was tested by carrying out an experiment in which the amount of acid activated clay mineral (in this case acid activated bentonite) was doubled. If this hypothesis is true, it would be expected that the system with the 10:1 acid activated clay mineral/ oil ratio will be more acidic and hence more toxic to microbial cells than the system with 5:1 acid activated clay mineral oil ratio, manifesting in reduced removal of TPH by biodgradation. Hence comparison was made between BA-500 (10:1) ratio and BA-250 (5:1) where the weight of the acid activated bentonite used has been increased from 250mg to 500mg (see Figure 5.12).

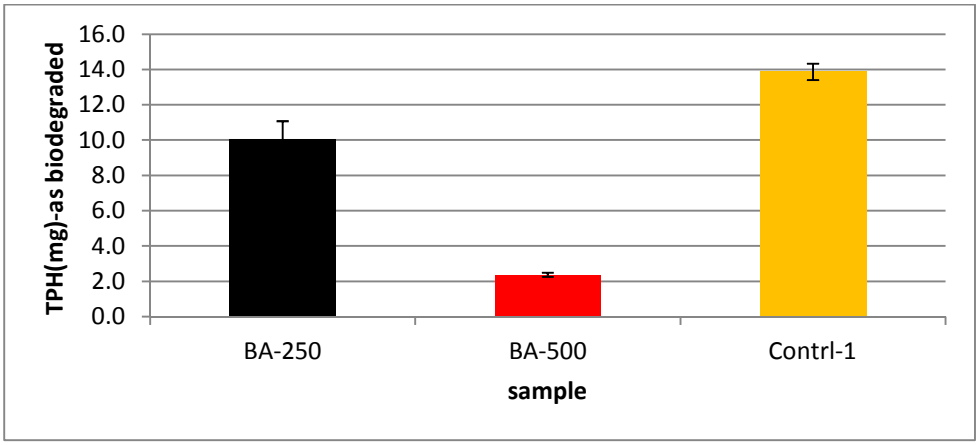

Figure 5.12 Effect of increasing the ratio of the acid activated-clay mineral/oil ratio from 5:1 (BA-250) to 10:1 (BA-500). Values are reported as mean ± one standard error.

The results presented in Figure 5.12 supports the indication that the acid-activated clay mineral affects microbial activity by lowering the pH. BA-500 having more acid-activated clay mineral in the medium will tend to increase the concentration of hydrogen ions hence

lowering the pH more than BA-250 and further inhibiting the biodegradation of the crude oil hydrocarbons. Thus the removal of TPH due to biodegradation has been reduced with BA-500. The indication of increased toxicity of BA-500 was supported by the results of the cell count experiments carried out as described in section 4.3.3 (Figure 4.7 and Table 4.4). At 95% CI, the 2-sample t-test shows that the P-value is 0.018 for BA-250 and BA-500 therefore the difference between the two samples are statistically significant.

The result of the second experiment on the effect of maintaining the medium at several pH ranging from pH2 to pH10 is presented in Table 5.4 and Figure 5.13.

Effect of pH on biodegradation of crude oil hydrocarbons

The effect of media pH during biodegradation of the crude oil hydrocarbons assessed by nC17/pristane and nC18/phytane ratios are presented in Table 5.4.

Table 5.4 nC17/pristane and nC18/phytane ratios-effect of pH. NM = not measurable

Sample	nC17/pristane	nC18/phytane
pH2	2.0	2.0
pH3	1.9	2.0
pH4	NM	NM
pH5	NM	NM
pH6	NM	NM
pH7	NM	NM
pH8	NM	NM
pH9	NM	NM
pH10	NM	NM

Table 5.4 indicates that at pH3 and pH2, there is hardly any microbial activity as the nC17/pristane and nC18/pristane ratios are both approximately 2.0 whereas at pH4-10 no ratio can be computed as both the normal alkanes and acyclic isoprenoids appear to have been degraded completely.

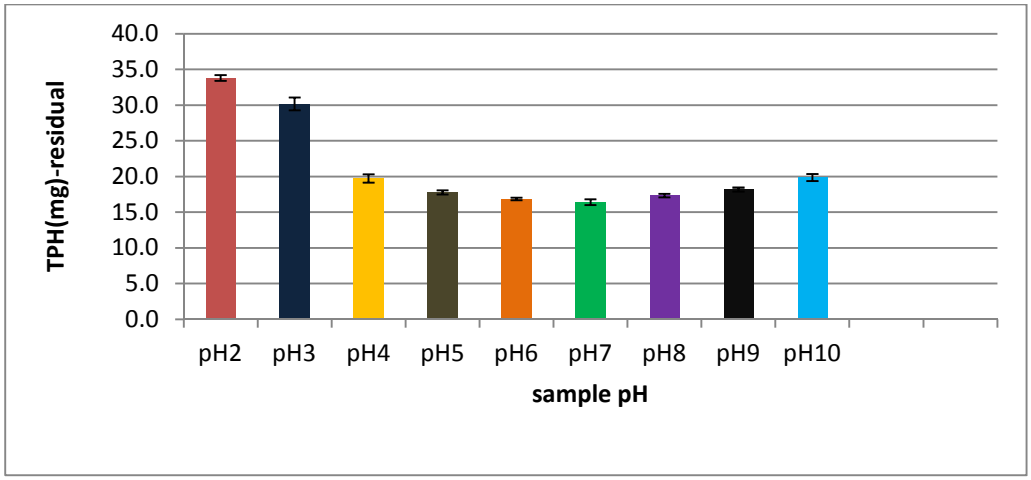

Figure 5.13 Effect of pH on the biodegradation of crude oil hydrocarbons. Values are reported as mean ± one standard error.

Figure 5.13 shows that pH affects the biodegradation of crude oil hydrocarbons. There is high residual TPH at pH 2 and 3 which is an indication of reduced activity of the microbial cells possibly due to the toxic effect of the relatively low pH of these two samples on the microbial cells. This corresponds with the observation with respect to nC17/pristane and nC18/phytane ratios. The residual TPH continues to fall gradually to reach a lowest value at pH 7 (which appears to be least toxic or non-toxic to the microbial cells) before gradually increasing. It is apparent therefore that the range of pH4-10 would not be as toxic to the microbial cells as that between pH2 and 3. The 2-sample t-test at 95% confidence interval (CI) performed to analyse for differences that may be statistically significant is as presented in Appendix 5.1. The optimum pH lies between pH5 and 8 as there is no statistical significant difference between pH7 and any of pH5, 6 and 8 (Appendix 5.1). It is therefore suggested that the repression of biodegradation by the acid activated clay samples is as a result of their lowering the pH of the medium and not by any other properties of the acid clay minerals.

5.3.4 Effect of organoclay minerals on biodegradation of crude oil hydrocarbons

The effect of organoclay minerals during biodegradation of the crude oil hydrocarbons assessed by nC17/pristane and nC18/phytane ratios are presented in Table 5.5.

Table 5.5 nC17/pristane and nC18/phytane-effect of organoclay

Sample	nC17/pristane	nC18/phytane
BO-250	NM	NM
SO-250	NM	NM
Control-1	NM	NM
CBO-250	2.0	2.1
CSO-250	2.0	2.1
Control-2	2.0	2.1

Table 5.5 shows that there is no microbial activity with the control samples whereas the test samples (BO-250,SO-250 and Control-1) have undergone considerable biodegradation as the isoprenoids and n-alkanes are degraded (see also the chromatograms Appendix 5.7C and 5.7D).

The result of the residual TPH is presented in Figure 5.14

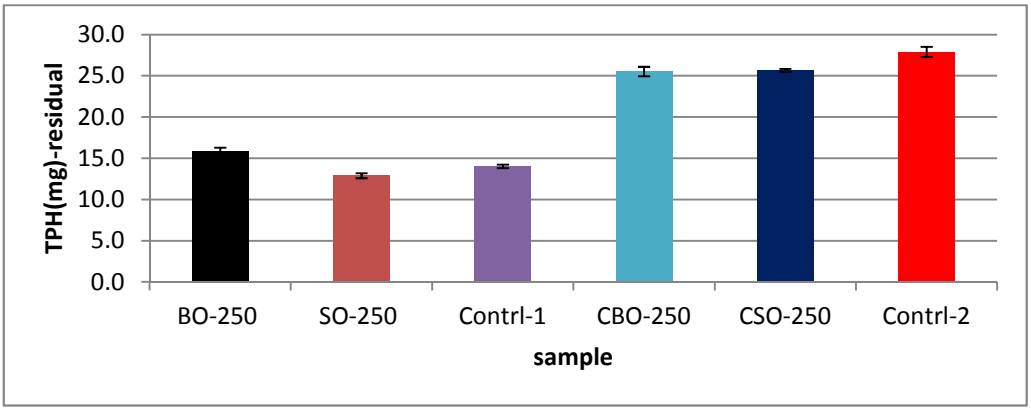

Figure 5.14 Residual TPH after biodegradation of crude oil hydrocarbons supported on organoclay samples. BO-250 = organobentonite; SO-250 = organosaponite; Control-1 =BH + oil + cells. Control-2= BH + oil. CBO-250 and CSO-250 are clay controls. Values are reported as mean ± one standard error.

The residual TPH is lowest with the SO-250 organo sample indicating that the removal of TPH is highest with this sample. However, it is apparent that all the removal of TPH may not be attributed to biodegradation. Figures 5.15 and 5.16 make it clearer which portion of the removal is due to biodegradation.

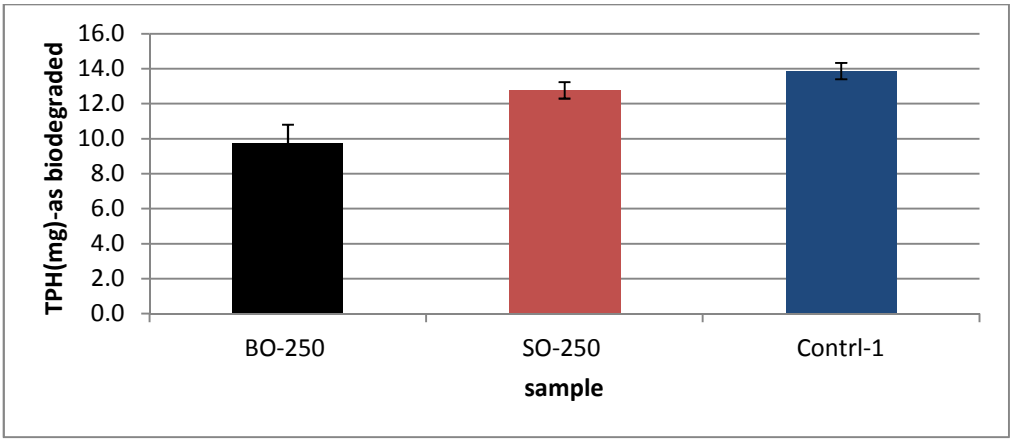

Figure 5.15 TPH biodegraded with organoclay samples. Values are reported as mean ± one standard error.

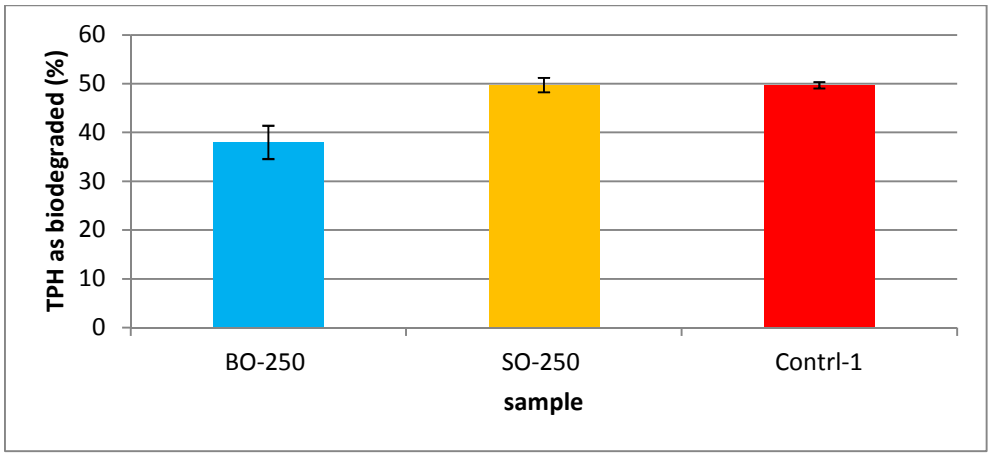

Figure 5.16 Percentage TPH biodegraded with organoclay samples. Values are reported as mean ± one standard error.

Figures 5.15 and 5.16 all indicate that generally, organo-clay minerals have not enhanced the biodegradation of crude oil hydrocarbons especially with organo-bentonite which seems to really inhibit the biodegradation of the hydrocarbons.

At 95% CI, the 2-sample t-test shows that the P-values are 0.121 and 0.071 for comparison between BO-250 and SO-250 and between BO-250 and Control-1 respectively. The P-value for Control-1 and SO-250 is 0.191. Therefore the difference among the samples is not statistically significant. On comparing the result of biodegradation of hydrocarbons with organoclay samples and the unmodified clay counterparts, the organoclay samples appear to repress the biodegradation.

Because DDDMA bromine used for preparing the organoclay is believed to be bactericidal, it became necessary to test whether the somewhat inhibitory behaviour of the organoclay especially BO-250 is due to free DDDMA bromine on the clay's surface or rather properties inherent in the organoclay. This test was carried out as described in section 5.2.3 and 2.3.3 and the result presented in Figure 5.17.

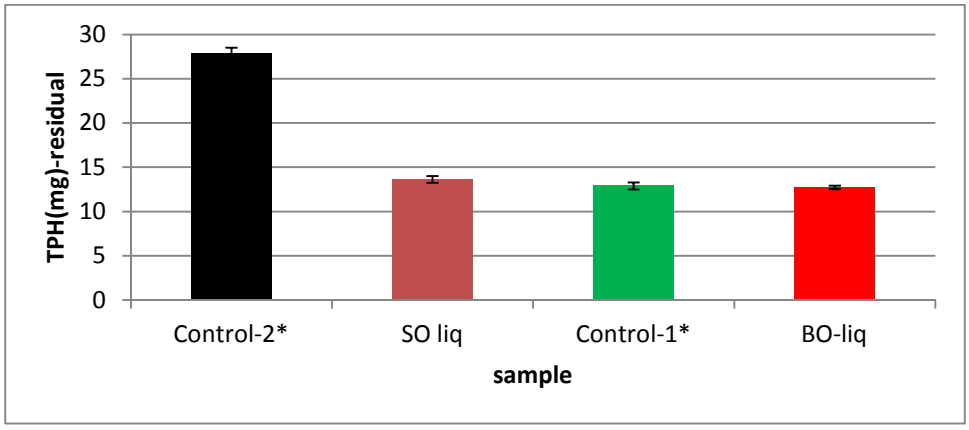

Figure 5.17 Test for free DDDMA Bromine on organoclay mineral surface. BO-liq = organobentonite spent water; SO-liq = organosaponite spent water; Control-1* = BH + oil + cells (prepared with de-ionized water). Control-2* = BH + oil. Values are reported as mean ± one standard error.

Figure 5.17 indicates that that extent of biodegradation is almost the same for BO-liq, SO-liq and Control-1*. The 2-sample t-test at 95% confidence interval (CI) performed to analyse for differences that may be statistically significant indicates that the P-values for Control-1* and Control-2*, Control-1 and BO-liq and Control-1 and SO-liq are 0.00, 0.742 and 0.272 respectively indicating that there is a statistical significant difference between Control-1* and Control-2* but no statistical significant difference between Control-1* and either of BO-liq or SO-liq. This implies that the organo-clays are unlikely to exert any bactericidal effect due to free DDDMA Br.

Their chromatograms are shown in Figures 5.18-5.21

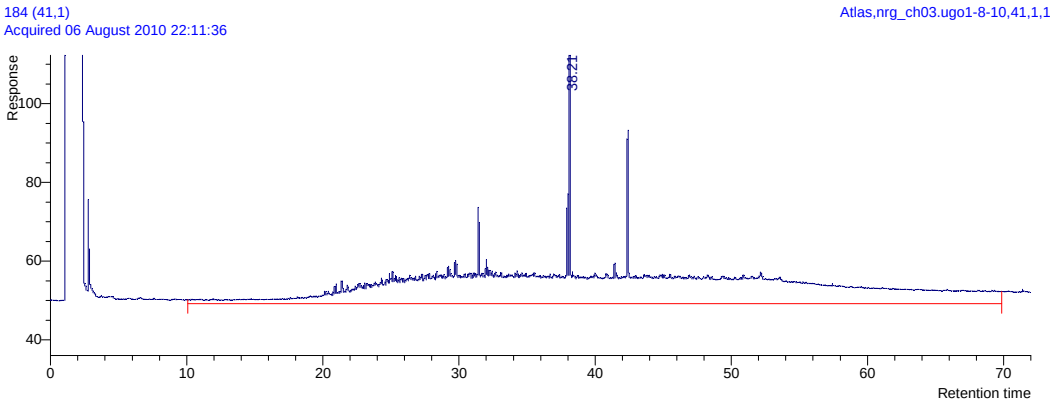

Figure 5.18 Chromatogram (TPH fraction) of Control-1*

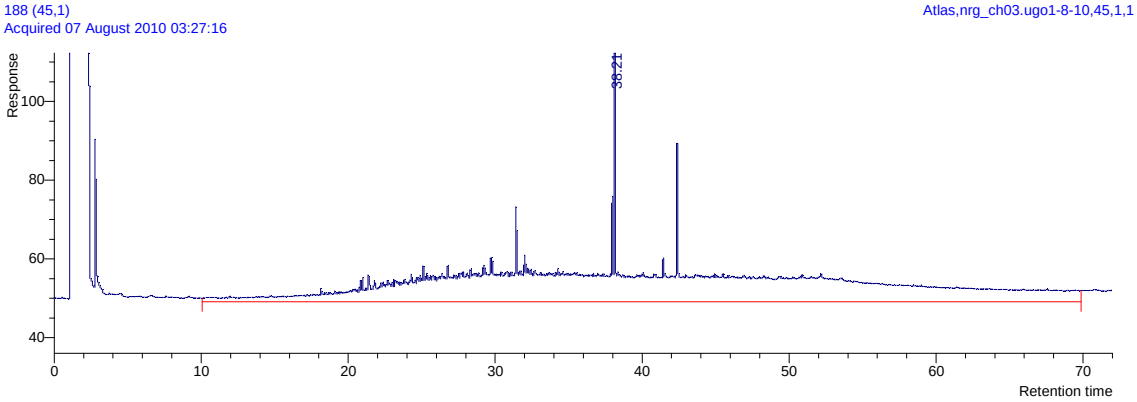

Figure 5.19 Chromatogram (TPH fraction) of BO-liq

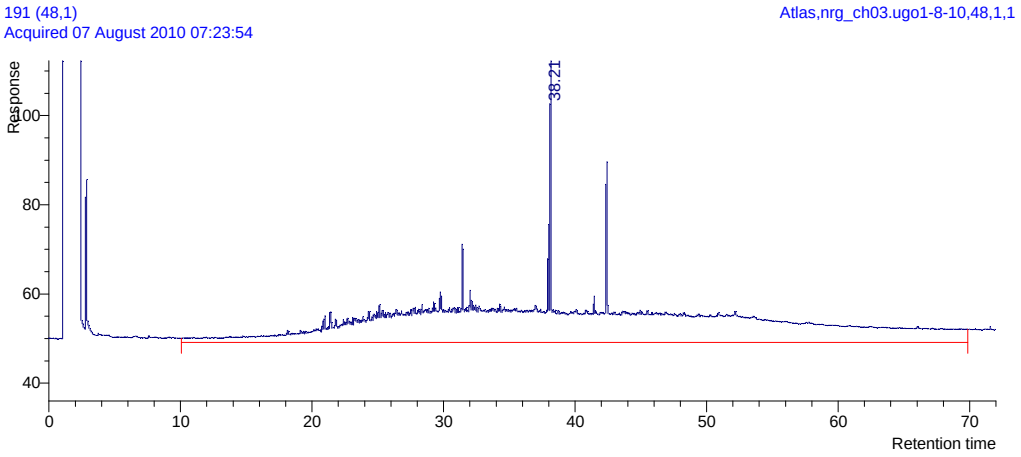

Figure 5.20 Chromatogram (TPH fraction) of SO-liq

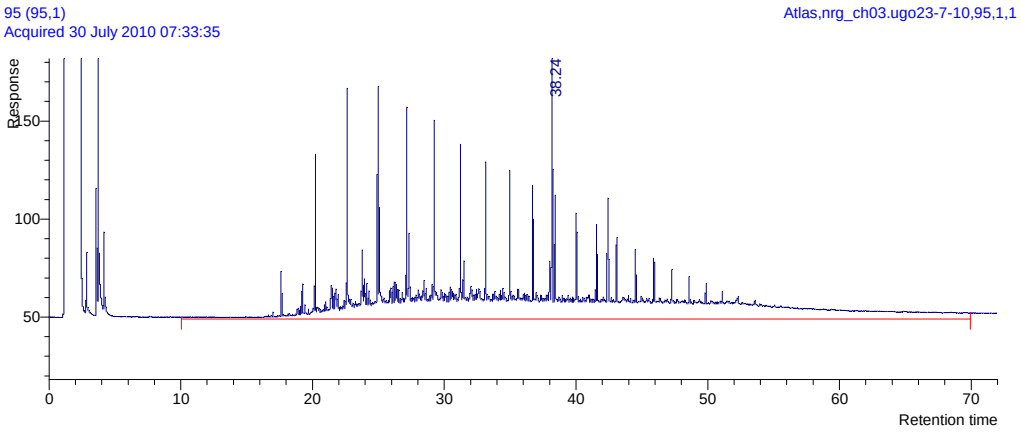

Figure 5.21 Chromatogram (TPH fraction) of Control-2*

The chromatograms as shown in Figures 5.18-5.21 indicate that the samples, BO-liq, SO-liq and Control1* have the same degree of biodegradation unlike in Control-2* where there was no microbial activity.

The nC17/pristane and nC18/phytane ratios for these samples are as given in Table 5.6

Table 5.6 nC17/pristane and nC18/phytane-bactericidal effect of organoclay

Sample	nC17/pristane	nC18/phytane
SO-liq	NM	NM
BO-liq	NM	NM
Control-1*	NM	NM
Control-2*	2.0	2.1

Table 5.6 shows that there is no microbial activity with the negative control (control-2*) as the nC17/pristane and nC18/phytane ratios are 2.0 and 2.1 respectively. The chromatograms as shown in Figures 5.18-5.21 indicate that n-alkanes and isoprenoids were substantially degraded by the microbes. Figures 5.17-5.21 indicate that the organoclay samples inhibited biodegradation as a result of their inherent nature and not because of free DDDMA Br.

5.3.5 Adsorption with unmodified, acid activated and organoclays

The behaviour of the clay samples (acid activated, organo and unmodified clay samples) with respect to adsorption are compared in Figures 5.22 and 5.23.

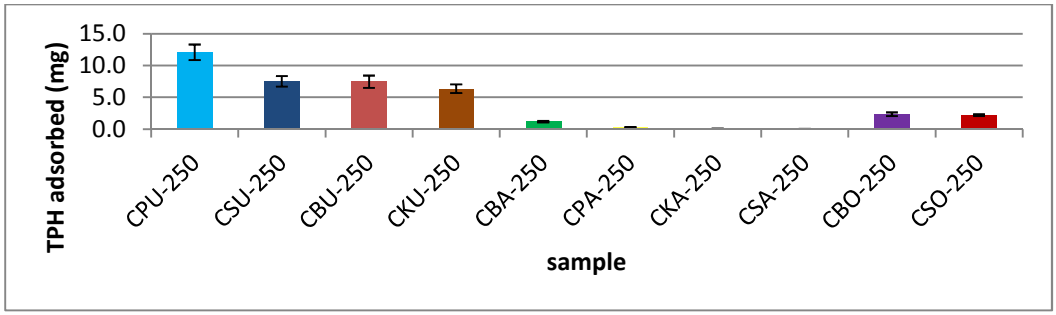

Figure 5.22 TPH adsorbed for unmodified, acid activated and organo clay samples. Values are reported as mean ± one standard error.

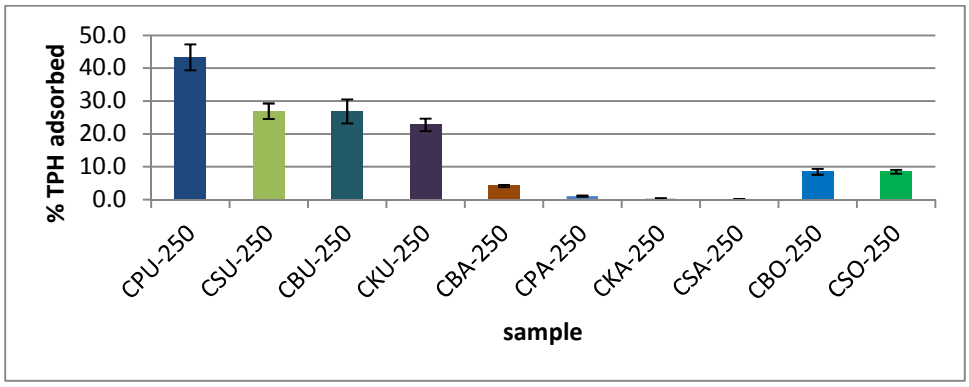

Figure 5.23 TPH (%) adsorbed for unmodified, acid activated and organoclay samples. Values are reported as mean ± one standard error.

The 2-sample t-test at 95% confidence interval (CI) performed to analyse for differences that may be statistically significant with respect to adsorption (on % adsorbed basis) indicate that unmodified palygorskite behaved differently from all other unmodified clay mineral samples as can be seen from their P-values as every other unmodified clay mineral sample behaved alike with comparable extent of adsorption as also indicated by their P-values amongst themselves (Appendix 5.4). The explanations of why unmodified palygorskite behaves this way, with good adsorptive capacity for crude oil hydrocarbons has been explained in section 5.5. As was observed, adsorption by unmodified kaolinites though comparable with unmodified bentonites and unmodified saponites was the least.

The general trend of the removal of TPH via biodegradation and adsorption is presented in the chart below.

The removal of TPH on a weight basis by both biodegradation and adsorption is as shown in Figure 5.24.

5.3.6 Biodegradation and Adsorption compared for unmodified, acid activated and organoclays

In this section a chart is presented to show the general trend of the effect of the clay samples (acid activated clay, organoclay and unmodified clay) with respect to biodegradation and adsorption (Figure 5.24).

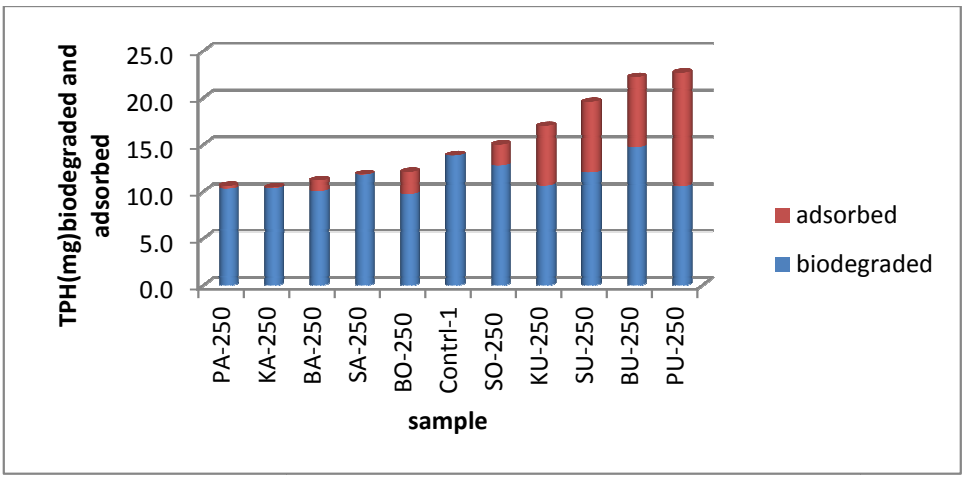

Figure 5.24 TPH(weight basis) as biodegraded and adsorbed with acid-activated clay minerals, organoclay minerals and unmodified clay minerals. Values are reported as mean

Figure 5.24 indicates that generally, biodegradation and adsorption increase from acid activated clay samples to unmodified clay mineral samples. Acid activated clay minerals and organoclay minerals appear to inhibit biodegradation and show minimum adsorption of the TPH.

Overall, removal of hydrocarbons is highest with unmodified palygorskite and bentonite in comparison with other unmodified clay mineral samples but significant part of the removal of TPH with palygorskite is due to adsorption as shown in Figure 5.24. Unmodified palygorskite shows an exceptional adsorptive capacity for the hydrocarbons as evidenced by significant TPH adsorption.

5.3.7 Effect of homoionic interlayer-cation clay minerals on hydrocarbon biodegradation

The effect of several interlayer-cation-exchanged clay minerals such as Na-bentonite, K-bentonite, Mg-bentonite, Ca-bentonite, Zn-bentonite, Al-bentonite, Cr-bentonite and Fe-bentonite on biodegradation of clay minerals is presented in this section (Figures 5.25-5.30). The nC17/pristane and nC18/phytane ratios are presented in Table 5.7.

Table 5.7 nC17/pristane and nC18/phytane- effect of homoionic interlayer-cation. NM = not measurable

Sample	nC17/pristane	nC18/phytane
B-Na	NM	NM
B-K	NM	NM
B-Mg	NM	NM
B-Ca	NM	NM
B-Zn	NM	NM
B-Al	NM	NM
B-Cr	NM	NM
B-Fe	NM	NM
Control-1	NM	NM
Control-2	2.0	2.1
CB-Na	2.0	2.1
CB-K	2.0	2.1
CB-Mg	2.0	2.1
CB-Ca	2.0	2.1
CB-Zn	2.0	2.1
CB-Al	2.0	2.1
CB-Cr	2.0	2.1
CB-Fe	2.0	2.1

Table 5.7 shows that the negative control samples have nC17/pristane and nC18/phytane ratios of 2.0 and 2.1 respectively indicating that there was no microbial activity. See also chromatograms in Appendix 5.7D-5.7F. The hydrocarbons in the test samples had undergone microbial degradation to the degree that the n-alkanes and acyclic isoprenoids are biodegraded. See Appendix 5.7D-5.7F

The result of the residual TPH after incubation for all samples (both the test and controls) are presented in Figure 5.25.

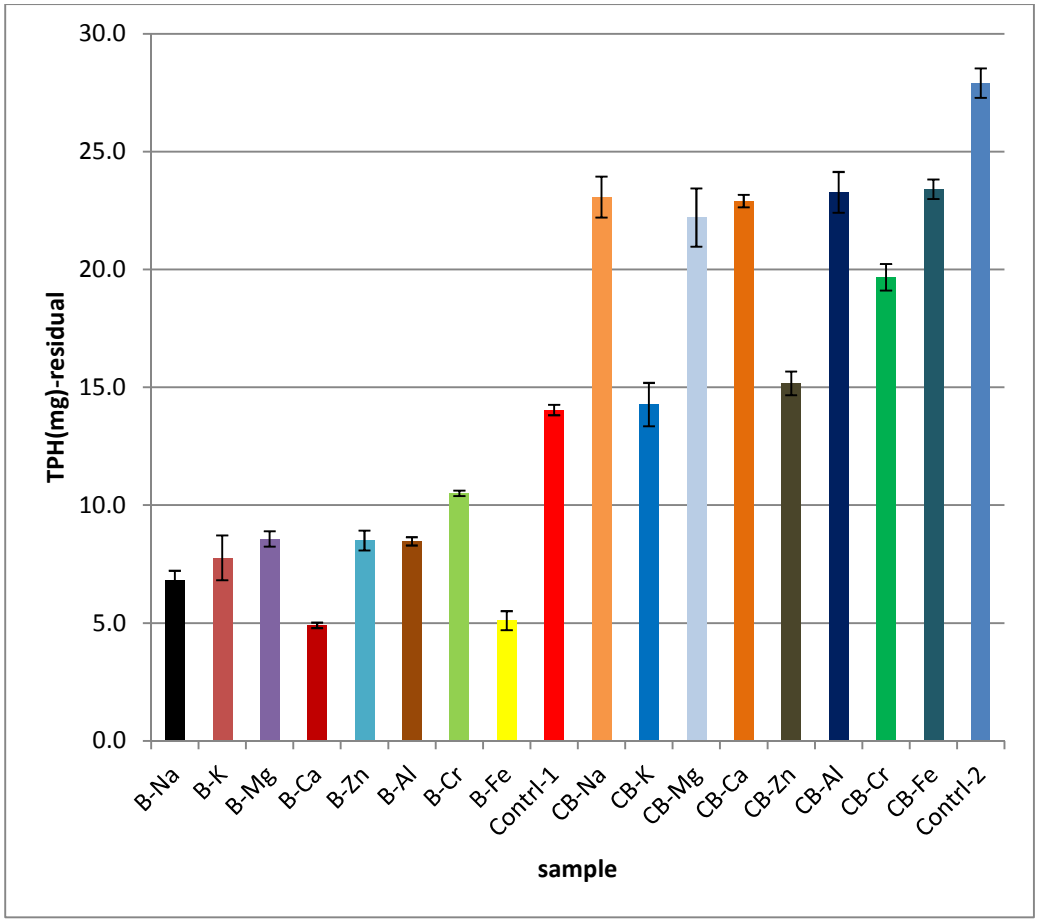

Figure 5.25 Residual TPH after biodegradation of crude oil hydrocarbons supported on the homoionic interlayer clay samples. B-Na = sodium-bentonite, CB-Na = sodium-bentonite control, B-K = potassium-bentonite, CB-K = potassium-bentonite control, B-Mg = magnesium-bentonite, CB-Mg = magnesium-bentonite control, B-Ca = Calcium-bentonite, CB-Ca = calcium-bentonite control, B-Zn = zinc-bentonite, CB-Zn = zinc-bentonite control, B-Al = aluminium-bentonite, CB-Al = aluminium-bentonite control, B-Cr = chromium-bentonite, CB-Cr = chromium-bentonite control, B-Fe = Iron (III)-bentonite, CB-Fe = iron (III)-bentonite control. Values are reported as mean ± one standard error. Control-1 and Control-2 are as earlier defined.

The low residual TPH for B-Ca and B-Fe as shown in Figure 5.25 is an indication that removal of hydrocarbons is highest with these two samples. However, see subsequent Figures (5.26 - 5.30) for portions of the removal that are due to biodegradation and adsorption. Also, of the control samples, two samples, CB-Zn and CB-K have the lowest TPH residual which is an

indication that an abiotic process such as adsorption must have taken place most in these two samples.

The removal of TPH as a result of biodegradation is shown in Figures 5.26 and 5.27 whereas removal of TPH due to adsorption is shown in Figures 5.28 and 5.29.

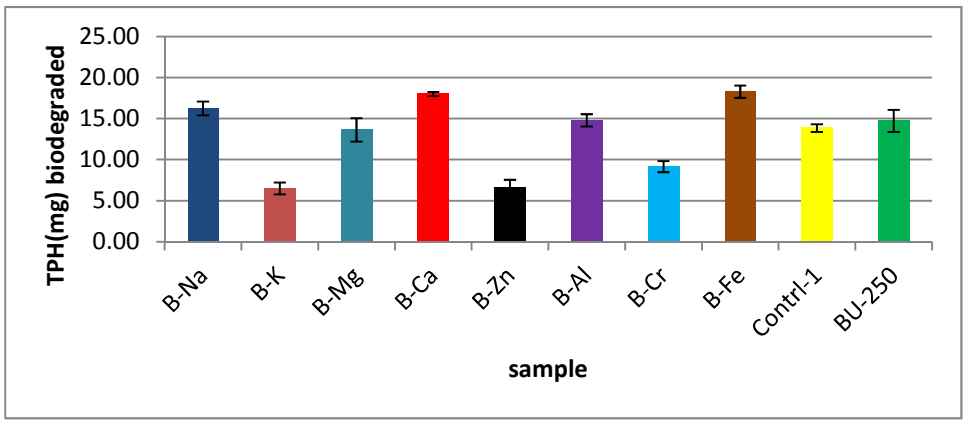

Figure 5.26 TPH biodegraded with homoionic interlayer clays. Values are reported as mean ± one standard error.

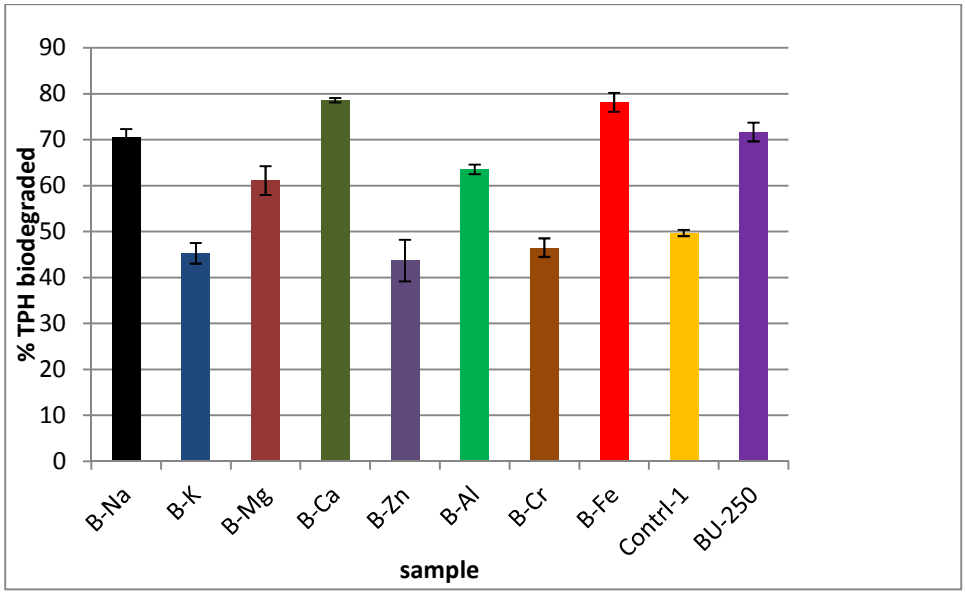

Figure 5.27 Percentage TPH biodegraded with homoionic interlayer clays. Values are reported as mean ± one standard error.

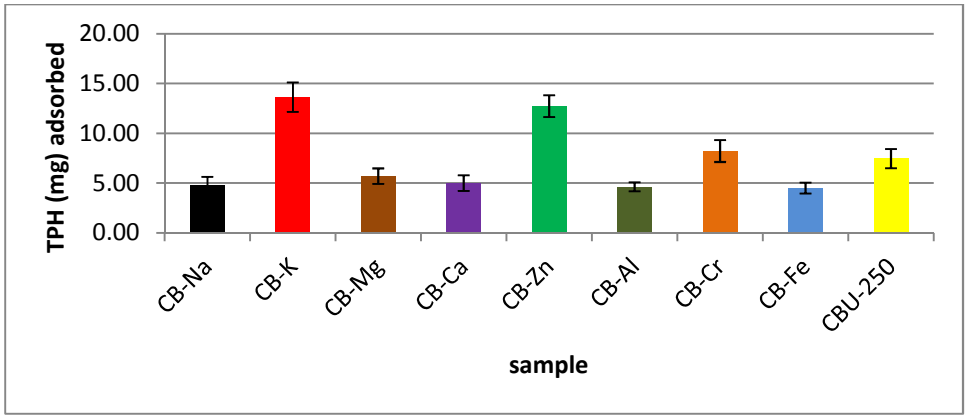

Figure 5.28 TPH removed due to adsorption by homoionic interlayer clays. Values are reported as mean ± one standard error.

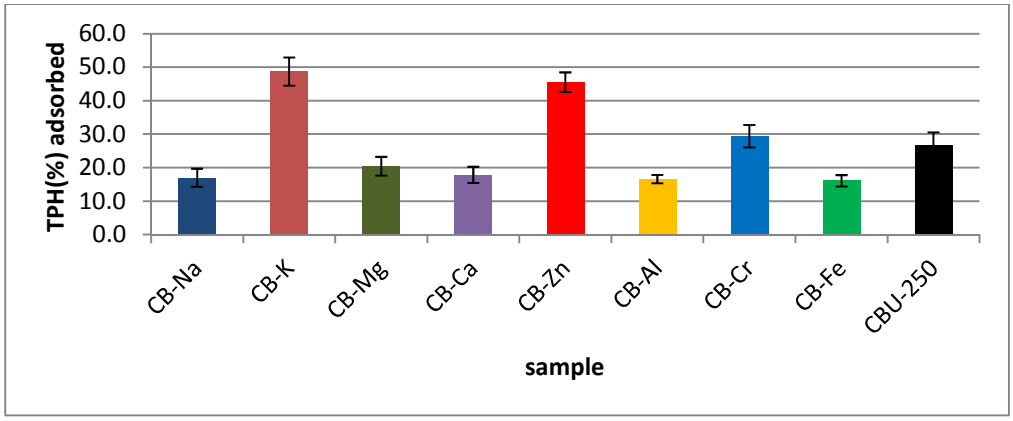

Figure 5.29 Percentage TPH removed due to adsorption by homoionic interlayer clays. Values are reported as mean ± one standard.

The general trend of the effect of the clay samples (homoionic interlayer cations) with respect to biodegradation and adsorption is shown in Figure 5.30.

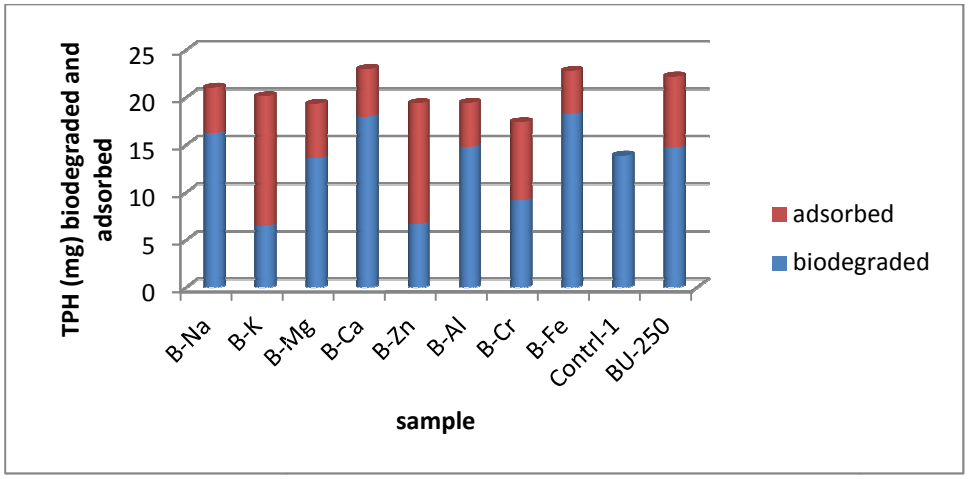

Figure 5.30 Removal of TPH by both adsorption and biodegradation with homoionic interlayer clay samples. Values are reported as mean.

Figure 5.30 shows that the homoionic interlayer clay samples affect both biodegradation and adsorption at varied extents indicating that the cation in the interlayer of clay minerals affects the extent of both biodegradation and adsorption. The 2-sample t-test at 95% confidence interval (CI) performed to analyse for differences that may be statistically significant with respect to biodegradation is as presented in Appendix 5.5. The P-values between B-Ca and control-1 and between B-Fe and Control-1 are very low especially for B-Ca where the P-value between it and Control-1 is zero. This same observation of very low P-value occurs with BU-250 and Control-1 also with B-Na and Control-1. These are all indications that these four clay mineral samples have the potential of enhancing the biodegradation of crude oil hydrocarbons. However, the ranking based on P-value seems to suggest that B-Zn, B-K and B-Cr behave alike as there is no significant statistical difference between B-K and B-Zn and between B-K and B-Cr. Also, there is no significant difference between B-K and Control-1 making it apparent that this group of cation exchanged clay minerals (B-K, B-Cr and B-Zn) behave differently from B-Na, BU-250, B-Ca and B-Fe with respect to supporting biodegradation of crude oil hydrocarbons. The 2-sample t-test at 95% confidence interval (CI) performed to analyse for differences that may be statistically significant with respect to adsorption is presented in Appendix 5.6. The statistical analysis indicate that though the behaviour of B-Cr, B-Zn and B-K are similar with respect to biodegradation of crude oil hydrocarbons as observed in Appendix 5.5, there is a slight difference in behaviour when it comes to adsorption as the P-value now indicates that the

difference in behaviour of B-Cr with respect to adsorption is statistically significant from that of B-K. From the results in Figures 5.26-5.30 and the statistical analysis, it is suggested that B-Na, B-Ca and B-Fe stimulate the biodegradation of crude oil hydrocarbons more than BU-250. However, each appears to show lower response to adsorption than BU-250. It is also observed from the same Figures and Tables that B-K and B-Zn while showing the highest response to adsorption, showed the least capability to support biodegradation.

5.4 Multivariate analysis-cluster analysis

Cluster analysis which is a form of multivariate analysis was used in this section to group the samples that are alike and are different from other samples in other groups. Minitab 15 statistical software was used to generate the dendrogram and other relevant data. The input variables namely, TPH biodegraded, TPH adsorbed and overall TPH removed are presented in Table 5.8

Table 5.8 Comparison of samples with respect to three variables-TPH biodegraded, adsorbed and as removed by both processes.

Sample name	Sample code	TPH (mg) biodegraded	TPH (adsorbed)	Total TPH (mg) Removed
BA-250	1	10.0	1.20	11.2
PA-250	2	10.3	0.3	10.6
KA-250	3	10.4	0.08	10.5
SA-250	4	11.8	0.03	11.8
Control-1	5	13.9	0	13.9
BO-250	6	9.7	2.4	12.1
SO-250	7	12.8	2.2	15.0
KU-250	8	10.6	6.4	17.0
SU-250	9	12.0	7.5	19.5
BU-250	10	14.7	7.5	22.2
PU-250	11	10.6	12.1	22.7
B-K	12	6.5	13.6	20.1
B-Zn	13	6.7	12.7	19.4
B-Cr	14	9.2	8.2	17.4
B-Mg	15	13.6	5.7	19.3
B-Al	16	14.8	4.6	19.4
B-Na	17	16.3	4.8	21.0
B-Fe	18	18.3	4.5	22.8
B-Ca	19	18.0	5.0	23.0

The dendrogram is shown in Figure 5.31.

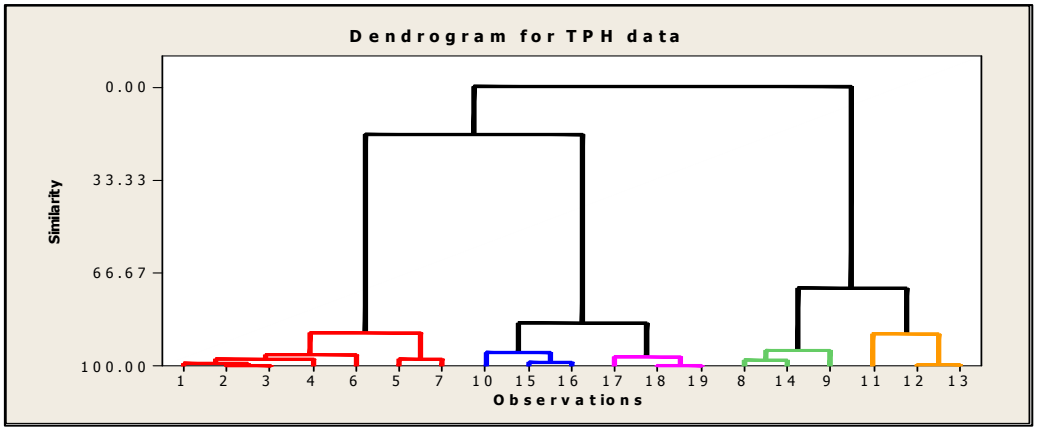

Figure 5.31 Dendrogram for cluster analysis of the samples with respect to adsorption and biodegradation of crude oil hydrocarbons.

Refer to Table 5.8 for sample names and number codes.

Cluster Analysis of Observations: TPH biodegraded, TPH adsorbed, Total TPH removed

Table 5.9 Standardized Variables, Squared Euclidean Distance, Complete Linkage- TPH biodegraded, TPH adsorbed, Total TPH removed

Step	Number of clusters	Similarity level	Distance level	Clusters joined	New cluster	Number of observations in new cluster
1	18	99.9756	0.0042	2 3	2	2
2	17	99.8642	0.0235	18 19	18	2
3	16	99.5790	0.0728	12 13	12	2
4	15	99.4101	0.1021	1 2	1	3
5	14	98.9332	0.1846	15 16	15	2
6	13	97.8554	0.3710	8 14	8	2
7	12	97.7937	0.3817	1 4	1	4
8	11	97.4591	0.4396	5 7	5	2
9	10	96.9473	0.5282	17 18	17	3
10	9	96.0008	0.6919	1 6	1	5
11	8	95.2118	0.8284	10 15	10	3
12	7	94.4123	0.9667	8 9	8	3
13	6	88.6609	1.9618	11 12	11	3
14	5	88.1578	2.0489	1 5	1	7
15	4	84.7785	2.6335	10 17	10	6
16	3	72.2252	4.8054	8 11	8	6
17	2	17.1545	14.3333	1 10	1	13
18	1	0.0000	17.3013	1 8	1	19

Final Partition
Number of clusters: 5

Cluster	Number of observations	Within cluster sum of squares	Average distance from centroid	Maximum distance from centroid
1	7	2.60917	0.572700	0.901791
2	3	0.63058	0.447835	0.544705
3	3	0.56758	0.422660	0.562905
4	3	1.32824	0.631491	0.928015
5	3	0.33836	0.318602	0.466629

From the dendrogram, samples of similarity are grouped together in the same cluster and are drawn in the same colour. However, in the same group, samples of higher similarity are further linked together.

Samples BA-250, PA-250, KA-250, SA-250, BO-250, Control-1 and SO-250 are in the same cluster, cluster 1 and therefore belong to same group.

Samples BU-250, B-Mg and B-Al are members of cluster 2 and therefore belong to same group.

Samples B-Na, B-Fe and B-Ca are members of cluster 3 and belong to same group.

Samples KU-250, SU-250 and B-Cr are in the same cluster, cluster 4 and therefore belong to the same group.

Samples PU-250, B-K and B-Zn also are all in cluster 5 and therefore belong to the same group.

Samples in cluster 1 are not expected to enhance the removal of hydrocarbons as they are similar to control 1. This is obvious if we examine both the TPH removed by biodegradation and adsorption.

Generally, samples in cluster 4 appear not to effect significant removal of hydrocarbons through biodegradation in comparison with control-1.

Samples in clusters 2 and 3 especially cluster 3 appear to enhance the removal of hydrocarbons via biodegradation significantly in addition to minor removal via adsorption. These samples especially B-Ca and B-Fe are therefore good candidates for supporting biodegradation of crude oil hydrocarbons.

Samples in cluster 5, achieve removal of hydrocarbons through both biodegradation and adsorption. The removal by adsorption is quite significant while the removal by biodegradation is generally poor except for PU-250 where the ratio of removal by biodegradation to adsorption is approximately 1:1.

5.5 Discussion

In this section, the results presented in previous sections are interpreted. Correlation of the clay properties (CEC & surface area) to biodegradation and adsorption are limited to unmodified and cation exchanged clay samples as they are neither hydrophobic (organo clays are) nor toxic to microbial cells (acid activated clays are somewhat toxic to microbial cells as seen previously).

Table 5.10 Clay properties and TPH biodegraded, adsorbed and overall removal

Sample	CEC (meq /100g)	Surface Area (m^2/g)	TPH (mg)		TPH (%)		Overall TPH removed	
			Biodegr.	Adsor.	Biodegr.	Adsor.	(mg)	(%)
BA-250	-	722	10	1.17	37	4.2	11.17	40
PA-250	-	567	10.3	0.3	37	1.1	10.6	40
KA-250	-	39	10.4	0.08	37	0.3	10.48	37.6
SA-250	-	532	11.8	0.03	42	0.1	11.83	42.4
Contrl-1	-	-	13.9	0	50	0	13.9	50
BO-250	-	471	9.7	2.37	38	8.5	12.07	43.3
SO-250	-	330	12.8	2.23	50	8.5	15.03	53.9
KU-250	3.5	36	10.6	6.4	49	22.7	17	60.9
SU-250	35.4	473	12	7.5	59	26.9	19.5	69.9
BU-250	83.3	645	14.7	7.5	72	26.8	22.2	79.6
PU-250	16.5	502	10.6	12.1	67	43.3	22.7	81.4
B-K	76.4	455	6.5	13.63	45	48.7	20.13	72.2
B-Zn	73.8	525	6.67	12.73	44	45.5	19.4	69.5
B-Cr	83	489	9.17	8.23	46	29.4	17.4	62.4
B-Mg	81.7	522	13.63	5.7	61	20.4	19.33	69.3
B-Al	65.9	513	14.8	4.63	64	16.6	19.43	69.6
B-Na	83	570	16.27	4.77	70	17	21.04	75.4
B-Fe	88	646	18.3	4.5	78	16.1	22.8	81.7
B-Ca	79.1	598	18	5	79	17.8	23	82.4

Table 5.10 shows the various extents of biodegradation and adsorption using different clay minerals.

Table 5.9 is used as the source of the data for correlation of the clay properties (CEC and surface area) to the extent of biodegradation and adsorption discussed subsequently.

The acid activated clay minerals inhibited biodegradation and is believed to do that by lowering the pH of the biodegradation system such that the toxic effect of the acidic medium reduced microbial activity. The clay sample with the lowest pH inhibited the biodegradation of crude oil hydrocarbons most. The pH of the acid activated clay samples (for samples of clay oil ratio of 5:1) was between 4.1 and 4.4 and inhibited the biodegradation mildly. However, for the acid activated clay sample with higher clay/oil ratio-10:1 the pH was 3.6 and the inhibition of biodegradation was quite significant. As the clay/oil ratio was increased from 5:1 to 10:1 therefore, the pH decreased leading to further inhibition of the biodegradation of crude oil hydrocarbons. The microbial communities responsible for biodegradation in this work appear to be active between pH4 and pH10 and inactive (or much reduced activity) below pH4. This result is consistent with the report of Alexander, (1999) that showed that at extremes of acidity or alkalinity, activity of microbes declines. Adsorption is insignificant and is probably due to the lack of interlayer cations. The surface area of the acid activated clay minerals is higher than the other forms of clay samples studied but this did not translate to increased adsorption or biodegradation because of the reasons stated above.

Organoclay was also inhibitory to biodegradation. Organobentonite which is richer in organic cations, was more inhibitory than organosaponite to hydrocarbon biodegradation. This suggests that the richness in organic cation intercalated in clays (which is a function of CEC) will determine the degree of inhibition to biodegradation. Clays with high CEC therefore, will be expected to form organoclay that are rich in organic phase and hence exhibit greater inhibition than clays with low CEC. The EGME- surface area of organoclay is lower than the other types and forms of clay. This is suggested to be mainly due to the existence of hydrophobicity (introduced into the clay by the organic cation) that hinders access to the interlayer surface by the EGME which is polar and hydrophilic. This hydrophobicity which is peculiar to the organoclay promotes interaction with crude oil

hydrocarbons (which are also hydrophobic). This hydrophobic interaction may render the adsorbed hydrocarbons unavailable for both biodegradation and volatilization during incubation. The amount of hydrocarbons adsorbed due to this hydrophobic interaction would be a function of the magnitude of the adsorptive sites of the organoclay. This hydrophobic interaction is suggested to be strong enough to render the hydrocarbons unavailable for biodegradation or volatilization but not strong enough to resist extraction with DCM during the extraction process of the EOM.

Unmodified clay minerals such as bentonite, saponite, kaolinite and palygorskite studied in this work affect biodegradation to varied degrees. Unmodified kaolinite (1:1 clay minerals) hindered biodegradation. Ideally, kaolinite does not have interlayer cations and therefore does not possess the ability to cause 'local bridging effect' (which as a result of reducing electric double layer repulsion, increases the contacts amongst clay, cells and nutrients). In addition to this, Kaolinite has the lowest EGME-surface area and CEC among the unmodified clay samples and indeed all other clay samples studied in this work. Adsorption of crude oil hydrocarbons is also not to the same degree with other unmodified clay samples and may be due to the absence of interlayer cations.

Unmodified bentonite is a dioctahedral 2:1 phyllosilicate with Na^+ as the predorminant interlayer cation (Moore and Reynold, 1997). This clay mineral has the highest ability to stimulate biodegradation of crude oil hydrocarbons among the unmodified clay minerals (see Table 5.9, Figures 5.5- 5.8). It has the highest EGME-surface area and CEC among the unmodified clay samples (Table 5.10). The extensive EGME-surface area of bentonite probably allows the accumulation of nutrients and microbes at its surface making it easier for the microbes to make contact with both the substrate and nutrients hence enhancing biodegradation.

Unmodified saponite has a lower EGME-surface area than both unmodified palygorskite and unmodified bentonite. This may account for why it did not stimulate biodegradation as much as bentonite. The ability of unmodified saponite to adsorb crude oil hydrocarbons is in the same order with that of unmodified bentonite. Because of the unique ability of these clay mineral samples (unmodified bentonite and saponite) to undergo hydration as a result of the attraction of water by cations in the interlayer, there is reduced ability to expose the

hydrophobic siloxane layer leading to reduced ability to adsorb hydrophobic compounds such as hydrocarbons (Bergaya et al., 2006).

Unmodified palygorskite exhibited a distinctive behaviour in that while having the ability to stimulate biodegradation of crude oil hydrocarbons, it also possessed the ability to adsorb hydrocarbons more extensively than any other unmodified clay samples studied. This ability by unmodified palygorskite to adsorb hydrocarbons is attributable to the unique structure of palygorskite in which a continuous tetrahedral sheet with occasional inversion that causes the octahedral sheet to be discontinuous at this point of inversion creates a channel with dimension ~ $4A^0$ by $6A^0$ (Moore and Reynolds, 1997) which can host the crude oil hydrocarbons that are eventually adsorbed.

The EGME-surface area of palygorskite is high and comes after that of bentonite but with a low CEC (Table 5.10). Though there is significant removal of hydrocarbons due to adsorption, there is equally high removal of hydrocarbons due to biodegradation making the overall removal of hydrocarbons by unmodified palygorskite higher than that of unmodified clay samples especially; unmodified kaolinite and unmodified saponite (see Table 5.9, Figure 5.8 and Figure 5.24). Palygorskite has structure that favours both processes.

From this study, it can be suggested that contrary to the study of Warr et al (2009), adsorption of hydrocarbons by palygorskite is significant as it accounts for about 45% of the removal of the hydrocarbons. Adsorption of crude oil hydrocarbons by other unmodified clay samples accounts for about 22%-30% which also is not insignificant (see Table 5.9, Figure 5.23).

The regression analysis and correlation of EGME-surface area to TPH biodegraded and TPH adsorbed are presented in Figures 5.32 and 5.33.

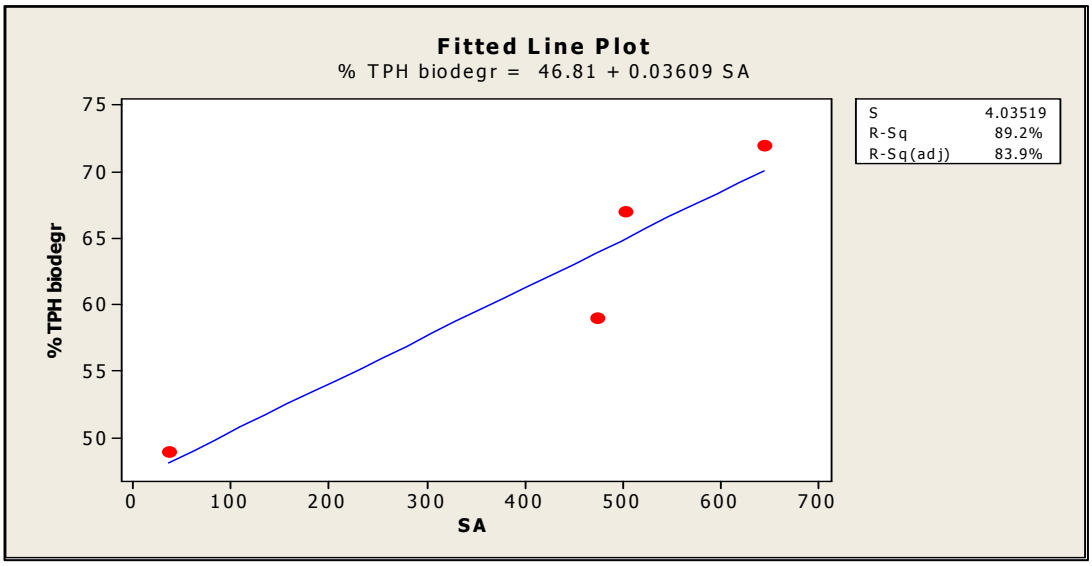

Figure 5.32 Regression analysis- Surface area (SA) with % TPH biodegraded for unmodified clay samples. The Pearson coefficient of correlation (r) of Surface area (SA) of unmodified clay and % TPH biodegraded = 0.945 and p = 0.055.

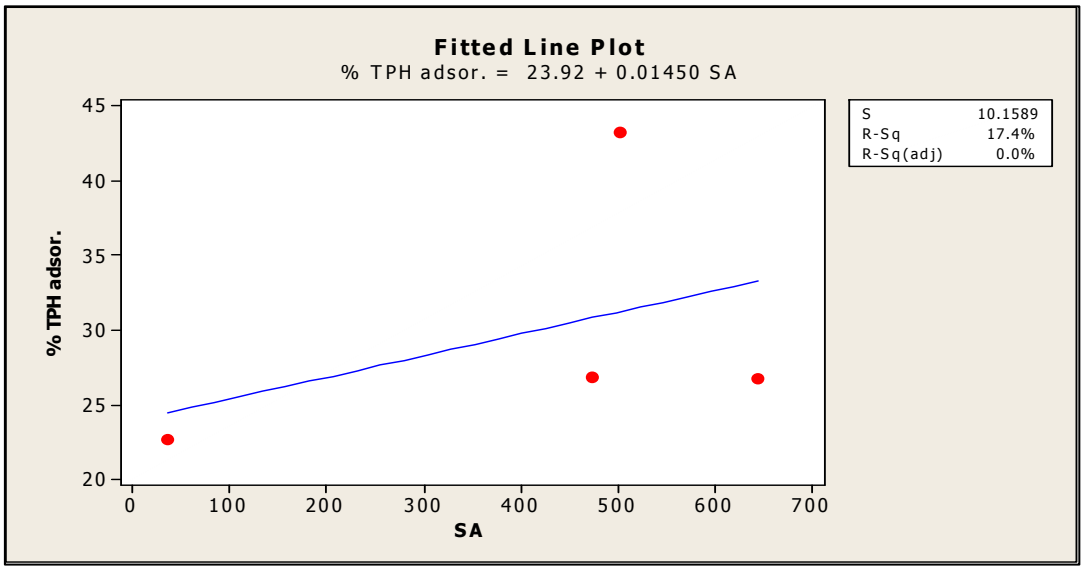

Figure 5.33 Regression analysis- Surface area (SA) with % TPH adsorbed for unmodified clay samples. The Pearson coefficient of correlation (r) of Surface area (SA) of unmodified clay and % TPH adsorbed = 0.418; P = 0. 582.

The regression analysis and correlation of CEC to TPH biodegraded and TPH adsorbed for unmodified clay samples are presented in Figures 5.34 and 5.35.

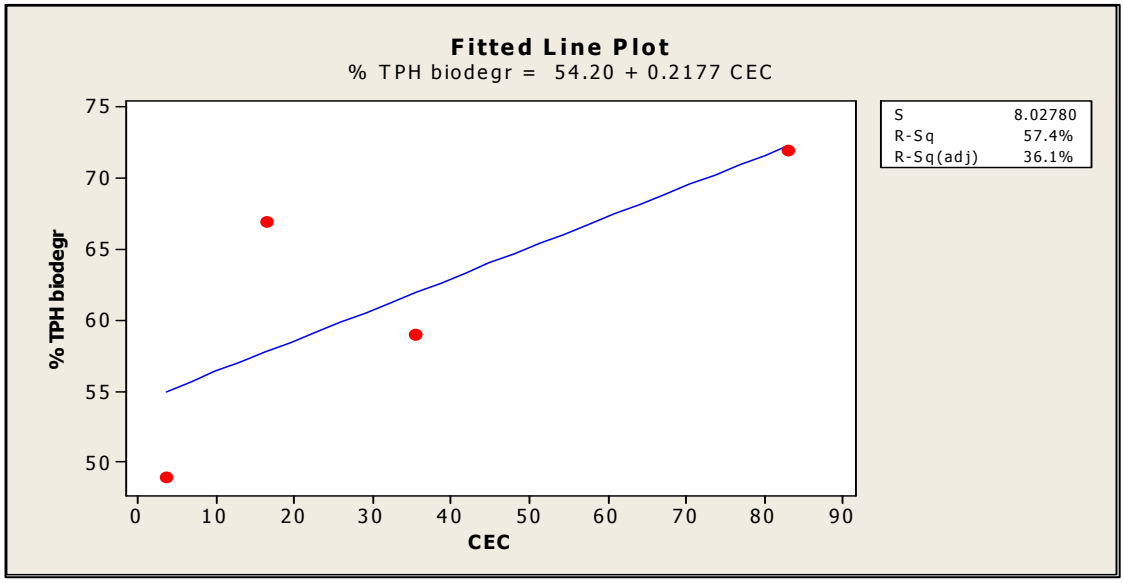

Figure 5.34 Regression analysis- CEC with % TPH biodegraded for unmodified clay samples. The Pearson coefficient of correlation (r) of CEC of unmodified clay and % TPH biodegraded = 0.758; P = 0.242.

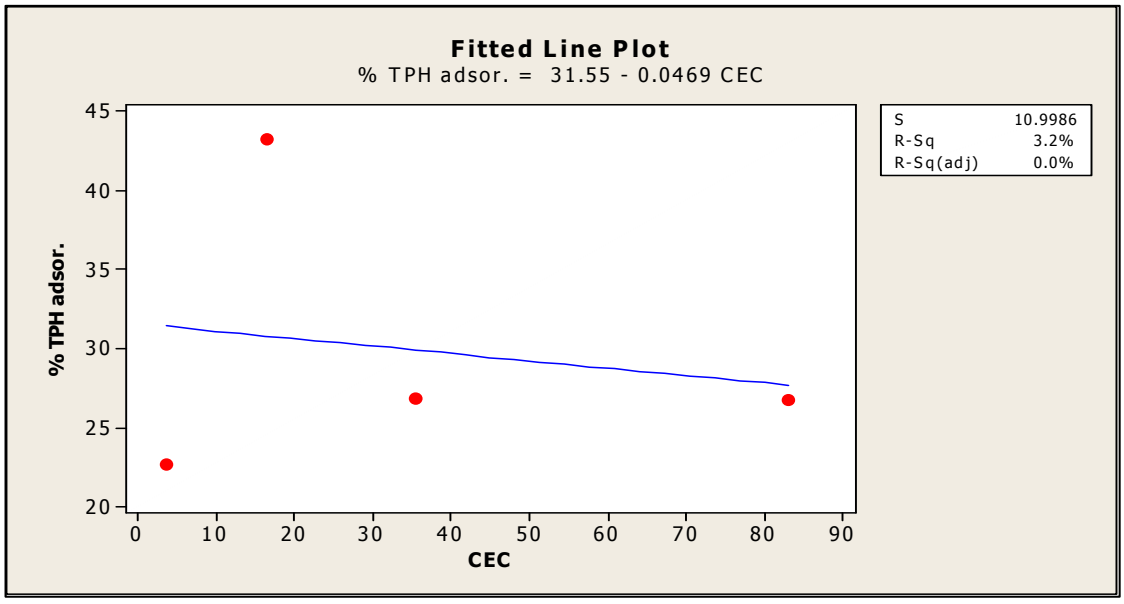

Figure 5.35 Regression analysis- CEC with % TPH adsorbed for unmodified clay samples.

The Pearson coefficient of correlation (r) of CEC of unmodified clay and % TPH adsorbed = -0.180; P = 0.820.

Figures 5.32-5.35 show that the R^2 value and r for the correlation between surface area (SA) and % TPH biodegraded and % TPH adsorbed are higher than those between CEC and the same variables. This indicates that surface area of clay minerals plays a more significant role than CEC during biodegradation of crude oil hydrocarbons.

Also, coefficient of correlation of surface area with % TPH biodegraded is higher than that with % TPH adsorbed indicating that biodegradation in the presence of clay minerals is more dependent on surface area than adsorption.

The regression analysis and correlation of EGME-surface area to TPH biodegraded and TPH adsorbed for homoionic interlayer cation clays samples are presented in Figures 5.36 and 5.37.

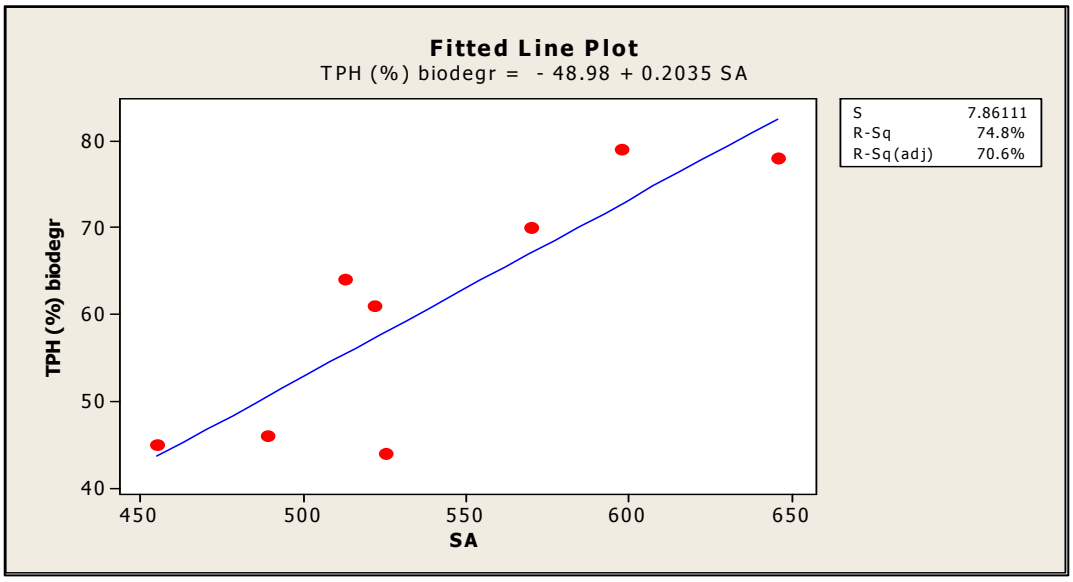

Figure 5.36 Regression analysis- Surface area (SA) with % TPH biodegraded for homoionic interlayer cation clay. The Pearson coefficient of correlation (r) of Surface area (SA) of homoionic interlayer cation clay and % TPH biodegraded = 0.865 and P= 0.006

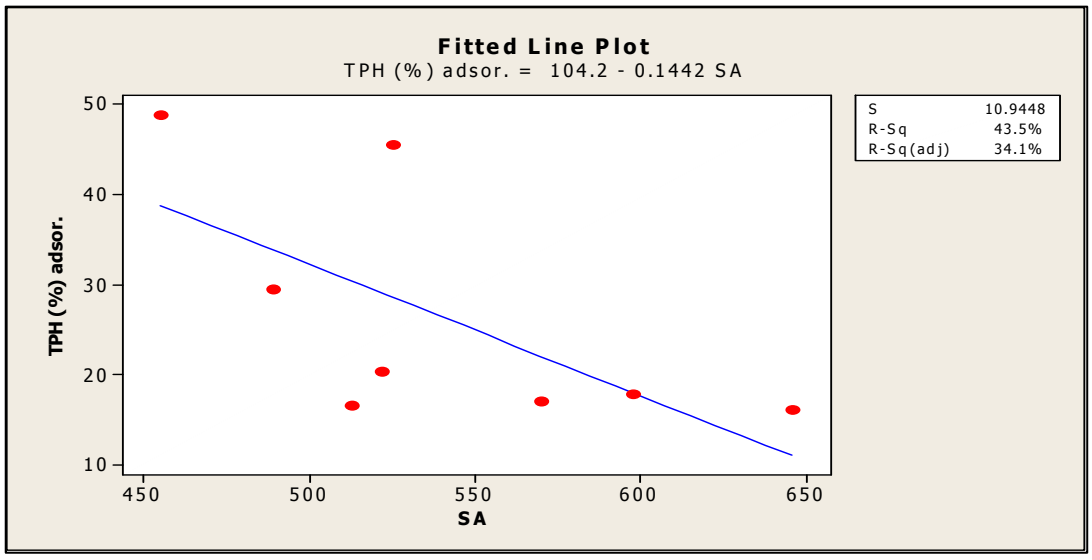

Figure 5.37 Regression analysis- Surface area (SA) with % TPH adsorbed for homoionic interlayer cation clay. The Pearson coefficient of correlation (r) of Surface area (SA) of homoionic interlayer cation clay and % TPH adsorbed = -0.659 and P= 0.075.

The regression analysis and correlation of CEC to TPH biodegraded and TPH adsorbed for homoionic interlayer cation clay samples are presented in Figures 5.38 and 5.39.

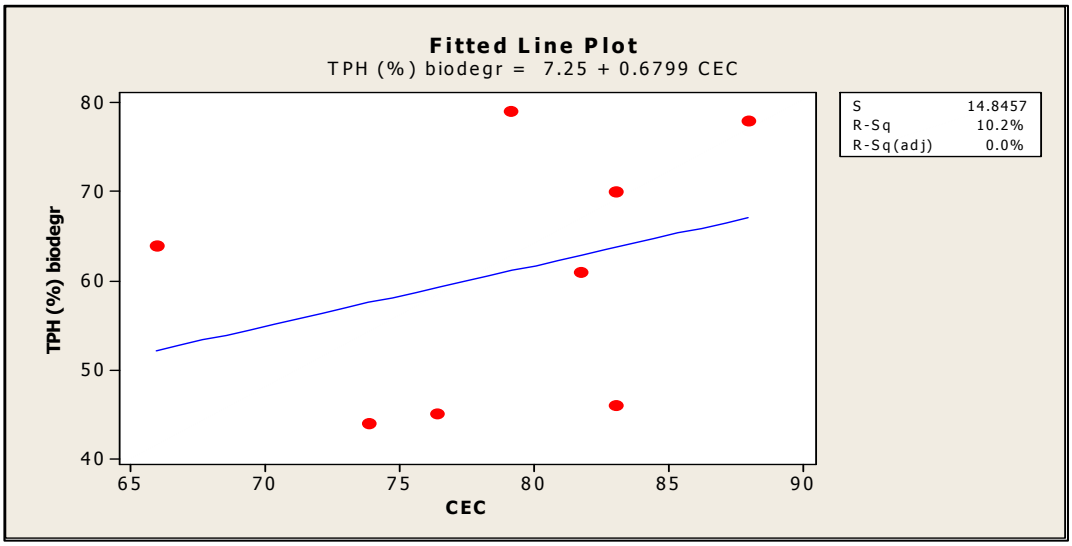

Figure 5.38 Regression analysis- CEC with % TPH biodegraded for homoionic interlayer cation clay. The Pearson coefficient of correlation (r) of CEC of homoionic interlayer cation clay and % TPH biodegraded = 0.320 and P= 0.440

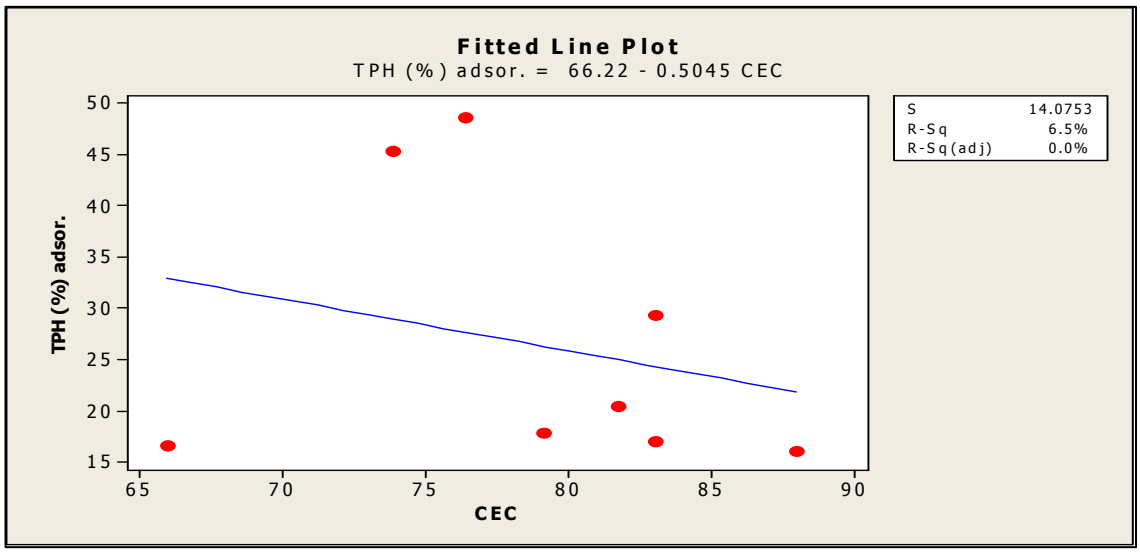

Figure 5.39 Regression analysis- CEC with % TPH adsorbed for homoionic interlayer cation clay. The Pearson coefficient of correlation (r) of CEC of homoionic interlayer cation clay and % TPH adsorbed = -0.255 and P= 0.542

Figures 5.36-5.39 show that the R^2 value and r for the correlation between surface area (SA) of homoionic interlayer cation clays and % TPH biodegraded, and % TPH adsorbed are higher than that between CEC and the same variables. This also indicates that the surface area of clay minerals plays a more significant role than CEC during biodegradation of crude oil hydrocarbons. Also, correlation of surface area with % TPH biodegraded is higher than that with % TPH adsorbed.

The clay samples with homoionic cations at their interlayer as reviewed in section 5.3.7 affected biodegradation and adsorption of the hydrocarbons to varied degrees indicating that the nature of the cation in the interlayer of the clay mineral would influence both processes of biodegradation and adsorption of crude oil hydrocarbons. However, there is no general trend in the extent of biodegradation or adsorption in going from monovalent to trivalent cation in the interlayer of the clay sample.

Between the monovalent cations (Na^+ and K^+) tested, Na-bentonite stimulated biodegradation of the hydrocarbons whereas K-bentonite inhibited the biodegradation. However, K-bentonite showed quite higher ability to adsorb crude oil hydrocarbons than Na-bentonite. The EGME-surface area and CEC of Na-bentonite are higher than that of K-bentonite. It appears that the implication of having K^+ in the interlayer of the clay is that the

attraction of water in the interlayer will be reduced due to the lower hydration energy of K^+ as its charge/radius ratio is relatively low (Jaynes and Boyd, 1991). This makes the interlayer of K-bentonite not as hydrophilic as Na-bentonite and coupled with the fact that K^+ has a relatively large size (that will expose the hydrophobic siloxane surface), this probably caused this clay sample to possess the ability to host hydrocarbons. The same reason of exposure of the hydrophobic siloxane surface accounts for why the surface area of K-bentonite is lower than that of Na-bentonite given that the EGME (which is a polar compound) would not be able to access the exposed hydrophobic siloxane surface in the interlayer of the clay sample.

Among the divalent interlayer cations, Ca-bentonite stimulated biodegradation of crude oil hydrocarbons most, whereas Zn-bentonite inhibited the biodegradation. Mg-bentonite stimulated the biodegradation but not as much as Ca-bentonite. Zn-bentonite showed the highest ability to adsorb crude oil hydrocarbons among the divalent cations. It is not clear how Zn^{2+} in the interlayer of the clay mineral accomplishes this. It has been proposed that Ca-bentonite is able to cause an excellent 'local bridging effect' (see below) that enhances the delivery of the nutrients and substrates to the microbes (Warr et al 2009). This may make Ca-bentonite able to effect significant biodegradation of the hydrocarbons.

Among the trivalent cations, Fe-bentonite achieved the highest stimulation of the biodegradation of crude oil hydrocarbons. Fe-bentonite has the highest CEC and EGME-surface area among all the clay samples studied. Adsorption of hydrocarbons by these clay samples is highest with Cr-bentonite though when compared with K-bentonite and Zn-bentonite, Cr-bentonite adsorbs hydrocarbons least.

Figure 5.40 explains the principle of local bridging effect and its relevance to the stimulation of biodegradation.

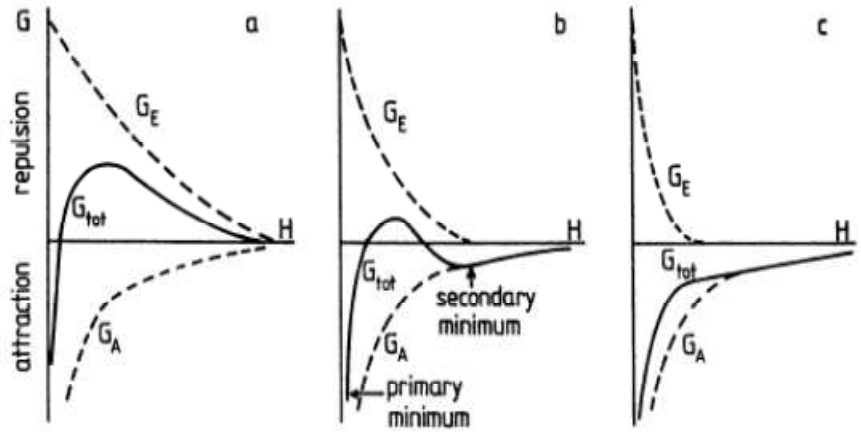

Figure 5.40 Gibb's energy of interaction between a sphere and a flat surface having the same charge sign according to DLVO theory (Rutter and Vincent 1984). Schematic representation for (a) low, (b) intermediate, and (c) high ionic strength. G_E, Electrostatic interaction; G_A, Van der Waals interaction; G_T, Total interaction; H, shortest separation distance between the two surfaces. (Modified from van Loosdrecht etal., 1990).

Particles with Gibb's free energy profile in (a) above where there is no primary or secondary minimum do not possess the ability to overcome the energy barrier due to repulsion and hence will not undergo adhesion whereas particles with higher ionic strength at (b) with primary and secondary minimum and at (c) with primary minimum will have the ability to overcome the energy barrier due to repulsion hence will undergo adhesion. However, adhesion at secondary minimum is not as strong as that at primary minimum and is reversible.

It is therefore believed that interlayer cations of clay minerals especially di and trivalent cations are able to increase the ionic strength of its suspension and hence impact positively on contacts between nutrients, cells and clay surface thereby stimulating microbial growth.

Warr et al (2009) suggested that this 'local bridging effect' produced by the divalent cations was responsible for why Ca-montmorillonite and palygorskite showed better stimulation of biodegradation than sodium-montmorillonite and therefore concluded that divalent cations in the interlayer will achieve a higher extent of biodegradation more than monovalent cations. This study however, has provided evidence that this is not generally true as Na-bentonite achieved a higher extent of biodegradation than Mg-bentonite and Zn-bentonite

which have divalent cations (Mg^{2+} and Zn^{2+}) in the interlayer. The cluster analysis carried out in this study identified Na-bentonite, Ca-bentonite and Fe-bentonite as having similar behaviour with respect to biodegradation of crude oil hydrocarbons eventhough they have different homoionic cations (mono, di and trivalent) in their interlayer respectively. If the 'local bridging effect' were to be the sole factor determining extent of biodegradation, trivalent cations in the interlayer of clay samples would produce the highest 'local bridging effect' and hence stimulate biodegradation most. It therefore follows that other factor(s) in addition to local bridging effect must be contributing to the overall influence of the interlayer cations on biodegradation of crude oil hydrocarbons.

It has been reported that clays dried to very low water contents behave like acids. The dried clay minerals of water content less than 5% have been reported to possess a high surface acidity equivalent to 90% by wt. of sulphuric acid (Theng, 1974; Pinnavaia, 1983; Lazlo, 1987). Interlayer cations have the ability to hydrolyse 'shells' of water in the interlayer of clay minerals producing protons that can increase the Bronsted acidity of the clay suspension(Pinnavaia, 1983; Lazlo, 1987 ; Soma and Soma 1989). The ability of the interlayer cation to hydrolyse the water in the interlayer of the clay mineral is a function of the charge/size ratio of the cation. Trivalent cations have the highest ability to polarize (hydrolyse) the interlayer water followed by divalent cations. This has the effect of reducing the pH of the system especially as the volume of water in the medium decreases which will ultimately reduce microbial activity as observed previously. This acidity (Bronsted acidity) which is common with smectites is derived from the dissociation of water that is directly coordinated to the interlayer cations as explained above. As the polarizing power of the interlayer cations increase, the acid strength increases. The smaller the amount of hydration water present, the greater the polarization of the remaining water molecules hence their ability to donate protons (Frenkel and Heller-Kallai, 1983).

The equilibrium reaction leading to the generation of protons responsible for the Bronsted acidity is as proposed by (Soma and Soma 1989).

$$[M(H_2O)_x]^{n+} \rightleftharpoons [(M(OH)(H_2O)_{x-1}]^{(n-1)+} + H^+ \quad \text{.....5.11}$$

Where:

M is the metal in the interlayer and x and n are integers.

This ability of interlayer cations to generate protons by polarizing interlayer water is suggested to be inhibitory to biodegradation of hydrocarbons. It is therefore also suggested that local bridging effect in addition to hydrolysis of interlayer water may be among the important roles played by the interlayer cations. Whereas local bridging effect will lead to enhanced biodegradation of the crude oil hydrocarbons, hydrolysis of the interlayer water by the interlayer cations is inhibitory to biodegradation of the crude oil hydrocarbons because of toxicity effect of increased acidity.

Ca-bentonite with charge/size ratio that is favourable to minimum hydrolysis of interlayer water would be minimally affected by the adverse effect of water hydrolysis. This could account for why this sample achieves high extent of biodegradation of crude oil hydrocarbons.

Fe (III)-bentonite, despite the inhibitory role of water hydrolysis which it is believed to have effected, was able to enhance biodegradation to almost the same degree as Ca-bentonite implying that the local bridging effect must have been very high. This sample has a very high CEC which could explain why the local bridging effect with this clay sample may have surpassed the other clay samples including Al-bentonite and Cr-bentonite. If the effect of water hydrolysis is suppressed during biodegradation, Fe-bentonite may effect a more significant enhancement of biodegradation than has been observed in this study.

The 2-sample t-test at 95% confidence interval and multivariate (cluster) analysis based on amount (mg) of hydrocarbons biodegraded, adsorbed and total removal by the clay minerals indicate the following:

Samples: BA-250, PA-250, KA-250, SA-250, BO-250, Control-1 and SO-250 are in the same group. Clay minerals in this group did not demonstrate significant differences in comparison with Control-1 with respect to biodegradation and are therefore inhibitory to biodegradation.

Samples: BU-250, B-Mg and B-Al are in the same group. These clay samples (especially BU-250) demonstrated significant percentage biodegradation of the hydrocarbons in comparison with Control-1 in addition to removal of the hydrocarbons via adsorption.

Samples: B-Na, B-Fe and B-Ca are in the same group. These clay samples showed minimum adsorption but significant enhancement of biodegradation of the crude oil hydrocarbons.
Samples KU-250, SU-250 and B-Cr are in the same group. These samples (especially KU-250 and B-Cr) did not demonstrate significant differences with respect to biodegradation in comparison with control-1. However, the overall removal of hydrocarbons which includes adsorption puts these samples outside the group where Control-1 is found. Nevertheless, these clays would not be the ones of choice if consideration is given to removal of hydrocarbons by biodegradation as they are inhibitory to biodegradation.
Samples PU-250, B-K and B-Zn are in the same group. These samples are grouped together principally because of their distinctive ability to adsorb hydrocarbons during biodegradation and adsorption of hydrocarbons by these samples is quite significant. However, B-K and B-Zn were inhibitory to biodegradation.

5.6 Conclusion

The acid activated clay minerals inhibited biodegradation and is believed to do that by lowering the pH of the biodegradation system such that the toxic effect of the acidic medium reduced microbial activity.

Organoclay was also inhibitory to biodegradation. Organobentonite which is richer in organic cations, was more inhibitory than organosaponite to hydrocarbon biodegradation. This suggests that the richness in organic cation intercalated in clays (which is a function of CEC) will determine the degree of inhibition to biodegradation. Clays with high CEC therefore, will be expected to form organoclay that are rich in organic phase and hence exhibit greater inhibition than clays with low CEC.

Unmodified bentonite and unmodified palygorskite are stimulatory to biodegradation of crude oil hydrocarbons and are believed to be able to do that as a result of local bridging effect and high surface area (Warr et al., 2009). Unmodified saponite is neither stimulatory nor inhibitory. Unmodified kaolinite is inhibitory and is suggested to be due to low surface area and lack of interlayer cations to cause local bridging effect. Unmodifed palygorskite has the highest ability to adsorb crude oil hydrocarbons among unmodified clays and is

suggested to be due to its fibrous structure which has channels that can host the hydrocarbons.

Among the homoionic cation interlayer clays, K-bentonite, Zn-bentonite and Cr-bentonite are inhibitory and this is suggested to be due to the ability of these clays especially K-bentonite and Zn-bentonite to adsorb crude oil hydrocarbons extensively. Na-bentonite, Fe-bentonite and Ca-bentonite are more stimulatory to biodegradation of the crude oil hydrocarbons than the other homoionic cation interlayer clays and are believed to be due to 'local bridging effect' and high surface area.

There is no general trend with respect to stimulation of biodegradation of crude oil hydrocarbons among the homoionic cation interlayer samples. The 'local bridging effect' by interlayer cations is suggested not to be the only factor influencing biodegradation. Hydrolysis of interlayer water by interlayer cations is suggested to be a factor that could affect biodegradation of crude oil hydrocarbons by generating protons that will lower the pH of the medium thereby inhibiting the biodegradation of the crude oil hydrocarbons.

6. BIODEGRADATION OF SELECTED CRUDE OIL AROMATICS

6.1 Introduction

There are a handful of biodegradation studies demonstrating the stimulatory role of some clay minerals. Such studies include the biodegradation of starch, uric acid, aldehydes and glucose in the presence of bentonite, montmorillonite and kaolinite (Filip, 1973; Kunc and Stotzky, 1977; Martin et al, 1976). Also reported is the hydrolysis of proteins by pseudomonas specie stimulated by kaolinite (Esterman and McLaren, 1959).

Over the last five years, studies have been carried out to investigate the effect of clay minerals on biodegradation of crude oil and such studies showed that while some clay minerals stimulated the microbial breakdown of hydrocarbons, others did not (Chaerun, 2005; Warr et al, 2009). It has been reported that surfactants produced by some microbes can desorb some aromatic hydrocarbons such as anthracene, phenanthrene and pyrene from solid surfaces such as soil (Liu et al 1991). Hence the surfactants produced by some microorganisms can facilitate the use of sorbed compounds by these microorganisms. However, the biodegradation of crude oil aromatic hydrocarbons supported on clay minerals has not been well reported hence this section of the work is aimed at studying how the various clay minerals affected the various classes of crude oil aromatic hydrocarbons during biodegradation.

In this chapter, the results of the biodegradation of selected aromatic compounds (dimethyl naphthalenes, trimethyl naphthalenes, fluorene and methyl fluorenes, phenanthrene and methyl phenanthrenes, dibenzothiophene and methyldibenzothiophenes, and triaromatic steroids) (for 60 days) supported on clay minerals are presented.

The main questions addressed in this chapter of the project are:

a. Do different clay minerals stimulate or inhibit the biodegradation of the above stated aromatic compounds?

b. Does modification of clays affect their ability to stimulate or inhibit the biodegradation of these aromatic compounds?

c. What factors can explain the different effects of both unmodified clays and modified clays?

6.2 Methods

6.2.1 Quantitation of aromatic compounds (analytes)

The internal standard used in the quantitation of the selected aromatic compounds was 1,1-binaphthyl.

6.2.2 Determination of Percentage biodegradation and adsorption of the selected aromatic compounds

The following equations were used to determine the weight and percentage of the aromatic compounds removed by biodegradation and adsorption.

Aromatic compound-as biodegraded (mg) = $Xcy - Xr$……Eq. 6.1

Aromatic compound-as biodegraded (%) = $\frac{(Xcy-Xr)}{Xcy} * 100$ ……Eq. 6.2

Xcy = weight(mg) of the residual aromatic compound for the clay control sample,

Xr = weight(mg) of the residual aromatic compound for the test sample.

Aromatic compound-as adsorbed (mg) = $Xc2 - Xcy$ ……Eq. 6.3

Aromatic compound-as adsorbed (%) = $\frac{Xc2-Xcy}{Xc2} * 100$ ……Eq. 6.4

Xc2 is the weight(mg) of the aromatic compound for the control-2.

X_{cy} retains its usual meaning.

All values are reported as mean ± one standard error.

6.3 Results

6.3.1 Biodegradation of Dimethylnaphthalenes

The results presented in this section considered the biodegradation of the following isomers of dimethylnaphthalene: 1,2-dimethylnaphthalene, 1,5-dimethylnaphthalene, 1,6-dimethylnaphthalene, 1,4+2,3-dimethylnaphthalene, 1,7+1,3-dimethylnaphthalene and 2,6+2,7-dimethylnaphthalene. However, unlike with other aromatic compounds in subsequent sections, the result of the biodegradation of these isomers will be presented as their total and not individual isomers. The effect of unmodified clay samples on biodegradation of dimethylnaphthalenes are presented in Figures 6.1 and 6.2

6.3.1.1 Effect of unmodified clay minerals on biodegradation of dimethylnaphthalenes

The effect of unmodified clay samples on biodegradation of dimethylnaphthalenes are presented in Figures 6.1 and 6.2

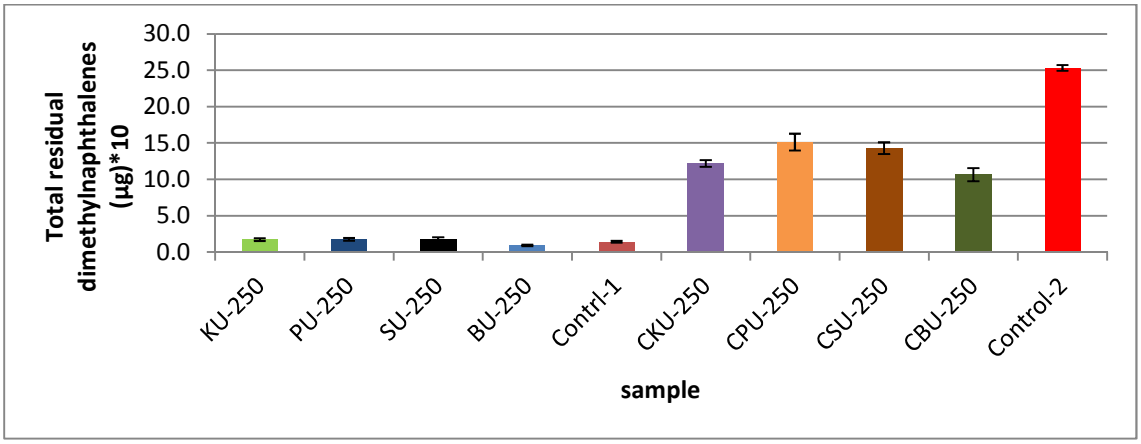

Figure 6.1 Residual dimethylnaphthalenes after biodegradation supported on unmodified clays. BU-250 = unmodified bentonite, CBU-250 = unmodified bentonite control, PU-250 = unmodified palygorskite, CPU-250 = unmodified palygorskite control, SU-250 = unmodified saponite, CSU-250 = unmodified saponite control, KU-250 = unmodified kaolinite, CKU-250 = unmodified kaolinite control, Control-1 = Positive control (BH + oil + cells) no clays, Control-2 = Negative control (BH + oil) no cells and no clays. Values are reported as mean ± one standard error.

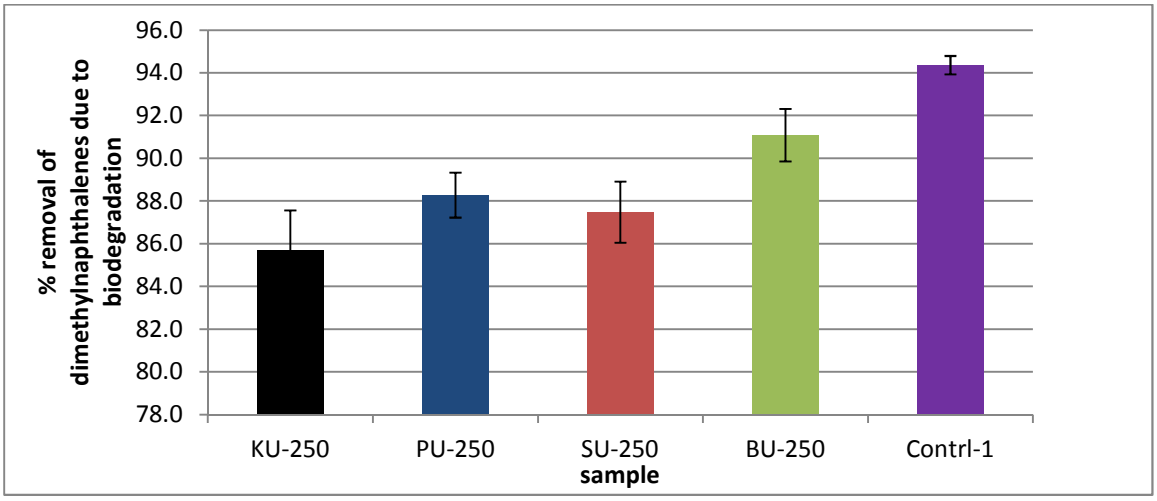

Figure 6.2 Percentage biodegradation of dimethylnaphthalenes supported on unmodified clays. Values are reported as mean ± one standard error.

Figure 6.1 shows that the residual dimethylnaphthalenes with CKU-250, CPU-250, CSU-250 and CBU-250 are all noticeably less than that of Control-2. This indicates that these control samples (CKU-250, CPU-250, CSU-250 and CBU-250) may have interacted with dimethylnaphthalenes that led to their adsorption. Figure 6.2 shows that the percent removal of dimethylnaphthalenes due to biodegradation is highest with Control-1 indicating that these unmodified clay samples actually inhibit the biodegradation of dimethylnaphthalenes especially with KU-250.

6.3.1.2 Effect of acid activated clay samples on biodegradation of dimethylnaphthalenes

The effect of acid activated clay samples on biodegradation of dimethylnaphthalenes are presented in Figures 6.3 and 6.4.

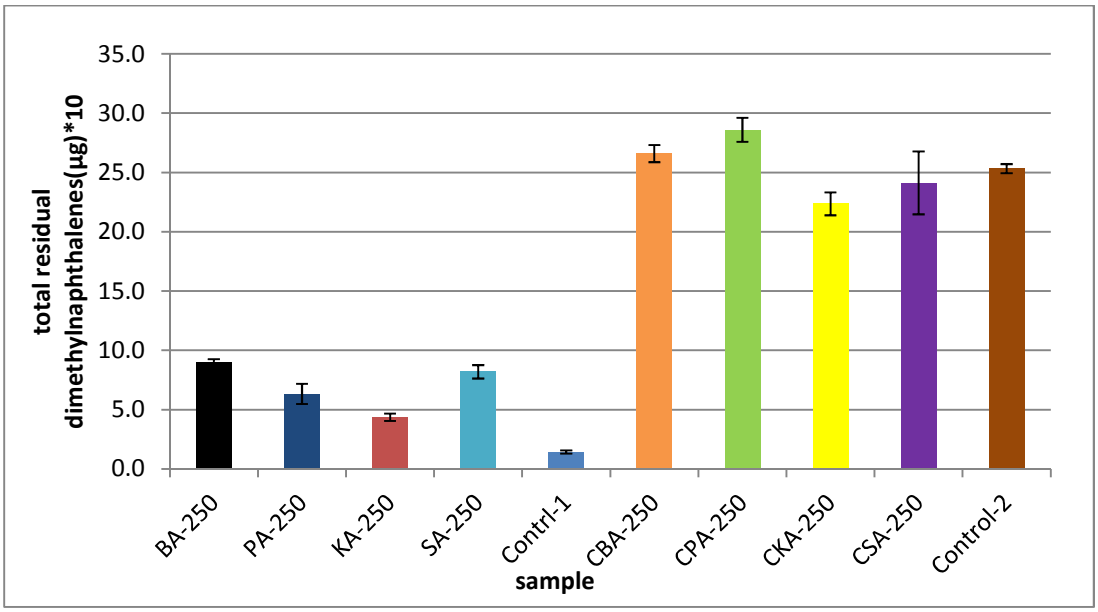

Figure 6.3 Residual dimethylnaphthalenes after biodegradation supported on acid activated clays. BA-250 = acid activated bentonite, CBA-250 = acid activated bentonite control, PA=250 = acid activated palygorskite, CPA-250 = acid activated palygorskite control, SA-250 = acid activated saponite, CSA-250 = acid activated saponite control, KA-250 = acid activated kaolinite, CKA-250 = acid activated kaolinite control. Control-1 and Control-2 retain their descriptions. Values are reported as mean ± one standard error.

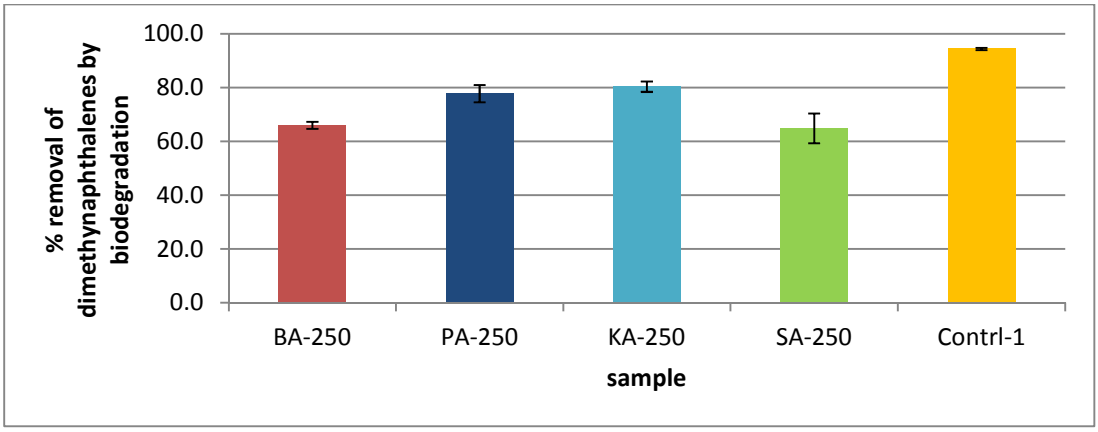

Figure 6.4 Percentage biodegradation of dimethylnaphthalenes supported on acid activated clays. Values are reported as mean ± one standard error.

Figure 6.3 shows that the residual dimethylnapthalenes are lowest with Control-1 and Figure 6.4 shows that the percent removal of dimethylnaphthalenes by biodegradation is highest with Control-1 indicating that the acid activated clay samples actually inhibited the biodegradation of dimethylnaphthalenes.

6.3.1.3 Effect of organo-clay on biodegradation of dimethylnaphthalenes

The effect of organoclay samples on biodegradation of dimethylnaphthalenes are presented in Figures 6.5 and 6.6

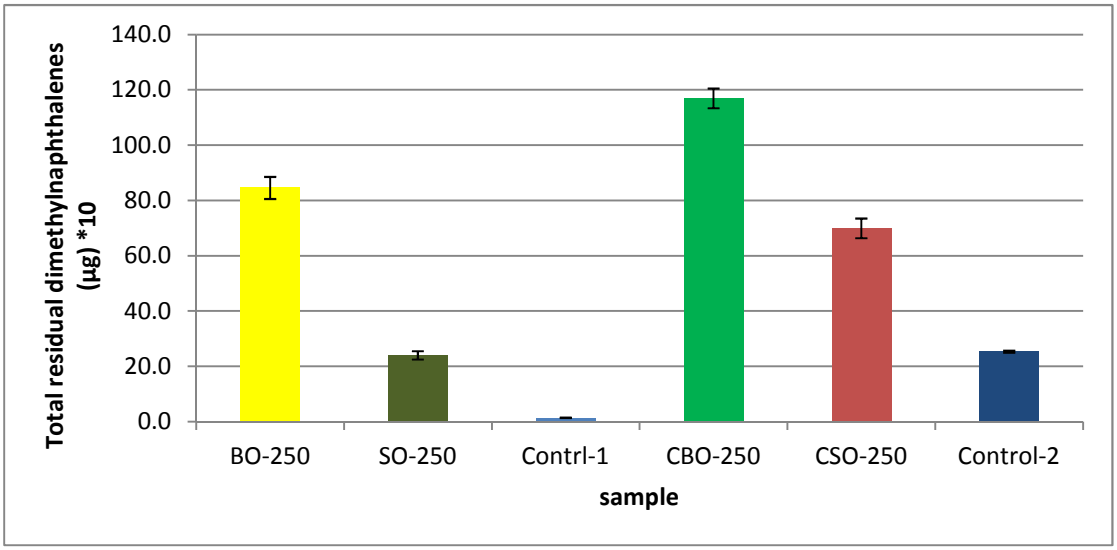

Figure 6.5 Residual dimethylnaphthalenes after biodegradation supported on organoclays. BO-250 = organobentonite; SO-250 = organosaponite; Control-1 =BH + oil + cells. Control-2=

BH + oil. CBO-250 and CSO-250 are clay controls. Values are reported as mean ± one standard error

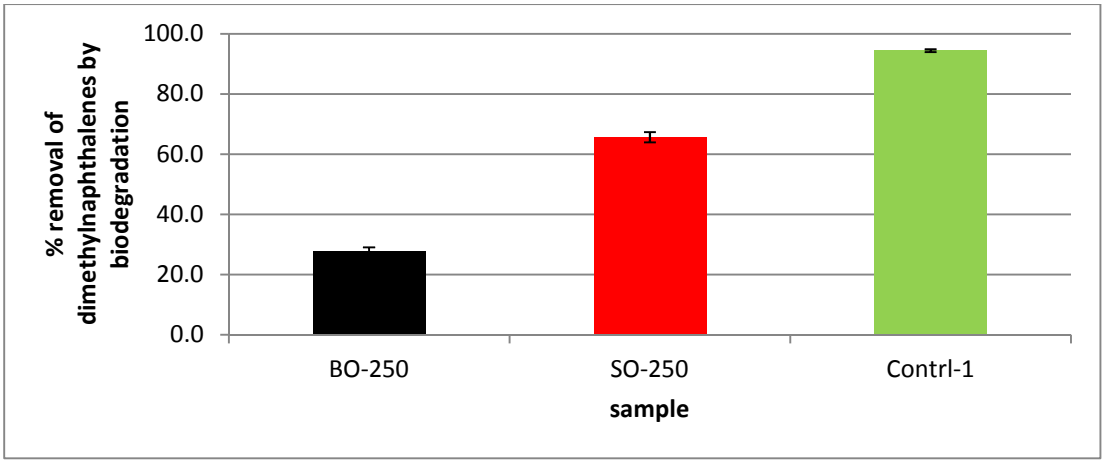

Figure 6.6 Percentage biodegradation of dimethylnaphthalenes supported on organoclays. Values are reported as mean ± one standard error

Figure 6.6 shows that on percentage basis, Control-1 effects more biodegradation than either BO-250 or SO-250 and leads to the conclusion that the organoclay minerals do not improve the biodegradation of dimethylnaphthalenes.

There is also a very strange behaviour as can be seen in Figure 6.5 in which there is a huge difference between CBO and CSO with respect to the residual dimethylnaphthalenes. There is also a huge difference generally between Control-2 and either of CBO-250 or CSO-250. This observation was not made in the case of the other clay controls in Figures 6.1, 6.3 and 6.7. The proposed explanation for this behaviour is given in the discussion section (6.5).

6.3.1.4 Effect of homoionic interlayer cation exchanged clay samples on biodegradation of dimethylnaphthalenes.

The effect of homoionic interlayer cation exchanged clay samples on biodegradation of dimethylnaphthalenes are presented in Figures 6.7 and 6.8.

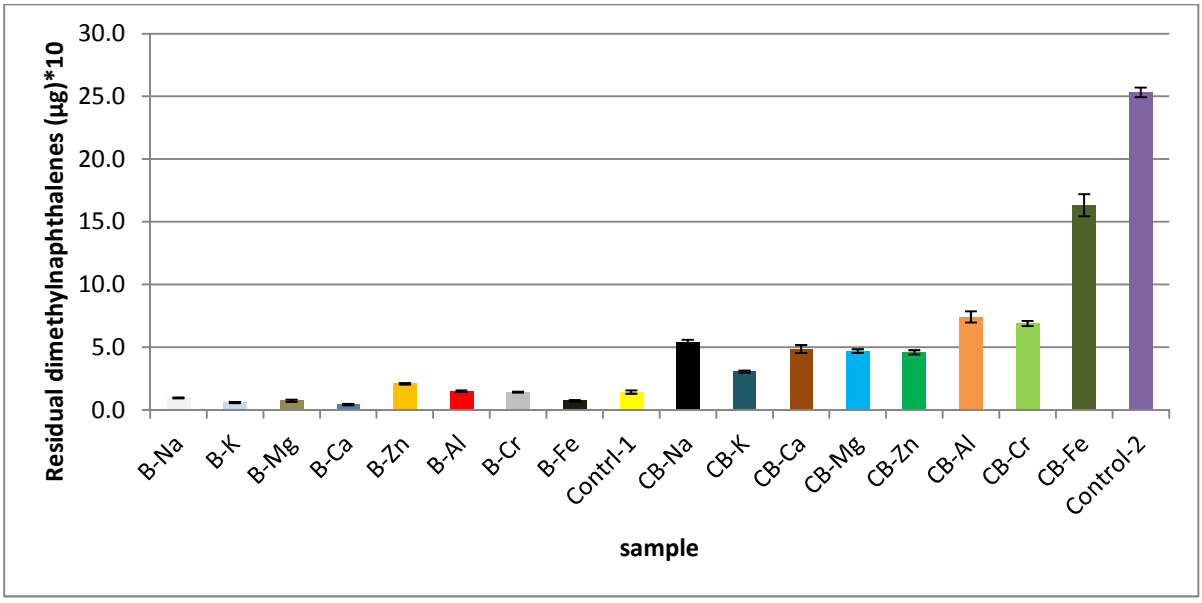

Figure 6.7 Residual dimethylnaphthalenes after biodegradation supported on homoionic cation interlayer clays. B-Na = sodium-bentonite, CB-Na = sodium-bentonite control, B-K = potassium-bentonite, CB-K = potassium-bentonite control, B-Mg = magnesium-bentonite, CB-Mg = magnesium-bentonite control, B-Ca = Calcium-bentonite, CB-Ca = calcium-bentonite control, B-Zn = zinc-bentonite, CB-Zn = zinc-bentonite control, B-Al = aluminium-bentonite, CB-Al = aluminium-bentonite control, B-Cr = chromium-bentonite, CB-Cr = chromium-bentonite control, B-Fe = Iron (III)-bentonite, CB-Fe = iron (III)-bentonite control. Control-1 and Control-2 are as earlier defined. Values are reported as mean ± one standard error

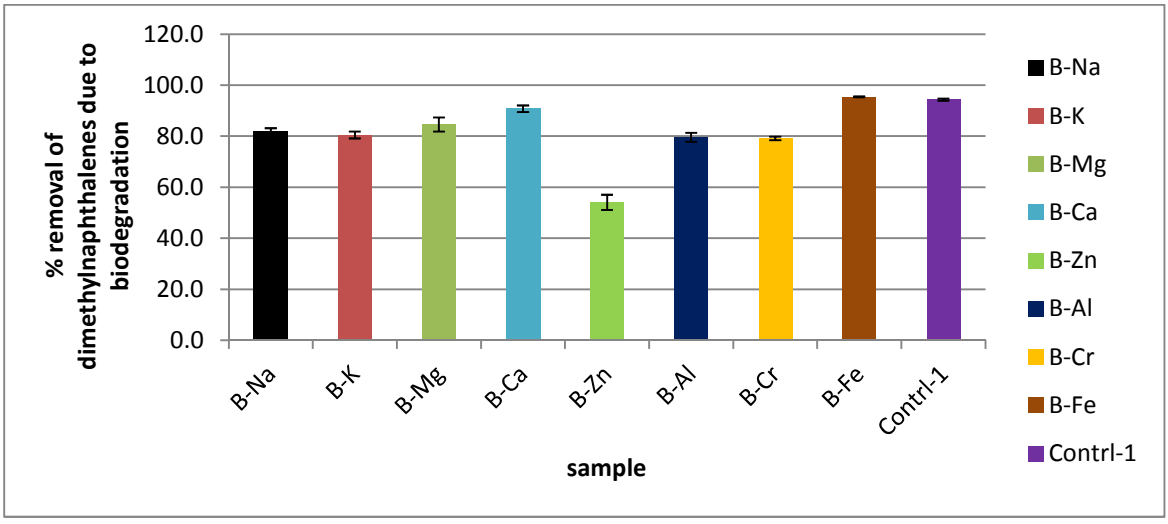

Figure 6.8 Percentage biodegradation of dimethylnaphthalenes supported on homoionic interlayer cation exchanged clays. Values are reported as mean ± one standard error.

Figures 6.7 and 6.8, show that the biodegradation of dimethylnaphthalenes for Control-1, B-Fe and B-Ca are comparable hence there is no improvement of the biodegradation of dimethylnaphthalenes with these samples (B-Fe and B-Ca). However, Control-1 obviously performs better than the rest clay samples with respect to the biodegradation of dimethylnaphthalenes with B-Zn clearly inhibiting the biodegradation of dimethylnaphthalenes.

6.3.2 Biodegradation of Trimethylnaphthalenes

The trimethylnaphthalene isomers that were analysed are: 1,3,7-trimethylnaphthalene, 1,3,6-trimethylnaphthalene, 2,3,6-trimethylnaphthalene, 1,3,5+1,4,6-trimethylnaphthalene and 1,2,7+1,6,7+1,2,6-trimethylnaphthalene.

The result will be presented for the individual isomers on removal by biodegradation on weight basis and for the total isomers (all the isomers collectively) on percent basis.

6.3.2.1 Effect of unmodified clays on biodegradation of trimethylnaphthalenes

The effect of unmodified clay samples on biodegradation of trimethylnaphthalenes are presented in Figures 6.9 and 6.10.

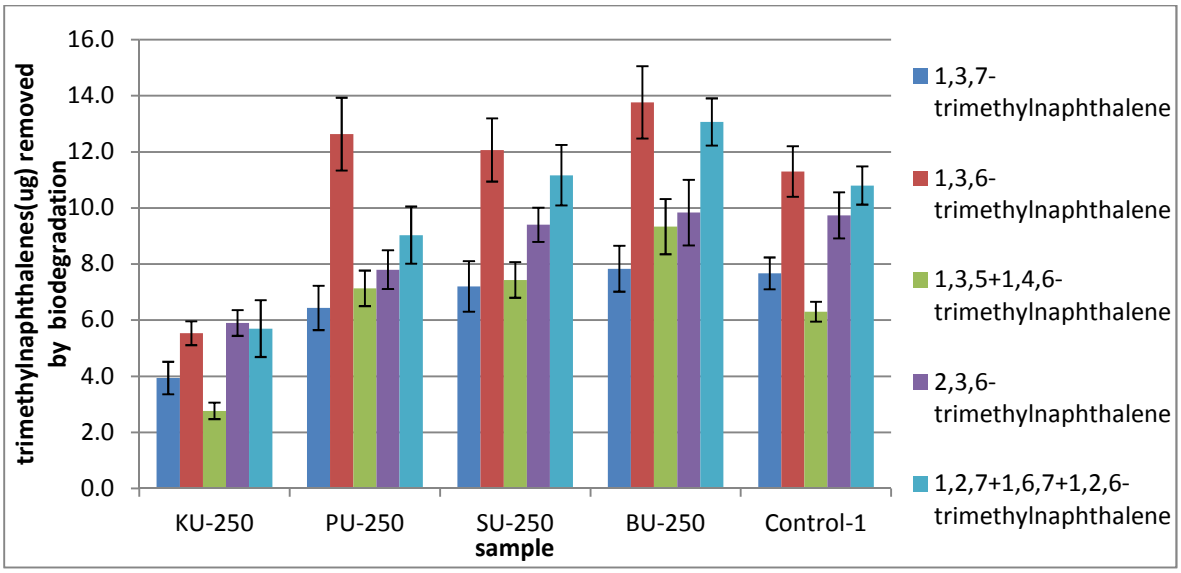

Figure 6.9 Biodegradation of trimethylnaphthalenes (on weight basis) supported on unmodified clays. Values are reported as mean ± one standard error.

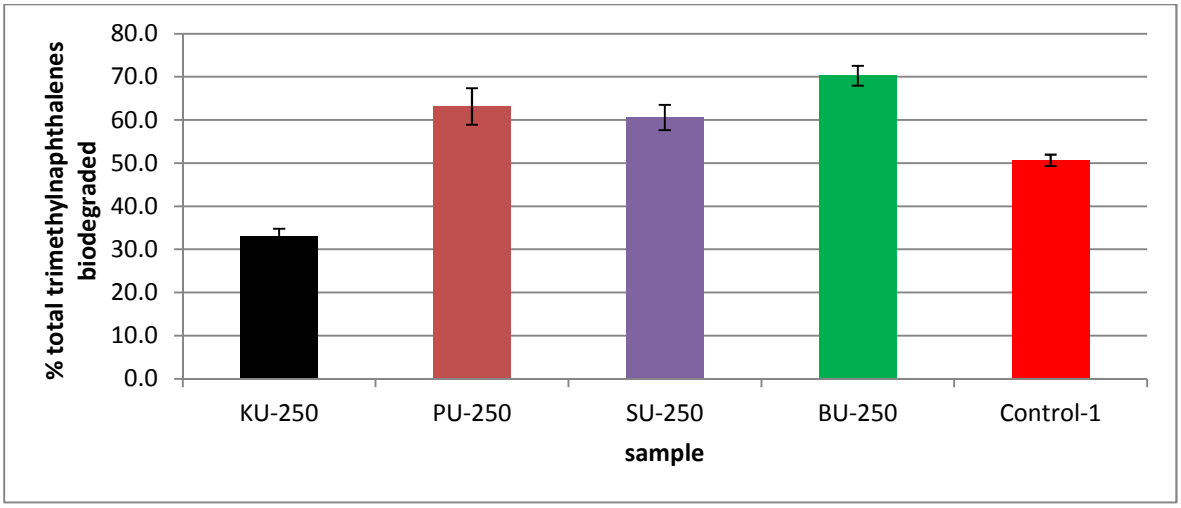

6.10 Percentage biodegradation of summed trimethylnaphthalenes supported on unmodified clays. Values are reported as mean ± one standard error.

The 2-sample t-test at 95% confidence interval (CI) performed to analyse for differences that may be statistically significant is presented in Appendix 6.5A. Figures 6.9 and 6.10 and Appendix 6.5A show that BU-250 significantly improves the biodegradation of trimethylnaphthalenes compared to Control-1 whereas KU-250 actually inhibits it. SU-250 and PU-250 are comparable with control-1 as their P-values indicate that there is no statistical significant difference.

6.3.2.2 Effect of acid activated clay minerals on biodegradation of trimethylnaphthalenes

The effect of acid activated clay samples on biodegradation of trimethylnaphthalenes are presented in Figures 6.11 and 6.12

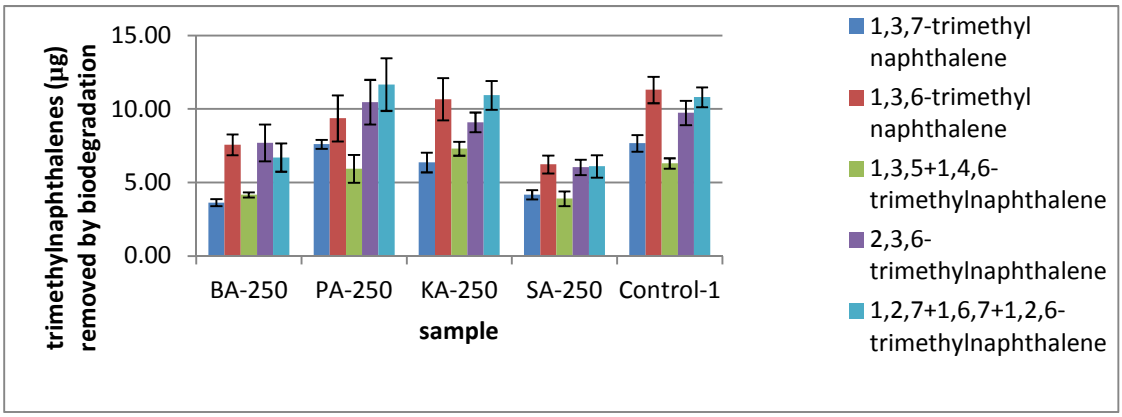

Figure 6.11 Biodegradation of trimethylnaphthalenes (weight basis) supported on acid activated clays. Values are reported as mean ± one standard error.

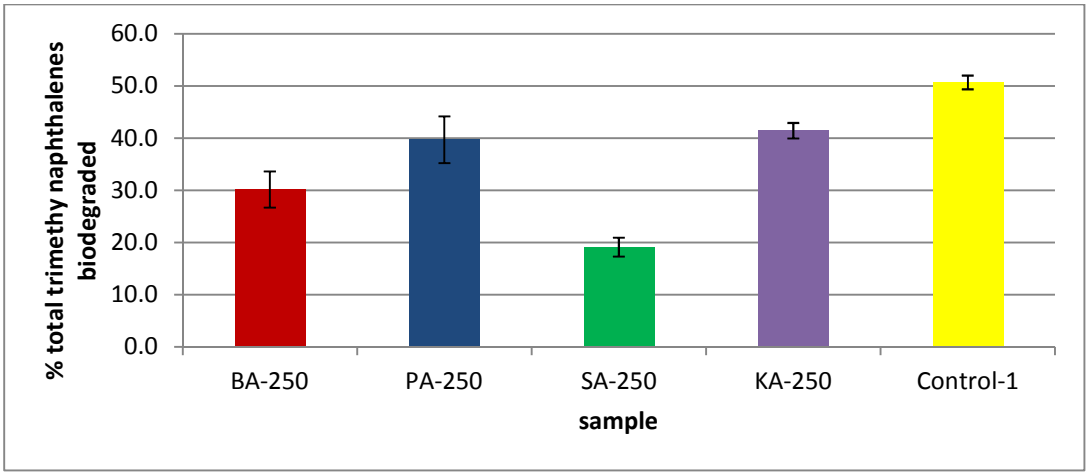

Figure 6.12 Percentage biodegradation of summed trimethylnaphthalenes supported on acid activated clays. Values are reported as mean ± one standard error.

The biodegradation of trimethylnaphthalenes as shown in Figures 6.11 and 6.12 shows that acid activated clay samples especially BA-250 and SA-250 appear not to support the biodegradation of the presented isomers of trimethylnaphthalenes.

6.3.2.3 Effect of organoclay

The effect of organoclay samples on biodegradation of trimethylnaphthalenes are presented in Figures 6.13 and 6.14

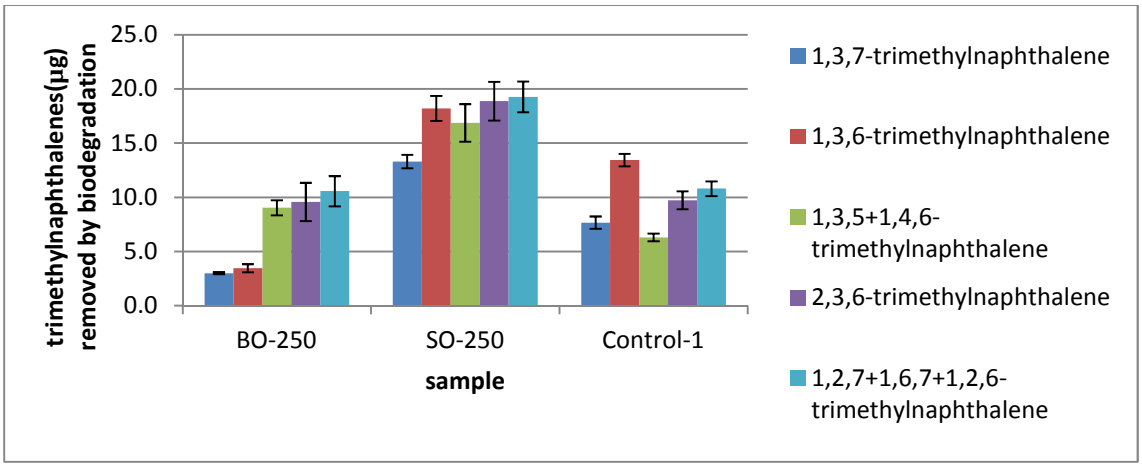

Figure 6.13 Biodegradation of trimethylnaphthalenes (weight basis) supported on organoclay. Values are reported as mean ± one standard error.

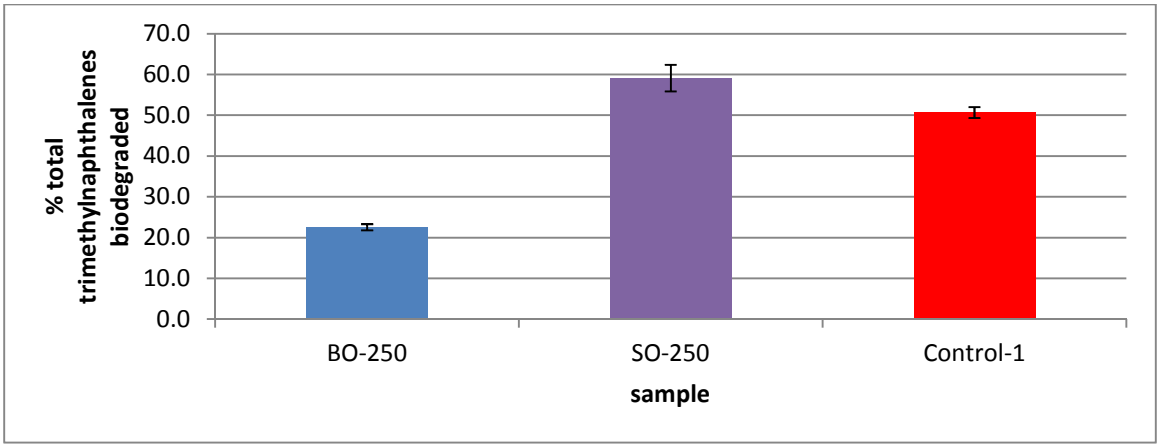

Figure 6.14 Percentage biodegradation of summed trimethylnaphthalenes supported on organoclay. Values are reported as mean ± one standard error.

Figure 6.13 shows that on a weight basis, the biodegradation of the trimethylnaphthalene isomers is higher with SO-250 than either control-1 or BO-250. However, Figure 6.14 shows that on % basis, the biodegradation with SO-250 and Control-1 becomes comparable, with P-value of 0.138 indicating that there is no significant statistical difference between the two samples. This is also an indication that SO-250 does not enhance the biodegradation of trimethylnaphthalenes though it does not inhibit it either.

From both Figures 6.13 and 6.14, BO-250 appears to be inhibitory to the biodegradation of trimethylnaphthalenes as the P-value between BO-250 and SO-250 and between BO-250 and Control-1 are 0.008 and 0.00 respectively.

6.3.2.4 Effect of homoionic interlayer cation exchanged clay samples on biodedgradation of trimethylnaphthalenes

The effect of homoionic interlayer cation exchanged clay samples on biodegradation of trimethylnaphthalenes are presented in Figures 6.15 and 6.16.

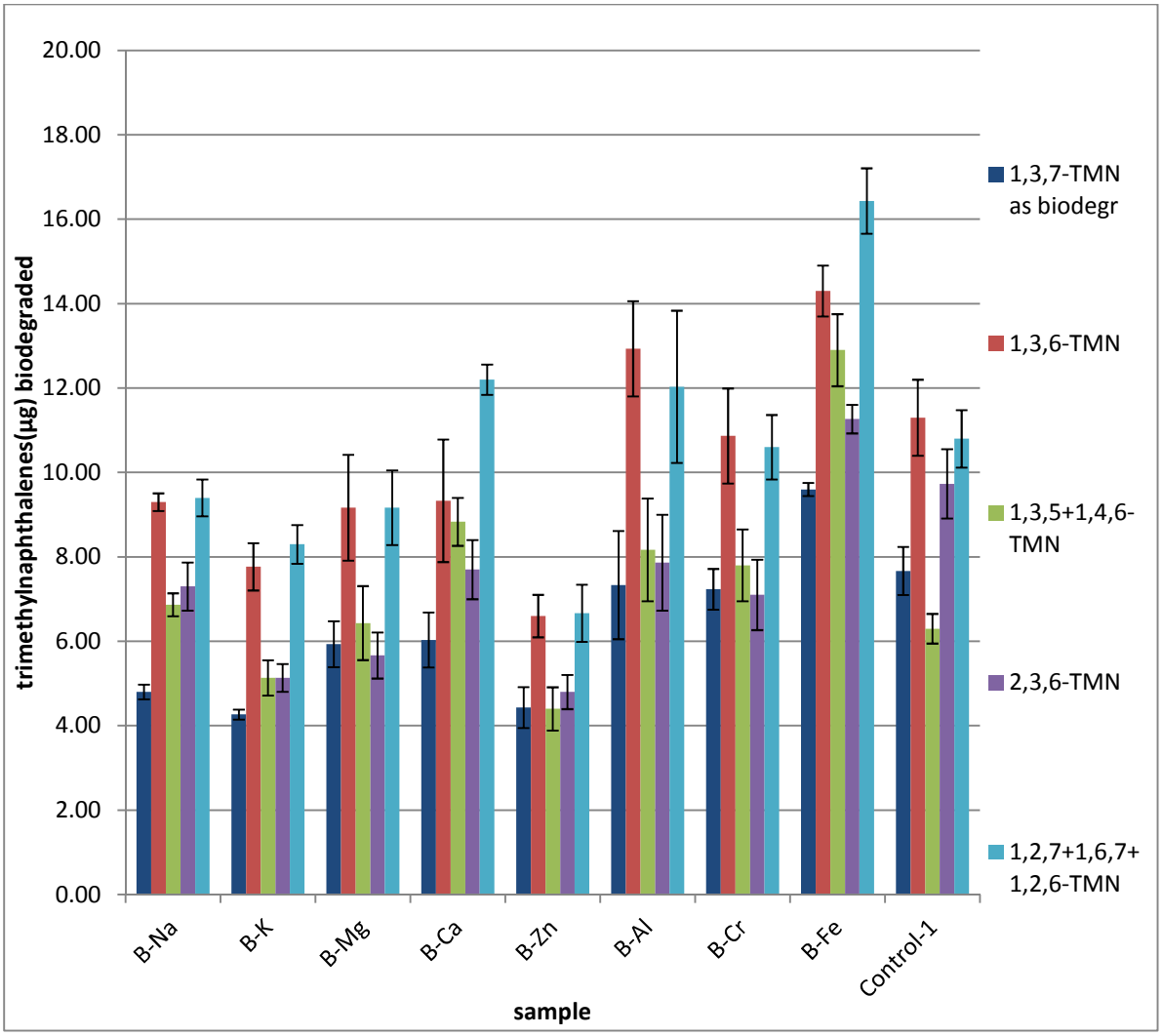

Figure 6.15 Biodegradation of trimethylnaphthalenes (weight basis) supported on homoionic cation interlayer clays. Values are reported as mean ± one standard error.

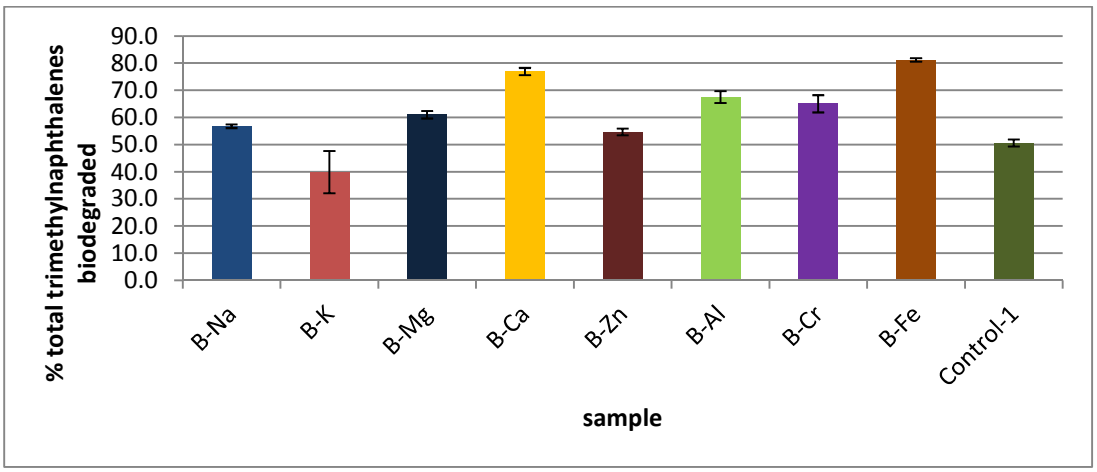

Figure 6.16 Percentage biodegradation of summed trimethylnaphthalenes supported on homoionic cation interlayer clays. Values are reported as mean ± one standard error.

The 2-sample t-test at 95% confidence interval (CI) performed to analyse for differences that may be statistically significant is presented in Appendix 6.5B. Figures 6.15, 6.16 and Appendix 6.5B all indicate that there is no statistical significant difference between Control-1 and any of B-Na, B-K, B-Cr and B-Zn with respect to the biodegradation of trimethylnaphthalenes. These samples therefore can be said to be unable to enhance the biodegradation of trimethylnaphthalenes.

However, B-Mg, B-Al, B-Ca and B-Fe appear to show statistical significant difference in comparison with Control-1 and therefore can be said to enhance the biodegradation of trimethylnaphthalenes. It is also observed that B-Ca and B-Fe are better enhancers of biodegradation of trimethylnaphthalenes than B-Mg and B-Al.

6.3.3 Biodegradation of fluorenes and methylfluorenes

The biodegradation of fluorenes and methylfluorenes is presented in this section. The results are also presented for the individual isomers on weight basis and for the total isomers (all the isomers collectively) on percent basis.

6.3.3.1 Effect of unmodified clays on biodegradation of fluorenes and methylfluorenes

The effect of unmodified clay samples on biodegradation of fluorenes and methylfluorenes are presented in Figures 6.17 and 6.18

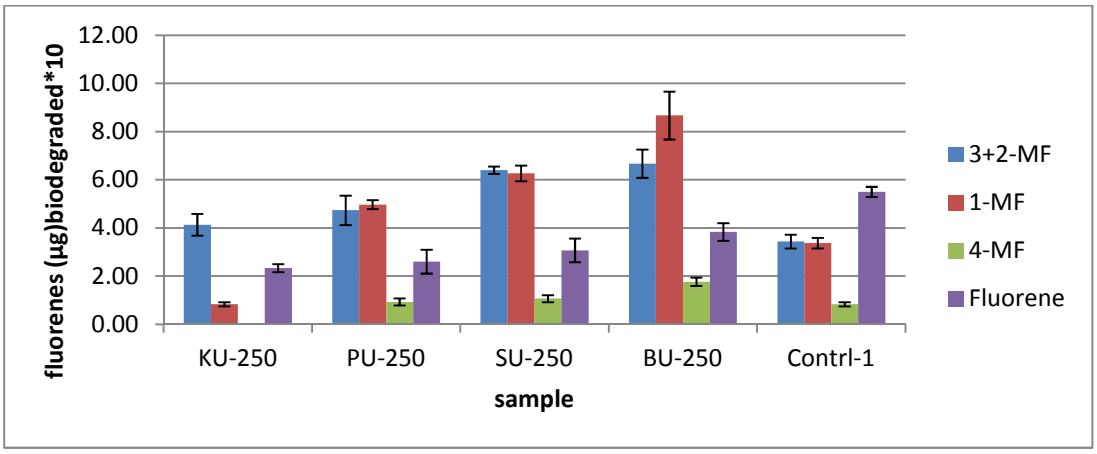

Figure 6.17 Biodegradation of Fluorene and methylfluorenes (weight basis) supported on unmodified clays. Values are reported as mean ± one standard error.

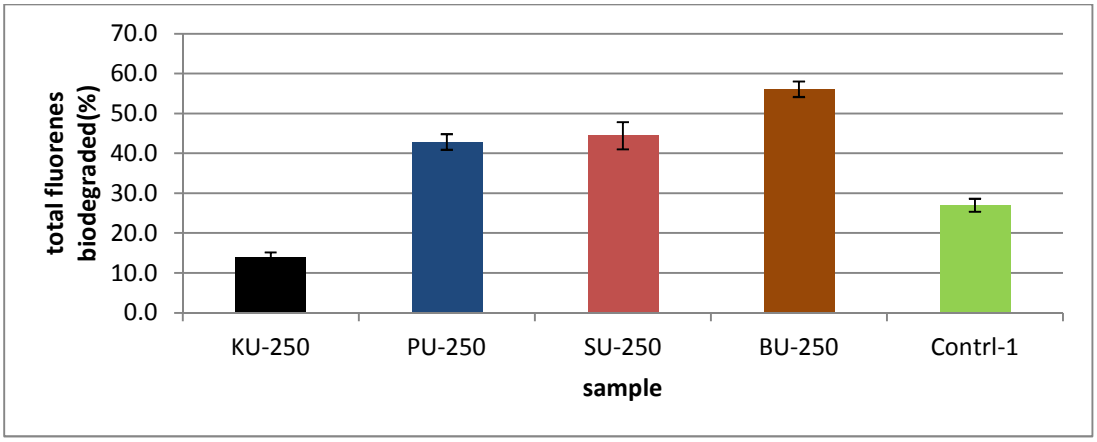

Figure 6.18 Percentage biodegradation of summed Fluorenes supported on unmodified clays. Values are reported as mean ± one standard error.

Figure 6.18 shows that unmodified clays enhance the biodegradation of total fluorenes especially unmodified bentonite (BU-250) with the exception of unmodified kaolinite (KU-250) which actually inhibits it. However, from Figure 6.17, Control-1 shows a far more superior biodegradation of fluorene to any of the unmodified clay samples.

6.3.3.2 Effect of acid activated clay minerals on biodegradation of fluorenes and methylfluorenes

The effect of acid activated clay samples on biodegradation of fluorenes and methylfluorenes are presented in Figures 6.19 and 6.20.

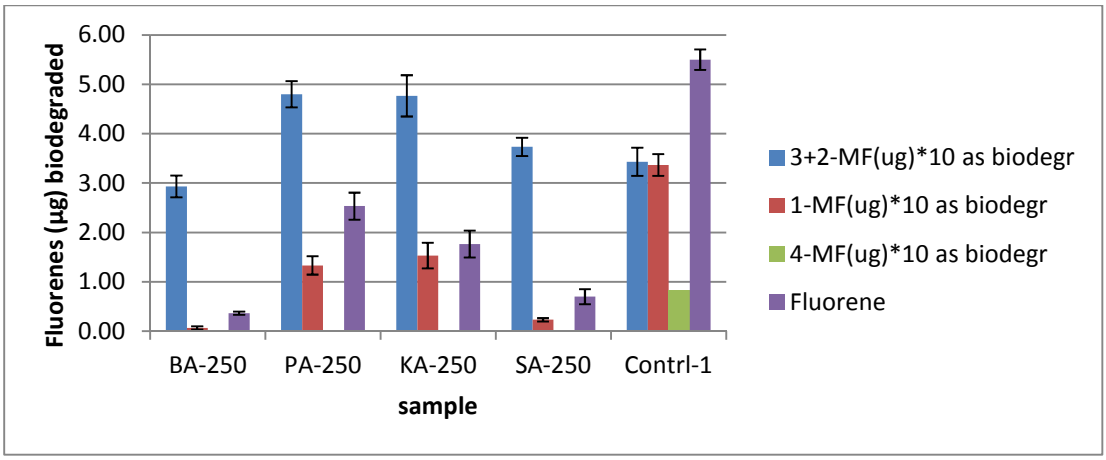

Figure 6.19 Biodegradation of Fluorene and methylfluorenes (on weight basis) supported on acid activated clays. Values are reported as ± one standard error.

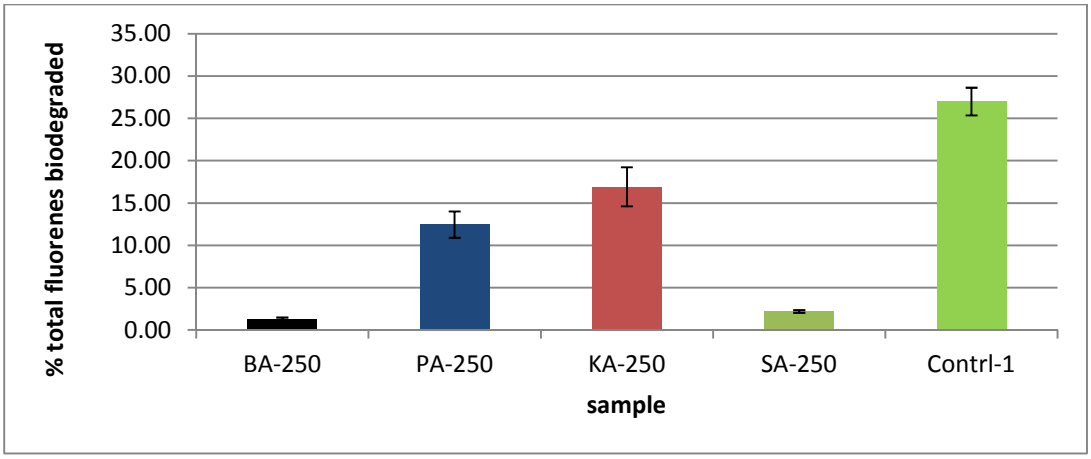

Figure 6.20 Percentage biodegradation of summed fluorenes supported on acid activated clays. Values are reported as mean ± one standard error.

It is obvious from Figure 6.19 and 6.20 that the acid activated clay minerals have not improved the biodegradation of fluorenes but rather inhibitted it.

6.3.3.3 Effect of organoclay on biodegradation of fluorenes and methylfluorenes

The effect of organoclay samples on biodegradation of fluorenes and methylfluorenes are presented in Figures 6.21 and 6.22

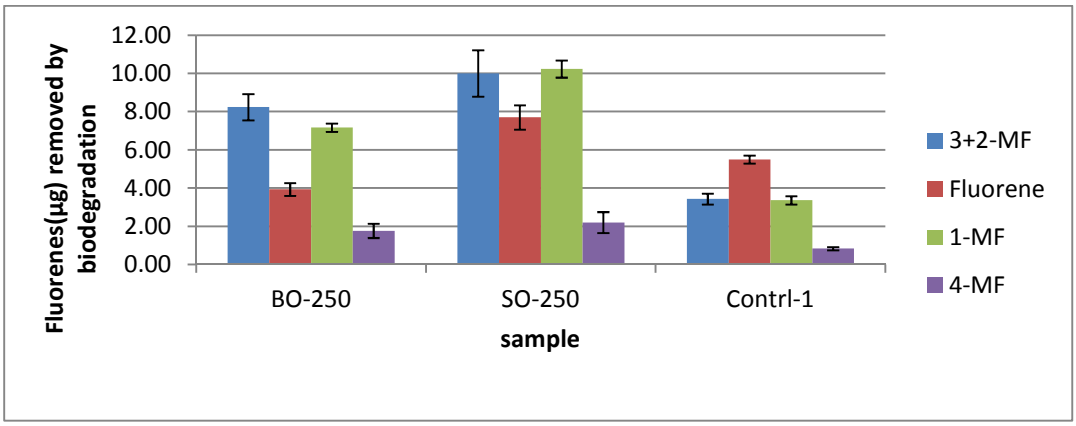

Figure 6.21 Biodegradation of Fluorene and methylfluorenes (on weight basis) supported on organoclay. Values are reported as mean ± one standard error.

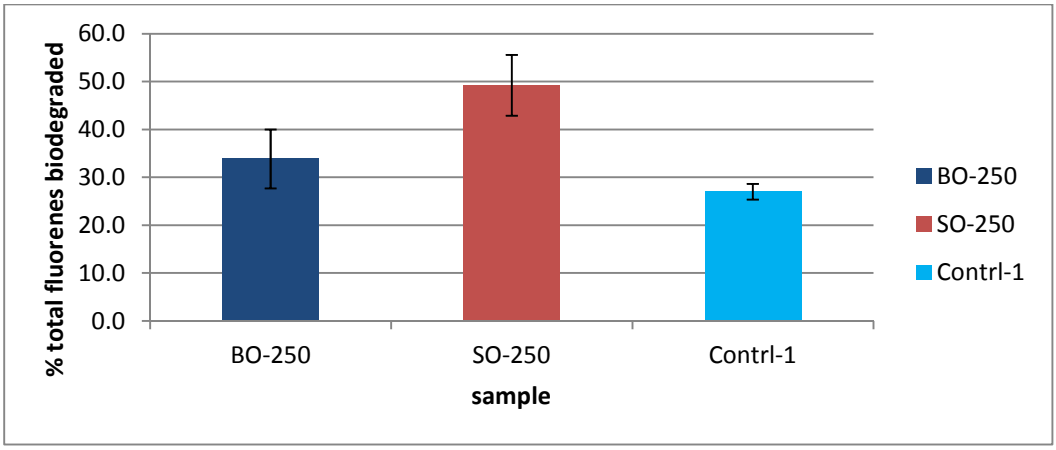

Figure 6.22 Percentage biodegradation of summed fluorenes supported on organoclays . Values are reported as mean ± one standard error.

The 2-sample t-test at 95% confidence interval (CI) performed to analyse for differences that may be statistically significant is presented in Appendix 6.5C.

Figure 6.19 shows that on a weight basis, SO-250 removes more Fluorenes by biodegradation than either BO-250 or Control-1. However, on a percent basis, the P-values (Appendix 6.5C) indicate that there is no statistical significant difference amongst them. Organoclay therefore do not seem to enhance the biodegradation of fluorenes.

6.3.3.4 Effect of homoionic interlayer cation exchanged clay minerals on biodegradation of fluorenes and methylfluorenes

The effect of homoionic interlayer cation exchanged clay minerals on biodegradation of fluorenes and methylfluorenes are presented in Figures 6.23 and 6.24.

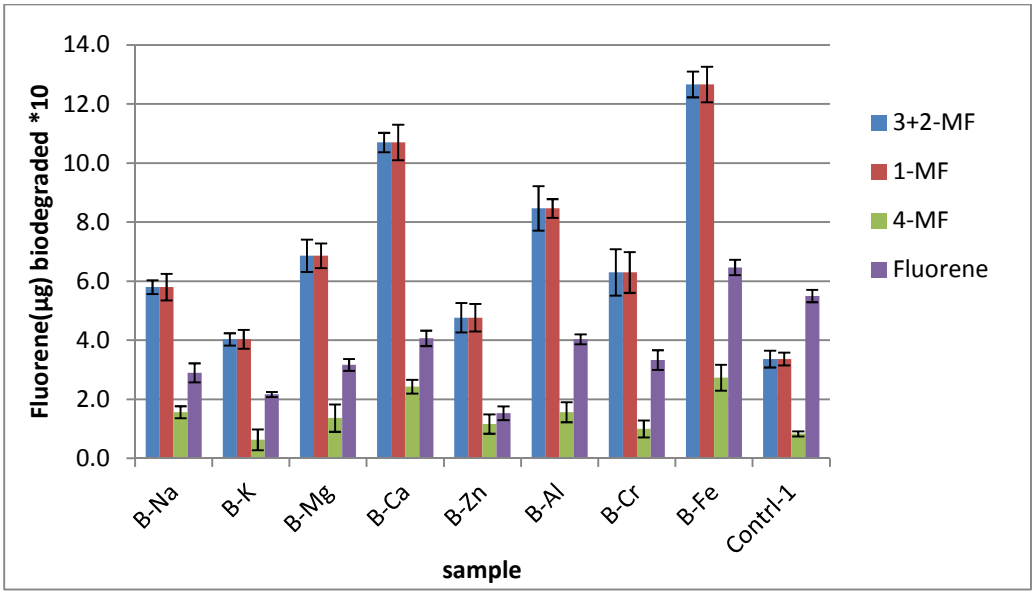

Figure 6.23 Biodegradation of fluorene and methyl fluorenes (on weight basis) supported on homoionic cation interlayer clays. Values are reported as mean ± one standard error.

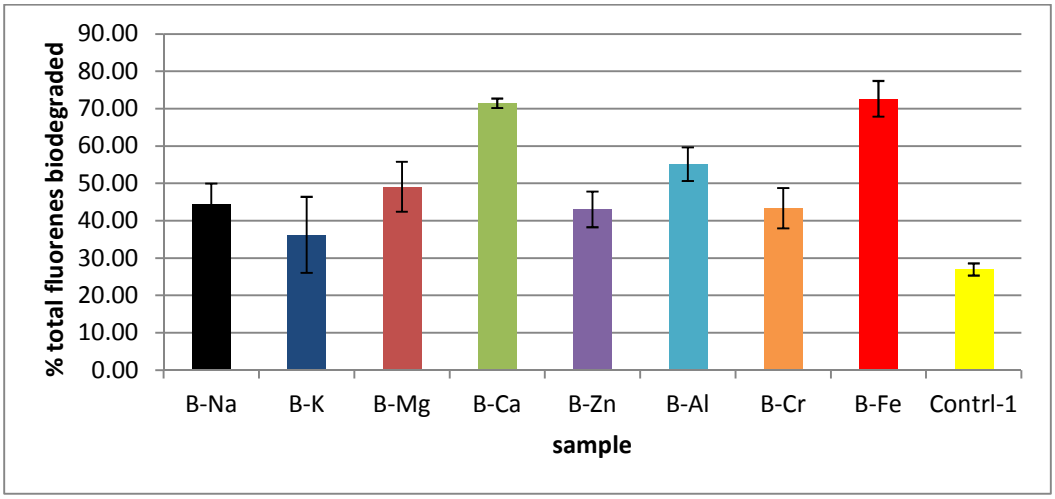

Figure 6.24 Percentage biodegradation of total fluorenes supported on homoionic cation interlayer clays. Values are reported as mean ± one standard error.

Figure 6.24 shows that on a % basis, all the interlayer cation exchanged clay samples enhance the biodegradation of total florenes especially B-Ca and B-Fe. However, from Figure 6.23, it appears that Control-1 allows the biodegradation of fluorene more than any other sample except B-Fe. B-Ca and B-Fe clearly enhances the biodegradation of total fluorenes.

6.3.4 Biodegradation of phenanthrene, methylphenanthrenes and dimethylphenanthrenes

The biodegradation of Phenanthrene, methyl phenanthrenes and dimethylphenanthrenes is presented in this section. Phenanthrene, methylphenanthrene and dimethylphenanthrene are represented in this section by P, MP and DMP respectively. For the purpose of this study, total phenanthrenes shall be regarded as the sum of phenanthrenes, methylphenanthrenes and dimethylphenanthrenes.

6.3.4.1 Effect of unmodified clays on biodegradation of Phenanthrene, methyl phenanthrenes and dimethylphenanthrenes.

The effect of unmodified clay samples on biodegradation of Phenanthrene, methyl phenanthrenes and dimethylphenanthrenes are presented in Figures 6.25, 6.26 and 6.27.

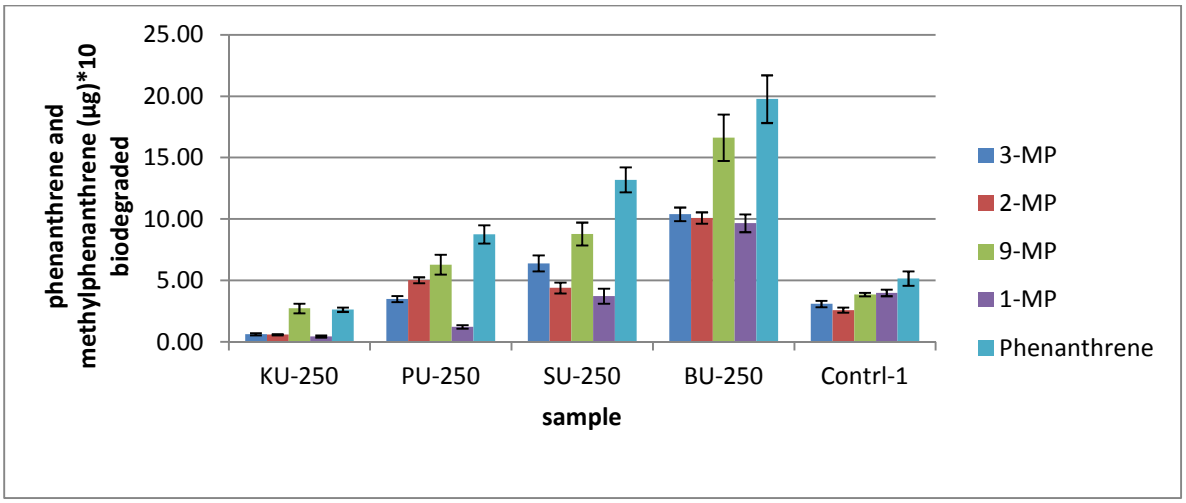

Figure 6.25 Biodegradation of phenanthrenes and methylphenanthrenes (on weight basis) supported on unmodified clays. Values are reported as mean ± one standard error.

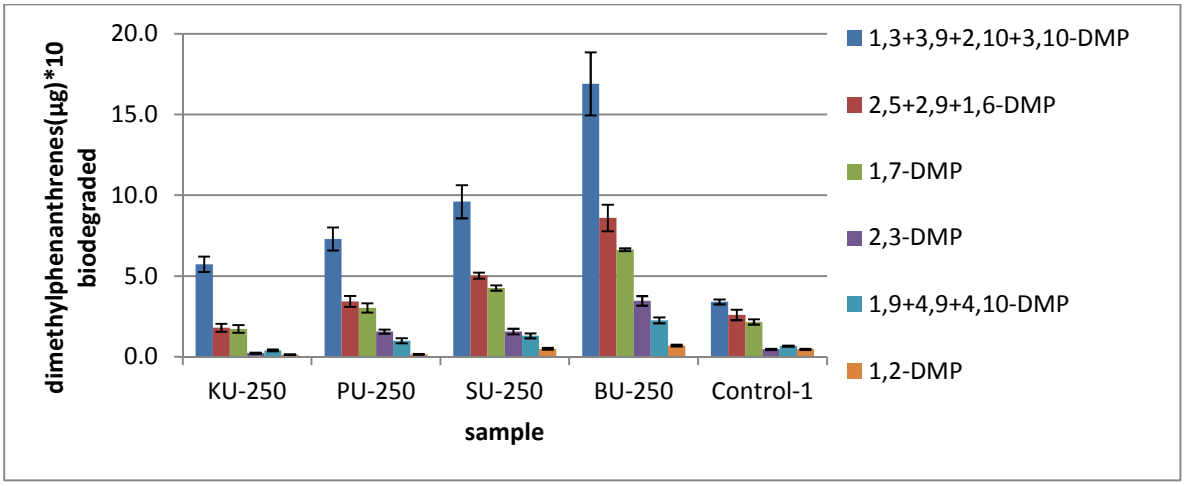

Figure 6.26 Biodegradation of dimethylphenanthrene(on weight basis) supported on unmodified clay

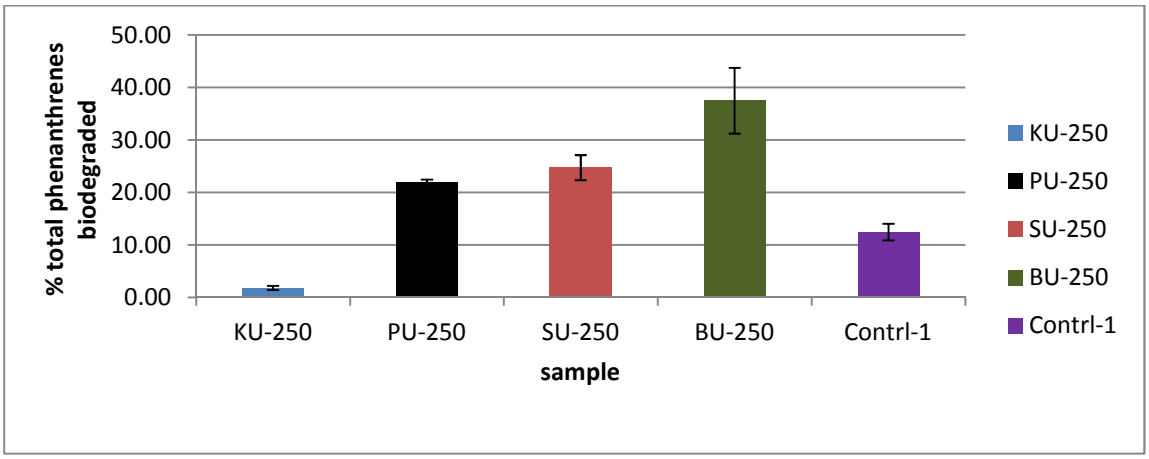

Figure 6.27 Biodegradation of summed phenanthrenes (on weight basis) supported on unmodified clay. Values are reported as mean ± one standard error.

From Figures 6.25-6.27, it is obvious that the unmodified clay samples such as PU-250, SU-250 and BU-250 enhance the biodegradation of phenanthrene, methylphenanthrene and dimethylphenanthrene. However, KU-250 appears to inhibit their biodegradation.

6.3.4.2 Effect of acid activated clay samples on biodegradation of Phenanthrene, methyl phenanthrenes and dimethylphenanthrenes.

The effect of acid activated clay samples on biodegradation of Phenanthrene, methyl phenanthrenes and dimethylphenanthrenes are presented in Figures 6.28, 6.29 and 6.30.

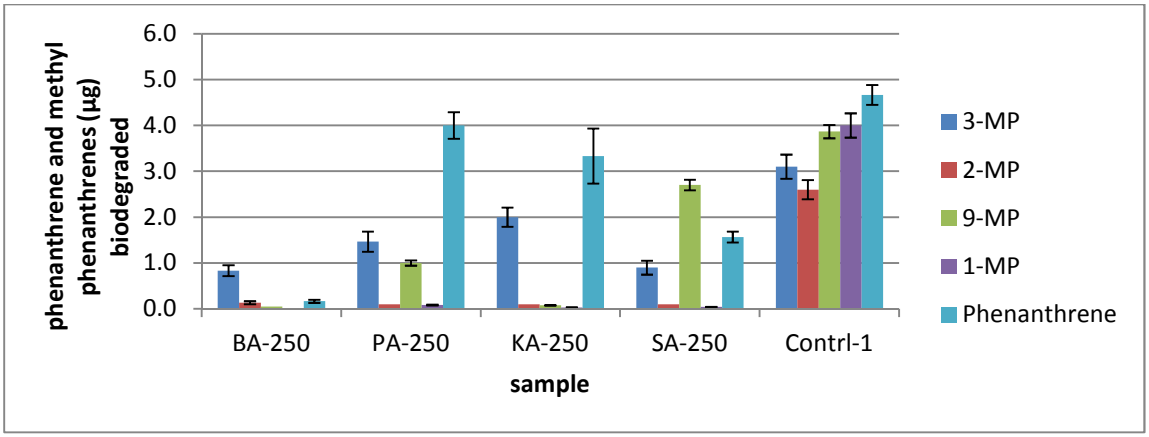

Figure 6.28 Biodegradation of phenanthrene and methyl phenanthrenes (on weight basis) supported on acid activated clays. Values are reported as mean ± one standard error.

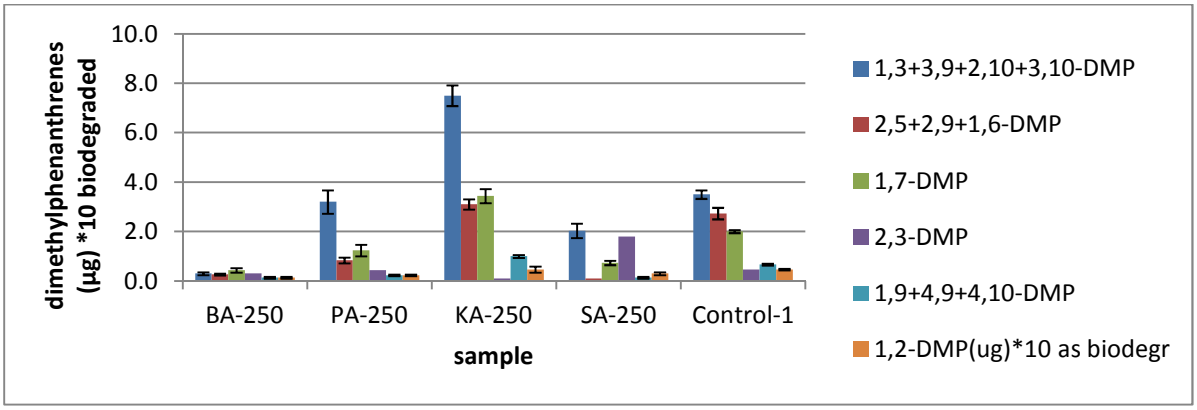

Figure 6.29 Biodegradation of dimethylphenanthrenes (on weight basis) supported on acid activated clays. Values are reported as mean ± one standard error.

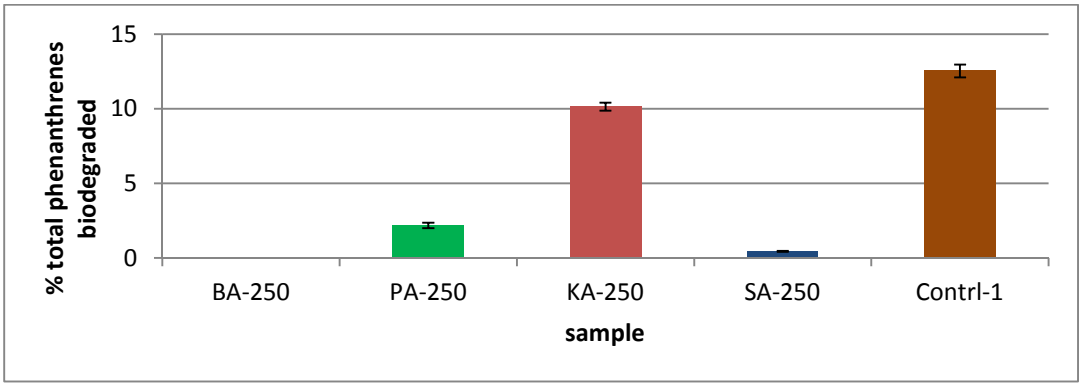

Figure 6.30 Percentage biodegradation of summed phenanthrenes supported on acid activated clays. Values are reported as mean ± one standard error.

Figures 6.28-6.30 show that acid activated clay minerals do not enhance the biodegradation of phenanthrenes particularly BA-250 which appears to have tremendous inhibitory property.

6.3.4.3 Effect of organoclay samples on biodegradation of Phenanthrene, methyl phenanthrenes and dimethylphenanthrenes.

The effect of organoclay samples on biodegradation of Phenanthrene, methyl phenanthrenes and dimethylphenanthrenes are presented in Figures 6.31, 6.32 and 6.33.

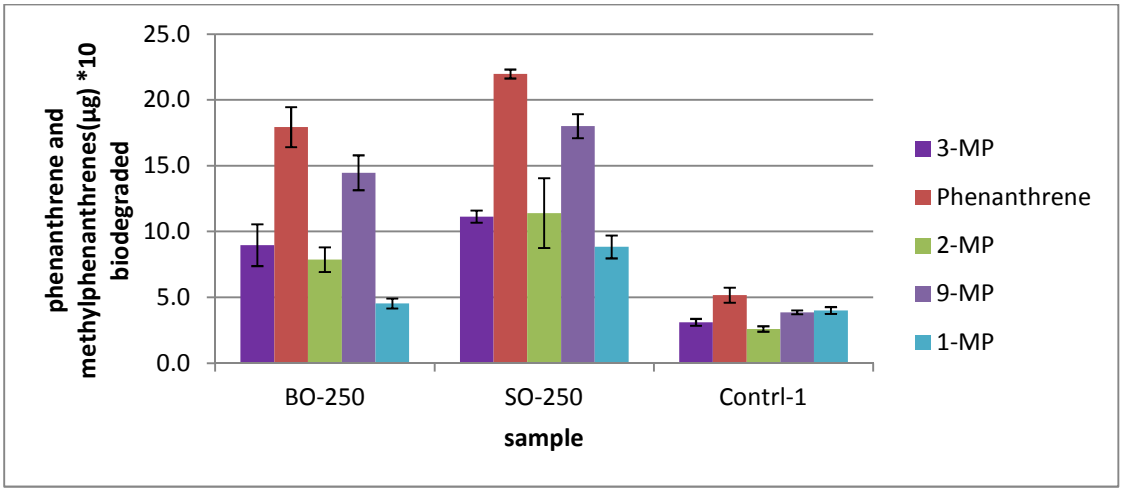

Figure 6.31 Biodegradation of phenanthrene and methylphenanthrenes (on weight basis) supported on organoclay. Values are reported as mean ± one standard error.

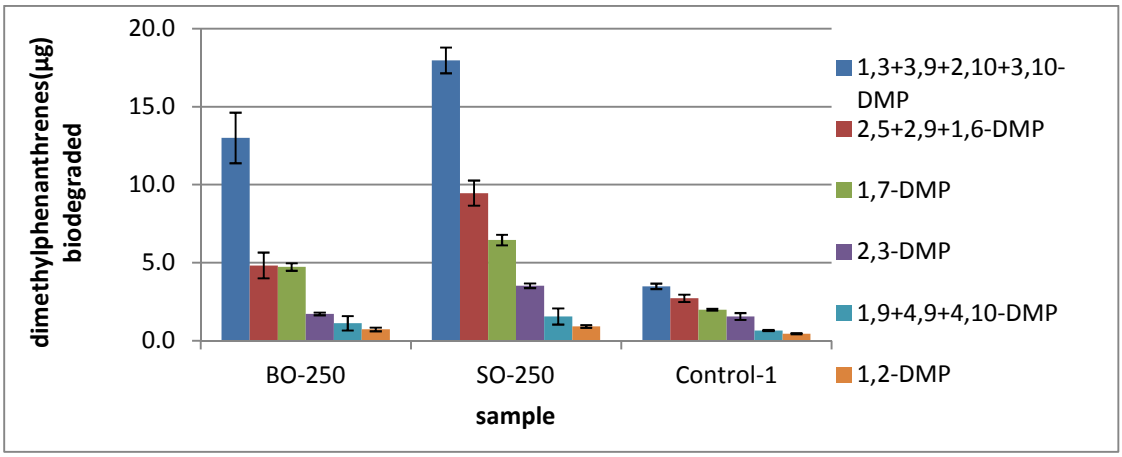

Figure 6.32 Biodegradation of dimethylphenanthrenes (on weight basis) supported on organoclay . Values are reported as mean ± one standard error.

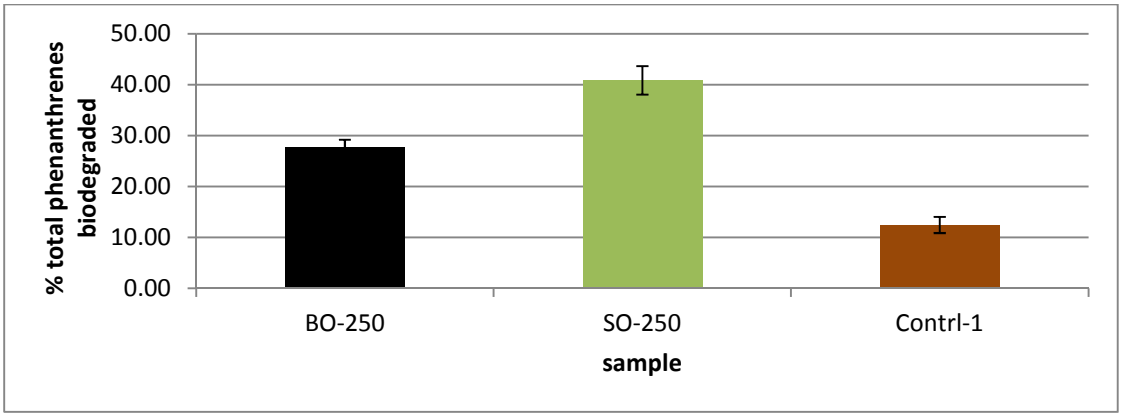

Figure 6.33 Percentage biodegradation of summed phenanthrenes supported on organoclay

The 2-sample t-test at 95% confidence interval (CI) performed to analyse for differences that may be statistically significant is presented in Appendix 6.5D.

Figures 6.31 – 6.33 and Appendix 6.5D show that there is significant difference statistically between Control-1 and either of BO-250 and SO-250. This indicates that organo clay enhances biodegradation of phenanthrene, methylphenanthrenes and dimethylphenanthrenes. However, on comparing BO-250 and SO-250 (Appendix 6.5D), SO-250 enhances the biodegradation of these aromatic compounds more than BO-250.

6.3.4.4 Effect of homoionic interlayer cation exchanged clay samples on biodegradation of Phenanthrene, methyl phenanthrenes and dimethylphenanthrenes.

The effect of homoionic interlayer cation exchanged clay samples on biodegradation of Phenanthrene, methyl phenanthrenes and dimethylphenanthrenes are presented in Figures 6.34, 6.35 and 6.36.

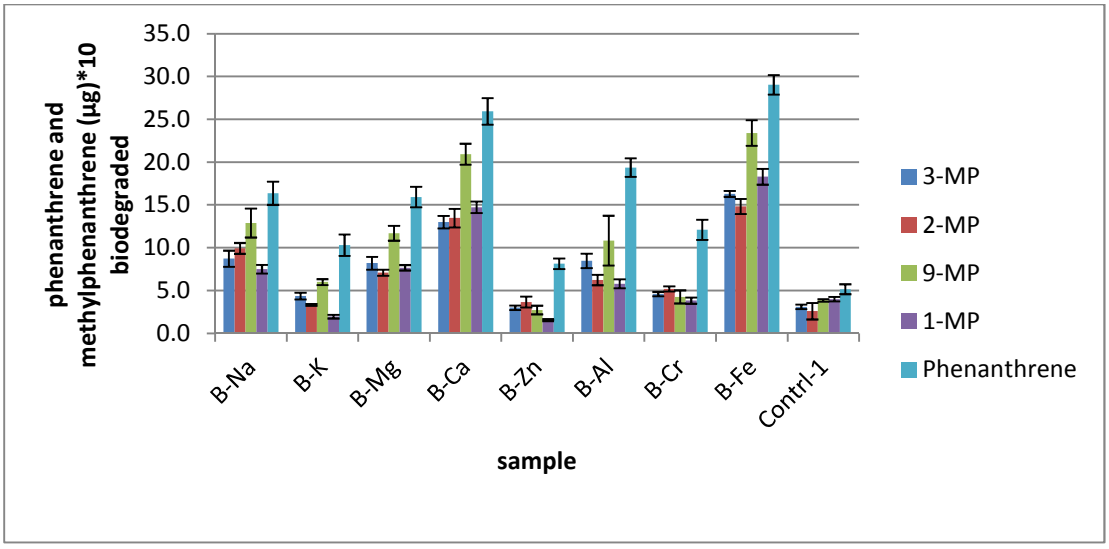

Figure 6.34 Biodegradation of phenanthrene and methylphenanthrenes (on weight basis) supported on homoionic interlayer cation clays. Values are reported as mean ± one standard error

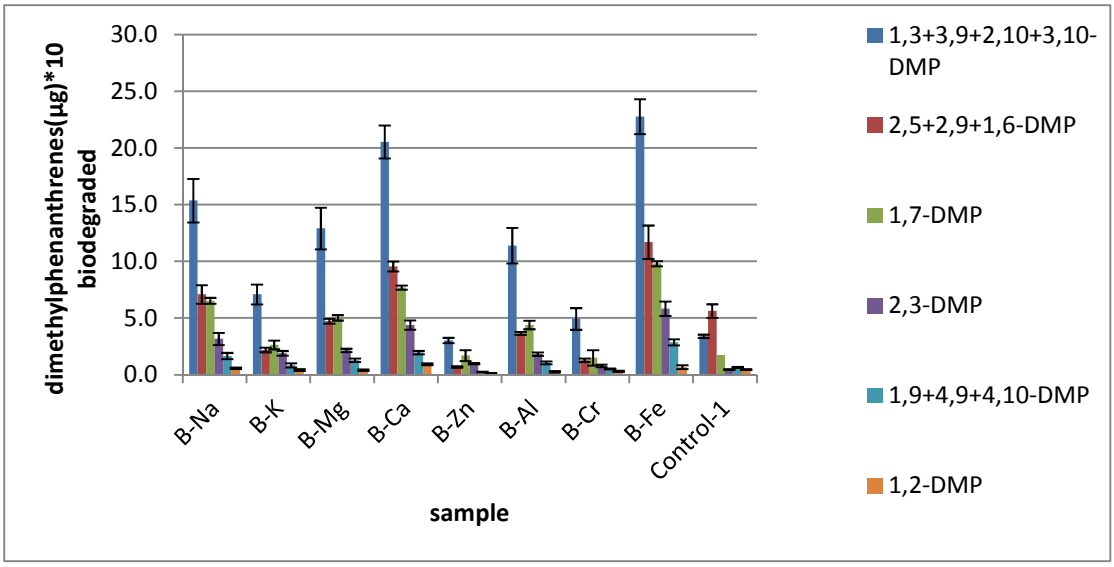

Figure 6.35 Biodegradation of dimethylphenanthrenes (on weight basis) supported on homoionic interlayer clays. Values are reported as mean ± one standard error.

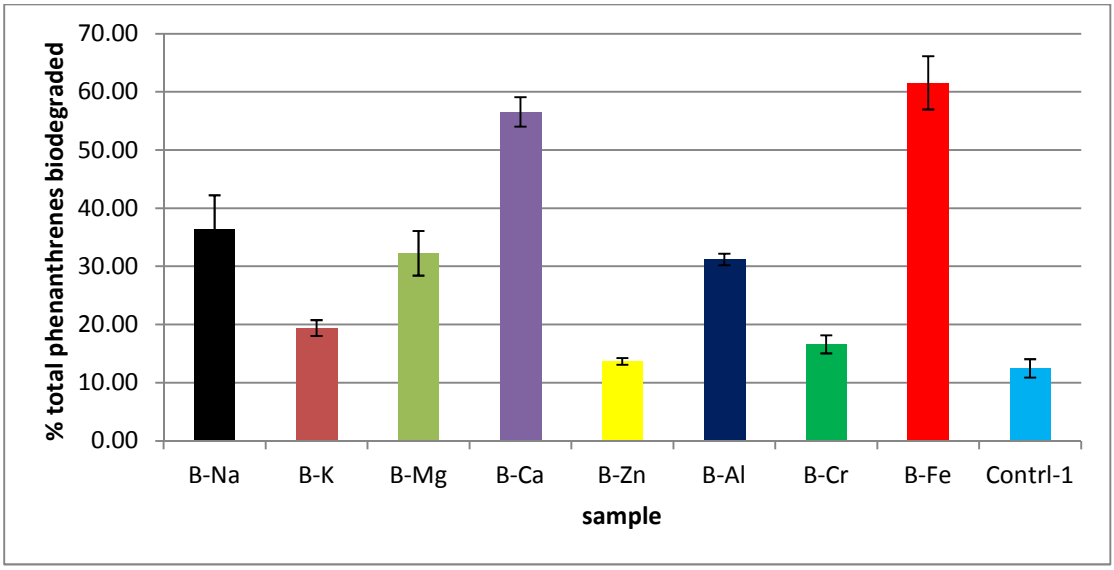

Figure 6.36 Percentage biodegradation of total phenanthrenes supported on homoionic interlayer cation clays

The 2-sample t-test at 95% confidence interval (CI) performed to analyse for differences that may be statistically significant is as presented in Appendix 6.5E

Figures 6.34-6.36 show that B-Na, B-K, B-Cr and especially B-Zn are comparable with Control-1 as can be seen from their P-values (Appendix 6.5E) and as such can be said not to have the ability to enhance the biodegradation of phenanthrene, methylphenanthrenes and dimethylphenanthrenes. The rest samples such as B-Al, B-Mg, especially B-Ca and B-Fe enhance the biodegradation of these compounds as the P-values indicate.

6.3.5 Biodegradation of Dibenzothiophene, methyldibenzothiophene, dimethyldibenzothiophene and ethyldibenzothiophene.

The biodegradation of Dibenzothiophene, methyldibenzothiophene, dimethyldibenzothiophene and ethyldibenzothiophene is presented in this section. Dibenzothiophene, methyldibenzothiophene, dimethyldibenzothiophene and ethyldibenzothiophene are represented by DBT, MDBT, DMDBT and EDBT respectively. Total dibenzothiophenes shall be regarded as the sum of dibenzothiophene, methyldibenzothiophene, dimethyldibenzothiophene and ethyldibenzothiophene.

6.3.5.1 Effect of unmodified clays on biodegradation of dibenzothiophene, methyldibenzothiophene, dimethyldibenzothiophene and ethyldibenzothiophene.

The effect of unmodified clay samples on biodegradation of dibenzothiophene, methyldibenzothiophene, dimethyldibenzothiophene and ethyldibenzothiophene are presented in Figures 6.37, 6.38 and 6.39

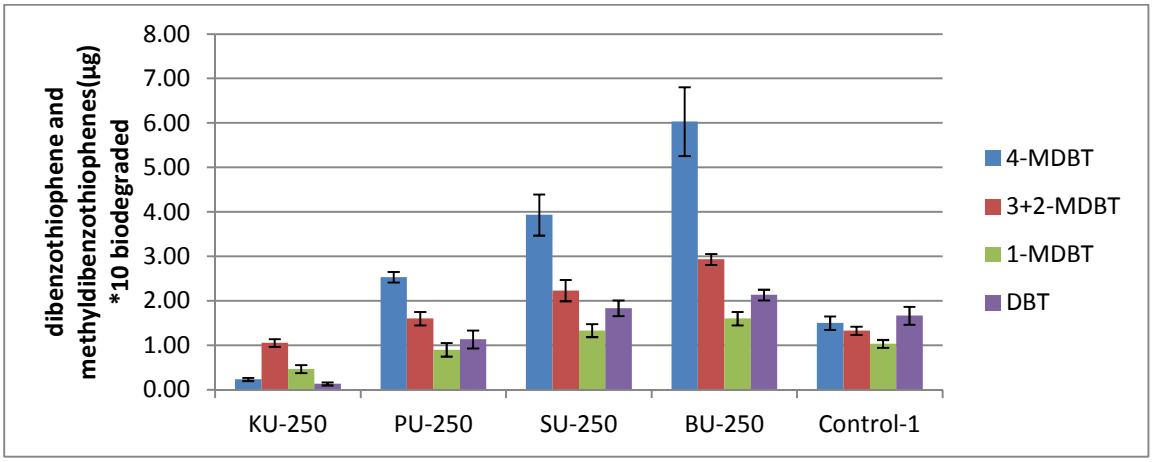

Figure 6.37 Biodegradation of dibenzothiophene and methyldibenzothiophene (on weight basis) supported on unmodified clay. Values are reported as mean ± one standard error.

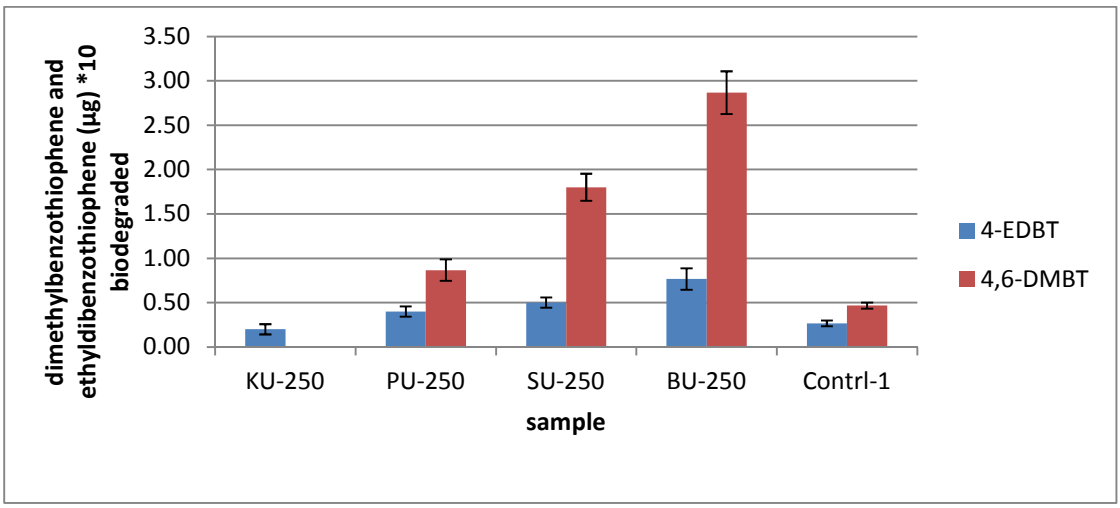

Figure 6.38 Biodegradation of dimethyldibenzothiophene and ethyldibenzothiophene (on weight basis) supported on unmodified clay. Values are reported as mean ± one standard error.

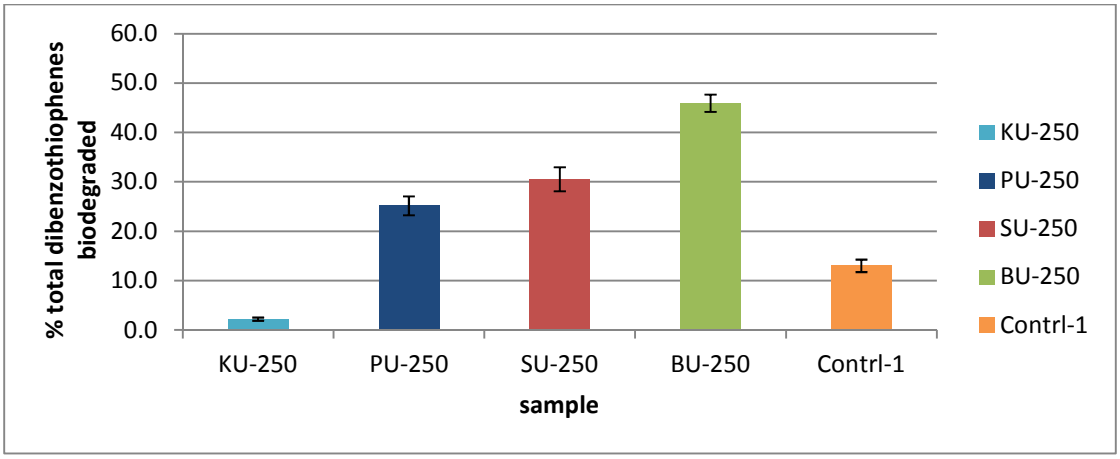

Figure 6.39 Percentage biodegradation of summed dibenzothiophenes supported on unmodified clay. Values are reported as mean ± one standard error.

Figures 6.37-6.39 show that unmodified clays such as PU-250, SU-250 and BU-250 enhance the biodegradation of dibenzothiophene, methyldibenzothiophenes, dimethyldibenzothiophene and ethyldibenzothiophene. KU-250 however, inhibits the biodegradation.

6.3.5.2 Effect of acid activated clays on biodegradation of dibenzothiophene, methyldibenzothiophene, dimethyldibenzothiophene and ethyldibenzothiophene.

The effect of acid activated clay samples on biodegradation of dibenzothiophene, methyldibenzothiophene, dimethyldibenzothiophene and ethyldibenzothiophene are presented in Figures 6.40, 6.41 and 6.42.

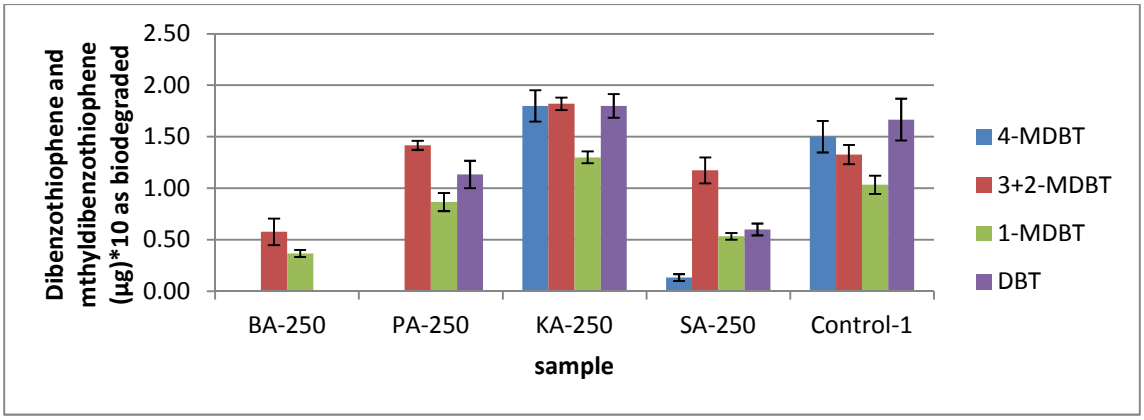

Figure 6.40 Biodegradation of dibenzothiophene and methyldibenzothiophenes (on weight basis) supported on acid activated clay. Values are reported as mean ± one standard error.

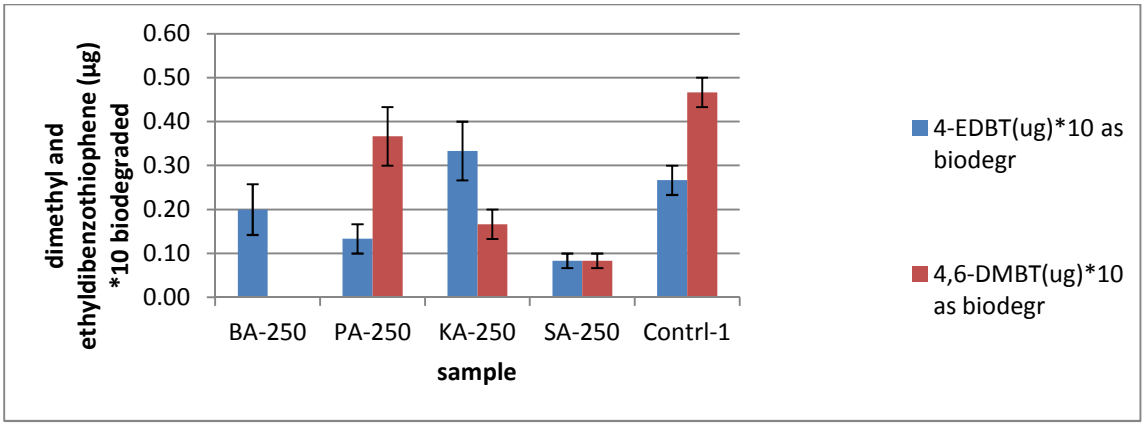

Figure 6.41 Biodegradation of dimethyldibenzothiophene and ethyldibenzothiophene (on weight basis) supported on acid activated clays. Values are reported as mean ± one standard error

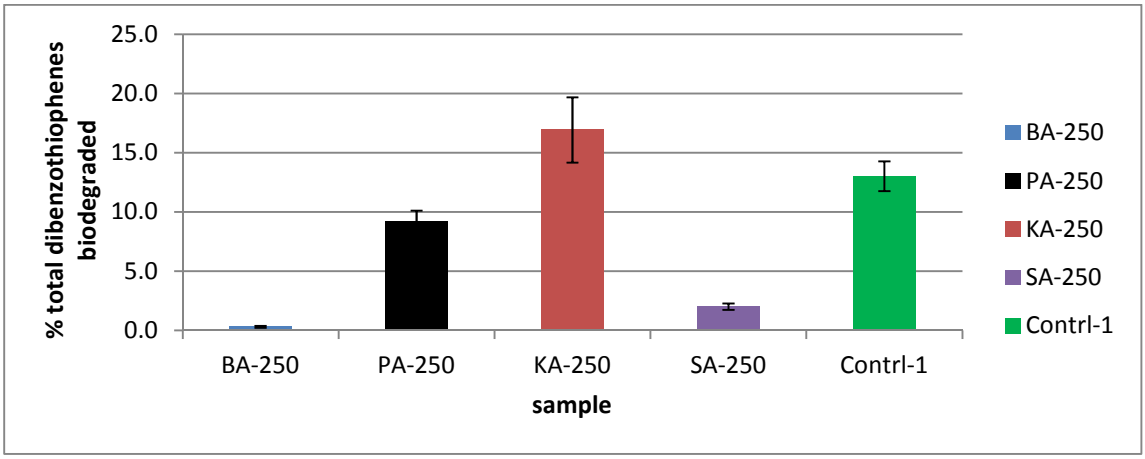

Figure 6.42 Percentage biodegradation of summed dibenzothiophenes supported on acid activated clay. Values are reported as mean ± one standard error

Figures 6.40-6.42 show that all the acid activated clay samples inhibit biodegradation of dibenzothiophene, methyldibenzothiophenes, dimethyl and ethyldibenzothiophenes though KA-250 tend to be comparable with control-1. BA-250 and SA-250 are highly inhibitory.

6.3.5.3 Effect of organoclay samples on biodegradation of dibenzothiophene, methyldibenzothiophene, dimethyldibenzothiophene and ethyldibenzothiophene.

The effect of organoclay samples on biodegradation of dibenzothiophene, methyldibenzothiophene, dimethyldibenzothiophene and ethyldibenzothiophene are presented in Figures 6.43, 6.44 and 6.45.

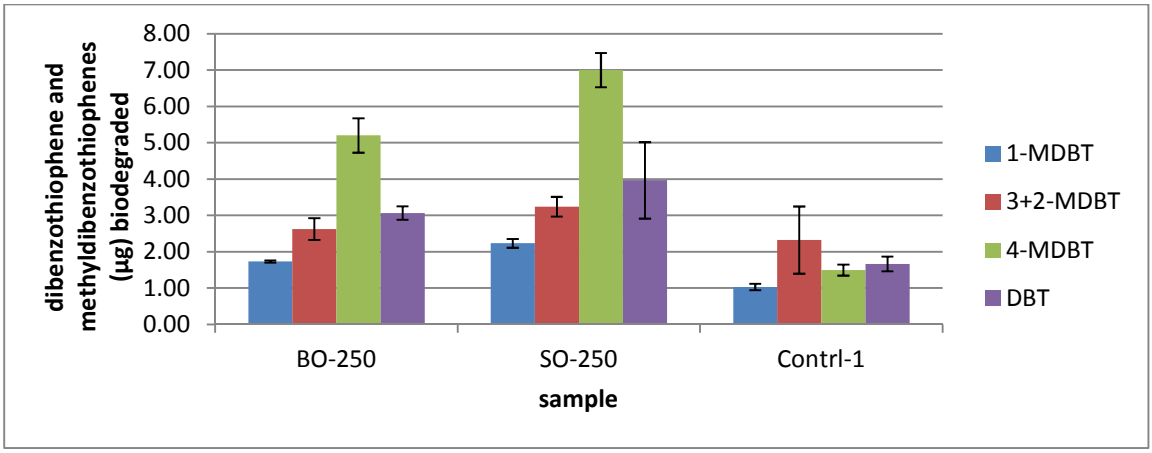

Figure 6.43 Biodegradation of dibenzothiophene and methydibenzothiophenes (on weight basis) supported on organo clay. Values are reported as mean ± one standard error.

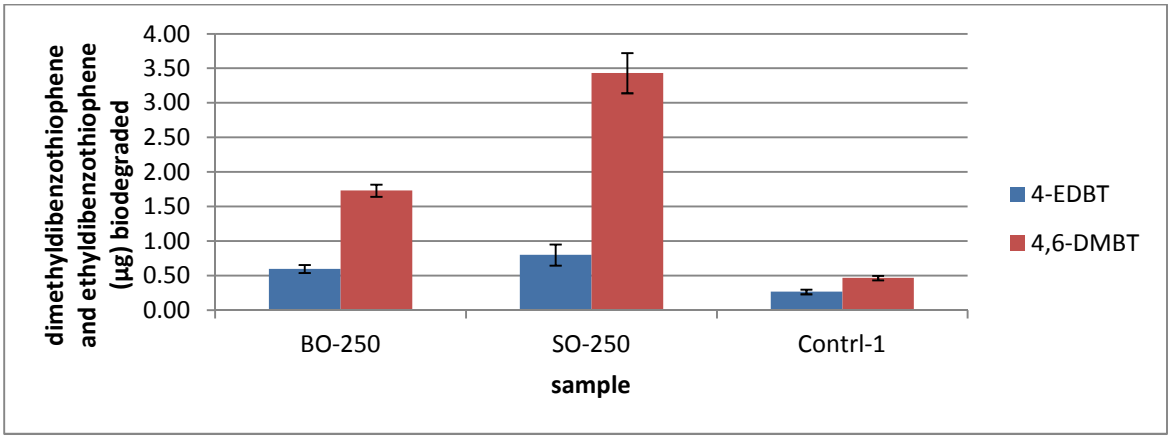

Figure 6.44 Biodegradation of methyl and ethyldibenzothiophenes (on weight basis) supported on organoclay. Values are reported as mean ± one standard error.

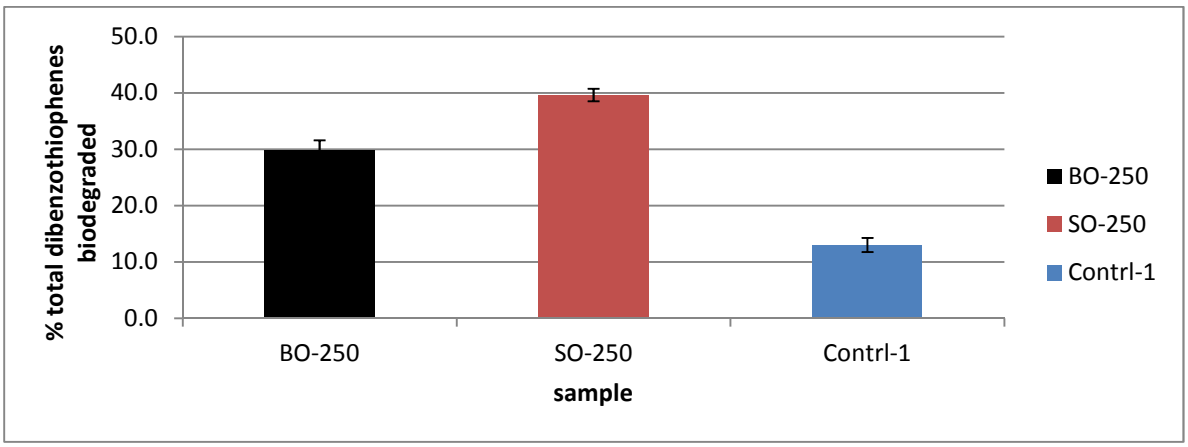

Figure 6.45 Percentage biodegradation of total dibenzothiophenes supported on organo clay. Values are reported as mean ± one standard error.

Figures 6.43-6.45 indicate that samples BO-250 and SO-250 (organoclay) enhance the biodegradation of dibenzothiophene, methyldibenzothiophene, dimethyldibenzothiophene and ethyldibenzothiophene.

6.3.5.4 Effect of homoionic interlayer cation clays on biodegradation of dibenzothiophene, methyldibenzothiophene, dimethyldibenzothiophene and ethyldibenzothiophene.

The effect of homoionic interlayer cation clay samples on biodegradation of dibenzothiophene, methyldibenzothiophene, dimethyldibenzothiophene and ethyldibenzothiophene are presented in Figures 6.46, 6.47 and 6.48

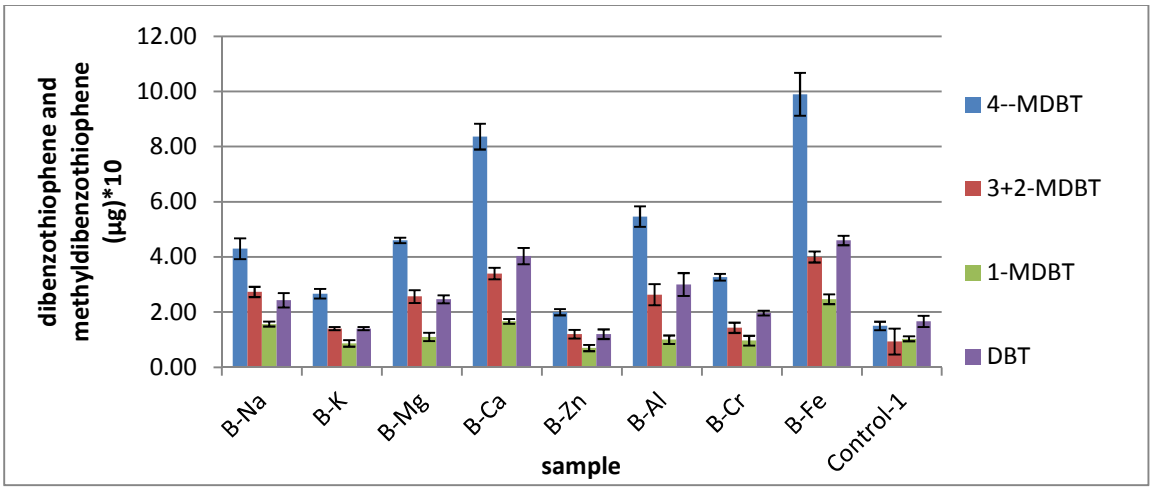

Figure 6.46 Biodegradation of methyldibenzothionphenes and dibenzothiophenes (on weight basis) supported on homoionic cation interlayer clays. Values are reported as mean ± one standard error.

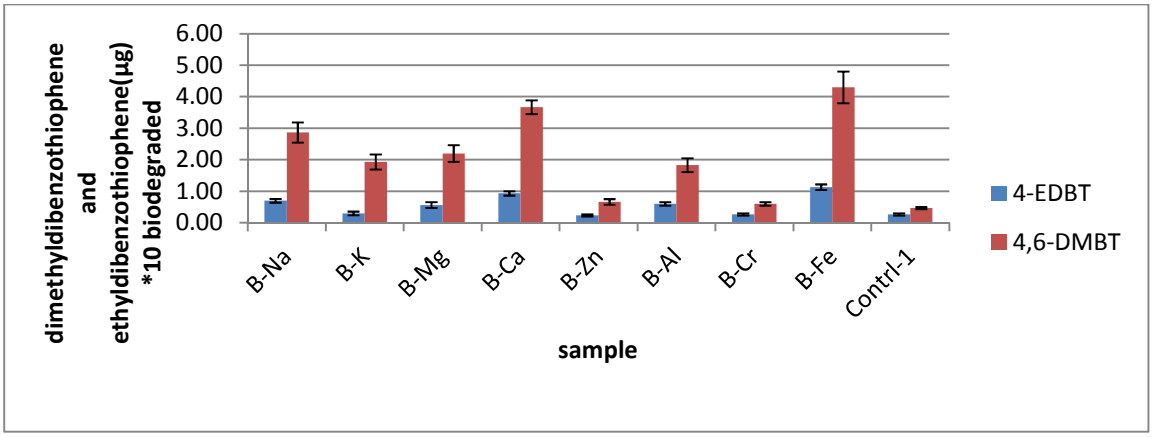

Figure 6.47 Biodegradation of dimethyldibenzothionphene and ethyldibenzothiophene (on weight basis) supported on homoionic cation interlayer clays. Values are reported as mean ± one standard error.

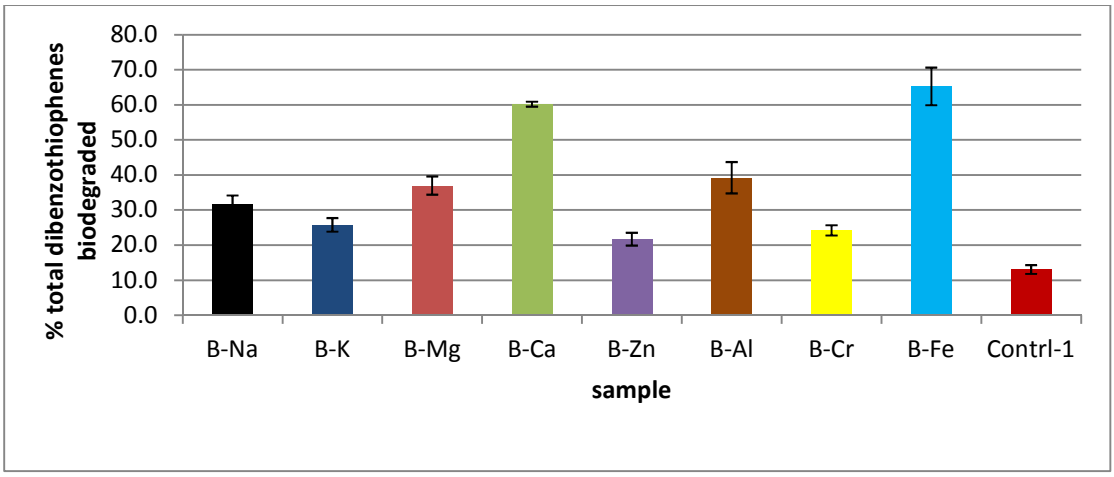

Figure 6.48 Percentage biodegradation of summed dibenzothiophenes supported on homoionic cation interlayer clays. Values are reported as mean ± one standard error.

Figures 6.46 to 6.48 show that the homoionic cation interlayer clays seem to enhance the biodegradation of dibenzothiophene, methyldibenzothiophenes, dimethyldibenzothiophene and ethyldibenzothiophene with B-Fe and B-Ca showing more enhancement of the biodegradation than the other clay samples.

6.3.6 Biodegradation of Triaromatic steroids

The biodegradation of triaromatic steroids are presented in this section**.** The biodegradation of the following isomers of triaromatic steroid are presented: (TAS): 26S, 27R, 28S, 28R and 26R+27S.

6.3.6.1 Effect of unmodified clay samples on biodegradation of triaromatic steroids

The effect of unmodified clay samples on biodegradation of triaromatic steroids are presented in Figures 6.49 and 6.50.

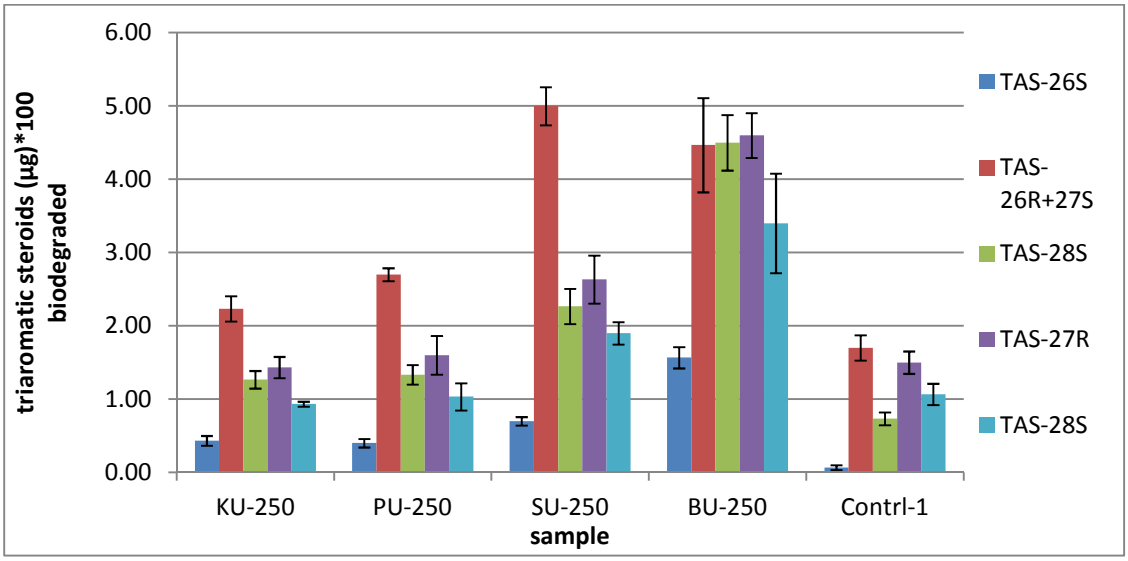

Figure 6.49 Biodegradation of triaromatic steroids (weight basis) supported on unmodified clay samples. Values are reported as mean ± one standard error.

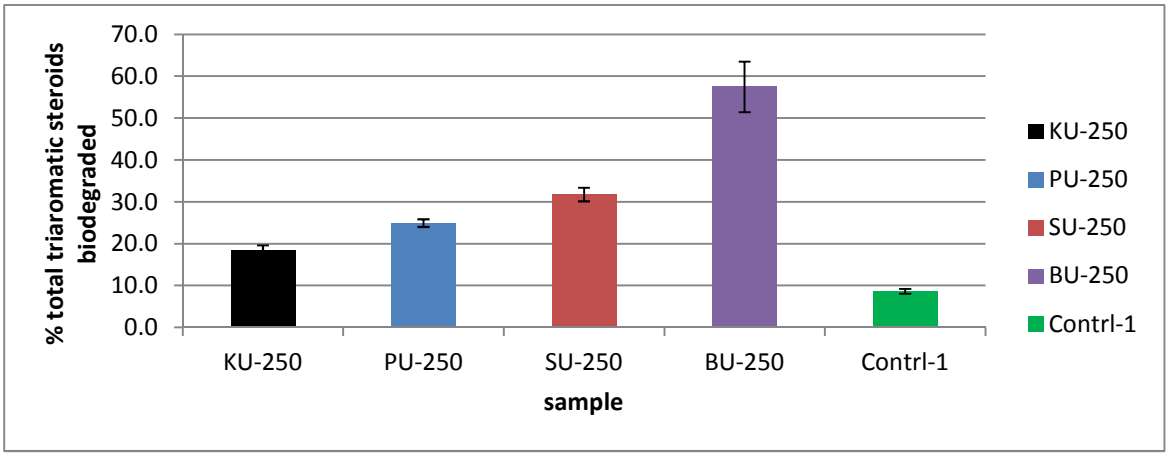

Figure 6.50 Percentage biodegradation of total triaromatic steroids supported on unmodified clay samples. Values are reported as mean ± one standard error

Figures 6.49 and 6.50 all show that the unmodified clays enhance the biodegradation of triaromatic steroids especially BU-250.

6.3.6.2 Effect of acid activated clay samples on biodegradation of triaromatic steroids

The effect of acid activated clay samples on biodegradation of triaromatic steroids are presented in Figures 6.51 and 6.52.

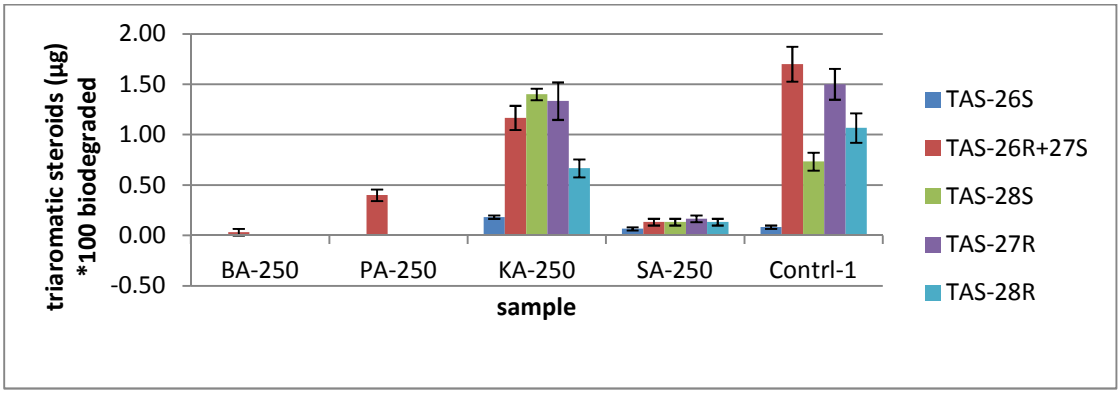

Figure 6.51 Biodegradation of triaromatic steroids (on weight basis) supported on acid activated clay samples. Values are reported as mean ± one standard error

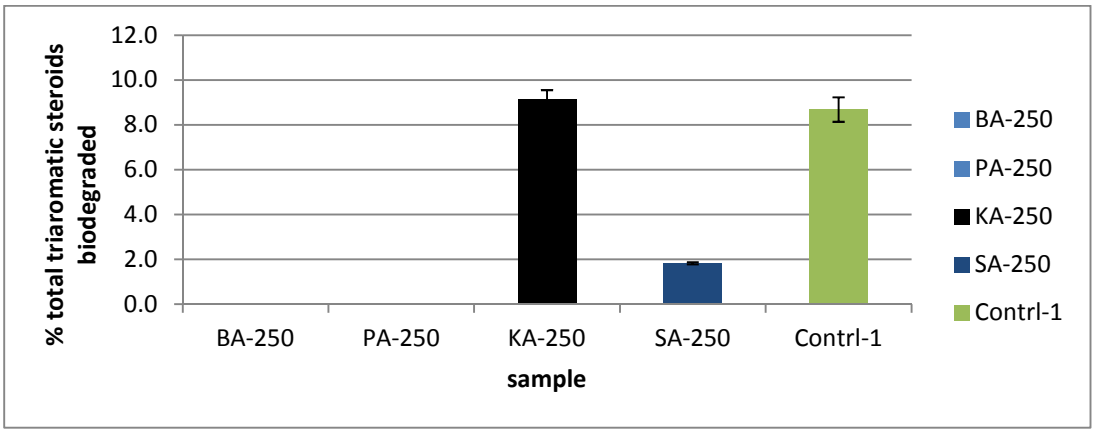

Figure 6.52 Percentage biodegradation of summed triaromatic steroids supported on acid activated clay samples. Values are reported as mean ± one standard error

The acid activated clay minerals are inhibitory to the biodegradation of triaromatic steroids except KA-250 which neither inhibits nor enhances the biodegradation.

6.3.6.3 Effect of organoclay samples on biodegradation of triaromatic steroids

The effect of organoclay samples on biodegradation of triaromatic steroids are presented in Figures 6.53 and 6.54.

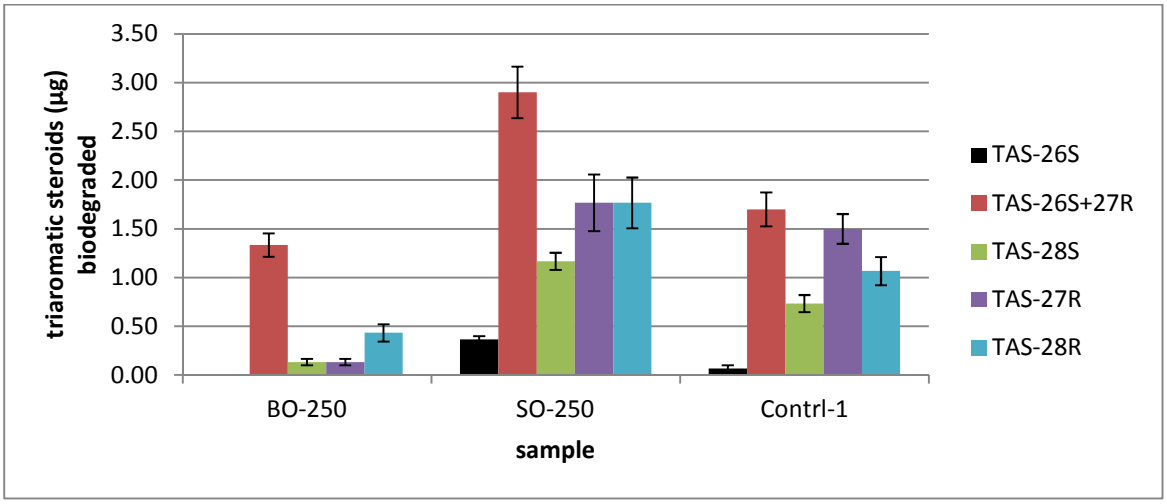

Figure 6.53 Biodegradation of triaromatic steroids (weight basis) supported on organoclays. Values are reported as mean ± one standard error.

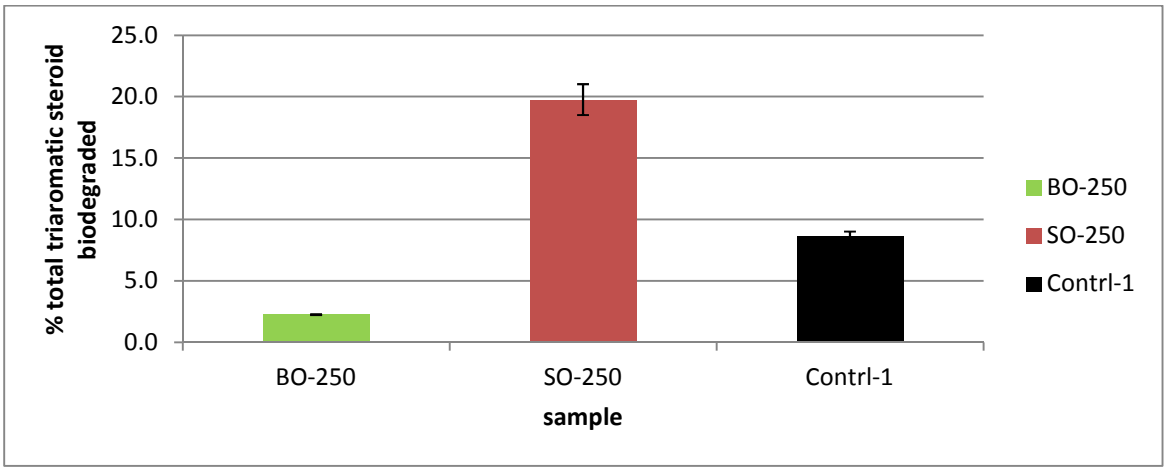

Figure 6.54 Percentage biodegradation of summed triaromatic steroids supported on organoclays. Values are reported as mean ± one standard error

Figures 6.53 and 6.54 as shown above show that BO-250 is inhibitory to the biodegradation of triaromatic steroids whereas SO-250 enhances the biodegradation.

6.3.6.4 Effect of homoionic interlayer clays samples on biodegradation of triaromatic steroids

The effect of homoionic interlayer clay samples on biodegradation of triaromatic steroids are presented in Figures 6.55 and 6.56.

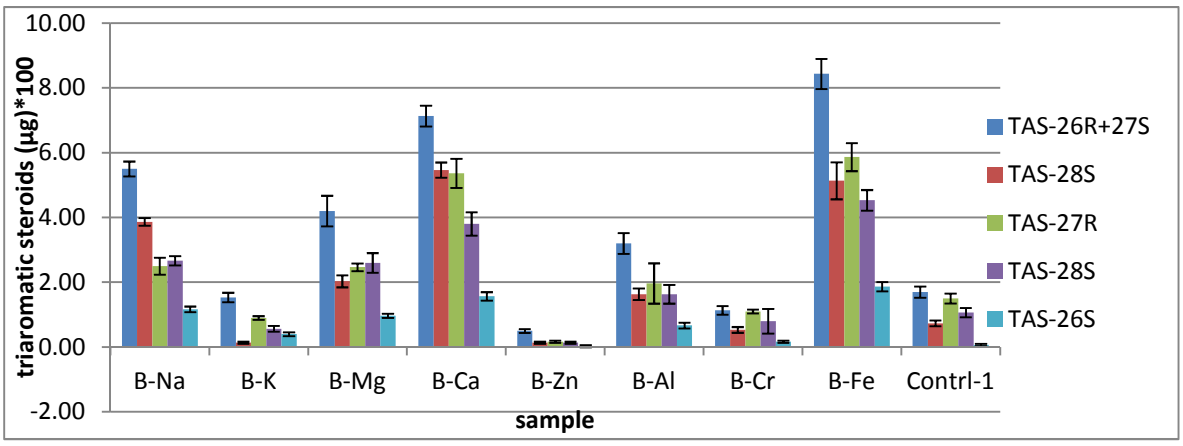

Figure 6.55 Biodegradation of triaromatic steroids (on weight basis) supported on homoionic interlayer clays. Values are reported as mean ± one standard error

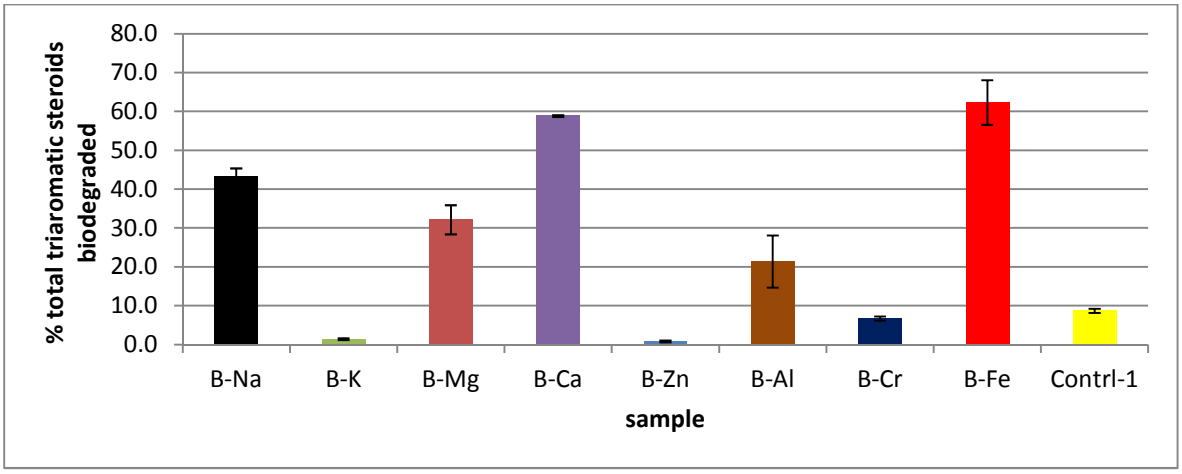

Figure 6.56 Percentage biodegradation of summed triaromatic steroids supported on homoionic interlayer clays. Values are reported as mean ± one standard error

Figures 6.55 and 6.56 indicate that whereas B-K, B-Zn, B-Al and B-Cr are inhibitory to the biodegradation of the triaromatic steroids, B-Na, B-Mg, and especially B-Ca and B-Fe enhance the biodegradation of triaromatic steroids

6. 3.7 Biodegradation of total aromatics

In this section, the analysed aromatic compounds have been grouped as follows:

All the isomers of dimethylnaphthalene - total dimethylnaphthalenes (TDMN),

All the isomers of trimethylnaphthalenes - total trimethylnaphthalenes (TTMN),

Fluorene and methylfluorenes - total fluorenes (TF)

Phenanthrene, methyl and dimethylphenanthrenes - total phenanthrenes (TP)

Dibenzothiophene, methyldibenzothiophenes, dimethylbenzothiophenes and ethyldibenzothiophenes – TDBT

The isomers of triaromatic steroids(26S, 27R, 28S, 28R and 26R+27S) - TTAS

Total aromatic compounds (TAC) = TDMN + TTMN + TF + TP + TDBT + TTAS

6.3.7.1 Effect of unmodified clay samples on biodegradation of TDMN, TTMN, TF, TP, TDBT, TTAS and TAC.

The effect of unmodified clay samples on biodegradation of TDMN, TTMN, TF, TP, TDBT, TTAS and TAC are presented in Figures 6.57-6.59.

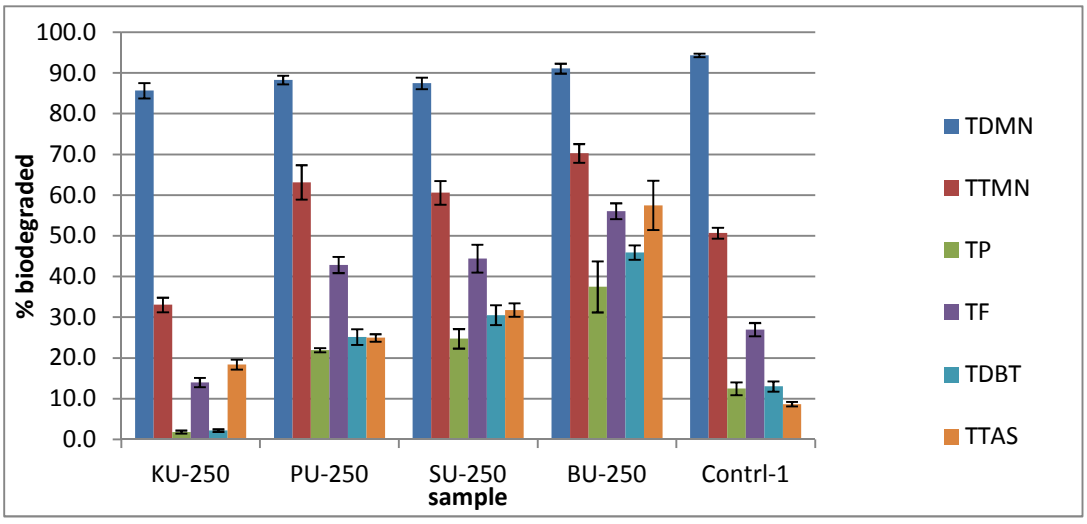

Figure 6.57 Percentage Biodegradation of various aromatic groups supported on unmodified clay samples. See description of legend above (6.3.7). Values are reported as mean ± one standard error

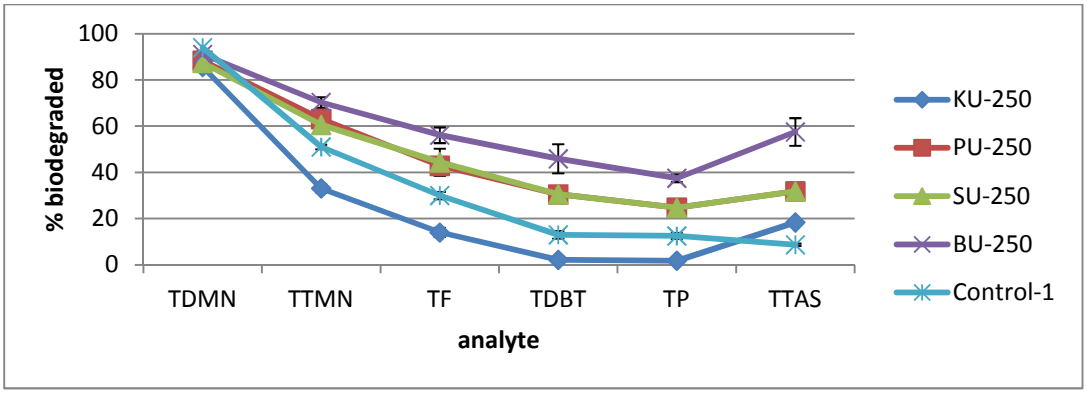

Figure 6.58 Percentage biodegradation of aromatics (as the number of benzene ring increases) supported on unmodified clays. Values are reported as mean ± one standard error

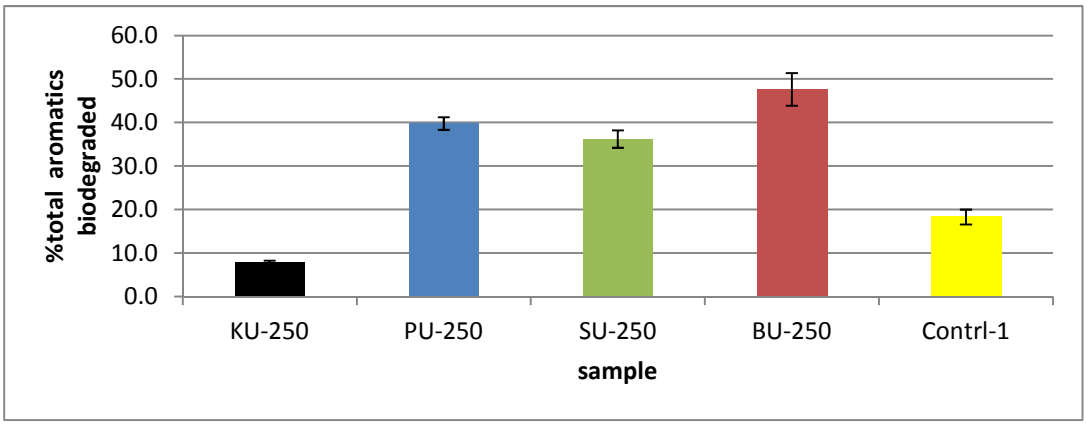

Figure 6.59 Percentage biodegradation of total aromatics supported on unmodified clay. Values are reported as mean ± one standard error

Figures 6.57-6.59 show that the unmodified clay samples enhanced the biodegradation of the aromatic compounds except unmodified kaolinite (KU-250) which only slightly enhanced the biodegradation of triaromatic steroids. From Figure 6.58, the minimum % biodegradation for unmodified clay minerals occured with TP. This behaviour appears to be different from that of other samples reviewed subsequently where the minimum was TTAS. The minimum % biodegradation for Control-1 occurred with TTAS. Unlike the organoclays, the unmodified clays all achieve a relatively high extent of biodegradation with TDMN though they have not enhanced its biodegradation. The unmodified clay samples seem to effect an increase in extent of biodegradation of the TTAS in comparison with Control-1. The percentage biodegradation of total aromatic compounds is highest with sample BU-250.

6.3.7.2 Effect of acid activated clay samples on biodegradation of TDMN, TTMN, TF, TP, TDBT, TTAS and TAC.

The effect of acid activated clay samples on biodegradation of TDMN, TTMN, TF, TP, TDBT, TTAS and TAC are presented in Figures 6.60-6.62.

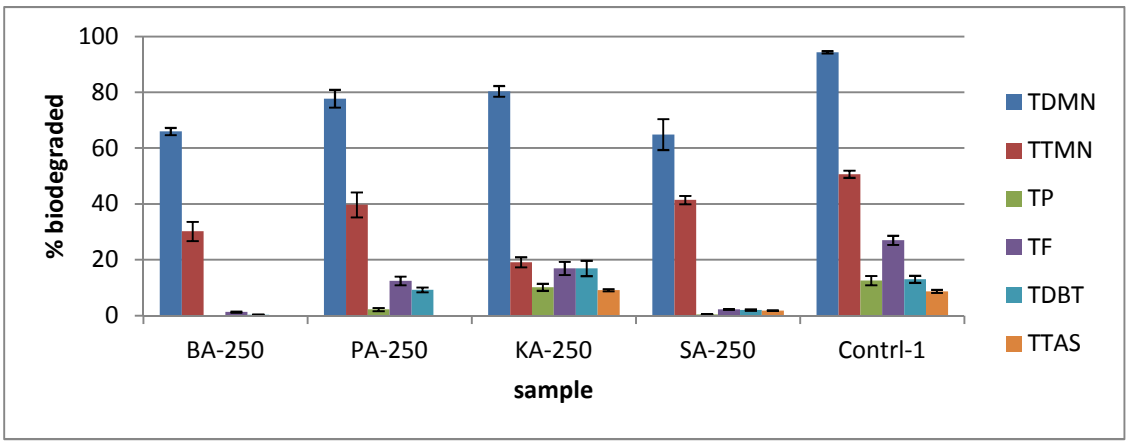

Figure 6.60 Percentage biodegradation of various aromatic groups supported on acid activated clay samples. Values are reported as mean ± one standard error

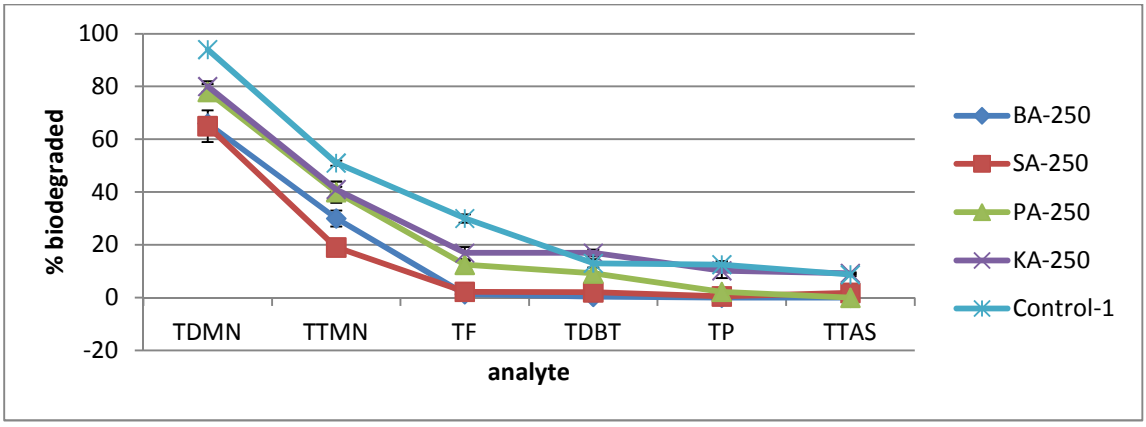

Figure 6.61 Percentage biodegradation of aromatics (as the number of fused benzene ring increases) supported on acid activated clay samples. Values are reported as mean ± one standard error.

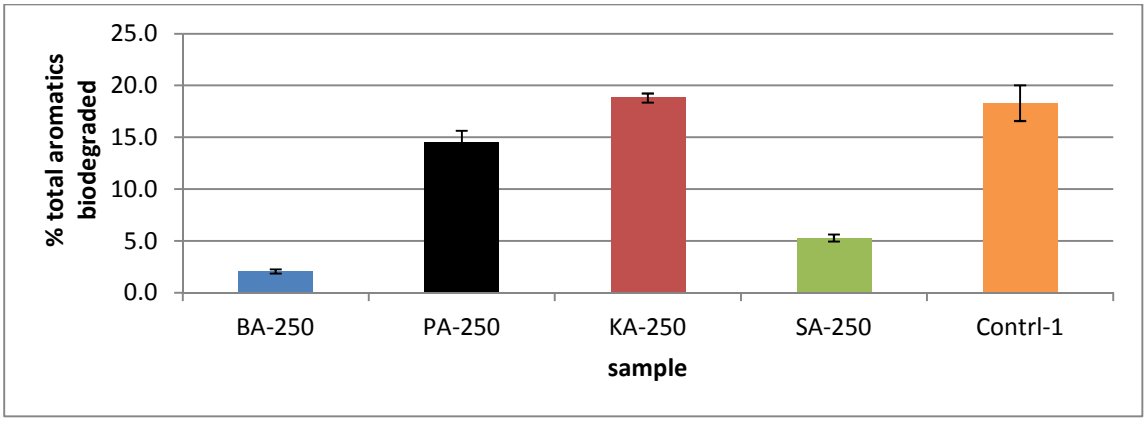

Figure 6.62 Percentage biodegradation of total aromatics supported on acid activated clays. Values are reported as mean ± one standard error.

The 2-sample t-test at 95% confidence interval (CI) performed to analyse for differences that may be statistically significant is as presented in Appendix 6.5F. Figures 6.60 and 6.62 and Appendix 6.5F show that none of the acid activated clay minerals enhanced the biodegradation of the aromatic compounds studied in this work. BA-250 and SA-250 are extremely inhibitory as they are both significantly different from Control-1 statistically. The statistical difference between Control-1 and either of PA-250 or KA-250 is not significant. Fig. 6.61 showing the extent of biodegradation as the aromatic compound increases in fused benzene rings appears to reveal the same pattern for the activated clay samples and Control-1. All the samples showed high biodegradation of dimethylnaphthalenes as they are relatively easy to biodegrade than the other aromatics studied. The % biodegradation of the different groups of aromatics falls steeply from TDMN to TF and gradually falls to TTAS as a result of increased difficulty in biodegrading the compounds.

6.3.7.3 Effect of organoclay samples on biodegradation of TDMN, TTMN, TF, TP, TDBT, TTAS and TAC.

The effect of organoclay samples on biodegradation of TDMN, TTMN, TF, TP, TDBT, TTAS and TAC are presented in Figures 6.63-6.65.

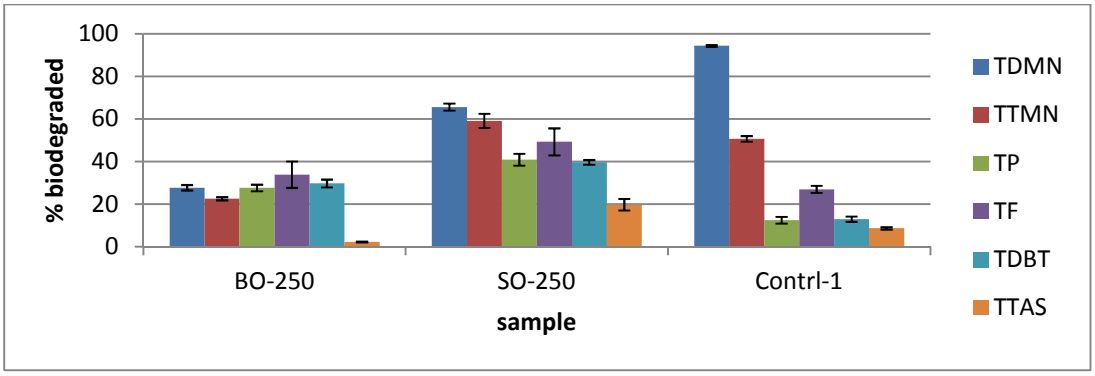

Figure 6.63 Percentage Biodegradation of various aromatic groups supported on organo-clay. Values are reported as mean ± one standard error

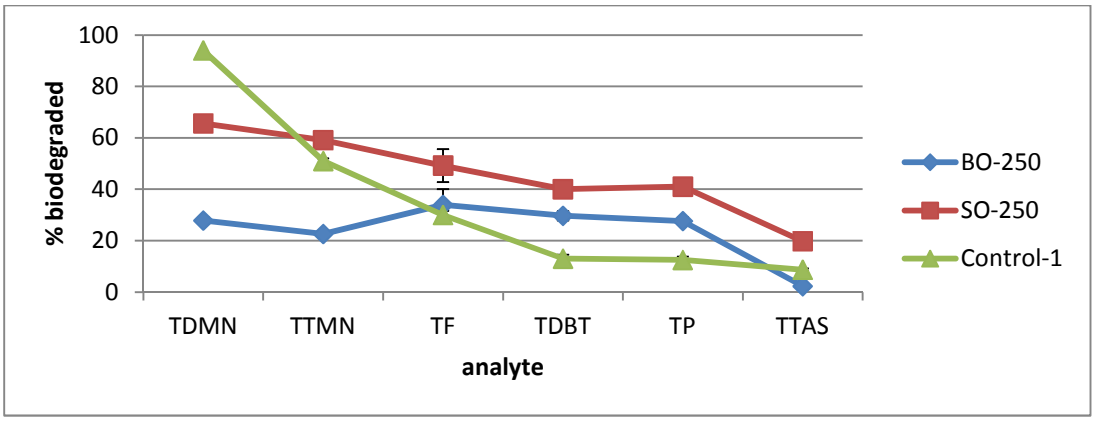

Figure 6.64 Percentage biodegradation of aromatics (as the number of benzene ring increases) supported on organo clays. Values are reported as mean ± one standard error

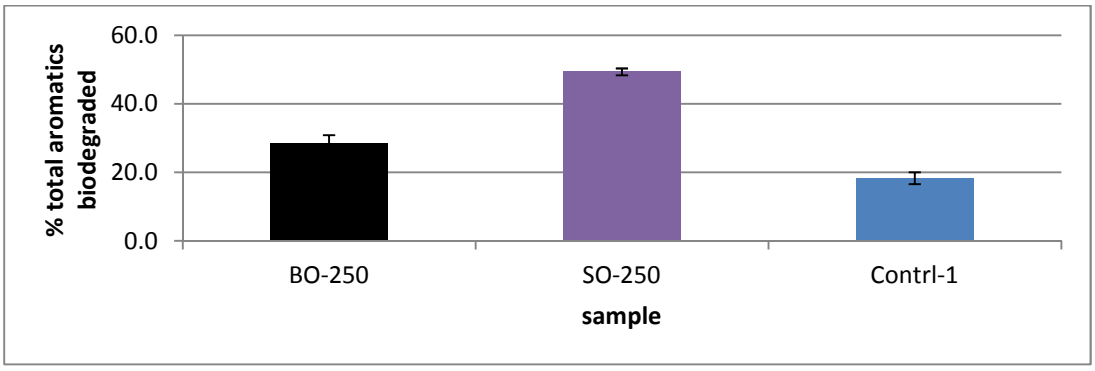

Figure 6.65 Percentage biodegradation of total aromatics supported on organo- clay. Values are reported as mean ± one standard error

Figure 6.65 shows that SO-250 enhanced the biodegradation of aromatics. However, the biodegradation of TDMN is highest with Control-1 as shown in Figures 6.63 and 6.64. The

organoclay samples especially BO-250 actually inhibits the biodegradation of low molecular weight organic compounds. The biodegradation of SO-250 falls gradually (unlike Control-1 which falls steeply) from TDMN to TP before falling steeply to TTAS. However, with BO-250, the % biodegradation of TDMN and TTMN are almost similar and increases to TF and tend to almost remain constant to TP before falling steeply to TTAS.

6.3.7.4 Effect of homoionic interlayer clay samples on biodegradation of TDMN, TTMN, TF, TP, TDBT, TTAS and TAC.

The effect of homoionic interlayer clay samples on biodegradation of TDMN, TTMN, TF, TP, TDBT, TTAS and TAC are presented in Figures 6.66-6.68.

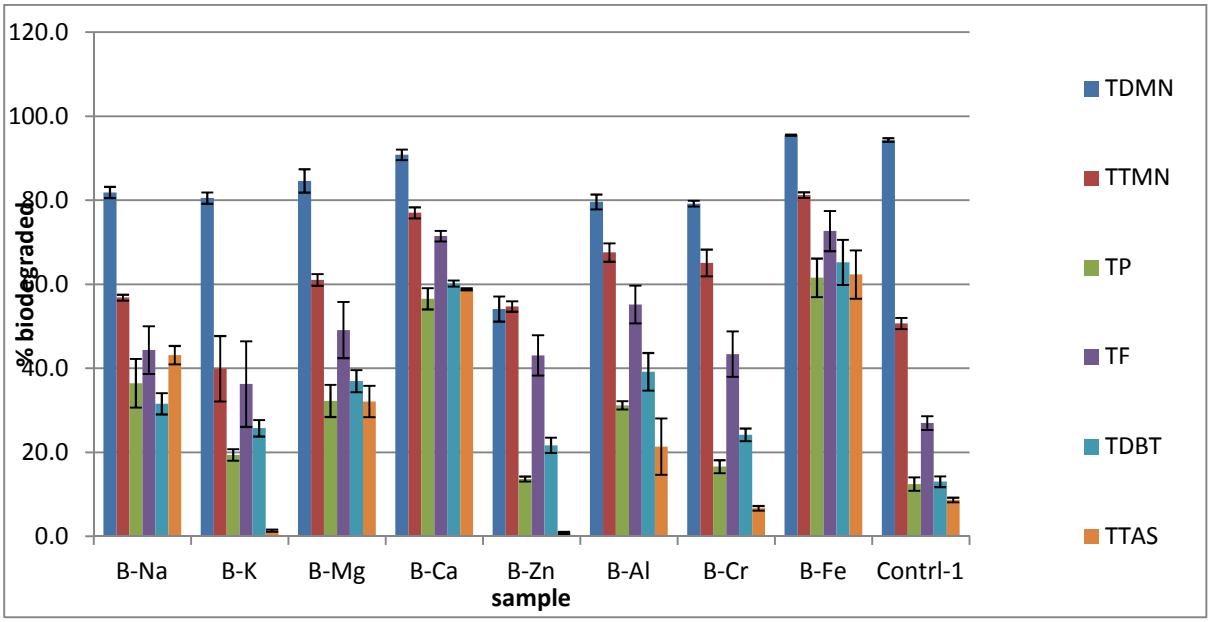

Figure 6.66 Percentage Biodegradation of various aromatic groups supported on homoionic interlayer clay samples. Values are reported as mean ± one standard error.

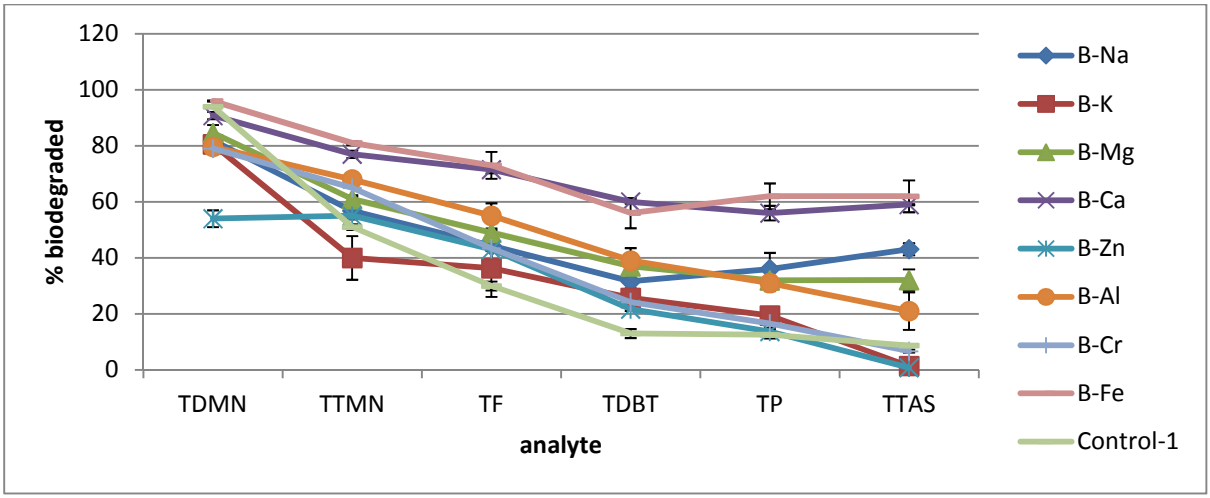

Figure 6.67 Percentage Biodegradation of aromatics (as the number of benzene ring increases) supported on homoionic interlayer clay samples. Values are reported as mean ± one standard error

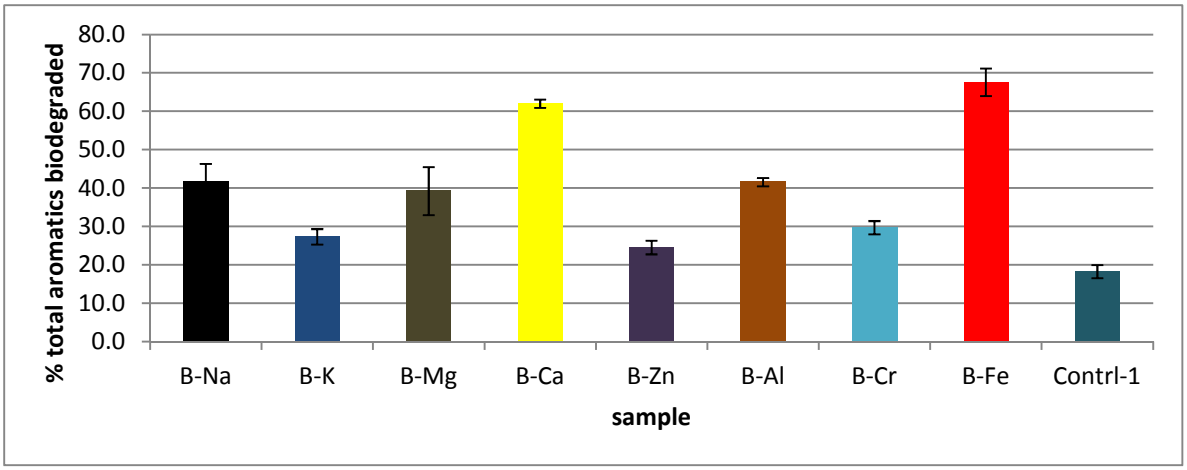

Figure 6.68 Percentage biodegradation of total aromatics supported on homoionic interlayer clay samples. Values are reported as mean ± one standard error

The 2-sample t-test at 95% confidence interval (CI) performed to analyse for differences that may be statistically significant is presented in Appendix 6.5G .

From the p-values shown in Appendix 6.5G, there is no statistical significant difference between Control-1 and either of B-Mg and B-Zn indicating that these two samples have not enhanced the biodegradation of the aromatics. Other cation-exchanged clays especially B-Ca and B-Fe appear to also enhance the biodegradation of aromatics as can be seen in Figures 6.66 - 6.68.

6. 3.8 Adsorption of aromatics

Adsorption of aromatics is presented in this section. The samples are named with a 'C' before it so as to distinguish adsorption data of aromatics from biodegradation data.

6.3.8.1 Adsorption of aromatics on acid activated, organoclay and unmodified clay

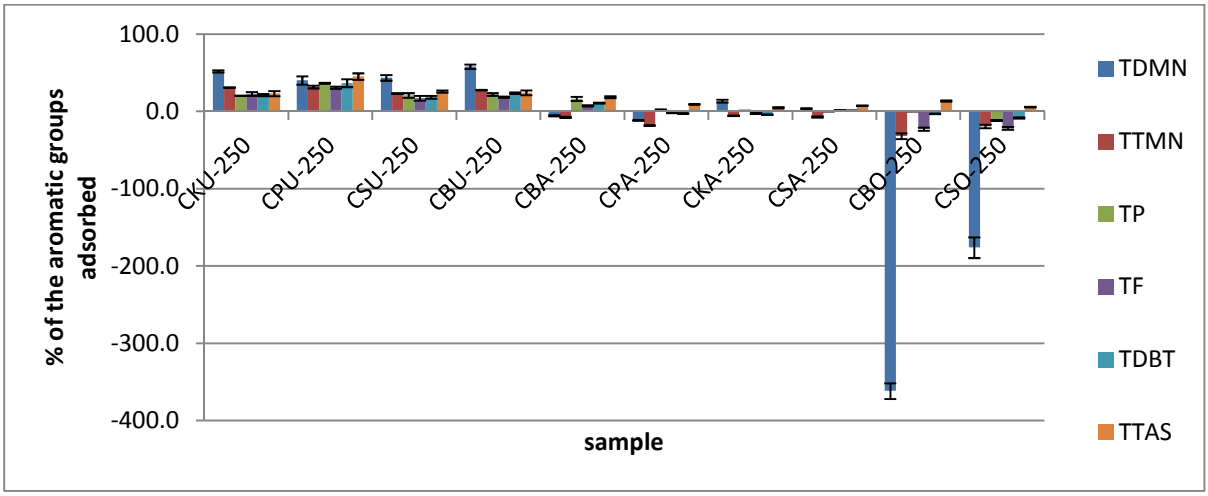

Figure 6.69 Percentage adsorption of different groups of aromatic compounds on acid activated clays, organoclays and unmodified clays. Values are reported as mean ± one standard error

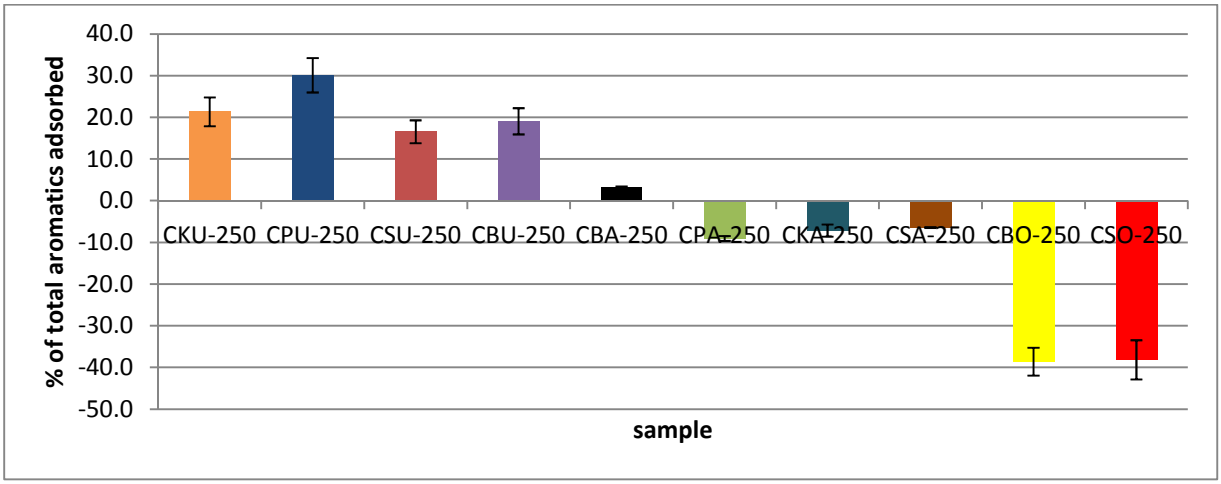

Figure 6.70 Percentage adsorption of total aromatic compounds on acid activated clays, organoclays and unmodified clays. Values are reported as mean ± one standard error

Figures 6.69 and 6.70 show that the adsorption of aromatics with respect to some samples especially organoclays is negative instead of being positive as with other samples. See

equations 6.3 and 6.4 to understand how the % adsorption was calculated. The implication of the negative adsorption is that the organoclay samples have retained the analytes more than the abiotic control, Control-2. With the organoclay, as shown in Figure 6.69, this negative adsorption tends to increase with low molecular weight of the aromatic compounds.

6.3.8.2 Adsorption of aromatics on homoionic interlayer cation exchanged clays

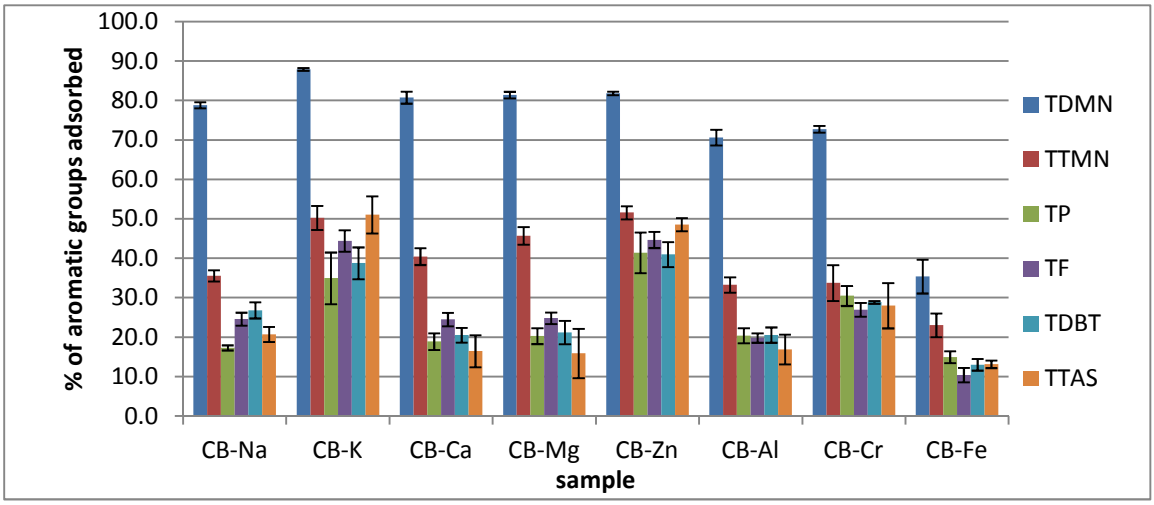

Figure 6.71 Percentage adsorption of different groups of aromatic compounds on homoionic cation interlayer clay samples. Values are reported as mean ± one standard error

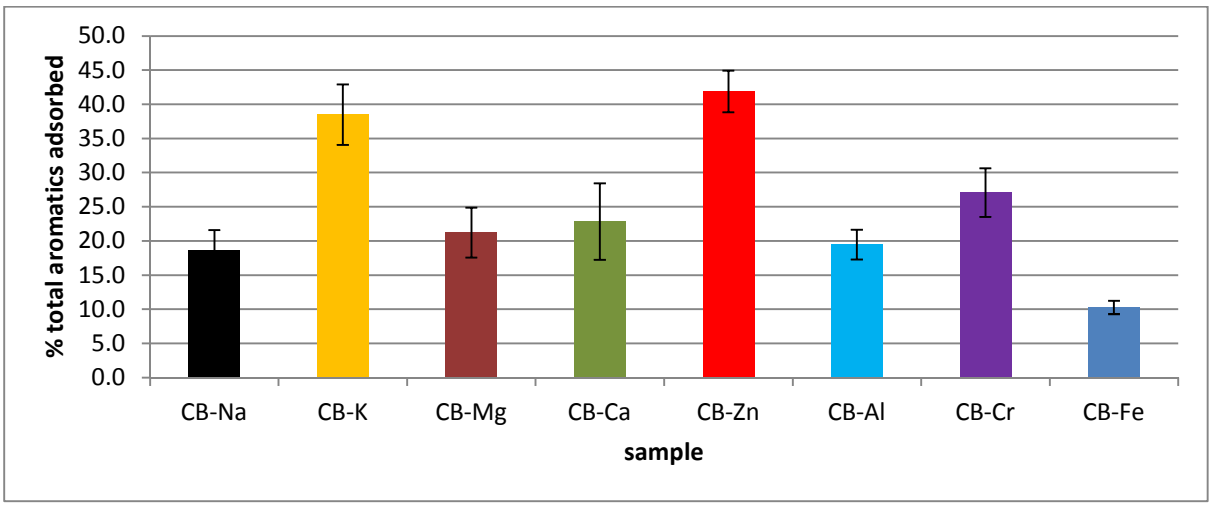

Figure 6.72 Percentage adsorption of total aromatic compounds on homoionic interlayer cation interlayer clay samples. Values are reported as mean ± one standard error.

Figures 6.71 and 6.72 show that CB-Zn and CB-K appear to achieve the highest adsorption of aromatics with CB-Fe achieving the lowest.

6.4 Cluster analysis of the biodegradation and adsorption of selected crude oil aromatics

Cluster analysis which is a form of multivariate analysis is used in this section to group the samples that are alike and are different from other samples in other groups as a result of the effects of the samples on biodegradation. Minitab 15 statistical software was used to generate the dendrogram and other relevant data. Samples with similarities with respect to biodegradation of TDMN, TTMN, TF, TDBT, TP and TTAS shall be grouped together. The same applies for adsorption.

6.4.1 Cluster analysis-biodegradation

Table 6.1 Cluster Analysis of Observations for biodegradation of aromatics: TDMN, TTMN, TF, TDBT, TP, TTAS

Standardized variables, squared eulidean distance, complete linkage

Amalgamation steps

Step	Number of clusters	Similarity level	Distance level	Clusters joined		New cluster	No. of obs. in new cluster
1	18	99.5064	0.2883	8	9	8	2
2	17	99.4359	0.3295	14	18	14	2
3	16	99.3188	0.3978	1	4	1	2
4	15	99.0577	0.5503	11	13	11	2
5	14	98.9311	0.6243	2	3	2	2
6	13	97.6172	1.3915	2	7	2	3
7	12	97.4912	1.4652	8	16	8	3
8	11	96.6494	1.9567	8	11	8	5
9	10	96.5056	2.0408	12	19	12	2
10	9	95.6039	2.5673	12	17	12	3
11	8	93.2823	3.9231	1	2	1	5
12	7	93.0083	4.0831	10	14	10	3
13	6	92.6438	4.2960	6	8	6	6
14	5	87.7328	7.1641	12	15	12	4
15	4	84.9311	8.8003	6	12	6	10
16	3	69.4516	17.8403	1	5	1	6
17	2	61.6346	22.4055	1	6	1	16
18	1	0.0000	58.4002	1	10	1	19

Final Partition

Number of clusters: 6

Cluster	Number of obs.	Within cluster sum of squares	Average distance from centroid	Maximum distance from centroid
1	5	4.04993	0.882978	1.08319
2	1	0.0000	0.0000	0.0000
3	6	4.60616	0.817149	1.44682
4	3	2.27066	0.806888	1.18489
5	3	2.26413	0.867663	0.91059
6	1	0.0000	0.0000	0.0000

Dendrogram

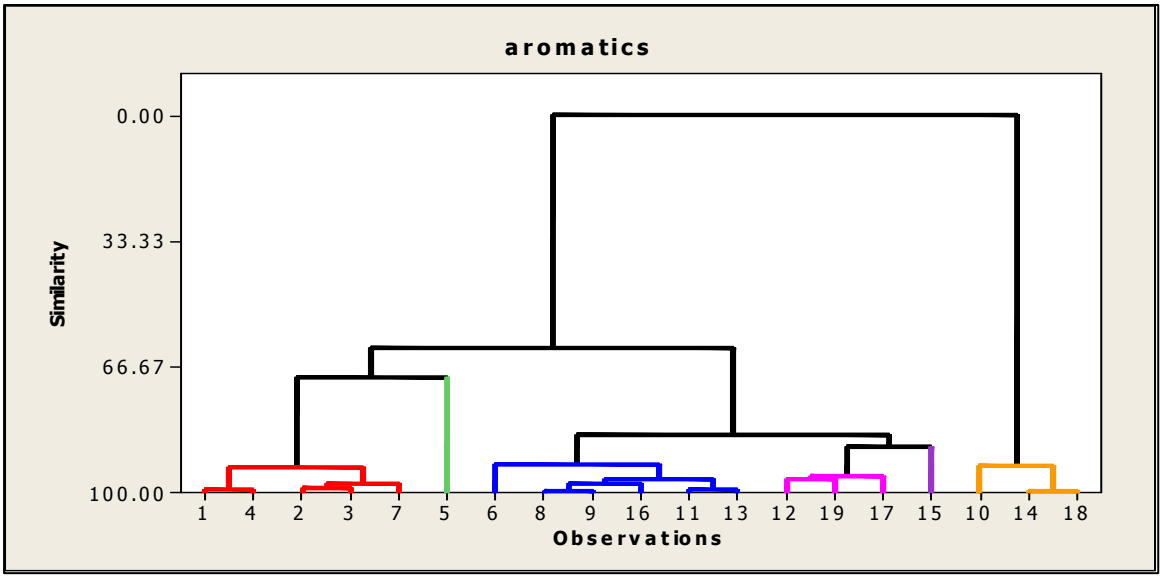

Figure 6.73 Dendrogram for the cluster analysis of biodegradation of aromatics based on TDMN, TTMN, TF, TDBT, TP, TTAS.
BA-250 = 1, PA-250 = 2, KA-250 = 3, SA-250 = 4, BO-250 = 5, SO-250 = 6, KU-250 = 7

PU-250 = 8, SU-250 = 9, BU-250 = 10, B-Na = 11, B-K = 12, B-Mg = 13, B-Ca = 14

B-Zn = 15, B-Al = 16, B-Cr = 17, B-Fe = 18, Control-1 = 19.
The above observations (samples) in the denogram are represented with numbers 1-19 and have been described above.

There are 6 clusters (groups) used in grouping the samples as follows:

Cluster (group) 1: BA-250, PA-250, KA-250, SA-250 and KU-250

Cluster (group) 2: BO-250

Cluster (group) 3: SO-250, PU-250, SU-250, B-Al, B-Na, B-Mg

Cluster (group) 4: B-K, B-Cr and Control-1

Cluster (group) 5: BU-250, B-Fe and B-Ca.

Cluster (group) 6: B-Zn

However, the greatest similarities are found among the following samples as shown by the % similarities in Table 7.8:

BA-250 and SA-250

PU-250 and SU-250

B-Na and B-Mg

B-Ca and B-Fe.

BU-250, B-Ca and B-Fe have been grouped together by the denogram and from previous analysis, these three samples appear to stimulate the biodegradation of the aromatic compounds. However, from the analysis of similarities, although these three are in the same group, B-Ca and B-Fe being more similar with each other than with BU-250, can further be said to stimulate the biodegradation of the aromatics more than BU-250. Therefore, B-Ca and B-Fe appear to have the most stimulatory properties for the biodegradation of aromatics.

6.4.2 Cluster analysis-adsorption

Table 6.2 Cluster Analysis of Observations for adsorption of aromatics: TDMN, TTMN, TP, TF, TDBT, TTAS.

Standardized variables, squared eulidean distance, complete linkage

Amalgamation steps

Step	No. of clusters	Similarity level	Distance level	Clusters joined	New cluster	No. of obs. in new cluster
1	17	98.7229	5.463	13 14	13	2
2	16	98.2669	7.413	12 15	12	2
3	15	98.0086	8.518	7 10	7	2
4	14	97.7178	9.762	11 16	11	2
5	13	97.2137	11.918	3 4	3	2
6	12	96.8009	13.683	11 13	11	4
7	11	96.3033	15.812	7 9	7	3
8	10	94.9932	21.415	11 17	11	5
9	9	94.2351	24.658	1 2	1	2
10	8	92.5626	31.812	8 12	8	3
11	7	92.2641	33.089	1 3	1	4
12	6	91.9311	34.513	11 18	11	6
13	5	87.6860	52.670	7 11	7	9
14	4	83.6523	69.923	7 8	7	12
15	3	75.1517	106.283	1 7	1	16
16	2	56.2655	187.065	5 6	5	2
17	1	0.0000	427.728	1 5	1	18

Final Partition

Number of clusters: 6

Cluster	Number of obs.	Within cluster sum of squares	Average distance from centroid	Maximum distance from centroid
1	4	843.84	13.7427	19.0191
2	1	0.00	0.0000	0.0000
3	1	0.00	0.0000	0.0000
4	3	165.29	7.2322	9.2740
5	3	647.41	13.9548	20.3295
6	6	1008.81	11.3157	22.2044

Dendrogram

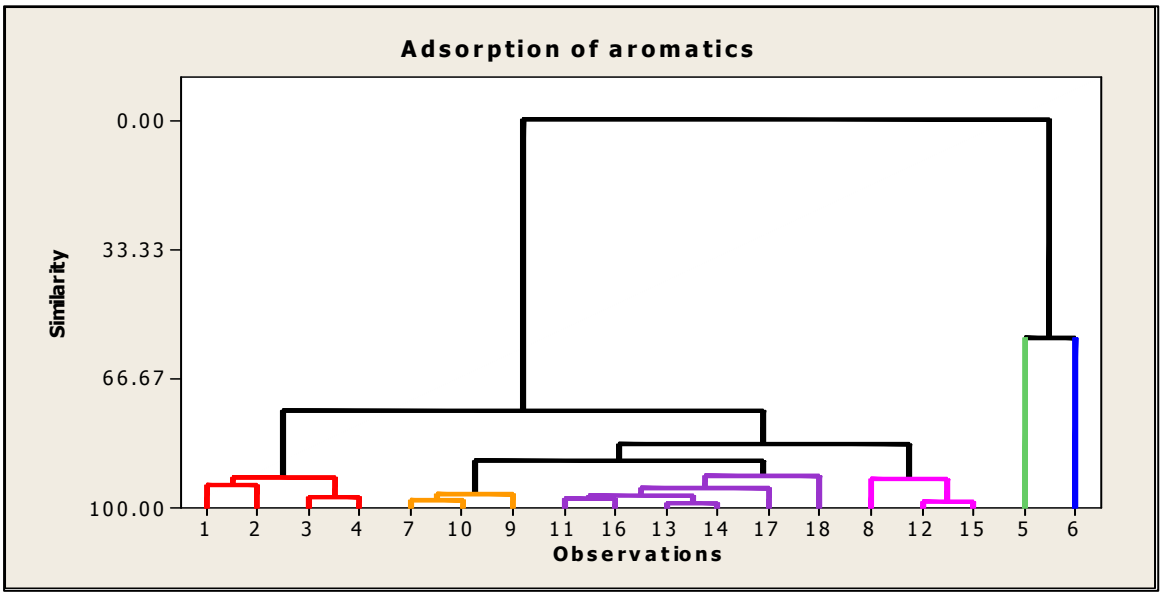

Figure 6.74 Dendrogram for the cluster analysis of adsorption of aromatics based on TDMN, TTMN, TF, TDBT, TP, and TTAS.

CBA-250 = 1, CPA-250 = 2, CKA-250 = 3, CSA-250 = 4, CBO-250 = 5, CSO-250 = 6, CKU-250 = 7, CPU-250 = 8, CSU-250 = 9, CBU-250 = 10, CB-Na = 11, CB-K = 12, CB-Mg = 13, CB-Ca = 14, CB-Zn = 15, CB-Al = 16, CB-Cr = 17, CB-Fe = 18.

Cluster (group) 1: CBA-250, CPA-250, CKA-250, CSA-250

Cluster (group) 2: CBO-250

Cluster (group) 3: CSO-250

Cluster (group) 4: CSU-250,CKU-250, CBU-250

Cluster (group) 5: CB-Fe,CB-Ca,CB-Al, B-Na, CB-Mg, CB-Cr

Cluster (group) 6 CPU-250, CB-Zn, CB-K.

6.5 Discussion

Acid activated clay minerals generally inhibited the biodegradation of crude oil aromatics. This is suggested to be due to their ability to lower the pH of the biodegradation system. The increase in acidity appears to be toxic to the microbial cells hence reducing the activity of the cells (Alexander, 1999). Adsorption of crude oil aromatics by acid activated clay samples is insignificant and is due to the lack of interlayer metallic cations as the interlayer cations have been replaced by protons. This eliminates adsorption due to pi-cation interaction (Zhu et al., 2004).

The organoclay samples especially organo-bentonite were inhibitory to the biodegradation of low molecular weight aromatic compounds such as dimethylnaphthalenes. The inhibitory properties of the organoclay tend to increase from Triaromatic steroids and phenanthrenes to Dimethylnaphthalenes. The proposed explanation is that the aromatic compounds (especially the low molecular weight aromatic compounds which would reach the adsorption sites of the organoclay first-as transport to the organic phase is most likely to be diffusion controlled) are able to interact with the organic phase of the organoclay via hydrophobic interaction which though is weak, is strong enough to cause these compounds to be rendered relatively unavailable for biodegradation. The adsorption of these relatively low molecular weight aromatic compounds (dimethylnaphthalenes) was hugely negative as shown in Figure 6.69 contributing largely to the adsorption of 'total aromatics' being negative. The main reason why these organoclay samples record negative adsorption is because they now contain more organic compounds than Control-2 (abiotic control that accounts for losses due to volatilization). This is because whereas Control-2 loses some

aromatic compounds (especially lower molecular weight aromatics like dimethylnaphthalenes) by volatilization, the organoclay holds them in the organic phase, making them to resist volatilization. However, during the extraction process with DCM, these organic compounds are extracted as the hydrophobic interaction is not strong enough to resist extraction by DCM. The hydrophobic interaction is therefore suggested to be strong enough to render these aromatic compounds (especially the low molecular weight ones) unavailable for both biodegradation and evaporation.

It is this strange behaviour that makes the organoclay achieve lower extent of biodegradation with respect to dimethylnaphthalenes and trimethylnaphthalenes when compared with other clay samples and Control-1.

Unmodified clay minerals such as bentonite, saponite, kaolinite and palygorskite studied in this work affected biodegradation of crude oil aromatics. Unmodified kaolinite (1:1 clay minerals) inhibited the biodegradation of crude oil aromatics. Ideally, kaolinite does not have interlayer cations and therefore does not possess the ability to cause 'local bridging effect' (which as a result of reducing electric double layer repulsion, increases the contacts between cells and nutrients on clay surface) as discussed previously. In addition to this, kaolinite has very low surface area in comparison with other clay samples studied in this work.

Other unmodified clay samples such as palygorskite, saponite and bentonite stimulated the biodegradation of crude oil aromatics with bentonite showing superior ability among them. These unmodified clay samples have the ability to cause local bridging effect to a degree that is sufficient enough to stimulate biodegradation of crude oil aromatics.

Unmodified palygorskite exhibited a unique behaviour in that while having the ability to stimulate biodegradation of crude oil aromatics, also possessed the ability to adsorb crude oil aromatics more extensively than any other unmodified clay samples studied. This ability is attributable to the unique structure of palygorskite which has a continuous tetrahedral sheet with inversion that causes the octahedral sheet to be discontinuous at this point of inversion creating a channel with approximate dimensions of 4Å by 6Å (Moore and Reynold, 1997) which can host the crude oil aromatics that are eventually adsorbed.

Generally, adsorption of crude oil aromatics by the unmodified clay samples is not insignificant. Cation – π interaction between the aromatic hydrocarbons and the interlayer cations of the clay is suggested to account for why these clay mineral samples show good adsorption for crude oil aromatic compounds (Zhu et al., 2004) .

The clay samples with homoionic cations at their interlayer affected biodegradation and adsorption of the crude oil aromatics to varied degrees indicating that the nature of the cation in the interlayer of the clay mineral would influence both processes of biodegradation and adsorption of crude oil aromatics. However, there is no general trend in the extent of biodegradation or adsorption in going from monovalent to trivalent cation in the interlayer of the clay sample.

Between the monovalent cations (Na^+ and K^+) tested Na-bentonite stimulated biodegradation of the crude oil aromatics more than K-bentonite. However, K-bentonite showed quite higher ability to adsorb crude oil aromatics than Na-bentonite. The interlayer of K-bentonite is not as hydrophilic as Na-bentonite. This, coupled with the fact that K^+ has a relative large size (that will make the K-bentonite expose its hydrophobic siloxane surface) caused this clay sample to possess the ability to host crude oil aromatic compounds. As the aromatic compounds get attracted into the hydrophobic siloxane surface, the cation – π interaction stated earlier would take over. See Figures 6.75 and 6.76 for a typical cation – π interaction and hydrophobic siloxane surface schemes repectively.

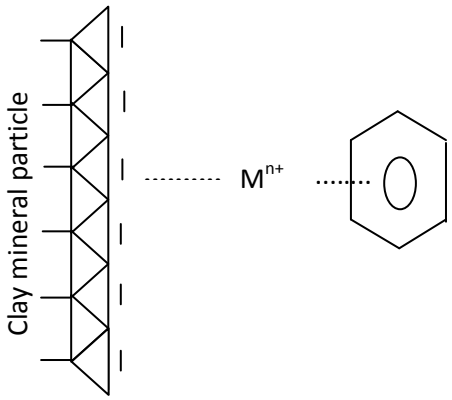

Figure 6.75 Schematic of cation – π interaction : M is a metal and n is an integer varying from 1 to 3 (modified from Zhu et al., 2004).

The pi-cation interaction represented above is a simplified form of interaction in which the benzene ring shown above could actually be any aromatic compound in the crude oil that is capable of donating pi electrons to the interlayer cation of the clay mineral. This interaction is probably largely responsible for the adsorptive capacity of clay minerals for crude oil aromatic compounds.

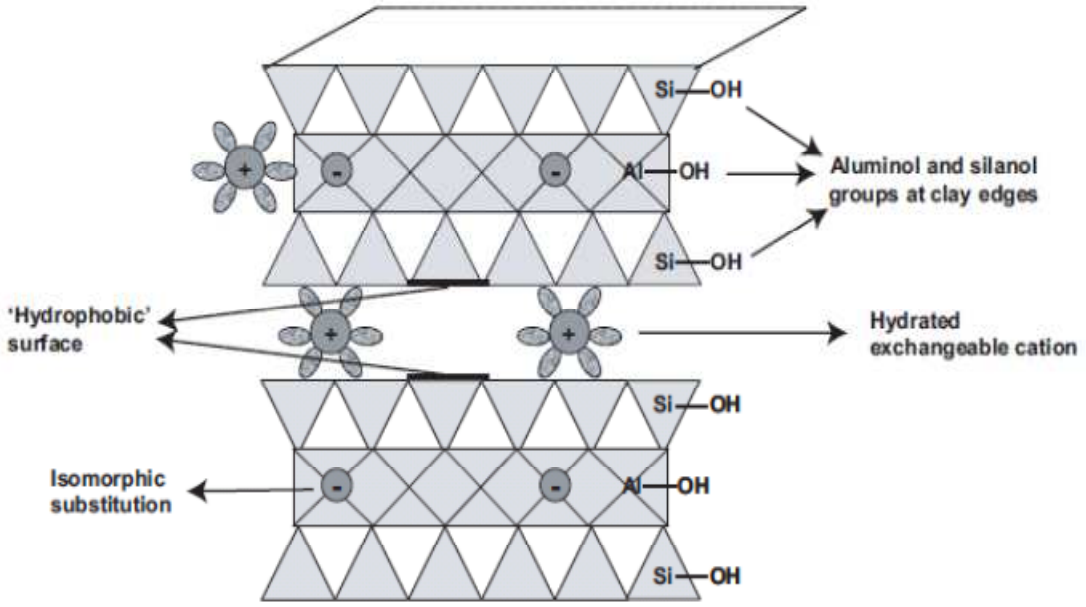

Figure 6.76 Schematics of the exposition of the hydrophobic siloxane surface of clay mineral (modified from Cornejo, 2008)

Figure 6.76 shows how the hydrophobic surface of clay minerals can actually be exposed for interaction with hydrophobic compounds such as crude oil aromatic hydrocarbons. The extent of hydration of the exchangeable cation is strictly a function of the cation and this in turn determines the accessibility of the hydrophobic siloxane surface. Not only is potassium ion large to open the interlayer, it has low hydration energy hence attracting water to the interlayer to a lower degree than metallic ions like sodium and calcium. This gives K-bentonite a unique ability to attract the crude oil aromatics into the hydrophobic surface where pi-cation interaction will eventually take place (Jaynes and Boyd, 1991).

Among the divalent interlayer cations, Ca-bentonite stimulated biodegradation of crude oil aromatics more than Zn-bentonite and Mg-bentonite. Zn-bentonite showed the highest ability to adsorb crude oil aromatics. It is not yet very clear how Zn^{2+} in the interlayer of the clay mineral accomplishes this. It has been proposed that Ca-bentonite is able to cause

excellent 'local bridging effect' that enhances the delivery of the nutrients and substrates to the microbial cells (Warr et al., 2009). This makes Ca-bentonite to effect significant biodegradation of the crude oil aromatics.

Among the trivalent cations, Fe-bentonite achieved the highest stimulation of the biodegradation of crude oil aromatics. Fe-bentonite has the highest CEC and EGME-surface area among all the clay samples studied. Adsorption of crude oil aromatics by these clay samples is highest with Cr-bentonite though when compared with K-bentonite and Zn-bentonite, Cr-bentonite adsorbs least.

6.6 Conclusion

Generally, the biodegradation of low molecular weight aromatic compounds such as dimethylnaphthalenes and fluorene does not appear to be enhanced by clay minerals. The stimulation of biodegradation of aromatic compounds by some clay samples appears to increase as the molecular weight or fused rings increases (Figure 6.67). Hence, trimethylnaphthalenes, methylfluorenes, phenanthrene, methyl- and dimethylphenanthrenes, dibenzothiophenes, methyl- and di-methyldibenzothiophenes and triaromatic steroids are enhanced by some clay minerals.

Unmodified kaolinites did not stimulate the biodegradation of any of the aromatic compounds studied and is possibly due to the lack of interlayer cations and very low surface area of kaolinites as explained in previous section. Unmodified clays such as saponites, palygorskite and bentonite stimulated the biodegradation of all the aromatic compounds except the dimethylnaphthalenes (Figures 6.57-6.59). Unmodified bentonite stimulated the biodegradation of the aromatic compounds more than all unmodified clays and is due to its high surface area and local bridging effect. The adsorption of the aromatic compounds is higher with unmodified palygorskite than the other unmodified clay samples and is due to the fibrous and channel structure of palygorskite. Cation-π interaction is believed to be responsible for the adsorption of aromatic compounds by the clay samples.

Acid activated clay samples are inhibitory to the biodegradation of all the aromatic compounds (Figures 6.60-6.62). This is due to the ability of the acid activated clay samples to lower the pH of the medium to a possible level of toxicity to the microbes.

Organoclay samples are inhibitory to biodegradation of the aromatic compounds and the inhibition increases with increased amount of organic phase in the organoclay hence organo-bentonite was more inhibitory than organo-saponite. It is suggested that the organoclay inhibits biodegradation by interacting with the aromatic hydrocarbons. This hydrophobic interaction though weak is strong enough to render the aromatic compounds unavailable for the microbes. This interaction also makes the low molecular weight aromatic compounds such as the dimethylnaphthalenes to resist volatilization (Figure 6.69).

The homoionic cation interlayer clays affect the biodegradation of the aromatic compounds at varied degrees. Fe-bentonite, Ca-bentonite, Na-bentonite, Al-bentonite and Mg-bentonite enhanced the biodegradation of the aromatic compounds with the exception of dimethylnaphthalenes. Ca-bentonite and Fe-bentonite stimulated the biodegradation of the aromatic compounds more than the other homoionic cation interlayer clays. High surface area and local bridging effect are likely to be responsible for why these clays are stimulatory. K-bentonite, Zn-bentonite and Cr-bentonite did not stimulate the biodegradation of the aromatic compounds. These clay samples especially K-bentonite and Zn-bentonite have the highest adsorptive capacity for the aromatic compounds and may account for why they are not able to stimulate biodegradation.

There is no general trend with respect to stimulation of biodegradation of crude oil aromatics among the homoionic cation interlayer samples. As noted in previous chapter, if the local bridging effect by interlayer cations were to be the only factor influencing biodegradation, the trivalent cations such as Fe-bentonite, Cr-bentonite and Al-bentonite would stimulate the biodegradation the most followed by divalent cations while monovalent cations would be least. However, this is not the case leading to the suggestion that another factor that could be inhibitory to biodegradation namely hydrolysis of interlayer water by interlayer cations could be present as well.

The order of ‘local bridging effect’ by clay samples due to homoionic cation interlayer is

Trivalent cations > divalent cations > monovalent cations (Moore and Reynold, 1997; Warr et al., 2009). This is also the same order of inhibition of biodegradation that is caused by the polarization of the interlayer water of the clay mineral.

7. Biodegradation of crude oil saturates supported on clay minerals

7.1 Introduction

Biodegradation of crude oil saturated hydrocarbons has been described in many studies. Alkanes such as n-alkanes are reported to be readily degraded. They are more readily degraded than the isoprenoids and hopanes (Bailey et al., 1973; Prince et al, 1994; Harayama et al, 1999; Gogoi et al, 2003; Huesemann et al, 2004;).

However, the biodegradation of crude oil saturates on solid supports such as clay minerals is not reported. The study of Warr et al., (2009) which studied the biodegradation of oil supported on some clays, dealt with the entire oil using Infra-red spectrophotometry for quantitation and did not investigate the crude oil saturates as a fraction.

Crude oil hydrocarbons consist of both saturates and aromatics and, it is important to understand how each of these fractions is affected by biodegradation in the presence of clay minerals. Also important is to understand whether the fractions are adsorbed on clay minerals during biodegradation and whether they do so to the same degree.

This part of the research therefore centred on studying the effect of acid activated clay, organoclay and unmodified clay on biodegradation of crude oil saturates.

The main questions addressed in this chapter of the project are:

a. Do different clay minerals stimulate or inhibit biodegradation of crude oil saturated hydrocarbons?

b. Does modification of clays affect their ability to stimulate or inhibit the biodegradation of crude oil saturated hydrocarbons?

c. What factors can explain the different effects of both unmodified clays and modified clays?

7.2 Methods

7.2.1 Assessment criteria for biodegradation of crude oil saturated hydrocarbons supported on clay minerals

The basis for the assessment of biodegradation of the crude oil saturated hydrocarbon is the determination of the total residual saturates (TRS) from the GC.

7.2.2 Determination of total residual saturates (TRS)

Determination of the TRS was done by measuring the total saturated hydrocarbon fraction GC area between 10 and 70 minutes above the baseline of a DCM blank.

TRS (mg) = $\frac{(TGC-PASS-BA)WS(ug)}{PAS} * \frac{1}{1000}$ .....Eq. 7.1

Where:

TRS = Total residual saturates

TGC = Total GC area

PA S = Peak area of surrogate standard (Squalane) also used for quantifying the TPH

PASS = Peak area of all standards including the surrogate standard

BA = Area of blank (DCM)

WS (µg) = Weight of surrogate standard (Squalane) in microgram

The equation for the determination of the % recovery of the surrogate standard (squalane) is as given in equation 5.4.

Equations 5.5-5.8 for estimating biodegradation and adsorption are all applicable in this chapter except that instead of TPH as found in equations 5.5-5.8, total residual saturates (TRS) applies.

Experiments and sample analysis were done in triplicate for statistical purposes. All the data are presented as the arithmetic mean ± standard error of the mean.

7.3 Results

7.3.1 Selected chromatograms showing degree of biodegradation of crude oil saturated hydrocarbons in this study

The chromatograms of selected samples showing the different degrees of biodegradation attained in this study are shown in Figures 7.1-7.3.

Undegraded

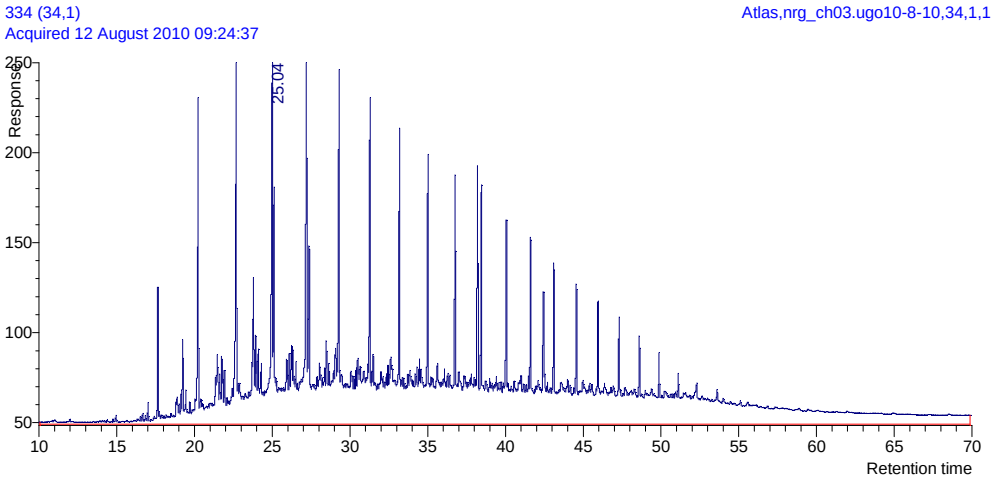

Figure 7.1 Gas chromatogram of the saturated hydrocarbon fraction of Control-2 showing absence of biodegradation. Control-2 = BH + crude oil saturated hydrocarbons. No cells and no clay.

Moderate biodegradation

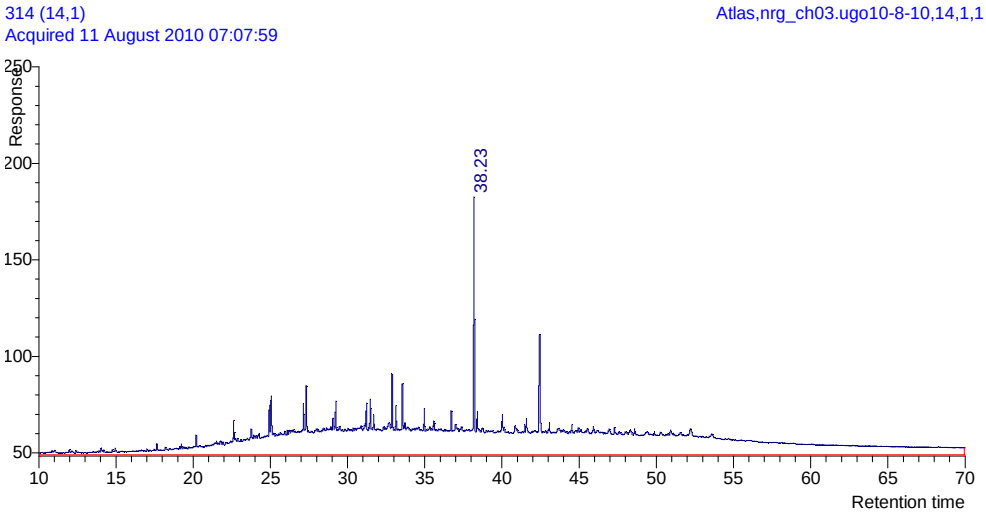

Figure 7.2 Gas chromatogram of the saturated hydrocarbon fraction of BO-250 showing moderate biodegradation. BO-250 = organobentonite.

Heavy biodegradation

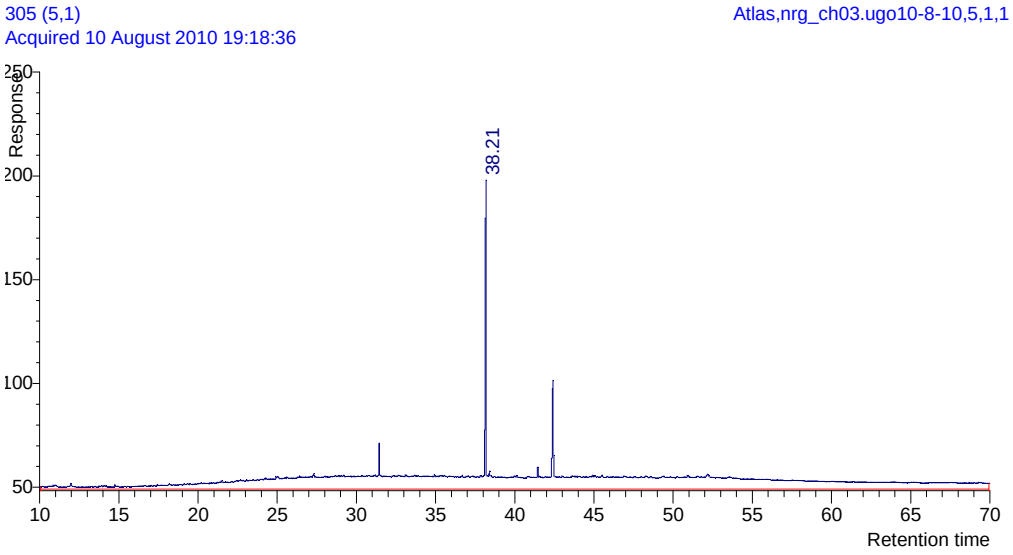

Figure 7.3 Gas chromatogram of the saturated hydrocarbon fraction of BU-250 showing heavy biodegradation. BU-250 = unmodified bentonite. Peaks remaining are for the standards namely, heptadecylcyclohexane, 5α-androstane, squalane.

Figures 7.1-7.3 show the gas chromatograms of the samples in which there was absence of biodegradation, moderate biodegradation and very heavy biodegradation. Control-2 (absence of biodegradation) is the negative control where there were no microbial cells. The chromatogram indicates that there was no substantial microbial degradation activity in this sample. BO-250 is the sample where there was moderate biodegradation of the saturates. BU-250 experiments allowed heavy biodegradation of the saturates as only the peaks corresponding to the standards remained prominent in the chromatogram.

7.3.2 Biodegradation of crude oil saturated hydrocarbons supported on unmodified clay samples

The biodegradation of crude oil saturated hydrocarbons supported on unmodified clay samples as assessed by nC17/pristane and nC18/phytane ratios are presented in Table 7.1

Table 7.1 nC17/pristane and nC18/phytane ratios-effect of unmodified clay minerals (nm = not measurable).

Sample	nC17/pristane	nC18/phytane
PU-250	nm	nm
SU-250	nm	nm
BU-250	nm	nm
KU-250	nm	nm
Control-1	nm	nm
CPU-250	2.0	2.0
CSU-250	2.0	2.0
CBU-250	2.0	2.0
CKU-250	2.0	2.0
Control-2	2.0	2.0

Table 7.1 shows that there is heavy biodegradation of the saturated hydrocarbons with the unmodified clay samples and positive control (Control-1) as the n-alkanes and isoprenoids are biodegraded giving unmeasurable values for the nC17/pristane and nC18/phytane ratios. However, the nC17/pristane and nC18/phytane ratios for the negative Control samples are similar with value of 2.0 indicating absence of microbial degradation. The residual saturates after biodegradation and the percentage biodegradation of saturated hydrocarbons supported on unmodified clay samples are presented in Figures 7.4 and 7.5.

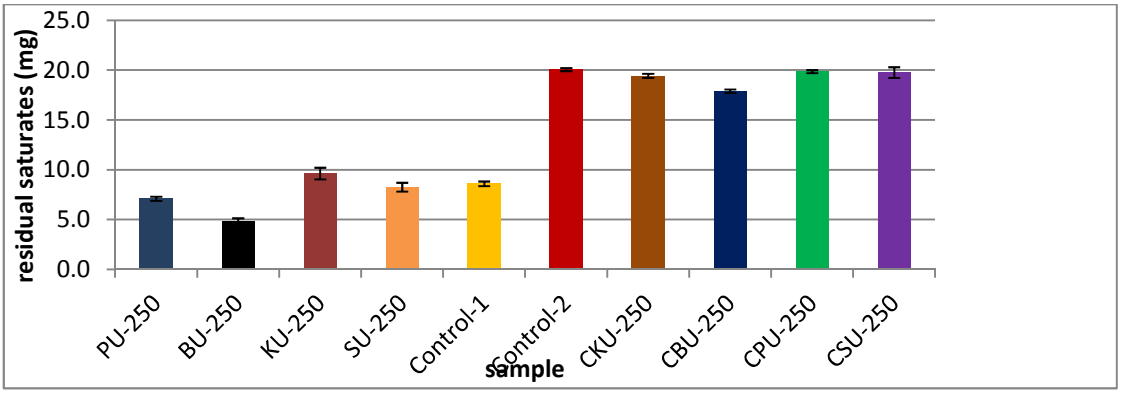

Figure 7.4 Residual saturated hydrocarbon after biodegradation supported on unmodified clays. BU-250 = unmodified bentonite, CBU-250 = unmodified bentonite control, PU-250 = unmodified palygorskite, CPU-250 = unmodified palygorskite control, SU-250 = unmodified saponite, CSU-250 = unmodified saponite control, KU-250 = unmodified kaolinite, CKU-250 = unmodified kaolinite control, Control-1 = Positive control (BH + oil + cells) no clays, Control-2 = Negative control (BH + saturates) no cells and no clays. Values are reported as mean ± one standard error.

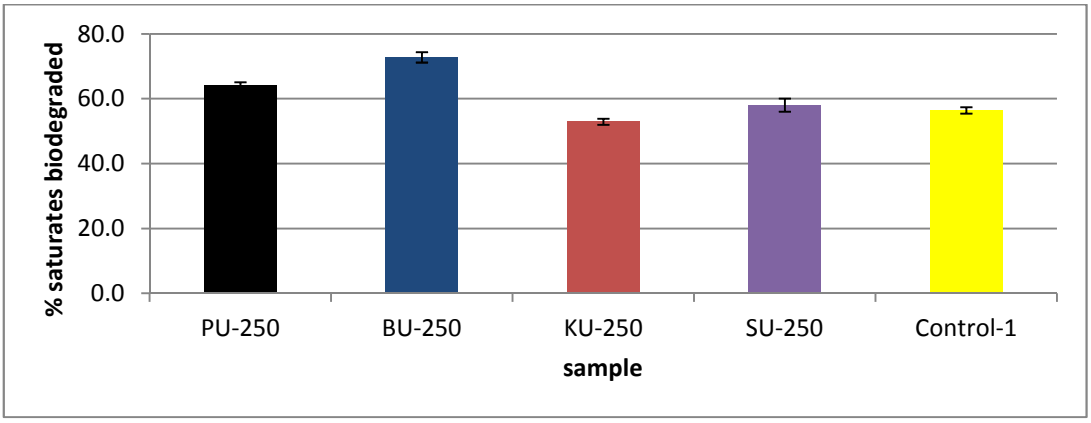

Figure 7.5 Percentage biodegradation of saturates supported on unmodified clays. Values are reported as mean ± one standard error.

Figures 7.4 and 7.5 and Appendix 7.3 show that KU-250 and SU-250 are not statistically different from Control-1 whereas PU-250 and BU-250 are statistically different from Control-1. This indicates that KU-250 and SU-250 did not enhance the biodegradation of crude oil saturated hydrocarbon whereas PU-250 and BU-250 enhanced the biodegradation of crude oil saturated hydrocarbon.

7.3.3 Biodegradation of crude oil saturated hydrocarbons supported on acid activated clays.

The biodegradation of crude oil saturated hydrocarbons supported on acid activated clay samples as assessed by nC17/pristane and nC18/phytane ratios are presented in Table 7.2

Table 7.2 nC17/pristane and nC18/phytane ratios-effect of acid activated clay (nm = not measurable).

Sample	nC17/pristane	nC18/phytane
KA-250	nm	nm
PA-250	nm	nm
SA-250	nm	nm
BA-250	nm	nm
CKA-250	2.0	2.0
CPA-250	2.0	2.0
CSA-250	2.0	2.0
CBA-250	2.0	2.0
Control-1	nm	nm
Control-2	2.0	2.0

Table 7.2 shows there is biodegradation with the acid activated clay samples and positive control (Control-1) as the n-alkanes and isoprenoids are biodegraded resulting in unmeasurable values for the nC17/pristane and nC18/phytane ratios. However, the nC17/pristane and nC18/phytane ratios for the negative Control samples are similar with a value of 2.0 signifying non-biodegradation. The residual saturates after biodegradation and the percentage biodegradation of saturated hydrocarbons supported on acid activated clay samples are presented in Figures 7.6 and 7.7.

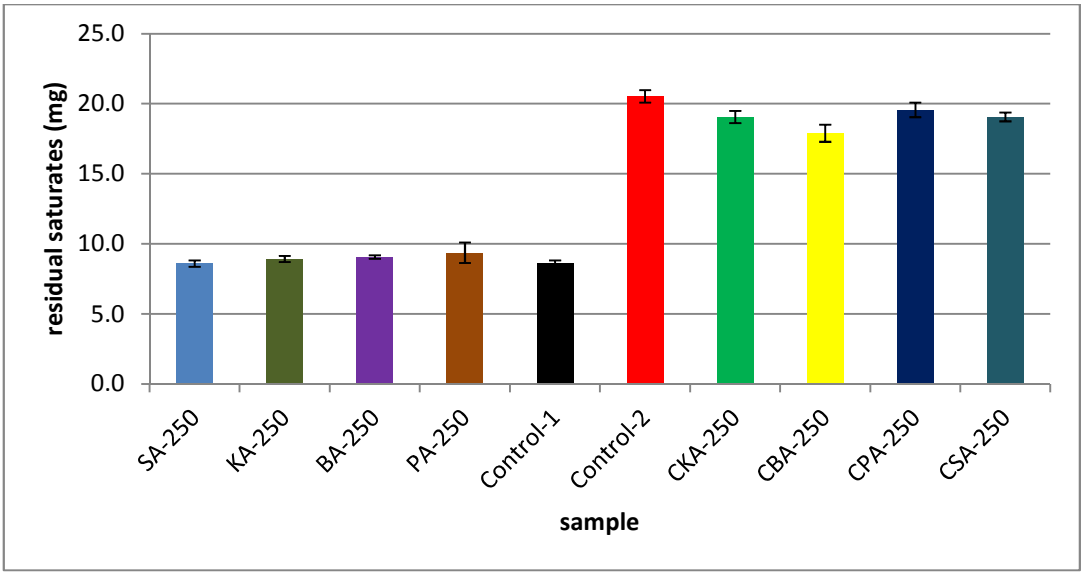

Figure 7.6 Residual saturated hydrocarbon after biodegradation supported on acid activated clay. KA-250 = acid activated kaolinite; SA-250 = acid activated saponite; PA-250 = acid activated palygorskite; BA-250 = acid activated bentonite. CBA-250, CKA-250, CPA-250 and CSA-250 are clay controls. Control-1 is the positive control (BH + oil + cells) without clay; Control-2 is the negative control (BH + saturates) without clay and cells. Values are reported as mean ± one standard error.

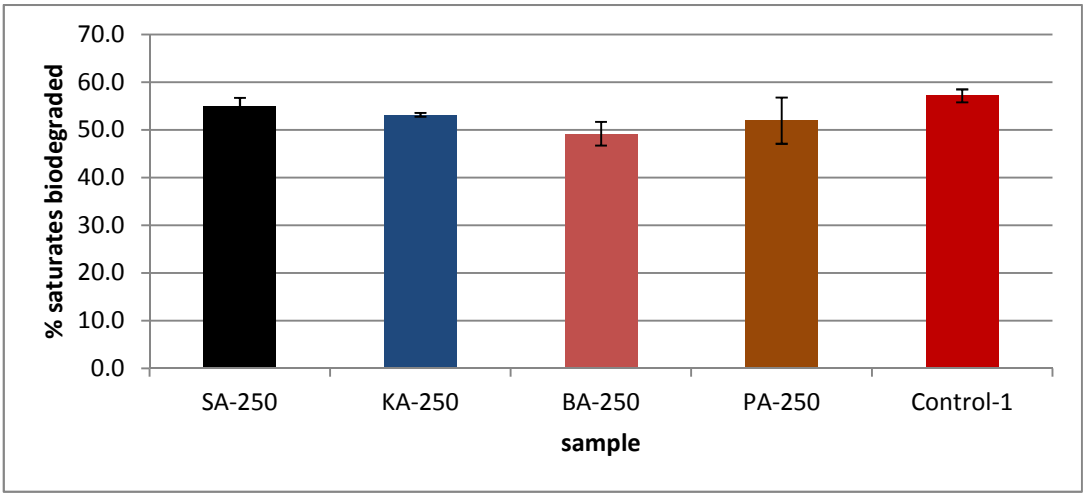

Figure 7.7 Percentage biodegradation of saturates supported on acid activated clays. Values are reported as mean ± one standard error.

Inasmuch as biodegradation had taken place in all the samples as indicated by Figures 7.6 and 7.7 and Table 7.2, there is no stimulation of biodegradation of saturated hydrocarbons

with the acid activated samples as none of the samples appear to do better than Control-1 (positive control).

The 2-sample t-test at 95% confidence interval (CI) performed to analyse for differences that may be statistically significant is presented in Appendix 7.2

The 2-sample t-test reveals that there is no statistical difference between any of the acid activated clay samples and Control-1 indicating that there is no stimulation of biodegradation of saturates by acid activated clays.

7.3.4 Biodegradation of crude oil saturated hydrocarbons supported on organoclays

The biodegradation of crude oil saturated hydrocarbons supported on organoclay samples as assessed by nC17/pristane and nC18/phytane ratios are presented in Table 7.3

Table 7.3 nC17/pristane and nC18/phytane-effect of organoclay

Sample	nC17/pristane	nC18/phytane
BO-250	0.4	0.3
SO-250	0.3	0.2
Control-1	nm	nm
CBO-250	2.0	2.0
CSO-250	2.0	2.0
Control-2	2.0	2.0

Table 7.3 shows, there is moderate biodegradation with organoclay samples giving values of 0.4 and 0.3 for the nC17/pristane and nC18/phytane ratios respectively. However, there is heavy biodegradation with Control-1 (positive control) as the n-alkane and isoprenoids are degraded giving unmeasurable nC17/pristane and nC18/phytane ratios. The nC17/pristane and nC18/phytane ratios for the negative control samples are similar with a value of 2.0 signifying absence of biodegradation. The residual saturates after biodegradation and the percentage biodegradation of saturated hydrocarbons supported on organoclay samples are presented in Figures 7.8 and 7.9.

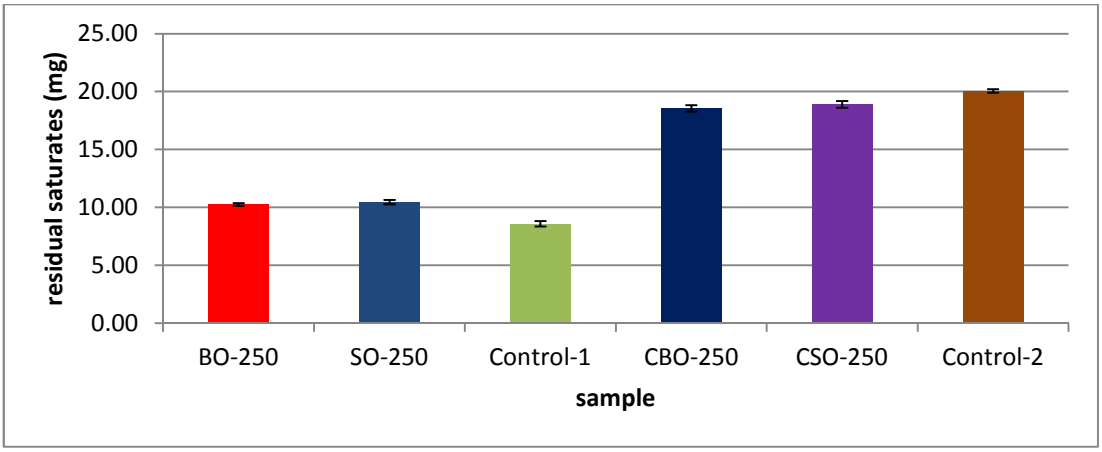

Figure 7.8 Residual saturated hydrocarbons after biodegradation supported on organoclay samples. Values are reported as mean ± one standard error.

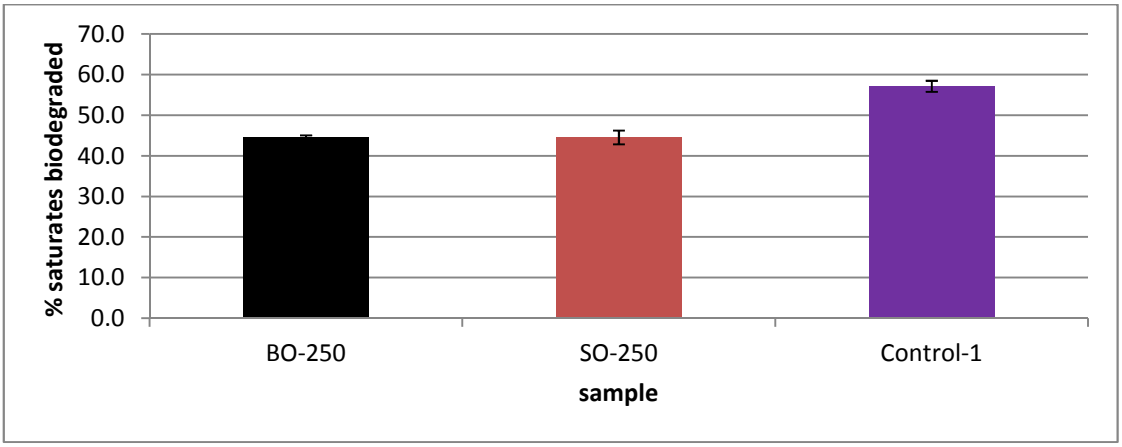

Figure 7.9 Percentage biodegradation of saturates supported on organoclay. BO-250 = organobentonite; SO-250 = organosaponite; Control-1 =BH + oil + cells. Control-2= BH + saturates. CBO-250 and CSO-250 are clay controls. Values are reported as mean ± one standard error.

The above Figures 7.8 and 7.9 and table 7.3 show that the organoclay samples seem to inhibit the biodegradation of crude oil saturated hydrocarbons. The P-values were 0.01 and 0.013 for Control-1 and SO-250 and Control-1 and BO-250 respectively indicating that the organoclay samples are both statistically different from Control-1 and that the organoclay samples inhibit the biodegradation of crude oil saturates.

7.3.5 Adsorption of crude oil saturated hydrocarbons on clay samples

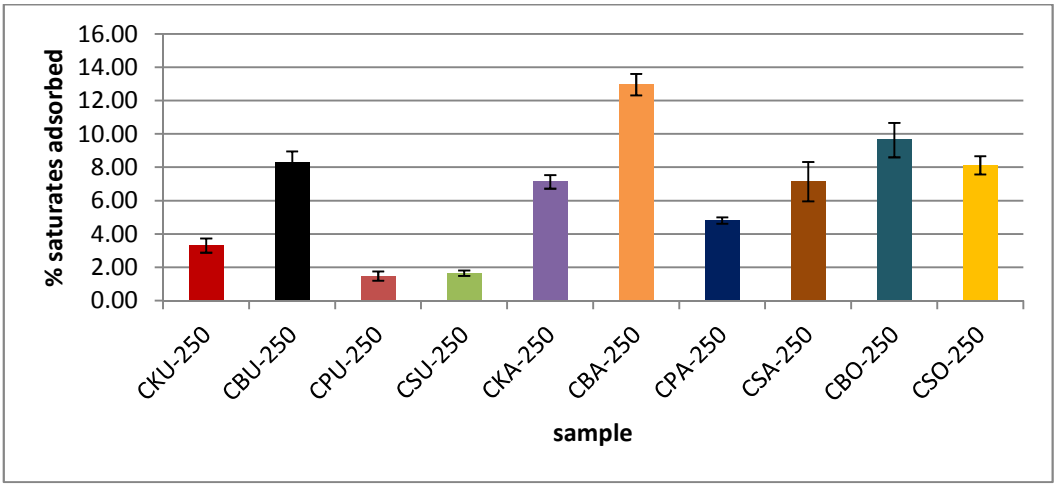

Figure 7.10 Percentage adsorption of crude oil saturated hydrocarbons on clay minerals. Values are reported as mean ± one standard error.

Figure 7.10 shows that the percent removal of saturates by adsorption on clay minerals was minor. However, there seemed to be an increase in the adsorption of crude oil saturates from unmodified clay samples to acid activated clay samples. CBA-250 appears to effect the highest adsorption (13% adsorption) of the crude oil saturates and has the lowest pH value as shown in Table 3.1.

7.4 Discussion

The acid activated clay samples namely, (BA-250, SA-250, PA-250 and KA-250) are inhibitory to biodegradation of crude oil saturates. This is suggested to be due to their ability to lower the pH of the biodegradation system. The increase in acidity would be toxic to the microbial cells hence reducing the activity of the cells (Alexander, 1999).

The organoclay samples were highly inhibitory to biodegradation of crude oil saturates. The inhibitory properties of the organoclay with crude oil saturates seems to be somewhat different from that of the crude oil aromatic hydrocarbons described earlier (Section 6.5). With crude oil saturates, the adsorptive sites of the organoclay would be occupied by some of the petroleum ether used as solvent for transfering the crude oil saturates into the flasks and serum bottles during the biodegradation experiment. The remaining portion of the PET ether in the system would volatilize as PET ether is highly volatile. As the hydrophobic

adsorptive sites of the organoclay could get fully occupied by PET ether, the crude oil saturates may therefore not be adsorbed by hydrophobic interaction with the organic phase of the organoclay and rather may be adsorbed by the hydrophobic siloxane surface of the clay. The inhibitory attribute of the organoclay probably arises mainly from the reduced 'local bridging effect' of these clays as the interlayer cations have been displaced by organic cations which cannot participate in 'local bridging effect'.

The unmodified clay minerals such as bentonite, saponite, kaolinite and palygorskite studied in this work affected biodegradation of crude oil saturates. Unmodified kaolinite (1:1 clay minerals) and saponite did not enhance the biodegradation of crude oil saturates. Theoretically, kaolinite does not have interlayer cations and therefore does not possess the ability to cause 'local bridging effect' (which as a result of reducing electric double layer repulsion, increases the contacts between cells and nutrients on clay surface) as discussed previously. In addition to this, Kaolinite has very low surface area in comparison with other clay samples studied in this work. Although saponite achieved a mean value of % saturates biodegraded higher than kaolinite, it is not significantly different from control-1 therefore it cannot be said to have enhanced biodegradation of crude oil saturates.

The other unmodified clay samples: palygorskite, and bentonite, stimulated the biodegradation of crude oil saturates with bentonite showing a superior ability to palygorskite. These unmodified clay samples probably have the ability to cause local bridging effect to a degree that is sufficient enough to stimulate biodegradation of crude oil saturates.

The regression analysis and correlation of crude oil saturated hydrocarbons biodegraded to surface area and CEC are presented in Figures 7.11 and 7.12.

Regression analysis and Correlation of crude oil saturates biodegraded to surface area and CEC of unmodified clay

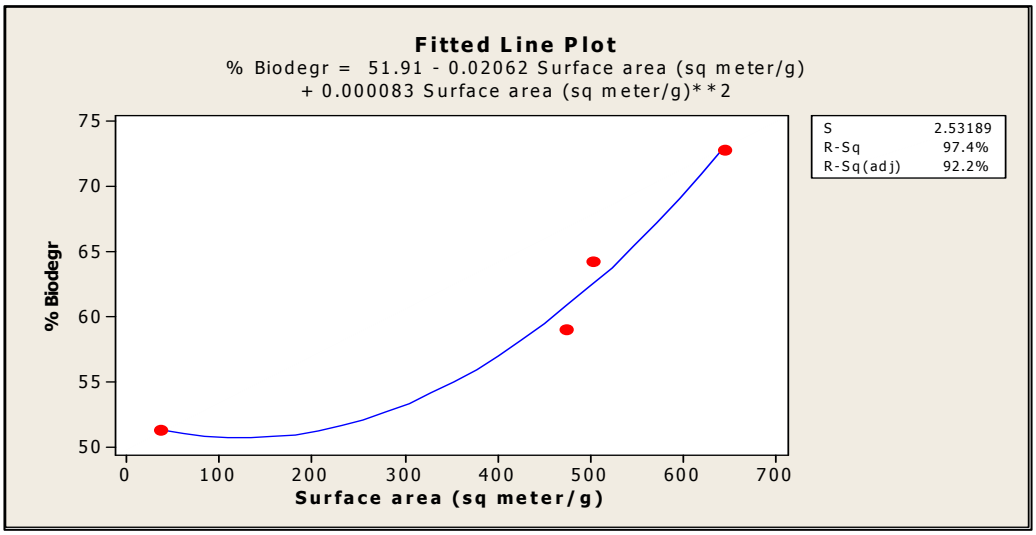

Figure 7.11 Regression analysis of surface area and % biodegradation of crude oil saturates.

The Pearson coefficient of correlation (r) of surface area of unmodified clay samples and % biodegradation of saturates = 0.872; P=0.128

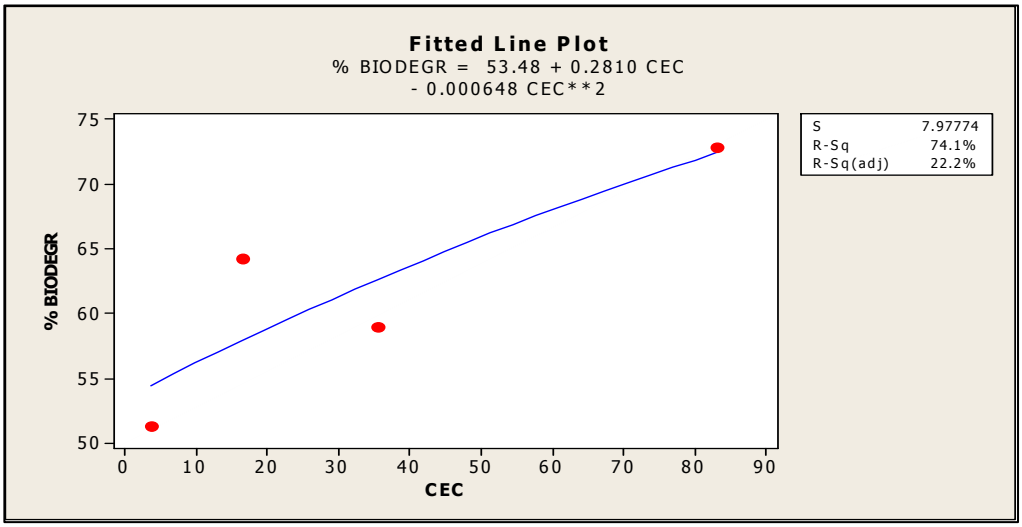

Figure 7.12 Regression analysis of CEC and % biodegradation of crude oil saturates

The Pearson coefficient of correlation (r) of surface area of unmodified clay samples and % biodegradation of saturates = 0.851; P=0.149

From Figures 7.11 and 7.12, the correlation of % biodegradation of crude oil saturates with the clay surface area is slightly higher than with its CEC. This indicates that the mechanism of biodegradation possibly involves the accumulation of nutrients and microbes on clay surface via reduction of electric double layer repulsion (local bridging effect).

Adsorption of crude oil saturates among the clay samples is low due to the absence of pi-cation interaction. However, acid activated bentonite showed the highest adsorption of the crude oil saturates of about 13%. This is suggested to be due to the protonation of alkanes in which the acid activated clay acts as a proton donor (Bronsted acid) and the alkane especially branched alkane as a proton acceptor (Bronsted base) though the alkanes are weak Bronsted bases. The reaction scheme below shows how acid activated clays especially acid activated bentonite can interact with saturates and hence get them adsorbed (Hunter et al, 2003; Xu et al, 2006).

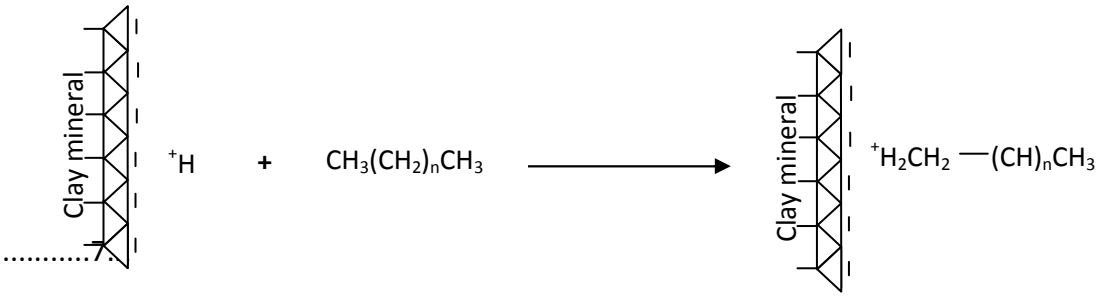

.....7.

This protonation reaction (equation 7.2) is quite relevant in the petrochemical industry where it is manipulated by employing favourable reaction conditions to crack the alkane and regenerate the catalyst (acid activated clay) (Hunter et al, 2003; Xu et al, 2006).

7.5 Conclusion

Unmodified clay minerals such as unmodified palygorskite and unmodified bentonite appear to stimulate the biodegradation of crude oil saturated hydrocarbons. The local bridging effect and high surface area are believed to account for the stimulatory role of some clay samples (Warr et al, 2009). Unmodified kaolinite is inhibitory and is possibly due to the lack of interlayer cations in kaolinite. Unmodified saponite is neither inhibitory nor stimulatory. The surface area of clay samples appears to play a more important role during the biodegradation of crude oil saturated hydrocarbons than the CEC as the coefficient of correlation between the surface area of the clay and the percentage biodegradation of the

saturated hydrocarbon is higher than that between the CEC and the percentage biodegradation of the saturated hydrocarbons.

The treated clay samples such as acid activated clay samples are inhibitory to the biodegradation of the saturated hydrocarbons. The inhibition of biodegradation of saturated hydrocarbons by acid activated clay samples is suggested to be due to the ability of the clay samples to lower the pH of the medium to a level that may be toxic to the microbes.

Organoclay samples are inhibitory to biodegradation and may be due to the drastically reduced ability of the organoclay to produce local bridging effect.

8. BULK COMPOSITION OF THE RESIDUAL OIL- IATRO SCAN

8.1 Introduction

Several studies have shown that Iatroscan which is thin layer chromatography-flame ionization detection (TLC-FID) can be used in the evaluation of compositional changes of petroleum arising from abiotic and biotic processes. Consequently, this tool has become very useful in monitoring the changes in composition of petroleum in environmental processes (Pollard et al., 1992; Napolotano et al., 1998; Stephens et al., 1998). The analysis of SARA fractions in biodegraded oils in order to estimate extent of biodegradation have been reported (Goto et al., 1994; Maki et al., 2001; Jirasripongpun, 2002; Ishiyama et al., 2007). Iatroscan is a semi-quantitative analytical tool and does not always produce highly reproducible measurements. However, it is a rapid means of revealing the changes in the % distribution of the SARA fractions of the oil (Pollard et al., 1992; Napolotano etal., 1998).

In this chapter, the results of the analysis of the residual oil (after incubation) with Iatroscan are presented. The key questions to be addressed are:

(a) What is the % distribution of the SARA fractions in the residual oil after the incubation of the experimental microcosm containing aqueous clay/oil and hydrocarbon degrading microbes for the test samples in comparison with the control samples?
(b) How are the losses of the hydrocarbons due to abiotic processes such as volatilization and adsorption estimated?
(c) How can the Iatroscan data be used to estimate the effect of the clays on the biodegradation of the crude oil hydrocarbons?

8.2 Methods

The quantitation of the SARA fractions was done with standard oil (North Sea oil) and the SARA fraction distribution generated in percentage.

To measure the weight distribution of the SARA fractions, the 2ml aliquot conserved as indicated in section 2.5 was carefully and slowly dried under nitrogen and the weight recorded. However, the original total volume of extract solution was 10ml, necessitating

conversion back to the weight of the extract in 10ml solution [using a conversion factor of 5 (ie 10ml/2ml)] to get the total weight of residual oil as extracted.

By multiplying through by the % distribution of fractions from the Iatro scan, the distribution of the fractions by weight was estimated.

The total weight (mg) of residual oil (EOM) and distribution by weight (mg) of SARA fractions in the residual oil was estimated as follows:

$W_{TS} = 5Y$……Eq. 8.1

Where:

W_{TS} = Total weight (mg) of residual oil (EOM) in a given sample

5 = conversion factor from 2ml to 10ml

Y = weight of oil residue (mg) in 2ml aliquot as conserved after extraction (see section 2.5)

$F_w = W_{TS} X$……Eq. 8.2

Where:

F_w = weight (mg) of a given SARA fraction in the oil residue

X = % of fraction as measured by Iatro scan

Weight (mg) of oil biodegraded,

$W_{ob} = W_{TS}$ (for control sample) - W_{TS} (for test sample).....Eq. 8.3

% of oil biodegraded,

$T_{ob\%} =$ [W_{ob}/ W_{TS} (for control sample-clay)] *100.....Eq. 8.4

Weight of oil adsorbed,

$W_{ads} = W_{TS}$ (for control-2) - W_{TS} (for control sample-clay).....Eq. 8.5

% of oil adsorbed = [W_{ads}/ W_{TS} (for control-2)] *100 .....Eq. 8.6

8.3 Results

8.3.1 Percentage distribution of SARA fractions in the residual oil samples

In this section, the arithmetic mean of the triplicate data of the % distribution of the SARA fractions of the residual oil both for control experiments where there was no microbial activities and test samples where there was microbial activities are presented. Values are reported as mean ± one standard error.

8.3.1.1 SARA fractions distribution with unmodified clay samples

The SARA fractions for unmodified clay samples after the biodegradation experiment is presented in Figure 8.1.

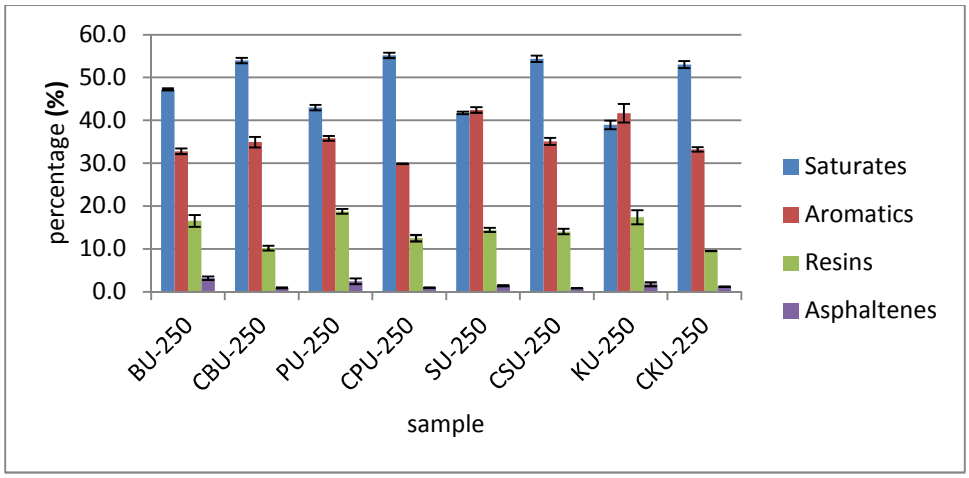

Figure 8.1 Percentage distributions of SARA fractions with unmodified clay samples. BU-250 = unmodified bentonite, CBU-250 = unmodified bentonite control, PU-250 = unmodified palygorskite, CPU-250 = unmodified palygorskite control, SU-250 = unmodified saponite, CSU-250 = unmodified saponite control, KU-250 = unmodified kaolinite, CKU-250 = unmodified kaolinite control. Values are reported as mean ± one standard error.

Figure 8.1 shows that the test unmodified clays such as BU-250 and PU-250 appear to behave alike in that the proportion of saturates in the residual oil is greater than that of aromatics. However, it is observed that with unmodified saponite and kaolinite, the aromatics in the residual oil is slightly greater than the saturates. Among the unmodified clay control experiments as shown in Figure 8.1, unmodified palygorskite shows the lowest proportion of aromatics (30%). The % saturates to % aromatics ratio is highest with a value

of 1.8 (Table 8.2) for the unmodified palygorskite clay control (CPU-250) among other unmodified clay controls. This is probably due to the adsorptive properties of palygorskite as discussed in section 5.4 (Figure 5.8) and section 5.5

8.3.1.2 SARA fractions distribution with acid activated samples

The SARA fractions for acid activated samples after the biodegradation experiment is presented in Figure 8.2.

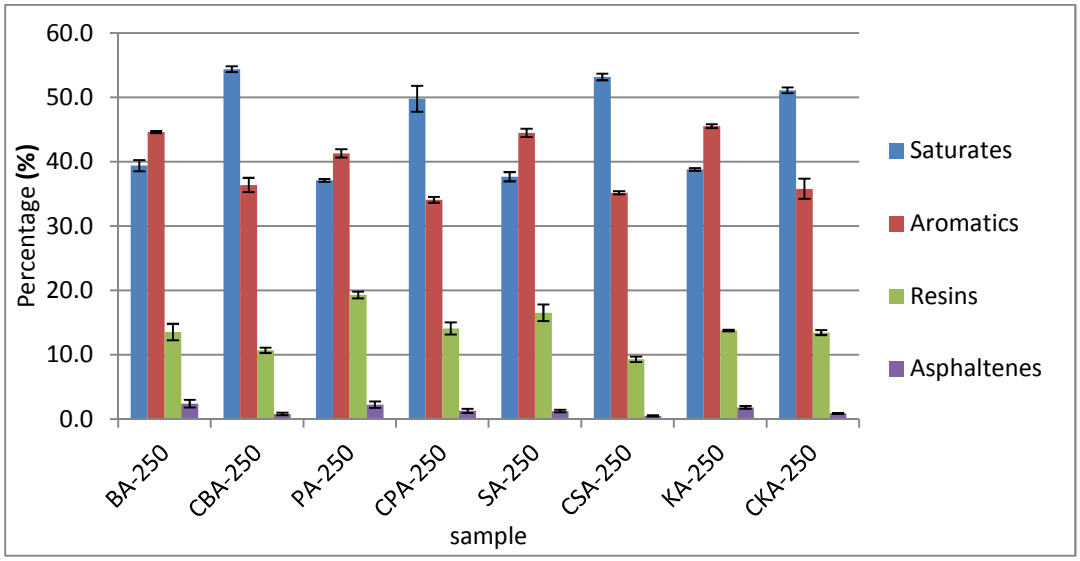

Figure 8.2 Percentage distributions of SARA fractions with acid activated samples. BA-250 = acid activated bentonite, CBA-250 = acid activated bentonite control, PA=250 = acid activated palygorskite, CPA-250 = acid activated palygorskite control, SA-250 = acid activated saponite, CSA-250 = acid activated saponite control, KA-250 = acid activated kaolinite, CKA-250 = acid activated kaolinite control. Values are reported as mean ± one standard error.

Figure 8.2 shows that there are changes in the distribution of SARA fractions with acid activated samples in comparison with their control counterparts. The aromatics are more in proportion in the test acid activated clay samples namely, BA-250, SA-250, PA-250 and KA-250 than in their respective control samples. These changes are most likely to be due to biodegradation which must have taken place with the test samples and appear to have affected saturates more than aromatics.

The effect of increasing the acid activated clay/oil ratio (w/w) from 5:1 to 10:1 is shown in Figure 8.3 as a test of how reduction of pH affects the SARA distribution during biodegradation.

Effect of increasing the acid activated clay/oil ratio (w/w) from 5:1 to 10:1

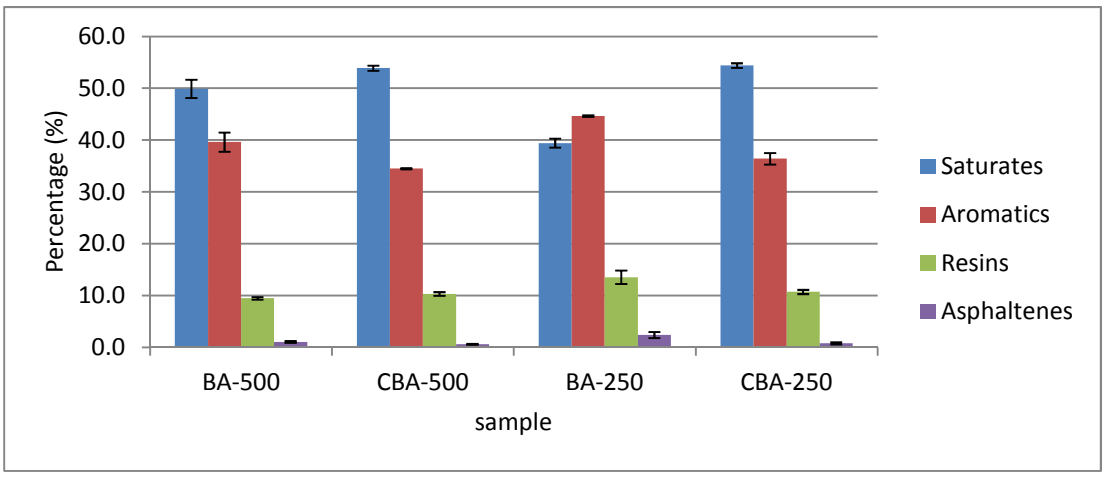

Figure 8.3 Percentage distribution of SARA fractions with acid activated samples -effect of increasing the acid activated clay/oil ratio from 5:1 to 10:1 (w/w). BA-250 and BA-500 represent 250mg and 500mg of acid activated bentonite respectively. CBA-250 and CBA-500 are the respective clay controls. Values are reported as mean ± one standard error.

Figure 8.3 shows that on increasing the clay/oil ratio from 5:1 to 10:1, the SARA distributions in BA-500 appear to have undergone little changes in comparison to the control sample, CBA-500. However, the saturates with BA-500 appears to have undergone mild biodegradation as its proportion in this test sample (BA-500) is lower than in the control sample (CBA-500). Generally, there have been significant changes in distribution of SARA fractions in the presence of acid activated bentonite at clay oil ratio of 10:1 compared with clay oil ratio of 5:1 (Figure 8.3). These significant changes in distribution of SARA fractions with BA-250 in comparison with BA-500 are highly suggested to be due to biodegradation which BA-250 supports more than BA-500 (see section 5.5 and Figure 5.12).

Further evidence of how reduction of pH affects SARA distribution during biodegradation is presented in Figure 8.4.

SARA fraction distribution at various pH's

The SARA fractions for samples maintained at various pH during the biodegradation experiment is presented in Figure 8.4.

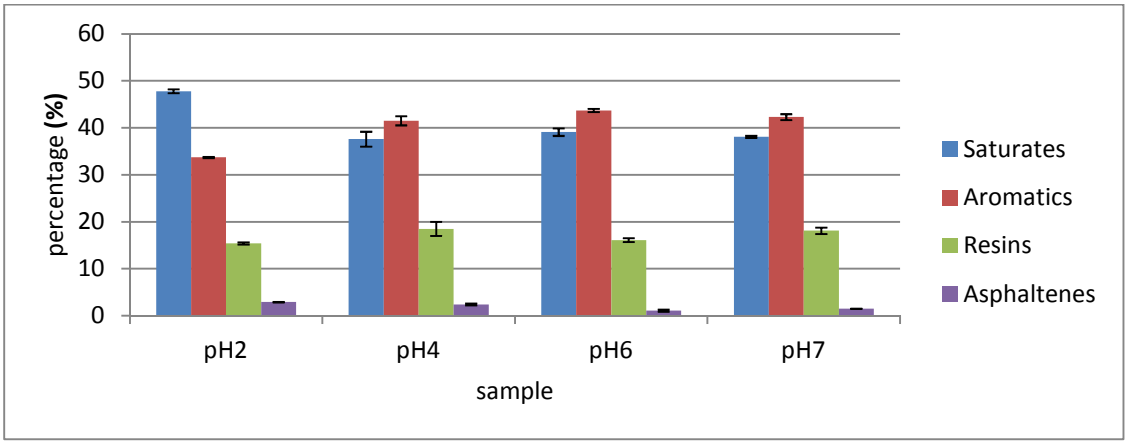

Figure 8.4 Percentage distributions of SARA fractions at various pH's. Values are reported as mean ± one standard error.

Figure 8.4 shows that at pH2, the % saturates of the residual oil exceeds that of the aromatics unlike at the other three pH's (4,6,and 7) where the converse is the case. From the GC analysis as observed in section 5.5 (Figure 5.13), there was hardly any biodegradation of the crude oil hydrocarbons at pH2 whereas there was biodegradation at pH's 4, 6 and 7. This perhaps accounts for why the proportion of saturates is higher than the aromatics at pH2. Because the aromatics are less susceptible to biodegradation than the saturates, during biodegradation, more of the saturates were removed than the aromatics hence the aromatics became higher in proportion than the saturates at pH's 4, 6 and 7.

8.3.1.3 SARA fractions distribution with Organoclay samples

The SARA fractions for organoclay samples after the biodegradation experiment is presented in Figure 8.5.

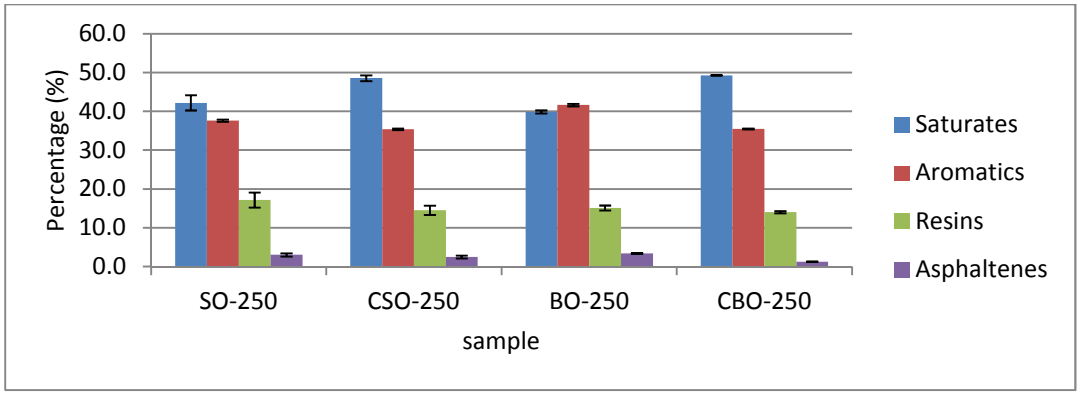

Figure 8.5 Percentage distributions of SARA fractions with organoclay samples. B0-250 = organobentonite, CBO-250 = organobentonite control, SO-250 = organo saponite, CSO-250 = organosaponite control. Values are reported as mean ± one standard error.

Figure 8.5 shows that the two organoclay samples, BO-250 and SO-250 behave differently. The proportion of aromatics in the residual oil is higher than saturates in sample BO-250 (similar to the acid activated samples) unlike in SO-250 where the proportion of saturates is higher than that of aromatics. This could be as a result of a more extensive removal of aromatics by SO-250 than BO-250 through the process of biodegradation.

8.3.1.4 Homoionic cation interlayer clays

The SARA fractions for homoionic interlayer clay samples after the biodegradation experiment is presented in Figure 8.6.

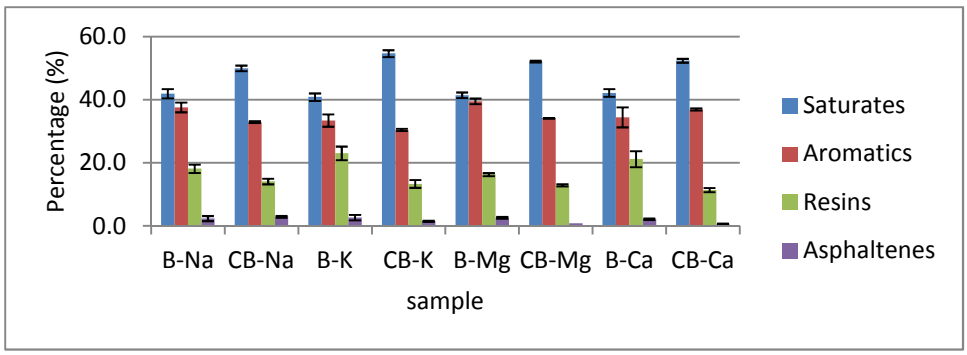

Figure 8.6 Percentage distributions of SARA fractions with homoionic interlayer clay samples. B-Na = sodium-bentonite, CB-Na = sodium-bentonite control, B-K = potassium-bentonite, CB-K = potassium-bentonite control, B-Mg = magnesium-bentonite, CB-Mg = magnesium-bentonite control, B-Ca = Calcium-bentonite, CB-Ca = calcium-bentonite control. Values are reported as mean ± one standard error.

Figure 8.6 shows that the proportions of saturates are higher than aromatics for both the test and control samples. However, the ratio of % saturates to % aromatics is lower with the test samples (B-Na, B-K, B-Mg and B-Ca) than the control samples (CB-Na, CB-K, CB-Mg and CB-Ca) (Figure 8.6 and Table 8.4) indicating that changes in the distributions of SARA fractions must have taken place as a result of biodegradation. However, among the control samples, potassium bentonite control (CB-K) has the lowest proportion of aromatics but with the highest % saturates to % aromatics ratio of 1.79 (Figure 8.6 and Table 8.2) indicating that it may have removed aromatics via an abiotic process such as adsorption.

The SARA distribution with the other homoionic interlayer clay samples are presented in Figure 8.7.

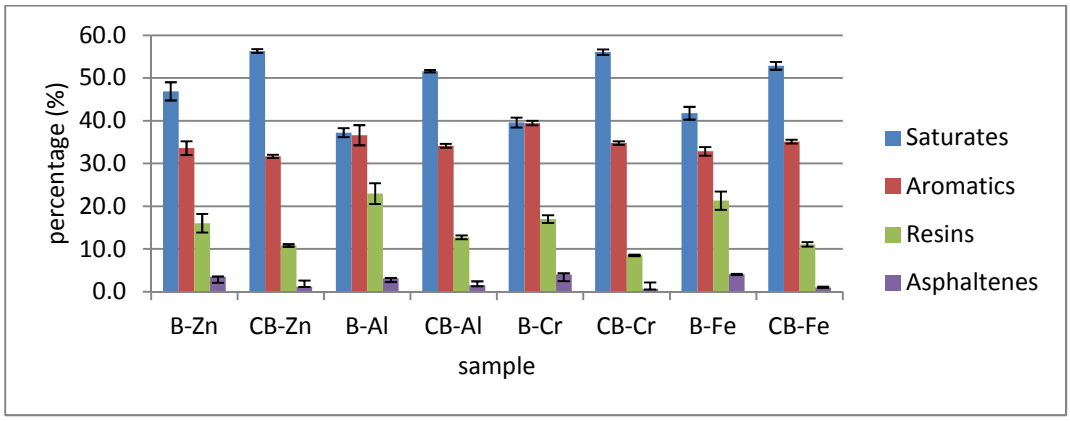

Figure 8.7 Percentage distributions of SARA fractions with homoionic interlayer clay samples. B-Zn = zinc-bentonite, CB-Zn = zinc-bentonite control, B-Al = aluminium-bentonite, CB-Al = aluminium-bentonite control, B-Cr = chromium-bentonite, CB-Cr = chromium-bentonite control, B-Fe = Iron (III)-bentonite, CB-Fe = iron (III)-bentonite control. Values are reported as mean ± one standard error.

Figure 8.7 shows that B-Zn and B-Fe have higher proportions of saturates than aromatics like their control counterparts (CB-Zn and CB-Fe). However, the ratio of % saturates to % aromatics is lower with B-Zn and B-Fe than with CB-Zn and CB-Fe respectively, indicating that changes in the distributions of SARA fractions had taken place probably as a result of microbial degradation. In contrast, B-Al and B-Cr appear to have nearly equal proportions of aromatics and saturates which also can be attributed to biodegradation. Among the control samples (Figure 8.7) zinc bentonite (CB-Zn) has the lowest proportion of aromatics but the

highest % saturates to % aromatics when compared with the other control samples indicating that it may have removed aromatics via an abiotic process such as adsorption.

8.3.1.5 SARA fractions distribution with control samples other than clay control samples.

The SARA fractions for control samples (other than clay control samples) after the biodegradation experiment is presented in Figure 8.8.

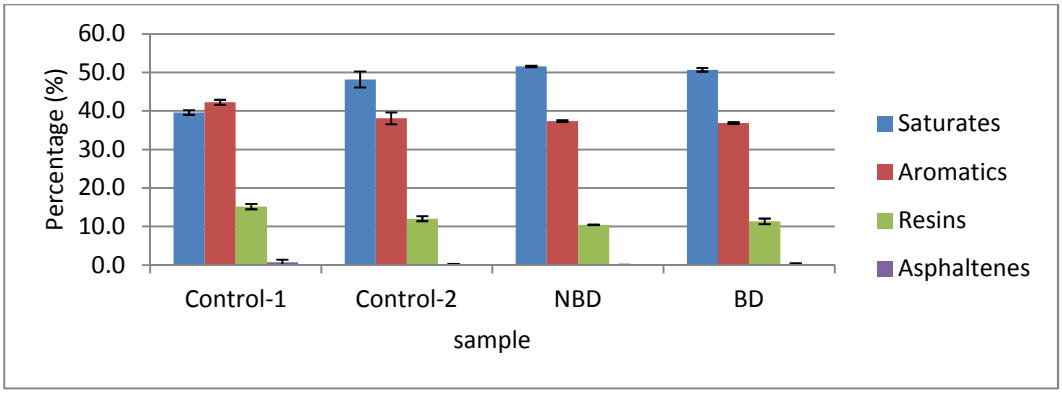

Figure 8.8 Percentage distributions of SARA fractions with controls other than clay controls. Control-1 = positive control (BH + oil + cells)-no clay, Control-2 = negative control (BH + oil)-no clay and no cells. NBD = fresh unincubated oil extracted, not blown down under nitrogen gas. BD = Fresh unincubated oil extracted and blown down under nitrogen gas. Values are reported as mean ± one standard error.

The distribution of SARA fractions in Control-1 (positive control) is different from that of Control-2 (negative control) in that unlike in Control-2, the aromatics are higher in proportion than saturates in Control-1 and indicates that biodegradation of saturates more than the aromatics must have taken place in control-1 (Figure 8.8). The SARA distribution in the unincubated samples (NBD & BD) is different from Control-1 but similar to Control-2 though the saturates fraction appears to have diminished slightly in Control-2 compared with NBD and BD.

8.3.2 Weight distribution of SARA fractions in the residual oil samples

8.3.2.1 SARA fractions in the control (non-clay) samples and unincubated oil samples

In this section, the estimation of the weight changes in the SARA fraction of the extracted oil that has undergone incubation with microbial degradation (Control-1) and without microbial

degradation (Control-2) in comparison with unincubated oil samples (NBD and BD) is presented. The fresh crude oil(50mg) that was not incubated was extracted from oil/water (10ml) mixture and blown down under nitrogen to have sample BD whereas the oil sample(50mg) that was extracted but not blown down is represented as sample NBD.

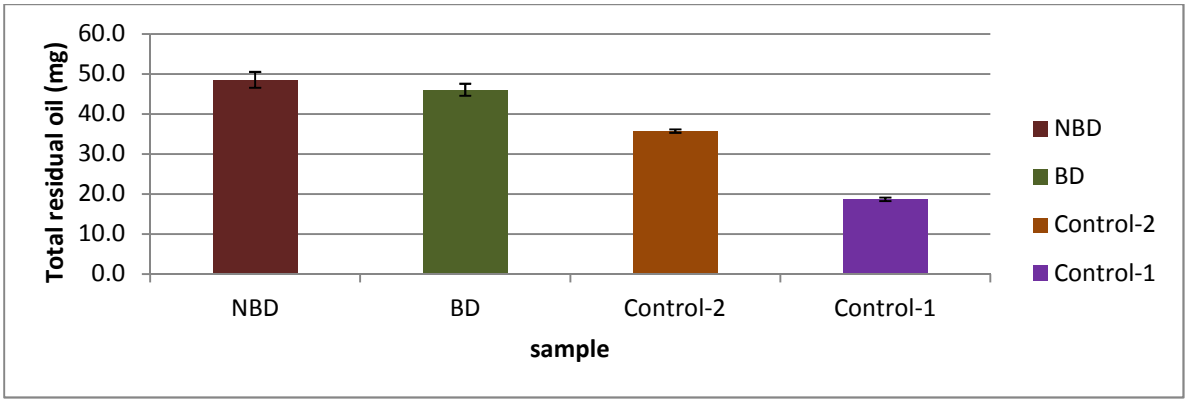

Figure 8.9 Total oil extracted (for estimating losses due to volatilization and microbial degradation). Sample codes retain their meanings. Values are reported as mean ± one standard error.

From Figure 8.9, the total residual oil value for Control-2 is about 77.6% of BD indicating that about 22.4% of the oil must have been lost during the experimental period of incubation of the samples via volatilization. On comparing BD and NBD in the same Figure 8.9, BD is about 95% of NBD indicating that about 5% of the oil is lost while the sample is blown down under nitrogen. Also from Figure 8.9, Control-1 is about 52% of Control-2 indicating that about 48% would have been lost by biotic process such as biodegradation.

The weight distribution with respect to saturates, aromatics and resins is presented in Figure 8.10 below.

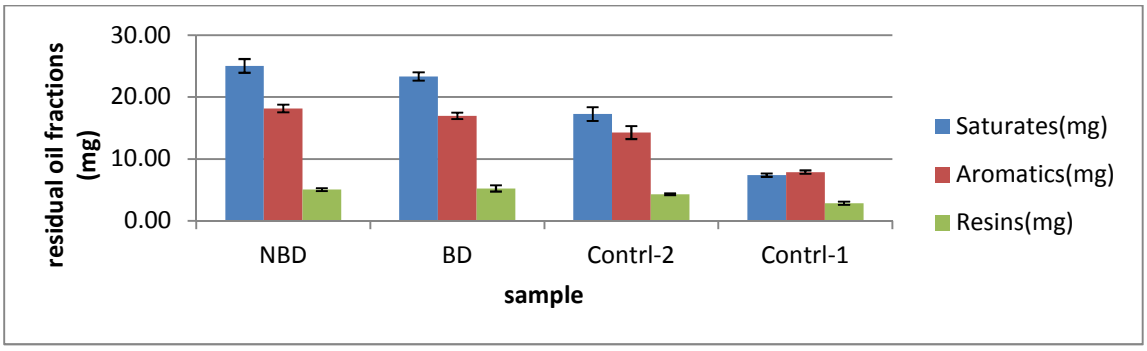

Figure 8.10 Saturates, aromatics and resins for control samples and unincubated samples.

Figure 8.10 shows that there is significant removal of saturates and aromatics with Control-1 which is most likely to be due to the process of biodegradation.

The removal of hydrocarbon in comparison with NSO's (resins and asphaltenes) among these control samples are further evaluated as shown in Figure 8.11.

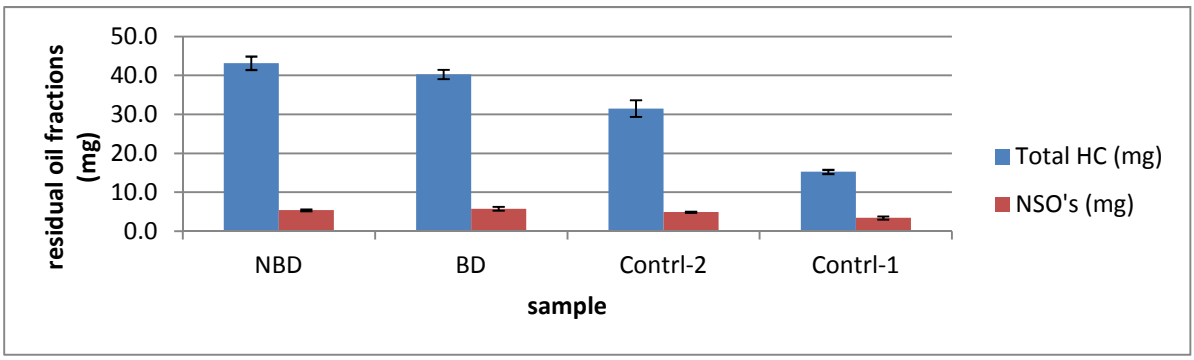

Figure 8.11 Weight distribution of hydrocarbons and NSO fractions in the control and unincubated samples.

Figure 8.11 further confirms the fact that depletion of hydrocarbons is more significant than depletion of NSO as we move from Control-2 to Control-1. This is due to the fact that most of the compounds grouped as the NSO's are more resistant to biodegradation than hydrocarbons.

8.3.2.2 Biodegradation of SARA fractions on Unmodified clay

The effect of unmodified clay on biodegradation of the SARA fractions is presented in Figures 8.12-8.14

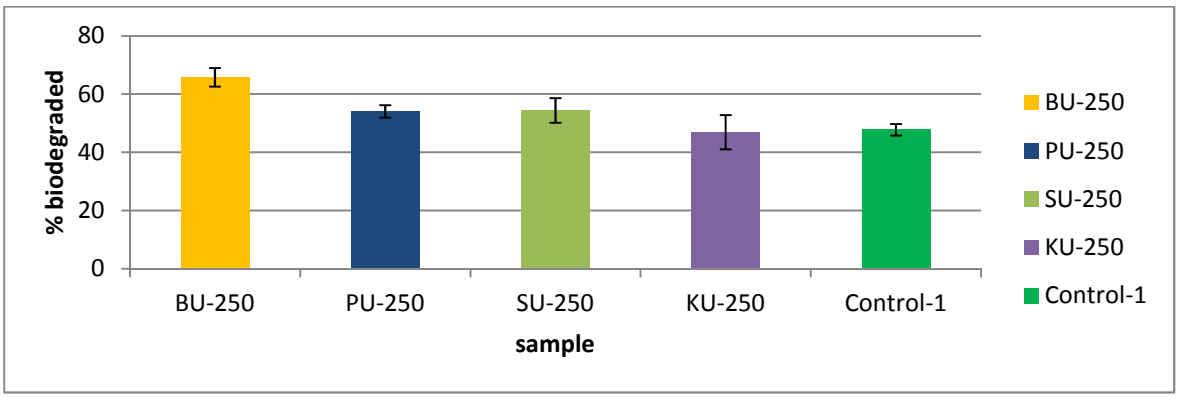

Figure 8.12 Percentage oil biodegraded with unmodified clay samples. Values are reported as mean ± one standard error.

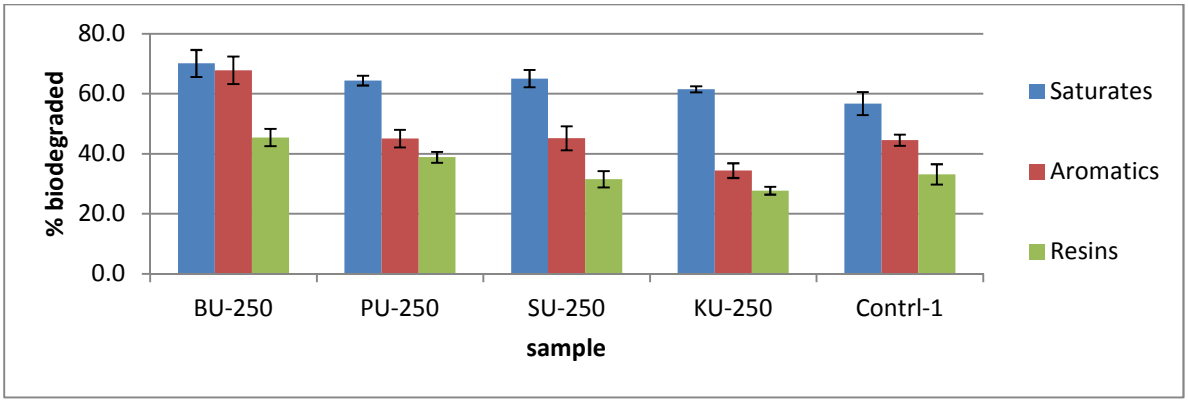

Figure 8.13 Percentage saturates, aromatics and resins biodegraded with unmodified clay samples. Values are reported as mean ± one standard error.

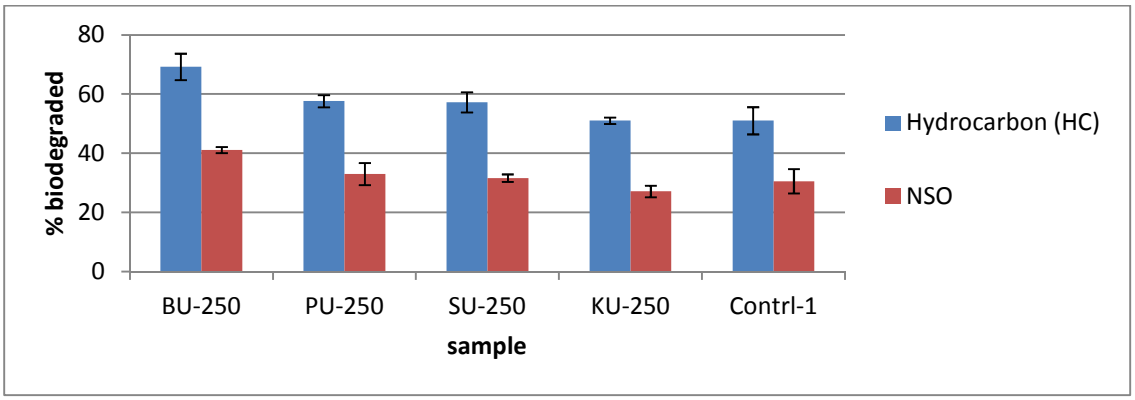

Figure 8.14 Hydrocarbons and NSO biodegraded with unmodified clay samples. Values are reported as mean ± one standard error.

The 2-sample t-test at 95% confidence interval (CI) performed to analyse for differences that may be statistically significant is presented in Appendix 8.1. From Figures 8.12-8.14 and Appendix 8.1, BU-250 appears to achieve a higher extent of biodegradation in all respects and statistically, it is significantly different from Control-1 as indicated by the P-value (Appendix 8.1).

8.3.2.3 Biodegradation of SARA fractions on acid activated clay samples

The effect of the acid activated clay minerals on biodegradation of SARA fractions is presented in Figures 8.15-8.17.

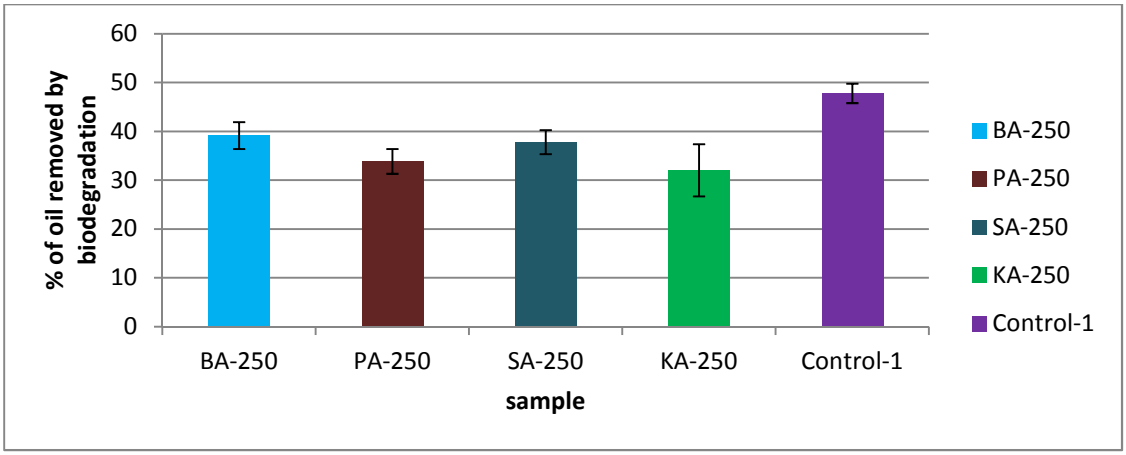

Figure 8.15 Percentage oil biodegraded with acid activated samples. Values are reported as mean ± one standard error.

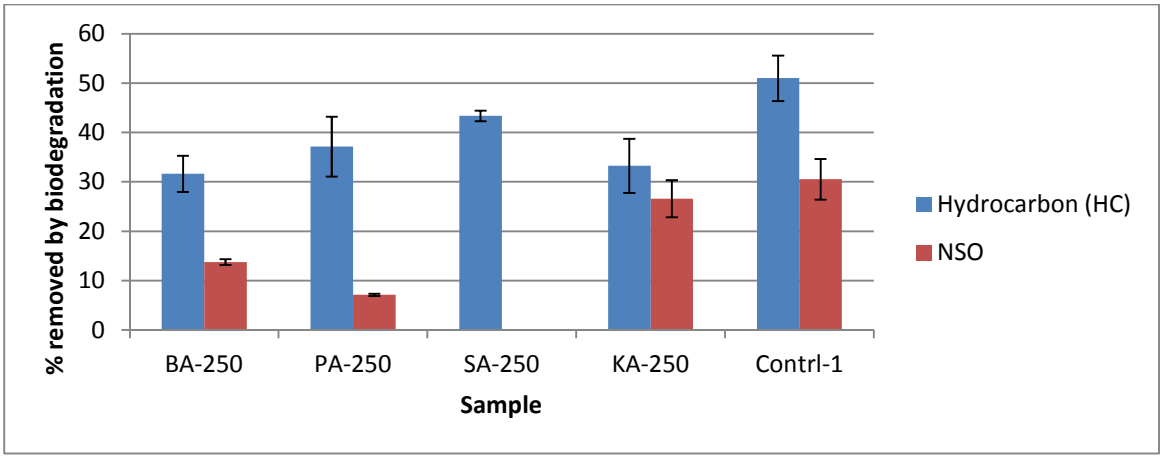

Figure 8.16 Percentage hydrocarbons and NSO biodegraded with acid activated samples. Values are reported as mean ± one standard error.

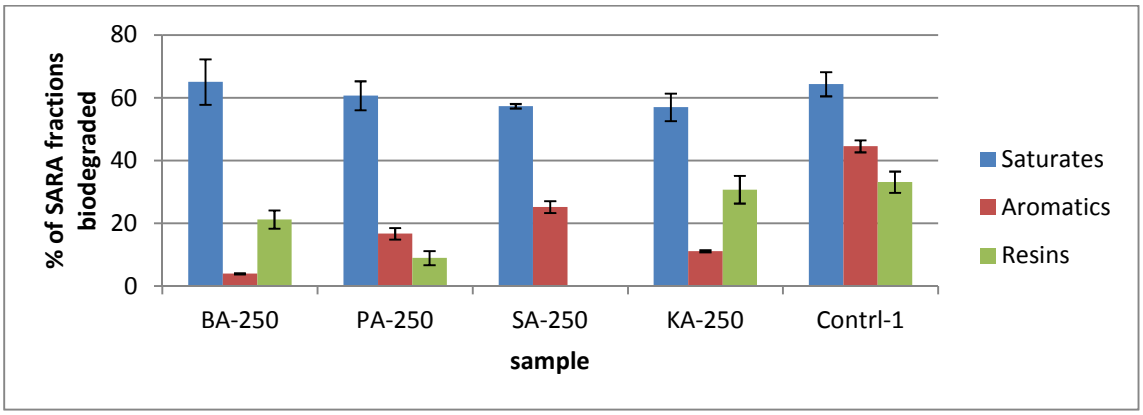

Figure 8.17 Percentage saturates, aromatics and resins biodegraded with acid activated samples. Values are reported as mean ± one standard error.

From Figures 8.15-8.17, Control-1 appears to effect more biodegradation than any of the acid activated clay samples. This seems to be true in all considerations (total oil, hydrocarbons and resins). However, to test whether the inhibition of microbial degradation by the acid activated clay minerals is as a result of lowering the pH or as a result of some other properties of the acid activated clay mineral, two more experiments were conducted. One of them was studying the effect of increasing the acid activated clay/oil ratio from 5:1 (w/w) to 10:1(w/w) hence instead of 250mg of acid activated clay, 500mg was used as this further reduced the pH to 3.6 (section 3.2, Table 3.1) . The second experiment was conducted with media at various pH. The result of the effect of increasing the acid activated clay/oil ratio from 5:1 (w/w) to 10:1(w/w) is presented in Figures 8.18-8.20.

Effect of increasing the acid activated clay/oil ratio from 5:1 to 10:1

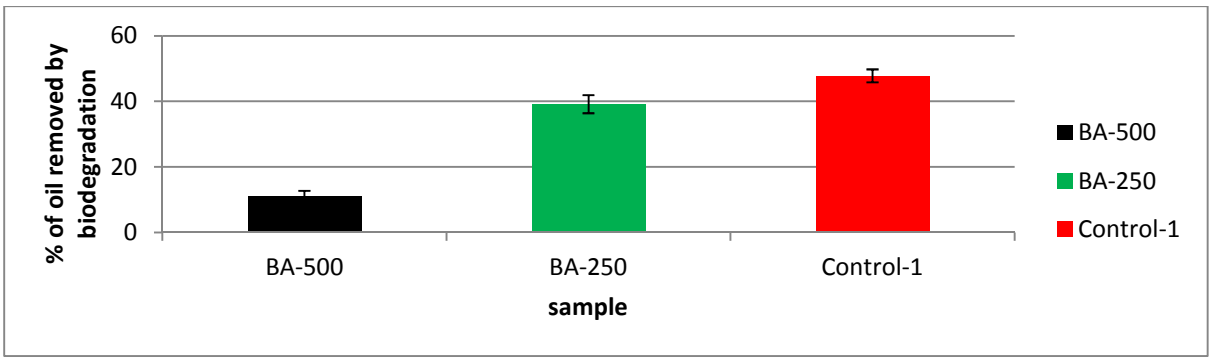

Figure 8.18: Percentage oil biodegraded with acid activated samples-effect of increasing the acid activated clay/oil ratio from 5:1 to 10:1(w/w).

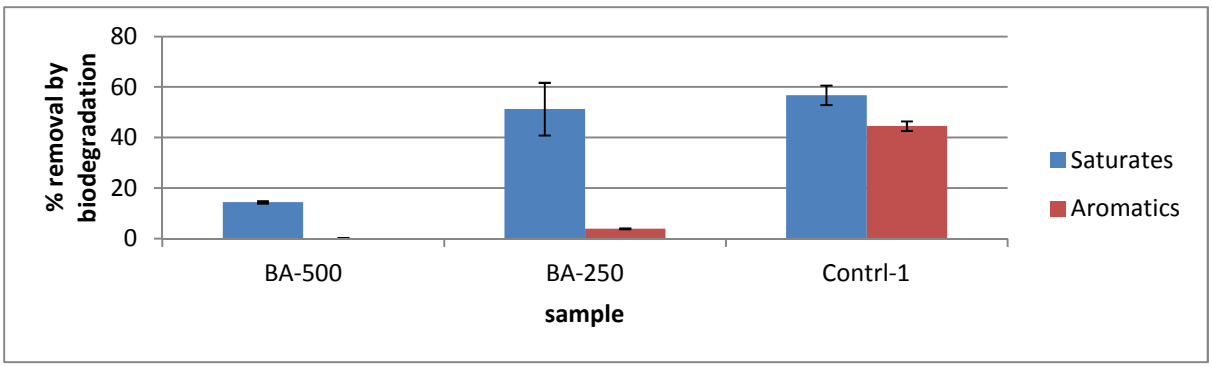

Figure 8.19 Percentage saturates and aromatics biodegraded with acid activated samples-effect of increasing the acid activated clay/oil ratio from 5:1 to 10:1(w/w). Values are reported as mean ± one standard error.

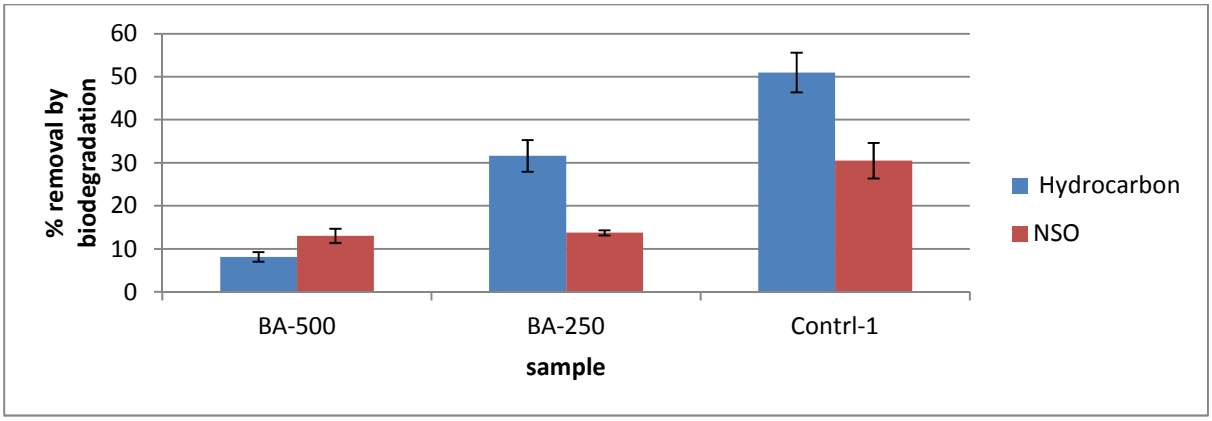

Figure 8.20 Hydrocarbons and NSO fractions biodegraded on acid activated samples-effect of increasing the acid activated clay/oil ratio from 5:1 to 10:1(w/w). Values are reported as mean ± one standard error.

From Figure 8.18-8.20, increasing the acid activated clay/oil ratio from 5:1 to 10:1 reduced the extent of biodegradation of the oil drastically. This reduction in biodegradation is mainly with hydrocarbons as shown in Figure 8.20.

The effect of pH is presented in Figures 8.21 and 8.22.

Weight distribution of SARA fractions at various pH's in the residual oil

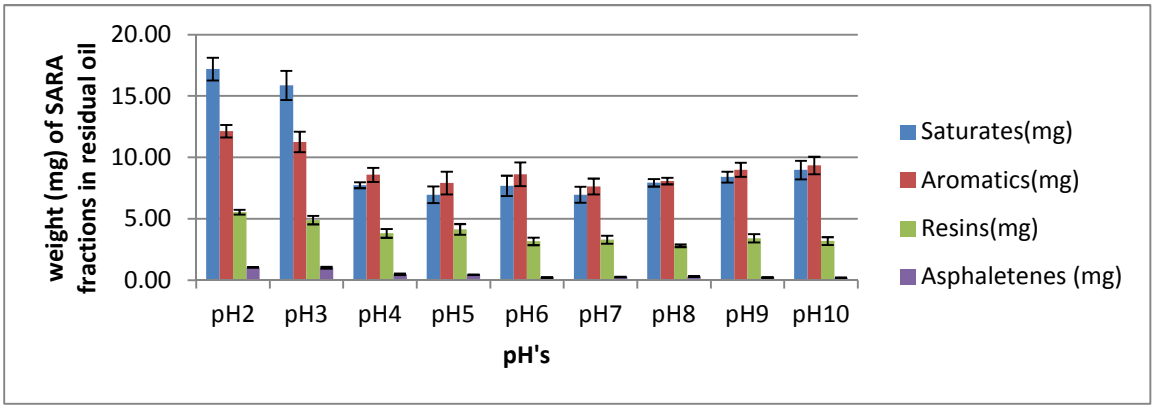

Figure 8.21: weight distribution of the residual SARA fractions at various pHs's. Values are reported as mean ± one standard error.

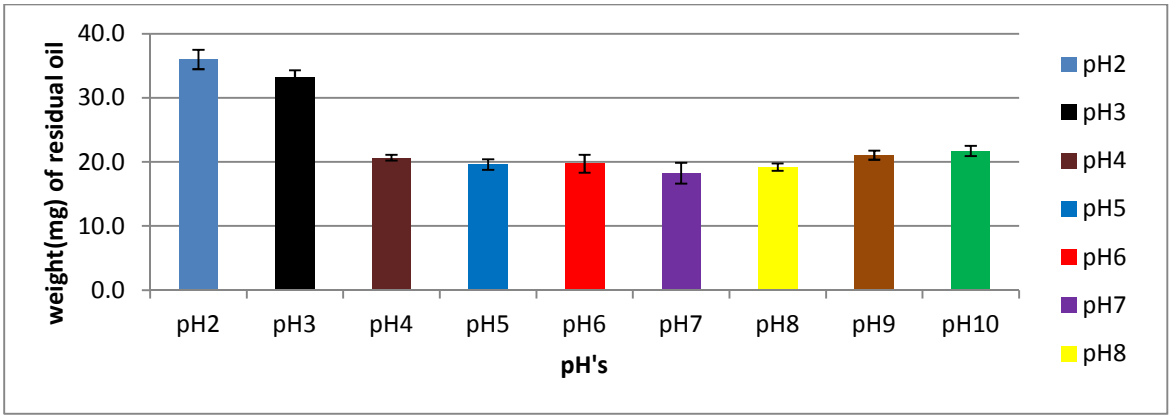

Figure 8.22 weight of the residual oil at various pH's. Values are reported as mean ± one standard error.

Figures 8.21 and 8.22 show that the residual oil and SARA components decrease as the pH increases and reaches a minimum at pH7 and then increases slightly until pH10 is reached. This indicates that biodegradation of the oil is favoured at or above pH4 and reaches maximum at pH7 before gradually declining.

This indicates that the acid activated clay minerals must have adversely affected the biodegradation of the oil because of their ability to reduce the pH to probably a somewhat toxic level to the microbes.

8.3.2.4 Biodegradation of SARA fractions on organoclay samples.

The effect of organoclay samples on biodegradation of SARA fractions is presented in Figures 8.23-8.25.

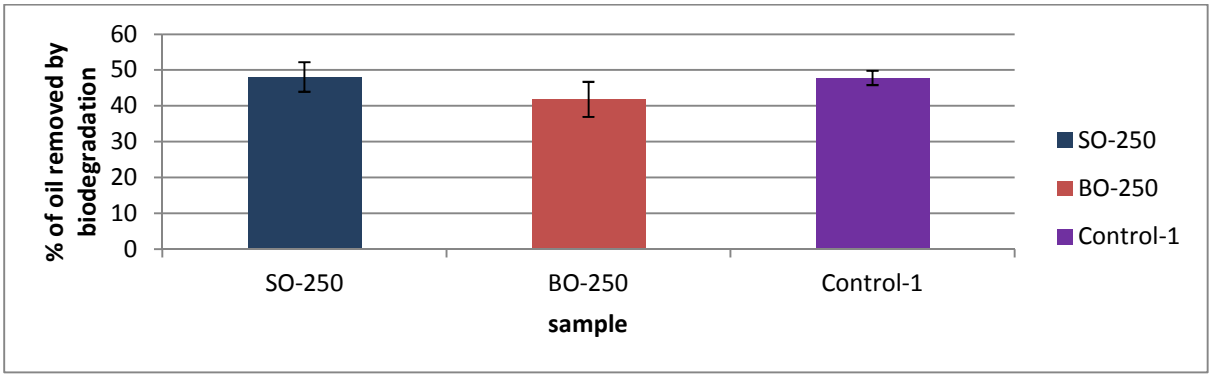

Figure 8.23 Percentage oil biodegraded on Organoclay samples. Values are reported as mean ± one standard error.

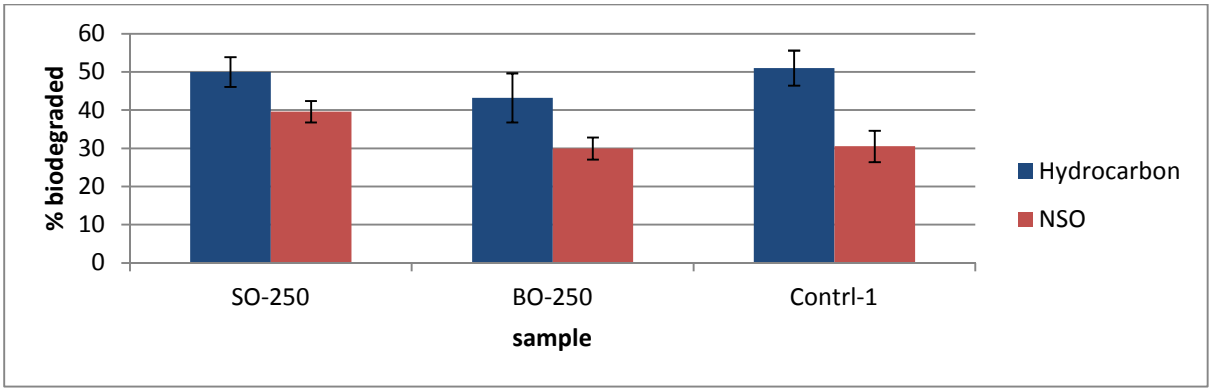

Figure 8.24 Hydrocarbons and NSO fractions biodegraded on organoclay samples. Values are reported as mean ± one standard error.

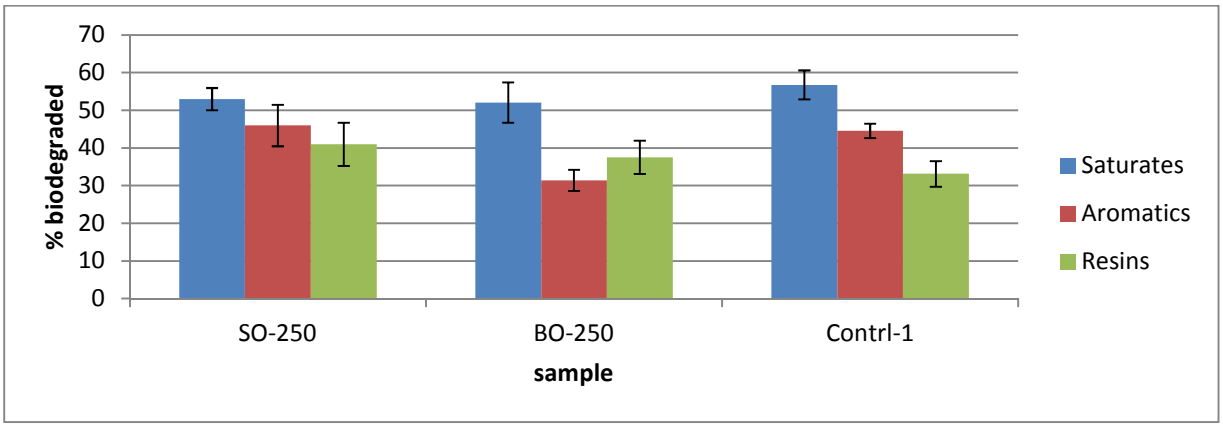

Figure 8.25 Percentage saturates, aromatics and resins biodegraded with organoclay samples. Values are reported as mean ± one standard error.

Figures 8.23-8.25 show that Control-1 is similar to SO-250 with respect to the extent of biodegradation of the total oil, hydrocarbons and resins. However, BO-250 achieves less biodegradation when compared with either SO-250 or Control-1 in all respects. BO-250 therefore cannot be said to enhance the biodegradation of the oil and the P-value between this sample and Control-1 is 0.217. SO-250 neither inhibits nor stimulates the biodegradation of the oil as its performance is akin to that of Control-1. The P-value between it and Control-1 is 1.0

8.3.2.5 Homoionic interlayer cation exchanged clays

The effect of homoionic interlayer clays on biodegradation of the SARA fractions is presented in Figures 8.26-8.28.

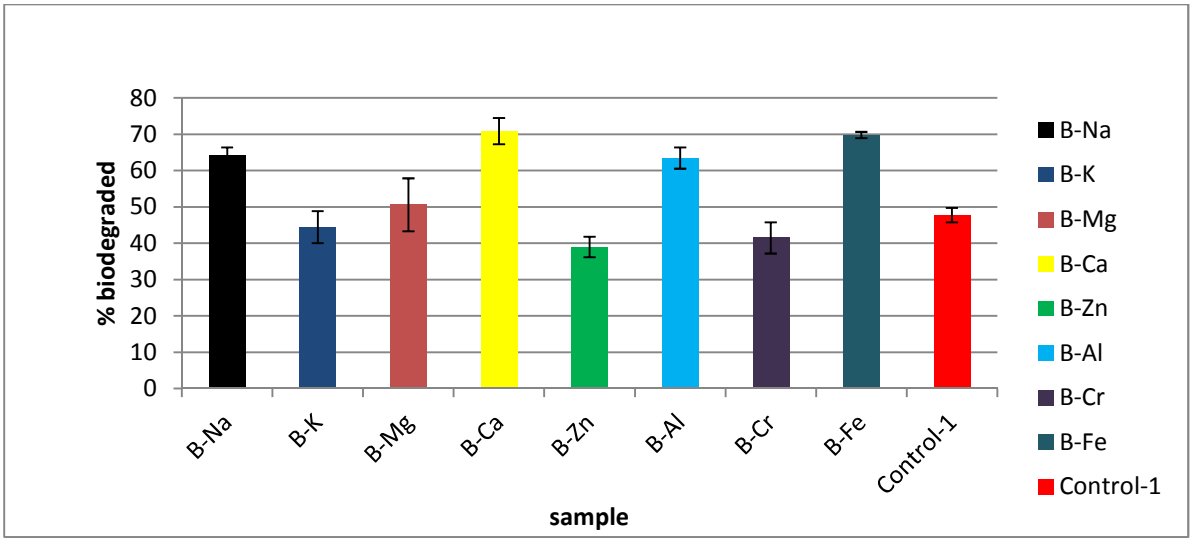

Figure 8.26 Percentage oil biodegraded with homoionic interlayer cation exchanged clay samples. Values are reported as mean ± one standard error.

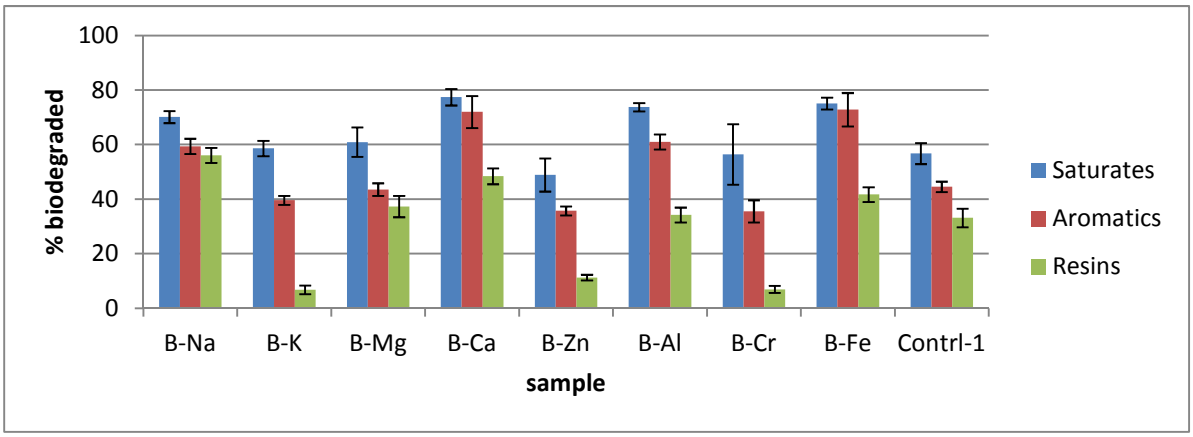

Figure 8.27 Percentage saturates, aromatics and resins biodegraded with homoionic cation exchanged samples. Values are reported as mean ± one standard error.

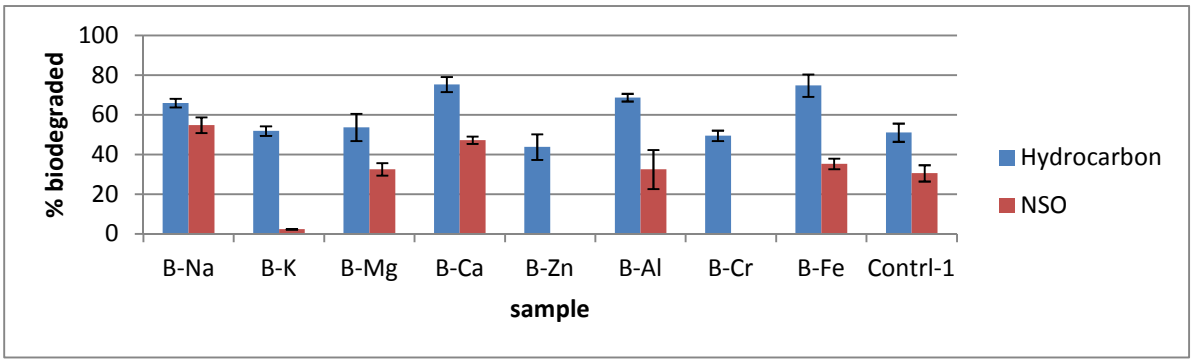

Figure 8.28 Percentage hydrocarbons and NSO fractions biodegraded with cation exchanged clay samples. Values are reported as mean ± one standard error.

Figures 8.26-8.28 show that Samples B-Na, B-Ca, B-Al and B-Fe appear to achieve a higher extent of biodegradation than Control-1 with respect to hydrocarbons and total oil. They are also significantly different from Control-1 (P-values less than 0.05 see Appendix 8.2) indicating that they enhanced the biodegradation of the oil. With samples B-Zn, B-Mg, B-K and B-Cr, there has not been any enhancement of biodegradation (P-values are more than 0.05).

8.3.3 Adsorption of the SARA fractions

8.3.3.1 Adsorption of Oil and SARA fractions on unmodified, acid activated and organoclay samples.

The adsorption of oil and SARA fractions on unmodified clays, acid activated clays and organoclays is presented in Figures 8.29-8.31.

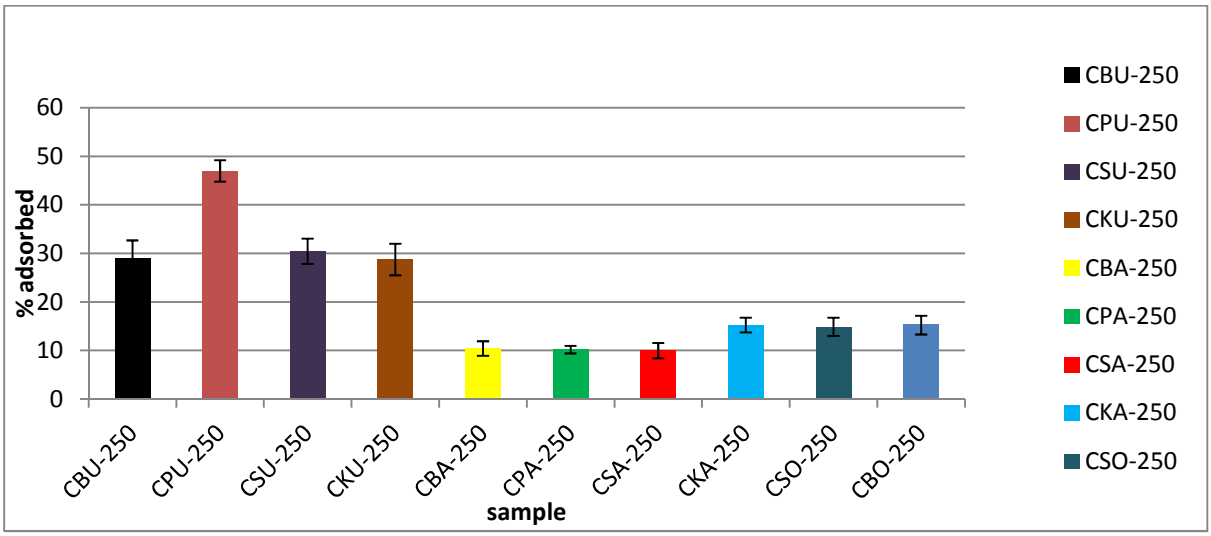

Figure 8.29 Adsorption of total oil on the clay samples on unmodified, acid activated and organoclay**.** Values are reported as mean ± one standard error.

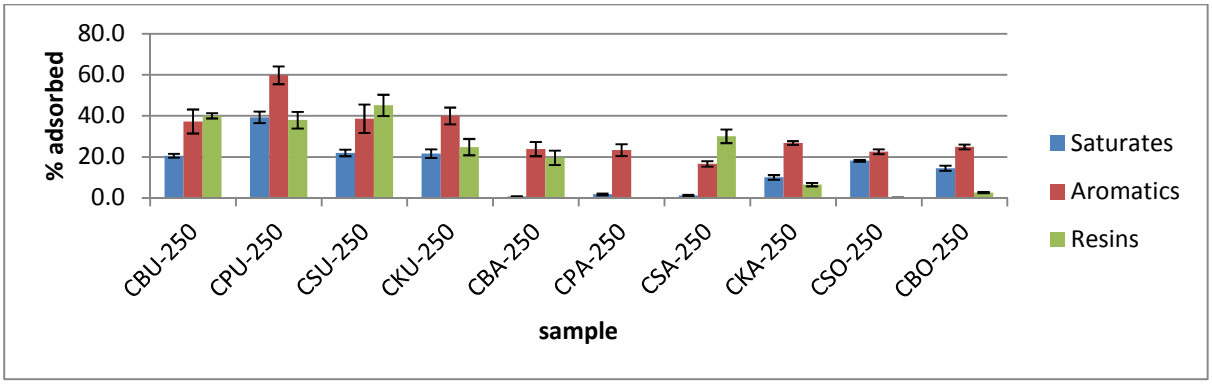

Figure 8.30 Adsorption of saturates, aromatics and resins on unmodified, acid activated and organoclay. Values are reported as mean ± one standard error.

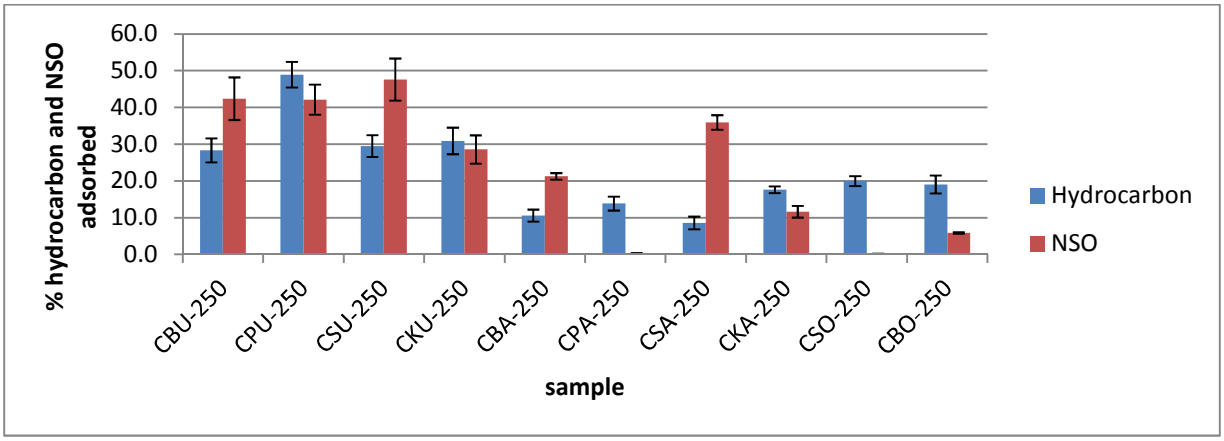

Figure 8.31 Adsorption of hydrocarbon and NSO on unmodified, acid activated and organoclay. Values are reported as mean ± one standard error.

Figures 8.29-8.31 show that CPU-250 appears to show significant adsorption of the oil and hydrocarbons. The unmodified clays, show superior adsorption to the organo and acid activated clays. The % of NSO adsorbed compared to hydrocarbons adsorbed by the same sample is highest with CSU among the unmodified clays indicating that unmodified saponite may have the preferred tendency to remove NSO's by adsorption rather than hydrocarbons. The removal of aromatics by the samples via adsorption is higher than that of saturates for all samples. Overall, CPU-250 with significant removal of NSO and Hydrocarbons by adsorption appears to contribute significantly to the removal of the oil during biodegradation.

8.3.3.2 Adsorption of SARA fractions on cation exchanged clay samples

The adsorption of oil and SARA fractions on unmodified clays, acid activated clays and organoclays is presented in Figures 8.32-8.34.

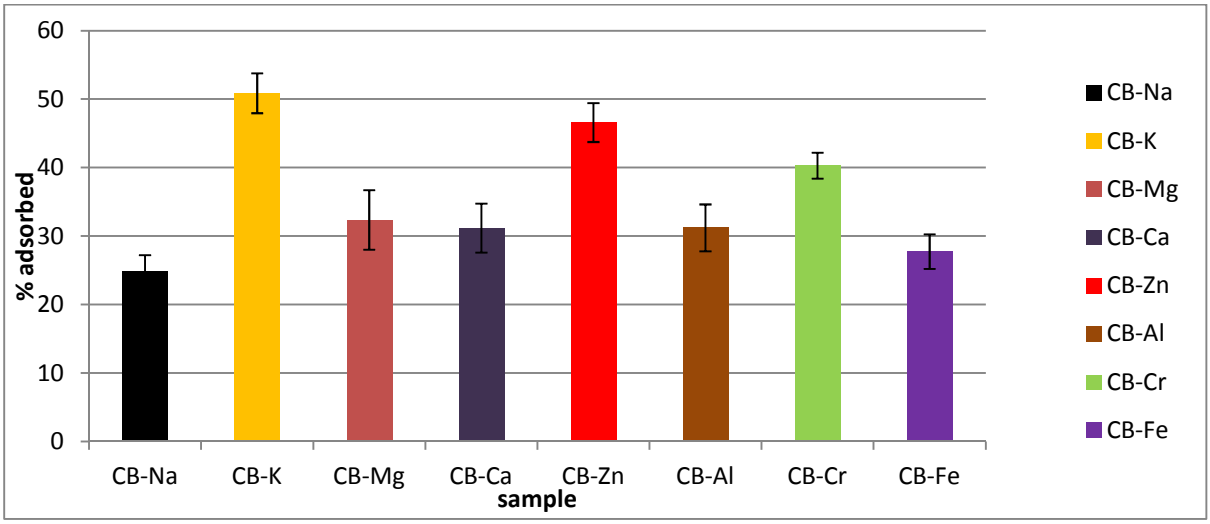

Figure 8.32 Adsorption of total oil on cation exchanged clays. Values are reported as mean ± one standard error.

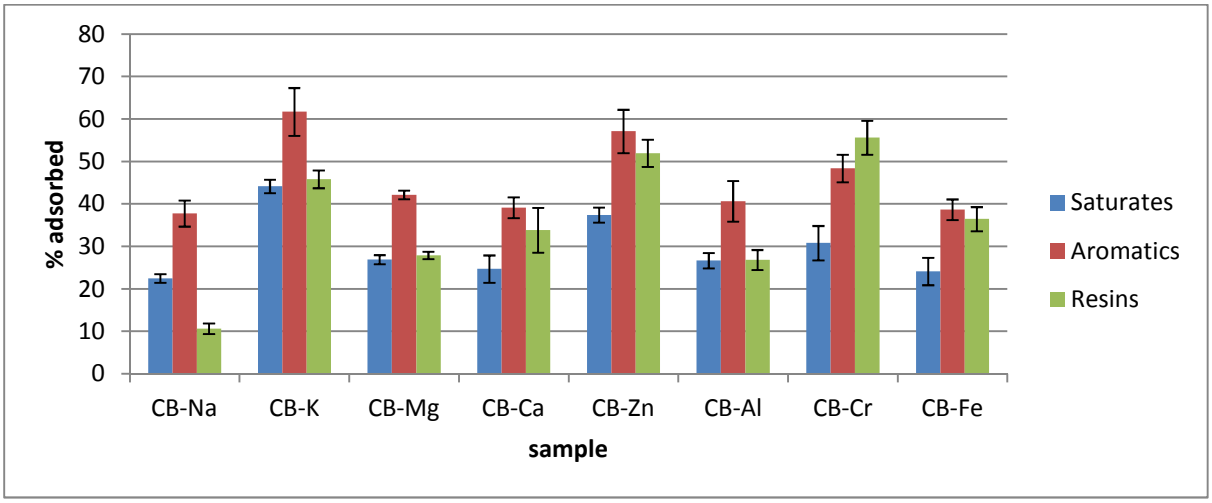

Figure 8.33 Adsorption of saturates, aromatics and resins on cation exchanged clays. Values are reported as mean ± one standard error.

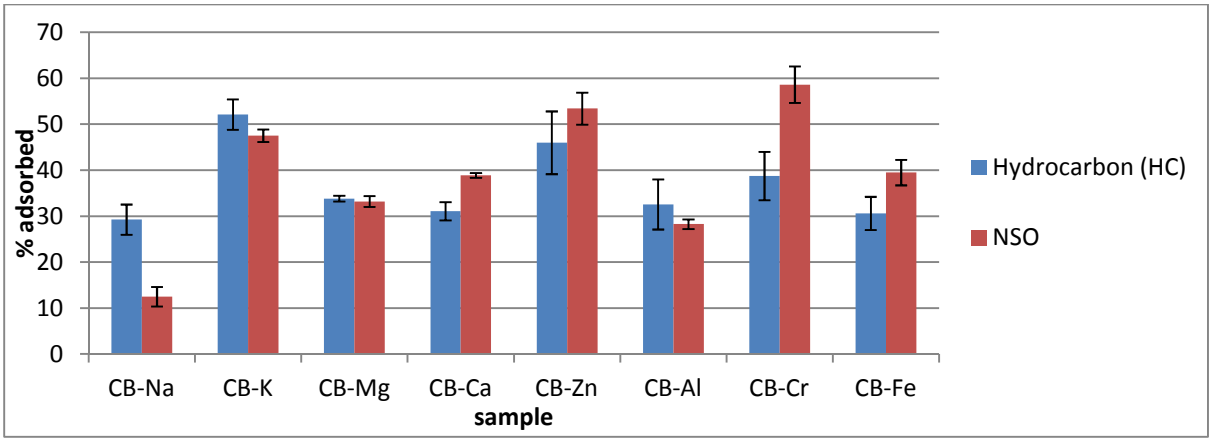

Figure 8.34 Adsorption of hydrocarbon and NSO on cation exchanged clay. Values are reported as mean ± one standard error.

Figures 8.32-8.34 show that CB-K and CB-Zn appear to remove the greatest amount of oil by adsorption, with aromatics (especially for CB-K) accounting for most of the removal. The % adsorption of resins is higher than either saturates or aromatics with CB-Cr unlike with other samples. The ratio of the % removal of NSO to that of hydrocarbon for all samples is highest with CB-Cr. It therefore follows that whereas CB-K and CB-Zn effect removal by adsorption of mainly aromatics, CB-Cr removes mainly the resins.

8.4 Multivariate analysis-cluster analysis

Cluster analysis was used in this section to group the samples that are alike and are different from other samples in other groups. The ten variables employed in the analysis are: % saturates, aromatics and resins biodegraded and adsorbed (six variables), % distribution of the SARA fractions (four variables) in the residual oil. The dendrogram is shown in Figure 8.35.

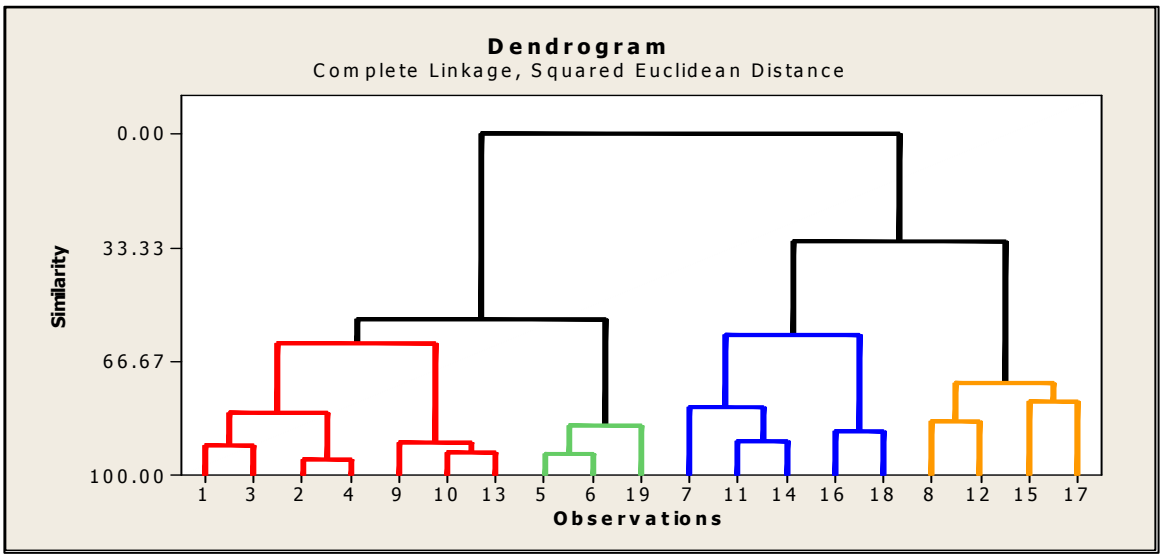

Figure 8.35 Dendrogram showing the groupings of the samples according to their similarities -IATRO SCAN analysis.

PA-250 = 1, BA-250 = 2, SA-250 = 3, KA-250 = 4, SO-250 =5, BO-250 =6, BU-250 =7, PU-250 =8, SU-250 =9, KU-250 =10, B-Na =11, B-K=12, B-Mg =13, B-Ca =14, B-Zn =15, B-Al =16, B-Cr =17 , B-Fe =18, Control-1 =19

The dendrogram has grouped samples that have at least 60% similarity (Table 8.1) together hence the following samples have been grouped together:

Group 1 (cluster 1): PA-250, BA-250, SA-250, KA-250, SU-250, KU-250 and B-Mg. However, the highest similarity in this group is observed between BA-250 and KA-250 whereas the least similarity is between PA-250 and SU-250 as shown in Table 8.1.

Group 2 (cluster 2): SO-250, BO-250 and Control-1. From Table 8.1, the similarity between SO-250 and BO-250 is higher than that between SO-250 and Control-1.

Group 3 (cluster 3): BU-250, B-Na, B-Ca, B-Fe, B-Al. The least similarity in this group is between B-Al and BU-250.

Group 4 (cluster4): PU-250, B-Zn, B-K and B-Cr.

Table 8.1 Cluster analysis -Standardized Variables, Squared Euclidean Distance, Complete Linkage Amalgamation Steps-data from Iatro-scan

Step	No. of clusters	Similarity level	Distance level	Clusters joined	New cluster	No. of obs in new cluster
1	18	95.2755	2.3322	2 4	2	2
2	17	93.6162	3.1513	5 6	5	2
3	16	93.4713	3.2228	10 13	10	2
4	15	91.2726	4.3082	1 3	1	2
5	14	90.6241	4.6283	9 10	9	3
6	13	90.2267	4.8245	11 14	11	2
7	12	87.2634	6.2873	16 18	16	2
8	11	85.6236	7.0968	5 19	5	3
9	10	84.0487	7.8742	8 12	8	2
10	9	81.6120	9.0771	1 2	1	4
11	8	80.126	9.8106	7 11	7	3
12	7	78.5418	10.5926	15 17	15	2
13	6	72.8609	13.3969	8 15	8	4
14	5	61.4428	19.0827	1 9	1	7
15	4	58.8168	20.3296	7 16	7	5
16	3	54.2374	22.5902	1 5	1	10
17	2	31.7174	33.7070	7 8	7	9
18	1	0.000	49.364	1 7	1	19

Final Partition

Number of clusters: 4

Clusters	No. of observ.	Within cluster sum of squares	Average dist. from centroid	Maximum dist from centroid
1	7	30.4270	2.06135	2.42558
2	3	5.1389	1.2920	1.54126
3	5	18.1993	1.86261	2.40589
4	4	17.0586	2.06346	2.14679

Group 1: Samples in this group appear not to be good candidates for stimulating the biodegradation of the oil.

Group 2 is where the positive control falls into and implies that samples in this group are not expected to stimulate the biodegradation of the oil.

Group 3: The samples in this group appeared to have effected the most biodegradation of the oil.

Group 4: Samples in this group appear to have more significant adsorptive capacity for the oil than other samples.

8.5 Discussion

The ratio of percentages of saturates to aromatics for Control-2, NBD and BD are 1.2, 1.4 and 1.4 respectively indicating that more saturates than aromatics had been lost in Control-2 in comparison with NBD and BD. This loss is suggested to be due to volatilization during incubation. On a closer comparison between BD and NBD (Figure 8.8), slightly more saturates had been lost in sample BD than in sample NBD indicating that some more volatile saturates must have been lost when the sample was blown down under nitrogen. The difference between Control-1 and Control-2 (Figure 8.9) which is about 48% of the oil retained by Control-2 is an indication that there was a biological removal process (biodegradation).

Table 8.2 Distributions of SARA fractions and EOM

	SARA Composition(%)				Ratios		
Sample	Sat	Aro	Resins	Asph	Sat/Aro	Sat/Res	EOM (mg)
SO-250	42.19	37.61	17.19	3.03	1.12	2.45	15.7
BO-250	39.84	41.63	15.12	3.4	0.96	2.63	17.6
BA-500	49	39.62	9.8	1.1	1.24	5	28.7
BA-250	39.41	44.64	13.54	2.4	0.88	2.91	19.4
PA-250	37.11	41.33	19.31	2.25	0.9	1.92	21.3
SA-250	37.69	44.51	16.54	1.26	0.85	2.28	20
KA-250	38.83	45.56	13.78	1.83	0.85	2.82	20.5
BU-250	47.22	32.81	16.54	3.17	1.44	2.86	8.5
PU-250	42.98	35.8	18.77	2.45	1.2	2.29	8.7
SU-250	41.73	42.44	14.43	1.4	0.98	2.89	11.1
KU-250	38.96	41.68	17.38	1.74	0.93	2.24	13.3
Control-1	39.57	42.23	15.17	3	0.94	2.61	18.7
Control-2	49	39.3	10	1.75	1.25	4.9	35.7
B-Na	41.9	37.58	18.15	2.37	1.11	2.31	9.5
B-K	40.85	33.42	23.05	2.68	1.22	1.77	9.7
B-Ca	42.15	34.44	21.21	2.19	1.22	1.99	6.8
B-Mg	41.44	39.51	16.31	2.61	1.05	2.54	11.7
B-Zn	46.87	33.59	16.02	3.51	1.4	2.93	11.6
B-Fe	41.75	32.83	21.31	4.12	1.27	1.96	7.8
B-Al	37.23	36.62	22.95	3.15	1.02	1.62	8.9
B-Cr	39.56	39.45	16.99	4	1	2.33	12.3
CB-Na	49.96	32.92	14.13	2.95	1.52	3.54	26.8
CB-K	54.64	30.47	13.36	1.52	**1.79**	4.09	17.6
CB-Mg	52.16	34.09	12.92	0.8	1.53	4.04	24.1
CB-Al	51.56	34.13	12.75	1.56	1.51	4.04	24.5
CB-Cr	56.06	34.77	8.53	0.62	1.61	**6.57**	19.1
CB-Fe	52.84	35.11	11.06	0.99	1.51	4.78	24.5
CB-Zn	56.31	31.66	10.82	1.21	**1.78**	5.2	21.3
CKU-250	53.03	35	11	1.18	1.52	4.82	25.8
CSU-250	51	36.1	12.1	0.87	1.41	4.21	25.5
CPU-250	55.16	29.84	12.5	0.94	**1.85**	4.41	18.9
CBU-250	53.98	34.91	10.18	0.93	1.55	5.3	24.8
CB-Ca	52.36	36.98	11.39	0.76	1.42	4.6	25.3
CBO-250	49.28	35.45	14.04	1.25	1.39	3.51	32.1
CSO-250	48.55	35.4	14.53	2.49	1.37	3.34	30.3
CBA-250	54.36	36.38	10.69	0.8	1.49	5.09	30.4
CPA-250	49.77	34.15	14.09	1.32	1.46	3.53	32
CKA-250	51.13	35.81	13.47	0.89	1.43	3.8	32.3
CSA-250	53.2	35.16	9.32	0.5	1.51	5.71	31.1
CBA-500	53.9	34.51	10.31	0.63	1.56	5.23	30.3
NBD	51.53	37.36	10.41	0.7	1.38	4.95	48.5
BD	50.66	36.85	11.33	1.17	1.37	4.47	46

From Table 8.2, it is observed that Control-1, all acid activated samples, KU-250, SU-250 and BO-250, have % Saturates/% Aromatics < 1 and % Saturates/% Resins ≤ 2.9. This indicates that these samples behave alike and have had more saturates removed than aromatics. The proportions of saturates in the residual SARA fractions are lower than aromatics with these samples as shown in Figures 8.1, 8.2 and 8.5 because there seemed to be far more removal of saturates than aromatics as a result of microbial degradation (Figures 8.13, 8.17 and 8.25). The clay samples, BA-250, SA-250, KA-250, PA-250, KU-250, BO-250 and SO-250 have been shown in previous sections to inhibit the biodegradation of crude oil hydrocarbons.

Acid activated samples with the ability of reducing the pH of the medium (which would increase the toxicity of the medium) would ultimately reduce the ability of the microbes to effect biodegradation of the oil. BA-500 was highly inhibitory to biodegradation of the oil and has pH value of 3.6 which is less than that of BA-250 (pH value of 4.1), supporting this suggestion. The experiment on the effct of pH also indicates that the amount of oil lost to biodegradation increases as the pH increases and reaches maximum at pH7. This implies that acid activated clay samples repress biodegradation by lowering the pH.

The extensive hydrophobic interaction between the hydrocarbons especially the low molecular weight hydrocarbons had been suggested in the previous chapter to be responsible for why BO-250 inhibited biodegradation of the hydrocarbons

BU-250, PU-250, SO-250, B-Na, B-K, B-Mg, B-Ca, B-Zn, B-Al, B-Cr and B-Fe have % Saturates/% Aromatics > 1 and % Saturates/% Resins ≤ 2.9. However, it can be observed that all the negative control samples have % Saturates/% Aromatics > 1 but % Saturates/% Resins ≥ 3.4. Therefore, the ratio of % Saturates/% Aromatics > 1 is not enough to indicate that there is a biotic or an abiotic process taking place. The ratio of % Saturates/% Resins provides additional information as to whether a biological process had taken place. The biological process would lead to a relative decrease in the saturates and increase in the resins fraction.

The ratio of % saturates to % aromatics for CB-Zn and CB-K and CPU-250 are 1.78, 1.79 and 1.85 respectively. These values are higher than the other samples and indicate that not all the aromatics removed by these samples are due to biodegradation. CB-Cr appears to have

the highest ratio of % saturates to % resins (6.57) indicating that this clay sample may have removed the resins more than the other control experiments via adsorption.

Table 8.2 provides evidence that the control samples have higher EOM and hence lower total oil removed than the corresponding test samples indicating that a biological process (biodegradation) must have taken place.

B-Ca, B-Fe, B-Na, B-K, PU-250 and BU-250 have EOM ranging between 6.8mg and 9.7mg which are the lowest of all the samples analysed indicating that these samples removed more oil than other samples. Generally the clay control samples have EOM value lower than Control-2 indicating that a non-microbial process, adsorption, had been responsible for some losses. The control samples corresponding to PU-250, B-Zn and B-K have the lowest EOM value which is consistent with the ratio analysis showed previously indicating that adsorption had been more extensive with these samples.

There is no significant difference between the EOM value of Control-1 and that of the acid activated or organoclays samples indicating that these clays are actually inhibitory to biodegradation.

There had been very low EOM with samples B-Ca, B-Fe, B-Na, B-Al and BU-250 indicating that oil had been lost most with these samples. In previous sections, we had shown that oil removal with these samples is mainly via a biological process (biodegradation).

8.6 CONCLUSION

The Iatro-scan has provided some evidence that changes in SARA distributions due to biodegradation and adsorption have taken place during incubation of the experimental microcosm containing aqueous clay/oil and hydrocarbon degrading microbes. The samples where there seemed to be either extensive adsorption of aromatics or extensive biodegradation of aromatics have saturates/aromatics ratio > 1.0 but < 1.5. One of the possible ways to tell which sample removed aromatics by extensive adsorption is if the corresponding clay control has relatively high saturates/aromatics ratio of about 1.75-1.8. The clay samples that are inhibitory to biodegradation appears to allow very little biodegradation of the aromatics hence with these samples, saturates/aromatics ratio ≤ 1.0.

The Iatroscan has also provided a means of assessing the ability of the clay samples to adsorb crude oil resins. Cr-bentonite appears to have the greatest ability to adsorb crude oil resins as it has the highest saturates/resins ratio of about 6.6.

The biodegradation of the crude oil hydrocarbons as evaluated by both the Iatro-scan and gravimetric methods indicate that unmodified bentonite, Al-bentonite, Na-bentonite, Ca-bentonite and Fe-bentonite seem to enhance biodegradation of the hydrocarbons. Acid activated clays and organo clays are inhibitory to biodegradation of hydrocarbons. Acid activated clay samples appear to have inhibited biodegradation of hydrocarbons as a result of reducing the pH of the medium which may have been toxic to the microbes. The organoclay is suggested to have inhibited biodegradation of the crude oil hydrocarbons by increasing the hydrophobic interaction between the hydrocarbons and the organoclay thereby making the hydrocarbons unavailable for microbial degradation. Samples such as kaolinite, saponite, Mg-bentonite, Zn-bentonite and K-bentonite did not enhance the biodegradation of crude oil hydrocarbons. The adsorption of hydrocarbons occurred most in K-bentonite, Zn-bentonite and unmodified palygorskite and this is mostly due to the adsorption of aromatic compounds via cation-π interactions.

This section of the study demonstrated that the % saturates / % aromatics removed via the process of biodegradation varies from 1.3-1.9 with samples such as Control-1, acid activated clay samples, organobentonite and unmodified kaolinite. This observation is consistent with the studies of (Maki et al., 2001 and Jirasripongpun, 2002) with (% saturates / % aromatics removed via the process of biodegradation of 1.7 and 1.4 respectively, although their studies did not involve solid support like clay minerals. However, with clay samples that stimulated biodegradation such as Fe-bentonite and Ca-bentonite, the % saturates / % aromatics removed via the process of biodegradation is less than 1.1 indicating that the clay samples that stimulate microbial growth actually boost the biodegradation of aromatics.

9. CONCLUSIONS AND FURTHER WORK

The presence of clay minerals affects the biodegradation of crude oil hydrocarbons, though whether the biodegradation will be inhibited or stimulated depends on the type and form of the clay minerals. Acid activated clay minerals and organoclay minerals are generally inhibitory to biodegradation of crude oil hydrocarbons and the inhibition occurs via different mechanisms. The clay minerals that stimulate biodegradation occur among the unmodified and homoionic interlayer cation clay samples (though not all of them are stimulatory) and seem to do so via the same mechanism.

The extent of adsorption as an abiotic process that takes place alongside the biodegradation is also a function of the type and form of the clay mineral.

There is good correlation between the EGME-surface area of the clay minerals (unmodified and homoionic cation interlayer clay samples) and the extent of biodegradation of the crude oil hydrocarbons. However, the correlation between the EGME-surface area and adsorption of the crude oil hydrocarbons is poor. Also, the correlation between the CEC of the clay samples and extent of biodegradation or adsorption is poor.

9.1 Acid activated clay samples

All the data from microbial growth kinetics, GC-FID, GC-MS and Iatro-scan analysis showed that acid activated clay minerals inhibited biodegradation of crude oil hydrocarbons. Acid activated clay minerals generally inhibit biodegradation by lowering the pH of the biodegradation system. The increase in acidity appears to be toxic to the microbial cells hence reducing the activity of the cells. It is important to note that the degree of inhibition of biodegradation of crude oil hydrocarbons by acid activated clays appears to be a function of the ability of the acid activated clay to lower the pH of the medium below a certain threshold. The ability of acid activated clay minerals to cause significant inhibition of biodegradation of crude oil hydrocarbons is thought to be brought about by extensive acid activation (to ensure that all the exchangeable cations are replaced by protons) and having the clay particles in a large enough proportion of the medium as to provide sufficient ‘population of protons’ for lowering the pH of the medium.

In an environment polluted with acid such as acid mine drainage, it is expected that the above conditions would be met thereby reducing the natural ability of the indigenous microbes to biodegrade any crude oil hydrocarbons contaminating such environment. Under this condition, it may be appropriate to treat this soil to reduce the acidity before any bioremediation approach should be adopted.

Adsorption of hydrocarbons by acid activated clay samples is insignificant and is due to the lack of interlayer metallic cations as the interlayer cations have been replaced by protons. This eliminates adsorption of aromatics due to pi-cation interaction as discussed subsequently. The surface area of the acid activated clay minerals is higher than the other forms of the clay samples studied. Generally, the surface area of acid activated clay minerals is higher than their unmodified counterparts as a result of the digestion of impurities in the clay such as carbonates during acid activation and leaching of octahedral metals such as Mg, Fe and Al. The EGME used for the determination of the surface area of the clay samples was not expected to have any problem accessing all the surfaces of the acid activated clay mineral as the surfaces of the acid activated clay mineral is hydrophilic. This hydrophilic nature was confirmed by the XRD data. However, the high surface area of the acid activated clay samples did not translate to increased biodegradation because of the toxic effect of the surface to the microbes that carry out the biodegradation.

This study therefore has provided further knowledge regarding the role acid activated clay minerals play in the environment during the biodegradation of crude oil hydrocarbons.

9.2 Organoclay samples

Organoclay is quite common in the environment as it is essentially the existence or intercalation of an organic cation in the interlayer of the clay mineral. In this study, there was adequate evidence (total organic carbon content data and FTIR) of the presence of organic phase with the organoclay samples and also adequate evidence (FTIR and XRD) that the organic cation (didecyldimethylammonium) was actually intercalated in the interlayer of the clay mineral. The organoclay with a richer organic phase (ie organobentonite) was more inhibitory to biodegradation. This suggests that the richness in organic phase intercalated in clays (which is a function of CEC) will determine the degree of inhibition to biodegradation. Clays with high CEC therefore, will be expected to form organoclay that are rich in organic

phase and hence exhibit greater inhibition than clays with low CEC. The EGME- surface area of organoclay is lower than the other types and forms of clay. This is mainly due to the existence of hydrophobicity (introduced into the clay by the organic cation) that hinders access to the interlayer surface by the EGME which is polar and hydrophilic. This hydrophobicity which is peculiar to the organoclay promotes interaction with crude oil hydrocarbons (which are also hydrophobic). This hydrophobic interaction renders the adsorbed hydrocarbons unavailable for both biodegradation and volatilization during incubation. The amount of hydrocarbons adsorbed due to this hydrophobic interaction would be a function of the magnitude of the adsorptive sites of the organoclay. The evidence provided by the GC-MS seemed to suggest that the lower molecular weight aromatic hydrocarbons such as naphthalene, methylnaphthalenes, and dimethynaphthalenes are adsorbed first. This is most probably because the movement of compounds to the vicinity of the organic phase of the organoclay where hydrophobic interaction takes place is diffusion controlled and therefore will favour low molecular weight compounds. If the adsorptive sites of the organoclay are exhausted (fully occupied), there could be chances for adsorption to proceed through other mechanisms that are common with unmodified clay samples. However, there was ample evidence that adsorption due to hydrophobic interaction is predominant. This hydrophobic interaction which is strong enough to render the hydrocarbons unavailable for biodegradation or volatilization is not strong enough to resist extraction with DCM during the EOM extraction process.

This shows that the organoclay can actually sequester organic compounds such as hydrocarbons from the environment into the organic phase of the organoclay. If the organoclay does not make contact with a strong solvent such as DCM, the pollutant (organic compound) would be successfully removed but not biodegraded hence if the aim is to achieve microbial degradation, organoclay would not be useful.

This study has thus also advanced our knowledge of the role organoclay plays during the biodegradation of crude oil hydrocarbons.

9.3 Unmodified clay samples

Unmodified clay minerals such as bentonite, saponite, kaolinite and palygorskite studied in this work affected biodegradation to varied degrees.

The unmodified kaolinite (1:1 clay minerals) used in this study contained traces of montmorillonite and illite (illite occurred in greater proportion than montmorillonite) and may be due to the intergrowth of these minerals with kaolinite. There was also hindered biodegradation of crude oil hydrocarbons by unmodified kaolinites. Ideally, kaolinite does not have interlayer cations and therefore does not possess the ability to cause 'local bridging effect' (which as a result of reducing electric double layer repulsion, increases the contacts amongst clay surface, cells and nutrients). The traces of montmorillonite and illite present may have actually contributed to local bridging effect but this is suggested to be insignificant. Unmodified kaolinite has the lowest EGME-surface area in comparison with the other clay samples studied in this work. The EGME method should not have any problem accessing the surface of unmodified kaolinite as it is hydrophilic (as a result of the OH groups) hence the low EGME-surface area is a good estimate of the surface area. The low value is attributable to the lack of interlayer surfaces and corresponds only to the external surface which represents the entire surface. Adsorption of crude oil hydrocarbons with kaolinites may be due to the little contamination with montmorillonites and mica.

Montmorillonite (from Bentonite) is a dioctahedral 2:1 phyllosilicate with either Na^+ or Ca^{2+}as the predominant interlayer cation. The unmodified bentonite used in this study contains Na^+ as the predominant interlayer cation. The sample contains traces of carbonates such as calcite, siderite and dolomite. There was also minor contamination with quartz. This contamination did not have any significant effect on this sample. This clay mineral had the highest ability to stimulate biodegradation of crude oil hydrocarbons among the unmodified clay minerals. It had the highest EGME-surface area as it has a quite extensive interlayer surface. The extensive surface area of bentonite allows the accumulation of nutrients and microbes at its surface making it easy for the microbes to make contact with both the substrate and nutrients hence enhancing biodegradation.

The interlayer cation of the sample is highly exchangeable leading to relatively high CEC values. However, because of the ability of this clay mineral to undergo hydration as a result of the attraction of water by Na^+ in the interlayer, there is reduced ability to expose the hydrophobic siloxane layer leading to reduced ability to adsorb hydrophobic compounds such as hydrocarbons when compared with 2:1 clays that are non-swelling such as pallygorskite.

This study has demonstrated that bentonite with Na^+ as the predominant cation in the interlayer of the clay mineral would have the ability to stimulate the biodegradation of crude oil hydrocarbons significantly.

Unmodified saponite is trioctahedral 2:1 phyllosilicate and could have a monovalent or a divalent cation in the interlayer. The unmodified saponite used in this study contains a divalent cation in the interlayer. The sample contains traces of calcite (as the only carbonate contaminant) and feldspars such as sanidine, microcline and albite. It has the lowest EGME-surface area among the unmodified clay samples with the exception of kaolinites. The CEC is however, higher than that of palygorskite but lower than that of bentonite. This may account for why it did not stimulate biodegradation as much as bentonite. Overall, this clay sample does not seem to be of great value with respect to increasing the biodegradation of crude oil hydrocarbons as it did not demonstrate significant biodegradation compared with the positive control sample (Control-1). The ability of unmodified saponite to adsorb crude oil hydrocarbons is in the same order as that of bentonite and the same explanation given for bentonite holds.

The unmodified palygorskite used in this study contained traces of carbonates (siderite and magnesite) and feldspar (sanidine). This sample exhibited a unique behaviour in that while having the ability to stimulate biodegradation of crude oil hydrocarbons, it also possessed the ability to adsorb hydrocarbons more extensively than any other unmodified clay samples studied. This ability by unmodified palygorskite to adsorb hydrocarbons is attributable to the unique structure of palygorskite in which a continuous tetrahedral sheet with occasional inversion that causes the octahedral sheet to be discontinuous at this point of inversion creates a channel with dimension ~ $4A^0$ by $6A^0$ which can host the crude oil hydrocarbons that are eventually adsorbed.

The EGME-surface area of palygorskite is high (and is attributable to its micro-porous nature) though lower than that of bentonite. The CEC of this clay sample is low.

Although there is significant removal of hydrocarbons due to adsorption, there is equally high removal of hydrocarbons due to biodegradation making the overall removal of hydrocarbons by unmodified palygorskite higher than that of any of the unmodified clay samples studied. Palygorskite has structure that favours both processes.

If the total removal of oil is a priority, unmodified palygorskite will be a clay sample of choice as this sample removed crude oil hydrocarbons significantly by both adsorption and biodegradation. However, if microbial biodegradation is a priority, other unmodified clay samples such as unmodified bentonite would be considered.

Palygorskite is not the only clay mineral with channel structure. Sepiolite which has an even more extensive channel structure would therefore be expected to adsorb hydrocarbons significantly during biodegradation of crude oil hydrocarbons. However, because sepiolite does not have a dominant dioctahedral character like palygorskite, the effect on biodegradation of hydrocarbons may be different.

From this study, contrary to the study of Warr et al (2009), adsorption of hydrocarbons by palygorskite is significant as it accounts for about 50% of the removal of the hydrocarbons. Adsorption of crude oil hydrocarbons by other unmodified clay samples accounts for about 25%-35% which is not insignificant. Hence, adsorption of crude oil hydrocarbons by unmodified clay minerals during the biodegradation of crude oil hydrocarbons is significant and highest with palygorskite.

Adsorption of hydrocarbons observed in this study is largely the contribution of adsorption of aromatic hydrocarbons. Cation – pi interaction between the aromatic hydrocarbons and the interlayer cations of the clay is suggested to account for why the clay mineral samples show good adsorption for aromatic hydrocarbons. Adsorption of saturates by unmodified clay mineral samples is insignificant.

9.4 Homoionic cation interlayer clay samples

The main contaminants present in some of the homoionic interlayer clay mineral samples are carbonates. The carbonates (siderite, calcite and dolomite) which are the main contaminants as found in Na-bentonite, K-bentonite, Mg-bentonite and Ca-bentonite were missing in the Al-bentonite.

Zn-bentonite contained little dolomite as siderite and calcite had been removed. Fe(III)-bentonite and Cr (III)- bentonite contained traces of siderite as dolomite and calcite have been completely removed.

Zn-bentonite, Al-bentonite, Cr-bentonite and Fe-bentonite are more acidic than the other homoionic clay samples (Table 3.1) and the acidity for these four samples increases in the order: Zn-bentonite < Fe-bentonite < Cr-bentonite < Al-bentonite. The removal ability by these four clay samples of the carbonates follows the same order.

The acidity of these clay samples arises from the ability of the cations especially the trivalent cations to hydrolyse water thereby generating protons that lower the pH and increases the acidity during the cation exchange reaction. Consequently, the carbonates were digested by the acidic medium.

The clay samples with homoionic cations at their interlayer affected biodegradation and adsorption of the hydrocarbons to varied degrees indicating that the nature of the cation in the interlayer of the clay mineral would influence both processes of biodegradation and adsorption of crude oil hydrocarbons. However, there is no general trend in the extent of biodegradation or adsorption in going from monovalent to trivalent cation in the interlayer of the clay sample.

Between the monovalent cations (Na^+ and K^+) tested, Na-bentonite stimulated biodegradation of the hydrocarbons whereas K-bentonite inhibited the biodegradation. However, K-bentonite showed quite higher ability to adsorb crude oil hydrocarbons than Na-bentonite. The EGME-surface area and CEC of Na-bentonite are higher than that of K-bentonite. It is apparent that the implication of having K^+ in the interlayer of the clay is that the attraction of water in the interlayer will be reduced due to the lower hydration energy of K^+ as its charge/radius ratio is relatively low. This makes the interlayer of K-bentonite not as hydrophilic as Na-bentonite. This, coupled with the fact that K^+ has a relative large size (that will make the K-bentonite expose its hydrophobic siloxane surface) caused this clay sample to possess the ability to host hydrocarbons. As the hydrocarbons get attracted into the hydrophobic siloxane surface, the cation – π interaction stated earlier would take over.

The same reason of exposition of the hydrophobic siloxane surface accounts for why the surface area of K-bentonite is lower than that of Na-bentonite given that the EGME (which is a polar compound) would not be able to access the exposed hydrophobic siloxane surface in the interlayer of the clay sample.

Among the divalent interlayer cations, Ca-bentonite stimulated biodegradation of crude oil hydrocarbons most whereas Zn-bentonite inhibited the biodegradation. Mg-bentonite stimulated the biodegradation but not as much as Ca-bentonite. Zn-bentonite showed the highest ability to adsorb crude oil hydrocarbons. It is not yet very clear how Zn^{2+} in the interlayer of the clay mineral accomplishes this. It has been proposed that Ca-bentonite is able to cause a strong 'local bridging effect' that enhances the delivery of the nutrients and substrates to the microbes. This makes Ca-bentonite to have a significant effect on biodegradation of the hydrocarbons.

Among the trivalent cations, Fe-bentonite achieved the highest stimulation of the biodegradation of crude oil hydrocarbons. Fe-bentonite has the highest CEC and EGME-surface area among all the clay samples studied and this is believed to account for why it showed the highest stimulatory ability among the other clays with trivalent cations at the interlayer. Adsorption of hydrocarbons by these clays with trivalent cations at the interlayer is highest with Cr-bentonite though when compared with K-bentonite and Zn-bentonite, Cr-bentonite adsorbs hydrocarbons least.

Warr et al., (2009) suggested that the 'local bridging effect' produced by the divalent cations was responsible for why Ca-montmorillonite and palygorskite showed better stimulation of biodegradation than sodium-montmorillonite and therefore concluded that divalent cations in the interlayer will stimulate biodegradation more than monovalent cations. This study however, has provided evidence that this is not always true as Na-bentonite stimulated biodegradation more than bentonite clays with divalent cations at the interlayer viz, Mg-bentonite and Zn-bentonite. The cluster analysis carried out in this study identified Na-bentonite, Ca-bentonite and Fe-bentonite as having similar behaviour with respect to biodegradation of crude oil hydrocarbons eventhough they have different homoionic cations (mono, di and trivalent, respectively) in their interlayers. Also, if the 'local bridging effect' were to be the sole factor determining extent of biodegradation, trivalent cations in the interlayer of clay samples would produce the highest 'local bridging effect' and hence stimulate biodegradation most. It therefore follows that other factor(s) in addition to the local bridging effect must be contributing to the overall influence of the interlayer cations on biodegradation of crude oil hydrocarbons.

Interlayer cations have the ability to hydrolyse 'shells' of water in the interlayer of clay minerals producing protons that can increase the Bronsted acidity of the clay suspension. The ability of the interlayer cation to hydrolyse the water in the interlayer of the clay mineral is a function of the charge/size ratio of the cation. Trivalent cations have the highest ability to polarize (hydrolyse) the interlayer water in comparison with monovalent and divalent cations. This has the effect of reducing the pH of the system especially as the volume of water in the medium decreases which will ultimately reduce microbial activity.

It is therefore suggested that local bridging effect is not the only role played by interlayer cations of clay minerals during the biodegradation of crude oil hydrocarbons rather, in addition, the hydrolysis of interlayer water by the interlayer cations is also involved.

9.5 Key findings

(i) Contrary to the report of (Chaerun and Tazaki (2005) and Warr et al., 2009) where it was assumed that adsorption of oil is insignificant during biodegradation, this study showed that adsorption of hydrocarbons by unmodified and homoionic interlayer clay minerals during the biodegradation of crude oil hydrocarbons is significant especially with unmodified palygorskite, potassium-bentonite and zinc-bentonite where at the experimental concentrations used, almost 43-50% of the hydrocarbons are adsorbed. Adsorption of hydrocarbons which is largely as a result of adsorption of aromatics is suggested to be mainly due to pi-cation interaction.

(ii) Warr et al (2009), reported that divalent cations (Ca^{2+} and Mg^{2+}) in the interlayer of bentonite are more stimulatory to biodegradation than monovalent cations such as (Na^{+})on the account of more effective local bridging effect. This study having carried out study with monovalent, divalent and trivalent cations (homoionic interlayer cations), showed that this is not generally true. Na-bentonite (monovalent) was more stimulatory to biodegradation than Mg-bentonite and Zn-bentonite which all have divalent cations in the interlayer. This study also showed that Fe-bentonite, Ca-bentonite and Na-bentonite stimulated biodegradation to almost the same degree and yet have different valency. It is therefore suggested from this study that the interlayer cation would, in addition to the local bridging effect which is stimulatory, cause the polarization of the interlayer water to produce acidity that would be inhibitory to biodegradation as the biodegradation progresses especially as

the moisture level decreases. The same order of stimulation of biodegradation due to local bridging effect which is trivalent cations > divalent cations > monovalent cations is the same order of inhibition due to interlayer water polarization. Hence, these opposing effects of the interlayer cations with respect to biodegradation would ultimately mean that it is wrong to generalize that divalent cations or trivalent cations in the interlayer clay would cause the stimulation of biodegradation most.

(iii) Acid activated clay and organoclay minerals are inhibitory to biodegradation. Whereas acid activated clay minerals are inhibitory by increasing the acidity of the medium that is believed to have a toxic effect to the microbes, the organoclay is inhibitory by causing extensive hydrophobic interaction with the crude oil hydrocarbons that render them unavailable for biodegradation.

(iv) Among the unmodified clay minerals, unmodified kaolinite which is 1:1 phyllosilicate with very low EGME-surface area is inhibitory to biodegradation. Unmodified saponite (2:1 trioctahedral phyllosilicate) is neither inhibitory nor actually stimulatory hence can be said not to be quite useful for bioremediation purposes. Unmodified bentonite and unmodified palygorskite are stimulatory to biodegradation and both have high surface area. These two clay minerals have good potential for bioremediation of crude oil polluted sites.

(v) The homoionic cation interlayer clay samples such as K-bentonite, Zn-bentonite and Cr-bentonite are inhibitory to biodegradation though with high adsorptive capacity for crude oil hydrocarbons as stated earlier. Cr-bentonite appears to show high adsorption for resins as observed with Iatro-scan analysis.

Mg-bentonite and Al-bentonite are slightly stimulatory to the biodegradation of crude oil hydrocarbons while Na-bentonite, Ca-bentonite and Fe-bentonite are the most stimulatory of all samples studied.

These three samples, especially Ca-bentonite and Fe-bentonite have potential for bioremediation of oil spill sites.

The effect of the clay samples during the biodegradation of crude oil hydrocarbons is summarized in Table 9.1 below:

Table 9.1 Summary of the effect of clay minerals during the biodegradation of crude oil hydrocarbons

Clay type	Treatment	Effect on:		
		Biodegr. of HC's	Adsorp. of HC's	Overall removal of HC's
Kaolinite	Untreated	Inhibitory	Medium	Low
Saponite	Untreated	Neutral/inhibitory	Medium	Medium
Bentonite	Untreated	Stimulatory	Medium	High
Palygorskite	Untreated	Stimulatory (mild)	High	Very High
Bentonite	Acid activated	Inhibitory	Low	Low
Palygorskite	Acid activated	Inhibitory	Low	Low
Kaolinite	Acid activated	Inhibitory	Low	Low
Saponite	Acid activated	Inhibitory	Low	Low
Bentonite	Organo	Inhibitory	Low	Low
Saponite	Organo	Neutral	Low	Low
Bentonite	Potassium-exchanged	inhibitory	High	Medium
Bentonite	Zinc-exchanged	inhibitory	High	Medium
Bentonite	Chromium-exchanged	inhibitory	Medium	Low
Bentonite	Magnesium-exchanged	Stimulatory (mild)	Low	Medium
Bentonite	Aluminium-exchanged	Stimulatory (mild)	Low	Medium
Bentonite	Sodium-exchanged	Stimulatory	Low	High
Bentonite	Calcium-exchanged	Highly stimulatory	Low	Very High
Bentonite	Iron (III)-exchanged	Highly stimulatory	Low	Very High

9.6 Further studies

There is the need to ascertain the composition of microbial communities responsible for the biodegradation of crude oil hydrocarbons as different microbial communities may behave differently with respect to microbial degradation of crude oil hydrocarbons in the presence of clay minerals.

From the microbial growth experiment carried out as described in chapter four of this work, the tested clay mineral samples affected the growth phase of the cells differently making it apparent that the kinetics of the biodegradation would be different for different clay samples. It is therefore suggested that time dependent measurement of hydrocarbon biodegradation in conjunction with microbial growth should be carried out in order to fully describe the kinetics of the biodegradation of crude oil hydrocarbons supported on clay minerals.

Given that the local bridging effect and hydrolysis of interlayer water of clay minerals are identified as the two main factors associated with the interlayer cations that influence biodegradation in opposite directions, further studies should be carried out to identify ways of boosting the local bridging effect (which is believed to be beneficial to the stimulation of biodegradation) and dampening the effect of hydrolysis of interlayer water of the clay (which is believed to have adverse effect on biodegradation).

Some of the metabolites produced during the biodegradation of crude oil hydrocarbons could be toxic to microbes and also recalcitrant to biodegradation, hence their removal by adsorption during biodegradation would be highly beneficial. The ability of clay minerals to adsorb metabolites produced during biodegradation of crude oil hydrocarbons should be investigated as this could be another factor that makes some clay mineral to stimulate biodegradation of crude oil hydrocarbons by removing toxic substances.

The application of this study to real life bioremediation of oil spill sites would require consideration of what to do with the spent clay at the site of spill bioremediation. Should the clay be left in the soil with some soil amendment for agricultural purposes or should other uses of the spent clay be explored such as road construction? This is an issue that should be addressed before field application of this study.

REFERENCES

ABE, A., INOUE, A., USAMI, R., MORIYA, K., AND HORIKOSHI, K. 1995. Degradation of polyaromatic hydrocarbons by organic solvent-tolerant bacteria from deep sea. Bioscience Biotechnology and Biochemistry, 59, 1154-1156.

ABOLLINO, O., ACETO, M., MALANDRINO, M., SARZANINI, C., MENTASTI, E., 2003. Adsorption of heavy metals on Na-montmorillonite. Effect of pH and organic substances. Water research 37, 1619-1627.

ALEXANDER, M., 1999. Acclimation, Kinetics, sorption and mechanism of utilization In: Biodegradation and Bioremediation (2nd edition) Academic press, Sandiego, California, USA p 9-150.

ALEXIS J. K., AND ELIMELECH, M., 2007. Impact of alginate conditioning film on deposition kinetics of motile and nonmotile pseudomonas aeruginosa strains. Applied and Environmental Microbiology, 5227–5234.

ALEXIS J.K., WERONSKI, P., ELIMELECH, M., 2007. Adhesion of nonmotile pseudomonas aeruginosa on “soft” polyelectrolyte layer in a radial stagnation point flow system: Measurements and model predictions, Langmuir, 23, 12301.

ANNABI-BERGAYA, F., CRUZ, M.I., GATINEAU, L., FRIPIAT, J.J. 1979. Adsorption of alcohols by smectites.I. Distinction between internal and external surfaces. Clay minerals 14, 249-258.

ARGUER, J.P., HERMOSIN, M.C., CALDERON, M.J., AND CORNEJO, J. 2000. Fenuron sorption by homoionic natural and modified smectites. Journal of Environmental Science and Health Part B, 35, 279-296.

ASCON-CABRERA, M.A., AND LEBEAULT, J.-M. 1995. Interfacial area effects of a biphasic aqueous/organic system on growth kinetic of xenobiotic-degrading microorganisms. Applied Microbiology and Biotechnology, 43, 1136-1141.

ASKE, N., 2002. Characterisation of crude oil components, asphaltene aggregation and emulsion stability by means of near infrared spectroscopy and multivariate analysis (PhD theses) Department of chemical engineering, Norwegian university of science and technology.

ATLAS, R.M. 1984. Pathways of hydrocarbon degradation In: Petroleum microbiology. Macmilian, New York, USA, 1-15.

ATLAS, R.M., AND BARTHA, R. 1972. Biodegradation of petroleum in seawater at low temperatures. Canadian Journal of microbiology, 18, 1851-1855.

ATLAS, R.M., AND BARTHA, R. 1992. Hydrocarbon biodegrdadtion and oil spill bioremediation. Advances in Microbiology and Ecology, 12, 287-338.

BAILEY S.W, 1980. Structures of layer silicates. In: Crystal structures of clay minerals and their X-ray identification (Brindley,G.W., and Brown G. eds.), Mineralogical society, London, pp1-123.

BAILEY, N.J.L, JOBSON, A.M., ROGERS, M.A., 1973. Bacterial degradation of crude oil: comparison of field and experimental data. Chemical Geology, 11, 203-221.

BALL, W.P. AND ROBERTS, P.V. 1991a. Long term sorption of halogenated organic chemicals by aquifer material. I Equilibrium. Environmental Science and Technology, 25, 1223-1237.

BALL, W.P. AND ROBERTS, P.V. 1991b. Long term sorption of halogenated organic chemicals by aquifer material. 2 Intraparticle diffusion. Environmental Science and Technology, 25, 1237-1249.

BECHER, P. 1965. Emulsions: Theory and practise. (Smith, A.L. ed.) Reinhold, New York.

BENNETT, B., CHEN, M., BRINCAT, D., GELIN, F.J.P., LARTER, S.R., 2002. Fractionation of benzocarbazoles between source rocks and petroleums. Organic Geochemistry, 33, 545-559.
BERGAYA, F., AND VAYER, M. 1997. CEC of clays: Measurement by adsorption of a copper ethylene diamine complex. Applied Clay Sccience, 12, 275-280.

BERGAYA, F., THENG, B.K.G., AND LAGALY, G. 2006: Surface area and porosity. In: Handbook of Clay science, Elsevier, Amsterdam, Netherlands pp 965.

BIRMAN, I. AND ALEXANDER, M. 1996a. Optimizing biodegradation of phenanthrene dissolved in nonaqueous-phase liquids. Appled Microbiology and Biotechnology 45, 263-266.

BLACK, J.G. 1996. Microbiology. Principles and Applications (3rd Edition), Prentice Hall. Upper Saddle River, New Jersey, USA. 136-140, 151-153.

BOCCHI, C., M. CARERI, A. CASNATI, AND G. MORI. 1995. Selectivity of calix[4]arene crown-6 for cesium ion in ISE-effect of the conformation Analytical Chemistry, 67, 4234–4238.

BOGAN, L.M. AND SULLIVAN, W.R. 2003. Physicochemical soil parameters affecting sequestration and mycobacterial biodegrdation of polycyclic aromatic hydrocarbon in soil. Chemosphere, 52, 1717-1726.

BOGAN, L.M., LAHNER, L.M., SULLIVAN, W.R. AND PATEREK, J.R. 2003. Degradation of straight-chain aliphatic and high-molecular-weight polycyclic aromatic hydrocarbons by a strain of mycobacterium austroafricanum. Journal of Applied Microbiology,94, 230-239.

BOLES J.R., FRANKS, S.G., 1979. Clay diagenesis in Wilcox sandstones of southwest Texas: implications of smectite diagenesis on sandstone cementation. Journal of Sediment Petrology, 49, 55-70.

BOSSERT , I., AND BARTHA, R. 1984. The fate of petroleum in soil ecosystem: In Petroleum Microbiology, Ed, Atlas, Macmillan, New York, USA, pp 435-473.

BOUCHEZ, M., BLANCHET, D., AND VANCASTEELE, J. –P. 1995. Substrate availability in phenanthrene biodegradation: transfer mechanism and influence on metabolism. Applied Microbiology and Biotechnology, 43, 952-960.

BOUCHEZ, M., BLANCHET, D., AND VANCASTEELE, J. –P. 1997. Microbiology, 143, 1087-1093.

BRADLEY, W.F. 1945. Molecular associations between montmorillonite and some polyfunctional organic liquids. Journal of American chemical society, 67 (6) 975-981.

BRAGG, J.R., PRINCE, R.C., HARNER, E.J., ATLAS, R.M. 1993 In proceedings of the 1993 International Oil Spill Conference; American Petroleum Institute: Washington D.C., pp 435-447.

BREEN, C., MADEJOVA, J., KOMADEL, P. 1995a. Correlation of catalytic activity with infra-red, ^{29}Si MAS NMR and acidity data for HCl-treated fine fractions of montmorillonites. Applied Clay Science 10, 219-230.

BREEN, C., MADEJOVA, J., KOMADEL, P. 1995b. Characterization of moderately acid-treated, size fractionated montmorillonites using IR and MAS NMR spectroscopy and thermal analysis. Journal of Materials Chemistry 5, 469-474.

BRIGHT, J.J., AND FLETCHER, M. 1983. Amino acid assimilation and electron transport system activity in attached and free living marine bacteria. Applied Environmental Microbiology, 45, 818-825.

BRUSSEAU, M.L. AND RAO, P.S.C. 1991. In: Rates of soil chemical process (D.L. Sparks and D.L. Sunrez, eds). Soil science society of America, Madison, USA, pp 281-302.

BURGER, A.E., 1993. Estimating the mortality of seabirds following oil spills: Effects of spill volume. Marine Pollution Bulletin. 26, (3), 140-143.

BURNS, K. A., GARRITY, S. D. AND LEVINGS, S. C.,1993. How many years until mangrove ecosystems recover from catastrophic oil-spills. Marine Pollution Bulletin, 26, 239-248.

BUSSCHER, H.J., WEERKAMP, A.H., VAN DER MEI, H.C., VAN PELT, W.J., DE JONG, H.P., AND ARENDS, J. 1984. Measurement of the surface free energy of bacterial cell surfaces and its relevance for adhesion. Applied environmental microbiology, 48, 980-983.

BUTLER, E.L., DOUGLAS, G.S., STEINHAUER, W.S., PRINCE, R.C., ACZEL, T., HSU, C.S., BRONSTON, M.T., CLARK, J.R., LINDSTROM, J.E. 1991. In: On-site reclamation. Processes for xenobiotic and hydrocarbon treatment ; Hinchee, R.E., Olfenbuttel, R.F., Eds. Butterworth-Heinemann: Boston, USA, pp 515-521

CALVILLO, Y.M. AND ALEXANDER, M., 1996. Mechanism of microbial utilisation of biphenyl sorbed to polyacrylic beads. Applied and Environmental Microbiology, 45, 383-390.

CAMEOTRA, S.S., SINGH, H.D., HAZARIKA, A.K. AND BANIAN, J.N. 1983. Mode of uptake of insoluble solid substrates by microorganisms. Biotechnology & Bioengineering, 25, 2945-2956.

CARTER, D.L., HEILMAN, M.D. AND GONZALEZ, C.L. 1965. Ethylene glycol monoethyl ether for determining surface area of silicate minerals. Journal of Soil Science, 100 (5), 356-360.

CASSANI, F. AND EGLINTON, G. 1991. Organic geochemistry of Venezuelan extra-heavy crude oils. 2. Molecular assessment of biodegradation. Chemical Geology, 91, 315-333.

CELIS, R., HERMOSIN, M.C., CARRIZOSA, M.J., AND CORNEJO, J. 2002a. Inorganic and organic clays as carriers for controlled release of the herbicide hexazinone. Journal of Agricultural and Food Chemistry, 50, 2324-2330.

CELIS, R., KOSKINEN, W.C., HERMOSIN, M.C., ULIBARRI, M.A., AND CORNEJO, J., 2000a. Triadimefon interactions with organoclays and organohydrotalcites. Soil science society of Amerca Journal, 64, 36-43.

CERNIGLIA, C.E. 1984. Microbial transformation of aromatic compounds. In: Petroleum Microbiology (Atlas, R.M. ed), Macmillian , New York, pp 99-128.

CHAERUN, S.K. AND TAZAKI, K. 2005. How kaolinite plays an essential role in remediating oil-polluted seawater. Clay minerals, 40, 481-491.

CHIOU C.T., in Reactions and movement of organic chemicals in soils (Sawhney B.L. and Brown, K. eds). Soil Science Society of America, Madison, USA, pp 1-29.

CHIOU, C.T., and Rutherford, D.W. 1997. Effects of exchanged cation layer charge on the sorption of water and EGME vapours on montmorillonite clays: Clays and clay minerals, 45 (6), 867-880.

CHIPERA, S.J. AND BISH, D.L., 2001. Baseline studies of the clay minerals society source clays: powder x-ray diffraction analysis. Clay and Clay Minerals, 49,398-409

CHRISTIDIS, G.E., SCOTT, P.W., Dunham, A.C., 1997. Acid activation and bleaching capacity of bentonites from the islands of Milos and Chios, Aegean, Greece. Applied Clay Science, 12, 329-347.

CHUNG, N. AND ALEXANDER, M. 1998. Differences in sequestration and bioavailabilty of organic compounds aged in dissimilar soils. Environmental Science and Technology, 32, 855-860.

CHURCHMAN, G.J., GATES, W.P., Theng, B.K.G., Yuan, G., 2006. Clays and clay minerals for pollution control. In: Handbook of Clay Science: Developments in Clay Science (Bergaya, F., THENG, B.K.G., LAGALLY, G. eds.), Elsevier, Amsterdam, vol. 1, pp 625-675.

COLE, G.M., 1994. Assessment and Remediation of petroleum contaminated sites. Lewis publishers, Boca Raton, USA.

CONNAN, J. 1984. Biodegradation of crude oils in reservoirs. Advanced Petroleum Geochemistry, 1, 299-333.

CONNAN, J., LACRAMPE-COULOUME, G. AND MAGOT, M. 1997. Anaerobic biodegradation in reservoirs: A widespread phenomenon in nature. 8th international meeting on organic geochemistry, September 22-26, Maastricht, The Netherlands, pp. 5-6.

COONEY, J.J., SILVER, S.A., AND BECK, E.A., 1985. Factors influencing hydrocarbon degradation in three fresh water lakes. Microbial Ecology, 11, 127-137.

CORMA, A. MISFUD, E. SANZ., 1987. Influence of the chemical composition and textural characteristic of palygorskite on the acid leaching of octahedral cations. Clays Clay Mineralogy, 22 , 225-231.

CORNEJO, J., CELIS, R., PAVLOVIC, I., AND ULIBARRI, M.A. 2008. Interactions of pesticides with clays and layered double hydroxides: a review. Clay minerals, 43, 155-175.

CRUZ-GUZMAN, M., CELIS, R., HERMOSIN, M.C., KOSKINEN, W.C., AND CORNEJO, J. 2005. Adsorption of pesticides from water by functionalized organobentonites. Journal of Agricultural and Food Chemistry, 53, 7402-7511.

CURIALE, J.A. 2002. A review of the occurrences and causes of migration-contamination in crude oil. Organic Geochemistry, 33, 1389-1400.

DALING, P.S., FAKSNESS, L-G., HANSEN, A.B. AND STOUT, S.A. 2002. Improved and standardized methodology for oil spill fingerprinting. Environmental Forensics, 3, 263-378.

DAS, K., MUKHERJEE, A.K. 2006. Crude petroleum-oil biodegradation efficiency of Bacillus subtilis and Pseudomonas aeruginosa strains isolated from a petroleum-oil contaminated soil from North-East India. Bioresource Technology, 98 (7) 1339-1345.

DEBYE, P.; HÜCKEL, E. (1923), "The theory of electrolytes. I. Lowering of freezing point and related phenomena", *Physikalische Zeitschrift* 24: 185–206

DELILLE, D., AND COULON, F., 2008. Comparative mesocosm study of biostimulation efficiency in two different oil-ammended sub-antarctic soils. Microbial ecology, 56, 243-252.

DERJAGUIN, B.; LANDAU, L.,1941. Theory of the stability of strongly charged lyophobic sols and of the adhesion of strongly charged particles in solutions of electrolytes, *Acta Physico Chemica URSS* 14: 633.

DIBBLE, J.T., AND BARTHA, R. 1976. Effect of iron on the biodegradation of petroleum in sea water. Applied Environmental Microbiology, 31,544-550.

DIDYK, B.M., SIMONEIT, B.R.T, BRASSELL, S.C. AND EGLINTON, G. 1978. Organic geochemical indicators of palaeo-environmental conditions of sedimentation. Nature, 272, 216-222.

DUBIKOVA, M., CAMBIER, P., SUCHA, V., CAPLOCICOVA, M., 2002. Experimental soil acidification. Applied Geochemistry 17, 245-257.

EADIE, B.J. MOREHEAD, N.R. AND LANDRUM, P.F. 1990. Three-phase partitioning of hydrophobic organic compounds in great lakes water, Chemosphere, 20, 161-178.
EBERL, D. 1984. Clay mineral formation and transformation in rocks and soils. Philosophical Transactions of the Royal Society London, A311, pp 241-257.

EFROYMSON, R.A. AND ALEXANDER, M. 1991. Biodegradation by an arthrobacter species of hydrocarbons partitioned into an organic solvent. Appled Environmental Microbiology, 57, 1441-1447.
EGBERONGBE, F.O.A., NWILO, P.C., BADEJO, O.T., 2006. Oil spill disaster monitoring along Nigerian Coastline. Shaping the change

EINSELE, A., SCHNEIDER, H., AND FIECHTER., A. 1975. Characterization of micro-emulsion in a hydrocarbon fermentation by electronmicroscopy. Journal of Fermentation and Technology 53, 241-243.

EL-NAHHAL, Y., NIR, S., POLUBESOVA, T., MARGULIES, L. AND RUBIN, B., 1998. Leaching, phytotoxicity, and weed control of new formulations of alachlor. Journal of Agricultural and Food Chemistry, 46, 3305-3313.

EL-NAHHAL, Y., NIR, S., SERBAN, C., RABINOVITZ, O., AND RUBIN, B., 2001. Organoclay formulation of acetochlor for reduced movement in soil. Journal of Agricultural and Food Chemistry, 49, 5364-5371. Environmental Conservation, 19, 253–258.

ENERGY, 2011. http://www.energy.eu/dictionary/data/383.html

ENVIRONMENTAL AGENCY., 2006. http://www.environment-agency.gov.uk/commondata/103601/poll_incidents_2005_1438766.xls Accessed Nov, 2007.

ESTERMAN, E.F., AND MCLAREN, A.D., 1959. Stimulation of bacterial proteolysis by adsorbents. Journal of Soil Science, 10, 64-78.

FARRIMOND, P., TAYLOR, A. AND TELNAES, N., 1998. Biomarkers maturity parameters. The role of generation and thermal degradation. Organic Geochemistry, 29, 1181-1197.

FILIP, Z., 1973. Clay minerals as a factor influencing the biochemical activity of soil microorganisms. Folia Microbiology (Prague), 18, 56-74.

FLETCHER, M AND MARSHALL, K.C., 1982. Are solid surfaces of ecological significance to aquatic bacteria? Advanced Microbial ecology,6, 199-236.

FLOODGATE, G.D., 1984. The fate of petroleum in marine ecosystems. In: Petroleum Microbiology (R.M. Atlas ed). Macmilan, New York, 354-397.

FRENKEL, M. AND HELLER-KALLAI, L. 1983. Interlayer cations as reaction directors in the transformation of limonene on montmorillonite. Clays and clay minerals, 31, (2) 92-96.

FU, M.H., AND ALEXANDER, M. 1995. Use of surfactants and slurrying to enhance the biodegradation in soil of compounds initially dissolved in nonaqueous-phase liquids. Applied Microbiology and Biotechnology, 43, 551-558.

FUKUMAKI, T., INOUE, A., MORIYA, K., AND HORIKOSHI, K. 1994. Isolation of a marine yeast that degrades hydrocarbon in the presence of organic solvent. Bioscience Biotechnology Biochemistry, 58, 1784-1788.

GALAN, E., CARRETERO, M.I., FERNANDEZ CALIANI, J.C. 1999: Effects of acid mine drainage on clay minerals suspended in the Tinto River (Rio Tinto, Spain). An experimental approach. Clay minerals, 34, 99-108.

GASTON, L.A., LOCKE, M.A. AND ZABLOTOWICZ, R.M., 1996. Sorption and degradation of bentazon in conventional- and no-till Dundee soil. Journal of Environmental Quality, 25, 120-126.

GHOSHAL, S., AND LUTHY, R.G., 1996. Bioavaialability of hydrophobic organic compounds from nonaqueous-phase liquids: the biodegradation of naphthalene from coal tar. Environmental Toxicology and Chemistry, 15, 1894-1900.

GIBBONS, J.A., AND ALEXANDER, M. 1989. Microbial degradation of sparingly soluble.organic chemicals: Phthalate esters Applied Environmental Toxicology and Chemistry. 8, (4), 283-291.

GIBSON, D.T., KOCH, J.R., AND KALIO, R.E. 1968. Oxidative degradation of aromatic hydrocarbons by microorganisms. I. Enzymatic formation of catechol from benzene. Biochemistry, 7, (7), 2653-2662.

GIEG, L.M. AND SUFLITA, J.M. 2005. Metabolic indicators of anaerobic hydrocarbon biodegradation in petroleum-laden environments. In Petroleum Microbiology, B. Oliver and M.Magot (eds.), Washington, DC: ASM Press, 277-300.

GODWIN, N.S., PARK, P.J.D., RAWLINSON, A.P., 1981. Crude oil biodegradation. In: advances in organic geochemistry, Bjoray, M., Ed; Wiley: Chichester, UK., pp 650-658.

GOGOI, B.K., DUTTA, N.N., GOSWAMI, P. AND MOHAN, T.R.K., 2003. A case study of bioremediation of petroleum-hydrocarbon contaminated soil at a crude oil spill site. Advances in Environmental Research, 7, 767-782.

GOSWAMI, P.C. AND SINGH, H.D.,1991. Different modes of hydrocarbon uptake by two pseudomonas species. Biotechnology and Bioengineering, 37, 1-11.

GOSWAMI, P.C., SINGH, H.D., BHAGAT, S.D., AND BARUAH, J.N., 1983. Mode of uptake of insoluble substrates by microorganisms I: sterol uptake by an arthrobacter species. Biotechnology and Bioengineering, 25, 2929-2943.

GOTO, M., KATO, M., ASAUMI, M., SHIRAI, K., VENKATESWARAN, K., 1994. TLC-FID method of evaluation of the crude oil degrading capability of marine microorganism. Journal of Marine Biotechnology, 2, 45-50.

GRIFFITH, S.M., AND THOMAS, R.L., 1979. Activity of immo- bilized pronase in the presence of montmorillonite. Soil Science Society of American Journal, 43,1138-1140.

GRIM, R.E., GUVEN,N.,1978. Bentonites. In: Geology, mineralogy, properties and uses. Developments in sedimentology, 24, Elsevier, Amsterdam.

GROISMAN, L., RAV-ACHA C., GERSTL Z. AND MINGELGRIN, U. 2004a. Sorption of organic compounds of varying hydrophobicities from water and industrial waste-water by long- and short- chain organoclays. Applied clay science, 24, 159-166.

GUERIN, W.F., BOYD, S.A. 1992. Differential bioavailabilty of soil sorbed naphthalene to two bacterial species. Applied and environmental microbiology, 58, 1142-1152.

GUGGENHEIM, S.; MARTIN, R.T.,1995. Definition of clay and clay mineral: Joint report of the AIPEA nomenclature and CMS nomenclature committees. Clays and clay minerals, 43, 255-256.

GUGGENHEIM, S.; MARTIN, R.T.,1995. Definition of clay and clay mineral: Joint report of the AIPEA nomenclature and CMS nomenclature committees. Clay minerals, 30, 257-259.

HALL, P.L. 1987. Clays: their significance, properties, origins and uses In: A handbook of determinative methods in clay mineralogy.(eds), Wilson, M.J. Blackie , Glasgow and London, UK, pp 1-25.

HARAYAMA, S. AND KANALY, R.A. 2000. Biodegradation of high-molecular-weight polycyclic aromatic hydrocarbons by bacteria. Journal of bacteriology, 182,(8),2059-2067.

HARAYAMA, S., KIRSHIRA, H., KASAI YUKI, AND SHUTSUBO, K. 1999. Petroleum biodegradation in marine environments. J. Molec. Microbiol. Biotechnol. 1, (1): 63-70.

HARDER, W., DIJKHUISEN, L., VELDKAMP, H. In: The microbe (Kelly, D.P., and Carr, N.G., eds), part II, P51-95 Cambridge University Press, Cambridge, UK.

HARMS, H., AND ZEHNDER, A.J.B., 1995. Bioavailability of Sorbed 3-Chlorodibenzofuran. Applied Environmental Microbiology, 61, 27-33.

HATZINGER, P.B., AND ALEXANDER, M., 1995. Effect of ageing of chemicals in soil on their biodegradability and extractability. Environmental Science and Technology 29, 537-545.

HEAD, I.M., JONES, D.M., LARTER, S.R. Biological activity in the deep subsurface and the origin of heavy oil. Nature, 2003, 426, 344-352.

HELD, T., DRAUDE, G., SCHMIDT, F.R.J., BROKAMP, A. AND REIS, K.H. 1997. Enhanced humification as an in-situ bioremediation technique for 2,4,6-trinitrotoluene (TNT). Environmental Technology, 18, 479-487.

HERMOSIN, M.C., ULIBARRI, M.A., MANSOUR, M. AND CORNEJO, J. 1992. Assaying sorbents for 2,4-dichlorophenoxyacetic acid from water. Fresenius Environmental Bulletin, 1, 472-481.

HIRSCH, D., NIR, S., BANIN,A., 1989. Prediction of cadmium complexation in solution and adsorption to montmorillonite. Soil Science Society of America Journal 53, 716-721.

HOFFMAN, R.W. AND BRINDLEY, G.W., 1960. Adsorption of non-ionic aliphatic molecules from aqueous solutions on montmorillonite. Clay-organic studies. Geochimca et Cosmochimca Acta, 20, 15-29.

HOLDEN, P.A., LAMONTAGNE, M.G., BRUCE, A.K., MILLER, W.G., AND LINDOW, S.E., 2002., Assessing the role of Pseudomonas aeruginosa surface-active gene expression in hexadecane biodegradation in sand. Applied Environmental Microbiology 68, 2509-2518.

HOWER, J, ESLINGER, E.V., HOWER, M.E., PERRY, E.A., 1976. Mechanism of burial and metamorphism of argillaceous sediments: 1. Mineralogical and chemical evidence. Geological society of American Bulletin, 87, 725-737.

HUESEMANN, M.H., HAUSMANN, T.S. AND FORTMAN, T.J. 2004. Does bioavailabilty limit biodegradation? A comparison of hydrocarbon biodegradation and desorption rates in aged soils. Biodegradation, 15, 261-274.

HUGHES, J.D., AND SIMPSON, G.H., 1978. Arylsulphatase-Clay Interactions II*. The effect of kaolinite and montmorillonite on arylsulphatase activity . Australian Journal of Soil Resources , 16,35-40.

HUNT, J.M. 1979. Petroleum Geochemistry and Geology. WH Freeman, SanFrancisco, USA, pp 617.

HUNT, J.M. 1996. Petroleum Geochemistry and Geology, 2nd ed. Freeman Press. USA.

HUNTER, K.C., SEITZ, C., EAST, A.L.L. 2003 A mechanistic study of the Bronsted -acid catalysis of n Hexane ⟶ Propane + Propene Featuring carbonium ions. Journal of physical chemistry, 107, 159-168.

IKEDA, A., AND S. SHINKAIS. 1997. Novel cavity design using calix[n]arene skeletons: Toward molecular recognition and metal binding Chem. Rev. 97:1713–1734.

ISHIYAMA, M., TANAKA, D., KATSUYUKI, K., KUTO, K., SATO, C., 2007. Characterization of two oil-degrading bacterial groups in the Nakhodka oil spill. International Biodeterioration and Biodegradation, 60, (3) 202-207.

ISRAELACHVILI, J.N., Intermolecular and Surface Forces, Academic Press (1985–2004),

JAYNES, W.F., AND BOYD, S.A. 1991a. Clay mineral type and organic compound sorption by hexadecyltrimethylammonium-exchanged clays. Soil science society of America Journal, 55, 43-48.

JAYNES, W.F., AND VANCE, G.F. 1996. BTEX sorption by organo-clays: cosorptive enhancement and equivalence of interlayer complexes. Soil science society of America Journal, 60, 1742-1749.

JAYNES, W.F., BOYD, S.A., 1991. Hydrophobicity of siloxane surfaces in smectites as revealed by aromatic hydrocarbon adsorption from water. Clays and clay minerals 39, 428-436.

JEREMY A.R., SHARON L. W. AND MENACHEM, E., 2004. Bacterial adhesion and transport in porous media: role of the secondary energy minimum, Environmental Science and Technololgy, 38, 1777-1785.

JIRASRIPONGPUN, K., 2002. The characterization of oil-degrading microorganisms from lubricating oil contaminated (scale) oil. Letters in Applied Microbiology, 35, 296-300.

JONES, B.F. AND GALAN, E.1988. Sepiolite and palygorskite. In: Bailey SW (eds) Hydrous phyllosilicates (exclusive of micas). Rev Mineral 19: 631-674

JOSEPH, W.K., CHANTAL, J.B., 1992. A review of issues related to measuring colonization of plant roots by bacteria. Canadian Journal of Microbiology, 38, 1219-1231.

JOTA, M.A.T. AND HASSET, J.P. 1991. Effect of environmental variable on binding of PCB congener by dissolved humic substances. Environmental Toxicology and Chemistry, 10, 483-491.

JOZEFACIUK, G., BOWANKO, G.,2002. Effect of acid and alkai treatments on surface areas and adsorption energies of selected minerals. Clays and clay minerals 50, 771-783.

JURY, W.A., RUSSO, D., STREILE, G. AND ELABD, H.1990. Evaluation of volatilization by organic chemicals residing below the soil surface. Water Resources Research., 26, (1), 13-20.

KAEPPELI, O. AND FIECHTER, A. 1976. The mode of interaction between the substrate and cell surface of the hydrocarbon-utilizing yeast candida tropicalis. Biotechnology and Bioengineering, 18, 967-974.

KANALY, R.A. AND HARAYAMA, S. 2000. Biodegradation of high-molecular-weight polycyclic aromatic hydrocarbons by bacteria. Journal of Bacteriology, 182, 2059-2067.

KAPLAN, I.R., GALPERIN, S., LU, T. AND LEE, R.P. 1997. Forensic environmental geochemistry. Differentiation of fuel types, their sources and release time. Organic Geochemistry, 27, 289-317.

KAPLAN, I.R., GALPERIN, Y. 1997. Applications of alkylcyclohexane distribution patterns for hydrocarbon fuel identification in environmental samples. In: Kostecki, P.T. and Calabrese, E.J., AND BONAZOUNTAS, M. (eds). Contaminated soils, Amherst scientific publishers, Amherst, M.A., 2, 65-78.

KAPPELI, O., WALTER, P., MUELLER, M., AND FIECHTER, A. 1984. Structure of cell surface of the yeast candida tropicalis and its relation to hydrocarbon transport. Archives of Microbiology, 138, 279-282.

KARLSEN, D.A. & LARTER, S.R., 1991. Analysis of petroleum fractions by TLC-FID: Applications to petroleum reservoir description. Organic Geochemistry, 17, 603-617.

KELSEY, J.W., AND ALEXANDER, M. 1997. Declining availability and inappropriate estimation of risk of persistent compounds. Environmental and Toxicology Chemistry, 16, 582-585.

KENNETH, E.H., 1995. Mechanisms for polycyclic aromatic hydrocarbon degradation by ligninolytic fungi. Environmental Health Perspective, 103, 41-43.

KEPLAN, I.R., LU, S.T., ALIMI, H.M., AND MACMURPHEY, J. 2001. Fingerprinting of high boiling hydrocarbon fuels, asphalts and lubricants. Environmental Forensics, 2, 231-248.

KHANAN, M., AND STOTZKY, G., 1992. Transformation of Bacillus subtilis by DNA bound on montmorillonite and effect of DNase on the transforming ability of bound DNA. Applied and Environmental Microbiology, 58, 1930-1939.

KHANNA, M., STOTZKY G., 1992. Transformation of Bacillus subtilis by DNA bound on montmorillonite and effect of DNase on the transforming ability of bound DNA. Applied and Environmental Microbiology, 58, 1930-1939.

KILE, D.E., AND CHIOU, C.T. 1989. Water solubility enhancements of DDT and trichlorobenzene by some surfactants below and above the critical micelle concentration. Enviromental Science Technology 23, 832-838.

KILPATRICK, P. K., SPIECKER, P. M. 2001. Asphaltene emulsion. In: *Encyclopedic Handbook of Emulsion Technology*. SJÖBLOM, J., (ed).Marcel Dekker, Amsterdam. 707-728.

KIM, J.H., SHIN, W.S., KIM, Y.H., CHOI S,J., JEON, Y.W., AND SONG, D.I. 2003 Sequential sorption and desorption of chlorinated phenols in organoclays. Water Science Technology, 47, 59.

KINGHORN, R.R.F. 1983. An introduction to the physics and chemistry of petroleum. J. Wiley & Sons, New York, USA.

KNAEBEL, D.B., FEDERLE, T.W., MCAVOY, D.C. & VESTAL, J.R. 1994. Effect of mineral and organic soil constituents on microbial mineralization of organic compounds in a natural soil. Applied Environmental Microbiology, 60, 4500-4508.

KOHLER, A., SCHUTOFF, M., BRYNICK, D. AND KNACKMUSS, H.J. 1994. Enhanced biodegradation of phenanthrene in a biphasic culture system. Biodegradation, 5, 93-103.

KOMADEL, P. 2003. Chemically modified smectites. Clay minerals, 38, 127-138.

KOMADEL, P., BUJDAK, J., MADEJOVA, J., SUCHA, V., ELSASS, F., 1996a. Effect of non-swelling layers on the dissolution of reduced-charge montmorillonite in hydrochloric acid. Clay minerals 31, 333-345.

KOMADEL, P., MADEJOVA, J.,JANEK, M., GATES, W.P., KIRKPATRICK, R.J., STUCKI, J.W., 1996b. Dissolution of hectorite in inorganic acids. Clays and clay minerals 44, 228-236.

KONYA, J., NAGY, N.M., 1998. The effect of complexing-forming agent (EDTA) on the exchange of manganese ions on calcium-montmorillonite I. Reaction scheme and calcium-montmorillonite-$Mn(ClO_4)_2$-Na_2EDTA system. Colloids and surfaces A136, 299-310.

KONYA, J., NAGY, N.M., KIRALY, R., GELENCSER, J., 1998. The effect of complexing-forming agent (EDTA) on the exchange of manganese ions on calcium-montmorillonite II. Calcium-montmorillonite-$Mn(ClO_4)_2$-Na_2EDTA system. Colloids and surfaces 136, 311-319.

KOSITA J.E.,DALTON, D.D. SKELTON, H., DOLLHOPF, S., AND STUCKI, J.W., 2002. Growth of iron(III)- reducing bacteria on clay minerals as the sole electron acceptor and comparison of growth yields on a variety of oxidized iron forms . Applied and environmental microbiology, 68, 6256-6262.

KUIPER, J. AND HANSTVEIT, A.O., 1984. Fate and effects of 4-chlorophenol and 2,4-dichlorophenol in marine plankton communities in experimental enclosures. Ecotoxicology and Environmental Safety., 8, 15-33.

KUNC, F., AND STOTZKY, G., 1977. Acceleration of aldehide decomposition in soil by montmorillonite. Soil Science, 124, 167-172.

KVENVOLDEN, K.A., HOSTETTLER, F.D., CARLSON, P.R., RAPP, J.B., THRELKELD, C.N. AND WARDEN, A. Ubiquitous tar balls with a California-source signature on the shorelines of Prince Willam Sound, Alaska. Environmental Science Technology, 29, 2684.

LARTER, S.R., BOWLER, B.F.J., LI, M., CHEN, M., BRINCAT, D., BENNETT, B., NOKE, K., DONOHOE, P., SIMONS, D., KOHNEN, M., ALLAN, J., TELAES, N., AND HORSTAD, I. 1996. Molecular indicators of secondary oil migration distances. Nature, 383, 593-597.

LASZLO, P. 1987 Chemical reactions on clays. Science. 235, 1473-1477.

LAZSLO, P., 1987. Preparative chemistry using supported reagents. Academic press, New York.

LEBARE, M.P., AND ALEXANDER, M. 1995. Enhanced mineralization of organic compounds in non-aqueous phase liquids. Environmental Toxicology and Chem. 14, 257-265.

LEE, J.F., MORTLAND, M.M., CHIOU, C.T., KILE, D.E. AND BOYD, S.A., 1990. Adsorption of benzene, toluene and xylene by two tetramethylammonium-smectites having different layer charge densities. Clays and Clay minerals, 38, 113-120.

LEMKE, S.L., GRANT, P.G., AND PHILLIPS, T.D. 1998. Adsorption of searalenone by organophilic montmorillonite clay. Journal of Agricultural and Food Chemistry, 46, 3789-3796.

LEVINE, S.; DUBE, G. P. (1940), "Interaction between two hydrophobic colloidal particles, using the approximate Debye-Huckel theory. I. General properties", *Transactions of the* Faraday Society 35: 1125–1141.

LI,Y. AND GUPTA, G. 1994. Adsorption of hydrocarbons by clay minerals from gasoline. Journal of Hazardous Materials 38, 105-112.

LIN, Z., PULS, R.W., 2000. Adsorption, desorption and oxidation of arsenic affected by clay minerals and aging process. Environmental Geology, 39, 753-759.

LIPSON, S.M., STOTZKY, G. 1983. Adsorption of reovirus to clay minerals: effects of cation-exchange capacity, cation saturation, and surface area. Applied and Environmental Microbiology, 46, 673-682.

LIPSON, S.M., STOTZKY, G. 1984. Effect of proteins on adsorption to clay minerals. Applied and Environmental Microbiology, 48, 525-530.

LIU, Z., LAHA, S., AND LUTHY, R.G. 1991. Surfactant Solubilization of Polycyclic Aromatic Hydrocarbon Compounds in Soil-Water SuspensionsWater Science and Technology, 24, 475-485.

LOER, R.C. AND WEBSTER, M.T. 1996. Behaviour of fresh vs aged chemicals in soil. Journal of Soil Contamination, 5, 361-383.

LUPTON, F.S., AND MARSHALL, K.C. 1979. Effectiveness of surfactants in the microbial degradation of oil. Geomicrobiology Journal, 1, 235-247.

MACKENZIE, A.S., PATIENCE, R.L. AND MAXWELL, J.R. 1980. Molecular parameters of maturation in the Toarcian shales, Paris Basin, France – 1. Changes in the configurations of acyclic isoprenoid alkanes, steranes and triterpanes. Geochim, Cosmochim. Acta, 44, 1709-1721.

MADIGAN, M.T, MARTINKO, J.M., PARKER, J. 2000. Metabolic diversity. In: Brock biology of microorganisms. Prentice hall inc., New York, USA. 575-622.

MAES, A., RASQUIN, E., CREMERS, A. 1982. Thermodynamic study of the influence of complexation on exchange equilibria in Wyoming bentonite clay. Journal of the Chemical society, Faraday Ttransactions I ,78, 2041-2049.

MAIER, R.M., PEPPER,I.L., AND GERBA, C.P. 2000. In: Environmental microbiology. San Diego. Academic Press.

MAKBOUL, H.E., AND OTTOWO, J.C., 1979. Michaelis constant (K_m) of acid phospatase as affected by montmorillonite, illite, and kaolinite clay minerals. Microbial Ecology, 5, 207-213

MAKI, H., SASAKI, T., HARAYAMA, S., 2001. Photo-oxidation of biodegraded crude oil and toxicity of the photo-oxidized products. Chemosphere, 44, (5) 1145-1151.

MALANDRINI, H., CLAUSS, F., PARTYKA, S., DOUILLARD, J.M., 1997. Interactions between talc particles and water and organic solvents. Journal of colloid and interface science 194, 183-193.

MARGULIES, L., ROZEN, H., NIR, S., 1988. Model for competitive adsorption of organic cations on clays. Clays and clay minerals 36, b270-b276.

MARTIN, J.P., FILIP, Z. AND HAIDER, K., 1976. Effect of montmorillonite and humate on growth and metabolic activity of some actinomycetes. Soil Biology and Biochemistry, 8, 409-413.

MATYASIK, I.A., STECZKO, A. AND PHILP, R.P. 2000. Biodegradation and migrational fractionation of oils from the Eastern Carpathians, Poland. Organic Geochemistry, 31, 1509-1523.

MEUNIER, A. 2005. The crystal structure of clay minerals. In: Clays, Springer, Berlin, Germany. pp 1-19.

MOLDOWAN, J.M., SEIFERT, W.K., GALLEGOS,.E.J., 1985. Relationship between petroleum composition and depositional environment of petroleum source rocks. American Association of Petroleum Geology Bulletin, 69, 1255-1268.

MOORE, D.M., AND HOWER, JOHN. 1986. Ordered interstratifications of dehydrated and hydrated Na-smectite: Clays and clay minerals 34, 379-84.

MOORE, D.M., REYNOLDS, R.C. 1997. Illite and Gauconite In: X-ray diffraction and the identification and analysis of clay minerals. Oxford university press, pp 233.

MOORE, D.M., Reynolds, R.C. 1997. Structure, nomenclature, and occurrences of individual clay minerals In: X-ray diffraction and the identification and analysis of clay minerals. Oxford university press, pp 139-192.

MORIYA, D.E., AND HORIKOSHI, K. 1993. J. Ferment. Bioteeng, 76, 168-173.

MORONTA, A. 2004. Catalytic and adsorption properties of modified clay surfaces. Pp 321-344 in: Clay surfaces: Fundamentals and Applications (F. Wypych and K.G. Satyanarayana, editors). Elsevier, Amsterdam.

MOSCHOPEDIS, S.E., FRYER, J.F., AND SPEIGHT, J.G., 1976. Investigation of asphaltene molecular weights. Fuel, 55, 227-232.

MUELLER, J.G., CERNIGLIA, C.E. AND PRITCHARD, P.H. 1996. Bioremediation of environments contaminated by polycyclic aromatic hydrocarbons. In Bioremediation: Principles and applications, Cambridge university press, Cambridge, UK, pp 125-194.

MULKINS-PHILLIPS, G.J., AND STEWART, J.E. 1974. Appl. Microbiol. 28, 547-552.

MURRAY, H.H. 2000: Traditional and new applications for kaolin, smectite and palygorskite: a general overview. Applied clay science, 17, 207-221.

MUSSER, B.J., KILPATRICK, P.K. 1998. Characterization of Libyan waxy crude oil, Energy & Fuels, 12, 715-725.

NAM, K. AND ALEXANDER, M. 1998. Role of nanoporosity and hydrophobicity in sequestration and bioavailability. Environmental Science and Technology, 32, 71-74

NAPOLOTANO, G.E., RICHMOND, J.E., STEWART, A.J. 1998. Characterization of petroleum-contaminated soils by thin layer chromatography with flame ionization detection. Journal of Soil contamination,7, (6) 709-724.

NEIDHARDT, F.C., INGRAHAM, J.L., SCHAECHTER, M., 1990. Physiology of the bacterial cell. Sinauer associates, Sunderland, MA.

NESTE, 2011. http://www.nesteoil.com/default

NIKOPOLOU, M., AND KALOGERAKIS, N. 2009. Biostimulation strategies for fresh and chronically polluted marine environments with petroleum hydrocarbons. Journal of chemical technology and biotechnology, 84, 802-807.

NIR, S., HIRSCH, D., NAVROT, J., BANIN, A., 1986. Specific adsorption of lithium, sodium, potassium, and strontium to montmorillonite: observations and predictions. Soil science society of America Journal 50, 40-45.

NIR, S., UNDABEYITA, T., YARON-MARCOVICH, D., EL-NAHHAL, Y., POLUBESOVA, T., SERBAN, C., RYTWO, G., LAGALY, G., AND RUBIN, B. 2000. Optimization of adsorption of hydrophobic herbicides on montmorillonite pre-adsorbed by monovalent organic cations: interaction between phenyl rings . Environmental Science and Technology, 34, 1269-1274.

OBERBREMER, A., MULLER-HURTIG, R. AND WAGNER, F. 1990. Effect of the addition of microbial surfactants on hydrocarbon degradation in a soil population in a stirred reactor. Applied Microbiology and Biotechnology 32, 485-489.

OEPEN, B.V., KORDEL, W. AND KLEIN, W. 1991. Sorption of nonpolar and polar compounds to soils: Processes and measurements and experience with the applicability of the modified OECD-Guideline 106 Chemosphere, 22, (3-4) 285-304.

ORTEGA-CALVO, J.J. AND SAIZ-JIMENEZ, C., 1998. Effect of humic fractions and clay on biodegradation of phenanthrene by a pseudomonas fluorescens strain isolated from soil. Applied and Environmental Microbiology, 64, 3123-3126.

ORTEGA-CALVO, J.-J., AND ALEXANDER, M. 1994. Appl. Environ. Microbiol., 60, 2643-2646.
Owens, E.H., Lee, K., 2003. Interaction of oil and mineral fines on shorelines: review and assessment. Marine pollution bulletin 47 (9-12), 397-405.

PAGE, D.S., BOEHM, P.D., DOUGLAS, G.S., AND BENCE, A.E. 1995. Identification of hydrocarbon sources in the benthic sediments of prince Williams sound and the gulf of Alaska following the Exxon Valdez oil spill In: Exxon Valdez oil spill. Fate and effects in Alaska waters, Wells, P.G., Butler, J.N., and Hughes J.S. (eds), ASTM STP 1219. American society testing materials, Phil., PA, 41-83.

PALKOVA, H., MADEJOVA, J., RIGHI, D., 2003. Acid dissolution of reduced-charge Li- and Ni-montmorillonites. Clays and clay minerals 51,133-142.

PALMER, S.E. 1993. Effects of biodegradation and water washing on crude oil composition. In: Engel, M.H. and Macko, S.A. (eds). Advances in Organic Geochemistry; Plenum press, New York. 511-533.

PARKER, S.L., ACEY, R.A. 1993. Environmental bioremediation and biodegradation, Journal of Cellular Biochemistry, 53, S17C, 181-200.

PETERS, K.E., MOLDOWAN, J.M., 1993. The biomarker guide: Interpreting molecular fossils in petroleum and ancient sediments. In ENGLEWOOD CLIFS, N.J., (eds). Prentice Hall, 363.

PETERS, K.E., MOLDOWAN, J.M., SCHOELL, M., HEMPKINS, W.B. 1986. Petroleum isotopic and biomarker composition related to source rock organic matter and depositional environment. Organic Geochemistry, 10, 17-27.

PINES, O., AND GUTNICK, D. 1986. Role for emulsan in growth of acinetobacter calcoaceticus RAG-1 on crude oil. Applied Environmental Microbiology, 51, 661-663.

PINNAVAIA, T. J. 1983. Intercalated clay catalysts. Science, 220 (4595) 365-371

PLATFORMLONDON, 2008. http://www.platform.org/carbonweb, accessed on June 20th.

POLLARD, S.J., HRUDEY, S.E., FUR B.J., ALEX, R.F., HOLLOWAY, L.R., TOSTO, F. 1992. Hydrocarbon wastes at petroleum and creosote-contaminated sites: Rapid characterization of component classes by thin layer chromatography with flame ionization detection. Environmental Science & Technology, 26, 2528-2534.

PRIESACK, E. 1991. Analytical solution of solute diffusion and biodegradation in spherical aggregates. Soil Science Society, American Journal, 55, 1227-1230.

PRINCE, R.C., ELMENDORF, D.L., LUTE J.R., HSU, C.S., HAITH, C.E., SENIUS, J.D, DOUGLAS, G.S. AND BUTLER, E.L. 1994. 17α(H), 21ß(H)-Hopane as a conserved internal marker for estimating the biodegradation of crude oil. Environmental science technology, 28,142-145.

PSYRILLOS, A., HOWE, J.H., MANNING, A.C. AND BURLEY, S.D., 1997. Geological controls on kaolin particle shape and consequences for mineral processing. Clay minerals,34, 193-208.

PUSHPALETHA, P., RUGMINI, S. AND LALITHAMBIKA, M., 2005. Correlation between surface properties and catalytic activity of clay catalysts. Applied Clay Science, 30, 141-153.

RABUS, R. 2005. Biodegradation of hydrocarbons under anoxic conditions. In petroleum microbiology B. Oliver and M.Magot (eds.), Washington, DC: ASM Press, pp 337-356.

RADKE, M. 1988. Application of aromatic compounds as maturity indicators in source rocks and crude oils. In: Advances in organic geochemistry, Butterworth & Co. Ltd, London.
RAVICHANDRAN, J., SIVASANKAR, B. 1997. Properties and catalytic activity of acid modified montmorillonite and vermiculite. Clay and clay minerals, 45 (6) 854-858.

READ, H. 1985. Improved sample application methods for the Iatroscan. Lipids, 20, 8.
REDDY, C.R., NAGENDRAPPA, G., JAI PRAKASH, B.S. 2007. Surface acidity study of Mn+-montmorillonite clay catalysts by FT-IR spectroscopy: Correlation with esterification activity. Catalysis communications, (8), 241-246.

RETZ, J.A., ALVAREZ, P.J. AND SCHNOOR, J.L. 2008. Benzo (a) pyrene degradation by sphingomonas yanoikuyae JAR02, Environmental pollution, 151, 669-677.

RIJNAARTS, H.H.M., BACHMANN, A., JUMELET, J.C., AND ZEHNDER, A.J.B. 1990. Effect of desorption and intraparticle mass transfer on the aerobic biomineralization of α-hexachlorocyclohexane in a contaminated calcareous soil. Environmental Science and Technology, 24, 1349-1354.

RITMANN, B.E. AND JOHNSON, N.M. 1989. Water Sci Technol, 21 (4/5), 209-219

ROBERTS, M.G., LI, H., TEPPEN, J., AND BOYD, S.A. 2006. Sorption of nitroaromatics by ammonium- and organic ammonium-exchanged smectite: shifts from adsorption/complexation to a partition-dominated processes. Clays and clay minerals, 54, 426-434.

ROBERTS, M.G., LI, H., TEPPEN, J., BOYD, S.A. 2006. Sorption of nitroaromatics by ammonium- and organic ammonium-exchanged smectite: shifts from adsorption/complexation to a partition-dominated processes. Clays and clay minerals, 54, 426-434.

ROCKNE, K.J AND REDDY, K.R. 2003. Bioremediation of contaminated sites. International e-conference on modern trends in foundation engineering: Geotechnical challenges and solutions. Indian institute of technology, Madra, India.

ROSENBERG, E., 1986. Miccrobial surfactants. CRC Crit Rev Biotechnol., 3, pp 109-132

ROSENBERG, E., LEGMANN, R., KUSHMARO, A., TAUBE, R., ALDER, E., Ron, E.Z., 1992., Petroleum Bioremediation: a multiphase problem. Biodegradation, 3, 337-350.

ROSENBERG, E., PERRY, A., GIBSON, D.T., AND GUTNICK, D.L. 1979. Emulsifier of Arthrobacter RAG-1: Specificity of hydrocarbon substrate. Applied Environmental Microbiology, 37, 409-413.

ROSENBERG, M., AND ROSENBERG, E. 1985. Bacterial adherence at the hydrocarbon-water interface. Oil Petrochemical Pollution 2, 155-162.

ROSENBERG, M., AND ROSENBERG, E.J., 1981. Role of Adherence in Growth of Acinetobacter calcoaceticus RAG-1 on Hexadecane. Journal of Bacteriology, 148, 51-57.

ROSENBERG, M., BAYER, E.A., DELAREA, J. AND ROSENBERG, E. 1982. Applied Environmental Microbiology, 44, 929-937.

ROZIC, L., NOVAKOVIC, T., PETROVIC, S. 2008. Process improvement approach to the acid activation of smectite using factorial and orthogonal central composite design methods. Journal of Serbian Chemical Society. 73 (4) 487-497.

RUBINSTEIN, I. AND ALBRECHT, P., 1975. The occurrence of nuclear methylated steranes in a shale. Journal of Chemical Society, Chemical communication, 957-958.

RUTTER, P. R., AND VINCENT, B. 1984. Physicochemical interactions of the substratum, microorganisms and the fluid phase, p.21-38. In K. C. Marshall (ed.), Microbial adhesion and aggregation.

RYTWO, G., BANNIN, A., NIR, S., 1996. Exchange reactions in the Ca-Mg-Na-montmorillonite system. Clays and clay minerals 44, 276-285.

SCHFFENBAUER, M., STOTZKY, G., 1982. Adsorption of coliphages T1 and T7 to clay minerals. Applied and Environmental Microbiology, 43, 590-596.

SCHOONHEYDT, R.A. AND JOHNSTON, C.T. 2006. Surface and interface chemistry of clay minerals. In: Handbook of clay science, Elsevier, Amsterdam

SCOW, K.M. AND ALEXANDER, M. 1992. Effects of diffusion on the kinetics of biodegradation: experimental results with synthetic aggregates. Soil Science Society of America Journal, 56, 128-134.

SCOW, K.M. AND HUTSON, J., 1992. Effect of diffusion and sorption on the kinetics of biodegradation: theoretical considerations Soil Science Society of American Journal, 56, 119-127.

SCRIBNER, S.L., BENZING, T.R., SUA, S. AND BOYD, S.A. 1992. Desorption and bioavailability of aged simazine residues in soil from a continuous corn field Journal of Environmental Quality, 21, 115-120.

SEIFERT, W.K., AND MOLDOWAN, J.M. 1978. Applicatrions of steranes, terpanes and monoaromatics to the maturation, migration and source of crude oils. Geochim, Cosmochim. Acta, 42, 77-95.

SEIFERT, W.K., MOLDOWAN, J.M. AND DEMAISON, G.J. 1984. Source correlation of biodegraded oils. Organic Geochemistry, 6, 633-643.

SELLEY, R.C. 1982. An introduction to sedimentology. Academic press, London pp 417

SHAW, D.G., 1992. The Exxon-valdez oil-spill-ecology and social consequences. Environmental conservation, 19, 3, 253-258.

SHAYAN, A., SANDERS, J.V., LANCUCKI, C.J. 1988. Hydrothermal alterations of Hisingerite material from a Basalt Quarry near Geelong, Victoria, Australia. Clay minerals,36, (4) 327-336.

SHELOBOLINA, E.S., ANDERSON, R.T., VODYANITSKII, Y.N., SIVTSOV, A.V., YURETICH, R. AND LOVLY, D.R., 2004. Importance of clay size minerals for Fe(III) respiration in a petroleum-contaminated aquifer. Geobiology, 2, 67 – 76.

SIMONEIT, B.R.T. 1986. Cyclic terpenoids of the geosphere. In: Biological markers in the sedimentary record. R.B. Johns (ed),; Elsevier, Amsterdam, the Netherlands. 43-99.

SINGER, M., AND FINNERTY, W.R.1984. In: Petroleum Microbiology (R.M. Atlas, ed). Mcmillan, New York pp 1-59.

SINGH, D.K., AND ARGAWAL, H.C. 1995. Persistence of DDT and nature of bound residues in soil at higher altitude. Environmental Science and Technology, 29, 2301-2304

SIROTA, E.B. 2005. Physical structure of asphaltenes. Energy and Fuels, 19, 1290-1296.

SITE D.A.2001. Factors affecting the sorption of organic compounds in natural sorbent/water systems and sorption coefficients for selected pollutants. A review. Journal of Physical Chemistry, 30, (1), 187-439.

SMITH, K.L., MILNES, A.R., AND EGGLETON, R.A., 1987. Weathering of basalt: formation of iddingsite. Clays and Clay Minerals, 35, 418-428.

SOMA, Y AND SOMA, M., 1989. Chemical reactions of organic compounds on clay surfaces. Environmental Health perspectives, 83, 205-214.

SPEIGHT, J.G. 1991.The chemistry and technology of petroleum, 2nd edition, Marcel Dekker, Inc., New York, NY.

SPEIGHT, J.G. 2007.The chemistry and technology of petroleum, 4th edition, Taylor and Francis Group, LLC, Boca Raton, Florida, USA, pp 223-237; 378.

SPEIGHT, J.G. AND MOSCHOPEDIS, S.E. 1977. Asphaltenes molecular weight by a cryospcopic method. Fuel, 56, 344.

SPOSITO, G. 1984. The surface chemistry of soils. Oxford university press, New York.

SPOSITO, G., SKIPPER, N.T., SUTTON, R., PARK, S.A., SOPER, A.K., GREATHOUSE, J.A., 1999. Surface geochemistry of the clay minerals. Proceedings of the National Academy of Science USA, 96, 3358-3364.

SRASRA, F., BERGAYA, H., ARGUIB, N.K., 1989. Surface properties of an activated bentonite — decolourization of rape-seed oil, Applied Clay Science **4**, 411–421

STEPHENS, F.L., BONNER, J.S., AUTENRIETH, R.L., 1998. TLC/FID Analysis of compositional hydrocarbon changes associated with bioremediation. International oil spill conference, no. 264.

STEPHENSON, T., LESTER, J.N., AND PERRY,R., 1984. Acclimatisation to nitrilotriacetic and in the activated sludge process. Chemosphere 13, (9)1033-1040.

STOTZKY, G. AND REM, L.T. 1966. Influence of clay minerals on microorganisms I. Montmorillonite and Kaolinite on bacteria. Canadian journal of microbiology, 12, 547-563.

STOUT, S.A. AND WANG, Z., 2007. Factors controlling the chemical fingerprints of spilled and discharged petroleum. In: Oil spill environmental forensics. Wang,Z., Stout, S.A (eds) Academic press, San Diego, California, USA., pp 13-15.

STOUT, S.A., UHLER, A.D., AND MCCARTHY, K.J. 2001. A strategy and methodology for defensibly correlating spilled oil to source candidates. Environmental forensics, 2, 87-98.

STROUD, J.L., PATON, G.I., SEMPLE, K.T., 2007. Microbe-aliphatic hydrocarbon interactions in soil: implications for biodegradation and bioremediation. Journal of Applied Microbiology, 102, 1239-1253.

STUCKI, G., ALEXANDER, M. 1987. Role of dissolution rate and solubility in biodegradation of aromatic compounds. Applied Environmental Microbiology, 53, 292-297.

SUBBA-RAO, R.V., AND ALEXANDER, M., 1982. Effect of Sorption on Mineralization of Low Concentrations of Aromatic Compounds in Lake Water Samples. Applied Environmental Microbiology, 44, 659-668.

SUNGGYU, L., 1995. Bioremediation of polycyclic aromatic hydrocarbon-contaminated soil. Journal of cleaner production, 3, 255.

SURDAM, R.C. AND CROSSLEY, L.J. 1985. Organic-inorganic reactions during progressive burial: key to porosity and permeability enhancement and preservation. Philos. Trans. Roy. Soc. London, A315, 135-156.

SUTHERSAN, S.S. 1999. Insitu-bioremediation In: Remediation engineering: design concepts, CRC Press LLC, Boca Raton, Florida, USA. 123.

TADMOR, R. 2001. Condensed matter, Journal of physics: 13 , L195–L202.

TALIBUDEEN, O., AND GOULDING, K.W.T., 1983a. Apparent charge heterogeneity in kaolins in relation to their 2:1 phyllosilicate content: Clays and clay minerals, 31, 137-142.

TANG, J., CARROGUINO, M.J., ROBERTSON, B.K., AND ALEXANDER, M., 1998. Combined effect of sequestration and bioremediation in reducing the bioavailability of polycyclic aromatic hydrocarbons in soil. Environmental Science Technology, 32, 3586-3590.

TAPP, H., STOTZKY, G., 1995. Insecticidal activity of the toxins from Bacillus thuringiensis subspecies kurstaki and tenebrionis adsorbed and bound on pure and soil clays. Applied and Environmental Microbiology, 61, 1786-1790.

TAYLOR, G.T., 1995. Microbial degradation of sorbed and dissolved protein in seawater. American Society of Limnology and Oceanography. 40, (5) 875-885.

TAZAKI, K., CHAERUN, S.K., 2008. Life in oil: Hydrocarbon-degrading bacterial mineralization in oil spill-polluted marine environment. Frontier material science China 2(2), 120-133.

THENG, B. K. G. 1974. The chemistry of clay-organic reactions. Adam Hilger Ltd, London, pp 343.

THEOCHARIS C.R., JACOB, K.J., GRAY, A.C. 1988. Enhancement of Lewis acidity in layer aluminosilicates. Journal of Chemical Society, Faraday Trans, 84, 1509-1516.

THOMAS, J.M., AND ALEXANDER, M. 1987. Colonization and mineralization of palmitic acid by pseudomonas pseudoflava. Microbial Ecology, 14, 75-80.

TISSOT, B.P., AND WELTE, D.H. 1984. Composition of crude oils. In: Petroleum formation and occurrence, 2nd ed., Springer-Verlag, New York, NY. pp 376-411.

TISSOT, B.P., AND WELTE, D.H. 1984. From kerogen to petroleum. In: Petroleum formation and occurrence, 2nd ed., Springer-Verlag, New York, NY. pp 160-198.

TISSOT, B.P., AND WELTE, D.H. 1984. Kerogen: Composition and classification. In: Petroleum formation and occurrence, 2nd ed., Springer-Verlag, New York, NY. pp 130-150.

TOURNASSAT, C., FERRAGE, E., POINSIGNON, C., CHARLET, L., 2004. The titration clay minerals II. Structure-based model and implications for clay reactivity. Journal of colloid and Interface science 273, 234-246.

TUCCILLO, M.E., COZZARELLI, I.M., HERMAND, S.J., 1999. Iron reduction in the sediments of a hydrocarbon contaminated aquifer. Applied geochemistry 14, 655-667.

TUNEGA, D., BENCO, L., HABERHAUER, G., GERZABEK, M.H., LISCHKA, H., 2002. Ab initio molecular dynamics study of adsorption sites on the (001) surfaces of 1:1 dioctahedral clay minerals. The Journal of physical chemistry B 106, 11515-11525.

VAN BEILEN, J.B., WUBBOLTS, M.G., AND WITHOLT, B. 1994. Genetics of alkane oxidation by pseudomonas oleovorans. Biodegradation, 5, 161-174.

VAN LOOSDRECHT, M.C.M, LYKLEMA, J., NORDE, W., ZEHNDER J.B., 1990. Influence of interfaces on microbial activity. Mirobiological Reviews, 54, 75-87.

VANLOOSDRECHT, M.C.M., LYKLEMA, J., NORDE, W. AND ZEHNDER, A.J.B. 1989. Bacterial adhesion: a physicochemical approach. Microbial ecology, 17, 1-15.

VENOSA, A.D., AND ZHU, X. 2003. Biodegradation of crude oil contaminating marine freshwater wetlands. Spill science & Technology Bulletin, 8, 163-178.

VERBUNG, K., BAVEYE, P., 1994. Hysterisis in the binary exchange of cations on 2:1 clay minerals: a critical review. Clays and clay minerals 42, 207-220.

VERWEY, E. J. W.; OVERBEEK, J. TH. G. 1948, Theory of the stability of lyophobic colloids, Elsevier, Amsterdam.

VETTORI, C., CALAMAI, L., YODER, M., STOTZKY, G., GALLORI, E., 1999. Adsorption and binding of AmpliTaq(R) DNA polymerase on the clay minerals, montmorillonite and kaolinite. Soil Biology Biochemistry, 31, 587-593.

VICENTE, M.A., SUAREZ BARRIOS, M., LOPEZ-GONZALEZ, J.D., BANARES-MUNOZ, M.A., 1994. Acid activation of a ferrous saponite (griffithite): Physico-chemical characterization and surface area of the products obtained. Clays and clay minerals 42, 724-730.

VIDALI, M. 2001. Bioremediation. An overview. In: T. Carney (eds), Contaminated land, Blackie academic and professionals, London , UK, 1993, pp 4

VIDALI, M. 2001. Bioremediation. An overview. Pure and applied chemistry, 73 (7), 1163-1172.

VOLKMAN, J.K. 1988. Biological marker compounds as indicators of depositional environments of petroleum source rocks. In: A.J. Fleets, Kelts, K., and Talbot, M.R. (eds) Lacusrine Petroleum Source Rocks, Geol. Soc. Spec. Publ. No. 40; Blackwell Scientific Publishers, Oxford.

VOLKMAN, J.K., REVILL, A.T., AND MURRAY, A.P. 1997. Application of biomarkers for identifying sources of natural and pollutant hydrocarbons in aquatic environment In: R.P. Eganhouse (ed), Molecular Markers in Environmental Geochemistry, American chemical society, Washingnton D.C, 110-132

WANG, Z., AND FINGAS, M. 2003. Development of oil hydrocarbon fingerprinting and identification technique. Mar pollution bulletin, 47,423-452.

WANG, Z., STOUT, S.A. AND FINGAS, M.F., HOLLEBONE, B.,YIM, U.H., OH, J.R,. 2007. Petroleum biomarker fingerprinting for oil spill characterization and source identification. In: Oil spill environmental forensics. Wang,Z., Stout, S.A (eds) Academic press, San Diego, California, USA., pp 73-150.

WANG,Z., STOUT, S.A. AND FINGAS, M.F., 2006. Biomarker fingerprinting for spill oil characterization and source identification. Environmental Forensics, 7 (2), 105-146.

WARR, L.N., PERDRIAL, J.N., LETT, M., HEINRICH-SALMERON, A., KHODJA, M. 2009. Clay mineral-enhanced bioremediation of marine oil pollution. Applied clay science 46, 337-345.

WATSON, J.S., JONES, D.M., SWANNELL, R.P.J AND VAN DUIN, A.C.T. 2002. Formation of carboxylic acids during aerobic biodegradation of crude oil and evidence of microbial oxidation of hopanes. Organic Geochemistry 33, 1153-1169.

WEBER, W.J., MC GINLEY, P.M. AND KATZ, L.E., 1991. Sorption phenomena in subsurface systems: Concepts, models and effects on contaminant fate and transport. Water Resources 25, 5, 499-528.

WHITE, J.C., KESLEY, J.W., HATZINGER, P.B., ALEXANDER, M. 1997. Factors affecting sequestration and bioavailability of phenanthrene in soils. Environmental Toxicology and Chemistry, 16, 2040-2045.

WHYTE, L.G., HAWARI, J., ZHOU, E., BOURBONNIERE, L., INNISS, W.E., AND GRIER, C.W., 1998. Biodegradation of variable-chain-length alkanes at low temperatures by a psychrotrophic rhodococcus sp. Applied Environmental Microbiology, 64, (7), 2578 2584.

WIGGINS, B.A., AND ALEXANDER, M., 1988a. Role of protozoa in microbial acclimation for mineralization of organic chemicals in sewage. Canadian Journal of microbiology, 34, 661-666.

WILKINS, R.W.T AND ITO, J. 1967. Infrared spectra of some synthetic talcs. American Mineralogist, 52, 1649-1661.

WILSON, M.J. 1987. Effects of water and inorganic cations In: A handbook of determinative methods in clay mineralogy. Blackie , Glasgow and London, UK, pp 60.

WILSON, M.J. 1987. Infrared methods-smectites In: A handbook of determinative methods in clay mineralogy. Blackie , Glasgow and London, UK, pp 145.

WILSON, M.J. 1987. Infrared methods-smectites In: A handbook of determinative methods in clay mineralogy. Blackie , Glasgow and London, UK, pp 154.

WILSON, M.J. 1994. Clay mineralogy: Spectroscopic and chemical determinative methods. Chapman & Hall, Alden Press, Oxford, Great Britain.

WITTHUHN, B., KLAUTH P., PERNYESZI, T., 2006. Organoclays for aquifer bioremediation: Adsorption of chlorobenzene on organoclays and its degradation by Rhdococcus B528. Water, Air and Soil Pollution, 6, 317-329.

WODZINSKI, R.S. AND BERTOLINI, D., 1972. Physical state in which naphthalene and bibenzyl are utilized by bacteria. Applied Microbiolgy, 23, 1077-1081.

WODZINSKI, R.S. AND COYLE, J.E. 1974. Physical State of phenanthrene for utilization by bacteria. Applied Microbiolgy, 27, 1081-1084

WODZINSKI, R.S. AND JOHNSON, M.J., 1968. Yields of Bacterial Cells from Hydrocarbons Applied Microbiolgy, 16, 1886-1891.

WODZINSKI, R.S. AND LAROCCA, D., 1977. Bacterial Growth Kinetics on Diphenylmethane and Naphthalene-Heptamethylnonane Mixtures. Applied Microbiolgy, 33, 660-665.

WSZOLEK, P.C., ALEXANDER, M.,1979. Effects of desorption rate on the biodegradation of nalkylamines bound to clay. Journal of Agricultural and Food Chemistry 27, 410–414.

WU, S.C. AND GSCHWEND, P.M. 1986. Sorption kinetics of hydrophobic organic compounds to natural sediments and soils. Environmental Science and Technology 20, 717-725.

XU, B., SIEVERS, C., HONG, S.B., PRINS, R., VAN BOKHOVEN, J.A. 2006 Catalytic activity of Bronsted acid sites in zeolite: Intrinsic activity, rate-limiting step and influence of the local structure of the acid sites. Journal of catalysis, 244, 163-168.

XU, S., AND BOYD, S.A. 1995. Cationic surfactant sorption to a vermiculitic subsoil via hydrophobic bonding . Environmental science and Technology, 29, 312-320.

ZHANG, Z.Z., SPARKS, D.L., SCRIVNER, N.C. 1993. Sorption and desorption of quaternary amine cations on clays. Environmental science and Technology, 27, 1625-1631.

ZHU, D., HERBERT, B.E., SCHLAUTMAN, M.A, CARRAWAY, E.R., AND HUR, J. 2004. Cation-∏ Bonding: A new perspective on the sorption of polycyclic aromatic hydrocarbons to mineral surfaces. Journal of environmental quality 33, 1322-1330.

APPENDIX

Appendix 3.1 Growth curve data from absorbance measurement-saturates as carbon source.

1st subculture: Weight of crude oil saturates as carbon source (0.2g).

Days	Absorbance			average	Std dev
0	0.15	0.12	0.16	0.14	0.02
2	0.28	0.25	0.31	0.28	0.03
4	0.59	0.65	0.57	0.60	0.04
6	0.77	0.78	0.73	0.76	0.03
8	0.81	0.86	0.79	0.82	0.04
10	0.8	0.85	0.78	0.81	0.04
12	0.73	0.79	0.72	0.75	0.04

9th subculture: Weight of crude oil saturates as carbon source (1.75g)

Day	Absorbance			average	std dev
0	1.8	1.9	1.7	1.8	0.1
2	3.1	3.2	3.5	3.3	0.2
4	6.3	6.1	5.5	6.0	0.4
6	8.3	7.8	8.9	8.3	0.6
8	9.0	8.6	9.4	9.0	0.4
10	8.8	9.2	8.3	8.8	0.5
12	7.8	8.5	8.2	8.2	0.4

Appendix 3.2 Growth curve data from absorbance measurement- crude oil as carbon source.

1st subculture : Weight of crude oil used as carbon source (0.5g)

Day	Absorbance			average	std dev
0	0.35	0.25	0.32	0.31	0.05
2	0.51	0.48	0.41	0.47	0.05
4	0.81	0.68	0.82	0.77	0.08
6	1.1	0.98	1.01	1.03	0.06
8	1.22	1.2	1.12	1.18	0.05
10	1.19	1.21	1.12	1.17	0.05
12	1.05	1.1	0.98	1.04	0.06

9th subculture : Weight of crude oil used as carbon source (2.0g)

Days	Absorbance			average	std dev
0	2.5	2.2	2.1	2.3	0.2
2	4.8	4.5	4.2	4.5	0.3
4	9.0	8.2	8.2	8.5	0.5
6	11.6	11.1	10.8	11.2	0.4
8	12.2	12.4	11.6	12.1	0.4
10	12.3	11.6	11.9	11.9	0.4
12	11.5	10.8	10.4	10.9	0.6

Appendix 3.3 Growth curve data from cell count-effect of pH

Sample	Cell count (CFU/ml)*10^{-8} from day 0 to day 12			
	Day 0	Day 4	Day 8	Day 12
	Mean value of cell count ± standard error			
pH 3	1.9 x 10^8 ± 2.1 x 10^7	2.5 x 10^8 ± 2.6 x 10^7	2.3 x 10^8 ± 1.8 x 10^7	2.4 x 10^8 ± 2.0 x 10^7
pH 4	1.9 x 10^8 ± 2.1 x 10^7	5.9 x 10^8 ± 2.8 x 10^7	7.5 x 10^8 ± 3.0 x 10^7	7.0 x 10^8 ± 3.7 x 10^7
pH 9	1.9 x 10^8 ± 2.1 x10^7	6.1 x 10^8 ± 5.8 x 10^7	8.0 x 10^8 ± 4.2 x 10^7	7.6 x 10^8 ± 3.5 x 10^7
pH 10	1.9 x 10^8 ± 2.1 x 10^7	5.8 x 10^8 ± 2.8 x 10^7	7.4 x 10^8 ± 3.9 x 10^7	6.8 x 10^8 ± 3.4 x 10^7

Appendix 3.4 Growth curve data from cell count-effect of acid activated clay samples

Sample	Cell count (CFU/ml)*10^{-8} from day 0 to day 12			
	Day 0	Day 4	Day 8	Day 12
	Mean value of cell count ± standard error			
KA-250	1.4 x 10^8 ± 1.5 x 10^7	6.5 x 10^8 ± 4.9 x 10^7	7.1 x 10^8 ± 3.8 x 10^7	6.5 x 10^8 ± 5.7 x 10^6
SA-250	1.4 x 10^8 ± 1.5 x 10^7	5.2 x 10^8 ± 3.0 x 10^7	6.2 x 10^8 ± 2.0 x 10^7	5.4 x 10^8 ± 8.0 x 10^7
PA-250	1.4 x 10^8 ± 1.5 x10^7	5.6 x 10^8 ± 5.5 x 10^7	6.6 x 10^8 ± 4.4 x 10^7	5.9 x 10^8 ± 2.4 x 10^7
BA-250	1.4 x 10^8 ± 1.5 x 10^7	4.7 x 10^8 ± 2.3 x 10^7	5.9 x 10^8 ± 2.4 x 10^7	4.8 x 10^8 ± 1.8 x 10^7
BA-500	1.4 x 10^8 ± 1.5 x 10^7	2.1 x 10^8 ± 2.0 x 10^7	2.5 x 10^8 ± 1.2 x 10^7	2.0 x 10^8 ± 1.2 x 10^7
Control-1	1.4 x 10^8 ± 1.5 x 10^7	6.4 x 10^8 ± 5.8 x 10^7	8.1 x 10^8 ± 3.2 x 10^7	7.1 x 10^8 ± 3.3 x 10^7

Control-2	0	0	0	0
CKA-250	0	0	0	0
CSA-250	0	0	0	0
CPA-250	0	0	0	0
CBA-250	0	0	0	0
CBA-500	0	0	0	0

Appendix 3.5 Growth curve data from cell count-effect of organoclay samples and spent water from organoclay (BO* and SO*).

Sample	Cell count (CFU/ml)*10^{-8} from day 0 to day 12			
	Day 0	Day 4	Day 8	Day 12
	Mean value of cell count ± standard error			
BO-250	$1.4 \times 10^8 \pm 1.5 \times 10^7$	$5.5 \times 10^8 \pm 5.5 \times 10^7$	$7.3 \times 10^8 \pm 2.0 \times 10^7$	$7.6 \times 10^8 \pm 9.0 \times 10^7$
SO-250	$1.4 \times 10^8 \pm 1.5 \times 10^7$	$5.7 \times 10^8 \pm 2.0 \times 10^7$	$8.2 \times 10^8 \pm 5.0 \times 10^7$	$8.4 \times 10^8 \pm 4.0 \times 10^7$
Control-1	$1.4 \times 10^8 \pm 1.5 \times 10^7$	$6.4 \times 10^8 \pm 5.0 \times 10^7$	$8.1 \times 10^8 \pm 3.2 \times 10^7$	$7.1 \times 10^8 \pm 3.3 \times 10^7$
BO*	$1.1 \times 10^8 \pm 1.4 \times 10^7$	$4.9 \times 10^8 \pm 3.2 \times 10^7$	$8.1 \times 10^8 \pm 4.1 \times 10^7$	$7.1 \times 10^8 \pm 1.8 \times 10^7$
SO*	$1.1 X 10^8 \pm 1.4 \times 10^7$	$5.4 \times 10^8 \pm 2.1 \times 10^7$	$7.9 \times 10^8 \pm 5.2 \times 10^7$	$7.1 \times 10^8 \pm 4.8 \times 10^7$
Control-3	$1.1 X 10^8 \pm 1.4 \times 10^7$	$6.0 \times 10^8 \pm 4.7 \times 10^7$	$8.0 \times 10^8 \pm 4.6 \times 10^7$	$7.1 \times 10^8 \pm 2.4 \times 10^7$
Control-2	0	0	0	0
CBO-250	0	0	0	0
CSO-250	0	0	0	0

Appendix 3.6 Growth curve data from cell count-effect of unmodified clay samples

Sample	Cell count (CFU/ml)*10^{-8} from day 0 to day 12			
	Day 0	Day 4	Day 8	Day 12
	Mean value of cell count ± standard error			
KU-250	$1.4 \times 10^8 \pm 1.5 \times 10^7$	$6.1 \times 10^8 \pm 6.4 \times 10^7$	$7.1 \times 10^8 \pm 4.2 \times 10^7$	$6.5 \times 10^8 \pm 5.0 \times 10^6$
SU-250	$1.4 \times 10^8 \pm 1.5 \times 10^7$	$6.4 \times 10^8 \pm 8.4 \times 10^7$	$8.0 \times 10^8 \pm 5.6 \times 10^7$	$8.3 \times 10^8 \pm 3.0 \times 10^7$
PU-250	$1.4 \times 10^8 \pm 1.5 \times 10^7$	$6.4 \times 10^8 \pm 5.1 \times 10^7$	$9.0 \times 10^8 \pm 4.6 \times 10^7$	$1.0 \times 10^9 \pm 3.0 \times 10^7$
BU-250	$1.4 \times 10^8 \pm 1.5 \times 10^7$	$6.9 \times 10^8 \pm 3.5 \times 10^7$	$1.0 \times 10^9 \pm 8.7 \times 10^7$	$1.12 \times 10^9 \pm 7.0 \times 10^7$
Control-1	$1.4 \times 10^8 \pm 1.5 \times 10^7$	$6.4 \times 10^8 \pm 5.8 \times 10^7$	$8.1 \times 10^8 \pm 3.2 \times 10^7$	$7.1 \times 10^8 \pm 3.3 \times 10^7$
Control-2	0	0	0	0
CKU-250	0	0	0	0
CSU-250	0	0	0	0
CPU-250	0	0	0	0
CBU-250	0	0	0	0
CBU-500	0	0	0	0

Appendix 3.7 Growth curve data from cell count-effect of homoionic interlayer cation clay samples

Sample	Cell count (CFU/ml)*10^{-8} from day 0 to day 12			
	Day 0	Day 4	Day 8	Day 12
	Mean value of cell count ± standard error			
B-Na	$1.7 \times 10^8 \pm 2.0 \times 10^7$	$6.9 \times 10^8 \pm 3.8 \times 10^7$	$1.0 \times 10^9 \pm 7.8 \times 10^7$	$1.2 \times 10^9 \pm 1.5 \times 10^8$
B-K	$1.7 \times 10^8 \pm 2.0 \times 10^7$	$6.3 \times 10^8 \pm 3.2 \times 10^7$	$8.0 \times 10^8 \pm 5.5 \times 10^7$	$8.2 \times 10^8 \pm 5.8 \times 10^7$
B-Mg	$1.7 \times 10^8 \pm 2.0 \times 10^7$	$7.3 \times 10^8 \pm 2.0 \times 10^7$	$9.0 \times 10^8 \pm 3.2 \times 10^7$	$1.0 \times 10^9 \pm 1.0 \times 10^8$
B-Ca	$1.7 \times 10^8 \pm 2.0 \times 10^7$	$7.3 \times 10^8 \pm 3.0 \times 10^7$	$1.2 \times 10^9 \pm 5.8 \times 10^7$	$1.4 \times 10^9 \pm 1.5 \times 10^7$
Control-1	$1.7 \times 10^8 \pm 2.0 \times 10^7$	$6.8 \times 10^8 \pm 3.8 \times 10^7$	$8.1 \times 10^8 \pm 5.4 \times 10^7$	$7.1 \times 10^8 \pm 3.5 \times 10^7$
B-Zn	$1.7 \times 10^8 \pm 2.0 \times 10^7$	$5.6 \times 10^8 \pm 3.6 \times 10^7$	$6.0 \times 10^8 \pm 7.0 \times 10^7$	$6.5 \times 10^8 \pm 5.0 \times 10^6$
B-Al	$1.7 \times 10^8 \pm 2.0 \times 10^7$	$7.1 \times 10^8 \pm 2.7 \times 10^7$	$1.0 \times 10^9 \pm 7.2 \times 10^7$	$1.1 \times 10^9 \pm 7.0 \times 10^7$
B-Cr	$1.7 \times 10^8 \pm 2.0 \times 10^7$	$6.5 \times 10^8 \pm 3.8 \times 10^7$	$8.0 \times 10^8 \pm 4.8 \times 10^7$	$8.1 \times 10^8 \pm 3.3 \times 10^7$
B-Fe	$1.7 \times 10^8 \pm 2.0 \times 10^7$	$7.5 \times 10^8 \pm 3.5 \times 10^7$	$1.3 \times 10^9 \pm 9.6 \times 10^7$	$1.3 \times 10^9 \pm 1.2 \times 10^8$
Control-2	0	0	0	0
CB-Na	0	0	0	0
CB-K	0	0	0	0
CB-Mg	0	0	0	0
CB-Ca	0	0	0	0

CB-Zn	0	0	0	0
CB-Al	0	0	0	0
CB-Cr	0	0	0	0
CB-Fe	0	0	0	0

Appendix 5.1: 2-sample t-test at 95% CI for the samples at various pH.

Two sample pH's compared	P-value	Comments
pH2 and pH3	0.066	Not significant
pH3 and pH4	0.002	Significant
pH4 and pH5	0.093	Not significant
pH4 and pH6	0.042	Significant
pH4 and pH7	0.018	Significant
pH5 and pH7	0.071	Not significant
pH6 and pH7	0.4	Not significant
pH7 and pH8	0.139	Not significant
pH7 and pH9	0.038	Significant
pH7 and pH10	0.012	Significant

Appendix 5.2: 2-sample t-test at 95% CI for the TPH biodegraded with acid activated samples

Samples compared	P-value for biodegradation on weight basis(mg)	P-value for biodegradation on % basis	Comments
BA-250 & PA-250	0.834	0.929	Not significant
BA-250 & KA-250	0.516	1.0	Not significant
BA-250 & SA-250	0.247	0.319	Not significant
BA-250 & Control-1	0.078	0.059	Not significant

Appendix 5.3: 2-sample t-test at 95% CI for the TPH biodegraded (%) with unmodified clay samples

Samples compared	P-value	Comment
Control-1 and PU-250	0.03	Significant
Control-1 and BU-250	0.009	Significant
BU-250 and KU-250	0.005	Significant
PU-250 and KU-250	0.018	Significant
BU-250 and SU-250	0.045	Significant
BU-250 and PU-250	0.253	Not significant
PU-250 and SU-250	0.175	Not significant
Control-1 and KU-250	0.796	Not significant
Control-1 and SU-250	0.11	Not significant
SU-250 and KU-250	0.089	Not significant

Appendix 5.4: 2-sample t-test at 95% CI for the TPH adsorbed (%) with unmodified, acid activated and organoclay samples.

Samples compared	P-value	Comments
CPU-250 and CSU-250	0.037	Significant
CPU-250 and CBU-250	0.055	Not significant
CPU-250 and CKU-250	0.042	Significant
CSU-250 and CBU-250	0.989	Not significant
CSU-250 and CKU-250	0.264	Not significant
CBU-250 and CKU-250	0.456	Not significant
CBO-250 and CBU-250	0.04	Significant
CBO-250 and CBA-250	0.045	Significant
CSO-250 and CSU-250	0.017	Significant
CSO-250 and CSA-250	0.005	Significant

Appendix 5.5: 2-sample t-test at 95% CI for the TPH biodegraded (%) with cation exchanged clay mineral samples.

Samples compared	P-value	Comments
B-Ca and B-Fe	0.782	Not significant
B-Ca and B-Na	0.047	Significant
B-Ca and B-Al	0.008	Very Significant
B-Ca and B-K	0.004	Very Significant
B-Ca and B-Zn	0.017	Significant
B-Ca and B-Mg	0.032	Significant
B-Ca and B-Cr	0.003	Very Significant
B-K and B-Zn	0.777	Not significant

B-K and B-Mg	0.027	Significant
B-K and B-Cr	0.75	Not significant
B-K and B-Na	0.003	Significant
B-K and B-Al	0.006	Significant
B-Ca and Control-1	0.000	Very significant
B-Fe and Control-1	0.006	Very significant
B-Na and Control-1	0.008	Very significant
B-Na and B-Fe	0.075	Not significant
BU-250 and B-Na	0.735	Not significant
B-Fe and BU-250	0.117	Not significant
B-Ca and BU-250	0.076	Not significant
BU-250 and Control-1	0.009	Significant

Appendix 5.6: 2-sample t-test at 95% CI for the TPH (%) adsorbed with cation exchanged clay mineral samples.

Samples compared	P-value	Comments
B-K and B-Zn	0.579	Not significant
B-K and B-Cr	0.037	Significant
B-K and B-Ca	0.008	Significant
B-K and B-Fe	0.019	Significant
B-K and B-Na	0.008	Significant
B-K and B-Al	0.018	Significant
B-K and B-Mg	0.011	Significant

Appendix 5.7A Chromatograms of BU-250, CBU-250, PU-250, CPU-250, SU-250, CSU-250

BU-250

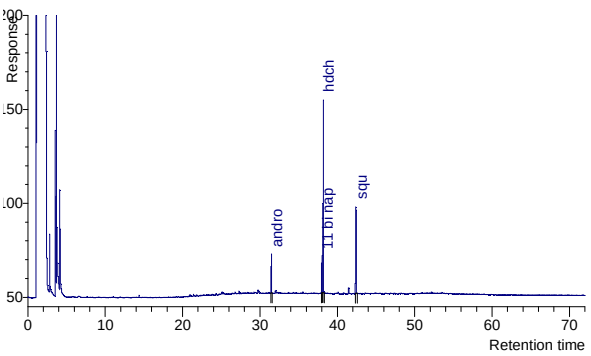

CBU-250

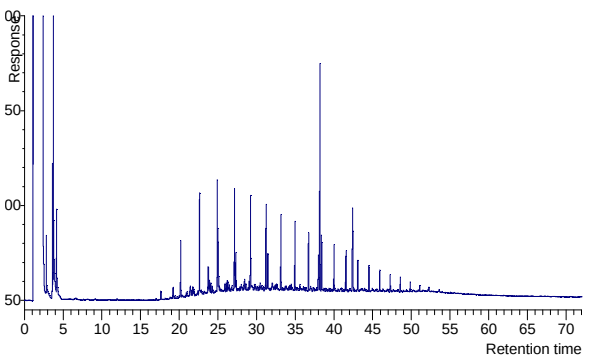

PU-250

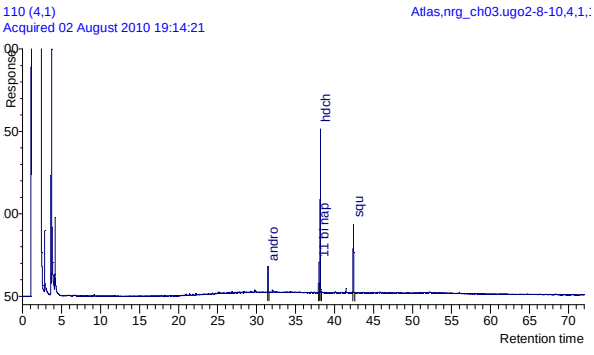

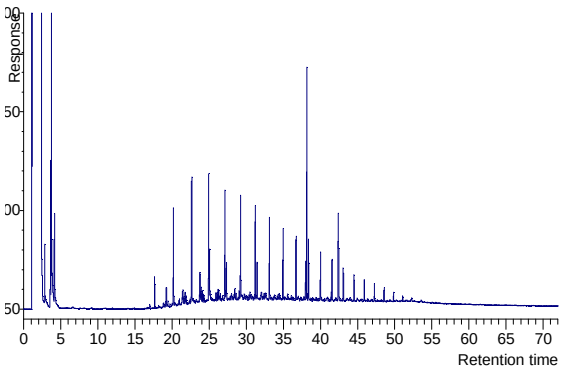

SU-250

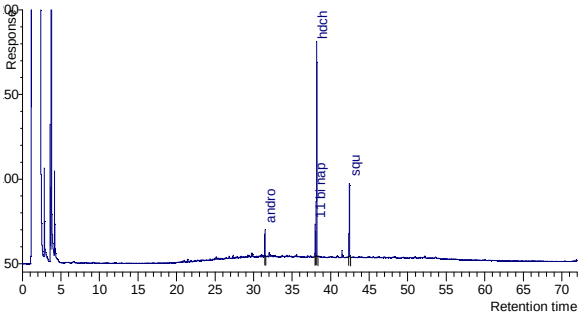

CSU-250

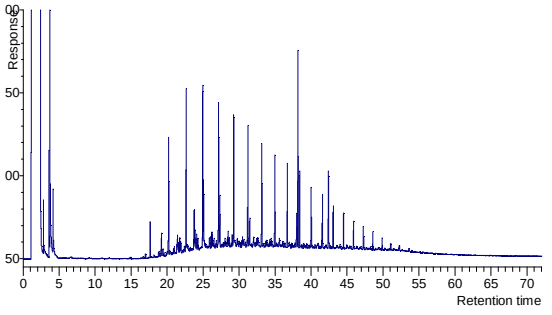

Appendix 5.7B Chromatograms of KU-250, CKU-250, BA-250, CBA-250, PA-250, CPA-250,

KU-250

104 (104,1) Atlas,nrg_ch03.ugo23-7-10,104,1,1
Acquired 30 July 2010 19:24:42

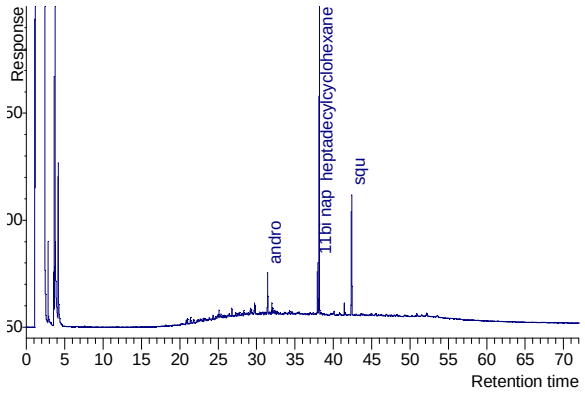

CKU-250

121 (15,1) Atlas,nrg_ch03.ugo2-8-10,15,1,1
Acquired 03 August 2010 09:40:44

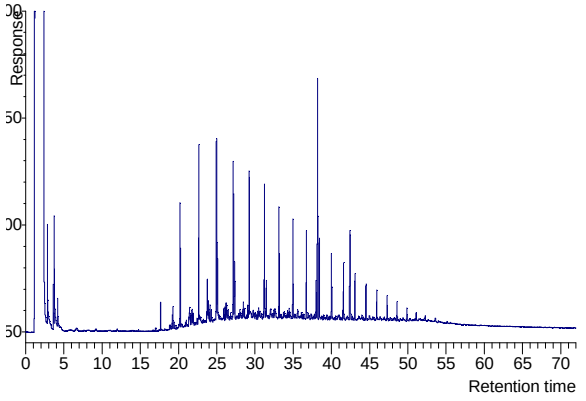

BA-250

29 (29,1) Atlas,nrg_ch03.ugo23-7-10,29,1,1
Acquired 26 July 2010 10:01:45

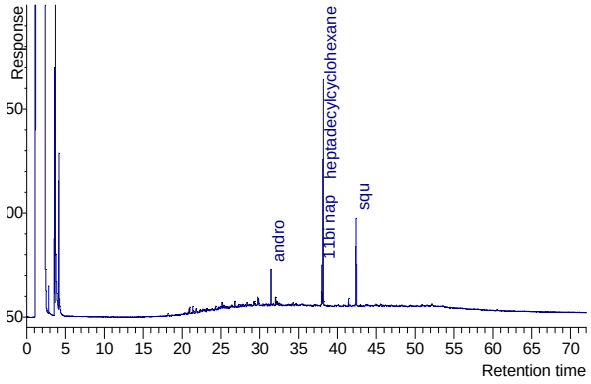

CBA-250

45 (45,1) Atlas,nrg_ch03.ugo23-7-10,45,1,1
Acquired 27 July 2010 13:44:39

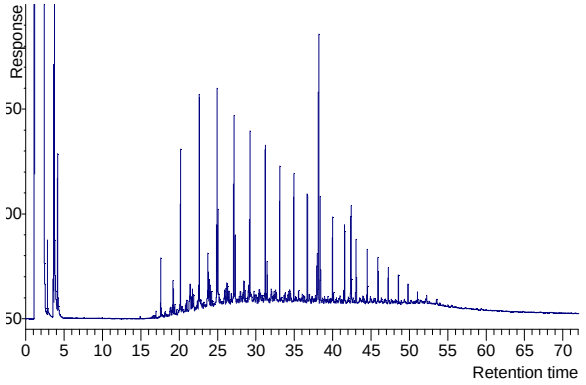

PA-250

35 (35,1) Atlas,nrg_ch03.ugo23-7-10,35,1,1
Acquired 26 July 2010 17:58:33

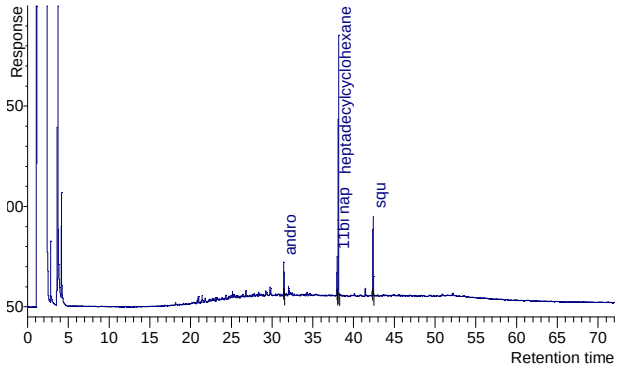

CPA-250

52 (52,1) Atlas,nrg_ch03.ugo23-7-10,52,1,1
Acquired 27 July 2010 22:59:18

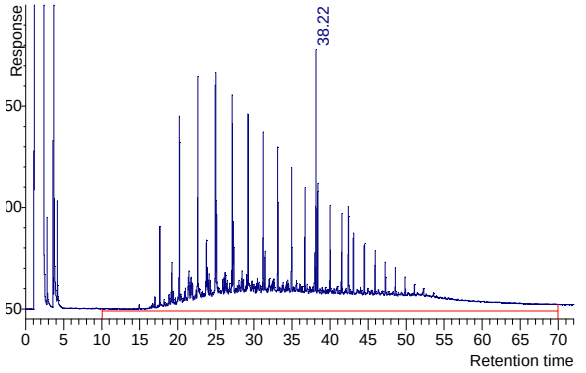

Appendix 5.7C Chromatograms of BO-250, CBO-250, SA-250, CSA-250, KA-250, CKA-250,

BO-250

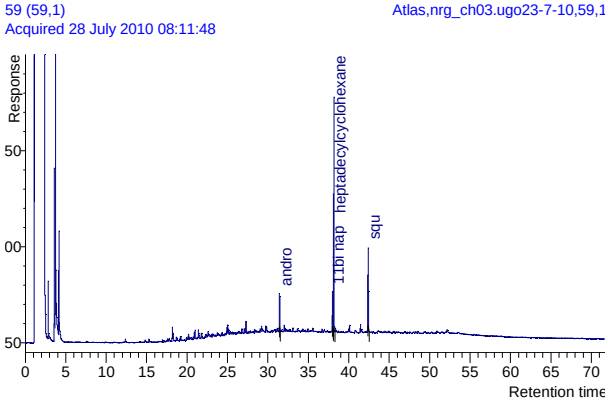

CBO-250

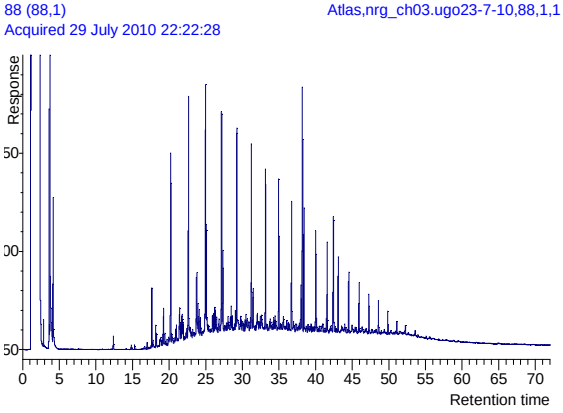

SA-250

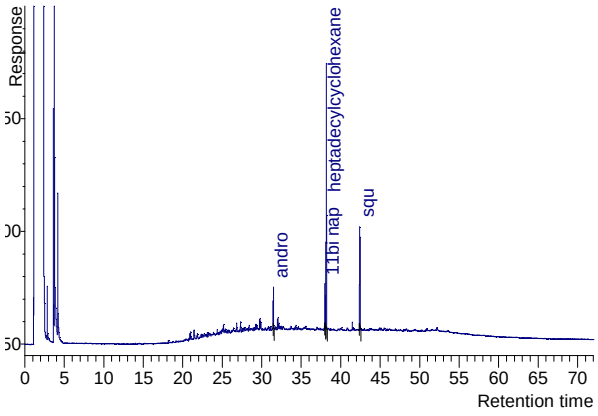

CSA-250

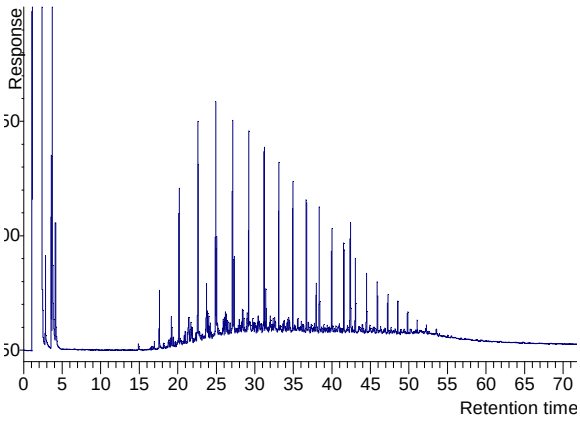

KA-250

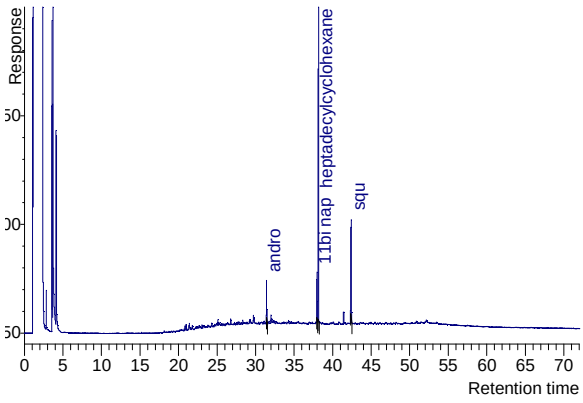

CKA-250

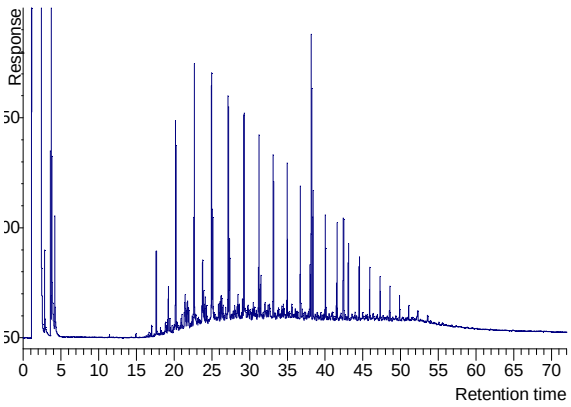

Appendix 5.7D Chromatograms of SO-250, CSO-250, B-Na, CB-Na, B-K, CB-K

SO-250

65 (65,1) Atlas,nrg_ch03.ugo23-7-10,65,1,
Acquired 28 July 2010 16:07:46

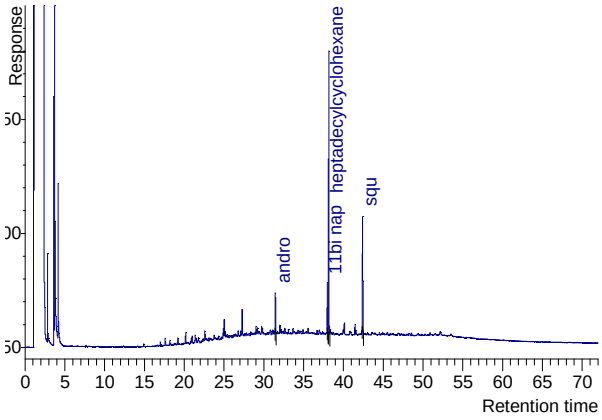

CSO-250

84 (84,1) Atlas,nrg_ch03.ugo23-7-10,84,
Acquired 29 July 2010 17:07:13

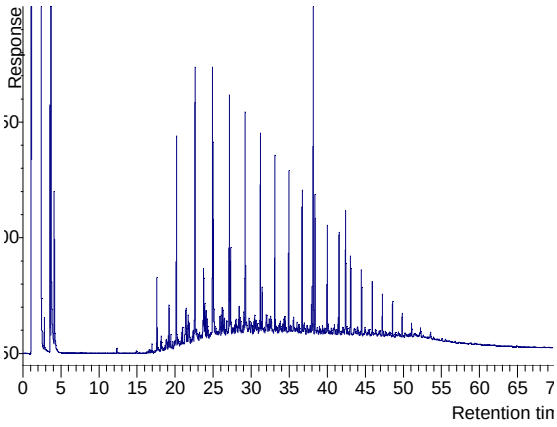

B-Na

136 1/1500ul (31,1) Atlas,nrg_ch03.ugo2-8-10,31,1,
Acquired 04 August 2010 07:05:42

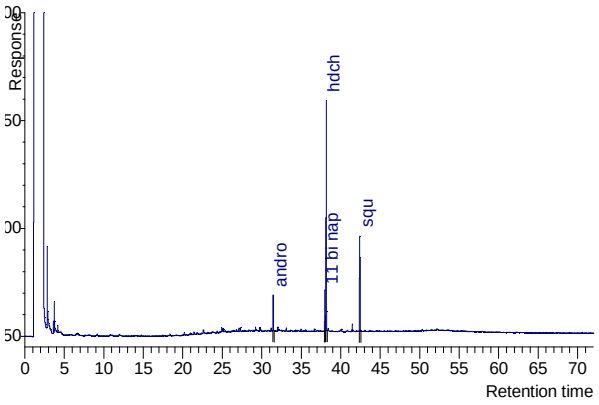

CB-Na

170 (27,1) Atlas,nrg_ch03.ugo1-8-10,27,1,1
Acquired 06 August 2010 03:47:08

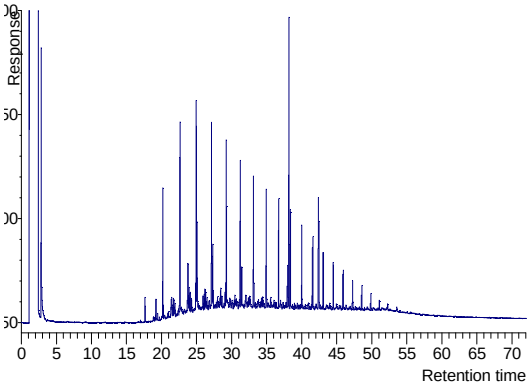

B-K

137 1/1500ul (32,1) Atlas,nrg_ch03.ugo2-8-10,32,
Acquired 04 August 2010 08:24:31

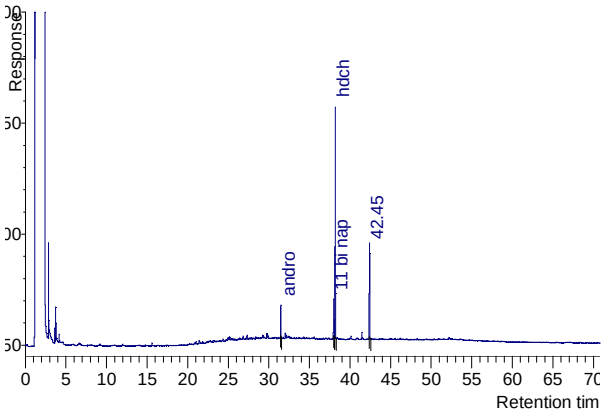

CB-K

163 (20,1) Atlas,nrg_ch03.ugo1-8-10,20,1,1
Acquired 05 August 2010 18:35:04

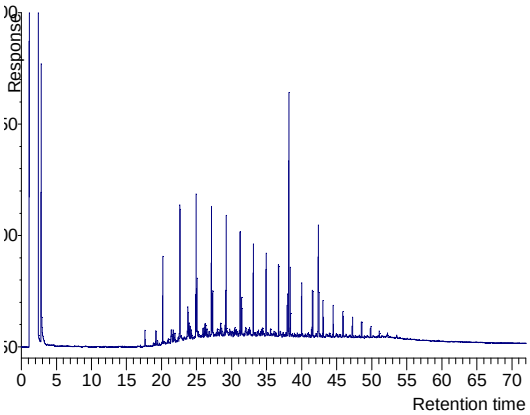

Appendix 5.7E Chromatograms of B-Mg, CB-Mg, B-Ca, CB-Ca, B-Zn, CB-Zn

B-Mg

142 1/1500ul (37,1) Atlas,nrg_ch03.ugo2-8-10,37,1,1
Acquired 04 August 2010 14:58:59

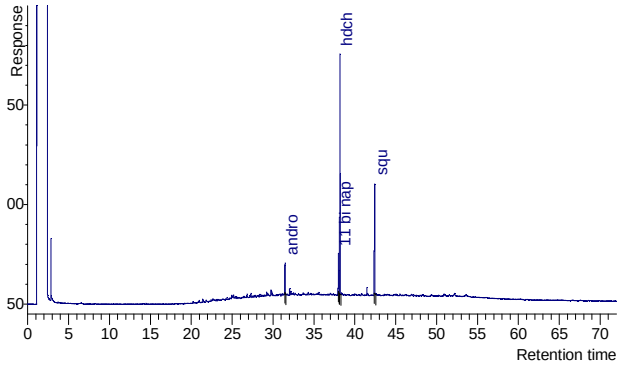

CB-Mg

161 (18,1) Atlas,nrg_ch03.ugo1-8-10,18,1,1
Acquired 05 August 2010 15:57:04

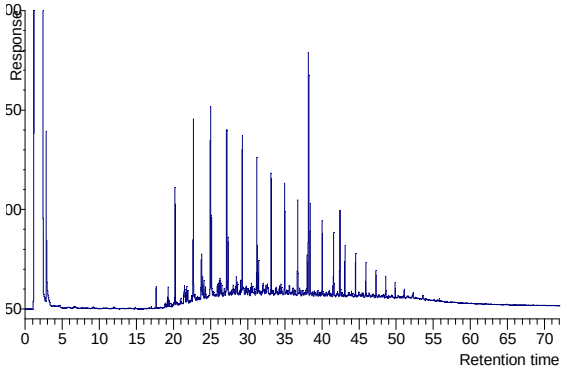

B-Ca

146 (3,1) Atlas,nrg_ch03.ugo1-8-10,3,1,
Acquired 04 August 2010 20:14:47

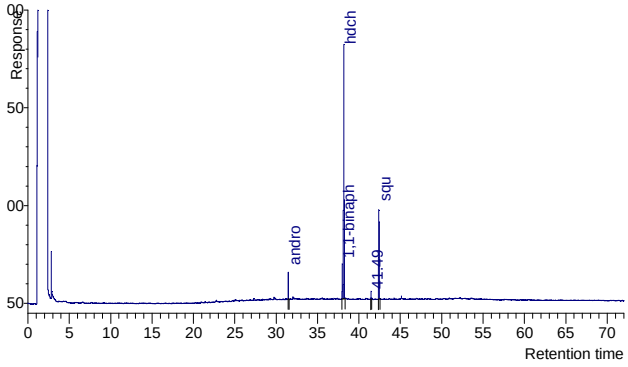

CB-Ca

167 (24,1) Atlas,nrg_ch03.ugo1-8-10,24,1,1
Acquired 05 August 2010 23:50:45

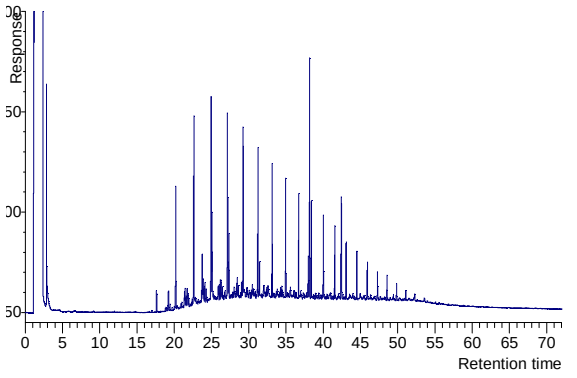

B-Zn

149 (6,1) Atlas,nrg_ch03.ugo1-8-10,6,1,1
Acquired 05 August 2010 00:11:30

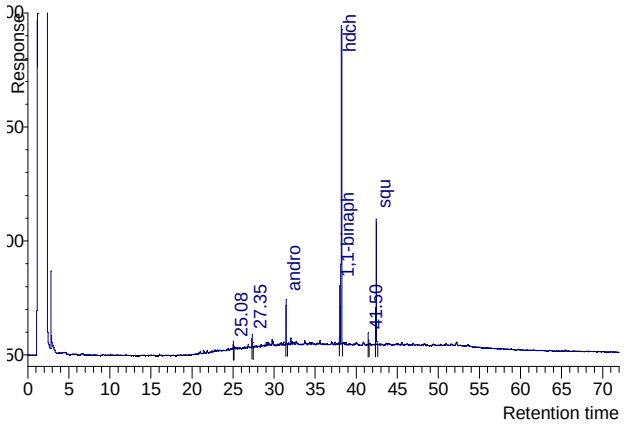

CB-Zn

174 (31,1) Atlas,nrg_ch03.ugo1-8-10,31,1,1
Acquired 06 August 2010 09:02:15

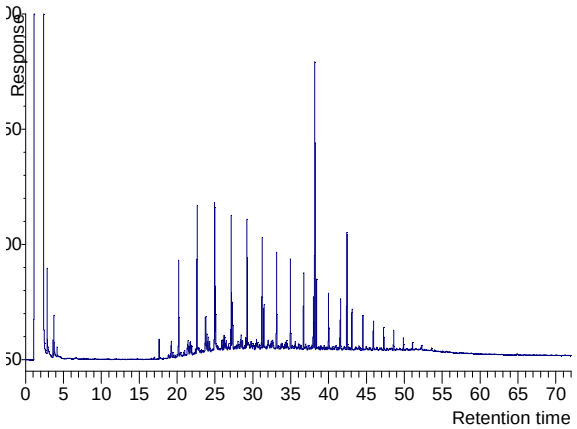

Appendix 5.7F Chromatograms of B-Al, CB-Al, B-Cr, CB-Cr, B-Fe, CB-Fe

B-Al

152 (9,1) Atlas,nrg_ch03.ugo1-8-10,9,1,1
Acquired 05 August 2010 04:07:48

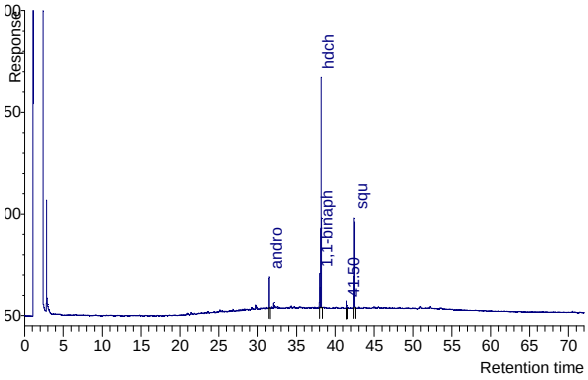

CB-Al

176 (33,1) Atlas,nrg_ch03.ugo1-8-10,33,1,1
Acquired 06 August 2010 11:39:44

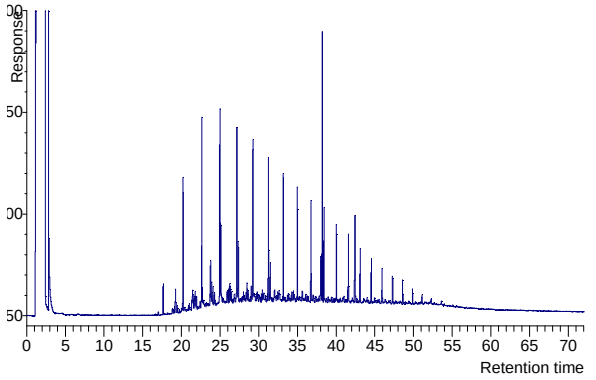

B-Cr

155 (12,1) Atlas,nrg_ch03.ugo1-8-10,12,1,1
Acquired 05 August 2010 08:04:00

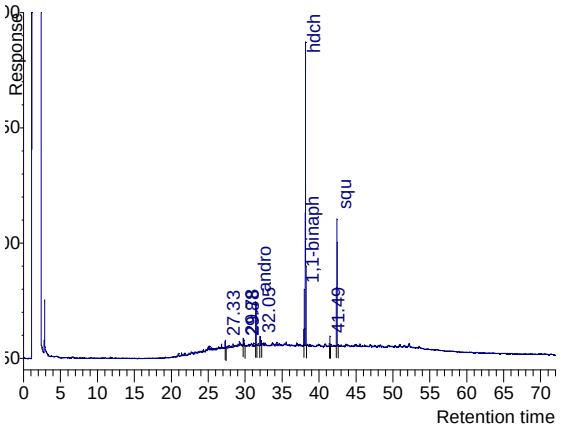

CB-Cr

179 (36,1) Atlas,nrg_ch03.ugo1-8-10,36,1,1
Acquired 06 August 2010 15:36:28

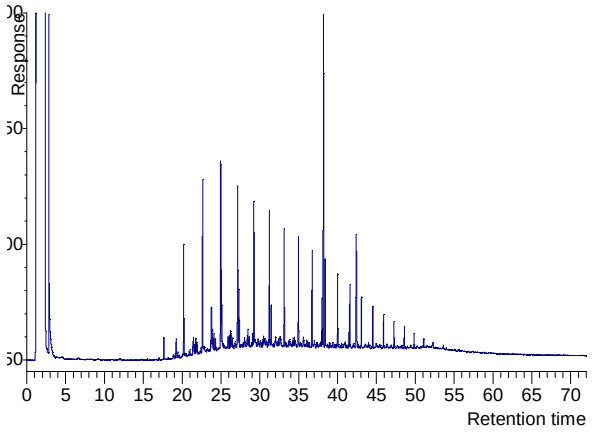

B-Fe

159 (16,1) Atlas,nrg_ch03.ugo1-8-10,16,1,1
Acquired 05 August 2010 13:19:17

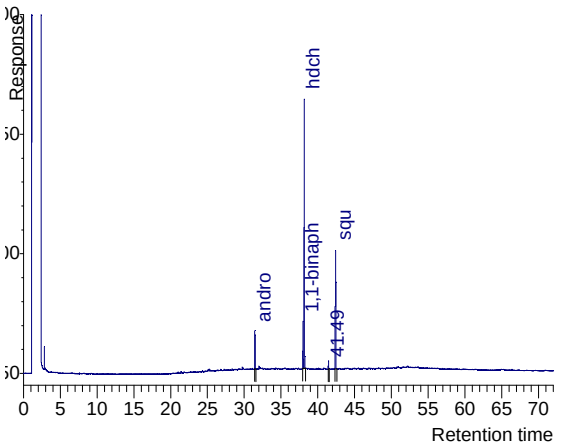

CB-Fe

183 (40,1) Atlas,nrg_ch03.ugo1-8-10,40,1,1
Acquired 06 August 2010 20:52:32

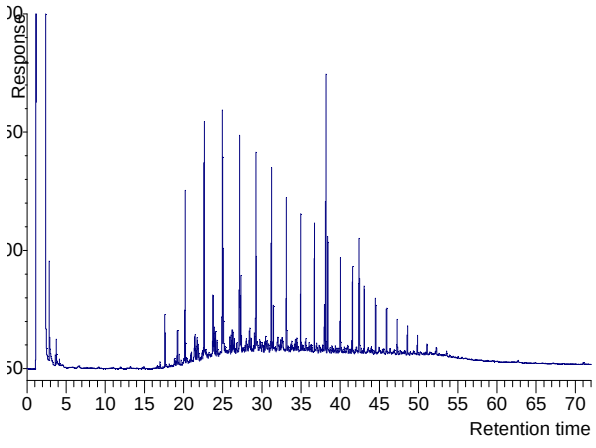

Appendix 5.8 Chromatograms of Blanks-SA, PA, SO, SU, KA, KU, BO, PU, BU and BA.

SA

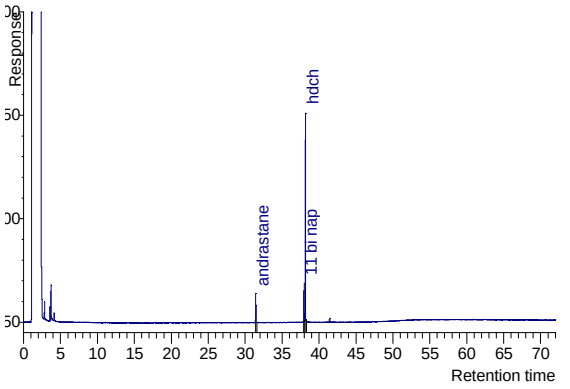

PA

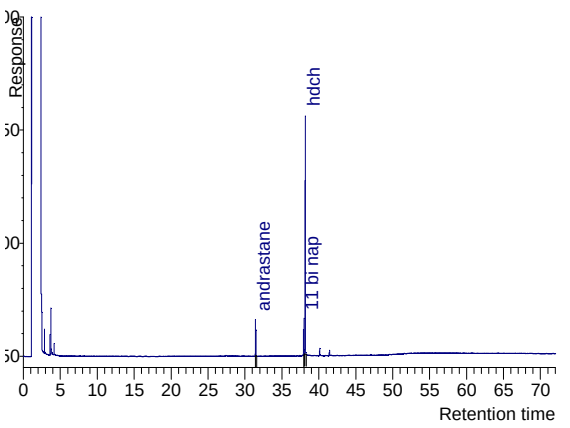

SO

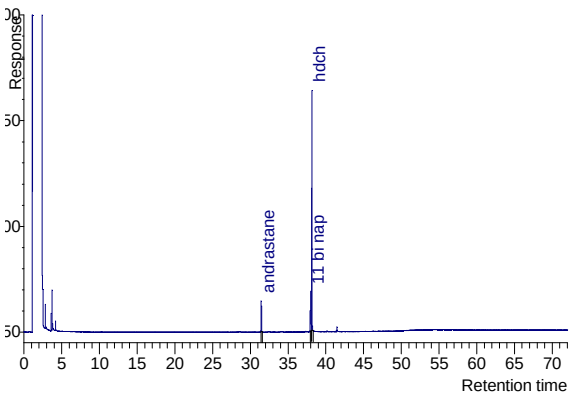

SU

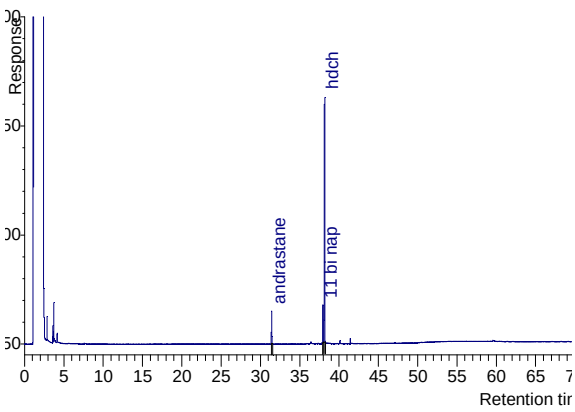

KA

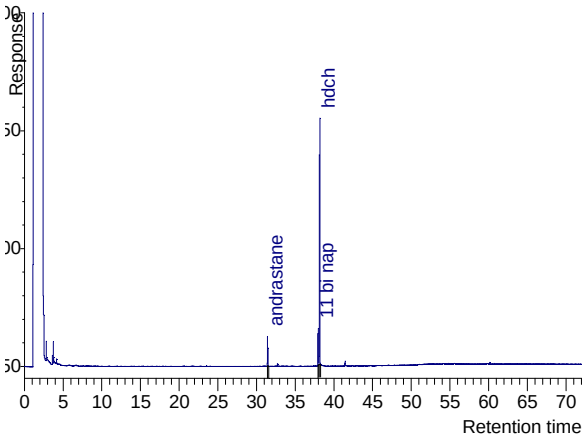

KU

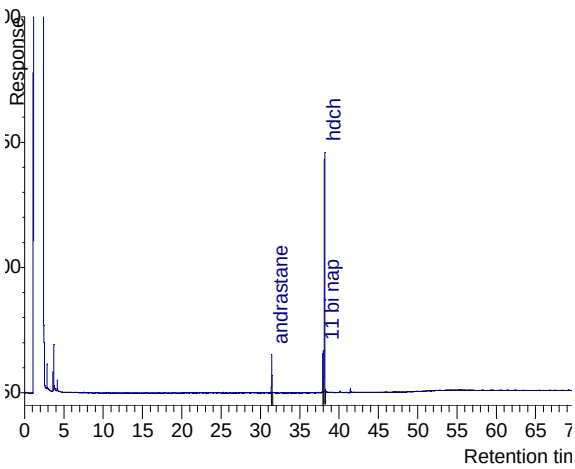

BO

201 (58,1) Atlas,nrg_ch03.ugo1-8-10,58,1,1
Acquired 09 August 2010 17:54:16

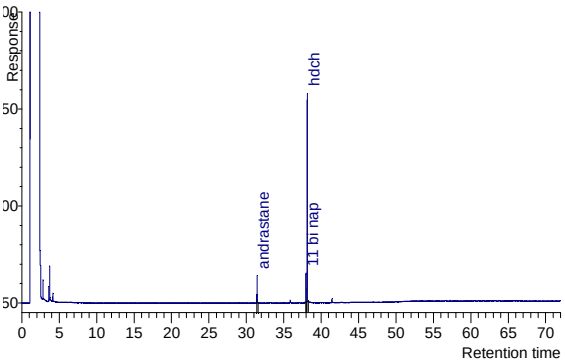

PU

202 (59,1) Atlas,nrg_ch03.ugo1-8-10,59,1,1
Acquired 09 August 2010 19:13:20

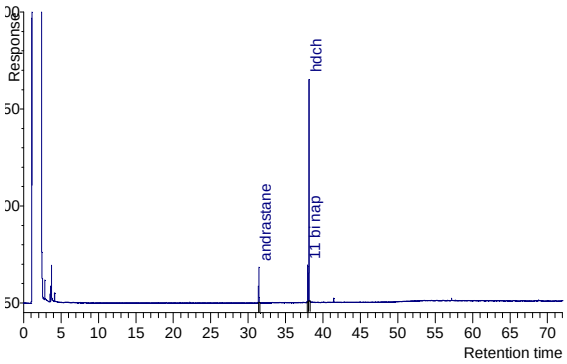

BU

203 (60,1) Atlas,nrg_ch03.ugo1-8-10,60,1
Acquired 09 August 2010 20:32:30

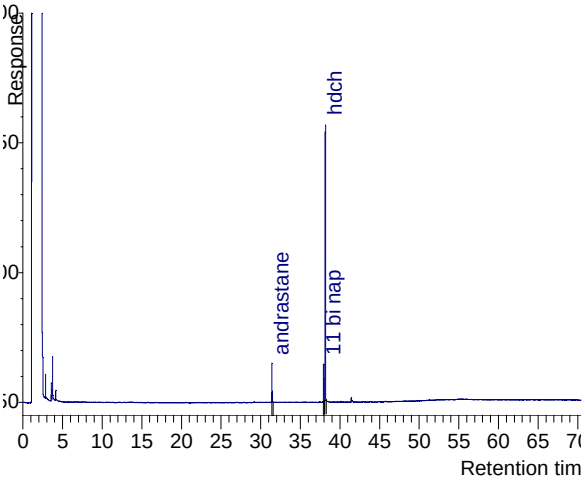

BA

204 (61,1) Atlas,nrg_ch03.ugo1-8-10,6
Acquired 09 August 2010 21:51:28

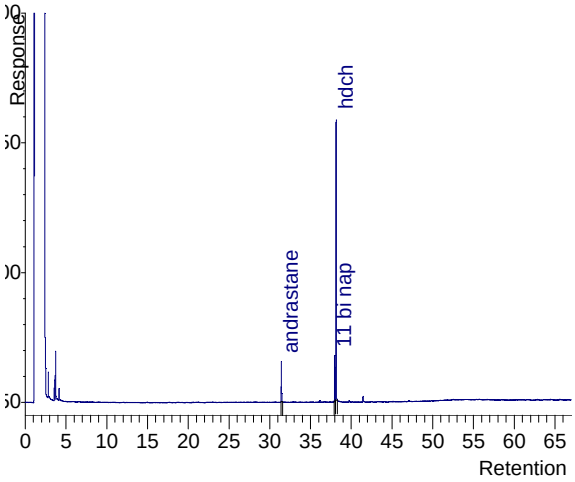

Appendix 5.9 Total petroleum hydrocarbon(TPH) remaining after biodegradation and % recovery of the surrogate standard (Squalane)

sample	TPH(mg)-residual	std error	% recovery	std error
pH2	33.8	0.40	87.5	2.5
pH3	30.2	0.90	91.4	0.4
pH4	19.7	0.58	84.6	1.1
pH5	17.8	0.29	82.9	3.6
pH6	16.9	0.19	81.6	1.4
pH7	16.4	0.40	84.8	0.8
pH8	17.3	0.23	85.8	6.6
pH9	18.2	0.29	86.9	3.0
pH10	19.9	0.49	81.8	4.3
BA-250	16.7	0.52	84.5	5.7
BA-500	24.9	0.42	83.3	2.8
PA-250	17.2	0.20	78.9	2.0
KA-250	17.4	0.12	76.8	2.7
SA-250	16.5	0.29	77.1	1.9
CBA-250	26.8	0.15	75.7	2.4
CBA-500	27.2	0.54	77.4	1.1
CSA-250	28.3	0.43	74.8	4.3
CPA-250	27.5	0.45	76.7	0.8
CKA-250	27.8	0.38	78.0	0.9
BO-250	15.8	0.50	75.2	1.7
SO-250	12.9	0.30	80.2	2.4
CSO-250	25.7	0.18	80.2	3.8
CBO-250	25.5	0.57	80.4	6.4
Contrl-2	27.9	0.62	81.1	1.1
Contrl-1	14.0	0.22	78.8	2.7
KU-250	10.9	0.35	80.5	2.7
PU-250	5.2	0.44	90.3	8.5
SU-250	8.3	0.44	82.7	3.7
BU-250	5.7	0.06	80.3	4.8
CKU-250	21.5	0.18	78.4	5.1
CPU-250	15.8	0.96	81.2	2.7
CSU-250	20.4	1.30	87.3	2.2
CBU-250	20.4	1.30	80.1	3.6
B-Na	6.8	0.42	82.9	1.0
B-K	7.8	0.95	80.9	1.3
B-Mg	8.6	0.33	82.4	6.7
B-Ca	4.9	0.12	80.8	4.9
B-Zn	8.5	0.42	78.3	6.9
B-Al	8.5	0.18	82.8	3.3
B-Cr	10.5	0.12	76.0	4.4
B-Fe	5.1	0.40	79.9	3.5

CB-Na	23.1	0.87	82.7	5.3
CB-K	14.3	0.92	83.1	4.2
CB-Ca	22.9	0.26	84.2	5.1
CB-Mg	22.2	1.23	80.2	3.3
CB-Zn	15.2	0.50	84.5	2.2
CB-Al	23.3	0.87	78.5	6.0
CB-Cr	19.7	0.57	83.7	5.3
CB-Fe	23.4	0.42	81.5	5.0
Control-1*	12.9	0.40	76.4	5.1
BO-liq	12.7	0.19	74.6	4.1
SO-liq	13.6	0.37	76.2	3.7

Appendix 5.10 TPH removed by biodegradation (on weight and % basis)

sample	TPH (mg) biodegr	std error	% TPH biodegr	std error
BA-250	10.03	1	37	5.0
BA-500	2.4	0.1	9	0.0
PA-250	10.3	0.4	37	2.0
KA-250	10.4	0.3	37	1.0
SA-250	11.8	0.7	42	3.0
BO-250	9.7	1.1	38	3.0
SO-250	12.8	0.5	50	1.0
Contrl-1	13.9	0.5	50	1.0
KU-250	10.6	0.5	49	2.0
PU-250	10.6	0.9	67	3.0
SU-250	12	1.3	59	3.0
BU-250	14.7	1.4	72	2.0
B-Na	16.3	0.8	71	1.8
B-K	6.5	0.7	45	2.3
B-Mg	13.6	1.4	61	3.2
B-Ca	18	0.3	79	0.5
B-Zn	6.7	0.9	44	4.5
B-Al	14.8	0.8	64	1.0
B-Cr	9.2	0.7	47	2.0
B-Fe	18.3	0.8	78	2.0

Appendix 5.11 TPH removed by adsorption (on weight and % basis)

sample	TPH(mg) adsorbed	std error	TPH % adsorbed	std error
BA-250	1.2	0.12	4.20	0.30
PA-250	0.3	0.06	1.10	0.20
KA-250	0.1	0.02	0.30	0.10
SA-250	0.1	0.00	0.10	0.00
BO-250	2.4	0.30	8.50	0.90
SO-250	2.2	0.20	8.50	0.60
KU-250	6.4	0.70	22.70	1.90
PU-250	12.1	1.20	43.30	3.90
SU-250	7.5	0.80	26.90	2.40
BU-250	7.5	1.00	26.80	3.70
B-Na	4.8	0.90	16.97	2.70
B-K	13.6	1.50	48.69	4.22
B-Mg	5.7	0.78	20.42	2.78
B-Ca	5.0	0.78	17.82	2.42
B-Zn	12.7	1.10	45.51	2.93
B-Al	4.6	0.44	16.56	1.27
B-Cr	8.2	1.11	29.37	3.37
B-Fe	4.5	0.55	16.08	1.69

Appendix 6.1 Aromatic compounds analysed with the GC-MS

Analyte	Ion monitored	Retention time (mins)
2,6 + 2,7-dimethylnaphthalene	156	18.136
1,7 + 1,3-dimethylnaphthalene	156	18.434
1,6-dimethylnaphthalene	156	18.519
1,4 + 2,3-dimethylnaphthalene	156	18.923
1,5-dimethylnaphthalene	156	19.008
1,2-dimethylnaphthalene	156	19.221
1,3,7-trimethylnaphthalene	170	20.945
1,3,5 + 1,4,6-trimethylnaphthalene	170	21.456
2,3,6-trimethylnaphthalene	170	21.520
1,2,7 + 1,6,7 + 1,2,6-trimethylnaphthalene	170	21.839
Phenanthrene	178	26.841
3-methylphenanthrene	192	29.183
2-methylphenanthrene	192	29.31
9-methylphenanthrene	192	29.672
1-methylphenanthrene	192	29.799
1,3 + 3,9 + 2,10 + 3,10-dimethylphenanthrene	206	31.652
2,5 + 2,9 + 1,6-dimethylphenanthrene	206	31.780
1,7-dimethylphenanthrene	206	31.886
1,9 + 4,9 + 4,10-dimethylphenanthrene	206	32.078
2,3-dimethylphenanthrene	206	32.227
Fuorene	166	22.286
3+2-methylfluorene	180	24.904
1-methylfluorene	180	25.032

4-methylfluorene	180	25.298
Dibenzothiophene	184	26.00
4-methyldibenzothiophene	198	28.14
3+2-methyldibenzothiophene	198	28.80
1-methyldibenzothiophene	198	29.24
4-ethyldibenzothiophene	212	30.20
4,6-dimethyldibenzothiophene	212	30.35
Triaromatic steroid-26S	231	45.70
Triaromatic steroid-26R + 27S	231	46.658
Triaromatic steroid-28S	231	47.446
Triaromatic steroid-27R	231	47.850
Triaromatic steroid-28R	231	48.808

Appendix 6.2 Residual total dimethylnaphthalenes(TDMN) and total trimethylnaphthalenes (TTMN) remaining after incubation. Values as mean and standard error.

Sample	TDMN(ug)*10	std error	TTMN (ug)*10	std error
BA-250	9.0	0.2	76.7	5.0
PA-250	6.3	0.8	72.3	4.1
KA-250	4.4	0.3	62.7	1.7
SA-250	8.2	0.6	87.0	3.1
CBA-250	26.6	0.7	109.7	2.8
CSA-250	24.1	2.6	93.3	5.0
CPA-250	28.6	1.0	120.3	3.0
CKA-250	22.4	1.0	107.0	1.5
BO-250	84.6	4.0	104.7	2.7
SO-250	24.0	1.5	49.3	1.2
CSO-250	69.9	3.6	122.0	8.4
CBO-250	116.9	3.6	128.0	8.5
Contrl-1	1.4	0.1	50.3	2.2
Control-2	25.3	0.4	93.3	3.3
KU-250	1.7	0.2	47.0	0.6
PU-250	1.8	0.2	25.3	2.0
SU-250	1.8	0.3	30.7	0.9
BU-250	0.9	0.1	21.7	0.9

CBU-250	10.7	0.9	73.3	3.5
CSU-250	14.3	0.8	78.3	3.7
CKU-250	12.2	0.5	70.3	2.4
CPU-250	15.1	1.2	69.3	3.5
B-Na	1.0	0.0	28.3	0.3
B-K	0.6	0.1	30.0	2.1
B-Mg	0.7	0.1	23.7	1.5
B-Ca	0.4	0.1	12.7	0.3
B-Zn	2.1	0.1	22.3	0.9
B-Al	1.5	0.1	22.0	1.2
B-Cr	1.4	0.0	23.3	1.5
B-Fe	0.7	0.1	14.7	0.3
CB-Na	5.4	0.2	65.7	0.9
CB-K	3.1	0.1	50.7	2.8
CB-Ca	4.9	0.3	55.3	2.2
CB-Mg	4.7	0.2	60.7	1.8
CB-Zn	4.6	0.2	49.3	1.5
CB-Al	7.4	0.4	68.0	1.7
CB-Cr	6.9	0.2	67.3	3.0
CB-Fe	16.3	0.9	78.3	1.2

Appendix 6.3 Residual total phenanthrenes (TP) and total fluorenes (TF) remaining after incubation. Values as mean and standard error.

Sample	TP(ug)*10	std error	TF(ug)*10	std error
BA-250	27.2	0.8	41.9	1.1
PA-250	28.6	0.9	40.7	1.4
KA-250	26.8	2.6	38.9	3.9
SA-250	29.9	1.1	44.4	0.9
CBA-250	24.9	0.6	42.1	1.1
CPA-250	29.2	1.4	46.4	1.0
CKA-250	29.6	0.6	46.8	0.7
CSA-250	29.4	0.8	45.2	1.6
BO-250	21.3	0.7	38.6	0.8
SO-250	19.8	1.4	29.1	1.7
CBO-250	29.6	2.1	59.3	4.6
CSO-250	33.8	3.5	58.4	4.3
Contrl-2	29.7	2.2	45.6	2.5
Contrl-1	26.6	1.3	33.2	1.6
KU-250	23.4	1.8	30.1	1.1
PU-250	14.7	1.0	17.9	1.1
SU-250	17.5	0.4	21.3	1.0
BU-250	14.5	2.1	16.3	0.1

CKU-250	23.6	1.8	35.1	2.4
CPU-250	18.8	1.3	31.5	2.8
CSU-250	23.4	2.0	37.8	3.8
CBU-250	23.1	1.4	37.1	2.6
B-Na	15.6	1.6	19.0	1.7
B-K	14.5	1.0	15.6	1.0
B-Mg	16.2	1.4	17.5	2.2
B-Ca	10.2	0.2	9.7	0.3
B-Zn	14.9	0.7	14.2	0.4
B-Al	16.2	0.6	16.2	1.0
B-Cr	17.4	0.6	18.6	0.8
B-Fe	9.6	1.5	11.1	2.1
CB-Na	24.5	0.3	34.3	1.2
CB-K	17.7	1.8	25.3	2.6
CB-Mg	24.0	0.5	34.4	0.9
CB-Ca	23.6	1.0	34.2	1.3
CB-Zn	17.3	1.3	25.2	1.7
CB-Al	23.6	1.6	36.5	2.6
CB-Cr	20.9	1.6	33.3	2.0
CB-Fe	25.2	0.6	40.8	1.4

Appendix 6.4 Residual total dibenzothiophenes (TDBT) and total triaromatic steroids (TTAS) remaining after incubation. Values reported as mean and standard error.

Sample	TDBT(ug)*10	std error	TTAS(ug)*100	std error
BA-250	41.0	0.5	42.4	0.9
PA-250	43.3	1.6	44.2	1.5
KA-250	39.9	3.8	41.2	2.0
SA-250	45.3	1.8	45.1	1.4
CBA-250	40.9	0.3	38.7	1.0
CPA-250	47.6	2.3	43.1	0.9
CKA-250	48.0	1.0	45.1	1.9
CSA-250	44.9	3.3	43.8	4.1
BO-250	33.2	1.4	40.2	1.6
SO-250	30.1	1.9	35.9	3.1
CBO-250	47.5	3.2	41.1	1.3
CSO-250	49.9	3.1	44.8	0.7
Contrl-2	46.1	2.2	47.5	1.0
Contrl-1	40.1	1.8	43.4	0.7
KU-250	35.4	2.7	29.9	2.8
PU-250	21.7	1.3	19.6	1.7
SU-250	26.0	0.8	24.0	2.7

BU-250	19.0	0.5	15.7	0.7
CKU-250	36.2	2.5	36.5	1.9
CPU-250	29.2	2.5	26.1	2.6
CSU-250	37.6	3.4	35.3	1.8
CBU-250	35.2	2.0	36.0	3.7
B-Na	22.9	2.3	21.4	2.7
B-K	20.9	1.3	23.4	2.5
B-Mg	23.1	2.2	26.9	2.2
B-Ca	14.4	0.4	16.4	1.0
B-Zn	21.2	0.7	26.5	1.0
B-Al	22.1	0.7	30.8	1.0
B-Cr	24.8	0.8	31.9	1.0
B-Fe	13.9	2.3	15.6	2.5
CB-Na	33.7	3.0	37.7	1.7
CB-K	28.1	2.6	23.2	2.2
CB-Mg	36.6	0.8	39.6	1.7
CB-Ca	36.3	1.5	39.8	2.2
CB-Zn	27.2	2.4	24.4	1.0
CB-Al	36.7	2.4	39.5	2.2
CB-Cr	32.8	2.2	34.3	3.4
CB-Fe	40.0	1.0	41.2	0.6

Appendix 6.5A 2-sample t-test at 95% CI for the total trimethylnaphthalenes biodegraded with unmodified clay samples.

Samples compared	P-value	Comments
Control-1 and KU-250	0.004	Significant
Control-1 and PU-250	0.107	Not significant
Control-1 and SU-250	0.091	Not significant
Control-1 and BU-250	0.005	Significant

Appendix 6.5B: 2-sample t-test at 95% CI for the total trimethyl naphthalenes biodegraded with cation exchanged clay samples.

Samples compared	P-value	Comment
B-Na and Control-1	0.054	Not significant
B-K and Control-1	0.307	Not significant
B-Mg and Control-1	0.012	Significant
B-Ca and Control-1	0.001	Significant
B-Zn and Control-1	0.113	Not significant
B-Al and Control-1	0.007	Significant
B-Cr and Control-1	0.052	Not significant
B-Fe and Control-1	0.002	Significant
B-Fe and B-Al	0.026	Significant
B-Ca and B-Al	0.033	Significant
B-Ca and B-Mg	0.004	Significant
B-Ca and B-Fe	0.1	Not significant

Appendix 6.5C: 2-sample t-test at 95% CI for the total fluorenes biodegraded with organoclay samples

Samples compared	P-value	Comment
BO-250 and SO-250	0.18	Not significant
BO-250 and Control-1	0.393	Not significant
SO-250 and control-1	0.077	Not significant

Appendix 6.5D 2-sample t-test at 95% CI for the total phenanthrenes biodegraded with organoclay samples

Samples compared	P-value	Comment
SO-250 and Control-1	0.003	Significant
BO-250 and Control-1	0.007	Significant
BO-250 and SO-250	0.025	Significant

Appendix 6.5E: 2-sample t-test at 95% CI for the total phenanthrenes biodegraded with cation exchanged clay samples

Samples compared	P-value	Comments
B-Na and Control-1	0.058	Not significant
B-Cr and Control-1	0.159	Not significant
B-Zn and Control-1	0.562	Not significant
B-Mg and Control-1	0.041	Significant
B-Al and Control-1	0.002	Significant
B-K and Control-1	0.045	Significant
B-Ca and Control-1	0.001	Significant
B-Fe and Control-1	0.01	Significant
B-Ca and B-Al	0.012	Significant
B-Fe and B-Al	0.023	Significant
B-Ca and B-Fe	0.41	Not significant

Appendix 6.5F 6.6: 2-sample t-test at 95% CI for the % total aromatics biodegraded with acid activated clay samples

Samples compared	P-value	Comments
BA-250 and Control-1	0.011	Significant
SA-250 and Control-1	0.017	Significant
PA-250 and Control-1	0.611	Not significant
KA-250 and Control-1	0.802	Not significant

Appendix 6.5G: 2-sample t-test at 95% CI for the % total aromatics biodegraded with acid activated clay samples.

Samples compared	P-value	Comments
B-Na and Control-1	0.043	Significant
B-K and Control-1	0.041	Significant
B-Mg and Control-1	0.084	Not significant
B-Ca and Control-1	0.000	Significant
B-Zn and Control-1	0.084	Not significant
B-Al and Control-1	0.001	Significant
B-Cr and Control-1	0.018	Significant
B-Fe and Control-1	0.006	Significant

Appendix 7.1 Total crude oil saturates remaining (residual saturates) after incubation and % recovery of the surrogate standard (squalane). Values reported as mean and standard error.

Sample	Residual saturates (mg)	std error	% recovery	Std error
PU-250	7.10	0.21	80	0
BU-250	4.87	0.27	86	2
KU-250	9.63	0.58	85	5
SU-250	8.27	0.44	85	5
BO-250	10.27	0.12	83	2
SO-250	10.47	0.19	89	5
SA-250	8.60	0.23	85	5
KA-250	8.93	0.22	79	2
BA-250	9.07	0.12	81	4
PA-250	9.37	0.73	88	5
Control-1	8.60	0.23	86	3
Control-2	20.53	0.44	88	4
CKA-250	19.07	0.43	83	2
CBA-250	17.90	0.61	95	12
CKU-250	19.43	0.20	84	4
CBU-250	17.90	0.17	88	7
CPU-250	20.20	0.21	88	2
CSU-250	19.77	0.54	93	7
CPA-250	19.57	0.52	85	7
CSA-250	19.07	0.32	78	1
CBO-250	18.57	0.27	91	5
CSO-250	18.90	0.29	83	3

Appendix 7.2: 2-sample t-test at 95% CI for the effect of acid activated clay on biodegradation of crude oil saturates

Samples compared	P-value	Comments
SA-250 and Control-1	0.4	Not significant
KA-250 and Control-1	0.11	Not significant
BA-250 and Control-1	0.068	Not significant
PA-250 and Control-1	0.41	Not significant

Appendix 7.3: 2-sample t-test at 95% CI for the effect of unmodified clay on biodegradation of crude oil saturates.

Samples compared	P-value	Comments
KU-250 and Control-1	0.089	Not significant
SU-250 and Control-1	0.071	Not significant
PU-250 and Control-1	0.022	Significant
BU-250 and Control-1	0.01	Significant

Appendix 8.1 2-sample t-test at 95% CI for % oil biodegraded with unmodified clay samples.

Samples compared	P-values	Comments
BU-250 and Control-1	0.017	Significant
PU-250 and Control-1	0.149	Not significant
SU-250 and Control-1	0.295	Not significant
KU-250 and Control-1	0.849	Not significant

Appendix 8.2: 2-sample t-test at 95% CI for % oil biodegraded with cation exchanged samples

Samples compared	P-value	Comments
B-Na and Control-1	0.01	Significant difference
B-K and Control-1	0.56	No significant difference
B-Mg and Control-1	0.73	No significant
B-Ca and Control-1	0.012	Significant difference
B-Zn and Control-1	0.09	No significant difference
B-Al and Control-1	0.02	Significant difference
B-Cr and Control-1	0.29	No significant difference
B-Fe and Control-1	0.01	Significant difference